

Special Collection on Cancer and mTOR

Rapatar increases lifespan in p53^{-/-} mice, see Comas, et al. - "New nanoformulation of rapamycin Rapatar extends lifespan in homozygous p53^{-/-} mice by delaying carcinogenesis."

**Cancer
and
mTOR**

AGING

AGING

www.aging-us.com

EDITORIAL BOARD

EDITORS-IN-CHIEF

Jan Vijn - Albert Einstein College of Medicine, Bronx, NY, USA

David A. Sinclair - Harvard Medical School, Boston, MA, USA

Vera Gorbunova - University of Rochester, Rochester, NY, USA

Judith Campisi - The Buck Institute for Research on Aging, Novato, CA, USA

Mikhail V. Blagosklonny - Roswell Park Cancer Institute, Buffalo, NY, USA

EDITORIAL BOARD

Frederick Alt - Harvard Medical School, Boston, MA, USA

Vladimir Anisimov - Petrov Institute of Oncology, St.Petersburg, Russia

Johan Auwerx - Ecole Polytechnique Federale de Lausanne, Switzerland

Andrzej Bartke - Southern Illinois University, Springfield, IL, USA

Nir Barzilai - Albert Einstein College of Medicine, Bronx, NY, USA

Elizabeth H. Blackburn - University of California, San Francisco, CA, USA

Maria Blasco - Spanish National Cancer Center, Madrid, Spain

Vilhelm A. Bohr - National Institute on Aging, NIH, Baltimore, MD, USA

William M. Bonner - National Cancer Institute, NIH, Bethesda, MD, USA

Robert M. Brosh, Jr. - National Institute on Aging, NIH, Baltimore, MD, USA

Anne Brunet - Stanford University, Stanford, CA, USA

Rafael de Caba - NIA, NIH, Baltimore, MD, USA

Ronald A. DePinho - Dana-Farber Cancer Institute, Boston, MA, USA

Jan van Deursen - Mayo Clinic, Rochester, MN, USA

Lawrence A. Donehower - Baylor College of Medicine, Houston, TX, USA

Caleb E. Finch - University of Southern California, Los Angeles, CA, USA

Toren Finkel - National Institutes of Health, Bethesda, MD, USA

Luigi Fontana - Washington University, St. Louis, MO, USA

Claudio Franceschi - University of Bologna, Bologna, Italy

David Gems - Inst. of Healthy Ageing, Univ. College London, UK

Myriam Gorospe - National Institute on Aging, NIH, Baltimore, MD, USA

Leonard Guarente - MIT, Cambridge, MA, USA

Andrei Gudkov - Roswell Park Cancer Institute, Buffalo, NY, USA

Michael Hall - University of Basel, Basel, Switzerland

Philip Hanawalt - Stanford University, CA, USA

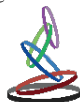
Nissim Hay - University of Illinois at Chicago, Chicago, IL, USA

Siegfried Hekimi - McGill University, Montreal, Canada
Stephen L. Helfand - Brown University, Providence, RI, USA
Jan H.J. Hoeijmakers - Erasmus MC, Rotterdam, The Netherlands
John O. Holloszy - Washington University, St. Louis, MO, USA
Stephen P. Jackson - University of Cambridge, Cambridge, UK
Heinrich Jasper - The Buck Institute for Research on Aging, Novato, CA, USA
Pankaj Kapahi - The Buck Institute for Research on Aging, Novato, CA, USA
Jan Karlseder - The Salk Institute, La Jolla, CA, USA
Cynthia Kenyon - University of California San Francisco, San Francisco, CA, USA
James L. Kirkland - Mayo Clinic, Rochester, MN, USA
Guido Kroemer - INSERM, Paris, France
Titia de Lange - Rockefeller University, New York, NY, USA
Arnold Levine - The Institute for Advanced Study, Princeton, NJ, USA
Michael P. Lisanti - University of Salford, Salford, UK
Lawrence A. Loeb - University of Washington, Seattle, WA, USA
Valter Longo - University of Southern California, Los Angeles, CA, USA
Gerry Melino - University of Rome, Rome, Italy
Simon Melov - The Buck Institute for Research on Aging, Novato, CA, USA
Alexey Moskalev - Komi Science Center of RAS, Syktyvkar, Russia
Masashi Narita - University of Cambridge, Cambridge, UK
Andre Nussenzweig - National Cancer Institute, NIH, Bethesda, MD, USA
William C. Orr - Southern Methodist University, Dallas, TX, USA
Daniel S. Peeper - The Netherlands Cancer Institute, Amsterdam, The Netherlands
Thomas Rando - Stanford University School of Medicine, Stanford, CA, USA
Michael Ristow - Swiss Federal Institute of Technology, Zurich, Switzerland
Igor B. Roninson - Ordway Research Institute, Albany, NY, USA
Michael R. Rose - University of California, Irvine, CA, USA
K Lenhard Rudolph - Hannover Medical School, Hannover, Germany
Paolo Sassone-Corsi - University of California, Irvine, CA, USA
John Sedivy - Brown University, Providence, RI, USA
Manuel Serrano - Spanish National Cancer Research Center, Madrid, Spain
Gerald S. Shadel - Yale University School of Medicine, New Haven, CT, USA
Norman E. Sharpless - University of North Carolina, Chapel Hill, NC, USA
Vladimir P. Skulachev - Moscow State University, Moscow, Russia
Sally Temple - NY Neural Stem Cell Institute, Albany, NY, USA
George Thomas - University of Cincinnati, Cincinnati, OH, USA
Jonathan L. Tilly - Massachusetts General Hospital, Boston, MA, USA
John Tower - University of Southern California, LA, CA, USA
Eric Verdin - University of California, San Francisco, CA, USA
Thomas von Zglinicki - Newcastle University, Newcastle, UK
Alex Zhavoronkov - Insilico Medicine, Baltimore, MD, USA

Aging (ISSN: 1945 - 4589) is published monthly by Impact Journals, LLC.
6666 East Quaker St., Suite 1B, Orchard Park, NY 14127

Abstracted and/or indexed in: PubMed/Medline (abbreviated as "Aging (Albany NY)"), PubMed Central (abbreviated as "Aging (Albany NY)"), Web of Science/Science Citation Index Expanded (abbreviated as Aging-US) & listed in the Cell Biology-SCIE and Geriatrics & Gerontology category, Scopus /Rank Q1(the highest rank) (abbreviated as Aging)- Aging and Cell Biology category, Biological Abstracts, BIOSIS Previews, EMBASE, META (Chan Zuckerberg Initiative), Dimensions (Digital Science's).

This publication and all its content, unless otherwise noted, is licensed under CC-BY 3.0 Creative Commons Attribution License.
Impact Journals, LLC meets Wellcome Trust Publisher requirements.
IMPACT JOURNALS is a registered trademark of Impact Journals, LLC.



Editorial and Publishing Office Aging

6666 E. Quaker St., Suite 1,
Orchard Park, NY 14127
Phone: 1-800-922-0957
Fax: 1-716-508-8254
e-Fax: 1-716-608-1380

Submission

Please submit your manuscript on-line at <http://aging.msubmit.net>

Editorial

For editorial inquiries, please call us or email editors@impactaging.com

Production

For questions related to preparation of your article for publication, please call us or email krasnova@impactaging.com

Indexing

If you have questions about the indexing status of your paper, please email kurenova@impactaging.com

Billing/Payments

If you have questions about billing/invoicing or would like to make a payment, please call us or email payment@impactaging.com

Media

If you have questions about post publication promotion, Altmetric, video interviews or social media, please email media@impactjournals.com

Printing

Each issue or paper can be printed on demand. To make a printing request, please call us or email printing@impactjournals.com

Publisher's Office

Aging is published by Impact Journals, LLC
To contact the Publisher's Office, please email: publisher@impactjournals.com, visit www.impactjournals.com, or call 1-800-922-0957

Aging (ISSN: 1945 - 4589) is published twice a month by Impact Journals, LLC.
6666 East Quaker St., Suite 1B, Orchard Park, NY 14127

Abstracted and/or indexed in: PubMed/Medline (abbreviated as "Aging (Albany NY)"), PubMed Central (abbreviated as "Aging (Albany NY)"), Web of Science/Science Citation Index Expanded (abbreviated as Aging-US) & listed in the Cell Biology-SCIE and Geriatrics & Gerontology category, Scopus /Rank Q1(the highest rank) (abbreviated as Aging) - Aging and Cell Biology category, Biological Abstracts, BIOSIS Previews, EMBASE, META (Chan Zuckerberg Initiative), Dimensions (Digital Science's).

This publication and all its content, unless otherwise noted, is licensed under CC-BY 3.0 Creative Commons Attribution License.
Impact Journals, LLC meets Wellcome Trust Publisher requirements.

IMPACT JOURNALS is a registered trademark of Impact Journals, LLC.



Table of Contents

Genetics of renal cancer: focus on MTOR

[Originally published in Volume 8, Issue 3 pp 421-422](#)

The PTEN tumor suppressor gene and its role in lymphoma pathogenesis

[Originally published in Volume 7, Issue 12 pp 1032-1049](#)

Rapamycin in preventive (very low) doses

[Originally published in Volume 6, Issue 3 pp 158-159](#)

Metformin and rapamycin are master-keys for understanding the relationship between cell senescent, aging and cancer

[Originally published in Volume 5, Issue 5 pp 337-338](#)

Temporal mTOR inhibition protects Fbxw7-deficient mice from radiation-induced tumor development

[Originally published in Volume 5, Issue 2 pp 111-119](#)

Rapamycin extends life span of Rb1^{+/-} mice by inhibiting neuroendocrine tumors

[Originally published in Volume 5, Issue 2 pp 100-110](#)

Potential anti-aging agents suppress the level of constitutive mTOR- and DNA damage- signaling

[Originally published in Volume 4, Issue 12 pp 952-965](#)

One-carbon metabolism: An aging-cancer crossroad for the gerosuppressant metformin

[Originally published in Volume 4, Issue 12 pp 894-898](#)

New nanoformulation of rapamycin Rapatar extends lifespan in homozygous *p53^{-/-}* mice by delaying carcinogenesis

[Originally published in Volume 4, Issue 10 pp 715-722](#)

Rapamycin extends lifespan and delays tumorigenesis in heterozygous *p53^{+/-}* mice

[Originally published in Volume 4, Issue 10 pp 709-714](#)

Rapamycin as longevity enhancer and cancer preventative agent in the context of *p53* deficiency

[Originally published in Volume 4, Issue 10 pp 660-661](#)

Tumor suppression by *p53* without apoptosis and senescence: conundrum or rapalog-like gerosuppression?

[Originally published in Volume 4, Issue 7 pp 450-455](#)

Molecular damage in cancer: an argument for mTOR-driven aging

[Originally published in Volume 3, Issue 12 pp 1130-1141](#)

Genome protective effect of metformin as revealed by reduced level of constitutive DNA damage signaling

[Originally published in Volume 3, Issue 10 pp 1028-1038](#)

Roles of the Raf/MEK/ERK and PI3K/PTEN/Akt/mTOR pathways in controlling growth and sensitivity to therapy-implications for cancer and aging

[Originally published in Volume 3, Issue 3 pp 192-222](#)

Potential of mTOR inhibitors for the treatment of subependymal giant cell astrocytomas in tuberous sclerosis complex

[Originally published in Volume 3, Issue 3 pp 189-191](#)

Phospho- Δ Np63 α /Rpn13-dependent regulation of LKB1 degradation modulates autophagy in cancer cells

[Originally published in Volume 2, Issue 12 pp 959-968](#)

Age-related mTOR in gynaecological cancers

[Originally published in Volume 9, Issue 2 pp 301-302](#)

Gerosuppression by pan-mTOR inhibitors

[Originally published in Volume 8, Issue 12 pp 3535-3551](#)

Towards specific inhibition of mTORC2

[Originally published in Volume 9, Issue 12 pp 2461-2462](#)

Fasting for stem cell rejuvenation

[Originally published in Volume 12, Issue 5 pp 4048-4049](#)

BMAL1 knockdown triggers different colon carcinoma cell fates by altering the delicate equilibrium between AKT/mTOR and P53/P21 pathways

[Originally published in Volume 12, Issue 9 pp 8067-8083](#)

BRD4 inhibition sensitizes renal cell carcinoma cells to the PI3K/mTOR dual inhibitor VS-5584

[Originally published in Volume 12, Issue 19 pp 19147-19158](#)

SPOCK1/SIX1axis promotes breast cancer progression by activating AKT/mTOR signaling

[Originally published in Volume 13, Issue 1 pp 1032-1050](#)

Deglycosylated EpCAM regulates proliferation by enhancing autophagy of breast cancer cells via PI3K/Akt/mTOR pathway

[Originally published in Volume 14, Issue 1 pp 316-329](#)

A comprehensive analysis of FOX family in HCC and experimental evidence to support the oncogenic role

of FOXH1

[Originally published in Volume 14, Issue 5 pp 2268-2286](#)

Ox-LDL-mediated ILF3 overexpression in gastric cancer progression by activating the PI3K/AKT/mTOR signaling pathway

[Originally published in Volume 14, Issue 9 pp 3887-3909](#)

Hallmarks of cancer and hallmarks of aging

[Originally published in Volume 14, Issue 9 pp 4176-4187](#)

Genetics of renal cancer: focus on MTOR

Arindam P. Ghosh and Sunil Sudarshan

Renal cell carcinoma (RCC) has multiple subtypes and may occur in hereditary and sporadic forms. Sporadic renal cell carcinomas are most commonly clear cell cancers (80%). Metastatic disease is found at presentation in almost 30% of patients with renal cell carcinoma and treatment of RCC metastases is greatly different from the treatment regimens of the primary tumor. Currently, several FDA approved therapies exist for metastatic clear cell RCC (ccRCC) which includes two rapamycin analogs- everolimus and temsirolimus. The mammalian target of rapamycin (mTOR) is a serine/threonine kinase and catalytic subunit of two biochemically distinct complexes called mTORC1 and mTORC2. Recently published TCGA data report aberrations in the PI3K/AKT/mTOR pathway in up to 28% of RCC cases [1]. Whether these aberrations predict for clinical benefit of mTOR-targeted therapy in ccRCC patients is debatable. Prior studies have identified hyperactivating point mutations in mTOR that remain sensitive to rapamycin [2] while other recent studies have identified a somatic mutation in mTOR that is resistant to allosteric mTOR inhibition while remaining sensitive to mTOR kinase inhibitors [3]. Mutations in *MTOR* are clustered in various regulatory domains in ccRCC. We focused our attention on a prominent cluster of hyperactivating mutations in the FAT (FRAP-ATM-TTRAP) domain of mTOR in ccRCC that led to an increase in both mTORC1 and mTORC2 activities and led to an increased proliferation of cells [4]. Several of the FAT domain mutants demonstrated a decreased binding of the intrinsic inhibitor DEPTOR (DEP domain containing mTOR-interacting protein), while a subset of these mutations showed altered binding of the negative regulator PRAS40 (proline rich AKT substrate 40). We also identified a recurrent mutation in *RHEB* (Ras homolog enriched in brain) in ccRCC patients that exclusively increased mTORC1 activity. Interestingly, mutations in the FAT domain of *MTOR* and in *RHEB* remained sensitive to rapamycin, though several of these mutations demonstrated residual mTOR kinase activity after treatment with rapamycin at clinically relevant doses. Overall, our data suggests that point mutations in the mTOR pathway may lead to downstream mTOR hyperactivation through multiple different mechanisms to confer a proliferative advantage to a tumor cell.

Given the central role of mTORC1 as a downstream target of PI3K activity, there exists a clear rationale for targeting mTORC1 in cancer and using rapalogs clinically. Unfortunately, the effectiveness of rapamycin as a single agent therapy is fraught with several limitations. mTORC1 promotes IRS-1 degradation [5] implying that the potential therapeutic benefit of inhibiting mTORC1 with rapamycin is opposed by the release of feedback inhibition of PI3K/AKT activation. In addition to inhibition of the feedback loop that restrains PI3K/AKT activation, everolimus treatment in breast cancer patients can increase ERK activation by a mechanism which is largely unknown, thereby adding a new level of complexity to allosteric inhibition of mTORC1 by rapalogs [5]. In an attempt to target the mTOR pathway more effectively, novel ATP competitive inhibitors that act at its catalytically active site are being developed. Active-site inhibitors have indeed proved more effective inhibitors of cell proliferation than rapamycin in a variety of tumor subtypes *in vitro* as they have a distinct advantage in that they inhibit 4E-BP1 phosphorylation at rapamycin resistant sites and also block AKT phosphorylation at Ser473 [6]. Significant homology in the kinase domains of PI3K and mTOR has made possible the development of dual active-site inhibitors. While these agents can circumvent the activation of PI3K/AKT feedback loops activated by rapalogs, dual PI3K/mTOR inhibitors could lead to activation of alternative compensatory pathways. The elucidation of the feedback loops that regulate the outputs of signaling networks is an area of fundamental importance for the rationale design of effective anticancer drugs that can be used in conjunction with PI3K/AKT/mTOR inhibitors.

While most of mTOR targeted therapies including everolimus and temsirolimus target mTORC1, mTORC2 is emerging as a pivotal player in many cancers. Defining mTORC2's role in the cellular milieu has been more challenging compared to mTORC1 because of its insensitivity to acute rapamycin treatment. As mTORC2 is a key regulator of cell proliferation and metabolic reprogramming of tumor cells [7], there is an increasing need to design therapeutic agents that specifically target mTORC2. Our *in vitro* data suggests that these hyperactivating mutations confer relative resistance to rapalog therapy

and these findings may have dosing implications for patients with ccRCC. These findings may be highly relevant from a clinical point of view, as *MTOR* mutations could serve as biomarker predicting tumor responses to mTOR allosteric inhibitors and explain acquired resistance to this class of drugs in humans.

REFERENCES

1. Cancer Genome Atlas Research N. *Nature*. 2013; 499:43-49.
2. Sato T, et al. *Oncogene*. 2010; 29:2746-2752.
3. Wagle N, et al. *N Engl J Med*. 2014; 371:1426-1433.
4. Ghosh AP, et al. *Oncotarget*. 2015; 6:17895-17910, DOI: 10.18632/oncotarget.4963.
5. Carracedo A, et al. *J Clin Invest*. 2008; 118:3065-3074.
6. Feldman ME, et al. *PLoS Biol*. 2009; 7:e38.
7. Masui K, et al. *Cell Metab*. 2013; 18:726-739.

Sunil Sudarshan: Department of Urology, University of Alabama at Birmingham, Birmingham , AL 35294, USA

Correspondence: Sunil Sudarshan

Email: sudarshan@uab.edu

Keywords: *mTOR, rapamycin, renal cancer, mutations*

Received: March 3, 2016

Published: March 26, 2016

The PTEN tumor suppressor gene and its role in lymphoma pathogenesis

Xiaoxiao Wang^{1,2}, Huiqiang Huang², and Ken H. Young^{1,3}

¹Department of Hematopathology, The University of Texas M. D. Anderson Cancer Center, Houston, TX 77230, USA;

²Department of Medical Oncology, Sun Yat-Sen University Cancer Center, Guangzhou, Guangdong, China;

³The University of Texas Graduate School of Biomedical Science, Houston, TX 77230, USA

Key words: PTEN, tumor suppressor, PI3K, AKT, mTOR, lymphoid malignancies, diffuse large B-cell lymphoma

Key points: PTEN deficiency is related to poor clinical outcomes in patients with a variety of tumors

Nuclear and cytoplasmic PTEN has distinct functions in tumor suppression

Received: 09/04/15; **Accepted:** 11/02/15; **Published:** 12/10/15

Correspondence to: Ken H. Young, MD/PhD; **E-mail:** khyoung@mdanderson.org

Copyright: Wang et al. This is an open-access article distributed under the terms of the Creative Commons Attribution License, which permits unrestricted use, distribution, and reproduction in any medium, provided the original author and source are credited

Abstract: The phosphatase and tensin homolog gene *PTEN* is one of the most frequently mutated tumor suppressor genes in human cancer. Loss of *PTEN* function occurs in a variety of human cancers via its mutation, deletion, transcriptional silencing, or protein instability. *PTEN* deficiency in cancer has been associated with advanced disease, chemotherapy resistance, and poor survival. Impaired *PTEN* function, which antagonizes phosphoinositide 3-kinase (PI3K) signaling, causes the accumulation of phosphatidylinositol (3,4,5)-triphosphate and thereby the suppression of downstream components of the PI3K pathway, including the protein kinase B and mammalian target of rapamycin kinases. In addition to having lipid phosphorylation activity, *PTEN* has critical roles in the regulation of genomic instability, DNA repair, stem cell self-renewal, cellular senescence, and cell migration. Although *PTEN* deficiency in solid tumors has been studied extensively, rare studies have investigated *PTEN* alteration in lymphoid malignancies. However, genomic or epigenomic aberrations of *PTEN* and dysregulated signaling are likely critical in lymphoma pathogenesis and progression. This review provides updated summary on the role of *PTEN* deficiency in human cancers, specifically in lymphoid malignancies; the molecular mechanisms of *PTEN* regulation; and the distinct functions of nuclear *PTEN*. Therapeutic strategies for rescuing *PTEN* deficiency in human cancers are proposed.

INTRODUCTION

The phosphatase and tensin homolog gene, *PTEN*, is one of the most commonly mutated tumor suppressors in human malignancies [1-5], and complete loss of *PTEN* protein expression is significantly associated with advanced cancer and poor outcome [6, 7]. The importance of *PTEN* as a tumor suppressor is further supported by the fact that germline mutations of *PTEN* commonly occur in a group of autosomal dominant syndromes, including Cowden Syndrome, which are characterized by developmental disorders, neurological deficits, and an increased lifetime risk of cancer and are

collectively referred to as *PTEN* hamartoma tumor syndromes (PHTS) [8, 9].

Biochemically, *PTEN* is a phosphatase that dephosphorylates phosphatidylinositol (3,4,5)-triphosphate (PIP₃), the lipid product of class I phosphoinositide 3-kinase (PI3K) [10]. To date, *PTEN* is the only lipid phosphatase known to counteract the PI3K pathway. Unsurprisingly, loss of *PTEN* has a substantial impact on multiple aspects of cancer development. Strikingly, *PTEN* has distinct growth-regulatory roles depending on whether it is in the cytoplasm or nucleus. In the cytoplasm, *PTEN* has

intrinsic lipid phosphatase activity that negatively regulates the cytoplasmic PI3K/AKT pathway, whereas in the nucleus, PTEN has AKT-independent growth activities. The continued elucidation of the roles of nuclear PTEN will help uncover the various functions of this essential tumor suppressor gene.

In this review, we describe the molecular basis of PTEN loss, discuss the regulation of PTEN expression in lymphoid malignancies, and summarize potential therapeutic targets in PTEN-deficient cancers.

STRUCTURE AND FUNCTION OF PTEN

PTEN structure

PTEN is a tumor suppressor gene located on chromosome 10q23.31 that encodes for a 403-amino acid protein that has both lipid and protein phosphatase activities. *PTEN* gene and protein structures are shown in Figure 1. The *PTEN* protein contains a sequence motif

that is highly conserved in members of the protein tyrosine phosphatase family. Structurally, the *PTEN* protein is composed of two major functional domains (a phosphatase domain and a C2 domain) and three structural regions (a short N-terminal phosphatidylinositol [4,5]-bisphosphate [PIP₂]-binding domain, a C-terminal tail containing proline-glutamic acid-serine-threonine sequences, and a PDZ-interaction motif) [11]. The PIP₂-binding site and adjacent cytoplasmic localization signal are located at the protein's N-terminal [12, 13].

The PI3K/PTEN/AKT/mTOR pathway

PTEN's tumor-suppressing function largely relies on the protein's phosphatase activity and subsequent antagonism of the PI3K/AKT/mammalian target of rapamycin (mTOR) pathway. Following *PTEN* loss, excessive PIP₃ at the plasma membrane recruits and activates a subset of pleckstrin homology domain-containing proteins to the cell membrane. These proteins

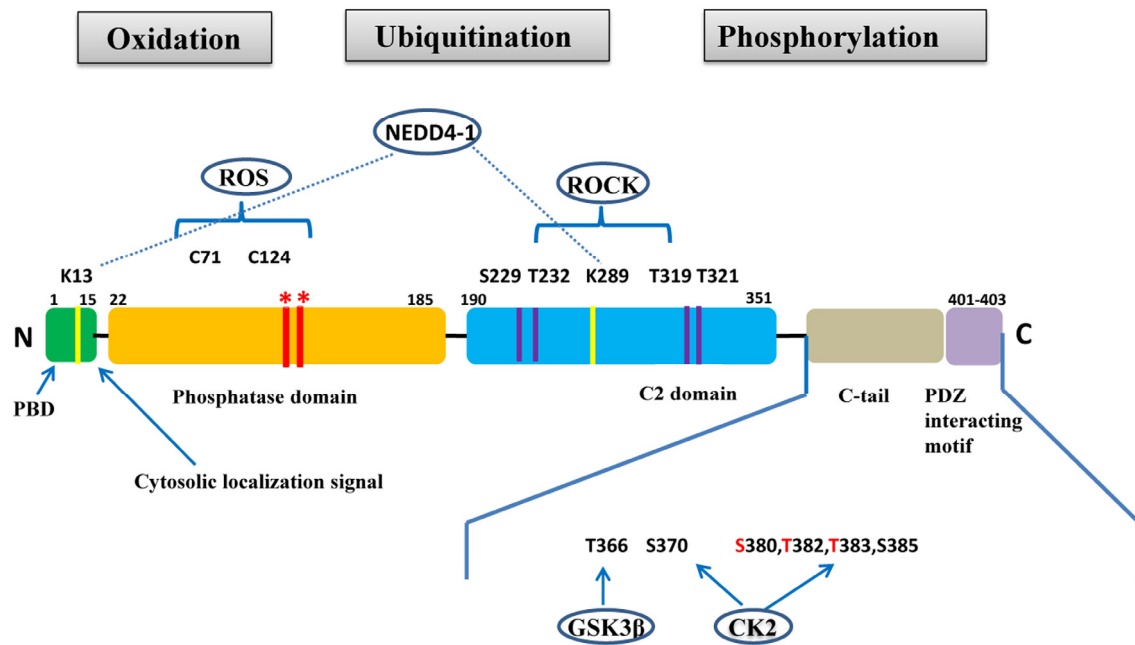


Figure 1. PTEN gene and protein structures. The *PTEN* protein is composed of 403 amino acids and contains an N-terminal PIP₂-binding domain (PBD), a phosphatase domain, a C2 domain, a C-terminal tail containing proline–glutamic acid–serine–threonine sequences, and a PDZ interacting motif at the end. *Mutations on the phosphatase domain that disrupt *PTEN*'s phosphatase activity include the C124S mutation, which abrogates both the lipid and protein phosphatase activity of *PTEN*, and the G129E mutation, which abrogates only the lipid phosphatase activity of *PTEN*. The C-terminal tail residues phosphorylated by glycogen synthase kinase 3 β (GSK3 β) and casein kinase 2 (CK2) are shown. Mutations of S380, T382, and T383 (referred to as the STT) can destabilize *PTEN* and increase its phosphatase activity. The PIP₂-binding site and adjacent cytoplasmic localization signal are located at the N-terminal. The N-terminal poly-basic region appears to selectively interact with PIP₂ and contribute to the nuclear accumulation of *PTEN*. Ubiquitination of *PTEN* has also been found on K13 and K289.

include phosphoinositide-dependent kinase-1 and AKT family members [14, 15]. AKT activation also leads to the activation of the mTOR kinase complex 1 through the inhibition of the phosphorylation of tuberous sclerosis complex tumor suppressors and consequent activation of the small GTPase rat sarcoma (RAS) homologue enriched in brain. The active mTOR complex 1 phosphorylates the p70 ribosomal protein S6 kinase (S6K) and inhibits 4E-binding protein 1 to activate protein translation [16]. Accordingly, the PTEN/PI3K/AKT/mTOR pathway is emerging as a vital target for anti-cancer agents, especially in tumors with mTOR pathway activation.

AKT-independent roles of PTEN

Although AKT pathway activation can explain many of the phenotypes associated with PTEN inactivation, *PTEN* gene targeting and genetic activation of *AKT* do not have completely overlapping biological consequences. Using transcriptional profiling, Vivanco et al. identified a new PTEN-regulated pathway, the Jun-N-terminal kinase (JNK) pathway, which was constitutively activated upon PTEN knockdown [17]. In the study, PTEN null cells had higher JNK activity than PTEN positive cells did, and genetic analysis indicated that JNK functioned parallel to and independently of AKT. Thus, the blockade of PI3K signaling may shift the survival signal to the AKT-independent PTEN-regulated pathway, implicating JNK and AKT as complementary signals in PIP₃-driven tumorigenesis and suggest that JNK may be a therapeutic target in *PTEN* null tumors.

In addition to its lipid phosphatase function, PTEN also has lipid phosphatase-independent roles. PTEN has been shown to inhibit cell migration through its C2 domain, independent of PTEN's lipid phosphatase activity [18]. In breast cancer, PTEN deficiency has been shown to activate, in a manner dependent on its protein phosphatase activity, the SRC proto-oncogene, non-receptor tyrosine kinase (SRC), thereby conferring resistance to human epidermal growth factor receptor 2 inhibition [19]. Furthermore, PTEN has been shown to directly bind to tumor protein 53 (p53), regulate its stability, and increase its transcription, thereby increasing P53 protein levels [20].

PTEN REGULATION

Genetic alteration of *PTEN*

PTEN loss of function occurs in a wide spectrum of human cancers through various genetic alterations that include point mutations (missense and nonsense mutations), large chromosomal deletions (homozygous/

heterozygous deletions, frameshift deletions, in-frame deletions, and truncations), and epigenetic mechanisms (e.g., hypermethylation of the *PTEN* promoter region) [21]. Somatic mutations are the main drivers of PTEN inactivation in human cancers, and have been reviewed extensively [22].

PTEN's tumor suppressor function is usually abrogated following mutations in its phosphatase domain, which is encoded by exon 5 [23] (Figure 1). These mutations typically include a C124S mutation that abrogates both lipid and protein phosphatase activity and a G129E mutation that abrogates lipid phosphatase but not protein phosphatase activity [24]. Although the N-terminal phosphatase domain is principally responsible for PTEN's physiological activity, approximately 40% of tumorigenic *PTEN* mutations occur in the C-terminal C2 domain (corresponding to exons 6, 7, and 8) and in the tail sequence (corresponding to exon 9), which encode for tyrosine kinase phosphorylation sites. This suggests that the C-terminal sequence is critical for maintaining PTEN function and protein stability [21, 23, 25, 26]. However, many tumor-derived *PTEN* mutants retain partial or complete catalytic function, suggesting that alternative mechanisms can lead to PTEN inactivation.

Transcriptional regulation

In addition to gene mutations, complete or partial loss of PTEN protein expression may impact PTEN's tumor suppression ability. The regulation of PTEN's functions and signaling pathway is shown in Figure 2. Positive regulators of PTEN gene expression include early growth response protein 1, peroxisome proliferator-activated receptor γ (PPAR γ) and P53, which have been shown to directly bind to the PTEN promoter region [27-29]. Early growth response protein 1, which regulates PTEN expression during the initial steps of apoptosis, has been shown to directly upregulate the expression of PTEN in non-small cell lung cancer. PPAR γ is a ligand-activated transcription factor with anti-inflammatory and anti-tumor effects. The activation of its selective ligand, rosiglitazone, leads to the binding of PPAR γ at two PTEN promoter sites, PPAR response element 1 and PPAR response element 2, thus upregulating PTEN and inhibiting PI3K activity. Negative regulators of PTEN gene expression include mitogen-activated protein kinase kinase-4, transforming growth factor beta (TGF- β), nuclear factor of kappa light polypeptide gene enhancer in B-cells (NF- κ B), IGF-1, the transcriptional cofactor c-Jun proto-oncogene, and the B-cell-specific Moloney murine leukemia virus insertion site 1 (BMI1) proto-oncogene, which have been shown to suppress PTEN expression in

several cancer models [30-32]. Research found that IGF-1 could affect cell proliferation and invasion by suppressing PTEN's phosphorylation. In pancreatic cancers, TGF- β significantly suppresses PTEN protein levels concomitant with the activation of AKT through transcriptional reduction of PTEN mRNA—induced growth promotion. c-Jun negatively regulates the expression of PTEN by binding to the activator protein 1 site of the PTEN promoter, resulting in the concomitant activation of the AKT pathway. *PTEN* transcription is also directly repressed by the leukemia-associated factor ecotropic virus integration site 1 protein in the hematopoietic system [33].

Intriguingly, recent studies reported a complex crosstalk between PTEN and other pathways. For example, RAS

has been found to mediate the suppression of PTEN through a TGF- β dependent mechanism in pancreatic cancer [34], and the mitogen-associated protein kinase/extracellular signal-related kinase pathway has been found to suppress PTEN transcription through c-Jun [35]. Finally, the stress kinase pathways including mitogen-activated protein kinase kinase kinase 4 and JNK promote resistance to apoptosis by suppressing PTEN transcription via direct binding of NF- κ B to the PTEN promoter [36]. These findings suggest that the pathways that are negatively regulated by PTEN can in turn regulate PTEN transcription, indicating a potential feedback loop. Studies have also shown that CpG islands hypermethylated in the *PTEN* promoter lead to the silencing of *PTEN* transcription in human cancer [37].

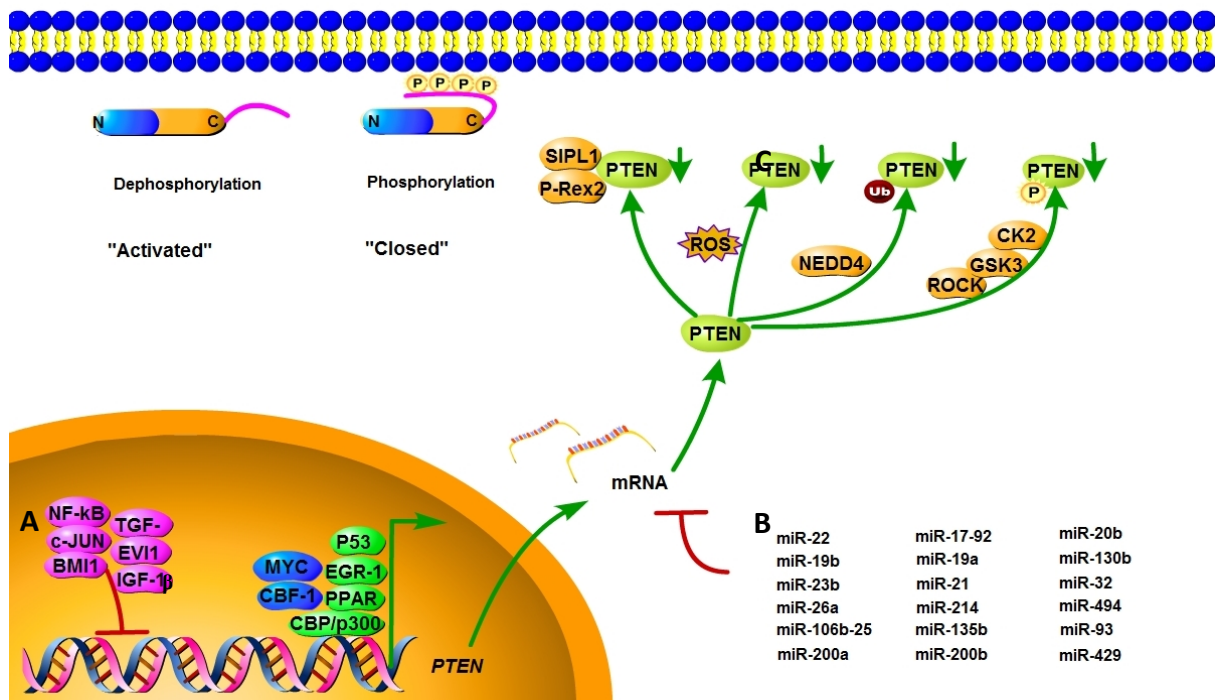


Figure 2. Mechanisms of PTEN regulation. PTEN is regulated at different levels. (A) PTEN mRNA transcription is activated by early growth response protein 1, P53, MYC, PPAR γ , C-repeat binding factor 1, and others, and inhibited by NF- κ B, proto-oncogene c-Jun, TGF- β , and BMI-1. (B) PTEN mRNA is also post-transcriptionally regulated by PTEN-targeting miRNAs, including miR-21, miR-17-92, and others. (C) Active site phosphorylation, ubiquitination, oxidation, acetylation, and protein-protein interactions can also regulate PTEN activity. The phosphorylation leads to a “closed” state of PTEN and maintains PTEN stability. Dephosphorylation of the C-terminal tail opens the PTEN phosphatase domain, thereby activating PTEN.

Table 1. MiRNAs which downregulate PTEN expression in human cancers

miRNA	Locus	Expression status	Tumor type	Reference
MiR-21	17q23.1	Upregulated	Colorectal, bladder, and hepatocellular cancer	[112-114]
MiR-19a	13q31.3	Upregulated	Lymphoma and CLL	[87, 115]
MiR-19b	Xq26.2	Upregulated	Lymphoma	[87]
MiR-22	17p13.3	Upregulated	Prostate cancer and CLL	[116, 117]
MiR-32	9q31.3	Upregulated	Hepatocellular carcinoma	[118]
MiR-93	7q22.1	Upregulated	Hepatocellular carcinoma	[119]
MiR-494	14q32.31	Upregulated	Cervical cancer	[120]
MiR-130b	22q11.21	Upregulated	Esophageal carcinoma	[121]
MiR-135b	1q32.1	Upregulated	Colorectal cancer	[122]
MiR-214	1q24.3	Upregulated	Ovarian cancer	[123]
MiR-26a	3p22.2 (MIR26A1) 12q14.1(MIR26A2)	Upregulated	Prostate cancer	[113]
MiR-23b	9q22.32	Upregulated	Prostate cancer	[114]

Abbreviations: CLL, chronic lymphocytic leukemia.

Translational and post-translational regulation

MicroRNAs (miRNAs) are a class of endogenous, 20- to 25-nucleotide single-stranded non-coding RNAs that repress mRNA translation by base-pairing with target mRNAs [38]. Various miRNAs are known to impact PTEN expression in both normal and pathological conditions. In multiple human cancers, PTEN expressions are downregulated by miRNAs, which are shown in Table 1.

Post-translational modifications, such as active site phosphorylation, ubiquitination, oxidation, and acetylation, can also regulate PTEN activity [39]. In its inactivated state, PTEN is phosphorylated on a cluster of serine and threonine residues located on its C-terminal tail, leading to a “closed” PTEN state in which PTEN protein stability is maintained. As PTEN is being activated, dephosphorylation of its C-terminal tail opens its phosphatase domain, thereby increasing PTEN acti-

vity (Figure 2). The phosphorylation of PTEN at specific residues of the C-terminal tail (Thr366, Ser370, Ser380, Thr382, Thr383, and Ser385) is associated with increased protein stability, whereas phosphorylation at other sites may decrease protein stability. Although S370 and S385 have been identified as the major sites for PTEN phosphorylation, mutations of these residues have minimal effects on PTEN function, whereas mutations of S380, T382, and T383 can destabilize PTEN and increase its phosphatase activity, thereby enhancing PTEN’s interaction with binding partners [40]. The “open” state of PTEN is more susceptible to ubiquitin-mediated proteasome degradation [13]. One recently identified E3 ligase of PTEN is neural precursor cell-expressed, developmentally down-regulated 4, E3 ubiquitin protein ligase 1 (NEDD4-1), which mediates PTEN mono- and poly-ubiquitination [41] (Figure 3). In cancer, the inhibition of NEDD4-1, whose expression has been found to be inversely correlated with PTEN levels in bladder cancer, may

upregulate PTEN levels [42]. Two major conserved sites for PTEN are K13 and K289, and ubiquitination of these sites is indispensable for the nuclear-cytoplasmic shuttling of PTEN (Figure 1).

Protein-protein interactions

PTEN contains a 3-amino acid C-terminal region that is able to bind to PDZ domain-containing proteins [43, 44]. PDZ domains are involved in the assembly of multi-protein complexes that may control the localization of PTEN and its interaction with other proteins. A number of PTEN-interacting proteins have been shown to regulate PTEN protein levels and activities. These interactions, which help recruit PTEN to the membrane, can be negatively modulated by the phosphorylation of PTEN on its C terminus [40, 45]. The phosphorylation of the C terminal end of PTEN has been attributed to the activities of casein kinase 2 and glycogen synthase kinase 3 β [46, 47]. In addition, evidence suggests that the C2 domain of PTEN can be phosphorylated by RhoA-associated kinase, which may have important roles in the regulation of chemoattractant-induced PTEN localization [48] (Figure 2).

Acetylation and oxidation also contribute to PTEN activity regulation. PTEN's interaction with nuclear histone acetyltransferase-associated p300/cAMP response element-binding protein (CREB)-binding protein (CBP)-associated factor can promote PTEN acetylation, and this acetylation negatively regulates the catalytic activity of PTEN [49]. Studies have shown that the PTEN protein becomes oxidized in response to the endogenous generation of the reactive oxygen species (ROS) stimulated by growth factors and insulin, and this oxidation correlates with a ROS-dependent activation of downstream AKT phosphorylation [50, 51]. Other studies have shown that the PIP₃-dependent Rac exchange factor 2 and SHANK-associated RH domain interactor proteins bind directly to PTEN to inhibit its lipid phosphatase activity [52, 53]. High P53 expression triggers proteasome degradation of the PTEN protein [54]. In addition to antagonizing the AKT-mouse double minute 2 homolog pathway in a phosphatase-dependent manner, PTEN also can interact with P53 directly in a phosphatase-independent manner, thereby stabilizing P53 [55, 56].

PTEN IN THE NUCLEUS

Growing evidence suggests that the translocation of PTEN from the nucleus to the cytoplasm leads to malignancy. In the nucleus, PTEN has important tumor-

suppressive functions, and the absence of nuclear PTEN is associated with aggressive disease in multiple cancers [57-59], implying that nuclear PTEN is a useful prognostic indicator. PTEN is predominantly localized to the nucleus in primary, differentiated, and resting cells, and nuclear PTEN is markedly reduced in rapidly cycling cancer cells [60, 61], which suggests that PTEN localization is related to cell differentiation status and cell cycle stage. High expression levels of nuclear PTEN have been associated with cell-cycle arrest at the G0/G1 phase, indicating a role of nuclear PTEN in cell growth inhibition [62]. PTEN's cytoplasmic and nuclear functions are shown in Figure 3.

PTEN enters the nucleus via its calcium-dependent interaction with the major vault protein [63], through passive diffusion [64], and by a Ran-GTPase-dependent pathway [65]. Moreover, monoubiquitination mediates PTEN's nuclear import, whereas polyubiquitination leads to PTEN's degradation in the cytoplasm [66] (Figure 3). The nuclear exportation of PTEN via a chromosome region maintenance 1-dependent mechanism during the G1-S phase transition is directly regulated by S6K, a downstream effector of the PI3K signaling pathway [67] (Figure 3). Thus, PTEN is preferentially expressed in the cytoplasm of tumor cells in which PI3K signaling is frequently activated. Nuclear PTEN has an essential role in the maintenance of chromosomal stability. First, PTEN directly interacts with centromere protein C in a phosphatase-independent manner. Second, PTEN transcriptionally regulates DNA repair by upregulating RAD51 recombinase in a phosphatase-dependent manner [68] (Figure 3). The disruption of nuclear PTEN results in centromere breakage and massive chromosomal aberrations. Nuclear PTEN may also play an important part in transcription regulation by negatively modulating the transcriptional activity of the androgen receptor, hepatocyte growth factor receptor, NF- κ B, CREB, and activator protein 1. Moreover, nuclear PTEN has been shown to promote p300/CREB-binding protein-mediated p53 acetylation in the response to DNA damage [69, 70].

Most of the functions of nuclear PTEN are independent of its phosphatase activity and do not involve the PI3K/AKT pathway. Not only PTEN but also activated PI3K and functional PIP₃ have been detected in the nucleus [71], indicating that nuclear PI3K signaling mediates PTEN's antiapoptotic effect through nuclear PIP₃ and nuclear AKT. Nevertheless, only limited evidence suggests that nuclear PTEN has lipid phosphatase functions, as the nuclear pool of PIP₃ is insensitive to PTEN [72].

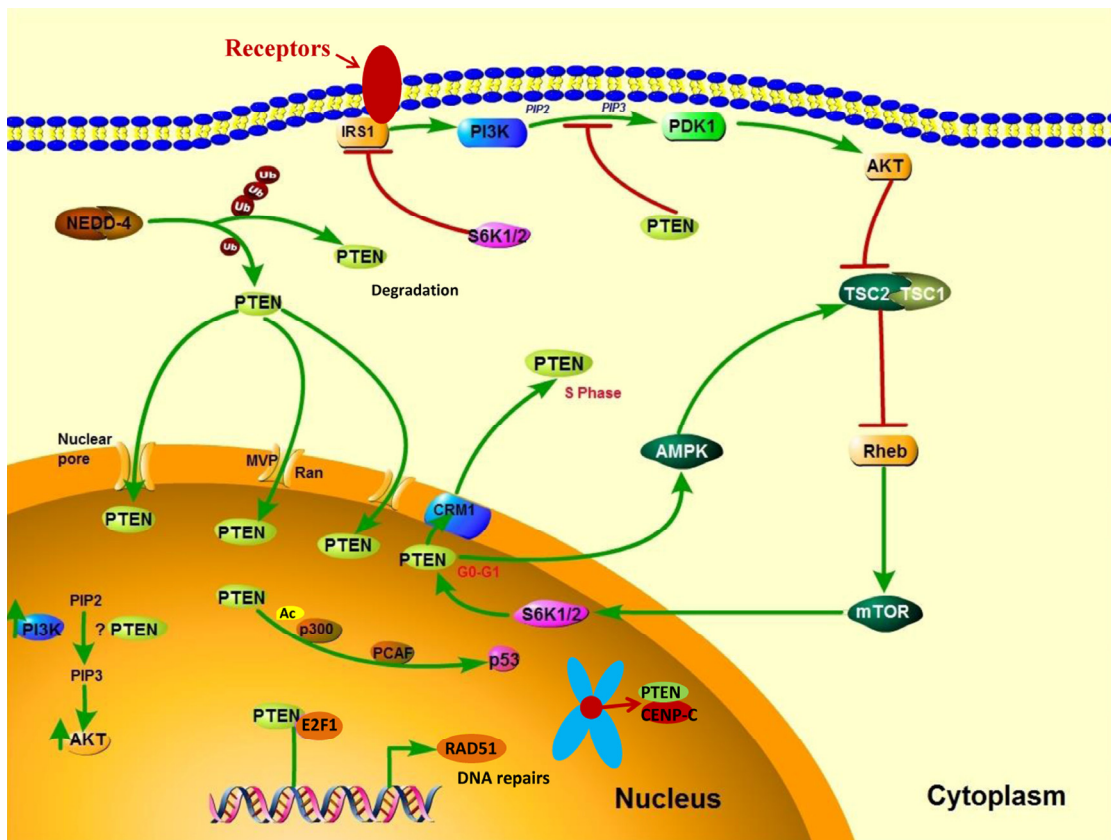


Figure 3. PTEN's cytoplasmic and nuclear functions. In the cytoplasm, PI3K is activated downstream of receptors that include receptor tyrosine kinases, G protein-coupled receptors, cytokine receptors, and integrins. PI3K activation converts PIP₂ to PIP₃, thereby leading to AKT activation, which enhances cell growth, proliferation, and survival. PTEN dephosphorylates PIP₃ and consequently suppresses the PI3K pathway. NEDD4-1 is an E3 ligase of PTEN that mediates PTEN ubiquitination. Polyubiquitination of PTEN leads to its degradation in the plasma, whereas monoubiquitination of PTEN increases its nuclear localization. PTEN can translocate into the nucleus through various mechanisms, including passive diffusion, Ran- or major vault protein-mediated import, and a monoubiquitination-driven mechanism. In the nucleus, PTEN promotes p300-mediated P53 acetylation in response to DNA damage to control cellular proliferation. Nuclear PTEN is also involved in maintaining genomic integrity by binding to centromere protein C (CENPC) and in DNA repair by upregulating RAD51 recombinase (RAD51).

PTEN DEFICIENCY IN LYMPHOMA

PTEN deficiency in T-cell acute lymphoblastic leukemia

PI3K signaling are frequently activated in T-cell acute lymphoblastic leukemia (T-ALL), which mainly due to the absent of PTEN function. Studies have shown that *PTEN* inactivation plays a prominent role in human T-ALL cell lines and primary patients [73-76]. Moreover, *PTEN* mutations have been shown induced resistance to γ -secretase inhibitors, which derepress the constitutively activated NOTCH1 signaling in T-ALL [77]. However, the *PTEN* mutations detected in these studies vary widely. Gutierrez et al. reported that T-ALL patients

had a *PTEN* mutation rate of 27% and a *PTEN* deletion rate of 9%, whereas Gedman et al. reported that 27 of 43 (63%) pediatric T-ALL specimens had *PTEN* mutations. In the latter study, the high frequency of *PTEN* mutations may have been due to the fact that approximately 50% of the specimens were patients with relapsed disease. Interestingly, all mutations were identified in the C2 domain of PTEN [75, 76], not in the phosphatase domain as has been reported for other solid tumors [78].

PTEN deficiency in diffuse large B-cell lymphoma

Published reports of *PTEN* gene alterations in lymphoid malignancies are summarized in Table 2. Studies have

reported unexpectedly low frequencies of *PTEN* mutations in DLBCL patients, ranging from 3% to 22% [79-83]. Lenz et al. performed gene expression profiling

in primary DLBCL and found that a recurrently altered minimal common region containing *PTEN* was lost in 11% GCB-DLBCL but not in other subtypes, suggesting

Table 2. Reported *PTEN* gene alterations in lymphoid malignancies

Alteration type	Exon	Domain	Disease	Frequency, %	Notes	Ref
Cell lines						
Del	3-9	PHOS, C2	DLBCL	28.6 (4/14)	Del in 4 of 11 GCB-DLBCL	[85]
Mut	2-5	PHOS, C2	DLBCL	35.7 (5/14)	Mut in 4 of 11 GCB- and 1 of 3 ABC-DLBCL	
Del and Mut	2-7	PHOS, C2		22.2 (6/27)		[82]
Biopsy tissue						
Del			DLBCL	15.3 (4/26)	Heterozygous Del in 3 of 18 GCB- and 1 of 8 ABC-DLBCL	[85]
Del	1	PB	NHL	3.4 (1/29)		[81]
Mut	5, 6	PHOS, C2		6.9 (2/29)		
Del and Mut	1, 8	PHOS, C2	NHL	4.6 (3/65)		[82]
Mut	8	C2	DLBCL	5 (2/39)		[79]
Del			GCB-DLBCL	13.9 (10/72)	Homozygous Del in 2, heterozygous Del in 8	[84]
Mut	1, 2, 7	PB, PHOS, C2	NHL	10 (4/40)		[109]
Mut	7	C2	T-ALL	8 (9/111)		[74]
Del	NA		T-ALL	8.7 (4/46)	Homozygous Del in 2, heterozygous Del in 2	[76]
Mut	7	C2		27.3 (12/44)		
Del and Mut			T-ALL	62.7 (27/43)	Homozygous Del in 8	[75]

Abbreviations: Del, deletion; PHOS, phosphatase; DLBCL, diffuse large B-cell lymphoma; GCB, germinal B-cell-like; Mut, mutation; ABC, activated B-cell-like; NHL, non-Hodgkin lymphoma; T-ALL, T-cell acute lymphoblastic leukemia; AML, acute myeloid leukemia; ALL, acute lymphoblastic leukemia; PB, phosphatidylinositol (4,5)-bisphosphate-binding; NA, not applicable.

that the alteration is exclusive to GCB-DLBCL [84]. More recently, Pfeifer and Lenz found that mutations involving both the phosphatase domain and C2 domain of *PTEN* were prominent in GCB-DLBCL cell lines. Interestingly, 7 of the 11 GCB-DLBCL cell lines had complete loss of PTEN function, whereas all ABC-DLBCL cell lines expressed PTEN, suggesting that *PTEN* mutation may be related to PTEN loss in GCB-DLBCL [85] (Table 2). In the GCB-DLBCL cell lines, PTEN loss was inversely correlated with the constitutive activation of the PI3K/AKT signaling pathway, whereas GCB-DLBCL cell lines with PTEN expression rarely had PI3K/AKT activation. In contrast, all ABC-DLBCL cell lines had PI3K/AKT activation regardless of PTEN status, which suggests that the activation of PI3K/AKT in GCB-DLBCL results from PTEN deficiency. Further, gene set enrichment analysis revealed that the MYC target gene set was significantly downregulated after PTEN induction. Also, inhibition of PI3K/AKT with either PTEN re-expression or PI3K inhibition significantly downregulated MYC expression, suggesting that PTEN loss leads to the upregulation of MYC through the constitutive activation of PI3K/AKT in DLBCL [85].

Although several studies have identified discrepancies in PTEN deficiency between DLBCL subtypes, few studies have investigated PTEN localization in different subcellular compartments, not to mention the prognostic value such information would have in de novo cases. Fridberg et al. found a trend towards a stronger staining intensity of cytoplasmic and nuclear PTEN in 28 non-GCB-DLBCL patients [59], most importantly, they found that the absence of nuclear PTEN expression was correlated with worse survival. This interesting evidence should be corroborated in a larger number of primary samples in further studies.

PTEN deficiency in other lymphomas

Previous studies of mantle cell lymphoma (MCL) showed that although the disease had no detectable genetic alterations of PTEN, it did have extremely low protein expression of PTEN. To determine whether the PI3K/AKT signaling pathway is involved in the pathogenesis of MCL, Rudelius et al. investigated pAKT and PTEN expression in primary MCL specimens and cell lines. Of the 31 MCL specimens, 6 had markedly decreased PTEN expression; of the 4 MCL cell lines, 3 had complete loss of PTEN expression [86]. The authors found no phosphatidylinositol 3-kinase catalytic subunit (*PIK3CA*) mutations in the primary specimens or cell lines, suggesting that loss of PTEN activates the PI3K/AKT pathway in MCL.

Loss of PTEN protein expression has also been reported in 32% of patients with primary cutaneous DLBCL–leg type and 27% of patients with primary cutaneous follicle center lymphomas. Remarkably, both the expression of miR-106a and that of miR-20a were significantly related to PTEN protein loss ($P < 0.01$). Moreover, low PTEN mRNA levels were significantly associated with shorter disease-free survival [87].

PTEN AND SPECIFIC PI3K ISOFORMS

PI3K comprises a regulatory p85 subunit and a catalytic p110 subunit. Of particular interest, Class IA PI3Ks include three p110 isoforms (p110 α , p110 β , and p110 δ), are primarily responsible for phosphorylating PIP₂. *PIK3CA*, the gene encoding the p110 α isoform is frequently mutated in various human cancers [88]. In one study, 59% of cases with mutant *PIK3CA* had increased p-AKT levels. Therefore, the constitutive activation of PI3K is another way by which the PTEN pathway can be disturbed in cancer. In their study of 215 DLBCL patients, Abubaker et al. reported that 8% had *PIK3CA* mutations and 37% had loss of PTEN. Both *PIK3CA* mutation and loss of PTEN were correlated with poor survival. However, correlation analysis revealed that most of the *PIK3CA* mutations occurred in cases with PTEN expression ($P = 0.0146$). Accordingly, 17 cases with *PIK3CA* mutations were screened for *PTEN* mutations, and none harbored both *PIK3CA* and *PTEN* mutations [89]. This suggests that *PIK3CA* mutation likely functions as an oncogene in DLBCL by contributing to PI3K pathway activation independently of PTEN deficiency.

Both p110 α and p110 β may generate distinct pools of PIP₃. In response to stimuli, p110 α produces an acute flux of PIP₃, which is efficiently coupled to AKT phosphorylation. In contrast, p110 β has been proposed to generate a basal level of PIP₃ with little effect on AKT phosphorylation [90]. Moreover, cells with AKT phosphorylation induced by PTEN loss were sensitive to a p110 β -specific inhibitor but not a p110 α inhibitor both in vitro and in vivo [91, 92], which suggests that the enhancement of basal PIP₃ drive oncogenesis in the absence of PTEN. Another study indicated that *PTEN*-mutant endometrioid endometrial carcinoma cells may not be sufficiently sensitive to the inhibition of p110 β alone and that combined targeted agents may be required for effective treatment [93]. This finding may have been due to the fact that mutations of *PTEN* and *PIK3CA* frequently coexist in endometrioid endometrial carcinoma. In contrast, cells with wild-type PTEN seem to engage the p110 α or p110 δ isoforms. Accordingly, clinical trials of isoform-specific inhibitors are warranted.

Table 3. Preclinical studies of targeted therapeutics in PTEN-deficient tumors

Inhibitor type	Drug	Study notes	Ref
<i>Class I-PI3K</i>			
Pan	Buparlisib (BKM120)	The drug elicited response in some PTEN-deficient tumors and induced cell death in DLBCL cell lines.	[124]
Pan	SAR245408 (XL147)	The drug significantly inhibited tumor growth in a PTEN-deficient prostate cancer model.	[109]
p110 α	BYL719	The drug had antitumor activity in cell lines harboring <i>PIK3CA</i> mutations but not in PTEN-deficient solid tumors	[110]
p110 β	AZD6482 (KIN-193)	The drug substantially inhibited tumor growth in PTEN-deficient cancer models.	[98]
p110 β	GSK2636771	<i>PTEN</i> -mutant EEC cell lines were resistant to the drug; the drug decreased cell viability only when combined with a p110 α selective inhibitor.	[93]
p110 β/δ	AZD8186	The drug inhibited the growth of PTEN-deficient prostate tumors.	[102]
p110 α/β	CH5132799	The drug inhibited the growth of some PTEN-deficient tumors in vitro.	[103]
p110 γ/δ	IPI-145	The drug significantly inhibited the Loucy cell lines in T-ALL.	[100]
<i>PI3K/mTOR</i>	SF1126	The drug significantly reduced the viability of PTEN-deficient but not PTEN-positive GCB-DLBCL cells.	[104]
<i>PI3K/HDAC</i>	CUDC-907	The drug inhibited growth in multiple cell lines; cell lines with <i>PIK3CA</i> or <i>PTEN</i> -mutation induced loss of PTEN were markedly sensitive to the drug.	[105]
<i>AKT</i>	MK-2206	The drug had antitumor activity in breast cancer cell lines with <i>PTEN</i> or <i>PIK3CA</i> mutations.	[106]
<i>mTORC1</i>	Everolimus (RAD001)	PTEN-deficient prostate cancer had greater sensitivity to the drug; glioblastoma cell lines were resistant to the drug.	[107]
	Temsirolimus (CCI-779)	Multiple PTEN-deficient cell lines were remarkably sensitive to the drug.	[108]

Abbreviations: DLBCL, diffuse large B-cell lymphoma; EEC, endometrioid endometrial carcinoma; MCL, mantle cell lymphoma; GCB, germinal B-cell-like.

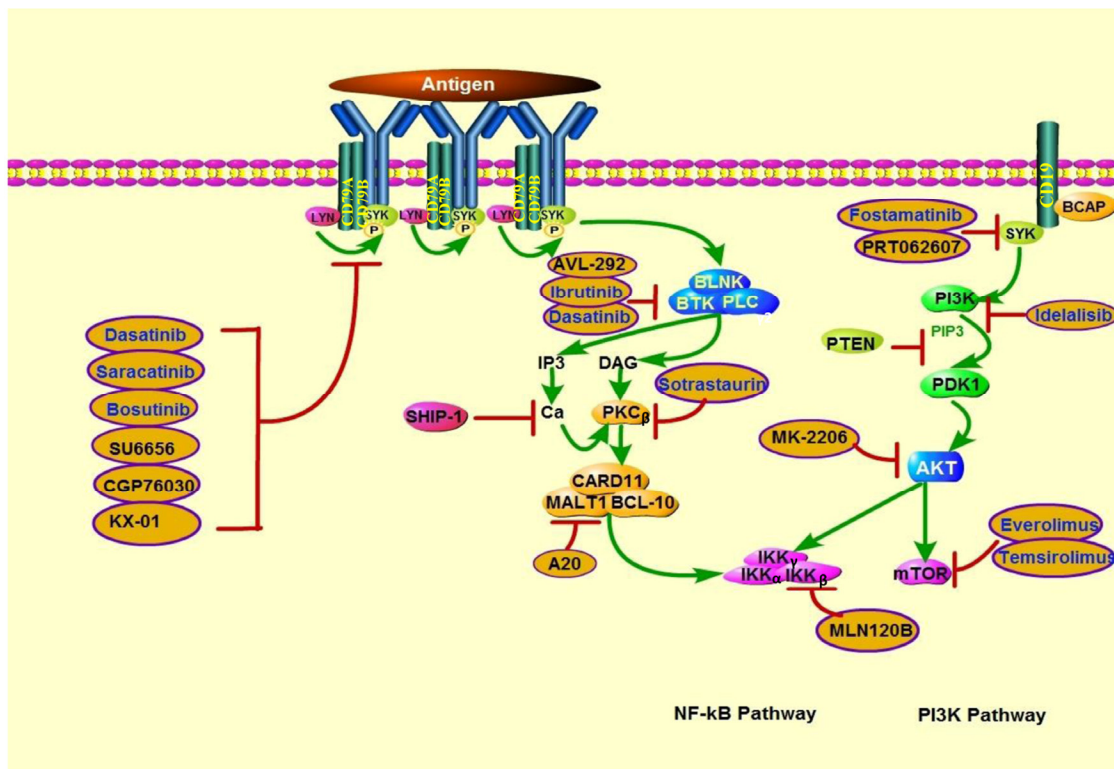


Figure 4. Actions of therapeutics targeting PTEN deficiency in lymphoid malignancies. PTEN deficiency is associated with increased sensitivity to PI3K, AKT, and mTOR inhibitors. In addition, because PI3K is involved in BCR signaling activation, BCR pathway inhibitors may also be effective in PTEN-deficient lymphoid malignancies. SRC family kinase inhibitors include dasatinib (which can also inhibit BTK), saracatinib, bosutinib, SU6656, CGP76030, and KX-01. BTK inhibitors include ibrutinib and AVL-292. Sotrastaurin is a PKC β inhibitor; A20, a MALT1 paracaspase inhibitor; and MLN120B, an IKK β inhibitor. SYK inhibitors include fostamatinib and PRT062607. Idelalisib is a PI3K δ -specific inhibitor. MK-2206 is an AKT inhibitor. mTOR inhibitors include everolimus and temsirolimus.

ENGAGEMENT OF THE PI3K PATHWAY IN B-CELL RECEPTOR SIGNALING

The survival of the majority of B-cell malignancies depends on functional B-cell receptor (BCR) signaling. The successful use of a Bruton tyrosine kinase (BTK) inhibitor to target the BCR pathway in DLBCL has yielded profound discoveries regarding the genetic and biochemical basis of BCR signaling. During BCR signaling, the SRC family kinase LYN phosphorylates the transmembrane protein cluster of differentiation 19, which recruits PI3K to the BCR. The transduction of BCR signaling finally results in the activation of the NF- κ B, PI3K, mitogen-associated protein kinase, and nuclear factor of activated T cells pathways, which

promote the proliferation and survival of normal and malignant B cells.

BCR signaling is directly affected by frequent mutations in CD79A (immunoglobulin α) and CD79B (immunoglobulin β)-mainly CD79B-which occur in approximately 20% of patients with ABC-DLBCL [94]. Tumor cells harboring CD79B mutations have longer and stronger activation of AKT signaling. Moreover, ABC-DLBCL cell lines with mutated CD79B are more sensitive to PI3K inhibition than those with wild-type CD79B are. Thus, CD79B mutations might be responsible for preventing the negative regulation that interferes with PI3K-dependent pro-survival BCR signaling [95].

Table 4. Preclinical studies of targeted therapeutics in PTEN-deficient tumors

Inhibitor type	Drug	Patient population	Phase	Identifier
PI3K	GSK2636771	Patients with advanced solid tumors with PTEN deficiency	1/2a	NCT01458067
	BKM120	Patients with recurrent glioblastoma with PTEN mutations or homozygous deletion of PTEN or with PTEN-negative disease	1b/2	NCT01870726
	BKM120	Patients with advanced, metastatic, or recurrent endometrial cancers with PIK3CA gene mutation, PTEN gene mutation, or null/low PTEN protein expression	2	NCT01550380
	AZD8186	Patients with advanced CRPC, sqNSCLC, TNBC, or known PTEN-deficient advanced solid malignancies	1	NCT01884285
PI3K/mTOR	BEZ235	Patients with advanced TCC; group 1 includes patients with no PI3K pathway activation, no loss of PTEN, and no activating PIK3CA mutation; group 2 includes patients with PI3K pathway activation as defined by PIK3CA mutation and/or PTEN loss	2	NCT01856101
	BEZ235	Patients with relapsed lymphoma or multiple myeloma	1	NCT01742988
AKT	MK-2206	Patients with previously treated metastatic colorectal cancer enriched for PTEN loss and PIK3CA mutation	2	NCT01802320
	MK-2206	Patients with advanced breast cancer with a PIK3CA mutation, AKT mutation, and/or PTEN loss or mutation	2	NCT01277757
	Pazopanib + everolimus	Patients with PI3KCA mutations or PTEN loss and advanced solid tumors refractory to standard therapy	1	NCT01430572
	Trastuzumab +RAD001	Patients with HER-2–overexpressing, PTEN-deficient metastatic breast cancer progressing on trastuzumab-based therapy	1/2	NCT00317720
	GDC-0068/ GDC-0980 +abiraterone	Patients previously treated prostate cancer with PTEN loss (currently in phase II)	1b/2	NCT01485861

Rapamycin (Temsirolimus)	Patients with advanced cancer and PI3K mutation and/or PTEN loss	1/2	NCT00877773
Ipatasertib (GDC- 0068) + paclitaxel	Patients with PTEN-low metastatic TNBC	2	NCT02162719

Abbreviations: CRPC, castrate-resistant prostate cancer; sqNSCLC, squamous non-small cell lung cancer; TNBC, triple-negative breast cancer; TCC, transitional cell carcinoma; HER-2, human epidermal growth factor receptor 2.

Previous studies have demonstrated that the transgenic expression of the constitutively active form of the PI3K catalytic subunit or PTEN knockout can rescue mature B cells from conditional BCR ablation. Moreover, BCR signaling is required for PI3K pathway engagement in both GCB-DLBCL and ABC-DLBCL. Specifically, PI3K engages BCR signaling by indirectly contributing to NF- κ B activity in ABC-DLBCL, whereas in GCB-DLBCL, PI3K pathway activation but not NF- κ B activity is required for survival. Briefly, the “chronic” BCR signaling in ABC-DLBCL is characterized by the many pathways involved with the CARD11-mediated activation of NF- κ B signaling, whereas the “tonic” BCR signaling in GCB-DLBCL is characterized by the constitutive activation of PI3K in promoting survival [96, 97].

Given these findings, the combination of PI3K pathway inhibitors with BCR pathway inhibitors may enhance the treatment response of PTEN-deficient tumors.

THERAPIES TARGETING FUNCTIONAL LOSS OF PTEN IN LYMPHOMA

PI3K/AKT/mTOR pathway inhibitors

Owing to PI3K’s critical roles in human cancers, PI3K targeting is one of the most promising areas of anticancer therapy development. Since the absent of PTEN is concomitant with PI3K signaling activation, inhibitors that targeting this pathway might play a significant role in the treatment of PTEN-deficient tumors. Growing evidence indicates that multiple solid tumor cell lines and several lymphoid malignancy cell lines with PTEN-deficient are hypersensitive to PI3K inhibitors, which are summarized in Tables 3 and Figure 4.

In addition to PI3K pan-inhibition, several isoform-selective PI3K inhibitors have been shown to repress the viability of PTEN-deficient tumors. Notably, the p110 β -specific PI3K inhibitor AZD6482 (KIN-193)

displayed remarkable antitumor activity in PTEN-null tumors but failed to block the growth of PTEN-wild-type tumors in mouse models [98]. However, another separate study showed that endometrioid endometrial cancer with *PTEN* mutation were resistant to p110 β -selective inhibition, cell lines’ viability was decreased only when p110 β -selective inhibition was combined with p110 α -selective inhibition. Recent findings have highlighted that there is a complex interplay between the Class I PI3K isoforms, inhibition of either α or β single isoform might be compensated by reactivation of another isoform at last [99]. Furthermore, it has been proposed that the dual γ/δ inhibitor CAL-130, specifically targeting p110 γ and p110 δ isoforms in *PTEN* deleted T-ALL cell lines [100]. By contrast, Lonetti et al. recently indicated that PI3K pan-inhibition developed the highest cytotoxic effects when compared with both selective isoform inhibition and dual p110 γ/δ inhibition, in T-ALL cell lines with or without *PTEN* deletion [101]. Nevertheless, which class of agents among isoform-specific or pan-inhibitors can achieve better efficacy is still controversial. Other target treatments including AKT, mTOR, dual PI3K/AKT and dual PI3K/mTOR inhibitors also show promising antitumor activity in cell line studies, and some of them have been testing under clinical trials [102-111] (Table 3, 4).

CONCLUSION

In summary, recent studies have identified PTEN as a tumor suppressor gene in various human cancers. It is clear that PTEN is far more than a cytosolic protein that acts as a lipid phosphatase to maintain PIP₃ levels. Therefore, we must reconsider the distinct roles PTEN have in specific subcellular compartments, identify the mechanisms underlying PTEN’s shuttling between different compartments, and investigate the significance of these mechanisms in predicting disease outcome. Future studies will further elucidate the mechanistic basis of PTEN deficiency in lymphoid malignancies, thereby aiding in the clinical management of lymphoid malignancies with PTEN loss or alteration.

Funding

This study was supported by the National Cancer Institute/National Institutes of Health (R01CA138688 and 1RC1CA146299 to KHY). XW is a recipient of hematology and oncology scholarship award. KHY is supported by The University of Texas MD Anderson Cancer Center Lymphoma Moonshot Program and Institutional Research and Development Award, an MD Anderson Cancer Center Lymphoma Specialized Programs on Research Excellence (SPORE) Research Development Program Award, an MD Anderson Cancer Center Myeloma SPORE Research Development Program Award, a Gundersen Lutheran Medical Foundation Award, and partially supported by the National Cancer Institute/National Institutes of Health (P50CA136411 and P50CA142509), and by MD Anderson's Cancer Center Support Grant CA016672.

Author contributions

Conception, design, manuscript writing and final approval of manuscript: XW and KHY.

Conflict of interest statement

KHY receives research support from Roche Molecular System, Gilead Sciences Pharmaceutical, Seattle Genetics, Dai Sanyo Pharmaceutical, Adaptive Biotechnology, Incyte Pharmaceutical and HTG Molecular Diagnostics.

REFERENCES

1. Wang SI, Puc J, Li J, Bruce JN, Cairns P, Sidransky D and Parsons R. Somatic mutations of PTEN in glioblastoma multiforme. *Cancer research*. 1997; 57:4183-4186.
2. Tashiro H, Blazes MS, Wu R, Cho KR, Bose S, Wang SI, Li J, Parsons R and Ellenson LH. Mutations in PTEN are frequent in endometrial carcinoma but rare in other common gynecological malignancies. *Cancer research*. 1997; 57:3935-3940.
3. Rasheed BKA, Stenzel TT, McLendon RE, Parsons R, Friedman AH, Friedman HS, Bigner DD and Bigner SH. PTEN gene mutations are seen in high-grade but not in low-grade gliomas. *Cancer research*. 1997; 57:4187-4190.
4. Wang SI, Parsons R and Ittmann M. Homozygous deletion of the PTEN tumor suppressor gene in a subset of prostate adenocarcinomas. *Clinical Cancer Research*. 1998; 4:811-815.
5. Cairns P, Evron E, Okami K, Halachmi N, Esteller M, Herman JG, Bose S, Wang SI, Parsons R and Sidransky D. Point mutation and homozygous deletion of PTEN/MMAC1 in primary bladder cancers. *Oncogene*. 1998; 16:3215-3218.
6. Nagata Y, Lan KH, Zhou X, Tan M, Esteva FJ, Sahin AA, Klos KS, Li P, Monia BP, Nguyen NT, Hortobagyi GN, Hung MC and Yu D. PTEN activation contributes to tumor inhibition by trastuzumab, and loss of PTEN predicts trastuzumab resistance in patients. *Cancer cell*. 2004; 6:117-127.
7. Berns K, Horlings HM, Hennessy BT, Madiredjo M, Hijmans EM, Beelen K, Linn SC, Gonzalez-Angulo AM, Stenke-Hale K, Hauptmann M, Beijersbergen RL, Mills GB, van de Vijver MJ, et al. A functional genetic approach identifies the PI3K pathway as a major determinant of trastuzumab resistance in breast cancer. *Cancer cell*. 2007; 12:395-402.
8. Trotman LC, Niki M, Dotan ZA, Koutcher JA, Di Cristofano A, Xiao A, Khoo AS, Roy-Burman P, Greenberg NM, Van Dyke T, Cordon-Cardo C and Pandolfi PP. Pten dose dictates cancer progression in the prostate. *PLoS biology*. 2003; 1:385-396.
9. Di Cristofano A, Pesce B, Cordon-Cardo C and Pandolfi PP. Pten is essential for embryonic development and tumour suppression. *Nature genetics*. 1998; 19:348-355.
10. Maehama T and Dixon JE. The tumor suppressor, PTEN/MMAC1, dephosphorylates the lipid second messenger, phosphatidylinositol 3,4,5-trisphosphate. *The Journal of biological chemistry*. 1998; 273:13375-13378.
11. Lee JO, Yang H, Georgescu MM, Di Cristofano A, Maehama T, Shi Y, Dixon JE, Pandolfi P and Pavletich NP. Crystal structure of the PTEN tumor suppressor: implications for its phosphoinositide phosphatase activity and membrane association. *Cell*. 1999; 99:323-334.
12. Denning G, Jean-Joseph B, Prince C, Durden DL and Vogt PK. A short N-terminal sequence of PTEN controls cytoplasmic localization and is required for suppression of cell growth. *Oncogene*. 2007; 26:3930-3940.
13. Leslie NR, Batty IH, Maccario H, Davidson L and Downes CP. Understanding PTEN regulation: PIP2, polarity and protein stability. *Oncogene*. 2008; 27:5464-5476.
14. Guertin DA and Sabatini DM. Defining the role of mTOR in cancer. *Cancer cell*. 2007; 12:9-22.
15. Manning BD and Cantley LC. AKT/PKB signaling: Navigating downstream. *Cell*. 2007; 129:1261-1274.
16. Ma XM and Blenis J. Molecular mechanisms of mTOR-mediated translational control. *Nature reviews Molecular cell biology*. 2009; 10:307-318.
17. Vivanco I, Palaskas N, Tran C, Finn SP, Getz G, Kennedy NJ, Jiao J, Rose J, Xie WL, Loda M, Golub T, Mellinghoff IK, Davis RJ, et al. Identification of the JNK signaling pathway as a functional target of the tumor suppressor PTEN. *Cancer cell*. 2007; 11:555-569.
18. Raftopoulos M, Etienne-Manneville S, Self A, Nicholls S and Hall A. Regulation of cell migration by the C2 domain of the tumor suppressor PTEN. *Science*. 2004; 303:1179-1181.
19. Zhang SY, Huang WC, Li P, Guo H, Poh SB, Brady SW, Xiong Y, Tseng LM, Li SH, Ding ZX, Sahin AA, Esteva FJ, Hortobagyi GN, et al. Combating trastuzumab resistance by targeting SRC, a common node downstream of multiple resistance pathways. *Nature medicine*. 2011; 17:461-U101.
20. Tang Y and Eng C. PTEN autoregulates its expression by stabilization of p53 in a phosphatase-independent manner. *Cancer research*. 2006; 66:736-742.
21. Waite KA and Eng C. Protean PTEN: form and function. *American journal of human genetics*. 2002; 70:829-844.
22. Keniry M and Parsons R. The role of PTEN signaling perturbations in cancer and in targeted therapy. *Oncogene*. 2008; 27:5477-5485.
23. Zhang S and Yu D. PI(3)king apart PTEN's role in cancer. *Clinical cancer research : an official journal of the American Association for Cancer Research*. 2010; 16:4325-4330.

24. Liaw D, Marsh DJ, Li J, Dahia PL, Wang SI, Zheng Z, Bose S, Call KM, Tsou HC, Peacocke M, Eng C and Parsons R. Germline mutations of the PTEN gene in Cowden disease, an inherited breast and thyroid cancer syndrome. *Nature genetics*. 1997; 16:64-67.
25. Sansal I and Sellers WR. The biology and clinical relevance of the PTEN tumor suppressor pathway. *Journal of clinical oncology : official journal of the American Society of Clinical Oncology*. 2004; 22:2954-2963.
26. Chalhoub N and Baker SJ. PTEN and the PI3-kinase pathway in cancer. *Annual review of pathology*. 2009; 4:127-150.
27. Patel L, Pass I, Coxon P, Downes CP, Smith SA and Macphree CH. Tumor suppressor and anti-inflammatory actions of PPARgamma agonists are mediated via upregulation of PTEN. *Current biology : CB*. 2001; 11:764-768.
28. Virolle T, Adamson ED, Baron V, Birle D, Mercola D, Mustelin T and de Belle I. The Egr-1 transcription factor directly activates PTEN during irradiation-induced signalling. *Nature cell biology*. 2001; 3:1124-1128.
29. Stambolic V, MacPherson D, Sas D, Lin Y, Snow B, Jang Y, Benchimol S and Mak TW. Regulation of PTEN transcription by p53. *Molecular cell*. 2001; 8(2):317-325.
30. Gericke A, Munson M and Ross AH. Regulation of the PTEN phosphatase. *Gene*. 2006; 374:1-9.
31. Lau MT, Klausen C and Leung PC. E-cadherin inhibits tumor cell growth by suppressing PI3K/Akt signaling via beta-catenin-Egr1-mediated PTEN expression. *Oncogene*. 2011; 30:2753-2766.
32. Meng X, Wang Y, Zheng X, Liu C, Su B, Nie H, Zhao B, Zhao X and Yang H. shRNA-mediated knockdown of Bmi-1 inhibit lung adenocarcinoma cell migration and metastasis. *Lung cancer*. 2012; 77:24-30.
33. Yoshimi A, Goyama S, Watanabe-Okochi N, Yoshiki Y, Nannya Y, Nitta E, Arai S, Sato T, Shimabe M, Nakagawa M, Imai Y, Kitamura T and Kurokawa M. Evi1 represses PTEN expression and activates PI3K/AKT/mTOR via interactions with polycomb proteins. *Blood*. 2011; 117:3617-3628.
34. Chow JY, Quach KT, Cabrera BL, Cabral JA, Beck SE and Carethers JM. RAS/ERK modulates TGFbeta-regulated PTEN expression in human pancreatic adenocarcinoma cells. *Carcinogenesis*. 2007; 28(11):2321-2327.
35. Vasudevan KM, Burikhanov R, Goswami A and Rangnekar VM. Suppression of PTEN expression is essential for antiapoptosis and cellular transformation by oncogenic ras. *Cancer research*. 2007; 67:10343-10350.
36. Xia DR, Srinivas H, Ahn YH, Sethi G, Sheng XY, Yung WKA, Xia QH, Chiao PJ, Kim H, Brown PH, Wistuba II, Aggarwal BB and Kurie JM. Mitogen-activated protein kinase kinase-4 promotes cell survival by decreasing PTEN expression through an NF kappa B-dependent pathway. *Journal of Biological Chemistry*. 2007; 282:3507-3519.
37. Leslie NR and Foti M. Non-genomic loss of PTEN function in cancer: not in my genes. *Trends in pharmacological sciences*. 2011; 32:131-140.
38. Bartel DP. MicroRNAs: target recognition and regulatory functions. *Cell*. 2009; 136:215-233.
39. Tamguney T and Stokoe D. New insights into PTEN. *J Cell Sci*. 2007; 120(4):4071-4079.
40. Vazquez F, Ramaswamy S, Nakamura N and Sellers WR. Phosphorylation of the PTEN tail regulates protein stability and function. *Molecular and cellular biology*. 2000; 20:5010-5018.
41. Wang XJ, Trotman LC, Koppie T, Alimonti A, Chen ZB, Gao ZH, Wang JR, Erdjument-Bromage H, Tempst P, Cordon-Cardo C, Pandolfi PP and Jiang XJ. NEDD4-1 is a proto-oncogenic ubiquitin ligase for PTEN. *Cell*. 2007; 128:129-139.
42. Drinjakovic J, Jung H, Campbell DS, Strohlic L, Dwivedy A and Holt CE. E3 ligase Nedd4 promotes axon branching by downregulating PTEN. *Neuron*. 2010; 65:341-357.
43. Georgescu MM, Kirsch KH, Akagi T, Shishido T and Hanafusa H. The tumor-suppressor activity of PTEN is regulated by its carboxyl-terminal region. *Proceedings of the National Academy of Sciences of the United States of America*. 1999; 96:10182-10187.
44. Wu X, Hepner K, Castelino-Prabhu S, Do D, Kaye MB, Yuan XJ, Wood J, Ross C, Sawyers CL and Whang YE. Evidence for regulation of the PTEN tumor suppressor by a membrane-localized multi-PDZ domain containing scaffold protein MAGI-2. *Proceedings of the National Academy of Sciences of the United States of America*. 2000; 97:4233-4238.
45. Vazquez F, Grossman SR, Takahashi Y, Rokas MV, Nakamura N and Sellers WR. Phosphorylation of the PTEN tail acts as an inhibitory switch by preventing its recruitment into a protein complex. *Journal of Biological Chemistry*. 2001; 276:48627-48630.
46. Al-Khoury AM, Ma YL, Togo SH, Williams S and Mustelin T. Cooperative phosphorylation of the tumor suppressor phosphatase and tensin homologue (PTEN) by casein kinases and glycogen synthase kinase 3 beta. *Journal of Biological Chemistry*. 2005; 280:35195-35202.
47. Miller SJ, Lou DY, Seldin DC, Lane WS and Neel BG. Direct identification of PTEN phosphorylation sites. *FEBS letters*. 2002; 528:145-153.
48. Li Z, Dong XM, Wang ZL, Liu WZ, Deng N, Ding Y, Tang LY, Hla T, Zeng R, Li L and Wu DQ. Regulation of PTEN by Rho small GTPases. *Nature cell biology*. 2005; 7:399-U342.
49. Okumura K, Mendoza M, Bachoo RM, DePinho RA, Cavenee WK and Furnari FB. PCAF modulates PTEN activity. *Journal of Biological Chemistry*. 2006; 281:26562-26568.
50. Leslie NR, Bennett D, Lindsay YE, Stewart H, Gray A and Downes CP. Redox regulation of PI 3-kinase signalling via inactivation of PTEN. *Embo J*. 2003; 22:5501-5510.
51. Seo JH, Ahn Y, Lee SR, Yeol Yeo C and Chung Hur K. The major target of the endogenously generated reactive oxygen species in response to insulin stimulation is phosphatase and tensin homolog and not phosphoinositide-3 kinase (PI-3 kinase) in the PI-3 kinase/Akt pathway. *Mol Biol Cell*. 2005; 16:348-357.
52. Fine B, Hodakoski C, Koujak S, Su T, Saal LH, Maurer M, Hopkins B, Keniry M, Sulis ML, Mense S, Hibshoosh H and Parsons R. Activation of the PI3K Pathway in Cancer Through Inhibition of PTEN by Exchange Factor P-REX2a. *Science*. 2009; 325:1261-1265.
53. He L, Ingram A, Rybak AP and Tang D. Shank-interacting protein-like 1 promotes tumorigenesis via PTEN inhibition in human tumor cells. *The Journal of clinical investigation*. 2010; 120:2094-2108.
54. Tang Y and Eng C. p53 down-regulates phosphatase and tensin homologue deleted on chromosome 10 protein stability partially through caspase-mediated degradation in cells with proteasome dysfunction. *Cancer research*. 2006; 66:6139-6148.
55. Mayo LD, Dixon JE, Durden DL, Tonks NK and Donner DB. PTEN protects p53 from Mdm2 and sensitizes cancer cells to chemotherapy. *The Journal of biological chemistry*. 2002; 277:5484-5489.

56. Freeman DJ, Li AG, Wei G, Li HH, Kertesz N, Lesche R, Whale AD, Martinez-Diaz H, Rozengurt N, Cardiff RD, Liu X and Wu H. PTEN tumor suppressor regulates p53 protein levels and activity through phosphatase-dependent and -independent mechanisms. *Cancer cell*. 2003; 3:117-130.
57. Tachibana M, Shibakita M, Ohno S, Kinugasa S, Yoshimura H, Ueda S, Fujii T, Rahman MA, Dhar DK and Nagasue N. Expression and prognostic significance of PTEN product protein in patients with esophageal squamous cell carcinoma. *Cancer*. 2002; 94:1955-1960.
58. Zhou XP, Loukola A, Salovaara R, Nystrom-Lahti M, Peltomaki P, de la Chapelle A, Aaltonen LA and Eng C. PTEN mutational spectra, expression levels, and subcellular localization in microsatellite stable and unstable colorectal cancers. *The American journal of pathology*. 2002; 161:439-447.
59. Fridberg M, Servin A, Anagnostaki L, Linderot J, Berglund M, Soderberg O, Enblad G, Rosen A, Mustelin T, Jerkeman M, Persson JL and Wingren AG. Protein expression and cellular localization in two prognostic subgroups of diffuse large B-cell lymphoma: higher expression of ZAP70 and PKC-beta II in the non-germinal center group and poor survival in patients deficient in nuclear PTEN. *Leuk Lymphoma*. 2007; 48:2221-2232.
60. Gimm O, Perren A, Weng LP, Marsh DJ, Yeh JJ, Ziebold U, Gil E, Hinze R, Delbridge L, Lees JA, Mutter GL, Robinson BG, Komminoth P, et al. Differential nuclear and cytoplasmic expression of PTEN in normal thyroid tissue, and benign and malignant epithelial thyroid tumors. *American Journal of Pathology*. 2000; 156:1693-1700.
61. Perren A, Komminoth P, Saremaslani P, Matter C, Feurer S, Lees JA, Heitz PU and Eng C. Mutation and expression analyses reveal differential subcellular compartmentalization of PTEN in endocrine pancreatic tumors compared to normal islet cells. *The American journal of pathology*. 2000; 157:1097-1103.
62. Ginn-Pease ME and Eng C. Increased nuclear phosphatase and tensin homologue deleted on chromosome 10 is associated with G0-G1 in MCF-7 cells. *Cancer research*. 2003; 63:282-286.
63. Minaguchi T, Waite KA and Eng C. Nuclear localization of PTEN is regulated by Ca²⁺ through a tyrosil phosphorylation-independent conformational modification in major vault protein. *Cancer research*. 2006; 66:11677-11682.
64. Liu FH, Wagner S, Campbell RB, Nickerson JA, Schiffer CA and Ross AH. PTEN enters the nucleus by diffusion. *Journal of cellular biochemistry*. 2005; 96:221-234.
65. Gil A, Andres-Pons A, Fernandez E, Valiente M, Torres J, Cervera J and Pulido R. Nuclear localization of PTEN by a ran-dependent mechanism enhances apoptosis: Involvement of an N-terminal nuclear localization domain and multiple nuclear exclusion motifs. *Mol Biol Cell*. 2006; 17:4002-4013.
66. Trotman LC, Wang X, Alimonti A, Chen Z, Teruya-Feldstein J, Yang H, Pavletich NP, Carver BS, Cordon-Cardo C, Erdjument-Bromage H, Tempst P, Chi SG, Kim HJ, et al. Ubiquitination regulates PTEN nuclear import and tumor suppression. *Cell*. 2007; 128:141-156.
67. Liu JL, Mao Z, LaFortune TA, Alonso MM, Gallick GE, Fueyo J and Yung WKA. Cell cycle-dependent nuclear export of phosphatase and tensin homologue tumor suppressor is regulated by the phosphoinositide-3-kinase signaling cascade. *Cancer research*. 2007; 67:11054-11063.
68. Shen WH, Balajee AS, Wang J, Wu H, Eng C, Pandolfi PP and Yin Y. Essential role for nuclear PTEN in maintaining chromosomal integrity. *Cell*. 2007; 128:157-170.
69. Li AG, Piluso LG, Cai X, Wei G, Sellers WR and Liu X. Mechanistic insights into maintenance of high p53 acetylation by PTEN. *Molecular cell*. 2006; 23:575-587.
70. Gu TT, Zhang Z, Wang JL, Guo JY, Shen WH and Yin YX. CREB Is a Novel Nuclear Target of PTEN Phosphatase. *Cancer research*. 2011; 71:2821-2825.
71. Tanaka K, Horiguchi K, Yoshida T, Takeda M, Fujisawa H, Takeuchi K, Umeda M, Kato S, Ihara S, Nagata S and Fukui Y. Evidence that a phosphatidylinositol 3,4,5-trisphosphate-binding protein can function in nucleus. *Journal of Biological Chemistry*. 1999; 274:3919-3922.
72. Lindsay Y, McCoull D, Davidson L, Leslie NR, Fairservice A, Gray A, Lucocq J and Downes CP. Localization of agonist-sensitive PtdIns(3,4,5)P3 reveals a nuclear pool that is insensitive to PTEN expression. *J Cell Sci*. 2006; 119:5160-5168.
73. Silva A, Yunes JA, Cardoso BA, Martins LR, Jotta PY, Abecasis M, Nowill AE, Leslie NR, Cardoso AA and Barata JT. PTEN posttranslational inactivation and hyperactivation of the PI3K/Akt pathway sustain primary T cell leukemia viability. *The Journal of clinical investigation*. 2008; 118:3762-3774.
74. Palomero T, Sulis ML, Cortina M, Real PJ, Barnes K, Ciofani M, Caparros E, Buteau J, Brown K, Perkins SL, Bhagat G, Agarwal AM, Basso G, et al. Mutational loss of PTEN induces resistance to NOTCH1 inhibition in T-cell leukemia. *Nat Med*. 2007; 13:1203-1210.
75. Larson Gedman A, Chen Q, Kugel Desmoulin S, Ge Y, LaFiura K, Haska CL, Cherian C, Devidas M, Linda SB, Taub JW and Matherly LH. The impact of NOTCH1, FBW7 and PTEN mutations on prognosis and downstream signaling in pediatric T-cell acute lymphoblastic leukemia: a report from the Children's Oncology Group. *Leukemia*. 2009; 23:1417-1425.
76. Gutierrez A, Sanda T, Grebliunaite R, Carracedo A, Salmena L, Ahn Y, Dahlberg S, Neuberg D, Moreau LA, Winter SS, Larson R, Zhang J, Protopopov A, et al. High frequency of PTEN, PI3K, and AKT abnormalities in T-cell acute lymphoblastic leukemia. *Blood*. 2009; 114:647-650.
77. Liu X, Karnell JL, Yin B, Zhang R, Zhang J, Li P, Choi Y, Maltzman JS, Pear WS, Bassing CH and Turka LA. Distinct roles for PTEN in prevention of T cell lymphoma and autoimmunity in mice. *The Journal of clinical investigation*. 2010; 120:2497-2507.
78. Bonneau D and Longy M. Mutations of the human PTEN gene. *Human mutation*. 2000; 16:109-122.
79. Gronbaek K, Zeuthen J, Guldberg P, Ralfkiaer E and Hou-Jensen K. Alterations of the MMAC1/PTEN gene in lymphoid malignancies. *Blood*. 1998; 91:4388-4390.
80. Dahia PL, Aguiar RC, Alberta J, Kum JB, Caron S, Sill H, Marsh DJ, Ritz J, Freedman A, Stiles C and Eng C. PTEN is inversely correlated with the cell survival factor Akt/PKB and is inactivated via multiple mechanisms in haematological malignancies. *Human molecular genetics*. 1999; 8:185-193.
81. Nakahara Y, Nagai H, Kinoshita T, Uchida T, Hatano S, Murate T and Saito H. Mutational analysis of the PTEN/MMAC1 gene in non-Hodgkin's lymphoma. *Leukemia*. 1998; 12:1277-1280.
82. Sakai A, Thieblemont C, Wellmann A, Jaffe ES and Raffeld M. PTEN gene alterations in lymphoid neoplasms. *Blood*. 1998; 92:3410-3415.
83. Butler MP, Wang SI, Chaganti RS, Parsons R and Dalla-Favera R. Analysis of PTEN mutations and deletions in B-cell non-Hodgkin's lymphomas. *Genes, chromosomes & cancer*. 1999; 24:322-327.

84. Lenz G, Wright GW, Emre NC, Kohlhammer H, Dave SS, Davis RE, Carty S, Lam LT, Shaffer AL, Xiao W, Powell J, Rosenwald A, Ott G, et al. Molecular subtypes of diffuse large B-cell lymphoma arise by distinct genetic pathways. *Proceedings of the National Academy of Sciences of the United States of America*. 2008; 105:13520-13525.
85. Pfeifer M and Lenz G. PI3K/AKT addiction in subsets of diffuse large B-cell lymphoma. *Cell cycle*. 2013; 12:3347-3348.
86. Rudelius M, Pittaluga S, Nishizuka S, Pham TH, Fend F, Jaffe ES, Quintanilla-Martinez L and Raffeld M. Constitutive activation of Akt contributes to the pathogenesis and survival of mantle cell lymphoma. *Blood*. 2006; 108:1668-1676.
87. Battistella M, Romero M, Castro-Vega LJ, Gapihan G, Bouhidel F, Bagot M, Feugeas JP and Janin A. The High Expression of the microRNA 17-92 Cluster and its Paralogs, and the Down-Regulation of the Target Gene PTEN are Associated with Primary Cutaneous B-cell Lymphoma Progression. *The Journal of investigative dermatology*. 2015; 135:1659-1667.
88. Samuels Y, Wang Z, Bardelli A, Silliman N, Ptak J, Szabo S, Yan H, Gazdar A, Powell SM, Riggins GJ, Willson JK, Markowitz S, Kinzler KW, et al. High frequency of mutations of the PIK3CA gene in human cancers. *Science*. 2004; 304:554.
89. Abubaker J, Bavi P, Al-Harbi S, Siraj A, Al-Dayel F, Uddin S and Al-Kuraya K. PIK3CA mutations are mutually exclusive with PTEN loss in diffuse large B-cell lymphoma. *Leukemia*. 2007; 21:2368-2370.
90. Knight ZA, Gonzalez B, Feldman ME, Zunder ER, Goldenberg DD, Williams O, Loewith R, Stokoe D, Balla A, Toth B, Balla T, Weiss WA, Williams RL, et al. A pharmacological map of the PI3-K family defines a role for p110 alpha in insulin signaling. *Cell*. 2006; 125:733-747.
91. Jia SD, Liu ZN, Zhang S, Liu PX, Zhang L, Lee SH, Zhang J, Signoretti S, Loda M, Roberts TM and Zhao JJ. Essential roles of PI(3)K-p110 beta in cell growth, metabolism and tumorigenesis. *Nature*. 2008; 454:776-U102.
92. Edgar KA, Wallin JJ, Berry M, Lee LB, Prior WW, Sampath D, Friedman LS and Belvin M. Isoform-Specific Phosphoinositide 3-Kinase Inhibitors Exert Distinct Effects in Solid Tumors. *Cancer research*. 2010; 70:1164-1172.
93. Weigelt B, Warne PH, Lambros MB, Reis-Filho JS and Downward J. PI3K pathway dependencies in endometrioid endometrial cancer cell lines. *Clin Cancer Res*. 2013; 19:3533-3544.
94. Davis RE, Ngo VN, Lenz G, Tolar P, Young RM, Romesser PB, Kohlhammer H, Lamy L, Zhao H, Yang Y, Xu W, Shaffer AL, Wright G, et al. Chronic active B-cell-receptor signalling in diffuse large B-cell lymphoma. *Nature*. 2010; 463:88-92.
95. Kloo B, Nagel D, Pfeifer M, Grau M, Duwel M, Vincendeau M, Dorken B, Lenz P, Lenz G and Krappmann D. Critical role of PI3K signaling for NF-kappaB-dependent survival in a subset of activated B-cell-like diffuse large B-cell lymphoma cells. *Proceedings of the National Academy of Sciences of the United States of America*. 2011; 108:272-277.
96. Chen L, Juszczynski P, Takeyama K, Aguiar RC and Shipp MA. Protein tyrosine phosphatase receptor-type O truncated (PTPROt) regulates SYK phosphorylation, proximal B-cell-receptor signaling, and cellular proliferation. *Blood*. 2006; 108:3428-3433.
97. Chen LF, Monti S, Juszczynski P, Daley J, Chen W, Witzig TE, Habermann TM, Kutok JL and Shipp MA. SYK-dependent tonic B-cell receptor signaling is a rational treatment target in diffuse large B-cell lymphoma. *Blood*. 2008; 111:2230-2237.
98. Li B, Sun A, Jiang W, Thrasher JB and Terranova P. PI-3 kinase p110beta: a therapeutic target in advanced prostate cancers. *Am J Clin Exp Urol*. 2014; 2:188-198.
99. Schwartz S, Wongvipat J, Trigwell CB, Hancox U, Carver BS, Rodrik-Outmezguine V, Will M, Yellen P, de Stanchina E, Baselga J, Scher HI, Barry ST, Sawyers CL, et al. Feedback Suppression of PI3K alpha Signaling in PTEN-Mutated Tumors Is Relieved by Selective Inhibition of PI3K beta. *Cancer cell*. 2015; 27:109-122.
100. Subramaniam PS, Whye DW, Efimenko E, Chen J, Tosello V, De Keersmaecker K, Kashishian A, Thompson MA, Castillo M, Cordon-Cardo C, Dave UP, Ferrando A, Lannutti BJ, et al. Targeting Nonclassical Oncogenes for Therapy in T-ALL. *Cancer cell*. 2012; 21:459-472.
101. Lonetti A, Cappellini A, Sparta AM, Chiarini F, Buontempo F, Evangelisti C, Evangelisti C, Orsini E, McCubrey JA and Martelli AM. PI3K pan-inhibition impairs more efficiently proliferation and survival of T-cell acute lymphoblastic leukemia cell lines when compared to isoform-selective PI3K inhibitors. *Oncotarget*. 2015; 6:10399-10414. DOI: 10.18632/oncotarget.3295.
102. Hancox U, Cosulich S, Hanson L, Trigwell C, Lenaghan C, Ellston R, Dry H, Crafter C, Barlaam B, Fitzek M, Smith PD, Ogilvie D, D'Cruz C, et al. Inhibition of PI3Kbeta signaling with AZD8186 inhibits growth of PTEN-deficient breast and prostate tumors alone and in combination with docetaxel. *Mol Cancer Ther*. 2015; 14:48-58.
103. Tanaka H, Yoshida M, Tanimura H, Fujii T, Sakata K, Tachibana Y, Ohwada J, Ebiike H, Kuramoto S, Morita K, Yoshimura Y, Yamazaki T, Ishii N, et al. The selective class I PI3K inhibitor CH5132799 targets human cancers harboring oncogenic PIK3CA mutations. *Clinical cancer research : an official journal of the American Association for Cancer Research*. 2011; 17:3272-3281.
104. Garlich JR, De P, Dey N, Su JD, Peng X, Miller A, Murali R, Lu Y, Mills GB, Kundra V, Shu HK, Peng Q and Durden DL. A vascular targeted pan phosphoinositide 3-kinase inhibitor prodrug, SF1126, with antitumor and antiangiogenic activity. *Cancer research*. 2008; 68:206-215.
105. Qian C, Lai CJ, Bao R, Wang DG, Wang J, Xu GX, Atoyan R, Qu H, Yin L, Samson M, Zifcak B, Ma AW, DellaRocca S, et al. Cancer network disruption by a single molecule inhibitor targeting both histone deacetylase activity and phosphatidylinositol 3-kinase signaling. *Clinical cancer research : an official journal of the American Association for Cancer Research*. 2012; 18:4104-4113.
106. Hirai H, Sootome H, Nakatsuru Y, Miyama K, Taguchi S, Tsujioka K, Ueno Y, Hatch H, Majumder PK, Pan BS and Kotani H. MK-2206, an allosteric Akt inhibitor, enhances antitumor efficacy by standard chemotherapeutic agents or molecular targeted drugs in vitro and in vivo. *Molecular cancer therapeutics*. 2010; 9:1956-1967.
107. Baselga J, Campone M, Piccart M, Burris HA, 3rd, Rugo HS, Sahmoud T, Noguchi S, Gnant M, Pritchard KI, Lebrun F, Beck JT, Ito Y, Yardley D, et al. Everolimus in postmenopausal hormone-receptor-positive advanced breast cancer. *The New England journal of medicine*. 2012; 366:520-529.
108. Elit L. CCI-779 Wyeth. *Curr Opin Investig Drugs*. 2002; 3:1249-1253.
109. Reynolds CP, Kang MH, Carol H, Lock R, Gorlick R, Kolb EA, Kurmasheva RT, Keir ST, Maris JM, Billups CA, Houghton PJ and

Smith MA. Initial testing (stage 1) of the phosphatidylinositol 3' kinase inhibitor, SAR245408 (XL147) by the pediatric preclinical testing program. *Pediatric blood & cancer*. 2013; 60:791-798.

110. Furet P, Guagnano V, Fairhurst RA, Imbach-Weese P, Bruce I, Knapp M, Fritsch C, Blasco F, Blanz J, Aichholz R, Hamon J, Fabbro D and Caravatti G. Discovery of NVP-BYL719 a potent and selective phosphatidylinositol-3 kinase alpha inhibitor selected for clinical evaluation. *Bioorg Med Chem Lett*. 2013; 23:3741-3748.

111. Hall CP, Reynolds CP and Kang MH. Modulation of glucocorticoid resistance in pediatric T-cell Acute Lymphoblastic Leukemia by increasing BIM expression with the PI3K/mTOR inhibitor BEZ235. *Clinical cancer research: an official journal of the American Association for Cancer Research*. 2015; in press.

112. Yang Y, Yang JJ, Tao H and Jin WS. MicroRNA-21 controls hTERT via PTEN in human colorectal cancer cell proliferation. *Journal of physiology and biochemistry*. 2015; 71:59-68.

113. Yang X, Cheng Y, Li P, Tao J, Deng X, Zhang X, Gu M, Lu Q and Yin C. A lentiviral sponge for miRNA-21 diminishes aerobic glycolysis in bladder cancer T24 cells via the PTEN/PI3K/AKT/mTOR axis. *Tumour biology : the journal of the International Society for Oncodevelopmental Biology and Medicine*. 2015; 36:383-391.

114. Meng F, Henson R, Wehbe-Janek H, Ghoshal K, Jacob ST and Patel T. MicroRNA-21 regulates expression of the PTEN tumor suppressor gene in human hepatocellular cancer. *Gastroenterology*. 2007; 133:647-658.

115. Calin GA, Liu CG, Sevignani C, Ferracin M, Felli N, Dumitru CD, Shimizu M, Cimmino A, Zupo S, Dono M, Dell'Aquila ML, Alder H, Rassenti L, et al. MicroRNA profiling reveals distinct signatures in B cell chronic lymphocytic leukemias. *Proceedings of the National Academy of Sciences of the United States of America*. 2004; 101:11755-11760.

116. Tian L, Fang YX, Xue JL and Chen JZ. Four microRNAs promote prostate cell proliferation with regulation of PTEN and its downstream signals in vitro. *PLoS one*. 2013; 8:e75885.

117. Palacios F, Prieto D, Abreu C, Ruiz S, Morande P, Fernandez-Calero T, Libisch G, Landoni AI and Oppezio P. Dissecting chronic lymphocytic leukemia microenvironment signals in patients with unmutated disease: microRNA-22 regulates phosphatase and tensin homolog/AKT/FOXO1 pathway in proliferative leukemic cells. *Leukemia & lymphoma*. 2015:1-6.

118. Yan SY, Chen MM, Li GM, Wang YQ and Fan JG. MiR-32 induces cell proliferation, migration, and invasion in hepatocellular carcinoma by targeting PTEN. *Tumour biology: the journal of the International Society for Oncodevelopmental Biology and Medicine*. 2015; 36:4747-4755.

119. Ohta K, Hoshino H, Wang J, Ono S, Iida Y, Hata K, Huang SK, Colquhoun S and Hoon DS. MicroRNA-93 activates c-Met/PI3K/Akt pathway activity in hepatocellular carcinoma by directly inhibiting PTEN and CDKN1A. *Oncotarget*. 2015; 6:3211-3224. DOI: 10.18632/oncotarget.3085.

120. Yang YK, Xi WY, Xi RX, Li JY, Li Q and Gao YE. MicroRNA494 promotes cervical cancer proliferation through the regulation of PTEN. *Oncology reports*. 2015; 33:2393-2401.

121. Yu TT, Cao RS, Li S, Fu MG, Ren LH, Chen WX, Zhu H, Zhan Q and Shi RH. MiR-130b plays an oncogenic role by repressing PTEN expression in esophageal squamous cell carcinoma cells. *BMC cancer*. 2015; 15:29.

122. Xiang SJ, Fang JQ, Wang SY, Deng B and Zhu L. MicroRNA-135b regulates the stability of PTEN and promotes glycolysis by

targeting USP13 in human colorectal cancers. *Oncology reports*. 2015; 33:1342-1348.

123. Yang H, Kong W, He L, Zhao JJ, O'Donnell JD, Wang J, Wenham RM, Coppola D, Kruk PA, Nicosia SV and Cheng JQ. MicroRNA expression profiling in human ovarian cancer: miR-214 induces cell survival and cisplatin resistance by targeting PTEN. *Cancer research*. 2008; 68:425-433.

124. Zang C, Eucker J, Liu H, Coordes A, Lenarz M, Possinger K and Scholz CW. Inhibition of pan-class I phosphatidylinositol-3-kinase by NVP-BKM120 effectively blocks proliferation and induces cell death in diffuse large B-cell lymphoma. *Leuk Lymphoma*. 2014; 55:425-434.

Rapamycin in preventive (very low) doses

Roman V. Kondratov and Anna A. Kondratova

In the recent paper of Popovich et al. published in *Cancer Biology and Therapy* [1], positive effects of low doses of rapamycin on survival of cancer-prone HER-2/neu mice have been reported. Inhibitors of the mTOR signaling pathway are already widely employed for anticancer therapy in humans. At the same time, over several last years a substantial body of evidence suggesting an anti-aging effect of at least one mTOR inhibitor, rapamycin, was accumulated. For example, rapamycin delayed death without changing the distribution of presumptive causes of death in genetically heterogeneous mice [2] and extended lifespan of cancer-prone mice, such as transgenic HER-2/neu mice [3]. Thus, a question was raised whether lifespan extension by rapamycin is a consequence of the anti-cancer effect of rapamycin (such as suppression of tumor initiation or slowing down tumor progression) or a direct result of its anti-aging properties (or both). Several studies supported effectiveness of rapamycin in delaying of aging independently from its anti-cancer activities. For example, Wilkinson et al. [4] demonstrated that rapamycin treatment significantly decreased numerous manifestations of aging and alleviated age-dependent decline in spontaneous activity in 20-22 month genetically heterogeneous mice (the age when the majority of mice survived). In the study of Anisimov et al. [5] conducted with inbred female mice, rapamycin treatment extended lifespan, inhibited age-related weight gain, and increased the percentage of mice having regular estrous cycle at 18 months. However, the question whether lifespan extension was in part a result of suppression of cancer was not answered in these studies. A recent work from our laboratory, conducted on *Bmal1*^{-/-} mice suffering from premature aging, provides an example of lifespan extension induced by rapamycin which is not due to inhibition of neoplastic diseases [6]. Strikingly, these mice, in spite of having many prominent aging phenotypes, virtually never develop cancer, and die from systemic failure due to progressive degeneration of nervous and cardiovascular and muscle systems. We found that rapamycin treatment extended lifespan of *Bmal1*^{-/-} mice from 8 to 12 months. Activity of mTORC1 in tissues of *Bmal1*^{-/-} was highly elevated, thus, treatment with rapamycin extended their lifespan mostly likely through suppression of mTOR signaling.

Therefore, this study helps to further separate the life-extending effect of rapamycin from its cancer-preventing properties. Taken together, these findings indicate that rapamycin can be considered as a good candidate for a preventive anti-aging medicine.

Using a substance as a preventive medicine immediately raises questions about its overall safety and potential side effects; these questions are even more principle here compared with the situation of disease treatment. For example, in cancer treatment the drugs are used under conditions when the disease has already been developed and is deadly dangerous. Therefore, administration of high doses of drugs (even in spite of particular side effects) is justified; additionally, drugs are often administered during relatively short periods of time. On the contrary, prevention suggests chronic exposure to a medicine before the actual disease is developed, which may not happen whatsoever even without taking the preventive medication (considered as a disease, aging is an apparent exception). Thus, an ideal chemopreventive medicine should not have any side effects. Rapamycin, like any other existing medicine, does have side effects. In addition to well-known side effects of high doses of rapamycin in humans [7], life-long chronic exposure to rapamycin, while preventing most age-related diseases and extending healthspan, was shown to increase incidence of cataracts and some other alterations in mice [4]. This type of known and potential side effects makes consideration of rapamycin as a chemopreventor much less attractive for a healthy individual. Several groups noticed another side effect, a general decrease in animal robustness, when treatment with rapamycin was started in very young mice [1, 8]; this underscores the importance of mTOR pathway activity during development and points out to the significance of another variable, the onset of treatment, in diminishing of side effects. Therefore, the question about safe dosage, timing and mechanisms of delivery of rapamycin is extremely important.

Popovich and colleagues reported the lifespan extension activity of low doses of rapamycin administered in the intermittent manner (with two-week breaks between two-week-long bi-daily treatments) in a mouse model of breast cancer. In this model, mammary carcinoma develops in female mice overexpressing oncogene

HER2; cancer advances very fast with average lifespan of about 9 months. Different regimes of treatment with low doses of rapamycin allowed increasing lifespan with or without significant cancer prevention (correlating with the age the treatment started). The present study is an extension of the previous work by this team of collaborators on anticancer/longevity effects of rapamycin given in doses corresponding to the therapeutic oral dose in humans in the same mouse model [3]. There, rapamycin reduced cancer incidents, suppressed development of tumors, and extended lifespan by almost two fold. The positive effect of low doses of rapamycin on longevity in the follow-up study supports previous observations. The most important advantage of the new study derives from the significant reduction of the dose used. The above-discussed side effects are generally a matter of dose: indeed, at particular doses any substance, even water, turns out to be toxic; thus, the ability of rapamycin to work at low doses makes it substantially more attractive as a candidate for a preventive medicine.

In conclusion, we would like to accentuate that indeed anti-cancer and anti-aging activities of rapamycin can be separated. In the case of HER2-overexpressing mice, whether rapamycin works through the delay of aging or other mechanisms are involved still has to be found. At the same time, it also supports the strategy to use rapamycin in combination with other anticancer drugs. Indeed, even if rapamycin on its own would not affect tumor, it still might improve survival and therapeutic outcome. It is worth testing at least in other animal models.

REFERENCES

1. Popovich IG et al. *Cancer Biol Ther.* 2014; 15 PMID: 24556924
2. Harrison DE et al. *Nature.* 2009; 460: 392-395.
3. Anisimov VN et al. *Am J Pathol.* 2010; 176: 2092-2097.
4. Wilkinson JE et al. *Aging Cell.* 2012; 11: 675-682.
5. Anisimov VN et al. *Cell Cycle.* 2011; 10: 4230-6.
6. Khapre RV et al. *Aging (Albany NY).* 2014; 6: 48-57.
7. Blagosklonny MV. *Oncoimmunology.* 2013;2:e26961.
8. Johnson SC et al. *Science.* 2013; 342: 1524-1528.

Roman V. Kondratov¹ and Anna A. Kondratova²

¹*Center for Gene Regulation in Health and Diseases, BGES, Cleveland State University, Cleveland, OH 44115; USA*

²*Department of Molecular Genetics, Lerner Research Institute, Cleveland Clinic, Cleveland, OH 44195; USA*
Email: r.kondratov@csuohio.edu; kondraa@ccf.org

Received: 3/4/14; Published: 3/22/14

Metformin and rapamycin are master-keys for understanding the relationship between cell senescent, aging and cancer

Vladimir N. Anisimov

During the last decade it was established that conservative growth hormone/ insulin-like growth factor-1 (IGF-1) and target of rapamycin (TOR) signaling pathways plays a key role in the control of aging and age-associated pathology in yeast, worms, insects and mammals [1-3]. mTORC1 (mammalian target of rapamycin complex 1) is activated by insulin and related growth factors through phosphatidylinositol-3-OH kinase and AKT kinase signaling and repressed by AMP-activated protein kinase, a key sensor of cellular energy status [1]. mTORC1 involved into promotion messenger RNA translation and protein synthesis through ribosomal protein S6 kinases (S6Ks) and 4E-BP protein. mTORC1 also stimulates lipid biosynthesis, inhibits autophagy, and through hypoxic response transcription factor HIF-1 α regulates mitochondrial function and glucose metabolism. The lifespan of S6K1 deficient female mice increased by 19% without effect on tumor development [see 1]. These data suggest that S6K1 plays a relevant role in lifespan regulation downstream of TORC1. Lamming et al. [4] have shown that decreased mTORC1 signaling is sufficient for lifespan prolongation independently from changes in glucose homeostasis. Rapamycin suppresses mTORC1 and indirectly mTORC2 that leads to metabolic lesions like glucose intolerance and abnormal lipid profile [1]. Treatment with rapamycin or its more soluble form rapatar increased the mean lifespan in various strain of mice [1-3,5-7]. It is worthy to note that the regulation of growth hormone and IGF-1, oxidative stress, DNA damage, and metabolic pathways by calorie restriction could simultaneously leads to its anti-aging and anti-tumor activities as well as to reduction of the number of senescent cells in some tissues [1,3].

It was shown that the treated with antidiabetic biguanide metformin diabetes type 2 patients have from 25% to 40% less cancer than those who receive insulin as therapy or treated with sulfonylurea drugs that increase insulin secretion from the pancreas [1-3]. It was shown that biguanides like inhibitor of mTOR rapamycin prolong the lifespan of animals from yeast to mammals [2,3]. It means that the targets as well as signaling pathways and regulatory signals are also similar. Moreover, there is also the sufficient similarity in

patterns of changes observed during normal aging and the process of carcinogenesis. There is a mounting evidence for the similarity between the aging and carcinogenesis in response patterns of these two signaling pathways to pharmacological intervention.

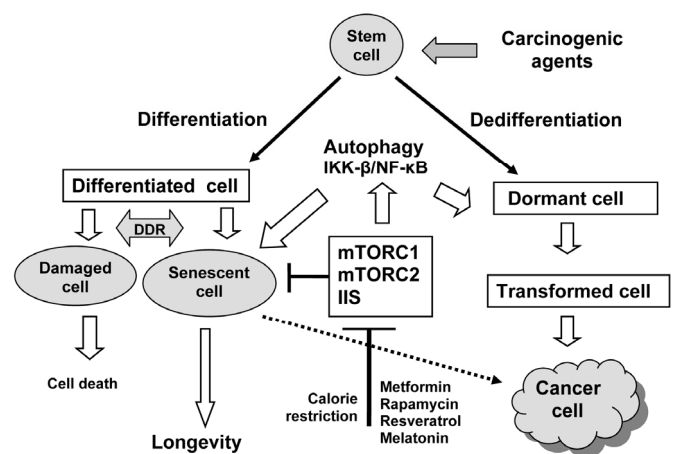


Figure 1. Relationship between aging and carcinogenesis: the key role of insulin/IGF-1-like signaling (IIS) and mTOR signaling. DNA damage induced by environmental and endogenous factors (ROS, chemicals, ionizing radiation, ultra-violet, constant illumination, oncogenes, some diets, etc.) may leads to cellular senescence or cellular lesions which could be deleted by apoptosis or autophagy. The same agents can induce damages which followed by neoplastic transformation thus leading to cancer. Metformin, rapamycin, and some other compounds with mTOR- and IIS-inhibitory potential (resveratrol, melatonin) are able to modify both the aging and carcinogenesis.

DNA damage response signaling seems to be the key mechanism of establishment and maintenance of the senescence programme as well as of the carcinogenesis [1-3]. The available data on cellular senescence *in vitro* and on accumulation in cells *in vivo* of various premalignant lesions provide evidence suggesting that senescence is effective natural cancer-suppressing

mechanism [1,2]. At the same time, adequate clinical application of therapy-induced ‘accelerated senescence’ for prevention or recurrence of human cancers is still not enough understood. The mechanisms underlying the bypass of senescence response in the progression of tumors should to be discovered. Recent studies reveal a negative side of cellular senescence, which is associated with the secreted inflammatory factors, and may alter the microenvironment in the favor of cancer progression designated as syndrome of cancerophilia or senescence-associated secretory phenotype (SASP) [1-3]. Thus, cellular senescence suppresses the initiation stage of carcinogenesis but is the promoter for initiated cells. We believe that the similarity of two fundamental processes – aging and carcinogenesis, – is a basis for understanding the two-side effects of biguanides and rapamycin on its (Figure 1). Recent finding provide the evidence of inhibitory effect of metformin and rapamycin on the SASP interfering with IKK- β /NF- κ B [1] – an important step in hypothalamic programming of systemic aging [8]. It remains to be shown whether antidiabetic biguanides and rapamycin can extend lifespan in humans.

Vladimir N. Anisimov

*Department of Carcinogenesis and Oncogerontology,
N.N.Petrov Research Institute of Oncology, St.Petersburg,
197758 Russia;*

Email: aqinq@mail.ru

Received: 5/18/13; Published: 5/25/13

REFERENCES

1. Johnson SC et al. *Nature*.2013;493:338-345.
2. Blagosklonny MV. *Aging (Albany NY)*.2012;4:861-867.
3. Anisimov VN, Bartke A. *Crit Rev Oncol Hematol*. 2013; Feb 21. doi:pii:S1040-8428(13)00031-0. 10.1016/j.critrevonc.2013.01.005.
4. Lamming DW et al. *Science*.2012;335:1638-1643.
5. Komarova EA et al. *Aging (Albany NY)*.2012;4:709-717.
6. Comas M et al. *Aging (Albany NY)*.2012;4:715-722.
7. Livi CB et al. *Aging (Albany NY)*.2013;5:100-110.
8. Zhang G et al. *Nature*.2013;497:211-218.

Temporal mTOR inhibition protects Fbxw7-deficient mice from radiation-induced tumor development

Yueyong Liu¹, Yurong Huang¹, Zeran Wang¹, Yong Huang², Xiaohua Li², Alexander Louie², Guangwei Wei^{3,1}, and Jian-Hua Mao¹

¹ Life Sciences Division, Lawrence Berkeley National Laboratory, Berkeley, CA 94720, USA;

² Drug Studies Unit, University of California at San Francisco, South San Francisco, CA 94080, USA;

³ Department of Anatomy, Shandong University School of Medicine, Jinan, Shandong, 250012 China

Key words: *Fbxw7*, mTOR, p53, radiation, tumorigenesis, rapamycin

Received: 1/16/13; **Accepted:** 2/22/13; **Published:** 2/24/13

Correspondence to: Jian-Hua Mao, PhD; **E-mail:** JHMao@lbl.gov

Copyright: © Liu et al. This is an open-access article distributed under the terms of the Creative Commons Attribution License, which permits unrestricted use, distribution, and reproduction in any medium, provided the original author and source are credited

Abstract: *FBXW7* acts as a tumor suppressor in numerous types of human cancers through ubiquitination of different oncoproteins including mTOR. However, how the mutation/loss of *Fbxw7* results in tumor development remains largely unknown. Here we report that downregulation of mTOR by radiation is *Fbxw7*-dependent, and short-term mTOR inhibition by rapamycin after exposure to radiation significantly postpones tumor development in *Fbxw7/p53* double heterozygous (*Fbxw7+/-p53+/-*) mice but not in *p53* single heterozygous (*p53+/-*) mice. Tumor latency of rapamycin treated *Fbxw7+/-p53+/-* mice is remarkably similar to those of *p53+/-* mice while placebo treated *Fbxw7+/-p53+/-* mice develop tumor significantly earlier than placebo treated *p53+/-* mice. Furthermore, we surprisingly find that, although temporal treatment of rapamycin is given at a young age, the inhibition of mTOR activity sustainably remains in tumors. These results indicate that inhibition of mTOR signaling pathway suppresses the contribution of *Fbxw7* loss toward tumor development.

INTRODUCTION

FBXW7 is one of the most important human tumor suppressor genes, which undergoes deletion and/or mutation in cancers from a wide spectrum of human tissues, such as breast, colon, endometrium, stomach, lung, ovary, pancreas, and prostate [1, 2]. The overall frequency of point mutation of *FBXW7* in human cancers is about 6% [3]. The *FBXW7* gene is essential for the ubiquitination of different oncoproteins, including c-Myc [4, 5], c-Jun [6], cyclin E [7, 8], Notch [9, 10], Klf5 [11, 12], Mcl-1 [13, 14], and Aurora-A [15, 16]. Haploinsufficient loss of *Fbxw7* is observed in most lymphomas in the mouse model, even those arising from *Fbxw7/p53* double heterozygous mice [17]. Similar observations of heterozygous mutations were subsequently made in human tumors [18]. These findings suggest that loss of only one copy of the gene can generate a substantial biological impact.

The mammalian target of rapamycin, mTOR, is a central component of several complex signaling networks that regulate cell growth, metabolism and proliferation. mTOR signaling is frequently dysregulated in a number of human diseases including cancer, cardiovascular disease and ageing, and thus has become an attractive target for therapeutic intervention. We and others have recently shown that mTOR is a target of *FBXW7* [19-21]. In this study, we investigated whether inhibition of mTOR signaling pathway by rapamycin was able to prevent the tumor development resulted from loss of *Fbxw7* in mice.

RESULTS

Fbxw7-dependent inhibition of mTOR by radiation

Our previous study has shown that *Fbxw7* can be transcriptionally activated by *p53* upon DNA damage

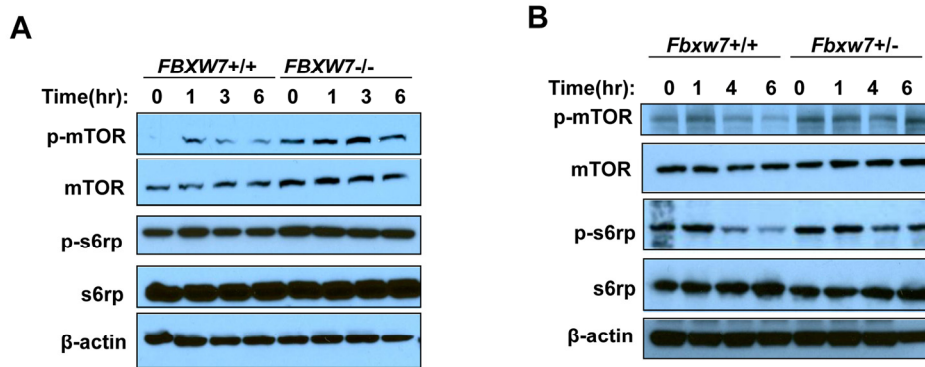


Figure 1. Radiation inhibits mTOR and its signaling in a FBXW7-dependent manner. mTOR and its signaling was assessed by Western blot assays with antibodies to p-mTOR (Ser2448), mTOR, p-S6rp (Ser240 and Ser244), S6rp, and β-Actin. **(A)** Detection of mTOR and its downstream signaling in HCT116 wild type and *FBXW7*^{-/-} cells at different time points after single dose of 4Gy X-ray radiation. **(B)** Detection of mTOR and its downstream signaling in thymuses from wild type and *FBXW7*^{+/-} mice that were collected at different time points after single dose of 4Gy X-ray radiation.

[17]. Thus we first sought to investigate the changes in mTOR signaling pathway after exposure to radiation. Western blot analysis showed that, at different time points post radiation, there is a decrease in the phosphorylation levels of mTOR (p-mTOR) in HCT116 *FBXW7*^{+/+} cells while there is no change in HCT116 *FBXW7*^{-/-} cells, which is confirmed by downstream the phosphorylation levels of s6 Ribosomal Protein (p-s6rp) (Fig. 1A). We also observed a significant increase in mTOR and p-mTOR level in HCT116 *FBXW7*^{-/-} cells compared to HCT116 *FBXW7*^{+/+} cells, consistent with our previous report [19]. These observations were further examined using *Fbxw7* wild-type (*Fbxw7*^{+/+}) and heterozygous (*Fbxw7*^{+/-}) mice (Fig. 1B). Loss of one copy of *Fbxw7* sufficiently blocked the radiation-induced decrease in level of total mTOR and p-mTOR (Fig. 1B). All these results clearly indicate that inhibition of mTOR and its signaling by radiation is FBXW7-dependent.

Temporal rapamycin treatment delays tumorigenesis in *Fbxw7/p53* double heterozygous (*Fbxw7*^{+/-}*p53*^{+/-}) mice, not in *p53* single heterozygous (*p53*^{+/-}) mice

Next, we investigated whether temporal mTOR inhibition by rapamycin can prevent mice from *Fbxw7* loss-induced tumor development. We decided upon administration using 10-week continuous release pellets embedded with rapamycin (at dose of 4mg/kg body weight/day) to standardize rapamycin treatment. First we examined blood levels of rapamycin in the treated

mice with this pellet at different time points using liquid chromatography-tandem mass spectrometry (details see Materials and Methods). We observed that in rapamycin-treated mice the average rapamycin level was about 20ng/ml and could not be detected at 15 weeks after pellet implantation, whereas in placebo-treated mice rapamycin concentration was always below the detection level (Supplementary Fig. S1). Next we assessed the biochemical effects of rapamycin by measuring the levels of p-s6rp in spleen. Western blotting analysis showed that the levels of total s6rp were similar between placebo and rapamycin treated groups (Fig. 2A). In contrast, we found that rapamycin reduced the levels of p-s6rp (Fig. 2A), suggesting that the kinase activity of mTOR was inhibited in the rapamycin-treated mice in comparison to the placebo-treated mice.

In order to investigate whether rapamycin can prevent mice from *Fbxw7* loss-induced tumor development, 60 *Fbxw7*^{+/-}*p53*^{+/-} mice were treated with a single dose of 4Gy whole body X-Ray irradiation at about 5-week old and were randomly divided into two groups (Supplementary Table S1). One week after irradiation, one group was treated with the 10-week continuous release rapamycin pellets and the other group was treated with placebo pellets (details see Materials and Methods). As a control, 57 *p53*^{+/-} mice were treated using the same protocol (Supplementary Table S1). We found that, in *Fbxw7*^{+/-}*p53*^{+/-} mice, temporal rapamycin treatment significantly delayed the tumor development (p=0.03) (Fig. 2B). In contrast, such

temporal rapamycin treatment is ineffective in *p53*^{+/-} mice ($p=0.43$), although showing a trend toward delay in tumor development in late life (Fig. 2B). Consistent with our previous finding [17], placebo-treated *Fbxw7*^{+/-}/*p53*^{+/-} mice developed tumors much earlier than *p53*^{+/-} mice ($p=0.014$) (Figure 2b). Strikingly, rapamycin-treated *Fbxw7*^{+/-}/*p53*^{+/-} mice were equivalent to *p53*^{+/-} mice in radiation sensitivity (Fig. 2B). Furthermore, the tumor spectra between placebo- and rapamycin-treated mice are similar (Supplementary Fig. S2). These results suggested that temporal rapamycin treatment fully blocked the contribution of *Fbxw7* loss to radiation-induced tumor development.

Sustained inactivation of mTOR signaling pathway in tumors from mice with temporal rapamycin treatment

Next we investigated the effects of temporal rapamycin treatment on mTOR signaling in the tumor tissues by Western blotting. Although there was no difference in

the levels of total s6rp among different genotype and treatment groups ($p=0.13$) (Fig. 3), one consistent observation was that tumors from rapamycin treated *Fbxw7*^{+/-}/*p53*^{+/-} mice retained the significantly lower average levels of p-s6rp in comparison to those from placebo treated *Fbxw7*^{+/-}/*p53*^{+/-} mice ($p<0.001$) (Fig. 3A and B). There are slightly lower average levels of p-s6rp in tumors from rapamycin treated *p53*^{+/-} mice than in those from placebo treated *p53*^{+/-} mice, but not significant difference ($p=0.12$) (Fig. 3B). Interestingly, tumors from rapamycin treated *Fbxw7*^{+/-}/*p53*^{+/-} mice showed a similar range of p-s6rp levels as those from rapamycin treated *p53*^{+/-} mice while tumors from placebo treated *Fbxw7*^{+/-}/*p53*^{+/-} mice showed significantly higher p-s6rp levels than these from placebo treated *p53*^{+/-} mice ($p<0.001$) (Fig. 3B), suggesting mTOR activity is elevated when loss of one copy of *Fbxw7*, and this elevation is inhibited by mTOR inhibitor, rapamycin. Presumably such inhibition by rapamycin subsequently suppresses the contribution of *Fbxw7* loss to tumor development.

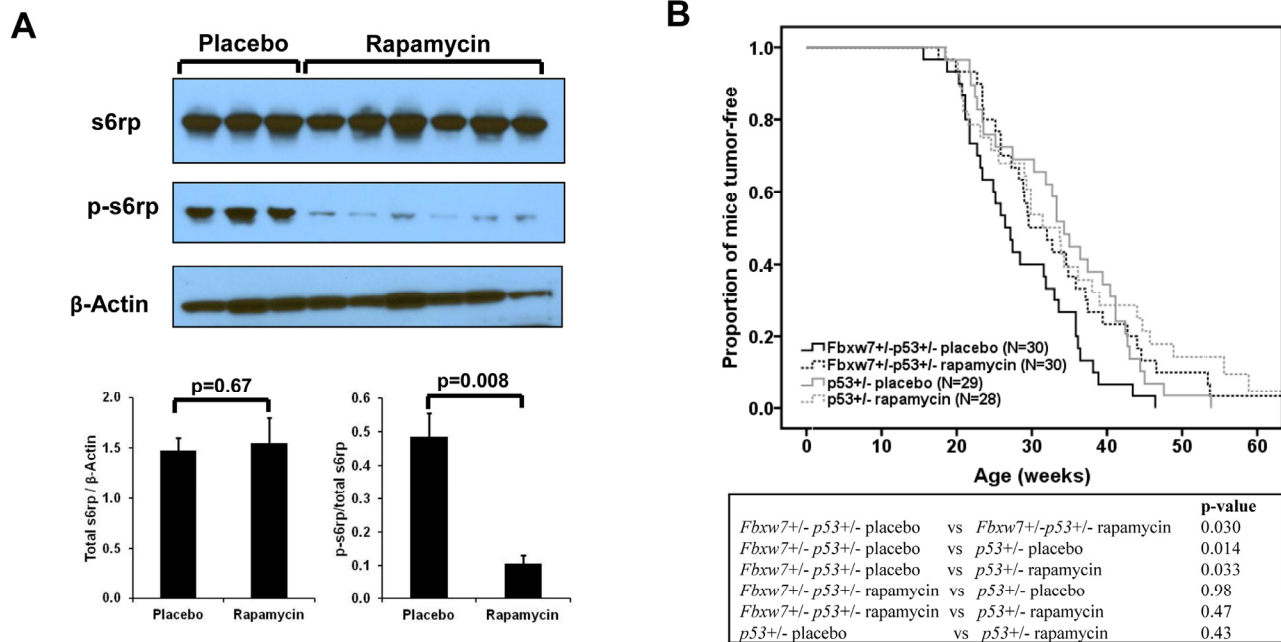


Figure 2. Effect of rapamycin on mTOR signaling and radiation-induced tumor development. **(A)** Western blotting and quantitative analysis of the blots shows decreased p-s6rp (Ser240 and Ser244) level in spleen when mice treated with rapamycin. No change was found in total s6rp. Mean values (\pm standard deviation) were presented. The p-values were obtained by t-test. **(B)** Radiation-induced tumorigenesis in *Fbxw7*^{+/-}/*p53*^{+/-} or *p53*^{+/-} mice with 10-week treatment of rapamycin or placebo that was given at 1 week post a single dose of 4Gy X-ray radiation. Top panel: Kaplan-Meier curves of tumor latency. Bottom panel: The p-values were obtained from long rank test by Kaplan-Meier analysis.

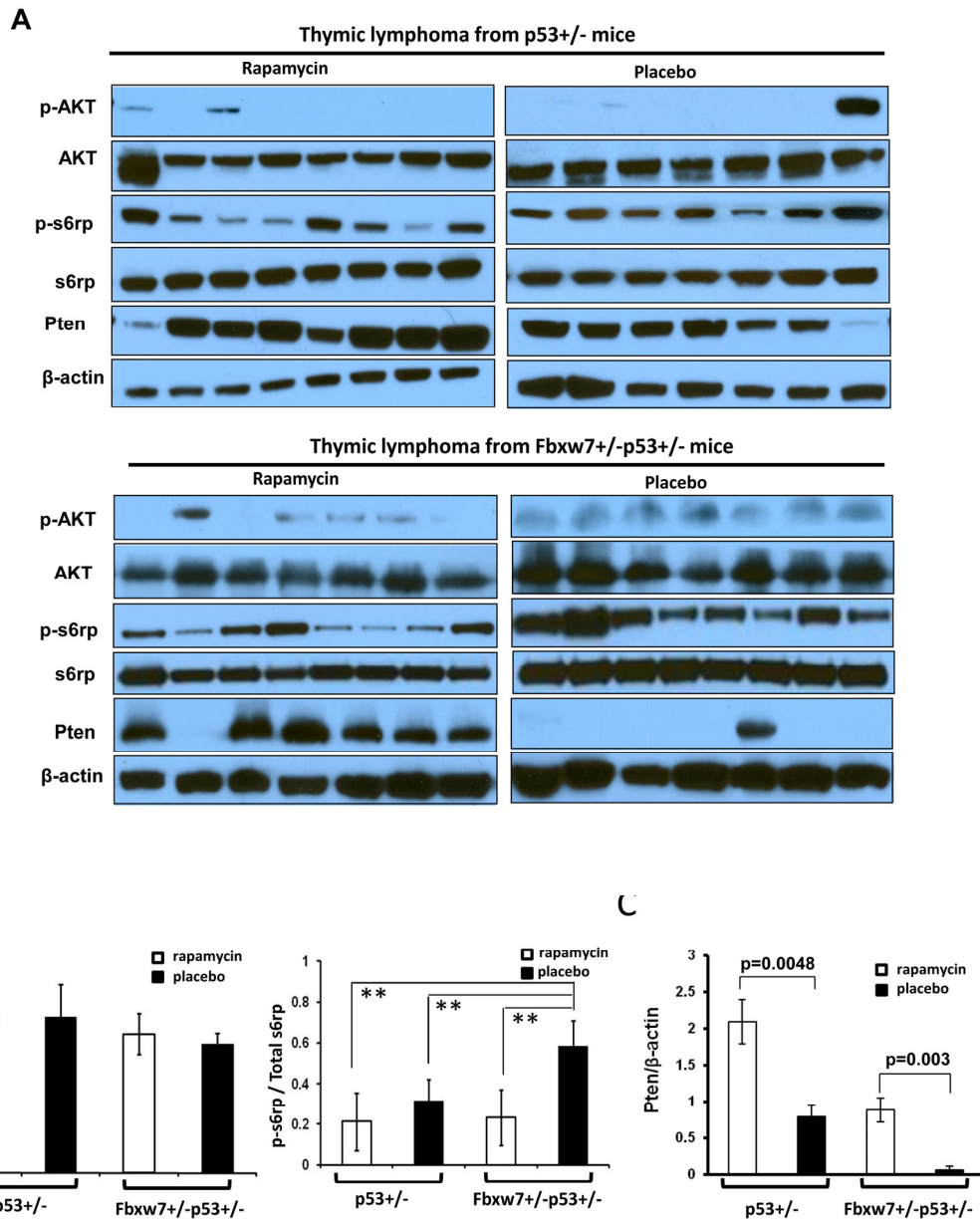


Figure 3. Inhibition of mTOR signaling sustains in tumors from rapamycin treated mice. **(A)** Detection of mTOR upstream and downstream signaling in the tumors from *Fbxw7*^{+/-}*p53*^{+/-} and *p53*^{+/-} mice treated with rapamycin or placebo by Western blot assays with antibodies to p-AKT (Ser473), AKT, p-S6rp (Ser240 and Ser244), S6rp, Pten, and β-Actin. **(B)** Quantitative analysis of the total s6rp and p-s6rp levels in the blots showed in **(A)**. Mean values (± standard deviation) were presented. **indicates $p < 0.001$. **(C)** Quantitative analysis of the Pten levels in the blots showed in **(A)**. Mean values (± standard deviation) were presented.

Another interesting finding was that the protein level of Pten had a significant increase in tumors from rapamycin treated *p53*^{+/-} and *p53*^{+/-}*Fbxw7*^{+/-} mice (Fig. 3C). Especially in those placebo treated *p53*^{+/-}*Fbxw7*^{+/-} mice, Pten level was only detected in one of

eight tumors. This observation was confirmed by immunochemical staining in tumors (Supplementary Fig. S3). The possible explanation for this is due to the complex feedback loops in mTOR pathway that has been reported [22].

DISCUSSION

Our results demonstrate that mTOR signaling pathway is inhibited following radiation exposure, which can be explained by that radiation activates p53, in turn p53 transcriptionally upregulates Fbxw7, subsequently Fbxw7 downregulates mTOR through ubiquitination. p53 inhibits mTOR through Fbxw7 and subsequently prevents cellular senescence [23-25]. This explanation is supported by that depletion of *Fbxw7* blocks radiation-induced mTOR inhibition. Interestingly, a recent study shows that PI3K-AKT-mTOR signaling pathway is activated in mouse mammary gland at 2 and 12 months post radiation exposure [26], suggesting that (a) mTOR signaling in different tissues possibly responds to radiation differently since we examined mTOR signaling in thymuses; and (b) long-term effect of radiation on mTOR signaling is possibly different from short-term one. Additional experiments are required to clarify this difference by systematic assessment of mTOR signaling in different tissues and at different time points and to examine the mechanisms underlying these different responses. It is possible that radiation modulates mTOR signaling via p53-Fbxw7 pathway at earlier time point whereas via different pathway(s) at long-term post exposure.

Fbxw7 regulates mTOR via its ubiquitination function [19-21]. Depletion of Fbxw7 leads to elevation of mTOR signaling, which drives many cell growth outputs. Thus we assume that inhibition of mTOR activity by rapamycin may act a major brake on tumor development in Fbxw7 deficient mice. Indeed, *Fbxw7*^{+/-}*p53*^{+/-} mice with temporal rapamycin treatment after radiation develop tumor same as *p53*^{+/-} mice, while *Fbxw7*^{+/-}*p53*^{+/-} mice with temporal placebo treatment develop tumor significantly faster than *p53*^{+/-} mice. Even more, tumors from rapamycin treated *Fbxw7*^{+/-}*p53*^{+/-} mice showed similar mTOR signaling as those from rapamycin treated *p53*^{+/-} mice while tumors from placebo treated *Fbxw7*^{+/-}*p53*^{+/-} mice showed significantly higher mTOR signaling than these from placebo treated *p53*^{+/-} mice. These results indicate that rapamycin inhibits mTOR signaling pathway and in turn, such inhibition fully suppresses the contribution of *Fbxw7* loss toward tumor development.

We observed that the same temporal inhibition of mTOR pathway could not sufficiently prevent *p53*^{+/-} mice from radiation-induced tumor development. This observation is different from the recent report about anti-cancer effect of rapamycin in *p53*^{+/-} mice [27] and that cellular senescence of normal cells predispose to cancer [28, 29]. This difference is possibly due to rapamycin treatment regimen. In their study, *p53*^{+/-}

mice were continuously treated with rapamycin beginning at a young age (<5 months) whereas we temporally treated *p53*^{+/-} mice with rapamycin at age about 1.5 through 4 months. Other possible reason is that they did not use radiation, tumor were spontaneous. In our study, mice were irradiated at 5 weeks old, and rapamycin treatment was given at 1 week after radiation. It is possible that we missed the window of prevention since it has been reported that rapamycin is better for prevention than treatment [29].

In conclusion, *FBXW7* has emerged as a major human tumor suppressor gene that lies at the nexus of several pathways which control cell growth, cell differentiation, and tumorigenesis, including those mediated by Ras, Myc, Jun, p53, Notch and mTor. How the decrease in Fbxw7 function results in tumor development remains largely unknown. Mutation/loss of the *Fbxw7* gene may cause impaired degradation of multiple targets, and as a result constitutive accumulation of these targets may cooperatively contribute to tumor development. Our results in this study showed that temporal pharmacological inhibition of mTOR pathway after radiation was sufficient to suppress the tumor development contributed by *Fbxw7* loss, suggesting that Fbxw7-mTOR pathway plays a major role in this radiation-induced carcinogenesis mouse model.

MATERIALS AND METHODS

Mice, tumor induction, and rapamycin treatment. *Fbxw7*^{+/-} mice was crossed with *p53*^{-/-} mice to generate *p53*^{+/-} and *p53*^{+/-}*Fbxw7*^{+/-} mice. The 5-week old *p53*^{+/-} and *p53*^{+/-}*Fbxw7*^{+/-} mice were exposed to a single dose of 4Gy whole body X-ray irradiation. One week after radiation treatment, mice were randomly divided into two groups. One group of mice was treated with rapamycin, the other with placebo. The treatment was administrated by subcutaneously implanting the 10-week continuous release pellets embedded with rapamycin or placebo. The rapamycin and placebo pellet were purchased from Innovative Research of America (Sarasota, Florida USA. Website: <http://www.innovrsrch.com/>). The rapamycin pellet released at a dose of 4mg/kg/day based upon the average mouse weight of 20g. Mice were observed daily until moribund, then euthanized and autopsied. Mice were bred and treated under the protocol approved by Animal Welfare and Research Committee at Lawrence Berkeley National Laboratory.

Measurement of Rapamycin concentration in blood. Whole blood was collected from rapamycin or Placebo treated mice by retro-orbital or tail vein bleeding into EDTA tubes and stored at -70°C until analysis.

Rapamycin was measured by liquid chromatography-tandem mass spectrometry (LC/MS/MS). The standard curve range for rapamycin was 1ng/ml to 400ng/ml. The standard curve samples were made by spiking blank blood with different amounts of rapamycin and processed along with the study samples. The blood sample (20µl) was diluted with 20µl of water and then 40µl of 70% acetonitrile was added. 20µl of internal standard, rapamycin-d3 (10ng/ml), was added to each sample. 100µl of methanol: 0.3M zinc sulfate (70:30) (v/v) was added and vortexed for 1min. The mixture was centrifuged at 3000 rpm for 10 min. Then the supernatant was transferred to an autosampler vial and 5µl was injected to the following LC/MS/MS system. The mass detector was an API 5000 triple quadrupole (Applied Biosystems, Foster City, CA), equipped with a Turbo Ion Spray source. The system was set in positive ionization mode. The ion spray voltage was 5500V and the source temperature was 400°C. The values for CAD, CUR, GS1, and GS2 were 8, 20, 75, and 75 respectively. The multiple reaction monitor was set at 931.8 – 864.7 *m/z* for rapamycin and 934.8 – 864.7 *m/z* for Sirolimus-d3. The values for DP, EP, CE, CXP were 80, 10, 22, and 45 respectively for rapamycin and Sirolimus-d3. A Shimadzu system was used for the HPLC, consisting of a pump, solvent degasser, autosampler and column oven. The column oven was set to 50°C and the autosampler was set to 4°C. The mobile phase, consisting of 65 % acetonitrile, 0.05 % formic acid containing 1mM ammonium acetate, was pumped through a Hypersil BDS C8 (3 x 50 mm, 5 µm particle size) column with a flow rate of 0.40 ml/min. Data was acquired and processed by Analyst 1.5.1 software.

Antibody and Immunoblotting. Western blot assays were performed with antibodies to phospho-mTOR (Ser2448), mTOR, phospho-S6 ribosomal protein at Ser240 and S244 (p-s6rp), s6 ribosomal protein (s6rp), phospho-AKT (S473), AKT, Pten, and beta-Actin. All antibodies were purchased from Cell Signaling Technology (Danvers, MA, USA).

Spleen tissue was dissected from mice that had been implanted a rapamycin pellet for 5 weeks. Thymic lymphomas were collected and stored at -80°C. Tissues were minced by blue pestle using M-PER lysis buffer (Pierce) supplemented with protease inhibitor cocktail (Roche), 10µM phenylmethylsulfonyl fluoride, and 1 mM sodium orthovanadate. Protein extract was separated on 10% SDS-PAGE electrophoresis gels. Proteins were transferred to Hybond P membranes (Amersham, Piscataway, NJ). Nonspecific bands were blocked in 5% non-fat milk for 1 hour at room temperature and then in appropriate primary antibody

overnight at 4°C. After incubating with a horseradish peroxidase-linked secondary antibody, proteins were visualized by enhanced chemiluminescence (Amersham). Images were digitally acquired using an HP ScanJet 5200C Scanner and quantified using AlphaEaseFC image analysis software.

Statistical Analysis. Comparison of Pten level, total s6rp and p-s6rp levels in either normal tissues or thymic lymphomas between treatment and genotype groups was carried out by the two-tailed Student's t test or ANOVA. The Kaplan–Meier method was used to compare the tumor development after irradiation of mice between different treatments and genotypes. Statistical analysis was performed using SPSS version 12.0 (SPSS, Chicago, IL).

ACKNOWLEDGEMENTS

We thank Dr. K.I. Nakayama for providing Fbxw7 knockout mice and Dr. Bert Vogelstein for providing HCT116 WT and FBXW7-/- cell lines. This work was supported by the National Institutes of Health, National Cancer Institute grant R01 CA116481, the Low Dose Scientific Focus Area, Office of Biological & Environmental Research, US Department of Energy (DE-AC02-05CH11231), and Laboratory Directed Research & Development Program (LDRD) (to J.H. M.).

Conflict of Interest Statement

No potential conflicts of interest were disclosed.

REFERENCES

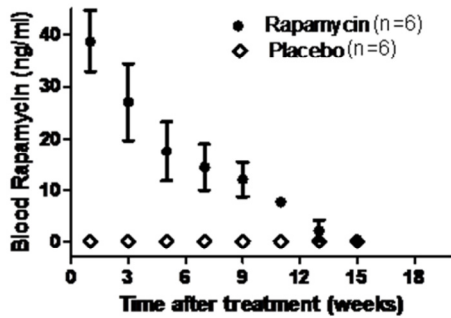
1. Welcker M, Clurman BE. FBW7 ubiquitin ligase: a tumour suppressor at the crossroads of cell division, growth and differentiation. *Nat Rev Cancer*. 2008; 8:83-93.
2. Cheng Y, Li G. Role of the ubiquitin ligase Fbw7 in cancer progression. *Cancer Metastasis Rev*. 2012; 31:75-87.
3. Akhoondi S, Sun D, von der Lehr N, Apostolidou S, Klotz K, Maljukova A, Cepeda D, Fiegl H, Dafou D, Marth C, Mueller-Holzner E, Corcoran M, Dagnell M. FBXW7/hCDC4 is a general tumor suppressor in human cancer. *Cancer Res*. 2007; 67:9006-9012.
4. Welcker M, Orian A, Grim JE, Eisenman RN, Clurman BE. A nucleolar isoform of the Fbw7 ubiquitin ligase regulates c-Myc and cell size. *Curr Biol*. 2004; 14:1852-1857.
5. Yada M, Hatakeyama S, Kamura T, Nishiyama M, Tsunematsu R, Imaki H, Ishida N, Okumura F, Nakayama K, Nakayama KI. Phosphorylation-dependent degradation of c-Myc is mediated by the F-box protein Fbw7. *Embo J*. 2004; 23:2116-2125.
6. Wei W, Jin J, Schlisio S, Harper JW, Kaelin WG Jr. The v-Jun point mutation allows c-Jun to escape GSK3-dependent recognition and destruction by the Fbw7 ubiquitin ligase. *Cancer Cell*. 2005; 8:25-33.

7. Koepp DM, Schaefer LK, Ye X, Keyomarsi K, Chu C, Harper JW, Elledge SJ. Phosphorylation-dependent ubiquitination of cyclin E by the SCFFbw7 ubiquitin ligase. *Science*. 2001; 294:173-177.
8. Rajagopalan H, Jallepalli PV, Rago C, Velculescu VE, Kinzler KW, Vogelstein B, Lengauer C. Inactivation of hCDC4 can cause chromosomal instability. *Nature*. 2004; 428:77-81.
9. Gupta-Rossi N, Le Bail O, Gonen H, Brou C, Logeat F, Six E, Ciechanover A, Israël A. Functional interaction between SEL-10, an F-box protein, and the nuclear form of activated Notch1 receptor. *J Biol Chem*. 2001; 276:34371-34378.
10. Oberg C, Li J, Pauley A, Wolf E, Gurney M, Lendahl U. The Notch intracellular domain is ubiquitinated and negatively regulated by the mammalian Sel-10 homolog. *J Biol Chem*. 2001; 276:35847-35853.
11. Liu N, Li H, Li S, Shen M, Xiao N, Chen Y, Wang Y, Wang W, Wang R, Wang Q, Sun J, Wang P. The Fbw7/human CDC4 tumor suppressor targets proliferative factor KLF5 for ubiquitination and degradation through multiple phosphodegron motifs. *J Biol Chem*. 2010; 285:18858-18867.
12. Zhao D, Zheng HQ, Zhou Z, Chen C. The Fbw7 tumor suppressor targets KLF5 for ubiquitin-mediated degradation and suppresses breast cell proliferation. *Cancer Res*. 2010; 70:4728-4738.
13. Inuzuka H, Shaik S, Onoyama I, Gao D, Tseng A, Maser RS, Zhai B, Wan L, Gutierrez A, Lau AW, Xiao Y, Christie AL, Aster J. SCF(FBW7) regulates cellular apoptosis by targeting MCL1 for ubiquitylation and destruction. *Nature*. 2011; 471:104-109.
14. Wertz IE, Kusam S, Lam C, Okamoto T, Sandoval W, Anderson DJ, Helgason E, Ernst JA, Eby M, Liu J, Belmont LD, Kaminker JS, O'Rourke KM. Sensitivity to antitubulin chemotherapeutics is regulated by MCL1 and FBW7. *Nature*. 2011; 471:110-114.
15. Fujii Y, Yada M, Nishiyama M, Kamura T, Takahashi H, Tsunematsu R, Susaki E, Nakagawa T, Matsumoto A, Nakayama KI. Fbxw7 contributes to tumor suppression by targeting multiple proteins for ubiquitin-dependent degradation. *Cancer Sci*. 2006; 97:729-736.
16. Kwon YW, Kim IJ, Wu D, Lu J, Stock WA Jr, Liu Y, Huang Y, Kang HC, DelRosario R, Jen KY, Perez-Losada J, Wei G, Balmain A, Mao JH. Pten regulates aurora-a and cooperates with fbxw7 in modulating radiation-induced tumor development. *Mol Cancer Res*. 2012; 10:834-844.
17. Mao JH, Perez-Losada J, Wu D, Delrosario R, Tsunematsu R, Nakayama KI, Brown K, Bryson S, Balmain A. Fbxw7/Cdc4 is a p53-dependent, haploinsufficient tumour suppressor gene. *Nature*. 2004; 432:775-779.
18. Kemp Z, Rowan A, Chambers W, Wortham N, Halford S, Sieber O, Mortensen N, von Herbay A, Gunther T, Ilyas M, Tomlinson I. CDC4 mutations occur in a subset of colorectal cancers but are not predicted to cause loss of function and are not associated with chromosomal instability. *Cancer Res*. 2005; 65:11361-11366.
19. Balamurugan K, Wang JM, Tsai HH, Sharan S, Anver M, Leighty R, Sterneck E. The tumour suppressor C/EBPdelta inhibits FBXW7 expression and promotes mammary tumour metastasis. *Embo J*. 2010; 29:4106-4117.
20. Fu L, Kim YA, Wang X, Wu X, Yue P, Lonial S, Khuri FR, Sun SY. Perifosine inhibits mammalian target of rapamycin signaling through facilitating degradation of major components in the mTOR axis and induces autophagy. *Cancer Res*. 2009; 69:8967-8976.
21. Mao JH, Kim IJ, Wu D, Climent J, Kang HC, DelRosario R, Balmain A. FBXW7 targets mTOR for degradation and cooperates with PTEN in tumor suppression. *Science*. 2008; 321:1499-1502.
22. Beauchamp EM, Platanias LC. The evolution of the TOR pathway and its role in cancer. *Oncogene*. 2012; doi: 10.1038/onc.2012.567. [Epub ahead of print]
23. Leontieva OV, Blagosklonny MV. DNA damaging agents and p53 do not cause senescence in quiescent cells, while consecutive re-activation of mTOR is associated with conversion to senescence. *Aging (Albany NY)*. 2010; 2:924-35.
24. Korotchkina LG, Leontieva OV, Bukreeva EI, Demidenko ZN, Gudkov AV, Blagosklonny MV. The choice between p53-induced senescence and quiescence is determined in part by the mTOR pathway. *Aging (Albany NY)*. 2010; 2:344-52.
25. Demidenko ZN, Korotchkina LG, Gudkov AV, Blagosklonny MV. Paradoxical suppression of cellular senescence by p53. *Proc Natl Acad Sci U S A*. 2010; 107: 9660-4.
26. Suman S, Johnson MD, Fornace AJ Jr, Datta K. Exposure to ionizing radiation causes long-term increase in serum estradiol and activation of PI3K-Akt signaling pathway in mouse mammary gland. *Int J Radiat Oncol Biol Phys*. 2012; 84:500-7.
27. Komarova EA, Antoch MP, Novototskaya LR, Chernova OB, Paszkiewicz G, Leontieva OV, Blagosklonny MV, Gudkov AV. Rapamycin extends lifespan and delays tumorigenesis in heterozygous p53+/- mice. *Aging (Albany NY)*. 2012; 4:709-14.
28. Mercier I, Camacho J, Titchen K, Gonzales DM, Quann K, Bryant KG, Molchansky A, Milliman JN, Whitaker-Menezes D, Sotgia F, Jasmin JF, Schwarting R, Pestell RG, Blagosklonny MV, Lisanti MP. Caveolin-1 and accelerated host aging in the breast tumor microenvironment: chemoprevention with rapamycin, an mTOR inhibitor and anti-aging drug. *Am J Pathol*. 2012; 181: 278-93.
29. Blagosklonny MV. Rapalogs in cancer prevention: Anti-aging or anticancer? *Cancer Biol Ther*. 2012; 13:1349-54.

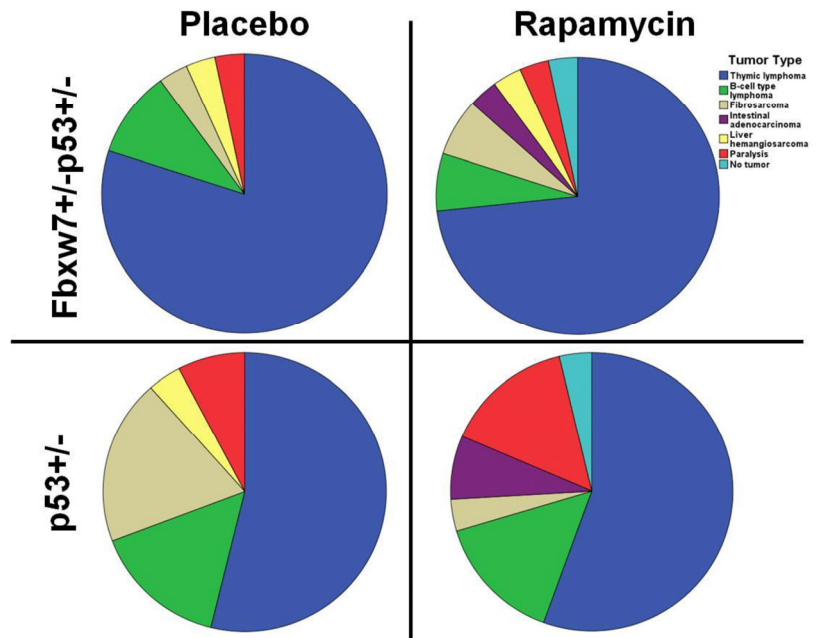
SUPPLEMENTARY DATA

Supplementary Table S1. Number of mice in different genotype and treatment groups

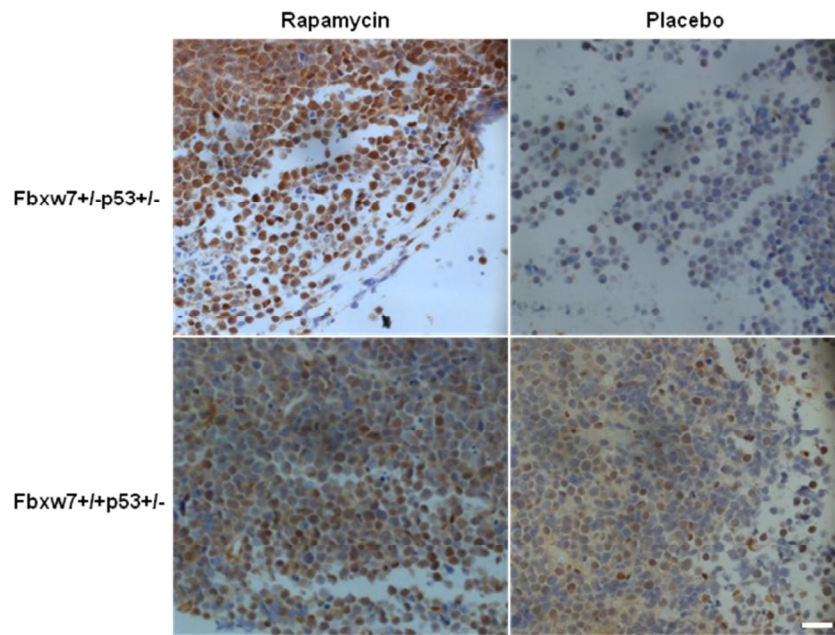
Genotype	Treatment group	Gender		Total
		Male	Female	
p53+/-Fbxw7+/-	Rapamycin	15	15	30
	Placebo	15	15	30
p53+/-Fbxw7+/+	Rapamycin	14	15	29
	Placebo	14	14	28



Supplementary Figure S1. Rapamycin levels in blood were measured by liquid chromatography-tandem mass spectrometry (LC/MS/MS) at different time points after rapamycin pellet implantation.



Supplementary Figure S2. Tumor spectrum in placebo or rapamycin treated Fbxw7+/- p53+/- or p53+/- mice.



Supplementary Figure S3. Immunohistochemical staining of Pten in tumor from placebo or rapamycin treated Fbxw7^{+/-} p53^{+/-} mice.

Rapamycin extends life span of $Rb1^{+/-}$ mice by inhibiting neuroendocrine tumors

Carolina B. Livi^{1,7,8}, Rulon L. Hardman², Barbara A. Christy^{1,7,8}, Sherry G. Dodds¹, Diane Jones¹, Charna Williams¹, Randy Strong^{4,7,8,9}, Alex Bokov⁶, Martin A. Javors^{3,7}, Yuji Ikono^{3,7,9}, Gene Hubbard^{3,7}, Paul Hasty^{1,7,8}, and Zelton Dave Sharp^{1,7,8}

¹ Department of Molecular Medicine and Institute of Biotechnology, University of Texas Health Science Center, San Antonio, TX 78229

² Department of Radiology, University of Texas Health Science Center, San Antonio, TX 78229;

³ Department of Pathology, University of Texas Health Science Center, San Antonio, TX 78229;

⁴ Department of Pharmacology, University of Texas Health Science Center, San Antonio, TX 78229;

⁵ Department of Epidemiology & Biostatistics, University of Texas Health Science Center, San Antonio, TX 78229;

⁶ Department of Psychiatry, University of Texas Health Science Center, San Antonio, TX 78229;

⁷ Barshop Institute for Longevity and Aging Studies, University of Texas Health Science Center, San Antonio, TX 78245

⁸ Cancer Therapy and Research Center, University of Texas Health Science Center, San Antonio, TX 78229

⁹ Geriatric Research, Education and Clinical Center, Research Service, South Texas Veterans Health Care System, San Antonio, TX 78229

Key words: mTOR; rapamycin; $Rb1$; neuroendocrine tumors

Received: 1/7/12; **Accepted:** 2/21/13; **Published:** 2/23/13

Correspondence to: Zelton Dave Sharp, PhD; **E-mail:** sharp@uthscsa.edu

Copyright: © Livi et al. This is an open-access article distributed under the terms of the Creative Commons Attribution License, which permits unrestricted use, distribution, and reproduction in any medium, provided the original author and source are credited

Abstract: Chronic treatment of mice with an enterically released formulation of rapamycin (eRapa) extends median and maximum life span, partly by attenuating cancer. The mechanistic basis of this response is not known. To gain a better understanding of these *in vivo* effects, we used a defined preclinical model of neuroendocrine cancer, $Rb1^{+/-}$ mice. Previous results showed that diet restriction (DR) had minimal or no effect on the lifespan of $Rb1^{+/-}$ mice, suggesting that the beneficial response to DR is dependent on pRb1. Since long-term eRapa treatment may at least partially mimic chronic DR in lifespan extension, we predicted that it would have a minimal effect in $Rb1^{+/-}$ mice. Beginning at 9 weeks of age until death, we fed $Rb1^{+/-}$ mice a diet without or with eRapa at 14 mg/kg food, which results in an approximate dose of 2.24 mg/kg body weight per day, and yielded rapamycin blood levels of about 4 ng/ml. Surprisingly, we found that eRapa dramatically extended life span of both female and male $Rb1^{+/-}$ mice, and slowed the appearance and growth of pituitary and decreased the incidence of thyroid tumors commonly observed in these mice. In this model, eRapa appears to act differently than DR, suggesting diverse mechanisms of action on survival and anti-tumor effects. In particular the beneficial effects of rapamycin did not depend on the dose of $Rb1$.

INTRODUCTION

Age is by far the biggest independent risk factor for a wide range of intrinsic diseases [1], including most types of cancer [2]. The age-adjusted cancer mortality rate for persons over 65 years of age is 15-times greater

than for younger individuals [3]. Numerous studies demonstrate that age retarding interventions reduce cancer by decreasing incidence and/or severity (Reviewed in [4]). Diet restriction (DR) has a long history of retarding cancer [5] and most of the other

age-associated diseases [6], consistent with life span extension in a wide range of organisms [7]. Genetic interventions resulting in pituitary dwarfism in mice, which causes growth factor reduction (GFR) and a reduction in associated signaling, also result in maximum lifespan extension [8], with a concomitant reduction in cancer severity [9, 10]. Thus, factors that inhibit growth appear to extend life span and reduce cancer.

mTORC1 (mechanistic Target of Rapamycin Complex 1) is central to cell growth by integrating upstream signals that include nutrients, growth factors and energy levels with stress responses for regulated cell growth. Thus, chronic mTORC1 inhibition could act similarly to DR and GFR. Supporting this possibility, the mTOR inhibitor rapamycin, increases life span in a variety of organisms including yeast [11], nematodes [12] and flies [13]. Using a chow containing a novel formulation of enterically delivered rapamycin (eRapa [14]), the NIA Intervention Testing Program [15] reported that long-term treatment extends both median and maximum lifespan of genetically heterogeneous mice (UM-HET3), even when started in late adulthood (20 months of age) [16], or at 9 months of age [17]. eRapa is the first drug reported to be capable of extending both median and maximum lifespan.

One explanation for the lifespan enhancement by eRapa is that chronic mTOR inhibition delays the onset and growth of neoplasms. Indeed, chronic eRapa (2.24 mg/kg/day diet) treatment reduced the incidence of lymphoma and hemangiosarcoma (two major cancers in the genetically heterogeneous mice studied by the ITP), and increased the mean age at death due to liver, lung and mammary tumors [16, 17]. Alternate possibilities are that the immune systems of treated mice better defend against their cancers or that the mice simply tolerate them longer. What is the basis of eRapa's ability to reduce cancer, and how does it compare to DR?

To gain an understanding of how chronic eRapa treatment compares with DR and affects cancer development, growth and progression, we used a mouse model deficient in the prototypical tumor suppressor,

Rb1. Rb1 regulates cell cycle checkpoints for differentiation and in response to stress and is important for genome maintenance [18]. *Rb1*^{+/-} mice are highly predisposed to cancers of neuroendocrine origin [19] including pituitary (intermediate and anterior lobe), thyroid C-cell (which can metastasize to lung), and adrenal. Tumorigenic cells form after losing the remaining functional copy of the Rb1 tumor suppressor gene. The complete penetrance of tumor formation, growth and progression results in a short lifespan for *Rb1*^{+/-} mice, which, unlike wild type mice, is minimally affected by diet restriction [20]. If eRapa acts in a similar manner to DR [16], we predicted that chronic eRapa treatment of *Rb1*^{+/-} mice would also have minimal effects on tumor development, growth, progression and life span. Surprisingly we find that eRapa treatment has a dramatic and positive effect on life span in both sexes of *Rb1*^{+/-} mice, which is associated with slower tumor development and growth.

RESULTS

To address the question of whether eRapa mimics DR in mice deficient for a prototypical tumor suppressor gene function, we initiated chronic treatment by feeding randomly grouped males and females chow that included either eRapa at the concentration previously shown to extend life span (14 mg/kg food), [16, 17] or Eudragit (empty capsule control). Treatment was begun at approximately 9 weeks of age (>80% of animals started between 8-10 weeks (minimum at 7 weeks and maximum at 12 weeks, Table S1). Mice continued on these diets for the remainder of their lives. Based on the average amount of chow consumed per day, this delivers an approximate rapamycin dose of 2.24 mg/kg body weight/day [16]. Blood levels of rapamycin (determined by a mass spectrometry) averaged 3.9 ng/ml for males, 3.8 ng/ml for females for *Rb1*^{+/-} mice and 3.4 for males and 4.6 ng/ml for females for *Rb1*^{+/+} mice (Figure S1). Hematocrits were performed on blood from *Rb1*^{+/+} mice between 18 and 24 months of age and readings indicated normal values for mice (between 40 and 49%), indicating that long-term eRapa treatment does not adversely effect red blood cell production (data not included).

Table 1. eRapa effects on survival of <i>Rb1</i> ^{+/-} mice					
	Coefficient	Hazard Ratio	SE	z	P
eRapa	-1.3177	0.2678	0.2400	-5.4909	0.00000004
Sex	0.1693	1.1844	0.2144	0.8005	0.42344718

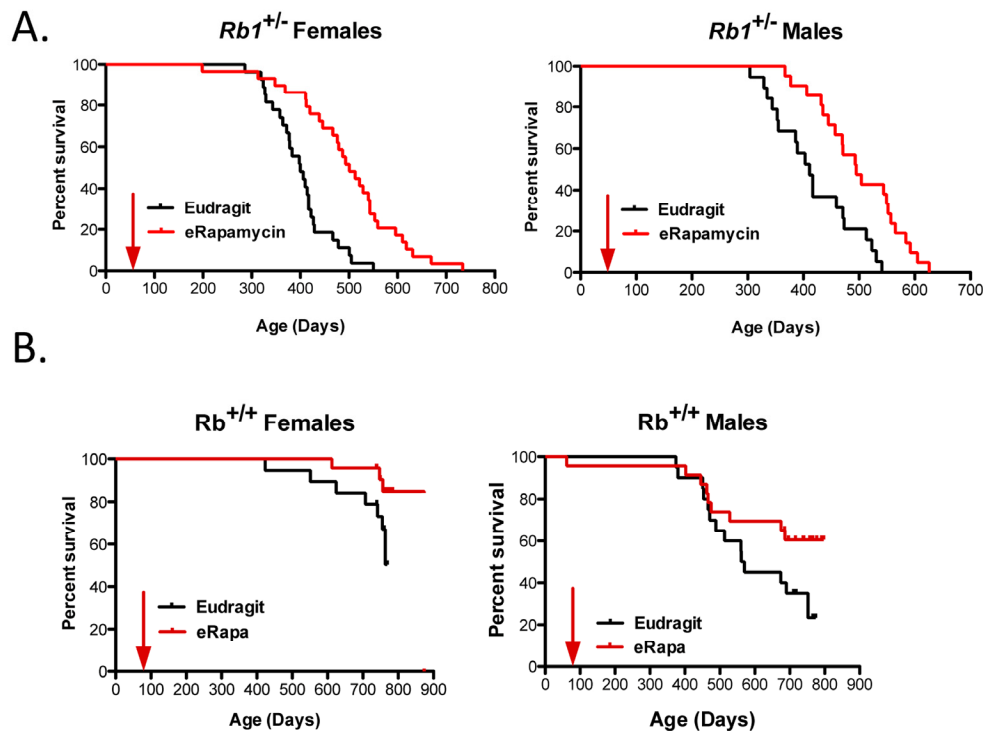


Figure 1. Survival plots for male and female $Rb1^{+/-}$ (A) and $Rb1^{+/+}$ (B) mice, comparing control-fed mice to those fed eRapa in the diet starting at approximately 9 weeks of age (indicated by arrow). Control (black line) and eRapa (red line) survival curves are shown. The horizontal axes represent life span in days and the vertical axes represent survivorship. $Rb1^{+/-}$ mice obtained from the NCI Mouse Repository were bred by the Nathan Shock animal core to obtain the cohorts of male and female mice used in this study. Genotype was confirmed as previously described [20]. eRapa mice were fed microencapsulated rapamycin-containing food (14mg/kg food designed to deliver approximately 2.24mg of rapamycin per kg body weight/day that achieved about 4 ng/ml blood [14]. Diets were prepared by TestDiet, Inc., Richmond, IN using Purina 5LG6 as the base [14]. Control diet was the same but with empty capsules. P values in (B) were calculated by the log-rank test.

eRapa extended life span of $Rb1^{+/-}$ mice

Unlike most mouse models of cancer [5], 50% DR had little (if any) effect on the development, growth and progression of neuroendocrine tumors or on life span of $Rb1^{+/-}$ mice [20]. Since rapamycin has been predicted to act in a similar way to DR [16], we investigated if eRapa would also have little effect in this model. In stark contrast to DR, Figure 1A shows that $Rb1^{+/-}$ males and females derive a significant longevity benefit from chronic treatment with eRapa. The Eudragit control-fed mice had a shorter mean life span than the eRapa-fed cohort for both females (377.5 versus 411 days) and males (mean age is 368.8 versus 419.8 days). Sex did

not modulate the effect of eRapa on $Rb1^{+/-}$ animals (Table 1).

Male and female $Rb1^{+/+}$ littermates of the $Rb1^{+/-}$ mice were also fed eRapa or control diets to ensure that this particular mutant strain (with a C57BL/6 background) is responsive to rapamycin. Once all $Rb1^{+/-}$ mice had died and the effects of eRapa were evident, the $Rb1^{+/+}$ littermates were euthanized. At this time, as expected, eRapa improved survival for both male and female $Rb1^{+/+}$ mice as well (Fig. 1B). Similar to the previous results from the Intervention Testing Program eRapa experiments [16, 17], lifespan was extended more in females than in males (Table 2) in wild type (WT) littermates.

	Coefficient	Hazard Ratio	SE	z	P
eRapa	-0.9305	0.3943	0.3631	-2.5625	0.01039082
Sex	-1.2818	0.2775	0.3840	-3.3382	0.00084312

	Eudragit	eRapa
Tumor Incidence		
Pituitary	97.5% (40)	100% ^a (39)
Thyroid	90.0% (40)	66.7% ^b (39)
Thyroid with lung metastases	37.5% (40)	28.2% ^c (39)
Thyroid with adrenal metastases	2.5% (40)	7.7% ^d (39)
Adrenal	30.0% (40)	23.1% ^e (39)

a, p = 0.9858, b, p = 0.0112; c, p = 0.3859; d, p = 0.5472, e, p = 0.4925
Two tailed, unpaired t test, GraphPad Prism.

eRapa effects on tumor incidence at the end of life

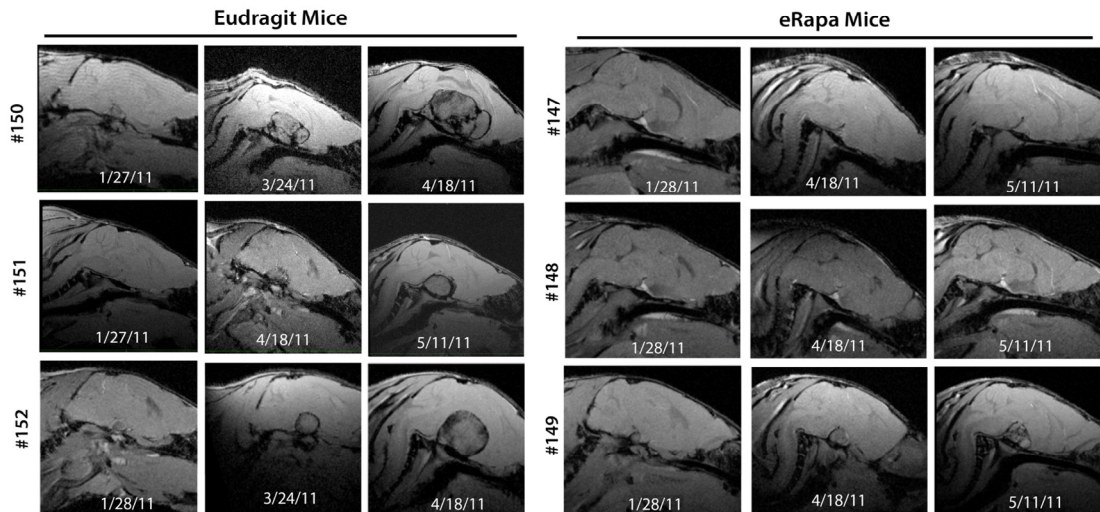
At necropsy, *Rb1*^{+/-} mice were evaluated for the presence of neuroendocrine tumors and lung metastases. As shown in Table 3, there were no differences in the eRapa and Eudragit control groups in terms of presence of pituitary tumors (although we did observe a delay in their detection and reduction in size by magnetic resonance imaging (MRI), discussed below). We did observe a decreased incidence of thyroid C-cell carcinomas in the eRapa treated group of *Rb1*^{+/-} mice (p = 0.0112). Except for the modest decrease in thyroid tumors, this tumor spectrum is similar to *Rb1* heterozygotes treated with DR compared to those fed *ad libitum* [20]. Along with the decrease in thyroid C-cell tumors, eRapa also tended to reduce the incidence and severity of C-cell lung metastases (Table 4). Thus mice have a decreased cancer burden and live with tumors longer.

eRapa delayed tumor development and slowed growth

Is delayed and/or reduced tumor growth the basis of life span extension by eRapa in this model? To address this question, we took advantage of the synchronous (spatial and temporal) development of tumors in this model Nikitin et al. [19, 21]. *Rb1*-deficient cells are first identified as atypical proliferates in the intermediate and

anterior lobes of the pituitary, thyroid and parathyroid glands and the adrenal medulla at about 12 weeks of postnatal development. Atypical proliferates eventually form gross tumors with varying degrees of malignancy by postnatal day 350. Since we started treatment at around 8 weeks of age, eRapa might have an effect on the initiating events leading to loss of heterozygosity and/or subsequent formation of atypically proliferating cells. Perhaps more likely, eRapa slows growth and development of proliferates to gross tumors, which had probably begun at or around the time treatment was started. To test this latter possibility, we used MRI to follow pituitary and thyroid tumor development and growth in a subset of eRapa-treated *Rb1*^{+/-} mice (8 mice per treatment group were imaged between 1 and 4 times up to twice a month). MRI is well suited for following head and neck tumors that correspond to the primary tumor types *Rb1*^{+/-} mice develop. An initial cohort was used to identify the best timeframe for MRI scans. For this, 6 female *Rb1*^{+/-} mice (3 per group) and 10 *Rb1*^{+/-} mice (3 per group in males and 2 per group in females) were imaged in a single session or with 2 serial scans. This study indicated the ideal timeframe to image pituitary tumors was a window between 9 and 12 months of age, which covers the time from initial detection through monitoring tumor growth.

A.



B.

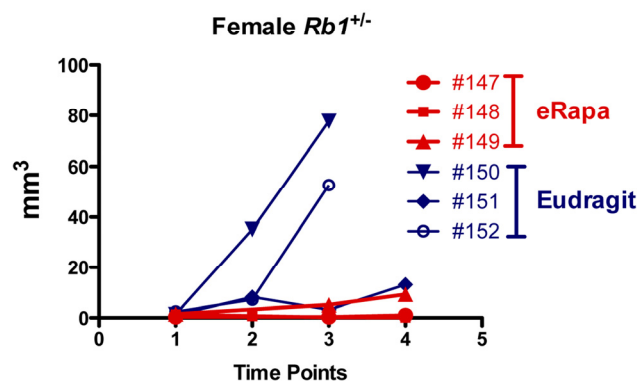


Figure 2. Effects of eRapa on pituitary and thyroid tumor development and growth. To identify effects on tumors, we used MRI as a non-invasive method to longitudinally monitor individual $Rb^{+/-}$ mice. High-resolution images were obtained on a very high field strength Bruker Pharmascan 7.0T animal MRI scanner using a coil to focus on pituitary and thyroid tumors. Images were acquired using a spoiled gradient echo named Fast low angle shot MRI (FLASH) on the scanner. Images were acquired to yield predominantly T1 weighted contrast with TE (echo time) 4.5 msec, TR (repetition time) 450 msec, FA (Flip angle) 40 degrees, FOV (field of view) 20 x 20 mm, in plane spatial resolution 0.078 x 0.078 mm. Tumor volume was determined for each time point. (A) Serially acquired MRI images from eRapa and Eudragit-fed control mice at 9, 11 and 12 months of age. (B) Tumor volumes calculated from MRI image stacks at each time point comparing individual mice at multiple ages. Tumors in two of the Eudragit-fed (control) mice are detected earlier and grow faster than the 3 eRapa-fed mice.

Age matched $Rb1^{+/-}$ females (3 per group) were scanned using MRI at 9, 11 and 12 months of age (Figure 2A shows sagittal plane sections of the serially acquired MRI images through the pituitary of eRapa and Eudragit treated mice). Calculated volumes based on the MRI image stacks (analyzed blind by a single radiologist, RLH) were plotted versus age at the date of

imaging. In concert with extended longevity, the detection of pituitary tumors was delayed with a decrease in their growth in the eRapa-treated mice. Figure 2B shows that eRapa delayed development and/or reduced tumor growth at each time point when mice were imaged. More $Rb1^{+/-}$ mice had detectable tumors identified during two separate MRI imaging

sessions from the Eudragit control cohort (4 pituitary and 2 thyroid tumors out of 8 mice in March 2011 scan and 7 pituitary and 4 thyroid tumors out of 8 mice in April 2011 scan) compared to the mice eRapa-fed cohort (1 pituitary and 0 thyroid tumors out of 8 mice in March

2011 scan and 2 pituitary and 3 thyroid tumors out of 8 mice in April 2011 scan). Longitudinal monitoring allowed us to conclude that chronic rapamycin delays both the development of visible tumors and inhibited the growth of tumors once they were present.

Table 4. Incidence and pathology of <i>Rb1</i> ^{+/-} lung metastases				
Grade	Eudragit		eRapa	
	Males	Females	Males	Females
0	6	6	5	11
1	1	1	1	3
2	3	7	1	2
3	1	1	1	2
4	0	1	0	0
Total (Gr 1-4)	5	10	4	7

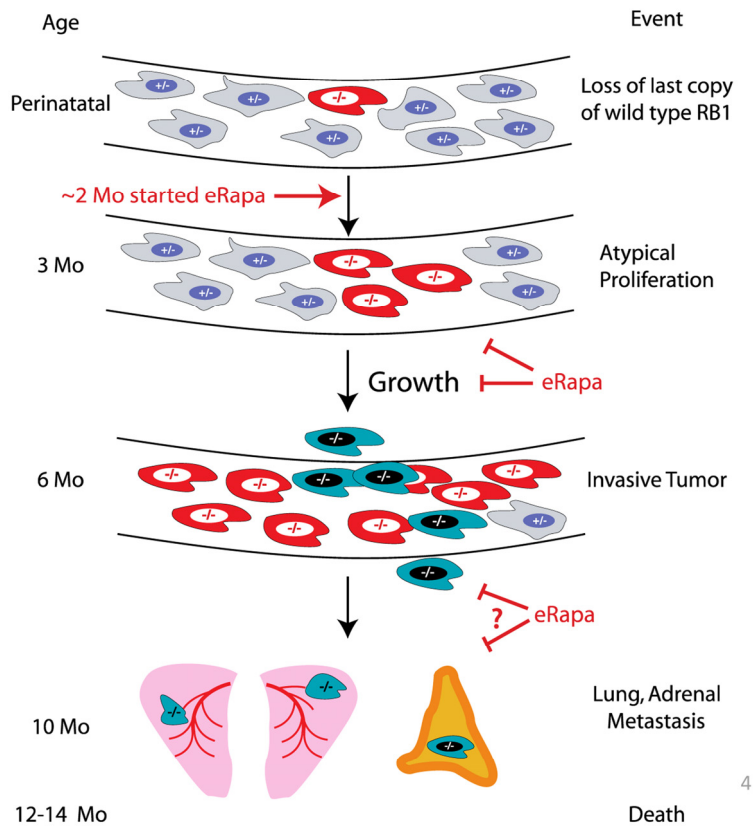


Figure 3. Summary of eRapa effects in the *Rb1*^{+/-} model of neuroendocrine tumorigenesis. Our MRI data are consistent with a delay of tumor development perhaps by inhibition of atypical proliferates and reduction in tumor growth. eRapa may inhibit lung metastasis and slow their growth.

DISCUSSION

In mice, pRb1 is critical for DR-mediated lifespan extension [20], but not rapamycin-mediated life span extension. It is unclear why this is the case, since both of these interventions chronically inhibit mTORC1 [22]. However, differences in the downstream *in vivo* effects of DR and rapamycin have been previously reported [22]. As previously described by Harrison et al. [16], a distinguishing feature of eRapa is its ability to extend median and maximum life when the intervention starts at a relatively old age (600 days) in mice. By comparison, DR in most [23] but not all [24] reports shows little if any longevity benefit when started after 550 days of age (equivalent to 60 human years). DR started at 6 weeks of age reduced body growth for *Rb1*^{+/-} mice but did not affect growth of *Rb1*^{+/-} tumors [20]. In contrast to DR, chronic eRapa treatment did not affect body weight of *Rb1*^{+/-} mice (Livi et al., in preparation), but did reduce tumor growth. Previous studies in fruit flies show that rapamycin extends life span through a mechanism that is at least partly independent of TOR [13]. Consistent with those results, we find that eRapa, but not DR, extended life span and reduced the growth of neuroendocrine tumors in the *Rb1*^{+/-} model. It will be interesting to determine if pRb1 might be at least partially involved in those settings where responses to chronic eRapa and DR diverge.

Based on the longitudinal imaging data acquired by MRI (Figure 2), eRapa appears to inhibit *Rb1*^{+/-} pituitary tumor development and growth in *Rb1*^{+/-} mice (summarized in Figure 3), which is likely a major factor in its ability to extend lifespan in this model. Since we started eRapa at between 2 and 3 months of age, it would be interesting to know if it affects loss of heterozygosity (LOH) (Figure 3) in neuroendocrine tissues. The significant reduction in the incidence of thyroid C-cell carcinoma at necropsy in eRapa treated *Rb1*^{+/-} mice (Table 3) also likely contributes to extended longevity. We also observed an apparent lessening of severity in lung metastases (Table 4), but this may be due to overall reduction of C-cell carcinomas. Metastasis of these to tumors to the adrenal (Table 3) has, to our knowledge, not been previously reported. A recent report linked an increase in metastasis with RAD001 treatment in a rat model of transplanted neuroendocrine tumors, which the authors attributed to alternations in tissue immune microenvironment [25]. Since RAD001 treatment was started subsequent to tumor implantation, it might be interesting to test this model in a prevention rather than treatment setting.

Two reports have linked pRb1 and mTOR. A genetic study in *D. melanogaster* established synergy between

deletion of mTOR and pRb1 using an *in vivo* synthetic lethality screen of *Rb*-negative cells [26]. These authors found that inactivation of *gig* (fly TSC2) and *rbf* (fly Rb) is synergistically responsible for oxidative stress leading to lethality. In a separate study, El-Naggar et al., [27] found that loss of the *Rb1* family (Rb1, Rb11 and Rb12) in primary cells derived from triple-knockout mice led to overexpression of mTOR and constitutive phosphorylation of Ser473 on Akt, which is oncogenic. The inhibition of tumor development and growth in *Rb1*^{+/-} mice by eRapa is also consistent with a recent report showing that mTOR inhibition partially alleviated tumor development in an *Rb*^{F/F};K14creERTM; *p107*^{+/-} model of squamous cell carcinoma [28], and with several reports demonstrating the effectiveness of rapamycin in mouse cancer models for tumor reduction and life span extension [29-31]. Potential mechanism may be by way of indirect effects or rapamycin on the tumor microenvironment [32] and/or senescent cells [33].

The reduction in lung metastases is consistent with ribosome profiling that revealed transcript-specific translational control mediated by oncogenic mTOR signaling, including a distinct set of pro-invasion and metastasis genes [34]. It will be interesting to determine whether chronic eRapa treatment affects these genes in thyroid C-cell neoplasms. We also observed metastasis of thyroid tumors to adrenal glands, albeit at a low frequency but eRapa treatment did not effect.

Neuroendocrine tumors are unique in their ability to secrete hormones or deleterious bioactive products [35]. It was previously reported that the rapalog Everolimus (RAD-001) in combination with ocreotide lanreotide (compared to placebo) improved the clinical picture of carcinoid patients by reducing circulating chromogranin A and 5-hydroxyindoleacetic acid, two tumor-secreted bioactive products responsible for some of the symptoms [36]. Thus, another potential mechanism for life span extension in *Rb1*^{+/-} mice by eRapa could be due the prevention of the production and/or secretion of hormones or deleterious bioactive factors.

Rb1 is known to have an important role in somatic growth regulation, since increased *RB1* dose reduced animal size [37]. Determining if there is a link between *Rb1* (a negative regulator of growth) and mTORC1 (a positive regulator of growth) in growth of tumors could suggest new therapeutic and prevention targets for drug development. One prediction is that mice over expressing pRb1 will have decreased mTOR activity and be long lived through prevention, delay or a reduction in severity of age-related diseases.

Here we show that eRapa extends the life span for *Rbl^{+/+}* mice. We find eRapa-fed mice exhibit a delay in the onset and/or progression of neuroendocrine tumors. These results are in direct contrast with DR. Thus, mTORC1 inhibition and DR likely use different modes for life span extension.

METHODS

Mice and life span. Mice (strain B6.129S2(Cg)-*Rbl^{tm1Tyj}*) for breeding were obtained from the NCI MMHCC Repository. Although they have similar phenotypes, the strain used in the diet restriction study by Sharp et al., [20] was different having been generated by Lee et al [38]. The procedures and experiments involving use of mice were approved by the Institutional Animal Care and Use Committee and are consistent with the NIH Principles for the Utilization and Care of Vertebrate Animals Used in Testing, Research and Education, the Guide for the Care and Use of Laboratory Animals and the Animal Welfare Act (National Academy Press, Washington, DC). Genotyping was done as described previously [20]. Cohorts of mice were fed microencapsulated rapamycin-containing food (14 mg/kg food designed to deliver ~2.24 mg of rapamycin per kg body weight/day to achieve about 4 ng/ml of rapamycin per kg body weight/day) prepared by TestDiet, Inc., Richmond, IN using Purina 5LG6 as the base [14]. Control diet was the same but with empty capsules.

Rapamycin food concentration. Rapamycin was quantified in food using HPLC with tandem mass spectrometry detection. Briefly, 100 mg of food for spiked calibrators and unknown samples were crushed with a mortar and pestle, then vortexed vigorously with 10 μ L of 250 μ g/mL ASCO (internal standard) and 4.0 ml of mobile phase A. The samples were then mechanically shaken for 10 min, centrifuged for 10 min, and then centrifuged in microfilterfuge tubes for 1 minute. Ten μ L of the final extracts was injected into the LC/MS/MS. The ratio of the peak area of rapamycin to that of the internal standard (response ratio) was compared against a linear regression of calibrator response ratios at rapamycin concentrations of 0, 2, 5, 10, 30, and 60 ng/mg of food to quantify rapamycin. The concentration of rapamycin in food was expressed as ng/mg food (parts per million).

Rapamycin blood measurements. Measurement of rapamycin used HPLC-tandem MS. RAPA and Ascomycin (ASCO) were obtained from LC Laboratories (Woburn, MA). HPLC grade methanol and acetonitrile were purchased from Fisher (Fair Lawn, NJ). All other reagents were purchased from Sigma

Chemical Company (St. Louis, MO). Milli-Q water was used for preparation of all solutions. RAPA and ASCO super stock solutions were prepared in methanol at a concentration of 1 mg/ml and stored in aliquots at -80°C. A working stock solution prepared each day from the super stock solutions at a concentration of 10 μ g/ml was used to spike the calibrators.

Calibrator and unknown whole blood samples (100 μ L) were mixed with 10 μ L of 0.5 μ g/mL ASCO (internal standard), and 300 μ L of a solution containing 0.1% formic acid and 10 mM ammonium formate dissolved in 95% HPLC grade methanol. The samples were vortexed vigorously for 2 min, and then centrifuged at 15,000 g for 5 min at 23°C (subsequent centrifugations were performed under the same conditions). Supernatants were transferred to 1.5 ml microfilterfuge tubes and centrifuged at 15,000 g for 1 min and then 40 μ L of the final extracts were injected into the LC/MS/MS. The ratio of the peak area of rapamycin to that of the internal standard ASCO (response ratio) for each unknown sample was compared against a linear regression of calibrator response ratios at 0, 1.25, 3.13, 6.25, 12.5, 50, and 100 ng/ml to quantify rapamycin.

The HPLC system consisted of a Shimadzu SCL-10A Controller, LC-10AD pump with a FCV-10AL mixing chamber (quaternary gradient), SIL-10AD autosampler, and an AB Sciex API 3200 tandem mass spectrometer with turbo ion spray. The analytical column was a Grace Alltima C18 (4.6 x 150 mm, 5 μ) purchased from Alltech (Deerfield, IL) and was maintained at 60°C during the chromatographic runs using a Shimadzu CTO-10A column oven. Mobile phase A contained 10 mM ammonium formate and 0.1% formic acid dissolved in HPLC grade methanol. Mobile phase B contained 10 mM ammonium formate and 0.1% formic acid dissolved in 90% HPLC grade methanol. The flow rate of the mobile phase was 0.5 ml/min. Rapamycin was eluted with a step gradient. The column was equilibrated with 100% mobile phase B. At 6.10 minutes after injection, the system was switched to 100% mobile phase A. Finally, at 15.1 min, the system was switched back to 100% mobile phase B in preparation for the next injection. The rapamycin transition was detected at 931.6 Da (precursor ion) and the daughter ion was detected at 864.5 Da. ASCO was detected at 809.574 Da and the daughter ion was 756.34 Da.

Survival Analysis Methods. An entry for each mouse in the study was created in a database used by the Nathan Shock Animal core. The age at which each animal died was recorded. Survival durations for animals that either lived past the end-date of the study, were terminated, or

died accidentally were treated as right-censored events. Cox proportional hazard models [39] were fitted to the wild type and *Rbl*^{+/-} subsets of the data, with eRapa and gender as additive predictor variables. Some animals were transferred to a different facility part-way through their life spans so the final facility at which they were housed was also added to the Cox models, as a stratifying variable. The R statistical language was used for the analysis [40, 41]. The mice in the life span studies were allowed to live out their life span, i.e., there was no censoring due to morbidity in the groups of mice used to measure lifespan of *Rbl*^{+/-} mice. Mice were euthanized only if they were either (1) unable to eat or drink, (2) bleeding from a tumor or other condition, or (3) when they were laterally recumbent, i.e., they fail to move when prodded or are unable to right themselves.

MRI Methods. Images were acquired on a Bruker Pharmascan 7.0T MRI scanner. Images were obtained in the sagittal plane through the brain and coronal plain through the neck (focused on the thyroid gland) using 2D spoiled gradient echo technique to quickly obtain high-resolution images (fast low angle shot magnetic resonance imaging - FLASH on our scanner). FLASH protocol was TE/TR 5 msec/450msec, Averages 1, Flip angle 40 deg, Field of view 20 mm x 20 mm, matrix size 256x256, In plane resolution was 0.078 x 0.078 mm, slice thickness 0.5 mm. The FLASH sequence shows predominantly T1 weighted image contrast. A single blinded radiologist (RLH) evaluated images for the presence and tumor volume used to plot detection and growth data. Images were analyzed using an open source image processing software, OsiriX, version 2.7.5. The pituitary gland was identified on all images and volume was calculated by measuring the greatest anterior-posterior, cranial-caudal, and right-left length. Volumes were then determined using prolate ellipse formula. Data were then parsed by treatment group and plotted in Prism (GraphPad).

Procedures for examination of pathology in mice. Fixed tissues (in 10% neutralized formalin) were embedded in paraffin, sectioned at 5 μ m, and stained with hematoxylin-eosin. Diagnosis of each histopathological change was made using histological classifications for aging mice as previously described [9, 20, 42, 43].

Pathology assessments. A list of lesions was compiled for each mouse. The severity of neoplastic lesions was assessed using the grading system previously described [9, 20, 42, 43]. Two pathologists separately examined all of the samples without knowledge of their genotype or age. Briefly, lung pathology grade is based on the area of the lung section infiltrated by metastatic tumor

tissue with 0 being no tumor cells observed and 4 being the largest area taken by tumor.

ACKNOWLEDGEMENTS

The authors gratefully acknowledge Gregory Friesenhahn for rapamycin blood level measurements, Jesse Usrey and Dr. Michael Duff Davis for technical assistance with MRI imaging. Viviane Diaz and the Nathan Shock Animal Core staff provided expert care for our mice. This work was supported by the following funding agencies: NIH (ISG 1RC2AG036613-01, Project 1, ZDS and PH; 2P01AG017242-12, PH; AG13319, YI; UL1RR025767, CTSA, Technology Transfer Resource to ZDS and CBL supported MRI imaging costs associated with this study), The Glenn Foundation for Medical Research (ZDS and YI), Department of Veteran Affairs (VA Merit Review Grant, YI). We would also like to thank the Cancer Therapy Research Center (CA054174), the NCRR (UL 1RR025767) and the RCMI (G12MD007591) for additional support.

Conflict of Interest Statement

ZDS and RS were unpaid consultants to Rapamycin Holdings, Inc. Other authors declare no conflicts.

REFERENCES

1. Kirkwood TB. Gerontology: Healthy old age. *Nature*. 2008; 455:739-740.
2. Blagosklonny MV, Campisi J. Cancer and aging: more puzzles, more promises? *Cell Cycle*. 2008; 7:2615-2618.
3. Altekruse SF, Kosary CL, Krapcho M, Neyman N, Aminou R, Waldron W, et al. SEER Cancer Statistics Review 1975-2007 Bethesda, MD: National Cancer Institute; 2010. Available from: http://seer.cancer.gov/csr/1975_2007/, based on November 2009 SEER data submission, posted to the SEER web site, 2010.
4. Sharp Z, Richardson A. Aging and cancer: can mTOR inhibitors kill two birds with one drug? *Targeted Oncology*. 2011; 6:41-51.
5. Hursting SD, Smith SM, Lashinger LM, Harvey AE, Perkins SN. Calories and carcinogenesis: lessons learned from 30 years of calorie restriction research. *Carcinogenesis*. 2010; 31:83-89.
6. Fontana L, Partridge L, Longo VD. Extending Healthy Life Span-From Yeast to Humans. *Science*. 2010; 328:321-326.
7. Weindruch R, Colman RJ, Pérez V, Richardson AG. How Does Calorie Restriction Increase the Longevity of Mammals? In: Guarente LP, Partridge L, Wallace DC, editors. *Molecular Biology of Aging*. Cold Spring Harbor, NY 11724: Cold Spring Harbor Laboratory Press; 2008; 409-426.
8. Bartke A. Growth hormone, insulin and aging: The benefits of endocrine defects. *Exp Gerontol*. 2011; 46:108-111.
9. Ikeno Y, Bronson RT, Hubbard GB, Lee S, Bartke A. Delayed Occurrence of Fatal Neoplastic Diseases in Ames Dwarf Mice: Correlation to Extended Longevity. *J Gerontol A Biol Sci Med Sci*. 2003; 58:B291-B296.

10. Ikeno Y, Hubbard GB, Lee S, Cortez LA, Lew CM, Webb CR, et al. Reduced Incidence and Delayed Occurrence of Fatal Neoplastic Diseases in Growth Hormone Receptor/Binding Protein Knockout Mice. *The Journals of Gerontology Series A: Biological Sciences and Medical Sciences*. 2009; 64A:522-529.
11. Powers RW, 3rd, Kaeberlein M, Caldwell SD, Kennedy BK, Fields S. Extension of chronological life span in yeast by decreased TOR pathway signaling. *Genes Dev*. 2006; 20:174-184.
12. Robida-Stubbs S, Glover-Cutter K, Lamming DW, Mizunuma M, Narasimhan SD, Neumann-Haefelin E, et al. TOR Signaling and Rapamycin Influence Longevity by Regulating SKN-1/Nrf and DAF-16/FoxO. *Cell Metabolism*. 2012;15:713-724.
13. Bjedov I, Toivonen JM, Kerr F, Slack C, Jacobson J, Foley A, et al. Mechanisms of Life Span Extension by Rapamycin in the Fruit Fly *Drosophila melanogaster*. *Cell Metabolism*. 2010; 11:35-46.
14. Nadon NL, Strong R, Miller RA, Nelson J, Javors M, Sharp ZD, et al. Design of aging intervention studies: the NIA interventions testing program. *AGE*. 2008; 30:187-199.
15. Nadon NL, Strong R, Miller RA, Nelson J, Javors M, Sharp ZD, et al. Design of aging intervention studies: the NIA interventions testing program. *Age (Dordr)*. 2008; 30:187-199.
16. Harrison DE, Strong R, Sharp ZD, Nelson JF, Astle CM, Flurkey K, et al. Rapamycin fed late in life extends lifespan in genetically heterogeneous mice. *Nature*. 2009; 460:392-395.
17. Miller RA, Harrison DE, Astle CM, Baur JA, Boyd AR, de Cabo R, et al. Rapamycin, But Not Resveratrol or Simvastatin, Extends Life Span of Genetically Heterogeneous Mice. *J Gerontol A Biol Sci Med Sci*. 2011; 66:191-201.
18. Zheng L, Lee WH. The retinoblastoma gene: a prototypic and multifunctional tumor suppressor. *Exp Cell Res*. 2001; 264:2-18.
19. Nikitin AY, Juarez-Perez MI, Li S, Huang L, Lee WH. RB-mediated suppression of spontaneous multiple neuroendocrine neoplasia and lung metastases in Rb^{+/-} mice. *Proc Natl Acad Sci U S A*. 1999 Mar 30; 96:3916-3921.
20. Sharp ZD, Lee WH, Nikitin AY, Flesken-Nikitin A, Ikeno Y, Reddick R, et al. Minimal effects of dietary restriction on neuroendocrine carcinogenesis in Rb^{+/-} mice. *Carcinogenesis*. 2003; 24:179-183.
21. Nikitin A, Lee WH. Early loss of the retinoblastoma gene is associated with impaired growth inhibitory innervation during melanotroph carcinogenesis in Rb^{+/-} mice. *Genes Dev*. 1996; 10:1870-1879.
22. Laplante M, Sabatini DM. mTOR Signaling in Growth Control and Disease. *Cell*. 2012; 149:274-293.
23. Masoro EJ. Overview of caloric restriction and ageing. *Mech Ageing Dev*. 2005;126:913-922.
24. Dhahbi JM, Kim HJ, Mote PL, Beaver RJ, Spindler SR. Temporal linkage between the phenotypic and genomic responses to caloric restriction. *Proc Natl Acad Sci U S A*. 2004; 101:5524-5529.
25. Pool SE, Bison S, Koelewijn SJ, van der Graaf LM, Melis M, Krenning EP, et al. mTOR inhibitor RAD001 promotes metastasis in a rat model of pancreatic neuroendocrine cancer. *Cancer Res*. 2013; 73:12-18.
26. Li B, Gordon GM, Du CH, Xu J, Du W. Specific killing of Rb mutant cancer cells by inactivating TSC2. *Cancer Cell*. 2010; 17:469-480.
27. El-Naggar S, Liu Y, Dean DC. Mutation of the Rb1 Pathway Leads to Overexpression of mTor, Constitutive Phosphorylation of Akt on Serine 473, Resistance to Anoikis and a Block in c-Raf Activation. *Mol Cell Biol*. 2009; 29:5710-5717.
28. Costa C, Santos M, Segrelles C, Duenas M, Lara MF, Agirre X, et al. A Novel Tumor suppressor network in squamous malignancies. *Sci Rep*. 2012; 2:828.
29. Anisimov VN, Zabezhinski MA, Popovich IG, Piskunova TS, Semenchenko AV, Tyndyk ML, et al. Rapamycin Extends Maximal Lifespan in Cancer-Prone Mice. *Am J Pathol*. 2010; 176:2092-2097.
30. Comas M, Toshkov I, Kuropatwinski KK, Chernova OB, Polinsky A, Blagosklonny MV, et al. New nanoformulation of rapamycin Rapatar extends lifespan in homozygous p53^{-/-} mice by delaying carcinogenesis. *Aging (Albany NY)*. 2012; 4: 715-722.
31. Komarova EA, Antoch MP, Novototskaya LR, Chernova OB, Paszkiewicz G, Leontieva OV, et al. Rapamycin extends lifespan and delays tumorigenesis in heterozygous p53^{+/-} mice. *Aging (Albany NY)*. 2012; 4:709-714.
32. Mercier I, Camacho J, Titcher K, Gonzales DM, Quann K, Bryant KG, et al. Caveolin-1 and accelerated host aging in the breast tumor microenvironment: chemoprevention with rapamycin, an mTOR inhibitor and anti-aging drug. *Am J Pathol*. 2012; 181:278-293.
33. Blagosklonny MV. Prevention of cancer by inhibiting aging. *Cancer Biol Ther*. 2008; 7:1520-1524.
34. Hsieh AC, Liu Y, Edlind MP, Ingolia NT, Janes MR, Sher A, et al. The translational landscape of mTOR signalling steers cancer initiation and metastasis. *Nature*. 2012; 485:55-61
35. Dogliotti L, Tampellini M, Stivanello M, Gorzegno G, Fabiani L. The clinical management of neuroendocrine tumors with long-acting repeatable (LAR) octreotide: comparison with standard subcutaneous octreotide therapy. *Ann Oncol*. 2001; 12:Suppl 2:S105-109.
36. Pavel ME, Hainsworth JD, Baudin E, Peeters M, Horsch D, Winkler RE, et al. Everolimus plus octreotide long-acting repeatable for the treatment of advanced neuroendocrine tumours associated with carcinoid syndrome (RADIANT-2): a randomised, placebo-controlled, phase 3 study. *Lancet*. 2011; 378:2005-2012.
37. Nikitin A, Shan B, Flesken-Nikitin A, Chang KH, Lee WH. The retinoblastoma gene regulates somatic growth during mouse development. *Cancer Res*. 2001; 61:3110-3118.
38. Lee EY, Chang CY, Hu N, Wang YC, Lai CC, Herrup K, et al. Mice deficient for Rb are nonviable and show defects in neurogenesis and haematopoiesis. *Nature*. 1992; 359:288-294.
39. Therneau TM. *Modeling Survival Data: Extending the Cox Model*. New York: Springer; 2000.
40. Therneau TM. *A package for Survival in S*. Rochester, MN: Mayo Foundation; 2012.
41. Team RDC. R: A Language and Environment for Statistical Computing 2012. Available from: <http://www.R-project.org>.
42. Bronson RT, Lipman RD. Reduction in rate of occurrence of age related lesions in dietary restricted laboratory mice. *Growth Dev Aging*. 1991; 55:169-184.
43. Ikeno Y, Hubbard GB, Lee S, Richardson A, Strong R, Diaz V, et al. Housing Density Does Not Influence the Longevity Effect of Calorie Restriction. *The Journals of Gerontology Series A: Biological Sciences and Medical Sciences*. 2005; 60:1510-1517.

SUPPLEMENTARY DATA

Table S1. Age (weeks) at treatment initiation					
	<i>Rb1</i> ^{+/-}		<i>Rb1</i> ^{+/+}		
Diet Start Range	#Mice	%	# Mice	%	
7-8	7	7.2	11	11.2	
8-9	49	50.5	47	48.0	
9-10	40	40.3	39	48.0	
12	1	1.0	1	1.0	
Average	8.9		8.8		
Youngest	7.0		7.0		
Oldest	12.0		12.0		

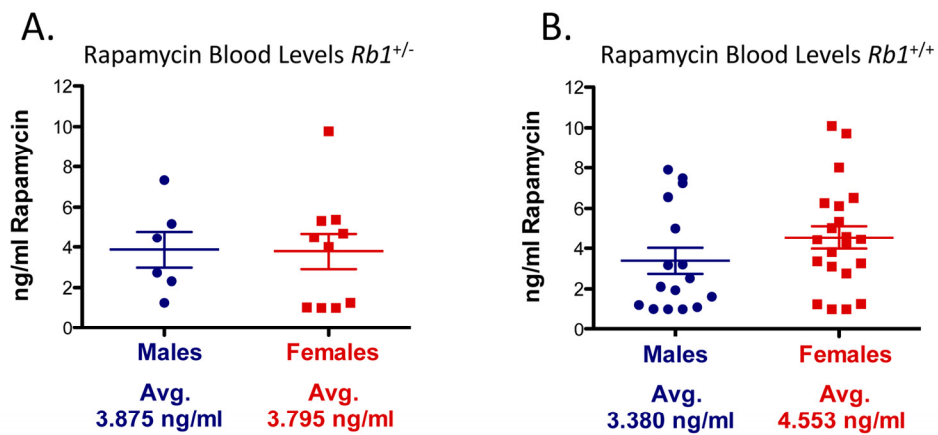


Figure S1. Rapamycin levels were quantified as described in Methods. The concentration of rapamycin was expressed as ng/ml of whole blood.

Potential anti-aging agents suppress the level of constitutive mTOR- and DNA damage- signaling

H. Dorota Halicka¹, Hong Zhao¹, Jiangwei Li¹, Yong-Syu Lee², Tze-Chen Hsieh², Joseph M. Wu², and Zbigniew Darzynkiewicz¹

¹ Brander Cancer Research Institute, Department of Pathology, New York Medical College, Valhalla, NY 10595, USA

² Department of Biochemistry and Molecular Biology, New York Medical College, Valhalla, NY 10595, USA

Key words: H2AX phosphorylation, ROS, ribosomal protein S6, calorie restriction, metformin, rapamycin, 2-deoxyglucose, rapamycin, berberine, vitamin D3, resveratrol, aspirin, replication stress, senescence, cell cycle, 4EBP1

Received: 12/6/12; **Accepted:** 12/28/12; **Published:** 12/30/12

Correspondence to: Zbigniew Darzynkiewicz, PhD; **E-mail:** darzynk@nymc.edu

Copyright: © Halicka et al. This is an open-access article distributed under the terms of the Creative Commons Attribution License, which permits unrestricted use, distribution, and reproduction in any medium, provided the original author and source are credited

Abstract: Two different mechanisms are considered to be the primary cause of aging. Cumulative DNA damage caused by reactive oxygen species (ROS), the by-products of oxidative phosphorylation, is one of these mechanisms (ROS concept). Constitutive stimulation of mitogen- and nutrient-sensing mTOR/S6 signaling is the second mechanism (TOR concept). The flow- and laser scanning- cytometric methods were developed to measure the level of the constitutive DNA damage/ROS- as well as of mTOR/S6- signaling in individual cells. Specifically, persistent activation of ATM and expression of γ H2AX in untreated cells appears to report constitutive DNA damage induced by endogenous ROS. The level of phosphorylation of Ser235/236-ribosomal protein (RP), of Ser2448-mTOR and of Ser65-4EBP1, informs on constitutive signaling along the mTOR/S6 pathway. Potential gero-suppressive agents rapamycin, metformin, 2-deoxyglucose, berberine, resveratrol, vitamin D3 and aspirin, all decreased the level of constitutive DNA damage signaling as seen by the reduced expression of γ H2AX in proliferating A549, TK6, WI-38 cells and in mitogenically stimulated human lymphocytes. They all also decreased the level of intracellular ROS and mitochondrial trans-membrane potential $\Delta\Psi_m$, the marker of mitochondrial energizing as well as reduced phosphorylation of mTOR, RP-S6 and 4EBP1. The most effective was rapamycin. Although the primary target of each on these agents may be different the data are consistent with the downstream mechanism in which the decline in mTOR/S6K signaling and translation rate is coupled with a decrease in oxidative phosphorylation, (revealed by $\Delta\Psi_m$) that leads to reduction of ROS and oxidative DNA damage. The decreased rate of translation induced by these agents may slow down cells hypertrophy and alleviate other features of cell aging/senescence. Reduction of oxidative DNA damage may lower predisposition to neoplastic transformation which otherwise may result from errors in repair of DNA sites coding for oncogenes or tumor suppressor genes. The data suggest that combined assessment of constitutive γ H2AX expression, mitochondrial activity (ROS, $\Delta\Psi_m$) and mTOR signaling provides an adequate gamut of cell responses to evaluate effectiveness of gero-suppressive agents.

INTRODUCTION

The cumulative DNA damage caused by reactive oxygen species (ROS), by-products of oxidative phosphorylation, for long time has been considered to be a key factor contributing both to cell aging as well as predisposing to neoplastic transformation [1-12]. Oxidative DNA damage generates significant number of DNA double-strand breaks (DSBs), the potentially

deleterious lesions. DSBs can be repaired either by the homologous recombination or nonhomologous DNA-end joining (NHEJ) mechanism. Recombinatorial repair which uses newly replicated DNA as a template restores DNA rather faithfully. It can take place however when cells have already the template, namely during late-S and G₂ phase. In the cells that lack a template (G₁, early-S) DNA repair relies on the NHEJ which is error-prone due to a possibility of a deletion or rearrangement

of some base pairs [13-17]. If the erroneously repaired DSBs are at sites of oncogenes or tumor suppressor genes this may result in somatic mutations that predispose cell to oncogenic transformation. Oxidative damage of telomeric DNA may lead to dysfunction of telomeres thereby driving cells to undergo replicative senescence [18-30].

Whereas DNA damage induced by endogenous (and exogenous) oxidants may indeed significantly contribute to cancer development its role as being the key factor accountable either for cellular or organismal aging is debatable [31-40]. There is growing body of evidence in support of the notion that the primary culprit of aging is the constitutive stimulation of the mitogen- and nutrient-sensing signaling pathways. Activation of these pathways enhances translation, leads to cell growth in size/mass and ultimately results in cell hypertrophy and senescence. Among these culprit pathways the mammalian target of rapamycin (mTOR) and its downstream target S6 protein kinase (S6K) play the key role [41-49]. Constitutive replication stress likely resulting from the ongoing oxidative DNA damage when combined with activation of mTOR/S6K appears to be the driving force leading to aging and senescence both at the cellular as well as organismal level [43-51].

We have recently reported that constitutive DNA damage signaling (CDDS) observed in the untreated normal or tumor cells, assessed as the level of expression of histone H2AX phosphorylated on Ser139 (γ H2AX) and of activated (Ser1981 phosphorylated) *Ataxia Telangiectasia mutated* protein kinase (ATM), is an indication of the ongoing DNA damage induced by endogenous ROS [52-55]. These phosphorylation events were detected with phospho-specific antibodies (Ab) and measured in individual cells by flow- or laser scanning- cytometry. Using this approach we have assessed several agents reported to have anti-oxidant and DNA-protective properties with respect to their ability to attenuate the level of CDDS [52-58]. In the present study we test effectiveness of several reported anti-aging modalities to attenuate the level of CDDS in individual TK6 and A549 tumor cell lines as well as in WI-38 and mitogenically stimulated normal lymphocytes.

In parallel, we also assess their effect on the level of constitutive state of activation of the critical mTOR downstream targets. Specifically, using phospho-specific Abs detecting activated status of ribosomal protein S6 (RP-S6) phosphorylated on Ser235/236 we measure effectiveness of these gero-suppressive agents along the mTOR/S6K signaling. We have also tested effects of these agents on the level of endogenous

reactive oxidants as well as mitochondrial electrochemical potential $\Delta\Psi_m$. The following agents, reported as having anti-aging and/or chemopreventive properties, were chosen in the present study: 2-deoxy-D-glucose (2dG) [59-62], metformin (MF) [63-71], rapamycin (RAP) [72-80], berberine (BRB) [81-85], vitamin D3 (Vit. D3) [86- 91], resveratrol (RSV) [92-97] and acetylsalicylic acid (aspirin) (ASA) [98-103].

RESULTS

Fig. 1 illustrates the effect of exposure of human lymphoblastoid TK6 cells for 24 h to the investigated presumed anti-aging agents on the level of constitutive expression of γ H2AX. Consistent with our prior findings [52-54] the expression γ H2AX in S and G₂M cells is distinctly higher than in the cells of G₁ phase. This is the case for both, the untreated (Ctrl) cells as well as the cells treated with these agents. It is also apparent that exposure of cells to each of the studied drugs led to the decrease in expression of γ H2AX in all phases of the cell cycle. In most treated cells, however, the decline in the mean expression γ H2AX was somewhat more pronounced in the S- compared to G₁ - or G₂M- phase cells. Analysis of DNA content frequency histograms reveals that the 24 h treatment with most of the drugs had no effect on the cell cycle distribution. The exception are the cells treated with 50 nM RP which show about 50% reduction in frequency of cells in S and G₂M which would indicate partial cells arrest in G₁ phase of the cell cycle. It should be noted that exposure of cells to these agents for 4 h led to rather minor (<15%) decrease in expression of γ H2AX whereas the treatment for 48 h had similar effect as for 24 h (data not shown).

The effect of exposure of TK6 cells to the investigated gero-suppressive agents on state of phosphorylation of ribosomal S6 protein is shown in Fig. 2. Unlike expression of γ H2AX the level of phosphorylation of RP-S6 shows no significant cell cycle phase-related differences, neither in control nor in the treated cultures. Somewhat higher expression of RP-S6^P in S- and G₂M- compared to G₁- cells is proportional to an overall increase in cell size during cell cycle progression. It is quite evident however that the treatment with each of these anti-aging agents led to a decrease in the level of phosphorylation of S6 protein. The most dramatic decrease (>95%) was seen in the cells treated with RAP. The cells treated with 2dG showed the smallest (32-38%) decrease. There was no evidence that treatment of TK6 cells with all these drugs for 4 h had any distinct effect on the cell cycle progression as detected by analysis of DNA content frequency histograms (not shown).

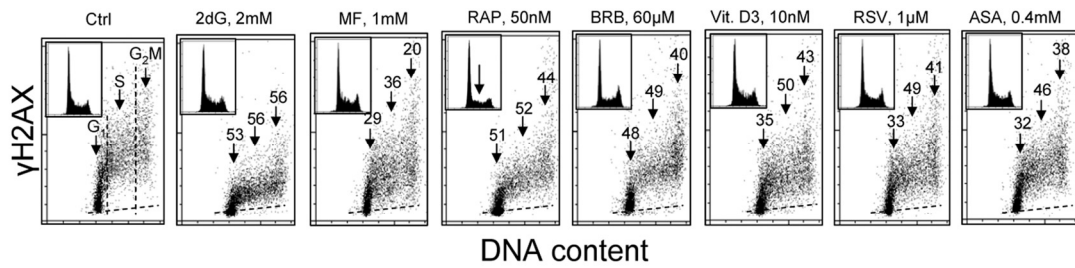


Figure 1. Effect of exposure of TK6 cells to different presumed anti-aging drugs on the level of constitutive expression of γ H2AX. Exponentially growing TK6 cells were untreated (Ctrl) or treated with the respective agents for 24 h at concentrations as shown. Expression of γ H2AX in individual cells was detected immunocytochemically with the phospho-specific Ab (AlexaFluor647), DNA was stained with DAPI; cellular fluorescence was measured by flow cytometry. Based on differences in DNA content cells were gated in the respective phases of the cell cycle, as marked by the dashed vertical lines. The percent decrease in mean fluorescence intensity of the treated cells in particular phases of the cell cycle, with respect to the respective untreated controls, is shown above the arrows. Inserts present DNA content frequency histograms from the individual cultures. The dashed skewed lines show the background level, the mean fluorescence intensity of the cells stained with secondary Ab only.

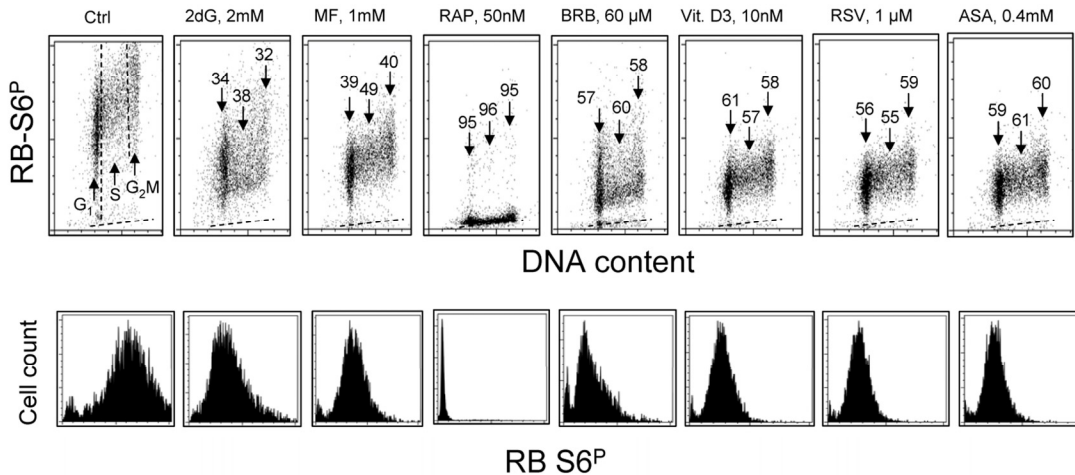


Figure 2. Effect of treatment of TK6 cells with different presumed anti-aging drugs for 4 h on the level of constitutive phosphorylation of ribosomal protein S6 (RP-S6). Exponentially growing TK6 cells were untreated (Ctrl) or treated with the respective agents at concentrations as shown. Phosphorylation status of ribosomal S6 protein was detected immunocytochemically with the phospho-specific Ab (AlexaFluor647), DNA was stained with DAPI; cellular fluorescence was measured by flow cytometry. **Top panels:** Based on differences in DNA content cells were gated in the respective phases of the cell cycle, as marked by the dashed vertical lines (Ctrl). The percent decrease in mean fluorescence intensity of the treated cells in particular phases of the cell cycle, with respect to the to the same phases of the untreated cells, is shown above the arrows. The dashed skewed lines show the background level, the mean fluorescence intensity of the cells stained with secondary Ab only. **Bottom panels:** Single parameter frequency histograms showing expression of phosphorylated ribosomal S6 protein (RB-S6^P) in all (G₁+S+G₂M) cells of the respective cultures.

Fig. 3 presents the effect of exposure of TK6 cells to MF, RAP or RSV at somewhat lower concentration for 24 h on the level of expression of RP-S6^P. Compared with cells exposed for 4 h (Fig. 1) the effect of MF, even at the lower concentration (50 μM), was more pronounced after 24 h. Also, after that time of exposure, more pronounced was the effect of RAP and RSV.

Analysis of the DNA content frequency histograms indicates that neither 50 – 500 μM MF nor RSV had an effect on the cell cycle progression. However, exposure to 0.1 μM RAP (similar to 50 nM, see Fig. 1) resulted in about 50% decrease in frequency of S and G₂M cells (insets, marked by arrows).

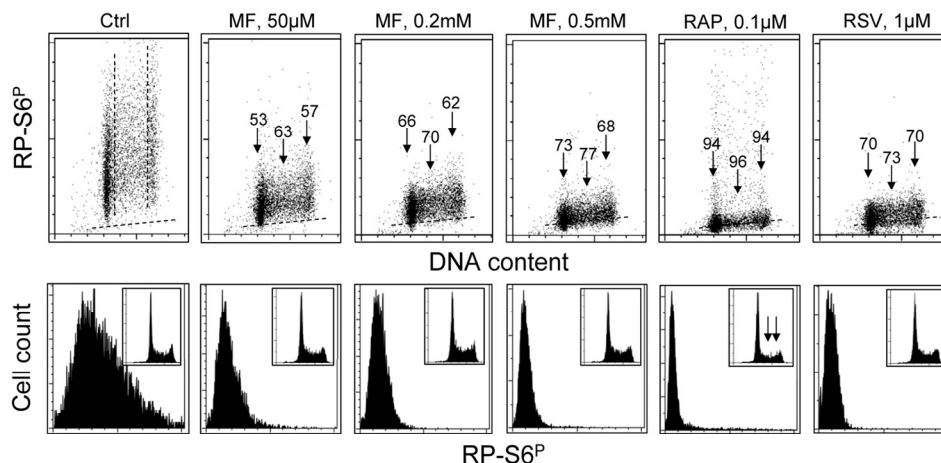


Figure 3. Effect of treatment of TK6 cells with MF, RAP or RSV for 24 h on the level of constitutive phosphorylation of S6 protein. TK6 cells were untreated (Ctrl) or treated with different concentrations of MF as well as with RAP or RSV for 24 h. Phosphorylation status of S6 was assessed as described in legend to Fig. 2. **Top panels:** The percent decrease in mean fluorescence intensity of the drug-treated cells in particular phases of the cell cycle is shown above the arrows. **Bottom panels:** Frequency histograms showing expression of RP-S6^P in all cells of the respective cultures. Insets show cellular DNA content histograms of cells in these cultures.

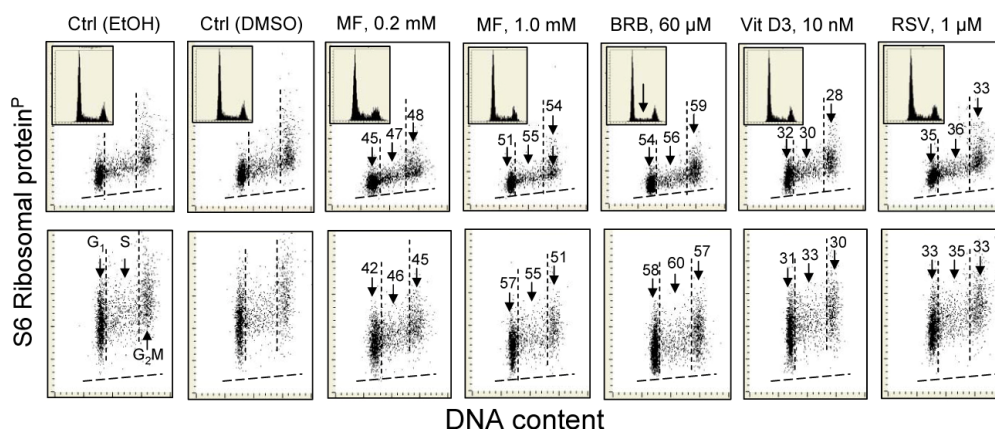


Figure 4. Reduction of the level of constitutive expression of RP-S6^P in A549 cells exposed to MF, BRB, Vit. D3 or RSV for 24 h. Exponentially growing in chamber slides A549 cells, were treated with the respective agents and their fluorescence was measured the laser scanning cytometry (LSC).⁷⁵ Top panels show RP-S6^P immunofluorescence integrated over the nuclei (reporting expression of RP-S6^P in the cytoplasm located over and below the nucleus); bottom panels present RP-S6^P immunofluorescence integrated over the cytoplasm aside of the nucleus. The percent decrease in expression of RP-S6^P in cells in particular phases of the cell cycle (mean values) is shown above the arrows. Because stock solutions of some of these agents were made in DMSO, other in MeOH or EtOH, the equivalent quantities of these solvents were included in the respective control culture and the percent decrease shown in the panels refers to the decrease compared to these controls shown are the cells from EtOH and DMSO containing controls. The insets present DNA content frequency histograms from the respective cultures.

The effect of some of these gero-suppressive drugs was also studied on human pulmonary adenocarcinoma A549 cells (Fig. 4). These cells grow attached and their fluorescence intensity was measured by imaging cytometry (laser scanning cytometer; LSC) [104]. The decrease in expression of RP-S6^P was seen in the cells treated with each of the drugs. The effect was essentially

of similar degree whether measured in cytoplasm over- and underlying the nucleus (Fig. 4 top panels) or in the cytoplasm at the nuclear periphery (bottom panels). The most pronounced decrease was induced by BRB. Also affected was the cell cycle progression, as evidenced by the decline in frequency of S-phase cells on the DNA histogram in BRB treated cells (inset, marked by arrow).

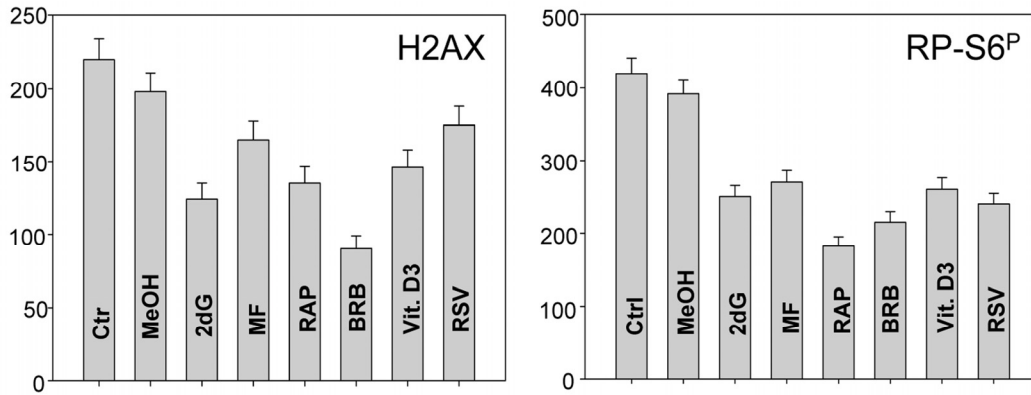


Figure 5. Effect of treatment of WI-38 cells with 2dG, MF, RAP, BRB, Vit. D3 or RSV for 24 h on the level of constitutive expression of γ H2AX (left panel) and RP-S6^P (right panel). Exponentially growing cells, were treated with the respective agents at concentrations as shown in Figs. 1 and 2, RP-S6^P was detected immunocytochemically and cell fluorescence was measured with the laser scanning cytometry (LSC). The bar graphs present the mean fluorescence intensity measured as an integral over the nucleus (γ H2AX) or over cytoplasm (RP-S6^P).

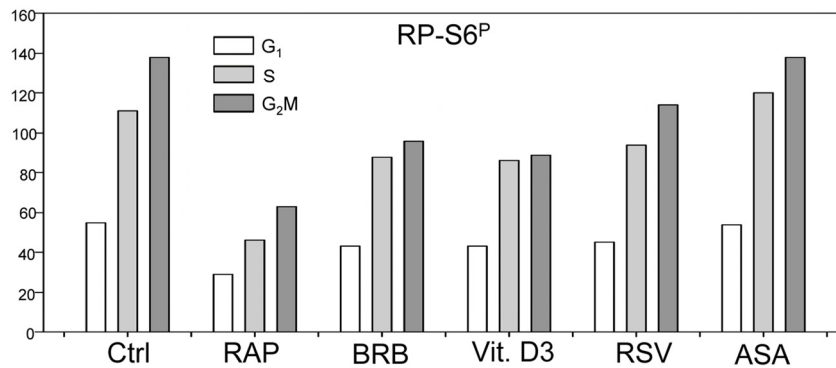


Figure 6. Effect of treatment of mitogenically stimulated human lymphocytes with RAP, BRB, Vit. D3, RSV or ASA for 4 h on the level of constitutive expression of RP-S6^P. Peripheral blood lymphocytes were mitogenically stimulated with phytohemagglutinin (PHA) for 72 h, the cells were then treated with the respective drugs at concentrations as shown in Figs. 1 and 2 for 4 h, RP-S6^P was detected immunocytochemically and cellular fluorescence measured by flow cytometry. The bar graphs present the mean values (+SD) of RP-S6^P immunofluorescence for G₁, S and G₂M cell subpopulations identified by differences in DNA content (intensity of DAPI fluorescence).

In addition to tumor cell lines we have also tested effects of the presumed gero-suppressive agents on non-tumor cells. Fig. 5 illustrates their effect on the WI-38 cells and Fig. 6 on mitogenically-stimulated human lymphocytes. A decrease in expression of γ H2AX was observed in WI-38 cells treated with each of the tested agents, the most pronounced reduction ($>50\%$) showed cells treated with BRB while the least affected ($<10\%$) were cells growing in the presence of RSV. A reduction in the level of phosphorylated RB-S6 was also evident in WI-38 cells exposed to each of these agents, the most pronounced ($>50\%$) after treatment with RAP. Because stock solutions of some of these agents were made in DMSO or MeOH equivalent quantities of these solvents were included in the respective control cultures. A minor suppressive effect of MeOH on expression of γ H2AX and RB-S6^P was observed (Fig. 5). Likewise, DMSO exerted also minor ($\sim 5\%$) but repeatable suppressive effect (not shown). As is evident RAP, BRB, Vit. D3 and RSV reduced the level of RP-S6^P in mitogenically stimulated human lymphocytes, in all phases of the cell cycle, while the effect of ASA on

these cells was minimal (Fig. 6).

To confirm the findings obtained by the flow- and laser scanning- cytometry based on measurement of individual cells we assessed effects of the gero-suppressive agents by measurement mTOR signaling in bulk, by western blotting. In this experiment, having available phospho-specific Abs that detect phosphorylation of mTOR, RP-S6 and the eukaryotic translation initiation factor 4E-binding protein (4EBP1) applicable to western blotting (not yet available for cytometry) we have been able to test effects of the studied gero-preventive agents on the level of constitutive phosphorylation of these proteins as well. As is evident in Fig. 7 and Table 1 exposure of TK6 cells to the gero-preventive agents lowered the level of phosphorylation status of mTOR, as well as its downstream targets RP-S6 and 4EBP1. The most pronounced effect was seen in the case of RAP, BRB and 2dG which lowered expression of RP-S6^P by 95%, 78 and 70%, respectively. RAP, BRB and 2dG were also quite effective in lowering the level of 4EBP1^P, by 52%, 51% and 51%.

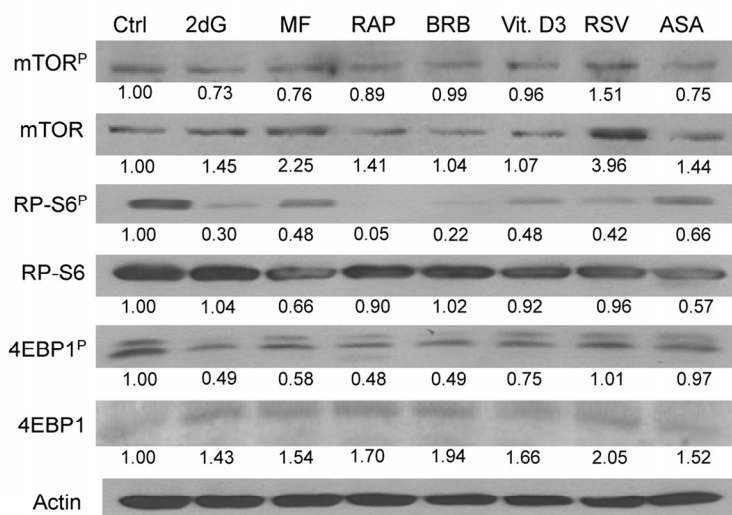


Figure 7. Effect of the studied gero-preventive agents on constitutive level of expression of mTOR-Ser2448^P, RP-S6-Ser235/236^P and 4EBP1-Ser65^P and their corresponding unphosphorylated forms in TK6 cells, detected by western blotting. TK6 cells were exposed to the studied agents at concentrations as shown in Figs 1 and 2 for 4 h. The protein expression level were determined by western blot analysis and the intensity of the specific immunoreactive bands were quantified by densitometry and normalized to actin (loading control). The numbers indicate the n-fold change in expression of the respective phospho-proteins in the drug-treated cultures with respect to the untreated cells (Ctrl).

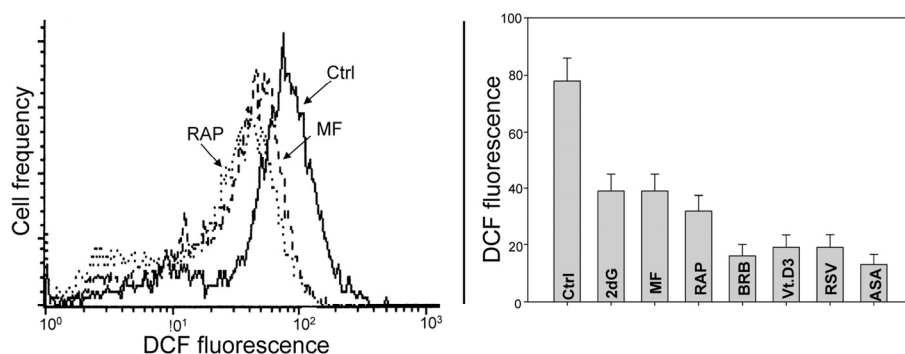


Figure 8. Effects of the studied gero-preventive agents on the intercellular level of ROS. TK6 cells, untreated (Ctrl) or treated for 24 h with the investigated agents, were exposed for 30 min to H₂DCF-DA and their fluorescence intensity was measured by flow cytometry. The cell-permeant non-fluorescent H₂DCF-DA upon cleavage of the acetate moiety by intercellular esterases and oxidation by ROS is converted to strongly fluorescent DCF and thus reports the ROS abundance. Left panel shows the frequency histograms of the untreated (Ctrl) as well MF and RAP-treated cells (note exponential scale of the DCF fluorescence). Right panel presents the mean values (+SD) of DCF fluorescence of the untreated (Ctrl) and treated cells.

Table 1. Effect of the studied gero-preventive agents on constitutive level of expression of mTOR-Ser2448^P, RP-S6-Ser235/236^P and 4EBP1-Ser65^P and their corresponding unphosphorylated forms, detected by western blotting (Fig. 7)

Agent	Ctrl	2dG	MF	RAP	BRB	Vit. D3	RSV	ASA
mTOR ^P	1.00	0.73	0.76	0.89	0.99	0.96	1.51	0.75
m-TOR	1.00	1.45	2.25	1.41	1.04	1.07	3.96	1.44
RATIO	1.00	0.50	0.34	0.63	0.95	0.90	0.38	0.52
RP-S6 ^P	1.00	0.30	0.48	0.05	0.22	0.48	0.42	0.66
S6	1.00	1.04	0.66	0.9	1.02	0.92	0.96	0.57
RATIO	1.00	0.29	0.73	0.06	0.22	0.52	0.44	1.16
4EBP1 ^P	1.00	0.49	0.58	0.48	0.49	0.75	1.01	0.97
4EBP1	1.00	1.43	1.54	1.7	1.94	1.66	2.05	1.52
RATIO	1.00	0.38	0.38	0.28	0.25	0.45	0.45	0.64

The numbers indicate the change in expression of the respective proteins in the drug-treated cultures with respect to the untreated ones. Densitometric quantification of phosphorylated and total proteins for mTOR, RP-S6 and 4EBP1 are presented as the *ratio* of actin-normalized phosphorylated to total protein level of expression (**Bold font**).

Most interesting, however, were the results reporting effects of the studied drugs on the total mTOR, RP-S6 and 4EBP1 protein content and on the ratios of the phosphorylated protein fractions to the total content of the respective proteins (Table 1). These data show that exposure of cells to each drug led to a distinct up-regulation of mTOR and 4EBP1 expression. This was not the case of RP-S6, which, with an exception of 2dG and BRB, showed a minor decline. However, compared with the apparent increase of total proteins content, the

level of the phosphorylated fractions of the respective proteins was more severely reduced. This over-compensated the upregulation and is expressed as the reduction of the ratio of phosphorylated to total content of the respective proteins. In the case of RP-S6 and 4EBP1, the downstream effectors of mTOR and the agents directly affecting the translation rate, the most effective was BRB and RAP, reducing proportion of the phosphorylated to total protein content by 75% and 72% respectively (Table 1).

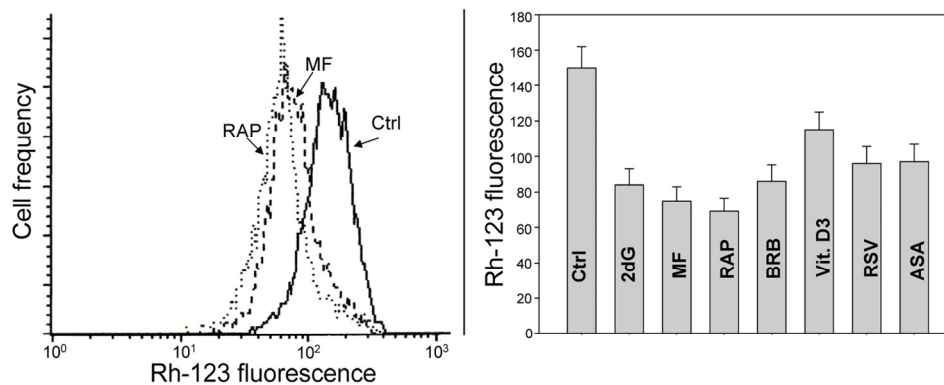


Figure 9. Effect of the studied gero-preventive agents on the mitochondrial transmembrane potential ($\Delta\Psi_m$). TK6 cells, untreated (Ctrl) or treated for 24 h with the investigated agents were exposed for 30 min to the mitochondrial probe rhodamine 123 (Rh-123) and their fluorescence intensity was measured by flow cytometry. Left panel shows the frequency histograms of the untreated (Ctrl) as well MF and RAP-treated cells (note exponential scale of the DCF fluorescence). Right panel presents the mean values (+SD) of Rh-123 fluorescence of the investigated cells.

In other set of experiments we assessed the effect of the studied gero-preventive agents on the level of endogenous ROS. As is evident in Fig. 8 exposure of TK6 cells to each of these agents led to a marked reduction of cells ability to oxidize $H_2DCF\text{-DA}$; its oxidation by ROS results in formation of the strongly fluorescent DCF which is considered to be a marker of ROS abundance. In this respect more effective appeared to be BRB, Vit. D3, RSV and ASA compared to RAP, MF or 2dG.

Fig. 9 illustrates changes in electrochemical transmembrane potential of mitochondria detected by cells capability to accumulate the mitochondrial probe rhodamine 123 (Rh-123) in TK6 cells treated with the investigated gero-preventive agents. The data show a reduction in the ability to accumulate Rh-123 in cells treated with each of these agents, the most pronounced in the case of treatment with RAP.

DISCUSSION

In the prior studies we have already observed that MF at concentrations 0.1 mM – 20 mM [55] and Vit. D (2 nM - 10 nM) [56] effectively reduced constitutive level of H2AX-Ser139 and ATM-Ser1981 phosphorylation. In the present study all seven agents, all reportedly having anti-aging and/or chemopreventive properties, including MF and Vit D3[59-103], have been tested with respect of their ability to affect both the level of constitutive DNA damage signaling as monitored γ H2AX expression as well as constitutive level of phosphorylation of ribo-

somal S6 protein (RP-S6^P). The data show that each of the drugs reduced both, the level of phosphorylation of both H2AX on Ser139 and RP-S6 on Ser235/236. RP-S6, a component of the 40S ribosomal subunit and the most downstream effector of mTOR signaling, is directly involved in regulation of translation [46] and considered to be a determinant of cell size [105,106]. As is evident from the western blotting data (Fig. 7) with an exception of RSV all the studied drugs reduced also the level of phosphorylation of mTOR, RP-S6 and 4EBP1. The latter protein is also considered to be a critical regulator of translation and cell size determinant [105-108].

Analysis of the mTOR vs. mTOR^P, RP-S6 vs. RP-S6^P and 4EBP1 vs. 4EBP1^P revealed up-regulation of mTOR and 4EBP1 in cells treated with each of the studied drugs (Table 1). The increase of total content of these proteins was overcompensated by the reduction in the extent of their phosphorylation, which led to decrease in the ratios of mTOR^P/mTOR, RP-S6^P/RP-S6 and 4EB1^P/4EB1. The upregulation of these proteins was unexpected but it suggests that the reduction of their phosphorylation status by the studied drugs may trigger compensatory synthesis (or reduced turnover rate) that leads to increase in their content. The distinctly reduced ratios of mTOR^P/mTOR, RP-S6^P/RP-S6 and 4EB1^P/4EB1, however, may provide a novel biomarker useful to assess the potential mTOR-inhibitory activities that relate to reduction of translation rate, cell size and thus may be of value in assessing anti-aging properties of the studied agents.

The reduction of RP-S6 phosphorylation by each of the gero-suppressive drugs was presently observed in all types of the cells, including tumor TK6 (Fig. 1-3,7) and A549 (Fig. 4) cell lines as well as in normal WI-38 (Fig. 5) and mitogenically stimulated human lymphocytes (Fig. 6). The results obtained by flow and laser scanning cytometry were confirmed by measurement in bulk, by western blotting. The western blotting approach allowed us also to measure phosphorylation level of mTOR and 4EBP1 to which the commercially available phospho-specific Abs are not fully applicable for flow or laser scanning cytometry. The cytometric approach has an advantage that it provides information regarding the cell cycle phase specificity of expression of γ H2AX or RP-S6. Furthermore, the cytometric approach has no potential risk of an artifact that the level of phosphorylation of the studied proteins may be altered as a result of disruption of cell integrity in preparation for blotting, which may provide contact of these proteins with active phosphatases and kinases. We observed, for example that when inhibitors of phosphatases were not rigorously used during cell preparation for western blotting the results (not shown) were entirely different than in Fig. 7.

According to the mTOR concept of the mechanism of aging the observed reduction of the level of phosphorylation of mTOR, 4EBP1 and RP-S6 by the studied agents would be consistent with their reported anti-aging properties. The gero-preventive mechanism of these agents thus would be similar to that of the calorie restriction which was definitely proven to extent life span of a variety of organisms [94-97,109].

Parallel to the reduction of constitutive mTOR/S6 signaling each of the investigated gero-suppressive agents also reduced CDDS, as seen by the decline in γ H2AX expression (Fig. 1). This corresponding response to these agents, concurrently by both the DNA damage- and mTOR- signaling pathways, suggests on mechanistic association between these two pathways that may converge on the aging-related processes. One of the mechanisms linking these pathways is straightforward as it may involve a decrease of intensity of oxidative phosphorylation in mitochondria. Namely, because the declined translation rate requires less energy the intensity of oxidative phosphorylation that generates ROS is reduced which results in attenuation of CDDS. Consistent with this mechanism is our prior observation that exposure of lymphocytes to Vit. D3 led to a three-fold decline in abundance of ROS [55]. Likewise, treatment of TK6 cells with MF resulted in a significant decrease in the level of ROS [56]. In the present study we confirmed these earlier findings as we observed that all studied drugs markedly lowered

abundance of ROS in TK6 cells (Fig. 8). Accordingly, mitogenic stimulation of lymphocytes known to dramatically enhance transcription and translation rates [110,111] also was seen to boost production of ROS and augment CDDS [112]. There are numerous linkages connecting DNA damage response with mTOR/RP-S6 pathways, primarily involving p53 signaling [113-118]. Of interest, and confirming the involvement of mitochondrial pathways in response to the studied gero-preventive agents, is also the observation that exposure of cells to each of them resulted in a decreased mitochondrial transmembrane potential ($\Delta\Psi$ m). The latter was detected by reduced cells capability to bind rhodamine 123 (Fig. 9), the probe known to be the marker of energized mitochondria [119-121].

Unlike constitutive phosphorylation of RP-S6 which was unrelated to the cell cycle phase, H2AX phosphorylation was cell cycle phase specific, distinctly higher in S- and G₂M- than in G₁- cells. This suggests that DNA replication stress may be a contributing factor to the observed CDDS. DNA lesions resulting from oxidative DNA damage caused by endogenous ROS could be responsible for the replication stress. As mentioned in the Introduction constitutive replication stress when concurrent with mTOR/S6K signaling is considered to be the predominant factor leading to aging and senescence. Thus, the present data that show that the investigated gero-preventive drugs suppress both, the mTOR/RP-S6 signaling and CDDS, would be consistent with the mechanism that involves attenuation of DNA replication stress.

Whereas mTOR/S6 signaling is the primary cause of aging and induction of premature cell senescence the DNA damage by reactive oxidants, since it induces DSBs which cannot always be faithfully repaired, predisposes to neoplastic transformation [1-7]. It is expected therefore that the anti-aging agents that reduce CDDS would have cancer preventive properties as well. Indeed such chemo-preventive properties have been described for each of the presently investigated drugs [122-128]. The present data indicate that the combined analysis of: (i) CDDS measured by γ H2AX expression, (ii) mitochondria activity (ROS, $\Delta\Psi$ m) and (iii) mTOR signaling (mTOR, S6K, 4EBP1 phosphorylation) in individual cells [129] may provide an adequate gamut of cell responses to evaluate potential gero- or chemo-preventive properties of suspected agents.

MATERIALS AND METHODS

Cells, Cell Treatment. Human lung carcinoma A549 cells, diploid lung WI-38 fibroblasts and lymphoblastoid TK6 cells were obtained from American Type

Culture Collection (ATCC CCL-185, Manassas, VA). Human peripheral blood lymphocytes were obtained by venipuncture from healthy volunteers and isolated by density gradient centrifugation. A549 cells were cultured in Ham's F12K, TK6, WI-38 and lymphocytes were cultured in RPMI 1640 with 2 mM L-glutamine, 1.5 g/L sodium bicarbonate and 10% fetal bovine serum (GIBCO/Invitrogen, Carlsbad, CA). Adherent A549 and WI-38 cells were grown in dual-chambered slides (Nunc Lab-Tek II), seeded with 10^5 cells/ml suspended in 2 ml medium per chamber. TK6 cells and lymphocytes were grown in suspension; lymphocyte cultures were treated with the polyvalent mitogen phytohemagglutinin (Sigma/Aldrich; St Louis, MO) as described [36]. MF (1,1-dimethylbiguanide) was obtained from Calbiochem, La Jolla, CA, 2dG, RAP, BRB, RSV and ASA from Sigma-Aldrich. The active form of vitamin D3 (1,25-dihydroxyvitamin D3) was kindly provided by Dr Milan Uskokovic [56]. Stock solutions of some of these agents were prepared either in DMSO, MeOH or EtOH as indicated by the vendor. The cells, during exponential phase of growth were treated with these agents, at concentrations and for duration as indicated in the figures or figure legends. Respective control cultures were treated with the equivalent volumes of solvents used for stock solutions. After exposure to the gero-preventive agents the cells were rinsed with phosphate buffered salt solution (PBS) and fixed in 1% methanol-free formaldehyde (Polysciences, Warrington, PA) for 15 min on ice. The cells were then transferred to 70% ethanol and stored at -20°C for up to 3 days until staining.

Immunocytochemical Detection of γH2AX and RP-S6^P. After fixation the cells were washed twice in PBS and with 0.1% Triton X-100 (Sigma-Aldrich) in PBS for 15 min and with a 1% (w/v) solution of bovine serum albumin (BSA; Sigma-Aldrich) in PBS for 30 min to suppress nonspecific antibody (Ab) binding. The cells were then incubated in 1% BSA containing a 1:300 dilution of phospho-specific (Ser139) γH2AX mAb (Biolegend, San Diego, CA) and/or with a 1:200 dilution of phosphospecific (Ser235/236) RP-S6 Ab (Epitomics, Burlingame, CA) at 4°C overnight. The secondary Ab was tagged with AlexaFluor 488 or 647 fluorochrome (Invitrogen/Molecular Probes, used at 1:100 dilution in 1% BSA). The incubation was at room temperature for 45 min. Cellular DNA was counterstained with 2.8 $\mu\text{g/ml}$ 4,6-diamidino-2-phenylindole (DAPI; Sigma-Aldrich) at room temperature for 15 minutes. Each experiment was performed with an IgG control in which cells were labeled only with the secondary AlexaFluor 488 Ab, without primary Ab incubation to estimate the extent of nonspecific adherence of the secondary Ab to the cells.

The fixation, rinsing and labeling of A549 and WI-38 cells was carried out on slides, and lymphocytes and TK6 cells in suspension. Other details have been described previously [53-56].

Detection of ROS and Mitochondrial Transmembrane Potential $\Delta\Psi\text{m}$. Untreated cells as well as the gero-protective agents drugs-treated TK6 cells were incubated 60 min with 10 μM 2',7'-dihydrodichlorofluorescein-diacetate ($\text{H}_2\text{DCF-DA}$) (Invitrogen/Molecular Probes) at 37°C . Cellular green fluorescence was then measured by flow cytometry. Following oxidation by ROS and peroxides within cells the non-fluorescent substrate $\text{H}_2\text{DCF-DA}$ is converted to the strongly fluorescent derivative DCF [97]. Mitochondrial potential $\Delta\Psi\text{m}$ was assessed by exposure of cells in tissue culture to 1 μM rhodamine 123 (Rh-123; Invitrogen/Molecular Probes) for 30 min prior to measurement of their fluorescence.

Analysis of Cellular Fluorescence. A549 and WI-38 cells: Cellular immunofluorescence representing the binding of the respective phospho-specific Abs as well as the blue emission of DAPI stained DNA was measured by Laser Scanning Cytometry (LSC) [131] (iCys; CompuCyte, Westwood, MA) utilizing standard filter settings; fluorescence was excited with 488-nm argon, helium neon (633 nm) and violet (405 nm) lasers. Intensities of maximal pixel and integrated fluorescence were measured and recorded for each cell. At least 3,000 cells were measured per sample. Gating analysis was carried out as described in Figure legends. **TK6 cells and lymphocytes:** Intensity of cellular fluorescence was measured using a MoFlo XDP (Beckman-Coulter, Brea, CA) high speed flow cytometer/sorter. DAPI fluorescence was excited with the UV laser (355-nm), AlexaFluor 488, DCF and Rh123 with the argon ion (488-nm) laser. Although berberine, one of the studied agents, is fluorescent [132] control experiments excluded the possibility that its fluorescence significantly contributed to analysis of the measured cells that could lead to a bias. Statistical evaluation of individual measurements (SD) was carried out assuming the Poisson distribution in evaluation of populations of cells in particular phases of the cell cycle. All experiments were repeated at least three times, representative data are presented.

Western Blotting. TK6 cells were exposed to the investigated agents at concentrations as shown in Figs. 1 and for 4 h. The cells were then collected and lysed by incubation on ice for 30 min in cold immunoprecipitation (RIPA) buffer, which contained 50 mM Tris, pH 7.4, 150 mM NaCl, 1 mM EDTA, 1% Triton X-100, 1% deoxycholate, 0.1% SDS, 1 mM

dithiothreitol (DTT) and 10 µl/ml protease inhibitor cocktail and 1% phosphatase inhibitor cocktail 3 (Sigma-Aldrich). The extracts were centrifuged and the clear supernatants were stored in aliquots at -80°C for further analysis. Protein concentrations of cell lysates were determined by Coomassie protein assay kit (Pierce, Rockford, IL) using BSA as standard. Aliquots of lysates (10 µg of protein) were resolved by 10% SDS-PAGE followed by western blot analysis. The primary antibody against total 4EBP1 (C-19) was purchased from Santa Cruz Biotechnology, Inc. (Santa Cruz, CA). The primary antibodies for mTOR-Ser2448^P, total mTOR, RP-S6-Ser235/236^P, Total RB-S6, and 4EBP1-Ser65^P were obtained from Cell Signaling Technology, Inc. (Beverly, CA). The blots were first incubated with specific primary antibodies followed by secondary antibodies. Specific immunoreactive bands was identified and detected by enhanced chemiluminescence (ECL) using protocol provided by the manufacturer (Kirkegaard & Perry Laboratories, Inc., Gaithersburg, MD). The expression of actin was monitored in parallel as loading control. The intensity of specific immunoreactive bands was quantified by densitometry and expressed as a ratio relative to the expression of actin [133].

ACKNOWLEDGEMENTS

Supported by: NCI, CA RO1 28704, 1 S10 RRO26548-1 and Robert A. Welke Cancer Research Foundation.

Conflict of Interest Statement

The authors of this manuscript have no conflict of interests to declare.

REFERENCES

1. Barzilai A, Yamamoto K. DNA damage responses to oxidative stress. *DNA repair (Amst)* 2004;3:1109-1115.
2. Moller P, Loft S. Interventions with antioxidants and nutrients in relation to oxidative DNA damage and repair. *Mutat Res* 2004;551:79-89.
3. Beckman KB, Ames BN. Oxidative decay of DNA. *J Biol Chem* 1997;272:13300-13305.
4. Vilenchik MM, Knudson AG. Endogenous DNA double-strand breaks: Production, fidelity of repair, and induction of cancer. *Proc Natl Acad Sci USA* 2003;100:12871-12876.
5. Karanjawala ZE, Lieber MR. DNA damage and aging. *Mech Ageing Dev* 2004;125:405-416.
6. Hudson D, Kovalchuk I, Koturbash I, Kolb B, Martin OA, Kovalchuk O. Induction and persistence of radiation-induced DNA damage is more pronounced in young animals than in old animals. *Aging (Albany NY)* 2011;609-620.
7. Schriener SE, Linford NJ, Martin GM, Treuting P, Ogburn CE, Emond M, Coskun PE, Ladiges W, Wolf N, Van Remmen H, Wallace DC, Rabinovitch PS. Extension of murine life span by

over expression of catalase targeted to mitochondria. *Science* 2005;308:1875-1878.

8. Parrinello S, Samper E, Krtolica A, Goldstein J, Melov S, Campisi J. Oxygen sensitivity severely limits the replicative lifespan of murine fibroblasts. *Nat Cell Biol* 2003;5:741-747.
9. Balliet RM, Capparelli C, Guido C, Pestell TG, Martinez-Outschoorn UE, Lin Z, Whitaker-Menezes D, Chiavarina B, Pestell RG, Howell A, Sotgia F, Lisanti MP. Mitochondrial oxidative stress in cancer-associated fibroblasts drives lactate production, promoting breast cancer tumor growth: understanding the aging and cancer connection. *Cell Cycle* 2011;10:4065-4073.
10. Erol A. Genotoxic stress-mediated cell cycle activities for the decision of cellular fate. *Cell Cycle* 2011;10:3239-3248.
11. Lisanti MP, Martinez-Outschoorn UE, Pavlides S, Whitaker-Menezes D, Pestell RG, Howell A, Sotgia F. Accelerated aging in the tumor microenvironment: connecting aging, inflammation and cancer metabolism with personalized medicine. *Cell Cycle* 2011;10:2059-2063.
12. Redon CE, Nakamura AJ, Martin OA, Parekh PR, Weyemi US, Bonner WM. Recent developments in the use of γ-H2AX as a quantitative DNA double-strand break biomarker. *Aging (Albany NY)* 2011;3:168-174.
13. Jeggo PA, Loblrich M. Artemis links ATM to double strand end rejoining. *Cell Cycle* 2005;4:359-362.
14. Seluanov A, Mittelman D, Pereira-Smith OM, Wilson JH, Gorbunova V. DNA end joining becomes less efficient and more error-prone during cellular senescence. *Proc Natl Acad Sci USA* 2004;101:7624-7629.
15. Bogomazova AN, Lagarkova MA, Tskhovrebova LV, Shutova MV, Kiselev SL. Error-prone nonhomologous end joining repair operates in human pluripotent stem cells during late G2. *Aging (Albany NY)* 2011;3:584-596.
16. Dever SM, Golding SE, Rosenberg E, Adams BR, Idowu MO, Quillin JM, Valerie N, Xu B, Povirk LF, Valerie K. Mutations in the BRCT binding site of BRCA1 result in hyper-recombination. *Aging (Albany)* 2011;3:515-532.
17. Dregalla RC, Zhou J, Idate RR, Battaglia CL, Liber HL, Bailey SM. Regulatory roles of tankyrase 1 at telomeres and in DNA repair: suppression of T-SCE and stabilization of DNA-PKcs. *Aging (Albany NY)* 2010;2:691-708.
18. Liu L, Trimarchi JR, Smith PJ, Keete DL. Mitochondrial dysfunction leads to telomere attrition and genomic instability. *Aging Cell* 2002;1:40-46.
19. Kurz DJ, Decary S, Hong Y, Trivier E, Akhmedov A, Erusalimsky JD. Chronic oxidative stress comprises telomere integrity and accelerates the onset of senescence in human endothelial cells. *J Cell Sci* 2004;117:2417-2426.
20. Passos JF, von Zglinicki T. Mitochondria, telomeres and cell senescence. *Exp Gerontol* 2005;40:466-472.
21. Richter T, Proctor C. The role of intracellular peroxide levels on the development and maintenance of telomere-dependent senescence. *Exp Gerontol* 2007;42:1043-1052.
22. Voghel G, Thorin-Trescases N, Mamarbachi AM, Villeneuve L, Malette FA, Farbeyre G, Farhat N, Perrault LP, Carrier M, Therin E. Endogenous oxidative stress prevents telomerase-dependent immortalization of human endothelial cells. *Mech Ageing Dev* 2010;131:354-363.
23. McNeely S, Conti C, Sheikh T, Patel H, Zabudoff S, Pommier Y, Schwartz G, Tse A. Chk1 inhibition after replicative stress activates a double strand break response mediated by ATM and DNA-dependent protein kinase. *Cell Cycle* 2010;9:995-1004.

24. Adams BR, Hawkins AJ, Povirk LF, Valerie K ATM-independent, high-fidelity nonhomologous end joining predominates in human embryonic stem cells. *Aging (Albany NY)* 2010;2:582-596.
25. Li B, Reddy S, Comai L. Depletion of Ku70/80 reduces the levels of extrachromosomal telomeric circles and inhibits proliferation of ALT cells. *Aging (Albany NY)* 2011;3:395-406.
26. Horikawa I, Fujita K, Harris CC. p53 governs telomere regulation feedback too, via TRF2. *Aging (Albany NY)*. 2011;3:26-32.
27. Mason M, Skordalakes E. Insights into Cdc13 dependent telomere length regulation. *Aging (Albany NY)* 2010;2:731-734.
28. Sheppard SA, Loayza D. LIM-domain proteins TRIP6 and LPP associate with shelterin to mediate telomere protection. *Aging (Albany NY)* 2010;2:432-444.
29. Kusumoto-Matsuo R, Opresko PL, Ramsden D, Tahara H, Bohr VA. Cooperation of DNA-PKcs and WRN helicase in the maintenance of telomeric D-loops. *Aging (Albany NY)* 2010;2:274-284.
30. Jee HJ, Kim AJ, Song N, Kim HJ, Kim M, Koh H, Yun J. Nek6 overexpression antagonizes p53-induced senescence in human cancer cells. *Cell Cycle*. 2010;9:4703-4710.
31. Doonan R, McElwee JJ, Matthijssens F, Walker GA, Houthoofd K, Back P, Matscheski A, Vanfleteren JR, Gems D. Against the oxidative damage theory of aging: superoxide dismutases protect against oxidative stress but have little or no effect on life span in *Caenorhabditis elegans*. *Genes Dev* 2008;22:3236-3241.
32. Gems D, Doonan R. Antioxidant defense and aging in *C. elegans*: Is the oxidative damage theory of aging wrong? *Cell Cycle* 2009;8:1681-1687.
33. Blagosklonny MV. Program-like aging and mitochondria: instead of random damage by free radicals. *J Cell Biochem* 2007;102:1389-1399.
34. Blagosklonny MV. Aging: ROS or TOR. *Cell Cycle*. 2008;7:3344-3354.
35. Blagosklonny MV. Paradoxes of aging. *Cell Cycle* 2007;6:2997-3003.
36. Blagosklonny MV. mTOR-driven aging: speeding car without brakes. *Cell Cycle* 2009;8:4055-4059.
37. Blagosklonny MV. Revisiting the antagonistic pleiotropy theory of aging: TOR-driven program and quasi-program. *Cell Cycle* 2010;9:3151-3156.
38. Cabreiro F, Ackerman D, Doonan R, Araiz C, Back P, Papp D, Braeckman BP, Gems D. Increased life span from overexpression of superoxide dismutase in *Caenorhabditis elegans* is not caused by decreased oxidative damage. *Free Radic Biol Med* 2011;51:1575-1582.
39. Lapointe J, Hekimi S. When a theory of aging ages badly. *Cell Mol Life Sci*. 2009;67:1-8.
40. Speakman JR, Selman C. The free-radical damage theory: Accumulating evidence against a simple link of oxidative stress to ageing and lifespan. *Bioessays* 2011;33:255-259.
41. Heeren G, Rinnerthaler M, Laun P, von Seyerl P, Kössler S, Klinger H, Hager M, Bogengruber E, Jarolim S, Simon-Nobbe B, Schüller C, Carmona-Gutierrez D, et al. The mitochondrial ribosomal protein of the large subunit, Afo1p, determines cellular longevity through mitochondrial back-signaling via TOR1. *Aging (Albany NY)*. 2009;1:622-636.
42. Hay N, Sonenberg N. Upstream and downstream of mTOR. *Genes Dev* 2004;18:1926-1945.
43. Hands SL, Proud CG, Wyttenbach A. mTOR's role in ageing: protein synthesis or autophagy? *Aging (Albany NY)* 2009;1:586-597.
44. Blagosklonny MV, Hall MN. Growth and aging: a common molecular mechanism. *Aging (Albany NY)* 2009;1:357-362.
45. Wullschleger S, Loewith R, Hall MN. TOR signaling in growth and metabolism. *Cell* 2006;124:471-484.
46. Magnuson B, Ekim B, Fingar DC. Regulation and function of ribosomal protein S6 kinase (S6K) within mTOR signalling networks. *Biochem J* 2012;441:1-21.
47. Loewith R, Hall MN. Target of rapamycin (TOR) in nutrient signaling and growth control. *Genetics* 2011;189:1177-1201.
48. Zoncu R, Efeyan A, Sabatini DM. mTOR: from growth signal integration to cancer, diabetes and ageing. *Nat Rev Mol Cell Biol* 2010;12:21-35.
49. Ma XM, Blenis J. Molecular mechanisms of mTOR-mediated translational control. *Nat Rev Mol Cell Biol* 2009;10:307-318.
50. Burhans WC, Weinberger M. DNA replication stress, genome instability and aging. *Nucleic Acids Res* 2007;35:7545-7556.
51. McKenna E, Traganos F, Zhao H, Darzynkiewicz Z. Persistent DNA damage caused by low levels of mitomycin C induces irreversible senescence of A549 cells. *Cell Cycle* 2012;11:3132-3140.
52. Huang X, Tanaka T, Kurose A, Traganos F, Darzynkiewicz Z. Constitutive histone H2AX phosphorylation on Ser-139 in cells untreated by genotoxic agents is cell-cycle phase specific and attenuated by scavenging reactive oxygen species. *Int J Oncol* 2006;29:495-501.
53. Tanaka T, Halicka HD, Huang X, Traganos F, Darzynkiewicz Z. Constitutive histone H2AX phosphorylation and ATM activation, the reporters of DNA damage by endogenous oxidants. *Cell Cycle* 2006;5:1940-1945.
54. Zhao H, Tanaka T, Halicka HD, Traganos F, Zarebski M, Dobrucki J, Darzynkiewicz Z. Cytometric assessment of DNA damage by exogenous and endogenous oxidants reports the aging-related processes. *Cytometry A* 2007;71A:905-914.
55. Halicka HD, Zhao H, Li J, Traganos F, Zhang S, Lee M, Darzynkiewicz Z. Genome protective effect of metformin as revealed by reduced level of constitutive DNA damage signaling. *Aging (Albany NY)* 2011;3:1028-1038.
56. Halicka HD, Zhao H, Li J, Traganos DF, Studzinski G, Darzynkiewicz Z. Attenuation of constitutive DNA damage signaling by 1,25-dihydroxyvitamin D3. *Aging (Albany NY)* 2012;4:270-278.
57. Zhao H, Tanaka T, Mitlitski V, Heeter J, Balazs EA, Darzynkiewicz Z. Protective effect of hyaluronate on oxidative DNA damage in WI-38 and A549 cells. *Int J Oncol* 2008;32:1159-1169.
58. Halicka HD, Ita M, Tanaka T, Kurose A, Darzynkiewicz Z. The biscoclaurine alkaloid cepharanthine protects DNA in TK6 lymphoblastoid cells from constitutive oxidative damage. *Pharmacol Rep* 2008;60:93-100.
59. Yang NC, Song TY, Chen MY, Hu ML. Effects of 2-deoxyglucose and dehydroepiandrosterone on intracellular NAD(+) level, SIRT1 activity and replicative lifespan of human Hs68 cells. *Biogerontology* 2011;12:527-536.
60. Ingram DK, Roth GS. Glycolytic inhibition as a strategy for developing calorie restriction mimetics. *Exp Gerontol* 2011;46:148-154.
61. Smith DL, Nagy TR, Allison DB. Calorie restriction: what recent results suggest for the future of ageing research. *Eur J Clin Invest* 2010;40:440-450.

62. Blagosklonny MV. Calorie restriction: decelerating mTOR-driven aging from cells to organisms (including humans) *Cell Cycle* 2010;9:683–688.
63. Anisimov VN, Berstein LM, Popovich IG, Zabezhinski MA, Egormin PA, Piskunova TS, Semenchenko AV, Tyndyk ML, Yurova MN, Kovalenko IG, Poroshina TE. If started early in life, metformin treatment increases life span and postpones tumors in female SHR mice. *Aging (Albany NY)*. 2011 Feb;3:148-157.
64. Menendez JA, Cufí S, Oliveras-Ferraro C, Vellon L, Joven J, Vazquez-Martin A. Gerosuppressant metformin: less is more. *Aging (Albany NY)* 2011;3:348-362.
65. Blagosklonny MV Metformin and sex: Why suppression of aging may be harmful to young male mice. *Aging (Albany NY)* 2010;2:897-899.
66. Anisimov VN, Piskunova TS, Popovich IG, Zabezhinski MA, Tyndyk ML, Egormin PA, Yurova MV, Rosenfeld SV, Semenchenko AV, Kovalenko IG, Poroshina TE, Berstein LM. Gender differences in metformin effect on aging, life span and spontaneous tumorigenesis in 129/Sv mice. *Aging (Albany)* 2010;2:945-958.
67. Mashhedi H, Blouin MJ, Zakikhani M, David S, Zhao Y, Bazile M, Birman E, Algire C, Aliaga A, Bedell BJ, Pollak M. Metformin abolishes increased tumor (18)F-2-fluoro-2-deoxy-D-glucose uptake associated with a high energy diet. *Cell Cycle*. 2011 Aug 15;10:2770-2778.
68. Bernstein LM. Metformin in obesity, cancer and aging: addressing controversies. *Aging (Albany)* 2012;4:320-329.
69. Bulterijs S. Metformin as a geroprotector. *Rejuvenation Res* 2011;14:469-482.
70. Anisimov VN, Metformin for aging and cancer prevention. *Aging (Albany NY)* 2010;2:760-774.
71. Pollak MN. Investigating metformin for cancer prevention and treatment: the end of the beginning. *Cancer discovery* 2012;2:778-790.
72. Zheng XF. Chemoprevention of age-related macular regeneration (AMD) with rapamycin. *Aging (Albany)*. 2012;4:375-376.
73. Blagosklonny MV. Once again on rapamycin-induced insulin resistance and longevity: despite of or owing to. *Aging (Albany)*. 2012;4:350-358.
74. Khanna A, Kapahi P. Rapamycin: killing two birds with one stone. *Aging (Albany NY)*. 2011;3:1043-1044.
75. Leontieva OV, Blagosklonny MV. DNA damaging agents and p53 do not cause senescence in quiescent cells, while consecutive re-activation of mTOR is associated with conversion to senescence. *Aging (Albany NY)*. 2010;2:924-235.
76. Wesierska-Gadek J. mTOR and its link to the picture of Dorian Gray - re-activation of mTOR promotes aging. *Aging (Albany NY)*. 2010;2:892-893.
77. Galluzzi L, Kepp O, Kroemer G. TP53 and MTOR crosstalk to regulate cellular senescence. *Aging (Albany NY)*. 2010;2:535-537.
78. Anisimov VN, Zabezhinski MA, Popovich IG, Piskunova, TS, Semenchenko, AV, Tyndyk ML, Yurova MN, Antoch MP, Blagosklonny MV. Rapamycin extends maximal lifespan in cancer-prone mice. *Am J Pathol* 2010;176:2092-2097
79. Pospelova TV, Leontieva OV, Bykova TV, Zubova SG, Pospelov VA, Blagosklonny MV. Suppression of replicative senescence by rapamycin in rodent embryonic cells. *Cell Cycle* 2012;11:2402-2407,
80. Wilkinson JE, Burmeister L, Brooks SV, Chan CC, Friedline S, Harrison DE, Hejtmancik JF, Nadon N, Strong R, Wood LK, Woodward MA, Miller RA. Rapamycin slows aging in mice. *Aging Cell* 2012;11:675-682.
81. Wang Q, Zhang M, Liang B, Shirwany N, Zhu Y, Zou MH. Activation of AMP-activated protein kinase is required for berberine-induced reduction of arteriosclerosis in mice: the role of uncoupling protein 2. *PLoS One* 2011; e25436.
82. Li H, Miyahara T, Tezuka Y, Tran OL, Seto H, Kadota S. Effect of berberine on bone mineral density in SAMP6 as a senile osteoporosis model. *Biol Pharma Bull* 2003;26:130-131.
83. Ki HF, Shen L. Berberine: a potential multipotent natural product to combat Alzheimer's Disease. *Molecules* 2011;16:6732-6740.
84. Cicero AF, Tartagani E. Antidiabetic properties of berberine: from cellular pharmacology to clinical effects. *Hosp Pract (Minneapolis)* 2012;40:56-63.
85. Shen N, Huan Y, Shen ZF. Berberine inhibits mouse insulin gene promoter through activation of AMP activated protein kinase and may exert beneficial effect on pancreatic β -cell. *Eur J Pharmacol* 2012; S0014-2099, 00697-8 (Epub).
86. Klotz B, Mentrup B, Regensburger M, Zeck S, Schneidereit J, Schupp N, Linded C, Merz C, Ebert R, Jakob F. 1,25-dihydroxyvitamin D3 treatment delays cellular aging in human mesenchymal stem cells while maintaining their multipotent capacity. *PLoS One* 2012;7:e29959 Epub Jan 5.
87. Haussler MR, Haussler CA, Whitfield GK, Hsieh JC, Thompson PD, Barthel TK, Bartik L, Egan JB, Wu Y, Kubicek JL, Lowmiller CL, Moffet EW, Forster RE, Jurutka PW. The nuclear vitamin D receptor controls the expression of genes encoding factors which feed the "Fountain of Youth" to mediate healthful Aging. *J Steroid Biochem Mol Biol* 2010;121:88-97.
88. Touhimm P. Vitamin D and aging. *J Steroid Biochem Mol Biol* 2009;114:78-84.
89. Lanske B, Razzaque MS. Vitamin D and aging: old concepts and new insights. *J Nutr Biochem* 2007;18:771-777.
90. Forster RE, Jurutka PW, Hsieh JC, Haussler CA, Lowmiller CL, Kaneko I, Haussler MR, Kerr WH. Vitamin D receptor controls expression of the anti-aging klotho gene in mouse and human renal cells. *Biochem Biophys Res Commun* 2011;414:557-562.
91. Yang J, Ikezoe T, Nishioka C, Ni L, Koeffler HP, Yokoyama, A. Inhibition of mTORC1 by RAD001 (everolimus) potentiates the effects of 1,25-dihydroxyvitamin D(3) to induce growth arrest and differentiation of AML cells in vitro and in vivo. *Exp Hematol* 2010;38:666-676.
92. Vetterli L, Maechler P. Resveratrol-activated SIRT1 in liver and pancreatic β -cells: a Janus head looking to the same direction of metabolic homeostasis. *Aging (Albany NY)*. 2011;3:444-449.
93. Gerhardt E, Graber S, Szego EM, Moisol N, Martins LM, Outeiro TF, Kermer P. Idebebone and resveratrol extend life span and improve motor function of Htra2 knockout mice. *PLoS One* 2011;6:e28855. Epub Dec 19.
94. Rascon B, Hubbard BP, Sinclair DA, Amdam GV. The lifespan extension effects of resveratrol are conserved in the honey bee and may be driven by a mechanism related to caloric restriction. *Aging (Albany NY)* 2012;4:499-508.
95. Chung JH, Manganiello V, Dyck JR. Resveratrol as a calorie restriction mimetic: therapeutic implications. *Trends Cell Biol* 2012; Aug 9 (Epub).
96. Timmers S, Auwerx J, Schrauwen P. The journey of resveratrol from yeast to human. *Aging (Albany NY)* 2012;4:146-158.

97. Bass TM, Weinkove G, Hourthoofd K, Gems D, Partridge L. Effects of resveratrol on lifespan in *Drosophila melanogaster* and *Caenorhabditis elegans*. *Mech Ageing Dev* 2007;128:546–552.
98. Ayyadevara S, Bharill P, Dandapat A, Hu C, Khaidakov M, Mitra S, Shmookler Reis RJ, Mehta JL. Aspirin inhibits oxidant stress, reduces age-associated functional declines, and extends lifespan of *Caenorhabditis elegans*. *Antioxid Redox Signal* 2012 Sept 7 Epub.
99. Bode-Boger SM, Martens-Lobenhoffer J, Tager M, Schroder H, Scalera F. Aspirin reduces endothelial cell senescence. *Biochem Biophys Res Commun* 2005;334:1226-1232.
100. Strong B, Miller RA, Astie CM, Floyd RA, Flurkey K, Hensley KL, Javors MA, Leeuwenburgh C, Nelson JF, Ongini E, Nadon NL, Warner HR, Harrison DE. Nordihydroguaiaretic acid and aspirin increase lifespan of genetically heterogeneous male mice. *Aging Cell* 2008;7: 641-650.
101. Yi TN, Zhao HY, Zhang JS, Shan HY, Meng X, Zhang J. Effect of aspirin on high glucose-induced senescence of endothelial cells. *Chin Med J (Engl)* 2009; 20:122:3055-3061.
102. McIlhatton MA, Tyler J, Kerepesi LA, Bocker-Edmonston T, Kucherlapati MH, Edelmann W, Kucherlapati R, Kopelovich L, Fishel L. Aspirin and low-dose nitric-oxide-donating aspirin increase life span in a Lynch syndrome mouse model. *Cancer Prev Res (Phila)* 2011;4:684-693.
103. Bulckaen H, Prevost G, Boulanger E, Robitaille G, Roquet V, Gaxatte C, Garcon G, Corman B, Gosset, P, Shirali P, Creusy C, Puisieux F. Low-dose aspirin prevents age-related endothelial dysfunction in a mouse model of physiological aging. *Am J Physiol Heart Circ Physiol* 2008;294:H1562-70.
104. Pozarowski P, Holden E, Darzynkiewicz Z. Laser scanning cytometry: Principles and applications. An update. *Meth Molec Biol* 2013;913:187-212.
105. Ruvinsky I, Sharon N, Lerer T, Cohen H, Stolovich-Rain M, Nir T, Dor Y, Zisman O, Meyuhav O. Ribosomal protein S6 phosphorylation is a determinant of cell size and glucose homeostasis. *Genes & Dev* 2005;19:2199-2211.
106. Fingar, D. Salama C., S., Tsou C., Harlow E., Blenis J. Mammalian cell size is controlled by mTOR and its downstream targets S6K1 and 4EBP1/eIF4E. *Genes Dev* 2002;16:1472–1487.
107. Nyfeler B, Bergman P, Triantafellow E, Wilson CJ, Zhu Y, Radetich B, Finan PM, Klionsky DJ, Murphy LO. Relieving autophagy and E4BP1 from rapamycin resistance. *Mol Cell Biol* 2011;31:2867-2876.
108. Chao SK, Horwitz SB, McDaid HM. Insights into 4E-bp1 and p53 mediated regulation of accelerated cell senescence. *Oncotarget* 2011;2:89-98.
109. Bartke A. Insulin and aging. *Cell Cycle* 2008;3338-3343.
110. Darzynkiewicz Z, Krassowski T, Skopinska E. Effect of phytohemagglutinin on synthesis of "rapidly labeled" ribonucleic acid in human lymphocytes. *Nature* 1965;207:1402-1403.
111. Darzynkiewicz Z, Traganos F, Sharpless T, Melamed MR. Lymphocyte stimulation: A rapid multiparameter analysis. *Proc Natl Acad Sci USA* 1976;73:2881-2884.
112. Tanaka T, Kajstura M, Halicka HD, Traganos F, Darzynkiewicz Z. Constitutive histone H2AX phosphorylation and ATM activation are strongly amplified during mitogenic stimulation of lymphocytes. *Cell Prolif* 2007;40:1-13.
113. Lai KP, Leong WF, Chau IF, Jia D, Zeng L, Liu H, He L, Hao A, Zhang H, Meek D, Velagapudi C, Habib SL, Li B. S6K1 is a multifaceted regulator of Mdm2 that connects nutrient status and DNA damage response. *EMBO J* 2010;29:2994-3006.
114. Ditch S, Paull TT. The ATM protein kinase and cellular redox signaling: beyond the DNA damage response. *Trends Biochem Sci* 2012;37:15-22.
115. Zajkovicz A, Rusin M. The activation of the p53 pathway by the AMP mimetic AICAR is reduced by inhibitors of the ATM or mTOR kinases. *Mech Ageing Dev* 2011;132:543-551.
116. Mukherjee B, Tomimatsu N, Amanchela K, Camacho CV, Pichamoorthy N, Burma S. The dual PI3K/mTOR inhibitor NVP-BEZ235 is a potent inhibitor of ATM- and DNA-PKCs-mediated DNA damage responses. *Neoplasia* 2012;14:34-43.
117. Darzynkiewicz Z. Another "Janus paradox" of p53: induction of cell senescence versus quiescence. *Aging (Albany NY)* 2010;2:329-330.
118. Darzynkiewicz Z. Running m(o)TOR with the brakes on leads to catastrophe at mitosis. *Cell Cycle* 2012, 11.
119. Darzynkiewicz Z, Traganos F, Staiano-Coico L, Kapuscinski J, Melamed MR. Interactions of rhodamine 123 with living cells studied by flow cytometry. *Cancer Res* 1982;42:799-806.
120. Darzynkiewicz Z, Staiano-Coico L, Melamed MR. Increased mitochondrial uptake of rhodamine 123 during lymphocyte stimulation. *Proc Natl Acad Sci USA* 1981;78:2383-2387.
121. Smith CP, Thersness PE. Formation of energized inner membrane in mitochondria with a gamma-deficient F1-ATPase. *Eukaryot Cell* 2005;4:2078-2086.
122. Li D. Metformin as an antitumor agent in cancer prevention and treatment. *J Diabetes* 2011;3:320-327.
123. Buitrago-Molina LE, Vogel A. mTOR as a potential target for the prevention and treatment of hepatocellular carcinoma. *Curr Cancer Drug Target* 2012; Aug 7 Epub.
124. Kajsar J. Will an aspirin a day keep cancer away? *Science* 2012; 337: 1471-1473.
125. Anis KV, Rajeshkumar NV, Kuttan R. Inhibition of chemical carcinogenesis by berberine in rats and mice. *J Pharm Pharmacol* 2001;53:763-768.
126. Zhu Z, Jiang W, McGinley JN, Thompson HJ. 2-Deoxyglucose as an energy restriction mimetic agent: effects on mammary carcinogenesis and on mammary tumor cell growth in vitro. *Cancer Res* 2005;65:7023-7030.
127. Juan ME, Alfaras I, Planas JM. Colorectal cancer chemoprevention by trans-resveratrol. *Pharmacol Res* 2012;65:584-5891.
128. Trump DL, Deeb KK, Johnson CS. Vitamin D: considerations in the continued development as an agent for cancer prevention and therapy. *Cancer J* 2010;16:1-9.
129. Darzynkiewicz Z, Zhao H, Halicka HD, Rybak P, Dobrucki J, Wlodkovic D. DNA damage signaling assessed in individual cells in relation to the cell cycle phase and induction of apoptosis. *Crit Rev Clin Lab Sci* 2012; 2012;49:199-217.
130. Rothe G, Klouche M. Phagocyte functions. *Meth Cell Biol* 2004;75:679-708.
131. Darzynkiewicz Z, Bedner E, Gorczyca W, Melamed MR. Laser scanning cytometry. A new instrumentation with many applications. *Exp Cell Res* 1999; 249:1-12.
132. Mikes V, Dadak V. Berberine derivatives are cationic fluorescent probes for the investigation of the energized state of mitochondria. *Biochim Biophys Acta* 1983;723:231-239.
133. Hsieh TC, Yang CJ, Lin CY, Lee YS, Wu JM. Control of stability of cyclin D1 by quinone reductase 2 in CWR22Rv1 prostate cancer cells. *Carcinogenesis*. 2012;33:670-677.

One-carbon metabolism: An aging-cancer crossroad for the gerosuppressant metformin

Javier A. Menendez^{1,2} and Jorge Joven³

¹ Metabolism & Cancer Group, Translational Research Laboratory, Catalan Institute of Oncology-Girona (ICO-Girona), Girona, Spain

² Molecular Oncology, Girona Biomedical Research Institute (IDIBGi), Girona, Spain

³ Unitat de Recerca Biomèdica (URB-CRB), Institut d'Investigació Sanitària Pere i Virgili (IISPV), Universitat Rovira i Virgili, Reus, Spain.

Key words: metformin, one-carbon metabolism, nucleotides, purines, AMP, ATP, AMPK, mTOR, gerosuppression, aging, cancer

Correspondence to: Javier A. Menendez, PhD; **E-mail:** jmenendez@iconcologia.net; jmenendez@idibgi.org

Copyright: © Menendez and Joven. This is an open-access article distributed under the terms of the Creative Commons Attribution License, which permits unrestricted use, distribution, and reproduction in any medium, provided the original author and source are credited

Abstract: The gerosuppressant metformin operates as an efficient inhibitor of the mTOR/S6K1 gerogenic pathway due to its ability to ultimately activate the energy-sensor AMPK. If an aging-related decline in the AMPK sensitivity to cellular stress is a crucial event for mTOR-driven aging and aging-related diseases, including cancer, unraveling new proximal causes through which AMPK activation endows its gerosuppressive effects may offer not only a better understanding of metformin function but also the likely possibility of repositioning our existing gerosuppressant drugs. Here we provide our perspective on recent findings suggesting that *de novo* biosynthesis of purine nucleotides, which is based on the metabolism of one-carbon compounds, is a new target for metformin's actions at the crossroads of aging and cancer.

It is perhaps not surprising that the cellular energy sensor adenosine monophosphate (AMP)-activated protein kinase (AMPK), a critical suppressor of the mTOR gerogene [1-17], has been once again highlighted as a conserved life span modulator linking bioenergetics, metabolism, and longevity [12-22]. What is certainly surprising is the *proximate* causation through which AMPK activation has now been shown to enable its pro-longevity effects. When searching for mutations capable of disrupting energy balance in metabolically active tissues and slowing aging in the fruit fly *Drosophila melanogaster*, Stenesen and colleagues [23] recently found that the inactivation of genes coding for enzymes involved in the *de novo* synthesis of the purine nucleotide AMP demonstrated the strongest pro-longevity effects. Interestingly, mutations in AMP biosynthetic enzymes capable of significantly extending the *Drosophila* lifespan impacted cellular bioenergetics by unexpectedly increasing the AMP:ATP and ADP:ATP ratios, thus

counter intuitively mimicking the effects of energy depletion (e.g., dietary restriction), despite disrupting AMP biosynthesis [23, 24]. AMPK, the cellular fuel gauge whose activity becomes significantly increased in long-lived flies, detects such energy imbalances to causally channel longevity effects resulting from genetically impaired *de novo* AMP synthesis. While the expression of a dominant-negative form of AMPK prevented the lifespan increases driven by heterozygous mutations in AMP biosynthetic enzymes, animals engineered to specifically exhibit AMPK gain-of-function in metabolic tissues also had lifespan increases equivalent to those observed in long-lived fly mutants. Therefore, enhanced AMPK activity appears to be sufficient to fully recapitulate the ability of AMP biosynthesis pathway mutations to increase the AMP:ATP ratio and longevity.

In the novel scenario illustrated by Stenesen and colleagues [23], it reasonably follows that small

molecule drugs capable of mimicking the energy imbalance imposed by mutations in the AMP biosynthesis pathway may be expected to increase healthy life spans by activating AMPK. Moreover, given that AMPK is a crucial gerosuppressor (and tumor-suppressor) that impedes mTOR-driven geroconversion (and mTOR-driven malignant transformation) [1-17], small molecules capable of activating AMPK by altering the *de novo* synthesis of purine nucleotides such as AMP should be expected to not only inhibit the pro-aging activity of mTOR gerogenes but also prevent aging-related diseases, such as cancer. The antidiabetic biguanide metformin may fulfill all of these requirements. First, epidemiological, preclinical, and clinical evidence from the last five years has demonstrated the multi-faceted capabilities of metformin in preventing and treating human carcinomas [25-35]. Second, metformin, independently of the insulin-signaling pathway, has been noted to significantly extend the healthy lifespan of not only non-diabetic mice but also the nematode *Caenorhabditis elegans* [36-42]. AMPK, which is activated in mammals by metformin treatment, has also been found to be an essential molecular operative for metformin healthspan benefits in *C. elegans* [42], thus suggesting that the metformin gerosuppressant activity largely depends on its ability to engage the same metabolic sensor, i.e., AMPK, which is highly conserved across phyla. Third, metformin prevents cancer and extends the lifespan of cancer-prone rodent strains. Moreover, metformin can also prolong lifespan without affecting cancers in non-cancer-prone rodent strains [36-41]. Although the latter discrepancy may suggest that metformin could delay aging (and prolong life) by mechanisms unrelated to its ability to suppress cancer, it may not if this discrepancy simply relies on a cancer-related enhancement of common proximate anti-aging mechanisms by which metformin can activate the gerosuppressor/tumor suppressor AMPK. One such mechanism may be one-carbon metabolism that drives the *de novo* synthesis of purine nucleotides (e.g., AMP).

It is well known that the relative contribution of nucleotide biosynthesis to nucleotide pool maintenance via the *de novo* and salvage pathways significantly varies in different cells and tissues. Proliferating cells, including cancer cells, usually require a functional *de novo* pathway to sustain their increased nucleotide demands. Indeed, this activity is the basis for the use of antifolate drugs in chemotherapy against cancer cells, which generally have higher DNA turnover. Crucially, a recently identified metabolomic fingerprint of human cancer cells treated with metformin revealed for the first time its previously unrecognized ability to significantly impair one-carbon metabolism and the *de novo*

biosynthesis of purine nucleotides in a manner that is functionally similar but mechanistically different than that of the antifolate class of chemotherapy drugs [43]. Of note, the ability of metformin to activate the AMPK metabolic tumor suppressor and inhibit cancer cell growth was notably prevented when the salvage branch of purine biosynthesis was promoted by exogenous supplementation with the pre-formed substrate hypoxanthine, a spontaneous deamination product of the purine adenine. Remarkably, Stenesen and colleagues [23] similarly found that dietary supplementation with adenine, the pre-formed substrate of AMP biosynthesis, not only markedly reversed the lifespan extension of AMP biosynthesis mutants but also the pro-longevity effects of dietary restriction. The recognition of *de novo* AMP biosynthesis, adenosine nucleotide ratios, and AMPK as determinants of the *Drosophila* adult lifespan and the finding that the anti-cancer activity of metformin could be explained in terms of the secondary activation of AMPK following the alteration of the essential carbon flow that leads to the *de novo* synthesis of purines both strongly suggest that the flow of one-carbon groups governing the *de novo* biosynthesis of purines could represent a crucial metformin-targeted intersection of aging with cancer (Fig. 1).

Because a ubiquitous event in cancer metabolism is the early, constitutive activation of one-carbon metabolism and because *de novo* nucleotide biosynthesis may influence cancer mortality due to its critical role in DNA synthesis and methylation, the repeatedly suggested reduction in cancer risk and mortality of diabetic patients chronically treated with metformin may therefore represent an unintended metronomic chemotherapy approach targeting the differential utilization of *de novo* one-carbon metabolism by malignant and non-malignant cells [43]. In light of the findings by Stenesen and colleagues [23], it may be reasonable to suggest that metformin treatment may silently operate not only to eliminate genetically damaged, initiated, or malignant cells addicted to higher nucleotide concentrations but also activate the gerosuppressant activity of AMPK by unbalancing the *de novo* biogenesis of the purine AMP in metabolically active tissues (Fig. 1). It may be argued that the ability of metformin to activate AMPK following the inhibition of one-carbon metabolism indicates its teratogenic potential [43, 44]. Although one study reported no alterations in embryonic growth and no major malformations during mouse embryogenesis, it is noteworthy that the metformin analog phenformin, an AMPK activator that is more potent than metformin, remarkably produced embryoletality and embryo malformations, including neural tube closure defects and craniofacial hypoplasia

[44]. Future studies may elucidate whether phenformin has a stronger inhibitory effect on *de novo* purine biosynthesis compared with metformin.

Nevertheless, we should acknowledge that while high doses of metformin have been reported to increase the lifespan of *C. elegans* in an AMPK-dependent manner [42], this metformin effect could not be observed in fruit flies [45]. Thus, while AMPK activation increases lifespan in *Drosophila*, metformin supplementation does not. Forthcoming studies should determine whether the lack of equivalence between feeding metformin and activating AMPK may be due to either off-target detrimental metformin effects or the detrimental effects of systemically activating AMPK in relevant *versus* non-relevant tissues for lifespan extension [24]. In this regard, it should also be considered that while previous studies in fibroblasts and rat hepatoma cells have shown that AMPK activation by metformin occurred by mechanisms other than changes in the cellular AMP:ATP ratio [46], recent evidence in

primary hepatocytes has revealed that metformin activates AMPK by decreasing the cellular energy status *via* a significant rise in the cellular AMP:ATP ratio [47]. Moreover, metformin has been reported to mimic a low-energy AMPK-activating state by increasing AMP levels through the inhibition of AMP deaminase (AMPD) in skeletal muscle cells and the development of fatty liver [48, 49]. Curiously, when Stenesen and colleagues [23] tested the longevity effects of an insertional mutation in AMPD that catalyzes the hydrolytic deamination of AMP into inosine monophosphate, i.e., the opposite direction of the longevity genes adenylosuccinate synthetase, adenylosuccinate lyase, adenosine kinase, and adenine phosphoribosyltransferase, they failed to observe any effects on lifespan. Whether the metformin ability to directly [48] or indirectly inhibit AMPD, such as through the accumulation of intermediates during the folate-dependent metabolism of one carbon unit [43], could counteract the longevity induced by AMPK activation certainly merits further exploration.

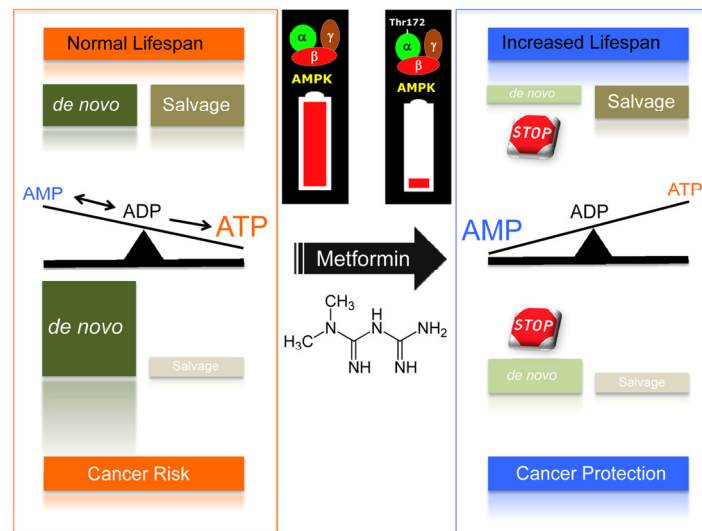


Figure 1. *De novo* biosynthesis of purine nucleotide at the crossroads of aging and cancer: A new target for the gerosuppressant metformin.

The molecular mechanism(s) through which the gerosuppressant metformin could increase life span and delay tumor formation and progression remain unclear. Most studies have focused on *ultimate causes*, which mostly involve the reasons why metformin has beneficial effects. An ever-growing experimental body of evidence strongly suggests that metformin operates as an efficient inhibitor of the mTOR/S6K1 gerogenic pathway due to its ability to ultimately activate the AMPK energy-sensor in a cell-autonomous manner. If an aging-related decline in the AMPK sensitivity to cellular stress is a crucial event for mTOR-driven aging and aging-related diseases, including cancer, it is now time to explore molecular events that primarily involve the “how” questions; unraveling new *proximal causes* through which AMPK activation endows its gerosuppressive effects may offer not only a better understanding of metformin function but also the likely possibility of repositioning our existing gerosuppressant drugs.

ACKNOWLEDGEMENTS

This work was financially supported by the Instituto de Salud Carlos III (Ministerio de Sanidad y Consumo, Fondo de Investigación Sanitaria (FIS), Spain, grants CP05-00090, PI06-0778 and RD06-0020-0028), the Fundación Científica de la Asociación Española Contra el Cáncer (AECC, Spain), and the Ministerio de Ciencia e Innovación (SAF2009-11579, Plan Nacional de I+D+I, MICINN, Spain).

Conflict of Interest Statement

The authors of this manuscript have no conflict of interests to declare.

REFERENCES

1. Blagosklonny MV. Rapamycin and quasi-programmed aging: four years later. *Cell Cycle*. 2010; 9:1859-1862.
2. Blagosklonny MV. Why men age faster but reproduce longer than women: mTOR and evolutionary perspectives. *Aging (Albany NY)*. 2010; 2:265-273.
3. Blagosklonny MV. Calorie restriction: decelerating mTOR-driven aging from cells to organisms (including humans). *Cell Cycle*. 2010; 9:683-688.
4. Blagosklonny MV. Increasing healthy lifespan by suppressing aging in our lifetime: preliminary proposal. *Cell Cycle*. 2010;9:4788-4794.
5. Blagosklonny MV. Why human lifespan is rapidly increasing: solving "longevity riddle" with "revealed-slow-aging" hypothesis. *Aging (Albany NY)*. 2010; 2:177-182.
6. Wang C, Maddick M, Miwa S, Jurk D, Czapiewski R, Saretzki G, Langie SA, Godschalk RW, Cameron K, von Zglinicki T. Adult-onset, short-term dietary restriction reduces cell senescence in mice. *Aging (Albany NY)*. 2010; 2:555-566.

7. Blagosklonny MV. Cell cycle arrest is not senescence. *Aging (Albany NY)*. 2011; 3:94-101.
8. Blagosklonny MV. Progeria, rapamycin and normal aging: recent breakthrough. *Aging (Albany NY)*. 2011; 3:685-691.
9. Anisimov VN, Zabezhinski MA, Popovich IG, Piskunova TS, Semenchenko AV, Tyndyk ML, Yurova MN, Rosenfeld SV, Blagosklonny MV. Rapamycin increases lifespan and inhibits spontaneous tumorigenesis in inbred female mice. *Cell Cycle*. 2011;10:4230-4236.
10. Leontieva OV, Blagosklonny MV. Yeast-like chronological senescence in mammalian cells: phenomenon, mechanism and pharmacological suppression. *Aging (Albany NY)*. 2011; 3:1078-1091.
11. Blagosklonny MV. Hormesis does not make sense except in the light of TOR-driven aging. *Aging (Albany NY)*. 2011; 3:1051-1062.
12. Blagosklonny MV. Molecular damage in cancer: an argument for mTOR-driven aging. *Aging (Albany NY)*. 2011; 3:1130-1141.
13. Blagosklonny MV. Cell cycle arrest is not yet senescence, which is not just cell cycle arrest: terminology for TOR-driven aging. *Aging (Albany NY)*. 2012; 4:159-165.
14. Blagosklonny MV. Prospective treatment of age-related diseases by slowing down aging. *Am J Pathol*. 2012; 181:1142-1146.
15. Komarova EA, Antoch MP, Novototskaya LR, Chernova OB, Paszkiewicz G, Leontieva OV, Blagosklonny MV, Gudkov AV. Rapamycin extends lifespan and delays tumorigenesis in heterozygous p53+/- mice. *Aging (Albany NY)*. 2012;4:709-714.
16. Comas M, Toshkov I, Kuropatwinski KK, Chernova OB, Polinsky A, Blagosklonny MV, Gudkov AV, Antoch MP. New nanoformulation of rapamycin Rapatar extends lifespan in homozygous p53-/- mice by delaying carcinogenesis. *Aging (Albany NY)*. 2012; 4:715-722.
17. Johnson SC, Rabinovitch PS, Kaeberlein M. mTOR is a key modulator of ageing and age-related disease. *Nature*. 2013; 493:338-345.
18. Menendez JA, Cufi S, Oliveras-Ferraro C, Martin-Castillo B, Joven J, Vellon L, Vazquez-Martin A. Metformin and the ATM DNA damage response (DDR): accelerating the onset of stress-induced senescence to boost protection against cancer. *Aging (Albany NY)*. 2011; 3:1063-1077.
19. Menendez JA, Cufi S, Oliveras-Ferraro C, Vellon L, Joven J, Vazquez-Martin A. Gerosuppressant metformin: less is more. *Aging (Albany NY)*. 2011; 3:348-362.
20. Menendez JA, Vellon L, Oliveras-Ferraro C, Cufi S, Vazquez-Martin A. mTOR-regulated senescence and autophagy during reprogramming of somatic cells to pluripotency: a roadmap from energy metabolism to stem cell renewal and aging. *Cell Cycle*. 2011;10:3658-3677.
21. Vazquez-Martin A, Vellon L, Quirós PM, Cufi S, Ruiz de Galarreta E, Oliveras-Ferraro C, Martin AG, Martin-Castillo B, López-Otín C, Menendez JA. Activation of AMP-activated protein kinase (AMPK) provides a metabolic barrier to reprogramming somatic cells into stem cells. *Cell Cycle*. 2012; 11:974-989.
22. Salminen A, Kaarniranta K. AMP-activated protein kinase (AMPK) controls the aging process via an integrated signaling network. *Ageing Res Rev*. 2012; 11:230-241.
23. Stenesen D, Suh JM, Seo J, Yu K, Lee KS, Kim JS, Min KJ, Graft JM. Adenosine Nucleotide Biosynthesis and AMPK Regulate Adult Life Span and Mediate the Longevity Benefit of Caloric Restriction in Flies. *Cell Metab*. 2013; 17:101-112.

24. Mair W. Tipping the Energy Balance toward Longevity. *Cell Metab.* 2013; 17:5-6.
25. Anisimov VN. Metformin for aging and cancer prevention. *Aging (Albany NY)*. 2010; 2:760-774.
26. Del Barco S, Vazquez-Martin A, Cufí S, Oliveras-Ferraros C, Bosch-Barrera J, Joven J, Martin-Castillo B, Menendez JA. Metformin: multi-faceted protection against cancer. *Oncotarget*. 2011; 2:896-917.
27. Apontes P, Leontieva OV, Demidenko ZN, Li F, Blagosklonny MV. Exploring long-term protection of normal human fibroblasts and epithelial cells from chemotherapy in cell culture. *Oncotarget*. 2011; 2:222-233.
28. Oliveras-Ferraros C, Cufí S, Vazquez-Martin A, Torres-Garcia VZ, Del Barco S, Martin-Castillo B, Menendez JA. Micro(mi)RNA expression profile of breast cancer epithelial cells treated with the anti-diabetic drug metformin: induction of the tumor suppressor miRNA let-7a and suppression of the TGF β -induced oncomiR miRNA-181a. *Cell Cycle*. 2011; 10:1144-1151.
29. Vazquez-Martin A, Oliveras-Ferraros C, Cufí S, Martin-Castillo B, Menendez JA. Metformin activates an ataxia telangiectasia mutated (ATM)/Chk2-regulated DNA damage-like response. *Cell Cycle*. 2011; 10:1499-1501.
30. Vazquez-Martin A, López-Bonet E, Cufí S, Oliveras-Ferraros C, Del Barco S, Martin-Castillo B, Menendez JA. Repositioning chloroquine and metformin to eliminate cancer stem cell traits in pre-malignant lesions. *Drug Resist Updat*. 2011; 14:212-223.
31. Oliveras-Ferraros C, Cufí S, Vazquez-Martin A, Menendez OJ, Bosch-Barrera J, Martin-Castillo B, Joven J, Menendez JA. Metformin rescues cell surface major histocompatibility complex class I (MHC-I) deficiency caused by oncogenic transformation. *Cell Cycle*. 2012;11:865-870.
32. Cufí S, Vazquez-Martin A, Oliveras-Ferraros C, Quirantes R, Segura-Carretero A, Micol V, Joven J, Bosch-Barrera J, Del Barco S, Martin-Castillo B, Vellon L, Menendez JA. Metformin lowers the threshold for stress-induced senescence: a role for the microRNA-200 family and miR-205. *Cell Cycle*. 2012;11:1235-1246.
33. Cufí S, Corominas-Faja B, Vazquez-Martin A, Oliveras-Ferraros C, Dorca J, Bosch-Barrera J, Martin-Castillo B, Menendez JA. Metformin-induced preferential killing of breast cancer initiating CD44+CD24-/low cells is sufficient to overcome primary resistance to trastuzumab in HER2+ human breast cancer xenografts. *Oncotarget*. 2012; 3:395-398.
34. Menendez JA, Oliveras-Ferraros C, Cufí S, Corominas-Faja B, Joven J, Martin-Castillo B, Vazquez-Martin A. Metformin is synthetically lethal with glucose withdrawal in cancer cells. *Cell Cycle*. 2012; 11:2782-2792.
35. Vazquez-Martin A, Cufí S, Lopez-Bonet E, Corominas-Faja B, Oliveras-Ferraros C, Martin-Castillo B, Menendez JA. Metformin limits the tumorigenicity of iPS cells without affecting their pluripotency. *Sci Rep*. 2012; 2:964.
36. Anisimov VN, Berstein LM, Egormin PA, Piskunova TS, Popovich IG, Zabezhinski MA, Tyndyk ML, Yurova MV, Kovalenko IG, Poroshina TE, Semenchenko AV. Metformin slows down aging and extends life span of female SHR mice. *Cell Cycle*. 2008; 7:2769-2773.
37. Anisimov VN, Egormin PA, Piskunova TS, Popovich IG, Tyndyk ML, Yurova MN, Zabezhinski MA, Anikin IV, Karkach AS, Romanukha AA. Metformin extends life span of HER-2/neu transgenic mice and in combination with melatonin inhibits growth of transplantable tumors in vivo. *Cell Cycle*. 2010; 9:188-197.
38. Martin-Castillo B, Vazquez-Martin A, Oliveras-Ferraros C, Menendez JA. Metformin and cancer: doses, mechanisms and the dandelion and hormetic phenomena. *Cell Cycle*. 2010; 9:1057-1064.
39. Anisimov VN, Piskunova TS, Popovich IG, Zabezhinski MA, Tyndyk ML, Egormin PA, Yurova MV, Rosenfeld SV, Semenchenko AV, Kovalenko IG, Poroshina TE, Berstein LM. Gender differences in metformin effect on aging, life span and spontaneous tumorigenesis in 129/Sv mice. *Aging (Albany NY)*. 2010; 2:945-958.
40. Anisimov VN, Berstein LM, Popovich IG, Zabezhinski MA, Egormin PA, Piskunova TS, Semenchenko AV, Tyndyk ML, Yurova MN, Kovalenko IG, Poroshina TE. If started early in life, metformin treatment increases life span and postpones tumors in female SHR mice. *Aging (Albany NY)*. 2011; 3:148-157.
41. Berstein LM. Metformin in obesity, cancer and aging: addressing controversies. *Aging (Albany NY)*. 2012; 4:320-329.
42. Onken B, Driscoll M. Metformin induces a dietary restriction-like state and the oxidative stress response to extend *C. elegans* healthspan via AMPK, LKB1, and SKN-1. *PLoS One*. 2010; 5:e8758.
43. Corominas-Faja B, Quirantes-Piné R, Oliveras-Ferraros C, Vazquez-Martin A, Cufí S, Martin-Castillo B, Micol V, Joven J, Segura-Carretero A, Menendez JA. Metabolomic fingerprint reveals that metformin impairs one-carbon metabolism in a manner similar to the antifolate class of chemotherapy drugs. *Aging (Albany NY)*. 2012; 4:480-498.
44. Denno KM, Sadler TW. Effects of the biguanide class of oral hypoglycemic agents on mouse embryogenesis. *Teratology*. 1994; 49:260-6.
45. Slack C, Foley A, Partridge L. Activation of AMPK by the putative dietary restriction mimetic metformin is insufficient to extend lifespan in *Drosophila*. *PLoS One*. 2012; 7:e47699.
46. Hawley SA, Gadalla AE, Olsen GS, Hardie DG. The antidiabetic drug metformin activates the AMP-activated protein kinase cascade via an adenine nucleotide-independent mechanism. *Diabetes*. 2002; 51:2420-2425.
47. Stephenne X, Foretz M, Taleux N, van der Zon GC, Sokal E, Hue L, Viollet B, Guigas B. Metformin activates AMP-activated protein kinase in primary human hepatocytes by decreasing cellular energy status. *Diabetologia*. 2011; 54:3101-3110.
48. Ouyang J, Parakhia RA, Ochs RS. Metformin activates AMP kinase through inhibition of AMP deaminase. *J Biol Chem* 2011; 286:1-11.
49. Lanaspá MA, Cicerchi C, Garcia G, Li N, Roncal-Jimenez CA, Rivard CJ, Hunter B, Andrés-Hernando A, Ishimoto T, Sánchez-Lozada LG, Thomas J, Hodges RS, Mant CT, Johnson RJ. Counteracting roles of AMP deaminase and AMP kinase in the development of fatty liver. *PLoS One*. 2012; 7:e48801.

New nanoformulation of rapamycin Rapatar extends lifespan in homozygous $p53^{-/-}$ mice by delaying carcinogenesis

Maria Comas^{1,5}, Ilia Toshkov², Karen K. Kuropatwinski¹, Olga B. Chernova³, Alexander Polinsky³, Mikhail V. Blagosklonny⁴, Andrei V. Gudkov⁴, and Marina P. Antoch¹

¹ Departments of Molecular and Cellular Biology, Roswell Park Cancer Institute, Buffalo, NY, USA

² Cleveland Biolabs, Buffalo, NY 14203, USA

³ Tartis Aging, Inc, Buffalo, NY14203, USA

⁴ Cell Stress Biology, Roswell Park Cancer Institute, Buffalo, NY USA;

⁵ Cancer Research Program, Garvan Institute of Medical Research, Darlinghurst, New South Wales, Australia

Key words: mTOR pathway, $p53^{-/-}$, lifespan, rapamycin, oral formulation, cancer prevention

Received: 8/30/12; **Accepted:** 10/27/12; **Published:** 10/29/12

Correspondence to: Marina P. Antoch, PhD; **E-mail:** marina.antoch@roswellpark.org

Copyright: © Comas et al. This is an open-access article distributed under the terms of the Creative Commons Attribution License, which permits unrestricted use, distribution, and reproduction in any medium, provided the original author and source are credited

Abstract: The nutrient-sensing mTOR (mammalian Target of Rapamycin) pathway regulates cellular metabolism, growth functions, and proliferation and is involved in age-related diseases including cancer, type 2 diabetes, neurodegeneration and cardiovascular disease. The inhibition of mTOR by rapamycin, or calorie restriction, has been shown to extend lifespan and delays tumorigenesis in several experimental models suggesting that rapamycin may be used for cancer prevention. This requires continuous long-term treatment making oral formulations the preferred choice of administration route. However, rapamycin by itself has very poor water solubility and low absorption rate. Here we describe pharmacokinetic and biological properties of novel nanoformulated micelles of rapamycin, Rapatar. Micelles of Rapatar were rationally designed to increase water solubility of rapamycin to facilitate oral administration and to enhance its absorption. As a result, bioavailability of Rapatar was significantly increased (up to 12%) compared to unformulated rapamycin, which concentration in the blood following oral administration remained below level of detection. We also demonstrated that the new formulation does not induce toxicity during lifetime administration. Most importantly, Rapatar extended the mean lifespan by 30% and delayed tumor development in highly tumor-prone $p53^{-/-}$ mice. Our data demonstrate that water soluble Rapatar micelles represent safe, convenient and efficient form of rapamycin suitable for a long-term treatment and that Rapatar may be considered for tumor prevention.

INTRODUCTION

Rapamycin (or Sirolimus) is a macrolide antibiotic that was first isolated from *Streptomyces hydropiscus* and was initially utilized as an antifungal agent [1, 2]. Under the name of Rapamune, it is now used as an immunosuppressant to prevent organ rejection after transplantation. Rapamycin inhibits the nutrient-sensing mTOR (mammalian Target of Rapamycin), a conserved protein kinase that controls cellular growth and metabolism. The mTOR signaling pathway is activated by nutrients, growth factors, hormones, cytokines, and

cellular energy status. When nutrients and growth factors are abundant, mTOR promotes protein synthesis, ribosome biogenesis, angiogenesis, cell cycle progression and cytoskeleton re-organization (reviewed in [3]-5)).

Recent data demonstrated that rapamycin extends life span in various model organisms including mammals [4-6]. The life-long administration of rapamycin inhibits age-related weight gain, decreases aging rate and increases lifespan of inbred [7] and genetically heterogeneous [6] mice. Previous data has

demonstrated that rapamycin significantly delayed the onset of spontaneous carcinogenesis both in normal (129/Sv [7]) and cancer-prone (HER-2/neu transgenic [8] and *p53*^{+/-} [9]) mice. Importantly, the anti-cancer effect of rapamycin in *p53*^{+/-} mice was blunted when treatment started at the age of 5 months [9] suggesting that rapamycin does not directly inhibit tumor growth but rather has an indirect effect.

Since rapamycin exhibits poor water solubility and instability in aqueous solutions, its clinical use through oral administration requires development of special drug design such as complex nanoparticle formulation to facilitate increased bioavailability and efficacy. Therefore, various oral formulations, such as inclusion complexes [10, 11], liposomes [12], nanocrystals [13], and solid dispersion [14] have been developed and tested in pre-clinical and clinical studies. In this study, we tested the biological activity of a novel formulation of rapamycin, Rapatar. This formulation is based on Pluronic block copolymers as nanocarriers, which serves to improve water solubility of the drug, and to enhance various biological responses favorable for therapeutics, such as activity of drug efflux transporters (reviewed in [15]). We show that Rapatar has significantly higher bioavailability after oral administration when compared to unformulated rapamycin. We also show that Rapatar effectively blocks mTOR in mouse tissues. Moreover, life-long administration of Rapatar increases lifespan and delays carcinogenesis in highly tumor-prone *p53*^{+/-} mice.

RESULTS

Rapatar is efficiently absorbed and systemically distributed and effectively inhibits mTOR *in vivo*

To compare the absolute and relative bioavailability and other pharmacokinetic properties of Rapatar with those of an unformulated rapamycin, we administered both

compounds as a single dose to female ICR mice. Rapatar was administered intravenously (IV) or orally (PO) at a dose of 0.4 mg/kg and 4 mg/kg respectively, while rapamycin was administered PO at 4 mg/kg. Blood samples were collected at different times after administration and analyzed for rapamycin by mass spectrometry (LC/MS/MS). Pharmacokinetic values of the area under the curve (AUC), the maximum drug concentration (C_{max}), the time of peak concentration (T_{max}), and the absolute bioavailability (F) were calculated from whole blood drug concentration-time data (Fig. 1A). Importantly, following oral administration, rapamycin could only be detected in whole blood samples of mice that received Rapatar whereas its concentration in blood of rapamycin-treated mice was beyond the level of detection. As shown in Table 1, when compared to unformulated rapamycin, Rapatar demonstrated very fast absorption (T_{max} 15 min) and significant increase in AUC value with mean $T_{1/2}$ extending to 6.4 hours. Consequently, a single oral administration of Rapatar resulted in 12% bioavailability, which is comparable with commercially available formulations used in clinical practice (14% when administered orally in combination with cyclosporine A).

Ribosomal protein S6 is a substrate of mTOR, and therefore phospho-ribosomal protein S6 is a marker of mTOR activity [16-19]. To test whether Rapatar inhibits mTOR activity *in vivo*, we compared levels of phosphorylated S6 (pS6) in livers of wild type C57Bl/6J mice, in which mTOR was suppressed by a period of food deprivation. Rapatar (0.5mg/kg or PBS) were given by gavage at a time when animals were allowed access to food. Fig. 1B shows that S6 is highly phosphorylated in livers of control animals indicating mTOR activation in response to food. In contrast, in animals that received Rapatar, S6 phosphorylation was reduced ~10-fold. Thus, Rapatar successfully inhibits mTOR activity in the liver *in vivo*.

Table 1. Pharmacokinetic parameters of unformulated rapamycin and Rapatar in C57Bl/6J mice. Abbreviations: C_{max} – the peak concentration; T_{max} – time taken to reach peak concentration; AUC – area under the curve; F – absolute bioavailability.

	Units	Rapamycin, IV 0.4mg/kg	Rapatar, PO 4mg/kg
Dose amount	ng	10.4	104
Dosage	ng/kg	400	4000
C_{max}	ng/ml	958	656
T_{max}	hr	0.04	0.25
AUC	ng-hr/ml	2634.6	3161.5
Half-life	hr	6.4	N/A
F	%	100	12

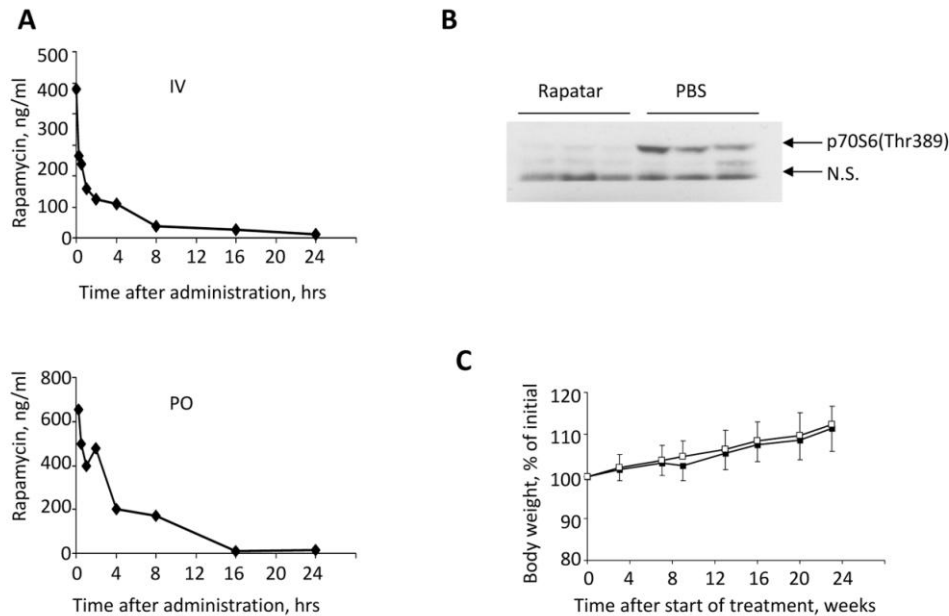


Figure 1. Pharmacokinetic and biological characteristics of Rapatar. **(A)** Rapamycin concentration–time profile in blood after intravenous (IV, top) and oral (PO, bottom) administration of Rapatar to mice (mean values, n = 3). A single dose of Rapatar was administered either IV (0.4mg/kg) or PO (4mg/kg). Blood samples were collected at designated times and analyzed for rapamycin by LC/MS/MS. **(B)** Rapatar blocks mTOR activation in vivo. Six C57/Bl/6J mice were food-deprived for 18 hrs. At the end of fasting period animals received either Rapatar (0.5mg/kg) or PBS via gavage and were allowed access to food. One hour later animals were sacrificed, livers were dissected and protein lysates were analyzed for mTOR activity by probing with p70S6(Thr389) antibody. **(C)** No acute or long-term toxicity are associated with PO administration of Rapatar. C57Bl/6J male mice received either Rapatar or PBS starting 8 weeks of age (10 mice/group) for 24 weeks according to the protocol described above. No loss in body weight was detected in experimental group throughout the treatment period. Both experimental and control groups showed similar gain in body weight with age.

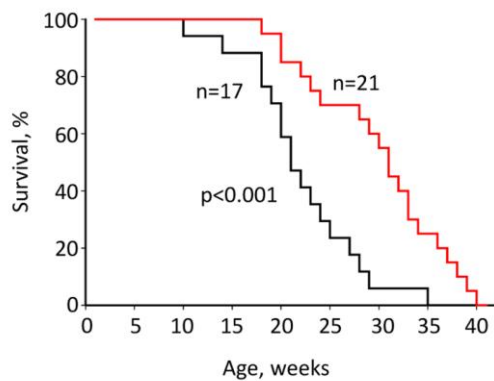


Figure 2. Rapatar increases lifespan in *p53*^{-/-} mice. Mice received Rapatar at 0.5 mg/kg via gavage according to the schedule described in Materials and Methods. Rapatar increased lifespan from 23 to 31 weeks (p<0.001, Mantel-Cox log-rank test).

To test whether life-long administration of Rapatar causes *in vivo* toxicity, we administered it to wild type C57Bl/6J mice at 0.5 mg/kg via gavage according to protocol described in Materials and Methods section. Rapatar- and PBS-treated animals were monitored for any signs of toxicity by visual inspection and body weight measurements. Mice receiving Rapatar maintained a healthy appearance with physical activities and body weights comparable to the control mice (Fig. 1C).

Rapatar increases lifespan of *p53*^{-/-} mice

Our data showed that Rapatar effectively inhibits mTOR *in vivo*. Suppression of mTOR by rapamycin has been shown to increase lifespan in various model organisms including mice [6-8, 20-25]. To test whether Rapatar can extend lifespan, we administered it to mice with targeted disruption of tumor suppressor p53. *p53*^{-/-}

mice are characterized by increased carcinogenesis and reduced lifespan (reviewed in [26]). Twenty $p53^{-/-}$ mice received Rapatar starting 8 weeks of age at a dose of 0.5mg/kg according to the schedule described in Material and Methods. Another group of 17 $p53^{-/-}$ mice received PBS as control. Throughout the experiment, animals were monitored for tumor development by visual inspection and total body weight measurements. Both Rapatar- and PBS-treated $p53^{-/-}$ mice die early in life due to a high rate of spontaneous carcinogenesis, which is characteristic for this mouse model. However, treatment with Rapatar resulted in an overall significant increase in median survival of $p53^{-/-}$ mice from 23 (± 10) weeks in the control group to 31 (± 1.5) weeks in the experimental group (Fig. 2A).

To gain insight into the potential mechanism of increase in survival of Rapatar-treated animals, we performed a detailed histological analysis of all tissues collected from each individual animal in the course of the exper-

iment (summarized in Table 2). Based on this analysis, 82% of mice in the control group (14 out of 17) developed lymphomas whereas 12% (2 out of 17) developed sarcomas. One animal showed the presence of both sarcoma and lymphoma and one animal developed myeloid leukemia. This spectrum of tumors is characteristic to $p53^{-/-}$ mice and comparable to previous reports [27]. The mice developed these spontaneous neoplasms from 2 to over 8 months of age with an average latency time of 161 days. When compared to the control group, Rapatar-treated mice showed later appearance and delayed progression of spontaneous tumors. They arose from 4.5 to over 9.5 months, with average latency of 261 days; one animal remained tumor-free until the end of the experiment. Interestingly, the incidence of sarcomas in Rapatar-treated mice was increased to 30% compared to 17% in control group (Table 2); however the number of animals used in the experiment was not enough to obtain a statistically significant difference.

Table 2. Summary of histological analysis. Tissues of 17 control and 20 Rapatar-treated $p53^{-/-}$ mice were evaluated for the presence of tumor cells. The type of tumors and the stage of their development were determined as described in Materials and Methods. The incidence of sarcomas in Rapatar-treated $p53^{-/-}$ mice was higher than in control group (30% and 17% respectively); however, due to a relatively small group size, statistical significance was not achieved ($p=0.2$; Fisher's exact test).

	Initial Lymphoma	Advanced Lymphoma	Sarcoma	Leukemia	Tumor-free
Rapatar	7 (35%)	6 (30%)	6 (30%)	1 (5%)	1 (5%)
PBS	4 (23%)	10 (58%)	3 (17%)	1 (6%)	0

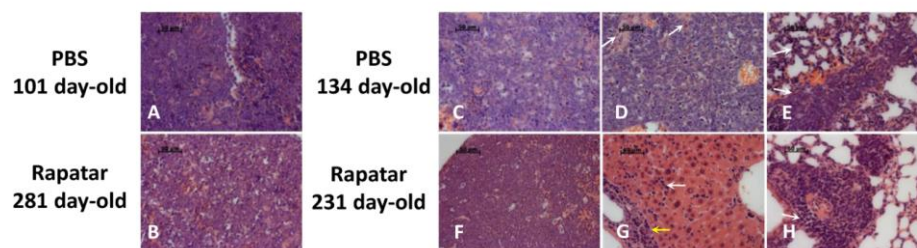


Figure 3. Rapatar delays development of lymphomas in $p53^{-/-}$ mice. (A) Representative initial lymphoma developed in control mouse at the age of 101 days. (B) Similar appearance of lymphoma in Rapatar-treated mouse at 281 days of age. Both A and B show monotonous infiltrate of medium-sized neoplastic cells with round nuclei, fine chromatin, indistinct nucleoli, and numerous mitotic figures and apoptotic cells. (C) Advanced lymphoma in 134-day old control mouse with metastases in liver (D) and lung (E). (D) Metastasis in liver showing the extensive spread of neoplastic cells effaces the normal structure and only minimal remnants of hepatocytes (marked by arrows). (E) Metastasis in the lung showing neoplastic infiltrates in perivascular area and in the alveolar walls (arrows) (F) Advanced lymphoma with pathological changes similar to shown in C in the thymus of 241day-old Rapatar-treated animal with metastasis in liver (G) and lung (H). (G) Metastasis in liver showing neoplastic infiltrates in portal tract (yellow arrow) and sinusoids (white arrow). (H) Metastasis in the lung showing perivascular neoplastic infiltrate (arrow).

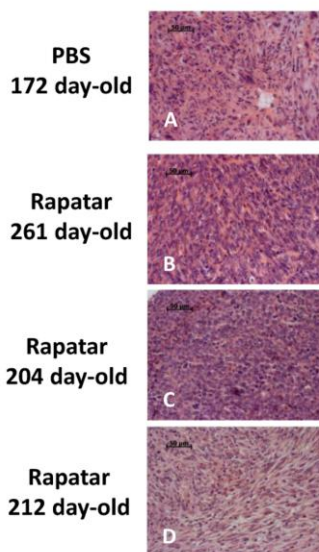


Figure 4. Rapatar delays development of sarcomas in $p53^{-/-}$ mice. (A) Liver sarcoma in 172-old control mouse. (B,C) Sarcoma developed in 261 day- and 204 day-old Rapatar-treated mice. No metastases are detected. D. Sarcoma in 212-day old Rapatar-treated mouse with metastases in the lung.

Since lymphomas represented the major type of tumor in both groups, we performed a detailed pathological evaluation of individual tumors. Based on the severity of pathological changes, the developmental stage, and involvement of non-lymphoid tissues, all lymphomas were graded as initial or advanced. Initial lymphomas mainly involved thymus and were presented macroscopically as enlarged masses. Under the microscope they were seen to be composed of broad sheets of densely packed rather uniform large lymphoblastic cells, with little or sparse cytoplasm that completely obliterated the normal thymus structure and cortical and medullary zones. In most cases, neoplastic lymphoid cells expanded through the thymic capsule and spread through the mediastinal fat, lymph nodes, along peritracheal and periaortal spaces, even infiltrating lungs and pericardium with limited penetration of the myocardium. Such lymphomas with predominantly local involvement were designated provisionally as initial. Tumors were graded as advanced when the rise of the malignancy and aggressiveness of the lymphoma cells resulted in metastases and infiltration into spleen, liver, lung, kidney, mesentery lymph nodes, testis, and bone marrow. Based on this designation, the proportion of the initial lymphomas in Rapatar-treated group was larger compared to controls (35% and 23% for experimental

and control groups respectively) suggesting that Rapatar slows down tumorigenesis. Consistently, the proportion of the advanced disseminated lymphomas, spreading to other organs in Rapatar-treated group was smaller than in control (30% and 58% respectively). Although histopathological appearance of lymphomas and sarcomas were very similar in control and experimental groups, Rapatar-treated mice develop tumors significantly later in life (Fig. 3 and 4). Based on these data we concluded that Rapatar increased lifespan of $p53^{-/-}$ mice by delaying tumorigenesis.

DISCUSSION

The mTOR signaling pathway is a key coordinator of cell growth and cell proliferation in response to a variety of environmental conditions. Its deregulation has been implicated in many pathological conditions, including those that are associated with aging, such as cancer, type 2 diabetes, neurological and cardiovascular disorders (reviewed in [28, 29]). Furthermore, the activation of the mTOR pathway is the most universal alteration in cancer [30]. Several analogs of rapamycin (rapalogs) have been approved for cancer therapy [31-35] and numerous clinical trials are underway. However, as anti-cancer drugs rapamycin and other rapalogs showed modest efficacy. There are several reasons that can explain relatively low therapeutic effect. First, rapamycin itself is not cytotoxic. Additionally, mTOR inhibition activates several feedback loops that drive mitogenic signaling (reviewed in [28, 36]). Therefore, it is still not quite clear whether rapamycin exhibits direct antitumor activity or whether it acts in a more indirect systemic way. Our previous data [9] and data presented here show that rapamycin delays carcinogenesis in tumor-prone $p53^{+/-}$ and $p53^{-/-}$ mice, most likely by slowing down the process of aging. If this is the case, than rapamycin can be considered as a tumor-preventive agent (i.e. administration is required before tumor initiation). This necessitates the development of efficacious nontoxic rapamycin-formulations that could be taken orally for extended periods of time. Here we show that oral administration of Rapatar results in high systemic bioavailability and does not induce toxicity during life-long administration. Importantly, biological effects of Rapatar were prominent at low doses (0.5 mg/kg) and intermittent schedules. Taken together, our data suggest that Rapatar is a promising candidate for clinical use as an effective cancer prevention drug.

MATERIALS AND METHODS

Materials. Rapamycin was purchased from LC Laboratories (Woburn, MA). Polymeric formulation of

rapamycin (Rapatar) was developed by Tartis Aging, Inc. using Pluronic block co-polymers [15] according to the following protocol. One gram of rapamycin was dissolved in 25 ml of ethanol. The resulting solution was mixed with 5 grams of Pluronic L-92 (BASF) and 2 grams of citric acid dissolved in 200 ml of 20% Pluronic F-127 (BASF) solution in ethanol and water mixture (97:3 v:v). The solution was then incubated at 20-25°C for 30 minutes with constant stirring. The ethanol was removed using Speedvac and the formulation was further dried using high vacuum.

Animals. ICR female mice were obtained from Charles River. C57Bl/6J mice were obtained from Jackson Laboratory. *p53*^{-/-} mice on C57Bl/6J background originally obtained from Jackson Laboratory, were housed and bred at the Department of Experimental Animal Resources of Roswell Park Cancer Institute. For pharmacokinetic analysis, three groups of 8 weeks old ICR female mice received a single dose of either Rapatar (2 groups) or rapamycin. Rapatar was administered via gavage at 4mg/kg in 0.5% methyl cellulose or IV at 0.4mg/kg in PBS. Rapamycin was administered via gavage at 4mg/kg in 0.5% methyl cellulose.

For estimating potential long-term toxic effects of Rapatar, two groups of C57BL/6J mice received the drug at a dose of 0.5 mg/kg via gavage once a day for 5 consecutive days, followed by 9-day interval without treatment. Mice were maintained on this treatment schedule for 24 weeks and were weighed weekly. Control mice receive PBS according to the same schedule.

For longevity studies, 38 *p53*^{-/-} male mice were randomly divided into two groups. Twenty one experimental animals received 0.5 mg/kg Rapatar and 17 animals received PBS according to the above described schedule. Treatment started at 8 weeks of age and continued until tumor appearance was visually observed or dramatic loss of weight, indicative of tumor appearance, was detected. At this point, mice were sacrificed and examined for gross pathological changes. Tumors, heart, kidney, liver, lungs, thymus and spleen were collected for histological evaluation. All procedures were approved by the Institutional Animal Care and Use Committee of Roswell Park Cancer Institute.

Pharmacokinetic study. Whole blood was collected into EDTA-blood tubes 0.5, 1, 2, 4, 8, 16 and 24 hours after administration of either Rapatar or unformulated rapamycin. Tubes were inverted a few times, and stored on ice in dark container during the experiment. At the end of the experiment, all samples were placed for storage at -70°C in a light-protected container. Frozen

blood samples were submitted to the Rocky Mountain Instrumental Laboratory (Fort Collins, Co) for LC/MS/MS analysis of rapamycin. Pharmacokinetic analysis was performed using data from individual mice for which the mean and standard error of the mean (SEM) were calculated for each group using PK Solutions software (Version 2.0).

Western blot analysis. In order to maximize and be able to detect p70S6 phosphorylation [37, 38], six C57Bl/6J mice were food-deprived for 18 hrs. At the end of the fasting period, animals received either Rapatar (0.5 mg/kg) or PBS via gavage and 15 minutes later were allowed access to food. One hour later animals were sacrificed; livers were dissected, lysed in RIPA buffer and loaded on a 8% SDS-PAGE gel. After separation and transfer to a PVDF membrane, protein lysates were analyzed for mTOR activation by probing with an antibody against phospho-*p70 S6 Kinase (Thr389)* (1:1000; Cell Signaling) and Actin (1:10000 Cell Signaling). After incubation with HRP conjugated secondary antibodies (Santa Cruz Biotechnologies), transferred proteins were visualized with the ECL detection kit (Jackson Research Laboratories).

Histopathology. The mice were visually inspected for tumor development and weighed weekly. Animals showing deteriorating clinical status manifested by constant weight loss or visual tumor appearance were sacrificed and evaluated for gross pathological changes by complete necropsy. For histological evaluation, all tissues were fixed in 10% neutral formalin for 24 hours, and then transferred to 70% ethanol. Samples were embedded in paraffin, sectioned and stained with hematoxylin and eosin. Histopathological examination was performed on tumors, gross lesions and target tissues using Zeiss AxioImager A1 with AxioCam MRc digital camera. The guidelines of Bethesda classification was used in determining the diagnosis [39].

Statistical Analyses. Differences in survival and tumor incidence were evaluated by the Mantel-Cox log-rank test.

ACKNOWLEDGEMENTS

We thank Mary Spengler for critical reading of the manuscript. This work was supported in part by NIH grant GM095874 and by Roswell Park Alliance Foundation (to M.P.A.) and Tartis, Inc. (to A.V.G.)

Conflict of Interest Statement

The authors of this manuscript have no conflict of interests to declare.

REFERENCES

1. Vézina C, Kudelski A and Sehgal S. Rapamycin (AY-22,989), a new antifungal antibiotic I. Taxonomy of the producing streptomycete and isolation of the active principle. *Journal of antibiotics*. 1975; 28:721-726.
2. Sehgal SN, Baker H and Vezina C. Rapamycin (AY-22,989), a new antifungal antibiotic. II. Fermentation, isolation and characterization. *Journal of antibiotics*. 1975; 28:727-732.
3. Wullschleger S, Loewith R and Hall MN. TOR Signaling in Growth and Metabolism. *Cell*. 2006; 124:471-484.
4. Kaeberlein M, Powers RW, 3rd, Steffen KK, Westman EA, Hu D, Dang N, Kerr EO, Kirkland KT, Fields S and Kennedy BK. Regulation of yeast replicative life span by TOR and Sch9 in response to nutrients. *Science*. 2005; 310:1193-1196.
5. Wilkinson JE, Burmeister L, Brooks SV, Chan CC, Friedline S, Harrison DE, Hejtmancik JF, Nadon N, Strong R, Wood LK, Woodward MA and Miller RA. Rapamycin slows aging in mice. *Aging Cell*.
6. Harrison DE, Strong R, Sharp ZD, Nelson JF, Astle CM, Flurkey K, Nadon NL, Wilkinson JE, Frenkel K, Carter CS, Pahor M, Javors MA, Fernandez E, et al. Rapamycin fed late in life extends lifespan in genetically heterogeneous mice. *Nature*. 2009; 460:392-395.
7. Spong A and Bartke A. Rapamycin slows aging in mice. *Cell Cycle*. 2012; 11:845.
8. Anisimov VN, Zabezhinski MA, Popovich IG, Piskunova TS, Semenchenko AV, Tyndyk ML, Yurova MN, Antoch MP and Blagosklonny MV. Rapamycin extends maximal lifespan in cancer-prone mice. *Am J Pathol*. 2010; 176:2092-2097.
9. Komarova E, Antoch M, Novototskaya L, Chernova O, Paszkiewicz G, Leontieva O, Blagosklonny M and Gudkov A. Rapamycin extends lifespan and delays tumorigenesis in heterozygous p53[±] mice. *Aging (Albany NY)*. 2012.
10. Baspinar Y, Bertelmann E, Pleyer U, Buech G, Siebenbrodt I and Borchert HH. Corneal permeation studies of everolimus microemulsion. *J Ocul Pharmacol Ther*. 2008; 24:399-402.
11. Buech G, Bertelmann E, Pleyer U, Siebenbrodt I and Borchert HH. Formulation of sirolimus eye drops and corneal permeation studies. *J Ocul Pharmacol Ther*. 2007; 23:292-303.
12. Alemdar AY, Sadi D, McAlister V and Mendez I. Intracerebral co-transplantation of liposomal tacrolimus improves xenograft survival and reduces graft rejection in the hemiparkinsonian rat. *Neuroscience*. 2007; 146:213-224.
13. Junghanns JU and Muller RH. Nanocrystal technology, drug delivery and clinical applications. *International journal of nanomedicine*. 2008; 3:295-309.
14. Kim MS, Kim JS, Park HJ, Cho WK, Cha KH and Hwang SJ. Enhanced bioavailability of sirolimus via preparation of solid dispersion nanoparticles using a supercritical antisolvent process. *International journal of nanomedicine*. 2011; 6:2997-3009.
15. Batrakov EV and Kabanov AV. Pluronic block copolymers: evolution of drug delivery concept from inert nanocarriers to biological response modifiers. *J Control Release*. 2008; 130:98-106.
16. Brown EJ, Beal PA, Keith CT, Chen J, Bum Shin T and Schreiber SL. Control of p70 S6 kinase by kinase activity of FRAP in vivo. *Nature*. 1995; 377:441-446.
17. Brunn GJ, Fadden P, Haystead TAJ and Lawrence JC. The Mammalian Target of Rapamycin Phosphorylates Sites Having a (Ser/Thr)-Pro Motif and Is Activated by Antibodies to a Region near Its COOH Terminus. *Journal of Biological Chemistry*. 1997; 272:32547-32550.
18. Brunn GJ, Hudson CC, Sekulić A, Williams JM, Hosoi H, Houghton PJ, Lawrence JC and Abraham RT. Phosphorylation of the Translational Repressor PHAS-I by the Mammalian Target of Rapamycin. *Science*. 1997; 277:99-101.
19. Burnett PE, Barrow RK, Cohen NA, Snyder SH and Sabatini DM. RAFT1 phosphorylation of the translational regulators p70 S6 kinase and 4E-BP1. *Proceedings of the National Academy of Sciences*. 1998; 95:1432-1437.
20. Miller RA, Harrison DE, Astle CM, Baur JA, Boyd AR, de Cabo R, Fernandez E, Flurkey K, Javors MA, Nelson JF, Orihuela CJ, Pletcher S, Sharp ZD, et al. Rapamycin, but not resveratrol or simvastatin, extends life span of genetically heterogeneous mice. *J Gerontol A Biol Sci Med Sci*. 2011; 66:191-201.
21. Moskalev AA and Shaposhnikov MV. Pharmacological inhibition of phosphoinositide 3 and TOR kinases improves survival of *Drosophila melanogaster*. *Rejuvenation Res*. 13:246-247.
22. Bjedov I, Toivonen JM, Kerr F, Slack C, Jacobson J, Foley A and Partridge L. Mechanisms of life span extension by rapamycin in the fruit fly *Drosophila melanogaster*. *Cell Metab*. 11:35-46.
23. Kapahi P, Chen D, Rogers AN, Katewa SD, Li PW, Thomas EL and Kockel L. With TOR, less is more: a key role for the conserved nutrient-sensing TOR pathway in aging. *Cell Metab*. 2010; 11:453-465.
24. Khanna A and Kapahi P. Rapamycin: killing two birds with one stone. *Aging (Albany NY)*. 2011; 3:1043-1044.
25. Ramos FJ, Chen SC, Garelick MG, Dai DF, Liao CY, Schreiber KH, Mackay VL, An EH, Strong R, Ladiges WC, Rabinovitch PS, Kaeberlein M and Kennedy BK. Rapamycin Reverses Elevated mTORC1 Signaling in Lamin A/C-Deficient Mice, Rescues Cardiac and Skeletal Muscle Function, and Extends Survival. *Sci Transl Med*. 2012; 4:144ra103.
26. Donehower LA. Using mice to examine p53 functions in cancer, aging, and longevity. *Cold Spring Harb Perspect Biol*. 2009; 1:a001081.
27. Donehower LA, Harvey M, Slagle BL, McArthur MJ, Montgomery CA, Jr., Butel JS and Bradley A. Mice deficient for p53 are developmentally normal but susceptible to spontaneous tumours. *Nature*. 1992; 356:215-221.
28. Laplante M and Sabatini DM. mTOR signaling in growth control and disease. *Cell*. 2012; 149:274-293.
29. Dazert E and Hall MN. mTOR signaling in disease. *Curr Opin Cell Biol*. 2011; 23:744-755.
30. Guertin DA and Sabatini DM. Defining the role of mTOR in cancer. *Cancer cell*. 2007; 12:9-22.
31. Hudes G, Carducci M, Tomczak P, Dutcher J, Figlin R, Kapoor A, Staroslawska E, Sosman J, McDermott D, Bodrogi I, Kovacevic Z, Lesovoy V, Schmidt-Wolf IG, et al. Temsirolimus, interferon alfa, or both for advanced renal-cell carcinoma. *The New England journal of medicine*. 2007; 356:2271-2281.
32. Motzer RJ, Hudes GR, Curti BD, McDermott DF, Escudier BJ, Negrier S, Duclos B, Moore L, O'Toole T, Boni JP and Dutcher JP. Phase I/II trial of temsirolimus combined with interferon alfa for advanced renal cell carcinoma. *J Clin Oncol*. 2007; 25:3958-3964.
33. Wander SA, Hennessy BT and Slingerland JM. Next-generation mTOR inhibitors in clinical oncology: how pathway complexity informs therapeutic strategy. *The Journal of clinical investigation*. 121:1231-1241.

- 34.** Chappell WH, Steelman LS, Long JM, Kempf RC, Abrams SL, Franklin RA, Basecke J, Stivala F, Donia M, Fagone P, Malaponte G, Mazarino MC, Nicoletti F, et al. Ras/Raf/MEK/ERK and PI3K/PTEN/Akt/mTOR inhibitors: rationale and importance to inhibiting these pathways in human health. *Oncotarget*. 2011; 2:135-164.
- 35.** Markman B, Dienstmann R and Tabernero J. Targeting the PI3K/Akt/mTOR pathway--beyond rapalogs. *Oncotarget*. 2010; 1:530-543.
- 36.** Garrett JT, Chakrabarty A and Arteaga CL. Will PI3K pathway inhibitors be effective as single agents in patients with cancer? *Oncotarget*. 2011; 2:1314-1321.
- 37.** Anand P and Gruppiso PA. The Regulation of Hepatic Protein Synthesis during Fasting in the Rat. *Journal of Biological Chemistry*. 2005; 280:16427-16436.
- 38.** Demirkan G, Yu K, Boylan JM, Salomon AR and Gruppiso PA. Phosphoproteomic Profiling of *In Vivo* Signaling in Liver by the Mammalian Target of Rapamycin Complex 1 (mTORC1). *PLoS ONE*. 6:e21729.
- 39.** Morse HC, 3rd, Anver MR, Fredrickson TN, Haines DC, Harris AW, Harris NL, Jaffe ES, Kogan SC, MacLennan IC, Pattengale PK and Ward JM. Bethesda proposals for classification of lymphoid neoplasms in mice. *Blood*. 2002; 100:246-258.

Rapamycin extends lifespan and delays tumorigenesis in heterozygous p53+/- mice

Elena A. Komarova¹, Marina P. Antoch², Liliya R. Novototskaya¹, Olga B. Chernova³, Geraldine Paszkiewicz¹, Olga V. Leontieva¹, Mikhail V. Blagosklonny¹, and Andrei V. Gudkov¹

¹ Department of Cell Stress Biology, Roswell Park Cancer Institute, BLSC, L3-312, Buffalo, NY 14263, USA;

² Department of Molecular & Cellular Biology, Roswell Park Cancer Institute, BLSC, L3-312, Buffalo, NY 14263, USA

³ Tartis Aging, Inc., Buffalo, NY 14203, USA

Key words: cancer, mutations, DNA damage, aging, mTOR

Received: 8/30/12; **Accepted:** 10/27/12; **Published:** 10/29/12

Correspondence to: Andrei V. Gudkov, PhD; **E-mail:** andrei.gudkov@roswellpark.org and Mikhail V. Blagosklonny, MD/PhD;

E-mail: blagosklonny@oncotarget.com

Copyright: © Komarova et al. This is an open-access article distributed under the terms of the Creative Commons Attribution License, which permits unrestricted use, distribution, and reproduction in any medium, provided the original author and source are credited

Abstract: The TOR (Target of Rapamycin) pathway accelerates cellular and organismal aging. Similar to rapamycin, p53 can inhibit the mTOR pathway in some mammalian cells. Mice lacking one copy of p53 (p53+/- mice) have an increased cancer incidence and a shorter lifespan. We hypothesize that rapamycin can delay cancer in heterozygous p53+/- mice. Here we show that rapamycin (given in a drinking water) extended the mean lifespan of p53+/- mice by 10% and when treatment started early in life (at the age less than 5 months) by 28%. In addition, rapamycin decreased the incidence of spontaneous tumors. This observation may have applications in management of Li-Fraumeni syndrome patients characterized by heterozygous mutations in the p53 gene.

INTRODUCTION

The mTOR (mammalian Target of Rapamycin) pathway plays a crucial role in the geroconversion from cell cycle arrest to senescence (geroconversion) [1]. Rapamycin suppresses or decelerates geroconversion, maintaining quiescence instead [2-8]. Furthermore, inhibition of the TOR pathway prolongs lifespan in model organisms, including mice [9-13]. In an organism, nutrients activate mTOR [14-16], whereas fasting or calorie restriction deactivates mTOR [17-19]. Calorie restriction slows down aging [20] and postpones tumorigenesis in several animal models [21, 22], including p53-deficient mice [23-25].

Similar to other tumor suppressors, p53 can inhibit mTOR in mammalian cells [26-31]. While causing cell cycle arrest, p53 can suppress geroconversion, thus preventing a senescent phenotype in the arrested cells [30, 31]. Therefore, it is not surprising that p53 inhibits hyper-secretory phenotype, a hallmark of senescence

[32] whereas p53-deficiency resulted in pro-inflammatory phenotype [33, 34]. Noteworthy, the activity of p53 is decreased with aging [35]. Lack of one p53-allele (p53+/-) accelerates carcinogenesis and shortens lifespan [36-41]. We propose that rapamycin can decelerate cancer development in p53+/- mice. Here we show experimental evidence supporting this hypothesis.

RESULTS

Rapamycin (approximate dose, 1.5 mg/kg/day) was given in drinking water. 75 mice were divided into two groups: control (n=38) and rapamycin-treated (n=37). The mean lifespan of animals in control group was 373 days and the last 10% of survivals lived as long as 520 days (Fig. 1 A). In rapamycin-treated mice, the mean lifespan was 410 days and lifespan of the last 10% of survivals could not be determined (Fig. 1 A). Mice in both groups were also monitored for tumor development. The data presented in Fig. 1B

demonstrate that carcinogenesis was significantly delayed in rapamycin-treated mice compared to control mice.

Since in our experiments animals started to receive rapamycin at different age, we sought to test whether this affected the outcome of the treatment.

For this, we further subdivided all mice used into two groups: “young” (receiving rapamycin from the age of 5 months or earlier) and “old” (receiving rapamycin starting at 5 months of age or older). Results of the data analysis for the “young” group are shown in Figure 1C and D. The mean lifespan in control group was 373 days, whereas in rapamycin-treated “young” mice the mean lifespan reached 480 days, 3.5 months increase over the control group. Furthermore, 40% of rapamycin-treated “young” mice survived 550 days (Fig. 1C) and by this age developed 2 times less tumors than control mice (Fig. 1D). In the “old” group the difference between control and treated group was blunted (data not shown).

Thus, the life-extending effect of rapamycin is more pronounced when treatment starts earlier in life. In order to confirm that rapamycin administered with drinking water has biological activity in vivo, we measured levels of phosphorylated ribosomal protein S6 (pS6), a marker of the mTOR activity in tissues of control and rapamycin-treated mice. After receiving rapamycin in drinking water for 2 days, mice were sacrificed and the levels of total S6 and pS6 were estimated by Western blot analysis and immunocytochemistry (Fig. 2).

As shown in Fig. 2A, levels of pS6 were reduced in the heart, kidney and liver of rapamycin-treated mice. Also, pS6/S6 ratios were lower in rapamycin-treated mice (Fig. S1).

These results were confirmed by immunohistochemical staining showing lower levels of pS6 in tissues of rapamycin-treated mice (Fig. 2B). The variability of pS6 levels among mice may explain the variability of biological effects of rapamycin.

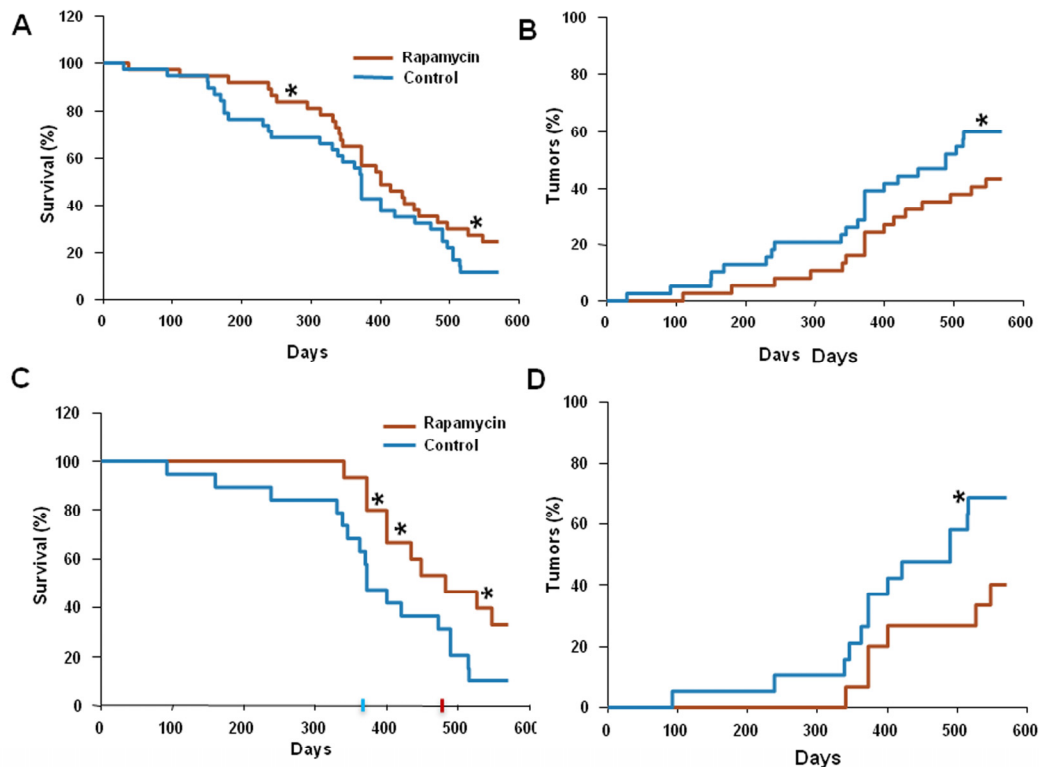


Figure 1. Administration of rapamycin extends lifespan and delays carcinogenesis in p53^{+/-} male mice. (A) Kaplan Meier survival curve of rapamycin-treated (red line) and control (blue line) mice. **(B)** Incidence of tumors in rapamycin-treated (red) and control (blue) mice. Animals received rapamycin starting at various ages at 1.5 mg/kg per day in drinking water throughout entire life. * p<0.05. **(C)** Kaplan Meier survival curve of rapamycin-treated (red line) and control (blue line) mice that start receiving rapamycin early in life (<5 months). **(D)** Incidence of tumors in rapamycin-treated (red) and control (blue) mice that start receiving rapamycin early in life (<5 months). * p<0.05 toph

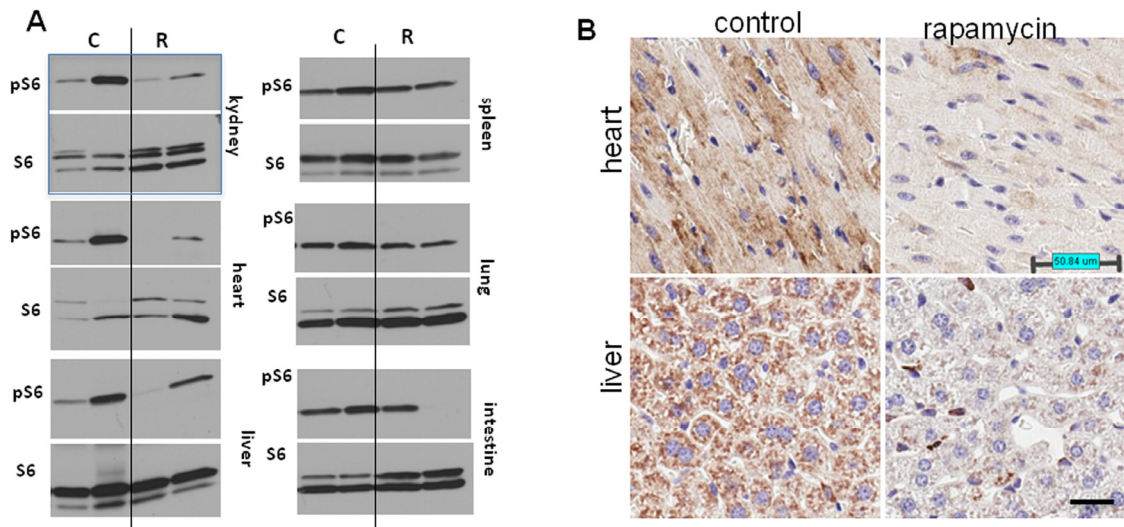


Figure 2. Administration of rapamycin in drinking water inhibits the mTOR pathway in p53^{+/-} male mice. (A) Western blot analysis of whole cell lysates of 6 organs of rapamycin-treated and control mice probed with antibodies specific to S6 and phospho-S6 (Ser240/244). Mice received rapamycin in drinking water for 2 days. (B) Immunohistochemistry. pS6 in the heart and the liver. Mice received rapamycin in drinking water for 2 days.

DISCUSSION

Previously it was shown that rapamycin prolongs lifespan in genetically heterogeneous mice [11], [12], inbred mice [42] and Her2-expressing mice [13]. In normal genetically heterogeneous mice, rapamycin extended life span even when its administration was started later in life [11]. Our data in p53^{+/-} mice show that the effect of rapamycin was blunted when treatment started at the age of 5 months or older.

This indicates that the anti-cancer effect of rapamycin is likely to be indirect and is imposed via its systemic effect at the level of an organism rather than through direct inhibition of tumor growth. To further address this question we plan to test the effect of rapamycin on animals with established tumors (by measuring tumor growth) along with evaluating the functional status of mTOR and the ability of rapamycin to suppress it in tumors and normal tissues. As we report here, administration of rapamycin starting early in life increased mean lifespan in p53^{+/-} male mice by 28%. Previous work has demonstrated that the life-extending effects of rapamycin [11, 12] as well as metformin [43, 44], calorie restriction [45] and genetic inhibition of the IGF-1/mTOR/S6K pathway [46, 47] were less pronounced in male mice compared with female mice. Moreover, in some cases, life span extension was achieved in female mice only [43, 47]. Therefore, the

observed increase in the median lifespan is dramatic, taking into account that it was achieved in male mice. However, because of low bioavailability of rapamycin, it was given constantly (in drinking water) without interruptions, whereas intermittent schedules may be more appropriate for future clinical developments as cancer-preventive interventions. In fact, a novel formulation of rapamycin (Rapatar) may be given intermittently, which still reveal even more pronounced extension of life span in p53-deficient mice (Comas et al, Aging 2012; this issue).

Our study suggests that rapamycin can be considered for cancer prevention in patients with Li-Fraumeni syndrome. Li-Fraumeni syndrome is an autosomal dominant disorder with a germline p53 mutation [48]. The incidence of cancer in carriers of mutation reaches 50% at the age of 40 and 90% at the age 60. Children of affected parents have an approximate 50% risk of inheriting the familial mutation [48]. Although functional assays have been established allowing for easy genetic testing for TP53 mutation, no effective chemopreventive therapy is currently available. The p53 rescue compounds may hold some promise in the future [48-50]; however these are not clinically approved drugs. In contrast, rapamycin has been used in the clinic for over a decade mostly in renal transplant patients. It was reported that rapamycin significantly decreased cancer incidence in renal transplant patients [51-53].

Our data suggest that rapamycin or its analogs can be considered for cancer prevention in Li-Fraumeni syndrome.

METHODS

Mice. All animal studies were conducted in accordance with the regulations of the Committee of Animal Care and Use at Roswell Park Cancer Institute. The colony of p53-knockout mice on a C57B1/6 background (originally obtained from Jackson Laboratories, Bar Harbor, ME) was maintained by crossing p53^{+/+} females with p53^{-/-} males followed by genotyping of the progeny (PCR) as described previously [54]. Heterozygous p53^{+/-} mice were generated by crossing p53^{-/-} males with wild type p53 females. Male mice were kept in polypropylene cages (30x21x10 cm) under standard light/dark regimen (12 hours light : 12 hours darkness) at 22 ± 2 °C, And received standard laboratory chow and water ad libitum.

Rapamycin treatment. Rapamycin (LC Laboratories, USA) was diluted in ethanol at concentration 15 mg/ml. Then the stock was diluted 1:1000 in drinking water. Drinking water was changed every week. Male mice were randomly divided into two groups. Mice of the first group (n=37) were given rapamycin in drinking water (approximately 1.5 mg/kg per day), whereas mice of the second group (n=38) were given tap water without rapamycin and served as control. Once a week all mice were palpated for detection of tumor mass appearance.

Pathomorphological examination. All animals were autopsied. Site, number and size of tumors were checked. All tumors, as well as the tissues and organs with suspected tumor development were excised and fixed in 10% neutral formalin. After the routine histological processing the tissues were embedded into paraffin. 5-7 µm thin histological sections were stained with haematoxylin and eosine and were microscopically examined. Tumors were classified according to International Agency for Research on Cancer recommendations.

Western blot analysis. Tissues were homogenized in Bullet blender using stainless steel 0.5 mm diameter beads (Next Advantage, Inc. NY, USA) and RIPA lysis buffer supplemented with protease and phosphatase inhibitors tablets (Roche Diagnostics, Indianapolis, IN, USA). Lysates were cleared by centrifugation at 4°C at 13000 rpm. Equal amounts of protein were separated on gradient Criterion gels (BioRad) and immunoblotting was performed with rabbit anti-phospho S6 (Ser 240/244) and mouse anti-S6 antibodies from Cell

Signaling Biotechnology as described previously [55], [56].

Immunocytochemistry. Dissected tissue samples were fixed in 10% buffered formalin, embedded into paraffin. 5-7 µm thin histological sections were stained with anti-phospho S6 (Ser240/244) antibody (Cell Signaling) and counterstained with Hematoxylin.

Statistical analyses. The SigmaStat software package was used for analysis. The P values were calculated using Fisher's Exact Test (2-tail). P<0.05 was considered as statistically significant.

Conflict of Interest Statement

The authors of this manuscript have no conflict of interests to declare.

REFERENCES

1. Blagosklonny MV. Cell cycle arrest is not yet senescence, which is not just cell cycle arrest: terminology for TOR-driven aging. *Aging (Albany NY)*. 2012; 4: 159-165.
2. Demidenko ZN, Zubova SG, Bukreeva EI, Pospelov VA, Pospelova TV, Blagosklonny MV. Rapamycin decelerates cellular senescence. *Cell Cycle*. 2009; 8: 1888-1895.
3. Gan B, Sahin E, Jiang S, Sanchez-Aguilera A, Scott KL, Chin L, Williams DA, Kwiatkowski DJ, DePinho RA. mTORC1-dependent and -independent regulation of stem cell renewal, differentiation, and mobilization. *Proc Natl Acad Sci U S A*. 2008; 105: 19384-19389.
4. Gan B, DePinho RA. mTORC1 signaling governs hematopoietic stem cell quiescence. *Cell Cycle*. 2009; 8: 1003-1006.
5. Chen C, Liu Y, Liu R, Ikenoue T, Guan KL, Zheng P. TSC-mTOR maintains quiescence and function of hematopoietic stem cells by repressing mitochondrial biogenesis and reactive oxygen species. *J Exp Med*. 2008; 205: 2397-2408.
6. Chen C, Liu Y, Zheng P. mTOR regulation and therapeutic rejuvenation of aging hematopoietic stem cells. *Sci Signal*. 2009; 2: ra75.
7. Adhikari D, Zheng W, Shen Y, Gorre N, Hamalainen T, Cooney AJ, Huhtaniemi I, Lan ZJ, Liu K. Tsc/mTORC1 signaling in oocytes governs the quiescence and activation of primordial follicles. *Human Molecular Genet*. 2010; 19:397-410.
8. Kolesnichenko M, Hong L, Liao R, Vogt PK, Sun P. Attenuation of TORC1 signaling delays replicative and oncogenic RAS-induced senescence. *Cell Cycle*. 2012; 11: 2391-2401.
9. Kapahi P, Zid BM, Harper T, Koslover D, Sapin V, Benzer S. Regulation of lifespan in *Drosophila* by modulation of genes in the TOR signaling pathway. *Curr Biol*. 2004; 14: 885-890.
10. Bjedov I, Toivonen JM, Kerr F, Slack C, Jacobson J, Foley A, Partridge L. Mechanisms of life span extension by rapamycin in the fruit fly *Drosophila melanogaster*. *Cell Metab*. 2010; 11: 35-46.
11. Harrison DE, Strong R, Sharp ZD, Nelson JF, Astle CM, Flurkey K, Nadon NL, Wilkinson JE, Frenkel K, Carter CS, Pahor M, Javors MA, Fernandez E, Miller RA. Rapamycin fed late in life extends

- lifespan in genetically heterogenous mice. *Nature*. 2009; 460: 392-396.
12. Miller RA, Harrison DE, Astle CM, Baur JA, Boyd AR, de Cabo R, Fernandez E, Flurkey K, Javors MA, Nelson JF, Orihuela CJ, Pletcher S, Sharp ZD, Sinclair D, Starnes JW, Wilkinson JE et al. Rapamycin, but not resveratrol or simvastatin, extends life span of genetically heterogeneous mice. *J Gerontol A Biol Sci Med Sci*. 2011; 66: 191-201.
13. Anisimov VN, al. e, Antoch M, Blagosklonny MV. *Am J Pathol*. 2010: in press.
14. Khamzina L, Veilleux A, Bergeron S, Marette A. Increased activation of the mammalian target of rapamycin pathway in liver and skeletal muscle of obese rats: possible involvement in obesity-linked insulin resistance. *Endocrinology*. 2005; 146: 1473-1481.
15. Tremblay F, Krebs M, Dombrowski L, Brehm A, Bernroider E, Roth E, Nowotny P, WaldhŠusl W, Marette A, Roden M. Overactivation of S6 kinase 1 as a cause of human insulin resistance during increased amino acid availability. *Diabetes*. 2005; 54: 2674-2684.
16. Krebs M, Brunmair B, Brehm A, Artwohl M, Szendroedi J, Nowotny P, Roth E, FŠyrnsinn C, Promintzer M, Anderwald C, Bischof M, Roden M. The Mammalian target of rapamycin pathway regulates nutrient-sensitive glucose uptake in man. *Diabetes*. 2007; 56: 1600-1607.
17. Jiang W, Zhu Z, Thompson HJ. Dietary energy restriction modulates the activity of AMP-activated protein kinase, Akt, and mammalian target of rapamycin in mammary carcinomas, mammary gland, and liver. *Cancer Res*. 2008; 68: 5492-5499.
18. Estep PWr, Warner JB, Bulyk ML. Short-term calorie restriction in male mice feminizes gene expression and alters key regulators of conserved aging regulatory pathways. *PLoS One*. 2009; 4: e5242.
19. Masternak MM, Panici JA, Bonkowski MS, Hughes LF, Bartke A. Insulin sensitivity as a key mediator of growth hormone actions on longevity. *J Gerontol A Biol Sci Med Sci*. 2009; 64: 516-521.
20. Wang C, Maddick M, Miwa S, Jurk D, Czapiewski R, Saretzki G, Langie SA, Godschalk RW, Cameron K, von Zglinicki T. Adult-onset, short-term dietary restriction reduces cell senescence in mice. *Aging (Albany NY)*. 2010; 2: 555-566.
21. Dirx MJ, Zeegers MP, Dagnelie PC, van den Bogaard T, van den Brandt PA. Energy restriction and the risk of spontaneous mammary tumors in mice: a meta-analysis. *Int J Cancer*. 2003; 106: 766-770.
22. Sarkar NH, Fernandes G, Telang NT, Kourides IA, Good RA. Low-calorie diet prevents the development of mammary tumors in C3H mice and reduces circulating prolactin level, murine mammary tumor virus expression, and proliferation of mammary alveolar cells. *Proc Natl Acad Sci U S A*. 1982; 79: 7758-7762.
23. Berrigan D, Perkins SN, Haines DC, Hursting SD. Adult-onset calorie restriction and fasting delay spontaneous tumorigenesis in p53-deficient mice. *Carcinogenesis*. 2002; 23: 817-822.
24. Hursting SD, Perkins SN, Phang JM. Calorie restriction delays spontaneous tumorigenesis in p53-knockout transgenic mice. *Proc Natl Acad Sci U S A*. 1994; 91: 7036-7040.
25. Hursting SD, Perkins SN, Brown CC, Haines DC, Phang JM. Calorie restriction induces a p53-independent delay of spontaneous carcinogenesis in p53-deficient and wild-type mice. *Cancer Res*. 1997; 57: 2843-2846.
26. Feng Z, Hu W, de Stanchina E, Teresky AK, Jin S, Lowe S, Levine AJ. The regulation of AMPK beta1, TSC2, and PTEN expression by p53: stress, cell and tissue specificity, and the role of these gene products in modulating the IGF-1-AKT-mTOR pathways. *Cancer Res*. 2007; 67: 3043-3053.
27. Feng Z, Zhang H, Levine AJ, Jin S. The coordinate regulation of the p53 and mTOR pathways in cells. *Proc Natl Acad Sci U S A*. 2005; 102: 8204-8209.
28. Levine AJ, Feng Z, Mak TW, You H, Jin S. Coordination and communication between the p53 and IGF-1-AKT-TOR signal transduction pathways. *Genes Dev*. 2006; 20: 267-275.
29. Budanov AV, Karin M. p53 target genes sestrin1 and sestrin2 connect genotoxic stress and mTOR signaling. *Cell*. 2008; 134: 451-460.
30. Demidenko ZN, Korotchkina LG, Gudkov AV, Blagosklonny MV. Paradoxical suppression of cellular senescence by p53. *Proc Natl Acad Sci U S A*. 2010; 9660-4: 9660-9664.
31. Korotchkina LG, Leontieva OV, Bukreeva EI, Demidenko ZN, Gudkov AV, Blagosklonny MV. The choice between p53-induced senescence and quiescence is determined in part by the mTOR pathway. *Aging (Albany NY)*. 2010; 2: 344-352.
32. CoppŽ JP, Patil CK, Rodier F, Sun Y, Mu-oz DP, Goldstein J, Nelson PS, Desprez PY, Campisi J. Senescence-associated secretory phenotypes reveal cell-nonautonomous functions of oncogenic RAS and the p53 tumor suppressor. *PLoS Biol*. 2008; 6: 2853-2868.
33. Komarova EA, Krivokrysenko V, Wang K, Neznanov N, Chernov MV, Komarov PG, Brennan ML, Golovkina TV, Rokhlin OW, Kuprash DV, Nedospasov SA, Hazen SL, Feinstein E, Gudkov AV. p53 is a suppressor of inflammatory response in mice. *FASEB J*. 2005; 19: 1030-1032.
34. Gudkov AV, Gurova KV, Komarova EA. Inflammation and p53: A Tale of Two Stresses. *Genes Cancer*. 2011; 2: 503-516.
35. Feng Z, Hu W, Teresky AK, Hernando E, Cordon-Cardo C, Levine AJ. Declining p53 function in the aging process: a possible mechanism for the increased tumor incidence in older populations. *Proc Natl Acad Sci U S A*. 2007; 104: 16633-16638.
36. Donehower LA, Harvey M, Slagle BL, McArthur MJ, Montgomery CA, Jr., Butel JS, Bradley A. Mice deficient for p53 are developmentally normal but susceptible to spontaneous tumours. *Nature*. 1992; 356: 215-221.
37. Harvey M, McArthur MJ, Montgomery CA, Jr., Butel JS, Bradley A, Donehower LA. Spontaneous and carcinogen-induced tumorigenesis in p53-deficient mice. *Nat Genet*. 1993; 5: 225-229.
38. Jacks T, Remington L, Williams BO, Schmitt EM, Halachmi S, Bronson RT, Weinberg RA. Tumor spectrum analysis in p53-mutant mice. *Curr Biol*. 1994; 4: 1-7.
39. Donehower LA, Harvey M, Vogel H, McArthur MJ, Montgomery CA, Jr., Park SH, Thompson T, Ford RJ, Bradley A. Effects of genetic background on tumorigenesis in p53-deficient mice. *Mol Carcinog*. 1995; 14: 16-22.
40. Venkatachalam S, Shi YP, Jones SN, Vogel H, Bradley A, Pinkel D, Donehower LA. Retention of wild-type p53 in tumors from p53 heterozygous mice: reduction of p53 dosage can promote cancer formation. *Embo J*. 1998; 17: 4657-4667.
41. Hinkal G, Parikh N, Donehower LA. Timed somatic deletion of p53 in mice reveals age-associated differences in tumor progression. *PLoS One*. 2009; 4: e6654.
42. Anisimov VN, Zabezhinski MA, Popovich IG, Piskunova TS, Semenchenko AV, Tyndyk ML, Yurova MN, Rosenfeld SV,

Blagosklonny MV. Rapamycin increases lifespan and inhibits spontaneous tumorigenesis in inbred female mice. *Cell Cycle*. 2011; 10: 4230-4236.

43. Anisimov VN, Piskunova TS, Popovich IG, Zabezhinski MA, Tyndyk ML, Egormin PA, Yurova MV, Rosenfeld SV, Semenchenko AV, Kovalenko IG, Poroshina TE, Berstein LM. Gender differences in metformin effect on aging, life span and spontaneous tumorigenesis in 129/Sv mice. *Aging (Albany NY)*. 2010; 2: 945-958.

44. Blagosklonny MV. Metformin and sex: Why suppression of aging may be harmful to young male mice. *Aging (Albany NY)*. 2010; 2: 897-899.

45. Turturro A, Duffy P, Hass B, Kodell R, Hart R. Survival characteristics and age-adjusted disease incidences in C57BL/6 mice fed a commonly used cereal-based diet modulated by dietary restriction. *J Gerontol A Biol Sci Med Sci*. 2002; 57: B379-389.

46. Holzenberger M, Dupont J, Ducos B, Leneuve P, Geloën A, Even PC, Cervera P, Le Bouc Y. IGF-1 receptor regulates lifespan and resistance to oxidative stress in mice. *Nature*. 2003; 421: 182-187.

47. Selman C, Tullet JM, Wieser D, Irvine E, Lingard SJ, Choudhury AI, Claret M, Al-Qassab H, Carmignac D, Ramadani F, Woods A, Robinson IC, Schuster E, Batterham RL, Kozma SC, Thomas G et al. Ribosomal protein S6 kinase 1 signaling regulates mammalian life span. *Science*. 2009; 326: 140-144.

48. Upton B, Chu Q, Li BD. Li-Fraumeni syndrome: the genetics and treatment considerations for the sarcoma and associated neoplasms. *Surg Oncol Clin N Am*. 2009; 18: 145-156, ix.

49. Glazer RI. A new therapeutic basis for treating Li-Fraumeni Syndrome breast tumors expressing mutated TP53. *Oncotarget*. 2010; 1: 470-471.

50. Herbert BS, Chanoux RA, Liu Y, Baenziger PH, Goswami CP, McClintick JN, Edenberg HJ, Pennington RE, Lipkin SM, Kopelovich L. A molecular signature of normal breast epithelial and stromal cells from Li-Fraumeni syndrome mutation carriers. *Oncotarget*. 2010; 1: 405-422.

51. Mathew T, Kreis H, Friend P. Two-year incidence of malignancy in sirolimus-treated renal transplant recipients: results from five multicenter studies. *Clin Transplant*. 2004; 18: 446-449.

52. Campistol JM, Eris J, Oberbauer R, Friend P, Hutchison B, Morales JM, Claesson K, Stallone G, Russ G, Rostaing L, Kreis H, Burke JT, Brault Y, Scarola JA, Neylan JF. Sirolimus Therapy after Early Cyclosporine Withdrawal Reduces the Risk for Cancer in Adult Renal Transplantation. *J Am Soc Nephrol*. 2006; 17: 581-589.

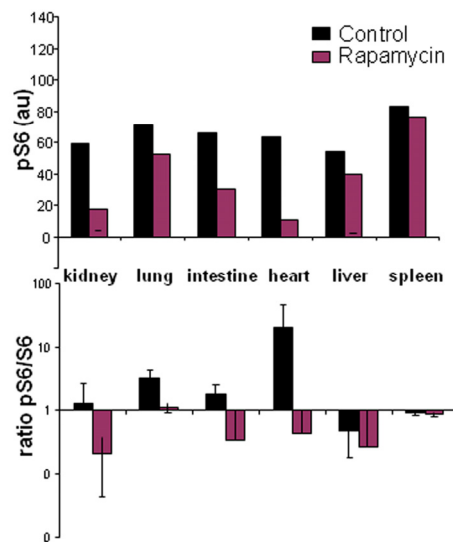
53. Blagosklonny MV. Prevention of cancer by inhibiting aging. *Cancer Biol Ther*. 2008; 7: 1520-1524.

54. Leonova KI, Shneyder J, Antoch MP, Toshkov IA, Novototskaya LR, Komarov PG, Komarova EA, Gudkov AV. A small molecule inhibitor of p53 stimulates amplification of hematopoietic stem cells but does not promote tumor development in mice. *Cell Cycle*. 2010; 9: 1434-1443.

55. Leontieva O, Gudkov A, Blagosklonny M. Weak p53 permits senescence during cell cycle arrest. *Cell Cycle*. 2010; 9: 4323-4327.

56. Leontieva OV, Blagosklonny MV. DNA damaging agents and p53 do not cause senescence in quiescent cells, while consecutive re-activation of mTOR is associated with conversion to senescence. *Aging (Albany NY)*. 2010; 2: 924-935.

SUPPLEMENTAL FIGURE



Supplemental Figure S1. Quantitative analysis of data shown in Figure 2A. Top panel - Intensity of phosphorylated S6 (pS6) signal was quantified using ImageJ program (intensity units, IU). Bottom panel - Intensity of pS6 and S6 signals were quantified and the ratio pS6/S6 was calculated.

Rapamycin as longevity enhancer and cancer preventative agent in the context of p53 deficiency

Lawrence A. Donehower

Since initial rodent studies in the mid-1930s, caloric restriction (CR) has been known to be an effective non-pharmacological intervention that can extend longevity in many species. Over the last 15-20 years, studies in yeast, worms, and flies have defined many of the signaling pathways mediating these CR-driven longevity effects. A prominent mediator of CR is the target of rapamycin (TOR) signaling pathway, which functions to monitor nutrient levels in the cell and modulate protein synthesis and cell growth in response. Dysfunctional regulation of TOR in humans has been associated with a number of aging-associated diseases such as diabetes, obesity, cardiovascular disease, and cancer [1]. On the other hand, downregulation of the TOR pathway in yeast, worms and flies by the inhibitory molecule rapamycin has been shown to significantly increase lifespan in each of those species. Moreover, in 2009, Miller, Harrison and colleagues showed that mixed inbred mice treated with rapamycin at a relatively late age (600 days) exhibited extended lifespans [2]. Recently, this group also showed that aging phenotypes were significantly delayed in the rapamycin-treated group, though testicular degeneration and cataracts increased [3].

Despite potential side effects, the rapamycin-induced longevity enhancement in a mammalian species has generated much excitement, and further studies in animal models have now indicated that cancer incidence is delayed by rapamycin treatment. This should not be too surprising, since rapamycin integrates signals initiated from a number of growth factor receptors, is upregulated in numerous cancers, and has been used as a cancer therapeutic drug in some contexts [1]. One such study by Anisomov et al. [4] showed that rapamycin treatment of HER-2 transgenic mammary cancer prone mice not only resulted in significantly extended lifespans, but also dramatically delayed tumor appearance and decreased tumor number and size. Thus, rapamycin may be a highly effective cancer preventative drug in addition to its many other beneficial effects.

To follow up and extend this initial exciting result, Gudkov, Blagosklonny, Antoch, and their colleagues have investigated the effects of rapamycin on tumor

incidence and longevity in p53-deficient mice. The results, appearing in two papers in this issue of *Aging*, confirm that the cancer preventative effects of rapamycin are significant and broad in scope [5,6]. The p53 tumor suppressor protects against an array of different tumors and p53-deficient mice succumb to lymphomas and many different types of sarcomas [7]. In the paper by Komarova et al. [5], mice heterozygous for a germline p53 null allele (p53^{+/-}) that were continuously treated with rapamycin in the drinking water beginning at a young age (<5 months) had a mean lifespan of 480 days compared to that of the control group's 373 day mean lifespan (a 28% increase). Importantly, these rapamycin-treated mice developed only half as many tumors as the control mice, a dramatic and significant anti-cancer effect. They also show direct inhibition of mTOR kinase activity in several tissues of the rapamycin-treated mice, an indicator that the rapamycin effects continuously inhibit mTOR signaling. In their discussion, the authors acknowledge that the anti-cancer effects of rapamycin are likely to be indirect, but don't speculate further. However, because mTOR integrates signals from so many growth signaling pathways, intersects with so many key growth signal transducers (such as AKT, PI-3 kinase, and Ras), and drives so many cell growth outputs, it's easy to argue that reduction of mTOR activity by rapamycin acts as a major brake on transformation. The authors suggest that the dramatic effects of rapamycin on p53^{+/-} mice could lead to use of this agent as a cancer preventative drug in Li-Fraumeni syndrome patients. Li-Fraumeni patients are analogous to p53^{+/-} mice, as they carry germline p53 mutations and are highly cancer prone at a young age [8]. This may be a good place to start in considering patients for rapamycin in clinical trials, though some of the side effects of rapamycin in mice indicated above [3] certainly need further evaluation.

In the second paper by Comas et al. [6], the authors treat p53 null (p53^{-/-}) mice with rapamycin from the age of 8 weeks. These mice are profoundly tumor prone and succumb to lymphomas by 4-6 months of age. In this paper, however, the bioavailability of the relatively insoluble rapamycin was enhanced by a novel rapamycin formulation called Rapatar that improved

water solubility. The authors showed that blood rapamycin levels were significantly increased in animals treated with Rapatar compared to the standard form of rapamycin. As with the p53+/- mice, Rapatar treatment of the p53-/- mice resulted in significant longevity extension and delayed cancer formation relative to untreated p53-/- mice. Mean tumor latencies for the control p53-/- mice and the Rapatar-treated p53-/- were 161 and 261 days, respectively, a very significant effect. The authors argue that improvement of rapamycin bioavailability through improved formulations is a necessity for clinical applications. They are uncertain whether the rapamycin effects are direct or indirect, but believe it to delay tumorigenesis by slowing aging. However, because the p53-/- mice are relatively young when they develop tumors, this interpretation seems less likely. Nevertheless, both papers represent exciting new advances that could lead us closer to pharmaceuticals that both enhance lifespan and delay cancer.

Lawrence A. Donehower, PhD
Departments of Molecular Virology & Microbiology, Molecular & Cellular Biology, and Pediatrics, Baylor College of Medicine,
Houston, TX 77030
Email: larryd@bcm.edu

Received: 10/25/12; Published: 10/27/12

REFERENCES

1. Zoncu R, Efeyan A, Sabatini DM. *Nat Rev Mol Cell Biol.* 2011; 12:21-35.
2. Harrison DE, Strong R, Sharp ZD et al. *Nature* 2009; 460:392-395.
3. Wilkinson JE, Burmeister L, Brooks SV et al. *Aging Cell.* 2012; 11:675-682.
4. Anisimov VN, Zabezhinski MA, Popovich IG et al. *Am J Pathol.* 2010; 176:2092-2097.
5. Komarova EA, Antoch MP, Novototskaya LR et al. *Aging.* 2012; 4: this issue
6. Comas M, Toshkov I, Kuropatwinski KK et al. *Aging.* 2012; 4
7. Donehower LA, Lozano G. *Nat Rev Cancer* 2009; 9:831-841.
8. Malkin D. *Genes Cancer.* 2011; 2:475-484.

Tumor suppression by p53 without apoptosis and senescence: conundrum or rapalog-like gerosuppression?

Mikhail V. Blagosklonny

Department of Cell Stress Biology, Roswell Park Cancer Institute, Buffalo, NY 14263, USA

Key words: tumor suppressors, aging, apoptosis, geroconversion

Received: 7/15/12; **Accepted:** 7/30/12; **Published:** 7/31/12

Correspondence to: Mikhail V. Blagosklonny, MD/PhD; **E-mail:** blagosklonny@oncotarget.com

Copyright: © Blagosklonny. This is an open-access article distributed under the terms of the Creative Commons Attribution License, which permits unrestricted use, distribution, and reproduction in any medium, provided the original author and source are credited

Abstract: I discuss a very obscure activity of p53, namely suppression of senescence (gerosuppression), which is also manifested as anti-hypertrophic, anti-hypermetabolic, anti-inflammatory and anti-secretory effects of p53. But can gerosuppression suppress tumors?

INTRODUCTION

Wt p53 can induce apoptosis, cell cycle arrest and senescence, which are sufficient to explain tumor suppression by p53 [1]. A recent paper in *Cell* described that these activities are dispensable for tumor suppression [2]. Mutant p53 (p53^{3KR}) that cannot cause arrest, senescence and apoptosis still suppressed tumors in mice [2, 3]. Why do then wt p53 induce apoptosis, cell cycle arrest and senescence? Before entertaining this intriguing question, I will focus on suppression of senescence (gerosuppression) by p53, overlapping with its anti-hypertrophic, anti-hypermetabolic, anti-inflammatory and anti-secretory effects.

P53 suppresses the conversion from arrest to senescence (geroconversion)

How can p53 suppress senescence, if it also can cause senescence? As recently suggested, induction of senescence is not an independent activity of p53 but a consequence of cell-cycle arrest [4-8]. This predicts that any mutant p53 that cannot cause arrest will not cause senescence too. In agreement, p53^{3KR} did not cause senescence [2]. This is not trivial. To create p53^{3KR}, wt p53 was altered to abolish apoptosis and cell-cycle arrest only [2]. Li et al did not modify p53 to abolish senescence as an independent activity. It was not needed, simply because p53 does not induce senescence as an independent effect. (Note: Seemingly in contrast, it was reported that mutant p53, which cannot induce

arrest in response to DNA damage, can cause senescence [9]. Although this mutant p53 did not cause instant arrest, it still arrested proliferation later and then senescence developed [9]. So there is no exception). p53 cannot induce senescence without inducing arrest. But p53 can induce quiescence, a reversible condition characterized by low protein synthesis and metabolism (see detailed definitions in ref. [7, 8]). It was assumed that when p53 causes quiescence, it simply fails to induce senescence. But another possibility is that in such cases p53 suppresses the conversion from cell-cycle arrest to senescence (geroconversion). How can that be tested? In some cell lines, induction of ectopic p21 causes irreversible senescence, whereas induction of p53 causes quiescence [4]. Does p53 suppresses a senescent program? This question can be answered by simultaneously inducing both p53 and ectopic p21. When both p21 and p53 were induced, then cells become quiescent not senescent [4]. p53 was dominant, actively suppressing senescence caused by p21... or by something else? In fact, p21 merely causes cell cycle arrest and does not inhibit mitogen-activated, nutrient-sensing and growth-promoting pathways such as Target of Rapamycin (mTOR) [4]. During several days, these pathways (gerogenic pathways, for brevity) convert p21-induced arrest into senescence. Rapamycin can decelerate geroconversion [10-13]. Also, p53 can inhibit the mTOR pathway [4-6, 14-17]. In some conditions, p53 can suppress senescence during arrest [4-6]. Wt p53 induces arrest and then if it fails to suppress senescence, then senescence prevails. Rather than p53, gerogenic

pathways drive senescence during cell-cycle arrest [18].

In summary, wt p53 seems to have three independent effects: apoptosis, cell-cycle arrest and gerosuppression. By inducing arrest, wt p53 primes cells for senescence, unless p53 is able or “willing” to suppress geroconversion. At high levels, gerosuppression by p53 is limited by apoptosis [6]. This predicts that p53^{3KR} would potentially suppress senescence because gerosuppression by p53^{3KR} will not be limited by apoptosis.

Hyper-metabolic senescent phenotype

Senescent cells are hyper-functional: hypertrophic, hypermetabolic, hyper-secretory and hyper-inflammatory [8]. Also, senescent cells may accumulate lipids, becoming not only large but also “fat” (Figure 1). Induction of p53 decreased both cellular hypertrophy and fat accumulation (Figure 1). This is in line with numerous metabolic effects of p53 including inhibition of glycolysis and stimulation of fatty acids oxidation [19-32]. Importantly, p53^{3KR} retained the ability to inhibit glycolysis and reactive oxygen species (ROS) [2]. (Noteworthy, ROS and mTOR co-activate each other [33] and N-Acetyl Cysteine (NAC), which decreases ROS, also inhibits mTOR [34]). Also, p53 decreases hyper-secretory phenotype also known as SASP [35] and suppresses a pro-inflammatory phenotype [36, 37]. How might gerosuppression contribute to tumor suppression? There are several overlapping explanations, from different points of view of the same process.

Gerogetic conversion and oncogenic transformation

In proliferating epithelial cells, pro-gerogenic conversion may contribute to carcinogenesis directly. The PI3K/mTOR pathway is universally activated in cancer [38-49]. p53 can inhibit the PI3K/mTOR pathway [4-6, 14-17, 50]. Like p53, many other tumor suppressors such as PTEN, AMPK, TSC2, LKB1, NF1 inhibit the PI3K/mTOR pathway [51].

Geroconversion of stromal cells creates carcinogenic microenvironment

First, senescence creates a selective disadvantage for normal cells, thus selecting for cancer [52-54]. Also, senescent stromal cells secrete factors that favors pre-cancer and cancer growth [37, 54-62]. Third, the senescent stroma is hyper-metabolic and thus promotes cancer by fueling cancer growth [59, 60, 63-71]. In a model of accelerated host aging, mTOR activity was increased in normal tissues [72]. This pro-senescent microenvironment accelerated growth of implanted tumors. The tumor-promoting effects of pro-senescent microenvironment were abrogated by rapamycin [72].

Cancer is an age-related disease

The incidence of cancer is increased exponentially in aging mammals. Manipulations that slow down aging delay cancer [73]. For example, calorie restriction delays cancer [74-76] including cancer in p53-deficient mice [77, 78]. Rapamycin, which decelerates aging, also postpones cancer in animals [73, 79-81] and in patients after renal transplantation [82-86].

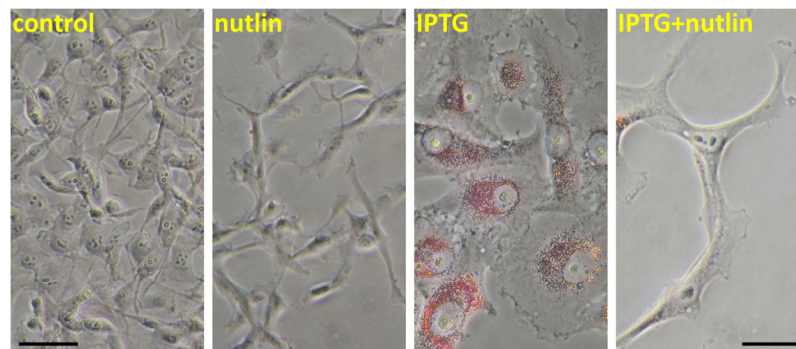


Figure 1. Nutlin-3a decreased lipid accumulation during IPTG-induced senescence. HT-p21 cells were treated with IPTG, nutlin-3a and IPTG+nutlin-3a (as indicated) for 3 days as described previously [4-6] and cells were stained with “oil red O” for lipids. In HT-p21 cells, IPTG induces ectopic p21 and senescence. As described previously, nutlin-3a induces endogenous p53 and suppresses IPTG-induced senescence [4-6].

Is aging accelerated in p53-deficient mice?

Inactivation of tumor suppressors accelerates both aging and cancer [87]. It was thought that p53 is an exception. Yet, given that p53 can suppress geroconversion, it may not be the exception after all. A complex role of p53 in cellular senescence and organismal aging was discussed [88-91]. Mice with increased, but normally regulated, p53 lives longer [92]. p53 knockout mice have both accelerated carcinogenesis and decreased longevity [93-98]. p53^{-/-} mice have a pro-inflammatory phenotype characteristic of accelerated aging [36,37]. Also, atherosclerosis is accelerated in p53^{-/-} animals [99-102]. While loss of p53 by itself makes cells prone to become tumorigenic, an increased rate of organismal aging in the absence of p53 may further accelerate carcinogenesis.

Rapalogs and p53

Rapamycin (sirolimus) and other rapalogs (everolimus and temsirolimus) are pharmacological tumor suppressors. Noteworthy, like p53, rapamycin decreases glycolysis [103] and lactate production [34] and stimulates oxidation of fatty acids [104, 105]. Furthermore, rapamycin slows cellular proliferation, and so, not surprisingly, p53^{3KR} inhibits clonogenicity too [2]. Yet, p53 affects metabolism and aging not only via mTOR but also via direct transactivation of metabolic enzymes, rendering it a more potent tumor suppressor.

Puzzles remain

Still, even if gerosuppression and anti-hypermetabolic effects can in part explain tumor suppression, puzzles remain. Why does wt p53 cause “unnecessary” apoptosis and “instant” (p21-dependent) arrest? Why is p53 needed at all? In the wild, most mice die from external/accidental causes and only a few would live long enough to die from cancer, regardless of p53 status. In the wild, starvation (natural calorie restriction) would delay cancer further. Yet, p53 is also needed very early in life, or technically speaking, even before life has begun, because p53 plays role in fertility and reproduction [106-113]. And is tumor suppression a late life function?

Alternatively, tumor suppression is a primary function of p53. And each of the three activities (apoptosis, arrest, gerosuppression) is partially sufficient for cancer prevention. In their combination, these activities are the most effective tumor suppressor. And each activity may be partially dispensable in some mice strains and in some conditions. For example, the gerosuppressive activity of p53 may be preferentially important in peculiar strains of laboratory mice, or mice fed *ad libitum*, which constantly activates mTOR and accelerates aging. In fact, calorie restriction, which

deactivates mTOR and decelerates aging, partially substitutes for the loss of p53 in mice.

ACKNOWLEDGEMENTS

I thank Wei Gu, Arnold Levine and Bert Vogelstein for critical reading of the manuscript and excellent suggestions.

CONFLICT OF INTERESTS STATEMENT

The author of this manuscript has no conflict of interest to declare.

REFERENCES

1. Vogelstein B, Lane DP, Levine AJ. Surfing the p53 network. *Nature*. 2000; 408: 307-310.
2. Li T, Kon N, Jiang L, Tan M, Ludwig T, Zhao Y, Baer R, Gu W. Tumor Suppression in the Absence of p53-Mediated Cell-Cycle Arrest, Apoptosis, and Senescence. *Cell*. 2012; 149: 1269-1283.
3. Hock AK, Vousden KH. Tumor Suppression by p53: Fall of the Triumvirate? *Cell*. 2012; 149: 1183-1185.
4. Demidenko ZN, Korotchkina LG, Gudkov AV, Blagosklonny MV. Paradoxical suppression of cellular senescence by p53. *Proc Natl Acad Sci U S A*. 2010; 107: 9660-9664.
5. Korotchkina LG, Leontieva OV, Bukreeva EI, Demidenko ZN, Gudkov AV, Blagosklonny MV. The choice between p53-induced senescence and quiescence is determined in part by the mTOR pathway. *Aging*. 2010; 2: 344-352.
6. Leontieva O, Gudkov A, Blagosklonny M. Weak p53 permits senescence during cell cycle arrest. *Cell Cycle*. 2010; 9: 4323-4327.
7. Blagosklonny MV. Cell cycle arrest is not senescence. *Aging*. 2011; 3: 94-101.
8. Blagosklonny MV. Cell cycle arrest is not yet senescence, which is not just cell cycle arrest: terminology for TOR-driven aging. *Aging*. 2012; 4: 159-165.
9. Brady CA, Jiang D, Mello SS, Johnson TM, Jarvis LA, Kozak MM, Kenzelmann Broz D, Basak S, Park EJ, McLaughlin ME, Karnezis AN, Attardi LD. Distinct p53 transcriptional programs dictate acute DNA-damage responses and tumor suppression. *Cell*. 2011; 145: 571-583.
10. Demidenko ZN, Blagosklonny MV. Growth stimulation leads to cellular senescence when the cell cycle is blocked. *Cell Cycle*. 2008; 7: 3355-3361.
11. Demidenko ZN, Zubova SG, Bukreeva EI, Pospelov VA, Pospelova TV, Blagosklonny MV. Rapamycin decelerates cellular senescence. *Cell Cycle*. 2009; 8: 1888-1895.
12. Demidenko ZN, Blagosklonny MV. Quantifying pharmacologic suppression of cellular senescence: prevention of cellular hypertrophy versus preservation of proliferative potential. *Aging*. 2009; 1: 1008-1016.
13. Pospelova TV, Demidenko ZN, Bukreeva EI, Pospelov VA, Gudkov AV, Blagosklonny MV. Pseudo-DNA damage response in senescent cells. *Cell Cycle*. 2009; 8: 4112-4118.
14. Feng Z, Levine AJ. The regulation of energy metabolism and the IGF-1/mTOR pathways by the p53 protein. *Trends Cell Biol*. 2010; 20: 427-434.

15. Feng Z, Hu W, de Stanchina E, Teresky AK, Jin S, Lowe S, Levine AJ. The regulation of AMPK beta1, TSC2, and PTEN expression by p53: stress, cell and tissue specificity, and the role of these gene products in modulating the IGF-1-AKT-mTOR pathways. *Cancer Res.* 2007; 67: 3043-3053.
16. Levine AJ, Feng Z, Mak TW, You H, Jin S. Coordination and communication between the p53 and IGF-1-AKT-TOR signal transduction pathways. *Genes Dev.* 2006; 20: 267-275.
17. Budanov AV, Karin M. p53 target genes sestrin1 and sestrin2 connect genotoxic stress and mTOR signaling. *Cell.* 2008; 134: 451-460.
18. Leontieva OV, Blagosklonny MV. DNA damaging agents and p53 do not cause senescence in quiescent cells, while consecutive re-activation of mTOR is associated with conversion to senescence. *Aging.* 2010; 2: 924-935.
19. Bensaad K, Tsuruta A, Selak MA, Vidal MN, Nakano K, Bartrons R, Gottlieb E, Vousden KH. TIGAR, a p53-inducible regulator of glycolysis and apoptosis. *Cell.* 2006; 126: 107-120.
20. Bensaad K, Vousden KH. p53: new roles in metabolism. *Trends Cell Biol.* 2007; 17: 286-291.
21. Kawachi K, Araki K, Tobiume K, Tanaka N. p53 regulates glucose metabolism through an IKK-NF-kappaB pathway and inhibits cell transformation. *Nat Cell Biol.* 2008; 10: 611-618.
22. Vousden KH, Ryan KM. p53 and metabolism. *Nat Rev Cancer.* 2009; 9: 691-700.
23. Vigneron A, Vousden KH. p53, ROS and senescence in the control of aging. *Aging.* 2010; 2: 471-474.
24. Cheung EC, Vousden KH. The role of p53 in glucose metabolism. *Curr Opin Cell Biol.* 2010; 22: 186-191.
25. Suzuki S, Tanaka T, Poyurovsky MV, Nagano H, Mayama T, Ohkubo S, Lokshin M, Hosokawa H, Nakayama T, Suzuki Y, Sugano S, Sato E, Nagao T, Yokote K, Tatsuno I, Prives C. Phosphate-activated glutaminase (GLS2), a p53-inducible regulator of glutamine metabolism and reactive oxygen species. *Proc Natl Acad Sci U S A.* 2010; 107: 7461-7466.
26. Jiang P, Du W, Wang X, Mancuso A, Gao X, Wu M, Yang X. p53 regulates biosynthesis through direct inactivation of glucose-6-phosphate dehydrogenase. *Nat Cell Biol.* 2011; 13: 310-316.
27. Zhu Y, Prives C. p53 and Metabolism: The GAMT Connection. *Mol Cell.* 2009; 36: 351-352.
28. Bensaad K, Cheung EC, Vousden KH. Modulation of intracellular ROS levels by TIGAR controls autophagy. *Embo J.* 2009; 28: 3015-3026.
29. Hu W, Zhang C, Wu R, Sun Y, Levine A, Feng Z. Glutaminase 2, a novel p53 target gene regulating energy metabolism and antioxidant function. *Proc Natl Acad Sci U S A.* 2010; 107: 7455-7460.
30. Ide T, Brown-Endres L, Chu K, Ongusaha PP, Ohtsuka T, El-Deiry WS, Aaronson SA, Lee SW. GAMT, a p53-inducible modulator of apoptosis, is critical for the adaptive response to nutrient stress. *Mol Cell.* 2009; 36: 379-392.
31. Park JY, Wang PY, Matsumoto T, Sung HJ, Ma W, Choi JW, Anderson SA, Leary SC, Balaban RS, Kang JG, Hwang PM. p53 improves aerobic exercise capacity and augments skeletal muscle mitochondrial DNA content. *Circ Res.* 2009; 105: 705-712.
32. Madan E, Gogna R, Bhatt M, Pati U, Kuppusamy P, Mahdi AA. Regulation of glucose metabolism by p53: emerging new roles for the tumor suppressor. *Oncotarget.* 2011; 2: 948-957.
33. Blagosklonny MV. Aging: ROS or TOR. *Cell Cycle.* 2008; 7: 3344-3354.
34. Leontieva OV, Blagosklonny MV. Yeast-like chronological senescence in mammalian cells: phenomenon, mechanism and pharmacological suppression. *Aging.* 2011; 3: 1078-1091.
35. Coppž JP, Patil CK, Rodier F, Sun Y, Mu-oz DP, Goldstein J, Nelson PS, Desprez PY, Campisi J. Senescence-associated secretory phenotypes reveal cell-nonautonomous functions of oncogenic RAS and the p53 tumor suppressor. *PLoS Biol.* 2008; 6: 2853-2868.
36. Komarova EA, Krivokrysenko V, Wang K, Neznanov N, Chernov MV, Komarov PG, Brennan ML, Golovkina TV, Rokhlin OW, Kuprash DV, Nedospasov SA, Hazen SL, Feinstein E, Gudkov AV. p53 is a suppressor of inflammatory response in mice. *Faseb J.* 2005; 19: 1030-1032.
37. Gudkov AV, Gurova KV, Komarova EA. Inflammation and p53: A Tale of Two Stresses. *Genes Cancer.* 2011; 2: 503-516.
38. Vogelstein B, Kinzler KW. Cancer genes and the pathways they control. *Nat Med.* 2004; 10: 789-799.
39. Shaw RJ, Cantley LC. Ras, PI(3)K and mTOR signalling controls tumour cell growth. *Nature.* 2006; 441: 424-430.
40. Janes MR, Fruman DA. Targeting TOR dependence in cancer. *Oncotarget.* 2010; 1: 69-76.
41. Guertin DA, Sabatini DM. Defining the role of mTOR in cancer. *Cancer Cell.* 2007; 12: 9-22.
42. Schmidt-Kittler O, Zhu J, Yang J, Liu G, Hendricks W, Lengauer C, Gabelli SB, Kinzler KW, Vogelstein B, Huso DL, Zhou S. PI3Kalpha inhibitors that inhibit metastasis. *Oncotarget.* 2010; 1: 339-348.
43. Martelli AM, Evangelisti C, Chiarini F, McCubrey JA. The phosphatidylinositol 3-kinase/Akt/mTOR signaling network as a therapeutic target in acute myelogenous leukemia patients. *Oncotarget.* 2010; 1: 89-103.
44. Zavel L. P3Kalpha: a driver of tumor metastasis? *Oncotarget.* 2010; 1: 315-316.
45. Zhang Z, Stiegler AL, Boggon TJ, Kobayashi S, Halmos B. EGFR-mutated lung cancer: a paradigm of molecular oncology. *Oncotarget.* 2010; 1: 497-514.
46. Shahbazian D, Parsyan A, Petroulakis E, Hershey J, Sonenberg N. eIF4B controls survival and proliferation and is regulated by proto-oncogenic signaling pathways. *Cell Cycle.* 2010; 9: 4106-4109.
47. Zhao L, Vogt PK. Hot-spot mutations in p110alpha of phosphatidylinositol 3-kinase (p13K): differential interactions with the regulatory subunit p85 and with RAS. *Cell Cycle.* 2010; 9: 596-600.
48. Bhatia B, Nahle Z, Kenney AM. Double trouble: when sonic hedgehog signaling meets TSC inactivation. *Cell Cycle.* 2010; 9: 456-459.
49. Fujishita T, Aoki M, Taketo MM. The role of mTORC1 pathway in intestinal tumorigenesis. *Cell Cycle.* 2009; 8: 3684-3687.
50. Galluzzi L, Kepp O, Kroemer G. TP53 and MTOR crosstalk to regulate cellular senescence. *Aging.* 2010; 2: 535-537.
51. Blagosklonny MV. Molecular damage in cancer: an argument for mTOR-driven aging. *Aging.* 2011; 3: 1130-1141.
52. Blagosklonny MV. NCI's provocative questions on cancer: some answers to ignite discussion. *Oncotarget.* 2011; 2: 1352-1367.
53. Henry CJ, Marusyk A, Zaberezhnyy V, Adane B, DeGregori J. Declining lymphoid progenitor fitness promotes aging-

associated leukemogenesis. *Proc Natl Acad Sci U S A.* 2010; 107: 21713-21718.

54. Henry CJ, Marusyk A, DeGregori J. Aging-associated changes in hematopoiesis and leukemogenesis: what's the connection? *Aging.* 2011; 3: 643-656.

55. Parrinello S, Coppe JP, Krtolica A, Campisi J. Stromal-epithelial interactions in aging and cancer: senescent fibroblasts alter epithelial cell differentiation. *J Cell Sci.* 2005; 118: 485-496.

56. Coppe JP, Patil CK, Rodier F, Sun Y, Munoz DP, Goldstein J, Nelson PS, Desprez PY, Campisi J. Senescence-associated secretory phenotypes reveal cell-nonautonomous functions of oncogenic RAS and the p53 tumor suppressor. *PLoS Biol.* 2008; 6: 2853-2868.

57. Davalos AR, Coppe JP, Campisi J, Desprez PY. Senescent cells as a source of inflammatory factors for tumor progression. *Cancer Metastasis Rev.* 2011; 29: 273-283.

58. Coussens LM, Werb Z. Inflammation and cancer. *Nature.* 2002; 420: 860-867.

59. Lisanti MP, Martinez-Outschoorn UE, Pavlides S, Whitaker-Menezes D, Pestell RG, Howell A, Sotgia F. Accelerated aging in the tumor microenvironment: connecting aging, inflammation and cancer metabolism with personalized medicine. *Cell Cycle.* 2011; 10: 2059-2063.

60. Balliet RM, Capparelli C, Guido C, Pestell TG, Martinez-Outschoorn UE, Lin Z, Whitaker-Menezes D, Chiavarina B, Pestell RG, Howell A, Sotgia F, Lisanti MP. Mitochondrial oxidative stress in cancer-associated fibroblasts drives lactate production, promoting breast cancer tumor growth: understanding the aging and cancer connection. *Cell Cycle.* 2011; 10: 4065-4073.

61. Campisi J. Senescent cells, tumor suppression, and organismal aging: good citizens, bad neighbors. *Cell.* 2005; 120: 513-522.

62. Vicente-Duenas C, Abollo-Jimenez F, Ruiz-Roca L, Alonso-Escudero E, Jimenez R, Cenador MB, Criado FJ, Cobaleda C, Sanchez-Garcia I. The age of the target cell affects B-cell leukaemia malignancy. *Aging.* 2010; 2: 908-913.

63. Bonuccelli G, Whitaker-Menezes D, Castello-Cros R, Pavlides S, Pestell RG, Fatatis A, Witkiewicz AK, Vander Heiden MG, Migneco G, Chiavarina B, Frank PG, Capozza F, Flomenberg N, Martinez-Outschoorn UE, Sotgia F, Lisanti MP. The reverse Warburg effect: glycolysis inhibitors prevent the tumor promoting effects of caveolin-1 deficient cancer associated fibroblasts. *Cell Cycle.* 2010; 9: 1960-1971.

64. Castello-Cros R, Bonuccelli G, Molchansky A, Capozza F, Witkiewicz AK, Birbe RC, Howell A, Pestell RG, Whitaker-Menezes D, Sotgia F, Lisanti MP. Matrix remodeling stimulates stromal autophagy, "fueling" cancer cell mitochondrial metabolism and metastasis. *Cell Cycle.* 2011; 10: 2021-2034.

65. Chiavarina B, Whitaker-Menezes D, Martinez-Outschoorn UE, Witkiewicz AK, Birbe RC, Howell A, Pestell RG, Smith J, Daniel R, Sotgia F, Lisanti MP. Pyruvate kinase expression (PKM1 and PKM2) in cancer-associated fibroblasts drives stromal nutrient production and tumor growth. *Cancer Biol Ther.* 2011; 12.

66. Bonuccelli G, Tsirigos A, Whitaker-Menezes D, Pavlides S, Pestell RG, Chiavarina B, Frank PG, Flomenberg N, Howell A, Martinez-Outschoorn UE, Sotgia F, Lisanti MP. Ketones and lactate "fuel" tumor growth and metastasis: Evidence that epithelial cancer cells use oxidative mitochondrial metabolism. *Cell Cycle.* 2010; 9: 3506-3514.

67. Migneco G, Whitaker-Menezes D, Chiavarina B, Castello-Cros R, Pavlides S, Pestell RG, Fatatis A, Flomenberg N, Tsirigos A,

Howell A, Martinez-Outschoorn UE, Sotgia F, Lisanti MP. Glycolytic cancer associated fibroblasts promote breast cancer tumor growth, without a measurable increase in angiogenesis: evidence for stromal-epithelial metabolic coupling. *Cell Cycle.* 2010; 9: 2412-2422.

68. Ko YH, Lin Z, Flomenberg N, Pestell RG, Howell A, Sotgia F, Lisanti MP, Martinez-Outschoorn UE. Glutamine fuels a vicious cycle of autophagy in the tumor stroma and oxidative mitochondrial metabolism in epithelial cancer cells: Implications for preventing chemotherapy resistance. *Cancer Biol Ther.* 2011; 12.

69. Martinez-Outschoorn UE, Pestell RG, Howell A, Tykocinski ML, Nagajyothi F, Machado FS, Tanowitz HB, Sotgia F, Lisanti MP. Energy transfer in "parasitic" cancer metabolism: mitochondria are the powerhouse and Achilles' heel of tumor cells. *Cell Cycle.* 2011; 10: 4208-4216.

70. Martinez-Outschoorn UE, Whitaker-Menezes D, Lin Z, Flomenberg N, Howell A, Pestell RG, Lisanti MP, Sotgia F. Cytokine production and inflammation drive autophagy in the tumor microenvironment: role of stromal caveolin-1 as a key regulator. *Cell Cycle.* 2011; 10: 1784-1793.

71. Capparelli C, Guido C, Whitaker-Menezes D, Bonuccelli G, Balliet R, Pestell TG, Goldberg AF, Pestell RG, Howell A, Sneddon S, Birbe R, Tsirigos A, Martinez-Outschoorn U, Sotgia F, Lisanti MP. Autophagy and senescence in cancer-associated fibroblasts metabolically supports tumor growth and metastasis via glycolysis and ketone production. *Cell Cycle.* 2012; 11: 2285-2302.

72. Mercier I, Camacho J, Titchen K, Gonzales DM, Quann K, Bryant KG, Molchansky A, Milliman JN, Whitaker-Menezes D, Sotgia F, Jasmin JF, Schwarting R, Pestell RG, Blagosklonny MV, Lisanti MP. Caveolin-1 and Accelerated Host Aging in the Breast Tumor Microenvironment: Chemoprevention with Rapamycin, an mTOR Inhibitor and Anti-Aging Drug. *Am J Pathol.* 2012; 181: 278-293.

73. Blagosklonny MV. Prevention of cancer by inhibiting aging. *Cancer Biol Ther.* 2008; 7: 1520-1524.

74. Hursting SD, Lavigne JA, Berrigan D, Perkins SN, Barrett JC. Calorie restriction, aging, and cancer prevention: mechanisms of action and applicability to humans. *Annu Rev Med.* 2003; 54: 131-152.

75. Longo VD, Fontana L. Calorie restriction and cancer prevention: metabolic and molecular mechanisms. *Trends Pharmacol Sci.* 2010; 31: 89-98.

76. Blagosklonny MV. Calorie restriction: Decelerating mTOR-driven aging from cells to organisms (including humans). *Cell Cycle.* 2010; 9: 683-688.

77. Hursting SD, Perkins SN, Phang JM. Calorie restriction delays spontaneous tumorigenesis in p53-knockout transgenic mice. *Proc Natl Acad Sci U S A.* 1994; 91: 7036-7040.

78. Berrigan D, Perkins SN, Haines DC, Hursting SD. Adult-onset calorie restriction and fasting delay spontaneous tumorigenesis in p53-deficient mice. *Carcinogenesis.* 2002; 23: 817-822.

79. Harrison DE, Strong R, Sharp ZD, Nelson JF, Astle CM, Flurkey K, Nadon NL, Wilkinson JE, Frenkel K, Carter CS, Pahor M, Javors MA, Fernandez E, Miller RA. Rapamycin fed late in life extends lifespan in genetically heterogeneous mice. *Nature.* 2009; 460: 392-396.

80. Anisimov VN, Zabezhinski MA, Popovich IG, Piskunova TS, Semenchenko AV, Tyndyk ML, Yurova MN, Antoch MP, Blagosklonny MV. Rapamycin extends maximal lifespan in cancer-prone mice. *Am J Pathol.* 2010; 176: 2092-2097.

- 81.** Anisimov VN, Zabezhinski MA, Popovich IG, Piskunova TS, Semenchenko AV, Tyndyk ML, Yurova MN, Rosenfeld SV, Blagosklonny MV. Rapamycin increases lifespan and inhibits spontaneous tumorigenesis in inbred female mice. *Cell Cycle*. 2011; 10: 4230-4236.
- 82.** Mathew T, Kreis H, Friend P. Two-year incidence of malignancy in sirolimus-treated renal transplant recipients: results from five multicenter studies. *Clin Transplant*. 2004; 18: 446-449.
- 83.** Kauffman HM, Cherikh WS, Cheng Y, Hanto DW, Kahan BD. Maintenance immunosuppression with target-of-rapamycin inhibitors is associated with a reduced incidence of de novo malignancies. *Transplantation*. 2005; 80: 883-889.
- 84.** Yakupoglu YK, Buell JF, Woodle S, Kahan BD. Individualization of Immunosuppressive Therapy. III. Sirolimus Associated With a Reduced Incidence of Malignancy. *Transplant Proc*. 2006; 38: 358-361.
- 85.** Campistol JM, Eris J, Oberbauer R, Friend P, Hutchison B, Morales JM, Claesson K, Stallone G, Russ G, Rostaing L, Kreis H, Burke JT, Braut Y, Scarola JA, Neylan JF. Sirolimus Therapy after Early Cyclosporine Withdrawal Reduces the Risk for Cancer in Adult Renal Transplantation. *J Am Soc Nephrol*. 2006; 17: 581-589.
- 86.** Stallone G, Schena A, Infante B, Di Paolo S, Loverre A, Maggio G, Ranieri E, Gesualdo L, Schena FP, Grandaliano G. Sirolimus for Kaposi's sarcoma in renal-transplant recipients. *N Engl J Med*. 2005; 352: 1317-1323.
- 87.** Pinkston JM, Garigan D, Hansen M, Kenyon C. Mutations that increase the life span of *C. elegans* inhibit tumor growth. *Science*. 2006; 313: 971-975.
- 88.** Poyurovsky MV, Prives C. P53 and aging: A fresh look at an old paradigm. *Aging*. 2010; 2: 380-382.
- 89.** Blagosklonny MV. Revisiting the antagonistic pleiotropy theory of aging: TOR-driven program and quasi-program. *Cell Cycle*. 2010; 9: 3151-3156.
- 90.** de Keizer PL, Laberge RM, Campisi J. p53: Pro-aging or pro-longevity? *Aging*. 2010; 2: 377-379.
- 91.** Chao SK, Horwitz SB, McDavid HM. Insights into 4E-BP1 and p53 mediated regulation of accelerated cell senescence. *Oncotarget*. 2011; 2: 89-98.
- 92.** Matheu A, Maraver A, Klatt P, Flores I, Garcia-Cao I, Borrás C, Flores JM, Vi-a J, Blasco MA, Serrano M. Delayed ageing through damage protection by the Arf/p53 pathway. *Nature*. 2007; 448: 375-379.
- 93.** Donehower LA, Harvey M, Slagle BL, McArthur MJ, Montgomery CA, Jr., Butel JS, Bradley A. Mice deficient for p53 are developmentally normal but susceptible to spontaneous tumours. *Nature*. 1992; 356: 215-221.
- 94.** Harvey M, McArthur MJ, Montgomery CA, Jr., Butel JS, Bradley A, Donehower LA. Spontaneous and carcinogen-induced tumorigenesis in p53-deficient mice. *Nat Genet*. 1993; 5: 225-229.
- 95.** Jacks T, Remington L, Williams BO, Schmitt EM, Halachmi S, Bronson RT, Weinberg RA. Tumor spectrum analysis in p53-mutant mice. *Curr Biol*. 1994; 4: 1-7.
- 96.** Donehower LA, Harvey M, Vogel H, McArthur MJ, Montgomery CA, Jr., Park SH, Thompson T, Ford RJ, Bradley A. Effects of genetic background on tumorigenesis in p53-deficient mice. *Mol Carcinog*. 1995; 14: 16-22.
- 97.** Venkatachalam S, Shi YP, Jones SN, Vogel H, Bradley A, Pinkel D, Donehower LA. Retention of wild-type p53 in tumors from p53 heterozygous mice: reduction of p53 dosage can promote cancer formation. *Embo J*. 1998; 17: 4657-4667.
- 98.** Hinkal G, Parikh N, Donehower LA. Timed somatic deletion of p53 in mice reveals age-associated differences in tumor progression. *PLoS One*. 2009; 4: e6654.
- 99.** Guevara NV, Kim HS, Antonova EI, Chan L. The absence of p53 accelerates atherosclerosis by increasing cell proliferation in vivo. *Nat Med*. 1999; 5: 335-339.
- 100.** Mercer J, Figg N, Stoneman V, Braganza D, Bennett MR. Endogenous p53 protects vascular smooth muscle cells from apoptosis and reduces atherosclerosis in ApoE knockout mice. *Circ Res*. 2005; 96: 667-674.
- 101.** Mercer J, Bennett M. The role of p53 in atherosclerosis. *Cell Cycle*. 2006; 5: 1907-1909.
- 102.** van Vlijmen BJ, Gerritsen G, Franken AL, Boesten LS, Kockx MM, Gijbels MJ, Vierboom MP, van Eck M, van De Water B, van Berkel TJ, Havekes LM. Macrophage p53 deficiency leads to enhanced atherosclerosis in APOE*3-Leiden transgenic mice. *Circ Res*. 2001; 88: 780-786.
- 103.** Edinger AL, Linardic CM, Chiang GG, Thompson CB, Abraham RT. Differential effects of rapamycin on mammalian target of rapamycin signaling functions in mammalian cells. *Cancer Res*. 2003; 63: 8451-8460.
- 104.** Sipula IJ, Brown NF, Perdomo G. Rapamycin-mediated inhibition of mammalian target of rapamycin in skeletal muscle cells reduces glucose utilization and increases fatty acid oxidation. *Metabolism*. 2006; 55: 1637-1644.
- 105.** Brown NF, Stefanovic-Racic M, Sipula IJ, Perdomo G. The mammalian target of rapamycin regulates lipid metabolism in primary cultures of rat hepatocytes. *Metabolism*. 2007; 56: 1500-1507.
- 106.** Hu W, Feng Z, Teresky AK, Levine AJ. p53 regulates maternal reproduction through LIF. *Nature*. 2007; 450: 721-724.
- 107.** Hu W, Feng Z, Atwal GS, Levine AJ. p53: a new player in reproduction. *Cell Cycle*. 2008; 7: 848-852.
- 108.** Roemer K. Are the conspicuous interdependences of fecundity, longevity and cognitive abilities in humans caused in part by p53? *Cell Cycle*. 2010; 9: 3438-3441.
- 109.** Levine AJ, Tomasini R, McKeon FD, Mak TW, Melino G. The p53 family: guardians of maternal reproduction. *Nat Rev Mol Cell Biol*. 2011; 12: 259-265.
- 110.** Mantovani R. More on the pro-fertility activity of p53: the blastocyst side. *Cell Cycle*. 2011; 10: 4205.
- 111.** Chen D, Zheng W, Lin A, Uyhazi K, Zhao H, Lin H. Pumilio 1 suppresses multiple activators of p53 to safeguard spermatogenesis. *Curr Biol*. 2012; 22: 420-425.
- 112.** McGee MD, Day N, Graham J, Melov S. cep-1/p53-dependent dysplastic pathology of the aging *C. elegans* gonad. *Aging*. 2012; 4: 256-269.
- 113.** Kang HJ, Feng Z, Sun Y, Atwal G, Murphy ME, Rebbeck TR, Rosenwaks Z, Levine AJ, Hu W. Single-nucleotide polymorphisms in the p53 pathway regulate fertility in humans. *Proc Natl Acad Sci U S A*. 2009; 106: 9761-9766.

Molecular damage in cancer: an argument for mTOR-driven aging

Mikhail V. Blagosklonny

Department of Cell Stress Biology, Roswell Park Cancer Institute, Elm and Carlton Streets, Buffalo, NY, 14263, USA

Key words: cancer, target, therapy, leukemia, anticancer drugs

Received: 12/7/11; **Accepted:** 12/31/11; **Published:** 12/31/11

Correspondence to: Mikhail V. Blagosklonny, MD/PhD; **E-mail:** blagosklonny@oncotarget.com

Copyright: © Blagosklonny. This is an open-access article distributed under the terms of the Creative Commons Attribution License, which permits unrestricted use, distribution, and reproduction in any medium, provided the original author and source are credited

Abstract: Despite common belief, accumulation of molecular damage does not play a key role in aging. Still, cancer (an age-related disease) is initiated by molecular damage. Cancer and aging share a lot in common including the activation of the TOR pathway. But the role of molecular damage distinguishes cancer and aging. Furthermore, an analysis of the role of both damage and aging in cancer argues against “a decline, caused by accumulation of molecular damage” as a cause of aging. I also discuss how random molecular damage, via rounds of multiplication and selection, brings about non-random hallmarks of cancer.

INTRODUCTION

Aging is defined as a decline caused by accumulation of all sorts of damage, in particular, molecular damage. This statement seemed so obvious that it was not questioned. Yet several lines of evidence rule out molecular damage as a cause of aging [1-15]. Yes, of course, molecular damage accumulates over time. But this accumulation is not sufficient to cause organismal death. Eventually it would. But the organism does not live long enough, because another cause terminates life first [8]. This cause is aging, a continuation of developmental growth. Definitely, developmental growth is not driven by accumulation of molecular damage, although molecular damage accumulates. Similarly, aging is not driven by damage.

Growth is stimulated in part by mitogen- and nutrient-sensing (and other) signaling pathways such as mTOR [16-35]. Aging, “an aimless continuation of developmental program”, is driven by the same signaling pathways including mTOR [8, 14, 24]. Aging in turn causes damage: not molecular damage but non-random organ damage (stroke, infarction, renal failure and so on) and death [13]. Seemingly, one objection to this concept is that cancer is caused by molecular damage. And cancer is often a cause of death in mammals. So how may one claim that damage does not drive aging, if it is involved in cancer. Let us discuss this.

Damage in cancer

Damage causes activate oncogenes and de-activate tumor suppressors due to genetic mutations, epigenetic alterations and microRNAs dysregulation [36-57]. Even according to alternative theories, cancer is caused by damage too [58]. So damage is involved in cancer. There are some exceptions, mostly related to embryonic cells. Also, in theory, extra-genetic alterations such as stable activation of oncogenic pathways via positive feedback loops can contribute to malignant phenotype [59]. Finally, positive feedback loops could be established between cancer and normal cells [59-61]. But in general molecular damage is a key factor in cancer origin. In agreement, cancer is associated with genetic instability [59, 62-69].

Not decline but robustness

Due to genetic instability, cancer cells accumulate high levels of unrepaired damage, resulting in genomic mutations and epigenetic alterations as well as aneuploidy [36-49, 70-80]. Despite of accumulation of damage, cancer is neither decline nor ‘wear and tear’. Cancer cells are robust and aggressive. Cancer cells damage organs, thus killing organism. If cancer cells with all damage are so robust, then how possibly aging of normal cells could be “a decline due to accumulation of molecular damage”. In fact, it does not.

Immortality of cancer cells

Cancer is associated with cellular immortality [38, 81-88]. Not only cancer cells can become cell lines but also they can become free-living organisms [89-96]. Such free-living cancer cells spread from one animal to another. Thus, venereal sarcoma in dogs spread as unicellular mammalian organisms for several millennia, once originated from a single cancer cell [89-96]. Thus accumulation of damage is associated with cellular immortality.

Damage is not sufficient to cause cancer

However, molecular damage is not sufficient either to cause cancer or to hurt organism. This damage is multiplied billions of times via cell replication. Also, cells with random mutations undergo non-random selection (Figure 1).

Multiplication and selection

A 1 cm tumor contains 10^9 (1 billion) cells. Therefore, damage does not passively accumulate but is actively

multiplied. Cells undergo clonal selection, analogous to Darwinian selection [70, 97-100]. Importantly, most mutations are so called “passenger” mutations that remain random and useless [72, 79, 80, 101]. But nevertheless they do not decrease cell vitality.

Selective microenvironment

Oncogenic mutations occur randomly. Cancer arises when cellular microenvironment favors oncogenic mutations, creating selective advantage to cells bearing oncogenic mutations. For example, carcinogens not only damage DNA but also cytostatic to normal cells, thus favoring selection of oncogenic mutations that render cells resistant to cytostatic/toxic carcinogens [102, 103]. This is especially apparent with non-damaging carcinogens such as phorbol esters [104]. Cancer therapy can select for additional oncogenic mutations (such as loss of p53), rendering cancer cells not only drug resistant but also increasingly oncogenic [102, 103, 105-108]. Inflammation and chronic infections also favor cancer [109-121]. And the aging microenvironment favors cancer [122-128].

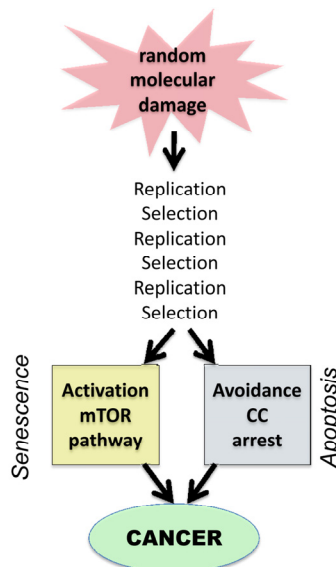


Figure 1. From random damage to cancer. Random damage undergoes multiple rounds of replication and selection. Aging is one of selection forces that favors cells with oncogenic mutations. Cancer cell is characterized by (a) activation of growth-promoting pathways such as mTOR and (b) loss of cell cycle (CC) control. Isolated activation of mTOR favors senescence, whereas isolated cell cycle progression may trigger apoptosis.

Aging as selective force

Organismal aging is the most important risk factor in common cancers such as prostate, breast, colon, gastric, lung, pancreatic, skin, brain, thyroid (and so on) cancers as well as melanomas and certain leukemias. Calorie restriction [129-137] and rapamycin [138-141], which decelerate aging, also postpone cancer. Why does aging favors cancer? One explanation is that aging stromal cells secrete factors that promote growth of pre-cancer cells [122, 123, 142-144] and aging is associated with pro-inflammation that favors cancer growth [145-147]. The pro-inflammatory NF- κ B pathway is involved in both DNA damage response (DDR), cancer and aging [60, 147-156].

One additional explanation is that chronic overactivation of mTOR renders normal cells irresponsive to growth factors [157]. (In fact, mTOR/S6K renders cells resistant to insulin and growth factors [158, 159]). Then, cancer cells, which are growth signal-independent, acquire selective advantage. In theory, by restoring responsiveness of normal cells to mitogenic signals, treatment with rapamycin can eliminate selective advantage for cancer cells. It was predicted that rapamycin can restore responsiveness of aging cells [157]. In fact, mTOR may cause exhaustion of the proliferative potential of stem cells and, in some studies, rapamycin improved the responsiveness of aging stem cells and immune cells [160-163]. As an example, activation of mTOR promoted leukemia-initiated cells, while depleting normal hematopoietic stem cell. Rapamycin not only depleted leukaemia-initiating cells but also restored normal stem cell function [160, 164]. Thus decreased proliferative potential of normal cells is associated with selective advantage to cancer cells.

Non-random activation of the PI3K/mTOR pathway

The PI3K/mTOR pathway is universally involved in cancer [37, 165-180]. It is activated by mutations in PI3K, Ras, Raf, non-receptor and growth factor receptor kinases and autocrine growth factors [165, 177, 181, 182]. Also, inactivation of tumor suppressors such as PTEN, AMPK, TSC2, LKB1, NF1 causes activation of this pathway [160, 169, 183-191]. In addition, the hypertrophic effect is often achieved via activation of downstream mTOR targets, translation factors [178]. Finally, p53, which is lost in cancer, is also a suppressor of the mTOR pathway [192-201]. Therefore, it can suppress conversion of cell cycle arrest to senescence [198-204]. In turn, the GF/PI3K/Akt/mTOR pathway drives cellular mass growth, hypersecretory phenotype,

HIF-1 expression, angiogenic phenotype, high levels of glycolysis and biosynthesis (metabolic switch) and apoptosis avoidance [16-35, 205-208]. In other words, it is involved in most of hallmarks of cancer [38, 88], with a notable exception of loss of cell cycle control. On the other hand, the mTOR pathway is involved in senescent phenotype. Therefore, the second alteration in cancer is deactivation of cell cycle checkpoints. Thus cancer cells can be viewed as cycling senescent cells.

Avoiding cell cycle arrest

In order to proliferate, cell with TOR-activating oncogenes must disable cell cycle control. Inactivation of tumor suppressors such p53, Rb, p16 and activation of c-myc, cyclins D and E, all disable cell cycle control, allowing "pro-senescent" cancer cell to proliferate [209-216]. Still, acute DNA damage, anticancer drugs and induction of p21 or p16 cause cell cycle arrest. Arrested cancer cells rapidly become senescent (geroconversion), revealing their pro-senescent phenotype.

Oncogenic transformation and gerogenic conversion

There are non-mutually exclusive ways to depict oncogenic transformation, as complementary activation/disabling of signaling pathways [88, 217-225]. Here to compare cancer with aging, I view oncogenic transformation as (a) activation of growth-promoting pathways such as mTOR and (b) loss of cell cycle control. Growth promoting pathways can drive either growth or aging, whereas avoidance of cell cycle arrest precludes aging (Fig. 1). In quiescent cells, activation of growth-promoting pathways (such as mTOR) converts quiescence into senescence, a process named *gerogenic conversion* or *geroconversion* [226, 227]. In proliferating cells, mTOR is fully activated. Induction of cell cycle arrest, without inhibition of mTOR causes gerogenic conversion too. When cell cycle is arrested, growth-promoting pathways drive hypertrophy and aging instead of growth. The difference between quiescence and senescence was recently discussed in detail [227]. Cellular hyper-functions and feedback signal resistance are manifestations of cellular senescence/aging that lead to age-related diseases [227]. These hallmarks result from excessive activation of signaling pathways not from accumulation of damage.

Why aging is not caused by accumulation of damage

To harbor the active mTOR pathway, cancer cells undergo multiple rounds of selection. In other words, numerous random mutations are selected for non-random activation of mTOR. In contrast it is resting non-dividing cells such as liver, muscle, fat, connective tissue, neurons

that undergo aging (geroconversion) in the organism. Not only levels of molecular damage are low in normal cells, but also there is no amplification and selection. So random damage hardly can cause non-random activation of mTOR. Noteworthy, calorie restriction (CR) inhibits mTOR. Even short-term CR suppresses cellular senescence in the organism [228, 229].

Extragenetic activation of mTOR in aging

mTOR pathway is activated by growth factors, hormones, mitogens, pro-inflammatory cytokines and other secretory molecules and nutrients. Cells can overactivate each other, via positive feedback loops. For example in the liver and fat, hyper-active mTOR causes insulin-resistance, which in turn leads to activation mTOR in beta-cells, which produce insulin. Insulin further activates mTOR in the liver and fat.

DNA damage response (DDR) and aging

In proliferating cells, mTOR is fully activated. Acute DNA damage induces DDR and cell cycle arrest. If mTOR is still active, such cells undergo geroconversion. Rapamycin and other inhibitors of the mTOR pathway decelerate geroconversion [198, 200, 206, 226, 230-236]. This is how accelerated senescence is usually induced in proliferating cells (in cell culture). However, in quiescent cells with inactive mTOR, DNA damage does not induce senescence, whereas activation of mTOR does [226, 237].

In oncogene-induced senescence (OIS), DDR causes cell cycle arrest, leading to senescence [238-245]. Noteworthy, most oncogenes that induce senescence (Ras, Raf, MEK, Akt and so on) activate the mTOR pathway. We can call them TOR-activating oncogenes or geroenes [14], because they are involved in aging from cells to organisms [14, 246, 247]. Loss of PTEN also activates the mTOR pathway, causing senescence [243]. In OIS, oncogenes induce cell cycle arrest but not necessary DNA damage or even DDR [248, 243, 249]. Furthermore, atypical DDR can occur without DNA damage (pseudo-DDR) [231, 236, 250-256]. DDR pathways and the mTOR pathway are interconnected [257-260]. And it seems that pseudo-DDR and DDR are markers of cellular hyper-activation associated with senescence [145] and can be blocked by rapamycin [231].

Cancer prevention and therapy

Prevention of DNA damage can decrease cancer incidence. For example, non-smoking prevents smoking-induced cancer. Also, cancer can be prevented by decelerating the aging process by calorie restriction

and rapamycin. Both calorie restriction and rapamycin delay cancer. Although rapalogs can directly affect cancer cells, rapalogs are only modestly effective as anti-cancer therapy [168, 261, 262], compared with their dramatic preventive effects. In any case, cancer can be prevented without decreasing levels of molecular damage. Furthermore, DNA damaging drugs are cornerstone of cancer therapy. And these drugs are also carcinogens, because anti-cancer and carcinogenic effects are two sides of the same coin [103].

CONCLUSION

Although molecular damage is typically necessary for cancer initiation, this damage limits life span not because of cellular decline but because of cellular robustness. Damage undergoes multiplication and selection. Aging by itself is a selective force that favors cancer probably because aging cells are signal resistant, thus providing selective advantage to cells that by-pass the need in mitogenic signals. In addition to non-random selection for oncogenic mutations, cancer cells accumulate even higher levels of random “passenger” mutations. Despite that cancer cells are robust. It must be expected that a lower rate of DNA damage in normal cells cannot cause cellular decline. Yes, molecular damage accumulates but is not a driving force for aging. Aging would occur in the absence of any molecular damage. On the other hand, yes, molecular damage is involved in something like cancer that can limit lifespan in mammals to some extent. Noteworthy, worms and flies do not die from cancer. Still they undergo PI3K/TOR-dependent aging [263-269].

As already discussed, if quasi-programmed TOR-driven aging would be eliminated, thus extending lifespan, then accumulation of molecular damage would become life-limiting [10]. In any case, in mammals, cellular aging (characterized by cellular overactivation, hyperfunction and secondary signal resistance) can cause diseases, which lead to organ damage. And cancer, an age-related disease, is not an exception: it kills not because cancer cells fail due to decline but because these cells damage organs. Perhaps, cancer is not the only one damage-related disease among aging-dependent conditions. But a subtle interference of molecular damage with TOR-driven aging will be a topic for another article, which will discuss the intricate relationship between non-random organ damage and random molecular damage.

CONFLICT OF INTERESTS STATEMENT

The author of this manuscript has no conflict of interest to declare.

REFERENCES

1. Doonan R, McElwee JJ, Matthijssens F, Walker GA, Houthoofd K, Back P, Matscheski A, Vanfleteren JR, Gems D. Against the oxidative damage theory of aging: superoxide dismutases protect against oxidative stress but have little or no effect on life span in *Caenorhabditis elegans*. *Genes Dev.* 2008; 22: 3236-3241.
2. Gems D, Doonan R. Antioxidant defense and aging in *C. elegans*: Is the oxidative damage theory of aging wrong? *Cell Cyce.* 2009; 8: 1681-1687.
3. Cabreiro F, Ackerman D, Doonan R, Araiz C, Back P, Papp D, Braeckman BP, Gems D. Increased life span from overexpression of superoxide dismutase in *Caenorhabditis elegans* is not caused by decreased oxidative damage. *Free Radic Biol Med.* 2011; 51: 1575-1582.
4. Lapointe J, Hekimi S. When a theory of aging ages badly. *Cell Mol Life Sci.* 2009; 67: 1-8.
5. Van Raamsdonk JM, Meng Y, Camp D, Yang W, Jia X, Benard C, Hekimi S. Decreased energy metabolism extends life span in *Caenorhabditis elegans* without reducing oxidative damage. *Genetics.* 2010; 185: 559-571.
6. Speakman JR, Selman C. The free-radical damage theory: Accumulating evidence against a simple link of oxidative stress to ageing and lifespan. *Bioessays.* 2011; 33: 255-259.
7. Ristow M, Schmeisser S. Extending life span by increasing oxidative stress. *Free Radic Biol Med.* 2011; 51: 327-336.
8. Blagosklonny MV. Aging and immortality: quasi-programmed senescence and its pharmacologic inhibition. *Cell Cycle.* 2006; 5: 2087-2102.
9. Blagosklonny MV. An anti-aging drug today: from senescence-promoting genes to anti-aging pill. *Drug Disc Today.* 2007; 12: 218-224.
10. Blagosklonny MV. Program-like aging and mitochondria: instead of random damage by free radicals. *J Cell Biochem.* 2007; 102: 1389-1399.
11. Blagosklonny MV. Paradoxes of aging. *Cell Cycle.* 2007; 6: 2997-3003.
12. Blagosklonny MV. Aging: ROS or TOR. *Cell Cycle.* 2008; 7: 3344-3354.
13. Blagosklonny MV. mTOR-driven aging: speeding car without brakes. *Cell Cycle.* 2009; 8: 4055-4059.
14. Blagosklonny MV. Revisiting the antagonistic pleiotropy theory of aging: TOR-driven program and quasi-program. *Cell Cycle.* 2010; 9: 3151-3156.
15. Blagosklonny MV. Why men age faster but reproduce longer than women: mTOR and evolutionary perspectives. *Aging.* 2010; 2: 265-273.
16. Hay N, Sonenberg N. Upstream and downstream of mTOR. *Genes Dev.* 2004; 18: 1926-1945.
17. Sarbassov dos D, Ali SM, Sabatini DM. Growing roles for the mTOR pathway. *Curr Opin Cell Biol.* 2005; 17: 596-603.
18. Inoki K, Corradetti MN, Guan KL. Dysregulation of the TSC-mTOR pathway in human disease. *Nat Genet.* 2005; 37: 19-24.
19. Wullschlegel S, Loewith R, Hall MN. TOR signaling in growth and metabolism. *Cell.* 2006; 124: 471-484.
20. Tee AR, Blenis J. mTOR, translational control and human disease. *Semin Cell Dev Biol.* 2005; 16: 29-37.
21. Dann SG, Selvaraj A, Thomas G. mTOR Complex1-S6K1 signaling: at the crossroads of obesity, diabetes and cancer. *Trends Mol Med.* 2007; 13: 252-259.
22. Hands SL, Proud CG, Wytttenbach A. mTOR's role in ageing: protein synthesis or autophagy? *Aging.* 2009; 1: 586-597.
23. Glazer HP, Osipov RM, Clements RT, Sellke FW, Bianchi C. Hypercholesterolemia is associated with hyperactive cardiac mTORC1 and mTORC2 signaling. *Cell Cycle.* 2009; 8: 1738-1746.
24. Blagosklonny MV, Hall MN. Growth and aging: a common molecular mechanism. *Aging.* 2009; 1: 357-362.
25. Kapahi P, Chen D, Rogers AN, Katewa SD, Li PW, Thomas EL, Kockel L. With TOR, less is more: a key role for the conserved nutrient-sensing TOR pathway in aging. *Cell Metab.* 2010; 11: 453-465.
26. Boguta M. Control of RNA polymerases I and III by the TOR signaling pathway. *Cell Cycle.* 2009; 8: 4023-4024.
27. Jiang Y. mTOR goes to the nucleus. *Cell Cycle.* 2009; 9: 868.
28. Dazert E, Hall MN. mTOR signaling in disease. *Curr Opin Cell Biol.* 2011; 23:744-55.
29. Loewith R, Hall MN. Target of Rapamycin (TOR) in Nutrient Signaling and Growth Control. *Genetics.* 2011; 189: 1177-1201.
30. Zoncu R, Efeyan A, Sabatini DM. mTOR: from growth signal integration to cancer, diabetes and ageing. *Nat Rev Mol Cell Biol.* 2010; 12: 21-35.
31. Conn CS, Qian SB. mTOR signaling in protein homeostasis: less is more? *Cell Cycle.* 2011; 10: 1940-1947.
32. Ma XM, Blenis J. Molecular mechanisms of mTOR-mediated translational control. *Nat Rev Mol Cell Biol.* 2009; 10: 307-318.
33. Proud CG. mTOR-mediated regulation of translation factors by amino acids. *Biochem Biophys Res Commun.* 2004; 313: 429-436.
34. Hall MN. mTOR-what does it do? *Transplant Proc.* 2008; 40: S5-8.
35. Magnuson B, Ekim B, Fingar DC. Regulation and function of ribosomal protein S6 kinase (S6K) within mTOR signalling networks. *Biochem J.* 2012; 441: 1-21.
36. Vogelstein B, Kinzler KW. The multistep nature of cancer. *Trends Genet.* 1993; 9: 138-141.
37. Vogelstein B, Kinzler KW. Cancer genes and the pathways they control. *Nat Med.* 2004; 10: 789-799.
38. Hanahan D, Weinberg RA. The hallmarks of cancer. *Cell.* 2000; 100: 57-70.
39. Jackson SP, Bartek J. The DNA-damage response in human biology and disease. *Nature.* 2009; 461: 1071-1078.
40. Lukas J, Lukas C, Bartek J. More than just a focus: The chromatin response to DNA damage and its role in genome integrity maintenance. *Nat Cell Biol.* 2011; 13: 1161-1169.
41. Baylin SB, Herman JG. DNA hypermethylation in tumorigenesis: epigenetics joins genetics. *Trends Genet.* 2000; 16: 168-174.
42. Egger G, Liang G, Aparicio A, Jones PA. Epigenetics in human disease and prospects for epigenetic therapy. *Nature.* 2004; 429: 457-463.
43. McKenna ES, Roberts CW. Epigenetics and cancer without genomic instability. *Cell Cycle.* 2009; 8: 23-26.
44. Timp W, Levchenko A, Feinberg AP. A new link between epigenetic progenitor lesions in cancer and the dynamics of signal transduction. *Cell Cycle.* 2009; 8: 383-390.
45. Johnson SM, Grosshans H, Shingara J, Byrom M, Jarvis R, Cheng A, Labourier E, Reinert KL, Brown D, Slack FJ. RAS is regulated by the let-7 microRNA family. *Cell.* 2005; 120: 635-647.
46. Calin GA, Ferracin M, Cimmino A, Di Leva G, Shimizu M, Wojcik SE, Iorio MV, Visone R, Sever NI, Fabbri M, Iuliano R, Palumbo T, Pichiorri F, Roldo C, Garzon R, Sevignani C et al. A MicroRNA signature associated with prognosis and progression

- in chronic lymphocytic leukemia. *N Engl J Med.* 2005; 353: 1793-1801.
47. Lujambio A, Esteller M. How epigenetics can explain human metastasis: a new role for microRNAs. *Cell Cycle.* 2009; 8: 377-382.
48. Burdach S, Plehm S, Unland R, Dirksen U, Borkhardt A, Staeger MS, Muller-Tidow C, Richter GH. Epigenetic maintenance of stemness and malignancy in peripheral neuroectodermal tumors by EZH2. *Cell Cycle.* 2009; 8: 1991-1996.
49. Chen SS, Sherman MH, Hertlein E, Johnson AJ, Teitell MA, Byrd JC, Plass C. Epigenetic alterations in a murine model for chronic lymphocytic leukemia. *Cell Cycle.* 2009; 8: 3663-3667.
50. Esquela-Kerscher A, Slack FJ. Oncomirs - microRNAs with a role in cancer. *Nat Rev Cancer.* 2006; 6: 259-269.
51. Kundu ST, Nallur S, Paranjape T, Boeke M, Weidhaas JB, Slack FJ. KRAS alleles: The LCS6 3'UTR variant and KRAS coding sequence mutations in the NCI-60 panel. *Cell Cycle.* 2012; 11.
52. Kasinski AL, Slack FJ. Epigenetics and genetics. MicroRNAs en route to the clinic: progress in validating and targeting microRNAs for cancer therapy. *Nat Rev Cancer.* 2011; 11: 849-864.
53. Croce CM. Causes and consequences of microRNA dysregulation in cancer. *Nat Rev Genet.* 2009; 10: 704-714.
54. Sozzi G, Pastorino U, Croce CM. MicroRNAs and lung cancer: from markers to targets. *Cell Cycle.* 2011; 10: 2045-2046.
55. Pekarsky Y, Croce CM. Is miR-29 an oncogene or tumor suppressor in CLL? *Oncotarget.* 2010; 1: 224-227.
56. Valastyan S, Weinberg RA. miR-31: a crucial overseer of tumor metastasis and other emerging roles. *Cell Cycle.* 2010; 9: 2124-2129.
57. Mavrakis KJ, Wendel HG. TargetScreen: an unbiased approach to identify functionally important microRNA targets. *Cell Cycle.* 2010; 9: 2080-2084.
58. Duesberg P, Li R. Multistep carcinogenesis: a chain reaction of aneuploidizations. *Cell Cycle.* 2003; 2: 202-210.
59. Blagosklonny MV. Molecular theory of cancer. *Cancer Biol Ther.* 2005; 4: 621-627.
60. Martinez-Outschoorn UE, Trimmer C, Lin Z, Whitaker-Menezes D, Chiavarina B, Zhou J, Wang C, Pavlides S, Martinez-Cantarín MP, Capozza F, Witkiewicz AK, Flomenberg N, Howell A, Pestell RG, Caro J, Lisanti MP et al. Autophagy in cancer associated fibroblasts promotes tumor cell survival: Role of hypoxia, HIF1 induction and NFκB activation in the tumor stromal microenvironment. *Cell Cycle.* 2010; 9: 3515-3533.
61. Liu D, Martin V, Fueyo J, Lee OH, Xu J, Cortes-Santiago N, Alonso MM, Aldape K, Colman H, Gomez-Manzano C. Tie2/TEK modulates the interaction of glioma and brain tumor stem cells with endothelial cells and promotes an invasive phenotype. *Oncotarget.* 2010; 1: 700-709.
62. Lengauer C, Kinzler KW, Vogelstein B. Genetic instabilities in human cancers. *Nature.* 1998; 396: 643-649.
63. Komarova NL, Lengauer C, Vogelstein B, Nowak MA. Dynamics of genetic instability in sporadic and familial colorectal cancer. *Cancer Biol Ther.* 2002; 1: 685-692.
64. Li L, Borodyansky L, Yang Y. Genomic instability en route to and from cancer stem cells. *Cell Cycle.* 2009; 8: 1000-1002.
65. Gupta A, Yang Q, Pandita RK, Hunt CR, Xiang T, Misri S, Zeng S, Pagan J, Jeffery J, Puc J, Kumar R, Feng Z, Powell SN, Bhat A, Yaguchi T, Wadhwa R et al. Cell cycle checkpoint defects contribute to genomic instability in PTEN deficient cells independent of DNA DSB repair. *Cell Cycle.* 2009; 8: 2198-2210.
66. Meyn RE. Linking PTEN with genomic instability and DNA repair. *Cell Cycle.* 2009; 8: 2322-2323.
67. Tuduri S, Crabbe L, Tourriere H, Coquelle A, Pasero P. Does interference between replication and transcription contribute to genomic instability in cancer cells? *Cell Cycle.* 2010; 9: 1886-1892.
68. Guirouilh-Barbat JK, Wilhelm T, Lopez BS. AKT1/BRCA1 in the control of homologous recombination and genetic stability: the missing link between hereditary and sporadic breast cancers. *Oncotarget.* 2010; 1: 691-699.
69. Ho CC, Hau PM, Marxer M, Poon RY. The requirement of p53 for maintaining chromosomal stability during tetraploidization. *Oncotarget.* 2010; 1: 583-595.
70. Beerenwinkel N, Antal T, Dingli D, Traulsen A, Kinzler KW, Velculescu VE, Vogelstein B, Nowak MA. Genetic progression and the waiting time to cancer. *PLoS Comput Biol.* 2007; 3: e225.
71. Wood LD, Parsons DW, Jones S, Lin J, Sjoblom T, Leary RJ, Shen D, Boca SM, Barber T, Ptak J, Silliman N, Szabo S, Dezso Z, Ustyanksky V, Nikolskaya T, Nikolsky Y et al. The genomic landscapes of human breast and colorectal cancers. *Science.* 2007; 318: 1108-1113.
72. Carter H, Chen S, Isik L, Tyekuceva S, Velculescu VE, Kinzler KW, Vogelstein B, Karchin R. Cancer-specific high-throughput annotation of somatic mutations: computational prediction of driver missense mutations. *Cancer Res.* 2009; 69: 6660-6667.
73. Zhao L, Vogt PK. Hot-spot mutations in p110α of phosphatidylinositol 3-kinase (p13K): differential interactions with the regulatory subunit p85 and with RAS. *Cell Cycle.* 2010; 9: 596-600.
74. Martinez AC, van Wely KH. Are aneuploidy and chromosome breakage caused by a CINgle mechanism? *Cell Cycle.* 2010; 9: 2275-2280.
75. McClelland SE, Burrell RA, Swanton C. Chromosomal instability: a composite phenotype that influences sensitivity to chemotherapy. *Cell Cycle.* 2009; 8: 3262-3266.
76. Baker DJ, van Deursen JM. Chromosome missegregation causes colon cancer by APC loss of heterozygosity. *Cell Cycle.* 2010; 9: 1711-1716.
77. Chen Z, Feng J, Saldivar JS, Gu D, Bockholt A, Sommer SS. EGFR somatic doublets in lung cancer are frequent and generally arise from a pair of driver mutations uncommonly seen as singlet mutations: one-third of doublets occur at five pairs of amino acids. *Oncogene.* 2008; 27: 4336-4343.
78. Torkamani A, Schork NJ. Prediction of cancer driver mutations in protein kinases. *Cancer Res.* 2008; 68: 1675-1682.
79. Loriaux MM, Levine RL, Tyner JW, Frohling S, Scholl C, Stoffregen EP, Wernig G, Erickson H, Eide CA, Berger R, Bernard OA, Griffin JD, Stone RM, Lee B, Meyerson M, Heinrich MC et al. High-throughput sequence analysis of the tyrosine kinome in acute myeloid leukemia. *Blood.* 2008; 111: 4788-4796.
80. Frohling S, Scholl C, Levine RL, Loriaux M, Boggon TJ, Bernard OA, Berger R, Dohner H, Dohner K, Ebert BL, Teckie S, Golub TR, Jiang J, Schittenhelm MM, Lee BH, Griffin JD et al. Identification of driver and passenger mutations of FLT3 by high-throughput DNA sequence analysis and functional assessment of candidate alleles. *Cancer Cell.* 2007; 12: 501-513.
81. Counter CM, Avilion AA, LeFeuvre CE, Stewart NG, Greider CW, Harley CB, Bacchetti S. Telomere shortening associated with chromosome instability is arrested in immortal cells which express telomerase activity. *Embo J.* 1992; 11: 1921-1929.

- 82.** Harley CB, Kim NW, Prowse KR, Weinrich SL, Hirsch KS, West MD, Bacchetti S, Hirte HW, Counter CM, Greider CW, et al. Telomerase, cell immortality, and cancer. *Cold Spring Harb Symp Quant Biol.* 1994; 59: 307-315.
- 83.** Counter CM, Hahn WC, Wei W, Caddle SD, Beijersbergen RL, Lansdorp PM, Sedivy JM, Weinberg RA. Dissociation among in vitro telomerase activity, telomere maintenance, and cellular immortalization. *Proc Natl Acad Sci U S A.* 1998; 95: 14723-14728.
- 84.** Hahn WC. Immortalization and transformation of human cells. *Mol Cells.* 2002; 13: 351-361.
- 85.** Lundberg AS, Randell SH, Stewart SA, Elenbaas B, Hartwell KA, Brooks MW, Fleming MD, Olsen JC, Miller SW, Weinberg RA, Hahn WC. Immortalization and transformation of primary human airway epithelial cells by gene transfer. *Oncogene.* 2002; 21: 4577-4586.
- 86.** Blagosklonny MV. Cell immortality and hallmarks of cancer. *Cell Cycle.* 2003; 2: 296-299.
- 87.** Bazarov AV, Hines WC, Mukhopadhyay R, Beliveau A, Melodyev S, Zaslavsky Y, Yaswen P. Telomerase activation by c-Myc in human mammary epithelial cells requires additional genomic changes. *Cell Cycle.* 2009; 8: 3373-3378.
- 88.** Hanahan D, Weinberg RA. Hallmarks of cancer: the next generation. *Cell.* 2011; 144: 646-674.
- 89.** Cohen D. The canine transmissible venereal tumor: a unique result of tumor progression. *Adv Cancer Res.* 1985; 43: 75-112.
- 90.** Liao KW, Hung SW, Hsiao YW, Bennett M, Chu RM. Canine transmissible venereal tumor cell depletion of B lymphocytes: molecule(s) specifically toxic for B cells. *Vet Immunol Immunopathol.* 2003; 92: 149-162.
- 91.** Leroi AM, Koufopanou V, Burt A. Cancer selection. *Nat Rev Cancer.* 2003; 3: 226-231.
- 92.** Pearse AM, Swift K. Allograft theory: transmission of devil facial-tumour disease. *Nature.* 2006; 439: 549.
- 93.** Siddle HV, Kreiss A, Eldridge MD, Noonan E, Clarke CJ, Pyecroft S, Woods GM, Belov K. Transmission of a fatal clonal tumor by biting occurs due to depleted MHC diversity in a threatened carnivorous marsupial. *Proc Natl Acad Sci U S A.* 2007; 104: 16221-16226.
- 94.** McAloose D, Newton AL. Wildlife cancer: a conservation perspective. *Nat Rev Cancer.* 2009; 9: 517-526.
- 95.** Murchison EP. Clonally transmissible cancers in dogs and Tasmanian devils. *Oncogene.* 2008; 27 Suppl 2: S19-30.
- 96.** Murchison EP, Tovar C, Hsu A, Bender HS, Kheradpour P, Rebbeck CA, Obendorf D, Conlan C, Bahlo M, Blizzard CA, Pyecroft S, Kreiss A, Kellis M, Stark A, Harkins TT, Marshall Graves JA et al. The Tasmanian devil transcriptome reveals Schwann cell origins of a clonally transmissible cancer. *Science.* 2010; 327: 84-87.
- 97.** Schollnberger H, Beerwinkel N, Hoogenveen R, Vineis P. Cell selection as driving force in lung and colon carcinogenesis. *Cancer Res.* 2010; 70: 6797-6803.
- 98.** Cahill DP, Kinzler KW, Vogelstein B, Lengauer C. Genetic instability and darwinian selection in tumours. *Trends Cell Biol.* 1999; 9: M57-60.
- 99.** Hempen PM, Zhang L, Bansal RK, Iacobuzio-Donahue CA, Murphy KM, Maitra A, Vogelstein B, Whitehead RH, Markowitz SD, Willson JK, Yeo CJ, Hruban RH, Kern SE. Evidence of selection for clones having genetic inactivation of the activin A type II receptor (ACVR2) gene in gastrointestinal cancers. *Cancer Res.* 2003; 63: 994-999.
- 100.** Zhang Y, Italia MJ, Auger KR, Halsey WS, Van Horn SF, Sathe GM, Magid-Slav M, Brown JR, Holbrook JD. Molecular evolutionary analysis of cancer cell lines. *Mol Cancer Ther.* 2010; 9: 279-291.
- 101.** Bozic I, Antal T, Ohtsuki H, Carter H, Kim D, Chen S, Karchin R, Kinzler KW, Vogelstein B, Nowak MA. Accumulation of driver and passenger mutations during tumor progression. *Proc Natl Acad Sci U S A.* 2010; 107: 18545-18550.
- 102.** Blagosklonny MV. Oncogenic resistance to growth-limiting conditions. *Nat Rev Cancer.* 2002; 2: 221-225.
- 103.** Blagosklonny MV. Carcinogenesis, cancer therapy and chemoprevention. *Cell Death Differ.* 2005; 12: 592-602.
- 104.** Dotto GP, Parada LF, Weinberg RA. Specific growth response of ras-transformed embryo fibroblasts to tumour promoters. *Nature.* 1985; 318: 472-475.
- 105.** Blagosklonny MV. Antiangiogenic therapy and tumor progression. *Cancer Cell.* 2004; 5: 13-17.
- 106.** Blagosklonny MV. Why therapeutic response may not prolong the life of a cancer patient: selection for oncogenic resistance. *Cell Cycle.* 2005; 4: 1693-1698.
- 107.** Fleenor CJ, Marusyk A, DeGregori J. Ionizing radiation and hematopoietic malignancies: altering the adaptive landscape. *Cell Cycle.* 2010; 9: 3005-3011.
- 108.** Aziz MH, Shen H, Maki CG. Acquisition of p53 mutations in response to the non-genotoxic p53 activator Nutlin-3. *Oncogene.* 2011; 30: 4678-4686.
- 109.** Uemura N, Okamoto S, Yamamoto S, Matsumura N, Yamaguchi S, Yamakido M, Taniyama K, Sasaki N, Schlemper RJ. Helicobacter pylori infection and the development of gastric cancer. *N Engl J Med.* 2001; 345: 784-789.
- 110.** Coussens LM, Werb Z. Inflammation and cancer. *Nature.* 2002; 420: 860-867.
- 111.** Karin M, Lawrence T, Nizet V. Innate immunity gone awry: linking microbial infections to chronic inflammation and cancer. *Cell.* 2006; 124: 823-835.
- 112.** Lin WW, Karin M. A cytokine-mediated link between innate immunity, inflammation, and cancer. *J Clin Invest.* 2007; 117: 1175-1183.
- 113.** Porta C, Subhra Kumar B, Larghi P, Rubino L, Mancino A, Sica A. Tumor promotion by tumor-associated macrophages. *Adv Exp Med Biol.* 2007; 604: 67-86.
- 114.** Shan W, Liu J. Inflammation: a hidden path to breaking the spell of ovarian cancer. *Cell Cycle.* 2009; 8: 3107-3111.
- 115.** Silvera D, Schneider RJ. Inflammatory breast cancer cells are constitutively adapted to hypoxia. *Cell Cycle.* 2009; 8: 3091-3096.
- 116.** Gonda TA, Tu S, Wang TC. Chronic inflammation, the tumor microenvironment and carcinogenesis. *Cell Cycle.* 2009; 8: 2005-2013.
- 117.** Wu Y, Zhou BP. Inflammation: a driving force speeds cancer metastasis. *Cell Cycle.* 2009; 8: 3267-3273.
- 118.** Paradisi A, Mehlen P. Netrin-1, a missing link between chronic inflammation and tumor progression. *Cell Cycle.* 2010; 9: 1253-1262.
- 119.** Barykova YA, Logunov DY, Shmarov MM, Vinarov AZ, Fiev DN, Vinarova NA, Rakovskaya IV, Baker PS, Shyshynova I, Stephenson AJ, Klein EA, Naroditsky BS, Gintsburg AL, Gudkov AV. Association of Mycoplasma hominis infection with prostate cancer. *Oncotarget.* 2011; 2: 289-297.
- 120.** Lisanti MP, Martinez-Outschoorn UE, Pavlides S, Whitaker-Menezes D, Pestell RG, Howell A, Sotgia F. Accelerated aging in

the tumor microenvironment: connecting aging, inflammation and cancer metabolism with personalized medicine. *Cell Cycle*. 2011; 10: 2059-2063.

121. Balliet RM, Capparelli C, Guido C, Pestell TG, Martinez-Outschoorn UE, Lin Z, Whitaker-Menezes D, Chiavarina B, Pestell RG, Howell A, Sotgia F, Lisanti MP. Mitochondrial oxidative stress in cancer-associated fibroblasts drives lactate production, promoting breast cancer tumor growth: Understanding the aging and cancer connection. *Cell Cycle*. 2011; 10: 4065-4073.

122. Krtolica A, Campisi J. Integrating epithelial cancer, aging stroma and cellular senescence. *Adv Gerontol*. 2003; 11: 109-116.

123. Campisi J. Senescent cells, tumor suppression, and organismal aging: good citizens, bad neighbors. *Cell*. 2005; 120: 513-522.

124. Vicente-Duenas C, Abollo-Jimenez F, Ruiz-Roca L, Alonso-Escudero E, Jimenez R, Cenador MB, Criado FJ, Cobaleda C, Sanchez-Garcia I. The age of the target cell affects B-cell leukaemia malignancy. *Aging*. 2010; 2: 908-913.

125. Henry CJ, Marusyk A, Zaberezhnyy V, Adane B, DeGregori J. Declining lymphoid progenitor fitness promotes aging-associated leukemogenesis. *Proc Natl Acad Sci U S A*. 2010; 107: 21713-21718.

126. Henry CJ, Marusyk A, DeGregori J. Aging-associated changes in hematopoiesis and leukemogenesis: what's the connection? *Aging*. 2011; 3: 643-656.

127. Lewis DA, Travers JB, Machado C, Somani AK, Spandau DF. Reversing the aging stromal phenotype prevents carcinoma initiation. *Aging*. 2011; 3: 407-416.

128. Campisi J, Andersen JK, Kapahi P, Melov S. Cellular senescence: A link between cancer and age-related degenerative disease? *Semin Cancer Biol*. 2011; 21: 354-359.

129. Hursting SD, Perkins SN, Phang JM. Calorie restriction delays spontaneous tumorigenesis in p53-knockout transgenic mice. *Proc Natl Acad Sci U S A*. 1994; 91: 7036-7040.

130. Berrigan D, Perkins SN, Haines DC, Hursting SD. Adult-onset calorie restriction and fasting delay spontaneous tumorigenesis in p53-deficient mice. *Carcinogenesis*. 2002; 23: 817-822.

131. Hursting SD, Smith SM, Lashinger LM, Harvey AE, Perkins SN. Calories and carcinogenesis: lessons learned from 30 years of calorie restriction research. *Carcinogenesis*. 2010; 31: 83-89.

132. Ingram DK, Zhu M, Mamczarz J, Zou S, Lane MA, Roth GS, deCabo R. Calorie restriction mimetics: an emerging research field. *Aging Cell*. 2006; 5: 97-108.

133. Ingram DK, Anson RM, de Cabo R, Mamczarz J, Zhu M, Mattison J, Lane MA, Roth GS. Development of calorie restriction mimetics as a longevity strategy. *Ann N Y Acad Sci*. 2004; 1019: 412-423.

134. Hursting SD, Lavigne JA, Berrigan D, Perkins SN, Barrett JC. Calorie restriction, aging, and cancer prevention: mechanisms of action and applicability to humans. *Annu Rev Med*. 2003; 54: 131-152.

135. Longo VD, Fontana L. Calorie restriction and cancer prevention: metabolic and molecular mechanisms. *Trends Pharmacol Sci*. 2010; 31: 89-98.

136. Fontana L, Partridge L, Longo VD. Extending healthy life span--from yeast to humans. *Science*. 2010; 328: 321-326.

137. Blagosklonny MV. Calorie restriction: Decelerating mTOR-driven aging from cells to organisms (including humans). *Cell Cycle*. 2010; 9: 683-688.

138. Blagosklonny MV. Prevention of cancer by inhibiting aging. *Cancer Biol Ther*. 2008; 7: 1520-1524.

139. Harrison DE, Strong R, Sharp ZD, Nelson JF, Astle CM, Flurkey K, Nadon NL, Wilkinson JE, Frenkel K, Carter CS, Pahor M, Javors MA, Fernandez E, Miller RA. Rapamycin fed late in life extends lifespan in genetically heterogeneous mice. *Nature*. 2009; 460: 392-396.

140. Anisimov VN, Zabezhinski MA, Popovich IG, Piskunova TS, Semenchenko AV, Tyndyk ML, Yurova MN, Antoch MP, Blagosklonny MV. Rapamycin extends maximal lifespan in cancer-prone mice. *Am J Pathol*. 2010; 176: 2092-2097.

141. Anisimov VN, Zabezhinski MA, Popovich IG, Piskunova TS, Semenchenko AV, Tyndyk ML, Yurova MN, Blagosklonny MV. Rapamycin increases lifespan and inhibits spontaneous tumorigenesis in inbred female mice. *Cell Cycle*. 2011; 10.

142. Krtolica A, Parrinello S, Lockett S, Desprez PY, Campisi J. Senescent fibroblasts promote epithelial cell growth and tumorigenesis: a link between cancer and aging. *Proc Natl Acad Sci U S A*. 2001; 98: 12072-12077.

143. Parrinello S, Coppe JP, Krtolica A, Campisi J. Stromal-epithelial interactions in aging and cancer: senescent fibroblasts alter epithelial cell differentiation. *J Cell Sci*. 2005; 118: 485-496.

144. Coppe JP, Patil CK, Rodier F, Sun Y, Munoz DP, Goldstein J, Nelson PS, Desprez PY, Campisi J. Senescence-associated secretory phenotypes reveal cell-nonautonomous functions of oncogenic RAS and the p53 tumor suppressor. *PLoS Biol*. 2008; 6: 2853-2868.

145. Rodier F, Coppe JP, Patil CK, Hoeijmakers WA, Munoz DP, Raza SR, Freund A, Campeau E, Davalos AR, Campisi J. Persistent DNA damage signalling triggers senescence-associated inflammatory cytokine secretion. *Nat Cell Biol*. 2009; 11: 973-979.

146. Davalos AR, Coppe JP, Campisi J, Desprez PY. Senescent cells as a source of inflammatory factors for tumor progression. *Cancer Metastasis Rev*. 2011; 29: 273-283.

147. Gudkov AV, Gurova KV, Komarova EA. Inflammation and p53: A Tale of Two Stresses. *Genes Cancer*. 2011; 2: 503-516.

148. Karin M, Greten FR. NF-kappaB: linking inflammation and immunity to cancer development and progression. *Nat Rev Immunol*. 2005; 5: 749-759.

149. Adler AS, Kawahara TL, Segal E, Chang HY. Reversal of aging by NFkappaB blockade. *Cell Cycle*. 2008; 7: 556-559.

150. Chauncey SS, Boothman DA, Habib AA. The receptor interacting protein 1 mediates a link between NFkappaB and PI3-kinase signaling. *Cell Cycle*. 2009; 8: 2671-2672.

151. Barre B, Coqueret O, Perkins ND. Regulation of activity and function of the p52 NF-kappaB subunit following DNA damage. *Cell Cycle*. 2010; 9: 4795-4804.

152. Donato AJ, Pierce GL, Lesniewski LA, Seals DR. Role of NFkappaB in age-related vascular endothelial dysfunction in humans. *Aging*. 2009; 1: 678-680.

153. Demchenko YN, Kuehl WM. A critical role for the NFkB pathway in multiple myeloma. *Oncotarget*. 2010; 1: 59-68.

154. Ohanna M, Giuliano S, Bonet C, Imbert V, Hofman V, Zangari J, Bille K, Robert C, Bressac-de Paillerets B, Hofman P, Rocchi S, Peyron JF, Lacour JP, Ballotti R, Bertolotto C. Senescent cells develop a PARP-1 and nuclear factor- κ B-associated secretome (PNAS). *Genes Dev*. 2011; 25: 1245-1261.

155. Vaughan S, Jat PS. Deciphering the role of nuclear factor-kappaB in cellular senescence. *Aging*. 2011; 3: 913-919.

- 156.** Moskalev A, Shaposhnikov M. Pharmacological inhibition of NF-kappaB prolongs lifespan of *Drosophila melanogaster*. *Aging*. 2011; 3: 391-394.
- 157.** Blagosklonny MV. Aging, stem cells, and mammalian target of rapamycin: a prospect of pharmacologic rejuvenation of aging stem cells. *Rejuvenation Res*. 2008; 11: 801-808.
- 158.** Shah OJ, Wang Z, Hunter T. Inappropriate activation of the TSC/Rheb/mTOR/S6K cassette induces IRS1/2 depletion, insulin resistance, and cell survival deficiencies. *Curr Biol*. 2004; 14: 1650-1656.
- 159.** Zhang H, Bajraszewski N, Wu E, Wang H, Moseman AP, Dabora SL, Griffin JD, Kwiatkowski DJ. PDGFRs are critical for PI3K/Akt activation and negatively regulated by mTOR. *J Clin Invest*. 2007; 117: 730-738.
- 160.** Yilmaz OH, Valdez R, Theisen BK, Guo W, Ferguson DO, Wu H, Morrison SJ. Pten dependence distinguishes haematopoietic stem cells from leukaemia-initiating cells. *Nature*. 2006; 441: 475-482.
- 161.** Chen C, Liu Y, Zheng P. The axis of mTOR-mitochondria-ROS and stemness of the hematopoietic stem cells. *Cell Cycle*. 2009; 8: 1158-1160.
- 162.** Castilho RM, Squarize CH, Chodosh LA, Williams BO, Gutkind JS. mTOR mediates Wnt-induced epidermal stem cell exhaustion and aging. *Cell Stem Cell*. 2009; 5: 279-289.
- 163.** Gan B, DePinho RA. mTORC1 signaling governs hematopoietic stem cell quiescence. *Cell Cycle*. 2009; 8: 1003-1006.
- 164.** Lee JY, Nakada D, Yilmaz OH, Tothova Z, Joseph NM, Lim MS, Gilliland DG, Morrison SJ. mTOR activation induces tumor suppressors that inhibit leukemogenesis and deplete hematopoietic stem cells after Pten deletion. *Cell Stem Cell*. 2010; 7: 593-605.
- 165.** Parsons DW, Wang TL, Samuels Y, Bardelli A, Cummins JM, DeLong L, Silliman N, Ptak J, Szabo S, Willson JK, Markowitz S, Kinzler KW, Vogelstein B, Lengauer C, Velculescu VE. Colorectal cancer: mutations in a signalling pathway. *Nature*. 2005; 436: 792.
- 166.** Shaw RJ, Cantley LC. Ras, PI(3)K and mTOR signalling controls tumour cell growth. *Nature*. 2006; 441: 424-430.
- 167.** Janes MR, Fruman DA. Targeting TOR dependence in cancer. *Oncotarget*. 2010; 1: 69-76.
- 168.** Markman B, Dienstmann R, Tabernero J. Targeting the PI3K/Akt/mTOR pathway--beyond rapalogs. *Oncotarget*. 2010; 1: 530-543.
- 169.** Cully M, You H, Levine AJ, Mak TW. Beyond PTEN mutations: the PI3K pathway as an integrator of multiple inputs during tumorigenesis. *Nat Rev Cancer*. 2006; 6: 184-192.
- 170.** Guertin DA, Sabatini DM. Defining the role of mTOR in cancer. *Cancer Cell*. 2007; 12: 9-22.
- 171.** Courtney KD, Corcoran RB, Engelman JA. The PI3K pathway as drug target in human cancer. *J Clin Oncol*. 2010; 28: 1075-1083.
- 172.** Schmidt-Kittler O, Zhu J, Yang J, Liu G, Hendricks W, Lengauer C, Gabelli SB, Kinzler KW, Vogelstein B, Huso DL, Zhou S. PI3Kalpha inhibitors that inhibit metastasis. *Oncotarget*. 2010; 1: 339-348.
- 173.** Dbouk HA, Backer JM. A beta version of life: p110beta takes center stage. *Oncotarget*. 2010; 1: 729-733.
- 174.** Martelli AM, Evangelisti C, Chiarini F, McCubrey JA. The phosphatidylinositol 3-kinase/Akt/mTOR signaling network as a therapeutic target in acute myelogenous leukemia patients. *Oncotarget*. 2010; 1: 89-103.
- 175.** Nucera C, Lawler J, Hodin R, Parangi S. The BRAFV600E mutation: what is it really orchestrating in thyroid cancer? *Oncotarget*. 2010; 1: 751-756.
- 176.** Zawal L. P3Kalpha: a driver of tumor metastasis? *Oncotarget*. 2010; 1: 315-316.
- 177.** Zhang Z, Stiegler AL, Boggon TJ, Kobayashi S, Halmos B. EGFR-mutated lung cancer: a paradigm of molecular oncology. *Oncotarget*. 2010; 1: 497-514.
- 178.** Shahbazian D, Parsyan A, Petroulakis E, Hershey J, Sonenberg N. eIF4B controls survival and proliferation and is regulated by proto-oncogenic signaling pathways. *Cell Cycle*. 2010; 9: 4106-4109.
- 179.** Bhatia B, Nahle Z, Kenney AM. Double trouble: when sonic hedgehog signaling meets TSC inactivation. *Cell Cycle*. 2010; 9: 456-459.
- 180.** Fujishita T, Aoki M, Taketo MM. The role of mTORC1 pathway in intestinal tumorigenesis. *Cell Cycle*. 2009; 8: 3684-3687.
- 181.** Roux PP, Ballif BA, Anjum R, Gygi SP, Blenis J. Tumor-promoting phorbol esters and activated Ras inactivate the tuberous sclerosis tumor suppressor complex via p90 ribosomal S6 kinase. *Proc Natl Acad Sci U S A*. 2004; 101: 13489-13494.
- 182.** De La OJ, Murtaugh LC. Notch and Kras in pancreatic cancer: at the crossroads of mutation, differentiation and signaling. *Cell Cycle*. 2009; 8: 1860-1864.
- 183.** Li J, Yen C, Liaw D, Podsypanina K, Bose S, Wang SI, Puc J, Miliareis C, Rodgers L, McCombie R, Bigner SH, Giovanella BC, Ittmann M, Tycko B, Hibshoosh H, Wigler MH et al. PTEN, a putative protein tyrosine phosphatase gene mutated in human brain, breast, and prostate cancer. *Science*. 1997; 275: 1943-1947.
- 184.** Di Cristofano A, Pesce B, Cordon-Cardo C, Pandolfi PP. Pten is essential for embryonic development and tumour suppression. *Nat Genet*. 1998; 19: 348-355.
- 185.** Ma L, Chen Z, Erdjument-Bromage H, Tempst P, Pandolfi PP. Phosphorylation and functional inactivation of TSC2 by Erk implications for tuberous sclerosis and cancer pathogenesis. *Cell*. 2005; 121: 179-193.
- 186.** Jones RG, Thompson CB. Tumor suppressors and cell metabolism: a recipe for cancer growth. *Genes Dev*. 2009; 23: 537-548.
- 187.** Shackelford DB, Shaw RJ. The LKB1-AMPK pathway: metabolism and growth control in tumour suppression. *Nat Rev Cancer*. 2009; 9: 563-575.
- 188.** Vazquez-Martin A, Oliveras-Ferreros C, Lopez-Bonet E, Menendez JA. AMPK: Evidence for an energy-sensing cytokinetic tumor suppressor. *Cell Cycle*. 2009; 8: 3679-3683.
- 189.** Peng C, Chen Y, Li D, Li S. Role of Pten in leukemia stem cells. *Oncotarget*. 2010; 1: 156-160.
- 190.** Green AS, Chapuis N, Lacombe C, Mayeux P, Bouscary D, Tamburini J. LKB1/AMPK/mTOR signaling pathway in hematological malignancies: from metabolism to cancer cell biology. *Cell Cycle*. 2011; 10: 2115-2120.
- 191.** Johannessen CM, Reczek EE, James MF, Brems H, Legius E, Cichowski K. The NF1 tumor suppressor critically regulates TSC2 and mTOR. *Proc Natl Acad Sci U S A*. 2005; 102: 8573-8578.
- 192.** Feng Z, Levine AJ. The regulation of energy metabolism and the IGF-1/mTOR pathways by the p53 protein. *Trends Cell Biol*. 2010; 20: 427-434.
- 193.** Feng Z, Hu W, Rajagopal G, Levine AJ. The tumor suppressor p53: cancer and aging. *Cell Cycle*. 2008; 7: 842-847.

- 194.** Feng Z, Hu W, de Stanchina E, Teresky AK, Jin S, Lowe S, Levine AJ. The regulation of AMPK beta1, TSC2, and PTEN expression by p53: stress, cell and tissue specificity, and the role of these gene products in modulating the IGF-1-AKT-mTOR pathways. *Cancer Res.* 2007; 67: 3043-3053.
- 195.** Feng Z, Zhang H, Levine AJ, Jin S. The coordinate regulation of the p53 and mTOR pathways in cells. *Proc Natl Acad Sci U S A.* 2005; 102: 8204-8209.
- 196.** Levine AJ, Feng Z, Mak TW, You H, Jin S. Coordination and communication between the p53 and IGF-1-AKT-TOR signal transduction pathways. *Genes Dev.* 2006; 20: 267-275.
- 197.** Budanov AV, Karin M. p53 target genes *sestrin1* and *sestrin2* connect genotoxic stress and mTOR signaling. *Cell.* 2008; 134: 451-460.
- 198.** Demidenko ZN, Korotchkina LG, Gudkov AV, Blagosklonny MV. Paradoxical suppression of cellular senescence by p53. *Proc Natl Acad Sci U S A.* 2010; 107: 9660-9664.
- 199.** Korotchkina LG, Leontieva OV, Bukreeva EI, Demidenko ZN, Gudkov AV, Blagosklonny MV. The choice between p53-induced senescence and quiescence is determined in part by the mTOR pathway. *Aging.* 2010; 2: 344-352.
- 200.** Leontieva O, Gudkov A, Blagosklonny M. Weak p53 permits senescence during cell cycle arrest. *Cell Cycle.* 2010; 9: 4323-4327.
- 201.** Galluzzi L, Kepp O, Kroemer G. TP53 and MTOR crosstalk to regulate cellular senescence. *Aging.* 2010; 2: 535-537.
- 202.** Long JS, Ryan KM. p53 and senescence: a little goes a long way. *Cell Cycle.* 2010; 9: 4050-4051.
- 203.** Santoro R, Blandino G. p53: The pivot between cell cycle arrest and senescence. *Cell Cycle.* 2010; 9: 4262-4263.
- 204.** Serrano M. Shifting senescence into quiescence by turning up p53. *Cell Cycle.* 2010; 9: 4256-4257.
- 205.** DeBerardinis RJ, Lum JJ, Hatzivassiliou G, Thompson CB. The biology of cancer: metabolic reprogramming fuels cell growth and proliferation. *Cell Metab.* 2008; 7: 11-20.
- 206.** Demidenko ZN, Blagosklonny MV. Quantifying pharmacologic suppression of cellular senescence: prevention of cellular hypertrophy versus preservation of proliferative potential. *Aging.* 2009; 1: 1008-1016.
- 207.** Demidenko ZN, Blagosklonny MV. The purpose of the HIF-1/PHD feedback loop: to limit mTOR-induced HIF-1alpha. *Cell Cycle.* 2011; 10: 1557-1562.
- 208.** Narita M, Young AR, Arakawa S, Samarajiwa SA, Nakashima T, Yoshida S, Hong S, Berry LS, Reichelt S, Ferreira M, Tavares S, Inoki K, Shimizu S. Spatial coupling of mTOR and autophagy augments secretory phenotypes. *Science.* 2011; 332: 966-970.
- 209.** Medema RH, Herrera RE, Lam F, Weinberg RA. Growth suppression by p16ink4 requires functional retinoblastoma protein. *Proc Natl Acad Sci USA.* 1995; 92: 62289-62293.
- 210.** de Jonge HJ, Woolthuis CM, de Bont ES, Huls G. Paradoxical down-regulation of p16 mRNA with advancing age in acute myeloid leukemia. *Aging (Albany NY).* 2009; 1: 949-953.
- 211.** Schmidt EV, Ravitz MJ, Chen L, Lynch M. Growth controls connect: interactions between c-myc and the tuberous sclerosis complex-mTOR pathway. *Cell Cycle.* 2009; 8: 1344-1351.
- 212.** Cannell IG, Bushell M. Regulation of Myc by miR-34c: A mechanism to prevent genomic instability? *Cell Cycle.* 2010; 9: 2726-2730.
- 213.** Haferkamp S, Tran SL, Becker TM, Scurr LL, Kefford RF, Rizos H. The relative contributions of the p53 and pRb pathways in oncogene-induced melanocyte senescence. *Aging.* 2009; 1: 542-556.
- 214.** Noonan EJ, Place RF, Basak S, Pookot D, Li LC. miR-449a causes Rb-dependent cell cycle arrest and senescence in prostate cancer cells. *Oncotarget.* 2010; 1: 349-358.
- 215.** Akakura S, Nochajski P, Gao L, Sotomayor P, Matsui S, Gelman IH. Rb-dependent cellular senescence, multinucleation and susceptibility to oncogenic transformation through PKC scaffolding by SSeCKS/AKAP12. *Cell Cycle.* 2010; 9: 4656-4665.
- 216.** Ertel A, Dean JL, Rui H, Liu C, Witkiewicz AK, Knudsen KE, Knudsen ES. RB-pathway disruption in breast cancer: differential association with disease subtypes, disease-specific prognosis and therapeutic response. *Cell Cycle.* 2010; 9: 4153-4163.
- 217.** Land H, Parada LF, Weinberg RA. Tumorigenic conversion of primary embryo fibroblasts requires at least two cooperating oncogenes. *Nature.* 1983; 304: 596-602.
- 218.** Kauffmann-Zeh A, Rodriguez-Viciano P, Ulrich E, Gilbert C, Coffey P, Downward J, Evan G. Suppression of c-Myc-induced apoptosis by Ras signalling through PI(3)K and PKB. *Nature.* 1997; 385: 544-548.
- 219.** Serrano M, Lin AW, McCurrach ME, Beach D, Lowe SW. Oncogenic ras provokes premature cell senescence associated with accumulation of p53 and p16INK4a. *Cell.* 1997; 88: 593-602.
- 220.** Hueber AO, Evan GI. Traps to catch unwary oncogenes. *Trends Genet.* 1998; 14: 364-367.
- 221.** Hahn WC, Counter CM, Lundberg AS, Beijersbergen RL, Brooks MW, Weinberg RA. Creation of human tumour cells with defined genetic elements. *Nature.* 1999; 400: 464-468.
- 222.** Podsypanina K, Politi K, Beverly LJ, Varmus HE. Oncogene cooperation in tumor maintenance and tumor recurrence in mouse mammary tumors induced by Myc and mutant Kras. *Proc Natl Acad Sci U S A.* 2008; 105: 5242-5247.
- 223.** Hoffman B, Liebermann DA. Apoptotic signaling by c-MYC. *Oncogene.* 2008; 27: 6462-6472.
- 224.** Chawla R, Procknow JA, Tantravahi RV, Khurana JS, Litvin J, Reddy EP. Cooperativity of Cdk4R24C and Ras in melanoma development. *Cell Cycle.* 2010; 9: 3305-3314.
- 225.** Debbas M, White E. Wild-type p53 mediates apoptosis by E1A, which is inhibited by E1B. *Genes Dev.* 1993; 7: 546-554.
- 226.** Leontieva OV, Blagosklonny MV. DNA damaging agents and p53 do not cause senescence in quiescent cells, while consecutive re-activation of mTOR is associated with conversion to senescence. *Aging (Albany NY).* 2010; 2: 924-935.
- 227.** Blagosklonny MV. Cell cycle arrest is not senescence. *Aging.* 2011; 3: 94-101.
- 228.** Wang C, Maddick M, Miwa S, Jurk D, Czapiewski R, Saretzki G, Langie SA, Godschalk RW, Cameron K, von Zglinicki T. Adult-onset, short-term dietary restriction reduces cell senescence in mice. *Aging.* 2010; 2: 555-566.
- 229.** Kirkland JL. Perspectives on cellular senescence and short term dietary restriction in adults. *Aging.* 2010; 2: 542-544.
- 230.** Demidenko ZN, Blagosklonny MV. Growth stimulation leads to cellular senescence when the cell cycle is blocked. *Cell Cycle.* 2008; 7: 3355-3361.
- 231.** Pospelova TV, Demidenko ZN, Bukreeva EI, Pospelov VA, Gudkov AV, Blagosklonny MV. Pseudo-DNA damage response in senescent cells. *Cell Cycle.* 2009; 8: 4112-4118.
- 232.** Blagosklonny MV. Aging-suppressants: cellular senescence (hyperactivation) and its pharmacologic deceleration. *Cell Cycle.* 2009; 8: 1883-1887.

- 233.** Demidenko ZN, Zubova SG, Bukreeva EI, Pospelov VA, Pospelova TV, Blagosklonny MV. Rapamycin decelerates cellular senescence. *Cell Cycle*. 2009; 8: 1888-1895.
- 234.** Demidenko ZN, Shtutman M, Blagosklonny MV. Pharmacologic inhibition of MEK and PI-3K converges on the mTOR/S6 pathway to decelerate cellular senescence. *Cell Cycle*. 2009; 8: 1896-1900.
- 235.** Demidenko ZN, Blagosklonny MV. At concentrations that inhibit mTOR, resveratrol suppresses cellular senescence. *Cell Cycle*. 2009; 8: 1901-1904.
- 236.** Romanov VS, Abramova MV, Svetlikova SB, Bykova TV, Zubova SG, Aksenov ND, Fornace AJ, Jr., Pospelova TV, Pospelov VA. p21(Waf1) is required for cellular senescence but not for cell cycle arrest induced by the HDAC inhibitor sodium butyrate. *Cell Cycle*. 2010; 9: 3945-3955.
- 237.** Wesierska-Gadek J. mTOR and its link to the picture of Dorian Gray - re-activation of mTOR promotes aging. *Aging*. 2010; 2: 892-893.
- 238.** Bartkova J, Rezaei N, Liontos M, Karakaidos P, Kletsas D, Issaeva N, Vassiliou LV, Kolettas E, Niforou K, Zoumpourlis VC, Takaoka M, Nakagawa H, Tort F, Fugger K, Johansson F, Sehested M et al. Oncogene-induced senescence is part of the tumorigenesis barrier imposed by DNA damage checkpoints. *Nature*. 2006; 444: 633-637.
- 239.** Di Micco R, Fumagalli M, Cicalese A, Piccinin S, Gasparini P, Luise C, Schurra C, Garre M, Nuciforo PG, Bensimon A, Maestro R, Pelicci PG, d'Adda di Fagagna F. Oncogene-induced senescence is a DNA damage response triggered by DNA hyper-replication. *Nature*. 2006; 444: 638-642.
- 240.** Mallette FA, Gaumont-Leclerc MF, Ferbeyre G. The DNA damage signaling pathway is a critical mediator of oncogene-induced senescence. *Genes Dev*. 2007; 21: 43-48.
- 241.** Bartek J, Lukas J, Bartkova J. DNA damage response as an anti-cancer barrier: damage threshold and the concept of 'conditional haploinsufficiency'. *Cell Cycle*. 2007; 6: 2344-2347.
- 242.** Halazonetis TD, Gorgoulis VG, Bartek J. An oncogene-induced DNA damage model for cancer development. *Science*. 2008; 319: 1352-1355.
- 243.** Alimonti A, Nardella C, Chen Z, Clohessy JG, Carracedo A, Trotman LC, Cheng K, Varmeh S, Kozma SC, Thomas G, Rosivatz E, Woscholski R, Cognetti F, Scher HI, Pandolfi PP. A novel type of cellular senescence that can be enhanced in mouse models and human tumor xenografts to suppress prostate tumorigenesis. *J Clin Invest*. 2010; 120: 681-693.
- 244.** Courtois-Cox S, Jones SL, Cichowski K. Many roads lead to oncogene-induced senescence. *Oncogene*. 2008; 27: 2801-2809.
- 245.** Reddy JP, Peddibhotla S, Bu W, Zhao J, Haricharan S, Du YC, Podsypanina K, Rosen JM, Donehower LA, Li Y. Defining the ATM-mediated barrier to tumorigenesis in somatic mammary cells following ErbB2 activation. *Proc Natl Acad Sci U S A*. 2010; 107: 3728-3733.
- 246.** Pinkston JM, Garigan D, Hansen M, Kenyon C. Mutations that increase the life span of *C. elegans* inhibit tumor growth. *Science*. 2006; 313: 971-975.
- 247.** Longo VD, Lieber MR, Vijg J. Turning anti-ageing genes against cancer. *Nat Rev Mol Cell Biol*. 2008; 9: 903-910.
- 248.** Toledo LI, Murga M, Gutierrez-Martinez P, Soria R, Fernandez-Capetillo O. ATR signaling can drive cells into senescence in the absence of DNA breaks. *Genes Dev*. 2008; 22: 297-302.
- 249.** Efeyan A, Murga M, Martinez-Pastor B, Ortega-Molina A, Soria R, Collado M, Fernandez-Capetillo O, Serrano M. Limited role of murine ATM in oncogene-induced senescence and p53-dependent tumor suppression. *PLoS One*. 2009; 4: e5475.
- 250.** McManus KJ, Hendzel MJ. ATM-dependent DNA damage-independent mitotic phosphorylation of H2AX in normally growing mammalian cells. *Mol Biol Cell*. 2005; 16: 5013-5025.
- 251.** Nelson G, Buhmann M, von Zglinicki T. DNA damage foci in mitosis are devoid of 53BP1. *Cell Cycle*. 2009; 8: 3379-3383.
- 252.** Soutoglou E, Misteli T. Activation of the cellular DNA damage response in the absence of DNA lesions. *Science*. 2008; 320: 1507-1510.
- 253.** Soutoglou E. DNA lesions and DNA damage response: even long lasting relationships need a "break". *Cell Cycle*. 2008; 7: 3653-3658.
- 254.** Bencokova Z, Kaufmann MR, Pires IM, Lecane PS, Giaccia AJ, Hammond EM. ATM activation and signaling under hypoxic conditions. *Mol Cell Biol*. 2009; 29: 526-537.
- 255.** Pankotai T, Hoffbeck AS, Boumendil C, Soutoglou E. DNA damage response in the absence of DNA lesions continued. *Cell Cycle*. 2009; 8: 4025-4026.
- 256.** Bouquet F, Ousset M, Biard D, Fallone F, Dauvillier S, Frit P, Salles B, Muller C. A DNA-dependent stress response involving DNA-PK occurs in hypoxic cells and contributes to cellular adaptation to hypoxia. *J Cell Sci*. 2011; 124: 1943-1951.
- 257.** Alexander A, Walker CL. Differential localization of ATM is correlated with activation of distinct downstream signaling pathways. *Cell Cycle*. 2010; 9: 3685-3686.
- 258.** Rodriguez-Jimenez FJ, Moreno-Manzano V, Mateos-Gregorio P, Royo I, Erceg S, Murguia JR, Sanchez-Puelles JM. FM19G11: A new modulator of HIF that links mTOR activation with the DNA damage checkpoint pathways. *Cell Cycle*. 2010; 9: 2803-2813.
- 259.** Guo Z, Deshpande R, Paull TT. ATM activation in the presence of oxidative stress. *Cell Cycle*. 2010; 9: 4805-4811.
- 260.** Cam H, Easton JB, High A, Houghton PJ. mTORC1 signaling under hypoxic conditions is controlled by ATM-dependent phosphorylation of HIF-1alpha. *Mol Cell*. 2010; 40: 509-520.
- 261.** Shor B, Gibbons JJ, Abraham RT, Yu K. Targeting mTOR globally in cancer: thinking beyond rapamycin. *Cell Cycle*. 2009; 8: 3831-3837.
- 262.** Benjamin D, Colombi M, Moroni C, Hall MN. Rapamycin passes the torch: a new generation of mTOR inhibitors. *Nat Rev Drug Discov*. 2011; 10: 868-880.
- 263.** Morris JZ, Tissenbaum HA, Ruvkun G. A phosphatidylinositol-3-OH kinase family member regulating longevity and diapause in *Caenorhabditis elegans*. *Nature*. 1996; 382: 536-539.
- 264.** Babar P, Adamson C, Walker GA, Walker DW, Lithgow GJ. P13-kinase inhibition induces dauer formation, thermotolerance and longevity in *C. elegans*. *Neurobiol Aging*. 1999; 20: 513-519.
- 265.** Vellai T, Takacs-Vellai K, Zhang Y, Kovacs AL, Orosz L, Muller F. Genetics: influence of TOR kinase on lifespan in *C. elegans*. *Nature*. 2003; 426: 620.
- 266.** Hansen M, Taubert S, Crawford D, Libina N, Lee SJ, Kenyon C. Lifespan extension by conditions that inhibit translation in *Caenorhabditis elegans*. *Aging Cell*. 2007; 6: 95-110.
- 267.** Kapahi P, Zid BM, Harper T, Koslover D, Sapin V, Benzer S. Regulation of lifespan in *Drosophila* by modulation of genes in the TOR signaling pathway. *Curr Biol*. 2004; 14: 885-890.

- 268.** Edman U, Garcia AM, Busuttil RA, Sorensen D, Lundell M, Kapahi P, Vijg J. Lifespan extension by dietary restriction is not linked to protection against somatic DNA damage in *Drosophila melanogaster*. *Aging Cell*. 2009; 8: 331-338.
- 269.** Katewa SD, Kapahi P. Role of TOR signaling in aging and related biological processes in *Drosophila melanogaster*. *Exp Gerontol*. 2011; 46: 382-390.

Genome protective effect of metformin as revealed by reduced level of constitutive DNA damage signaling

H. Dorota Halicka¹, Hong Zhao¹, Jiangwei Li¹, Frank Traganos¹, Sufang Zhang², Marietta Lee², and Zbigniew Darzynkiewicz¹

¹ Brander Cancer Research Institute and Department of Pathology, New York Medical College, Valhalla, NY 10595, USA

² Department of Biochemistry and Molecular Biology, New York Medical College, Valhalla, NY 10595, USA

Key words: DNA replication stress, Reactive oxidant species (ROS), H2AX phosphorylation, ATM activation, cell cycle

Received: 9/22/11; **Accepted:** 10/26/11; **Published:** 10/28/11

Correspondence to: Z. Darzynkiewicz, PhD; **E-mail:** darzynk@nymc.edu

Copyright: © Halicka et al. This is an open-access article distributed under the terms of the Creative Commons Attribution License, which permits unrestricted use, distribution, and reproduction in any medium, provided the original author and source are credited

Abstract: We have shown before that constitutive DNA damage signaling represented by H2AX-Ser139 phosphorylation and ATM activation in untreated normal and tumor cells is a reporter of the persistent DNA replication stress induced by endogenous oxidants, the by-products of aerobic respiration. In the present study we observed that exposure of normal mitogenically stimulated lymphocytes or tumor cell lines A549, TK6 and A431 to metformin, the specific activator of 5'AMP-activated protein kinase (AMPK) and an inhibitor of mTOR signaling, resulted in attenuation of constitutive H2AX phosphorylation and ATM activation. The effects were metformin-concentration dependent and seen even at the pharmacologically pertinent 0.1 mM drug concentration. The data also show that intracellular levels of endogenous reactive oxidants able to oxidize 2',7'-dihydro-dichlorofluorescein diacetate was reduced in metformin-treated cells. Since persistent constitutive DNA replication stress, particularly when paralleled by mTOR signaling, is considered to be the major cause of aging, the present findings are consistent with the notion that metformin, by reducing both DNA replication stress and mTOR-signaling, slows down aging and/or cell senescence processes.

INTRODUCTION

In live cells, DNA is continuously being damaged by reactive oxygen species (ROS), the by-products of aerobic respiration in mitochondria [1-6]. Exogenous oxidants originating from environmental pollutants [7], phagocyte-oxidative burst [8-10], and even iatrogenic factors [11], additionally contribute to DNA damage. Such DNA damage involves oxidation of the constituent DNA bases, particularly of guanine by formation of 8-oxo-7,8-dihydro-2'-deoxyguanosine (oxo8dG), base ring fragmentation, modification of deoxyglucose, crosslinking of DNA and protein, and induction of DNA double strand breaks (DSBs) [12,13]. Another important injurious effect of endogenous and exogenous oxidants is peroxidation of lipids in cell membranes [14].

The extent of ROS-induced DNA damage varies widely in different studies [1-6]. According to one rather con-

servative estimate, about 5,000 DNA single-strand lesions (SSLs) are generated per nucleus during a single cell cycle of approximately 24 h duration [6]. About 1% of those lesions become converted to DSBs, mostly during DNA replication. This leads to formation of ~50 "endogenous DSBs", the most severe and potentially mutagenic lesions [6]. DSBs can be repaired by two mechanisms, recombinatorial repair or nonhomologous DNA-end joining (NHEJ). The template-assisted recombinatorial repair is essentially error-free but takes place only when cells have already replicated their DNA which can serve as a template, namely in late-S and G₂ phase of the cell cycle. DNA repair in cells lacking a template such as in G₁ and early S phase occurs via the NHEJ mechanism. The latter is error-prone and may result in deletion of some base pairs [15,16]. When such change occurs at the site of an oncogene or tumor suppressor gene it may promote carcinogenesis [17,18]. It can also lead to [translocations](#) and [telomere](#) fusion, hallmarks of [tumor](#) cells [19]. The

progressive accumulation of DNA damage with each sequential cell cycle has been considered to be the primary cause of cell aging and senescence [20]. However, the notion that persistent stimulation of mTOR-driven pathways (rather than the ROS-induced DNA damage) is the major mechanism responsible for aging appears to have more merit [21-27]. Oxidative DNA damage, on the other hand, by contributing to replication stress may be a factor enhancing the TOR-driven aging or senescence process [28].

Strategies for preventing cancer or slowing down aging are often directed at protecting DNA from oxidative damage. Protective agents can be identified by their ability to reduce formation of "endogenous DSBs". The direct detection of endogenous DSBs in individual cells has been difficult because the leading methodology, single cell electrophoresis (comet) assay [29], lacks the desired sensitivity. The TUNEL assay, developed to label DSBs in apoptotic cells, also lack sufficient sensitivity [30,31]. While the assays of DNA damage measurement in bulk offer greater sensitivity, these approaches do not allow one to relate the damage to individual cells, reveal any heterogeneity within cell populations, or the relationship of DSBs to cell cycle phase or apoptosis.

Among the early and most sensitive reporters of DNA damage, and in particular formation of DSBs, is the activation of the Ataxia Telangiectasia mutated protein kinase (ATM) through its autophosphorylation on Ser1981 [32], and the phosphorylation of histone H2AX on Ser139; the phosphorylated H2AX is designated as γ H2AX [33]. Immunocytochemical detection of these events offers high sensitivity in assessment of DSBs formation in individual cells [34-37]. These biosensors of DNA damage have been used in conjunction with flow- or image-cytometry to assess DNA damage in cells exposed to a variety of exogenous genotoxins (reviews, [31,38]). In fact, the high sensitivity of these biomarkers makes it possible to use them to detect and measure the extent of constitutive DNA damage induced by the metabolically generated ROS in untreated cells [39-41]. Furthermore, these markers can be used to explore the effectiveness of factors protecting nuclear DNA from endogenous oxidants [42-45]. Thus, the anti-oxidants (N-acetyl-L-cysteine, ascorbate, Celecoxib), inhibitors of glycolysis and oxidative phosphorylation (2-deoxy-D-glucose and 5-bromopyruvate), hypoxia (3-5% O₂), confluency, low serum concentration, were all shown to distinctly reduce the level of constitutive ATM activation and H2AX phosphorylation [40-45]. Conversely, the factors enhancing metabolic activity (aerobic glycolysis) such as cell mitogenic activation, glucose, or dichloroacetate

amplified the level of constitutive expression of γ H2AX and activated ATM [42-45]. Collectively, these observations provide strong evidence that the extent of the ongoing DNA damage imposed by endogenous oxidants as well as the effectiveness of factors that protect from (or enhance) the damage can be assessed by analysis of the level of constitutive DNA damage signaling.

In the present study we tested whether metformin, a drug widely prescribed to treat type 2 diabetes, has the ability to modulate the level of constitutive DNA damage signaling. Metformin is a specific activator of 5'AMP-activated protein kinase (AMPK), a phylogenetically conserved serine/threonine kinase that plays a key role in cellular energy homeostasis (reviews, [46-52]). AMPK is the energy sensor ("fuel gauge") monitoring and regulating cellular energy in response to metabolic needs and nutritional environmental variations. This kinase is activated by low cellular energy status (increased AMP/ATP ratio) and responds by: (i) activating ATP-producing catabolic pathways such as glycolysis and fatty acids oxidation and (ii) suppressing the energy (ATP)-consuming anabolic pathways such as lipogenesis, gluconeogenesis and protein synthesis. Another effect of AMPK activation is inhibition of mammalian target of rapamycin (mTOR), the downstream effector of growth factor signaling pathways [51]. AMPK affects these activities by phosphorylating proteins regulating these pathways (instant effect) as well as by modulating transcription of genes encoding proteins of these pathways (delayed effect) [53-55]. AMPK itself is activated by the upstream mediator liver kinase B1 (LKB1) [52]. Activation of AMPK by metformin was shown to reduce intracellular reactive oxygen species (ROS) levels *via* upregulation of expression of the antioxidant thioredoxin through the AMPK-FOXO3 pathway [55].

There is a growing body of evidence that metformin may be considered a promising anti-aging candidate, applicable for life span extension, prevention and even treatment of cancer [22-27,50,56]. Given the above, it is of additional interest to know how metformin affects the level of constitutive DNA signaling in normal and tumor cells. Our present data show that in normal lymphocytes, as well as in cells of tumor lines the level of constitutive ATM activation and γ H2AX expression was distinctly attenuated upon exposure to metformin. Also reduced was the level of intracellular ROS.

RESULTS

The effect of metformin was tested on the level of constitutive expression of γ H2AX and Ser1981-

phosphorylated ATM in human lung adenocarcinoma A549 cells. The cells were grown attached on slides and the expression of these phospho-proteins was measured by laser scanning cytometry (LSC) [57]. The data provide clear evidence that expression of γ H2AX in A549 cells growing in the presence of metformin for 48 h was reduced (Figure 1). The reduction was apparent at 1 mM, and was progressively more pronounced following exposure to 5 and 20 mM concentrations of metformin.

Across all the three metformin concentrations, the degree of reduction in γ H2AX expression was more distinct in G₂M- and S- phase cells compared to cells in the G₁-phase of the cycle. The DNA content frequency histograms did not show major changes in the cell cycle distribution following 48 h treatment with up to 10 mM metformin, while only a modest decrease in the proportion of S-phase cells was apparent following exposure to 20mM metformin (Figure 1, insets).

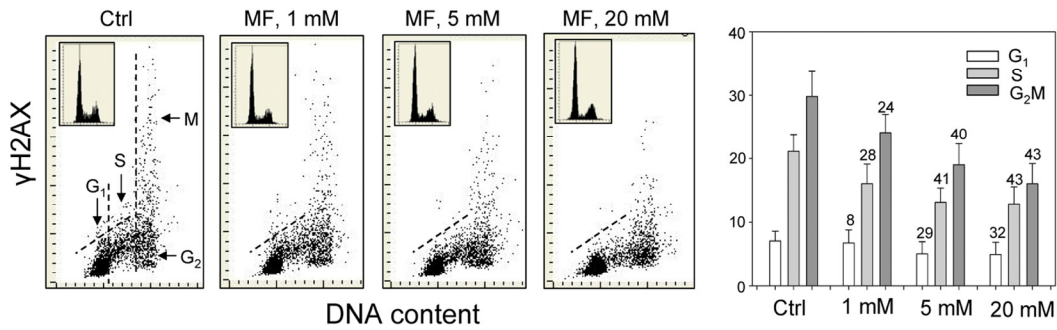


Figure 1. Effect of metformin (MF) on the level of constitutive γ H2AX expression in A549 cells. Exponentially growing A549 cells were left untreated (Ctrl) or treated with 1, 5 or 20 mM metformin for 48 h. Left panels present bivariate distributions of cellular DNA content *versus* intensity of γ H2AX immunofluorescence (IF) detected with H2AX-Ser139 phospho-specific Ab in cells of these cultures; fluorescence of individual cells was measured by laser scanning cytometry (LSC) [76]. Based on differences in DNA content the cells were gated in G₁, S and G₂M phases of the cell cycle, as shown in the left panel, and the mean values of γ H2AX IF for cells in each of these cell cycle phases by were obtained gating analysis. These mean values (+SD) are presented as the bar plots (right panel). The percent decrease in mean values of γ H2AX expression of the metformin-treated cells with respect to the same phase of the cell cycle of the untreated cells is shown above the respective bars. The skewed dash line shows the upper level of γ H2AX IF intensity for 97% of G₁- and S- phase cells in Ctrl. The insets show cellular DNA content frequency histograms in the respective cultures.

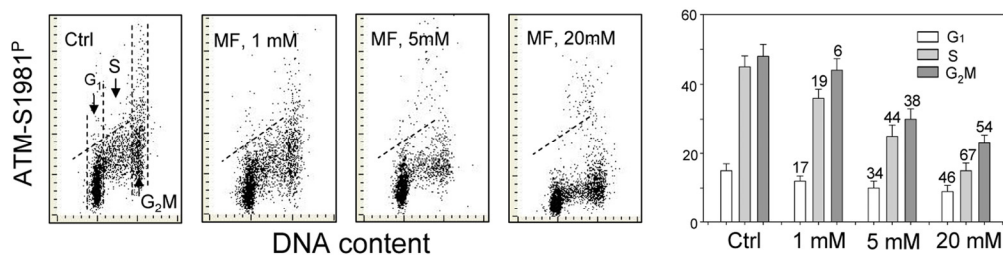


Figure 2. Effect of metformin (MF) on the level of constitutive ATM phosphorylation on Ser1981 in A549 cells. Similar as in Figure 1, the cells were treated with 1, 5 or 20 mM MF for 48 h. Left panels present bivariate distributions of cellular DNA content vs intensity of ATM-S1981^P IF. The mean values of ATM-S1981^P for cells in G₁, S, and G₂M were obtained by gating analysis and are shown (+SD) as the bar plots (right panel). The skewed dash line shows the upper level of ATM-S198^P IF intensity for 97% of G₁- and S- phase cells in Ctrl.

The effect of metformin on the level of constitutive expression of ATM phosphorylated on Ser1981 in A549 cells was strikingly similar to that of γ H2AX (Figure 2). The degree of reduction of ATM-S1981^P was metformin-concentration dependent. While the decline in ATM activation was seen in all phases of the cell cycle, the most pronounced reduction was evident in S-phase cells (Figure 2).

In the next set of experiments we have tested the effect of metformin on human lymphoblastoid TK6 cells. These cells grow in suspension and their fluorescence,

upon staining with phospho-specific Abs, was measured by flow cytometry [57]. The data show that, similar to A549, the expression of γ H2AX was also reduced in TK6 cells exposed to metformin (Figure 3). The effect could be seen (7 – 10% decrease) even at a metformin concentration as low as 0.1 mM, and was more pronounced (up to 44% reduction) at higher concentrations. In TK6 cells the reduction in γ H2AX was more pronounced in G₁ and S phase than in G₂M phase cells. The level of constitutively activated ATM was also decreased in TK6 cells growing in the presence of metformin (Figure 4).

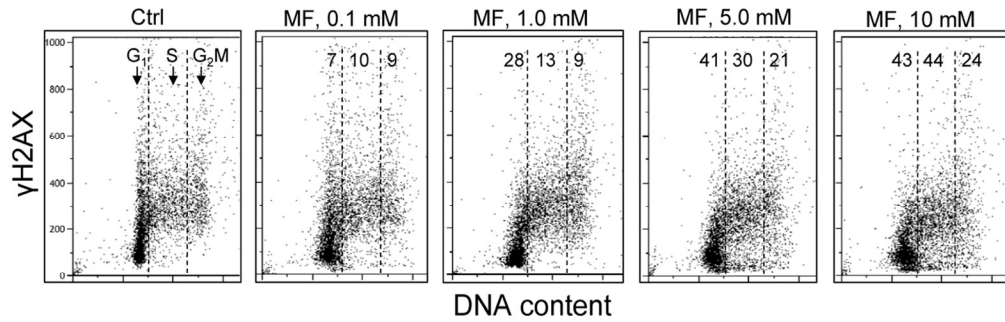


Figure 3. Effect of metformin on the level of constitutive expression of γ H2AX in TK6 cells. Exponentially growing TK6 cells were untreated (Ctrl) or were grown in the presence of 0.1, 1.0, 5.0 and 10 mM metformin (MF) for 48 h. The expression of γ H2AX was detected with phospho-specific (Ser139-P) Ab and cell fluorescence was measured by flow cytometry. Based on differences in DNA content the cells were gated in G₁, S and G₂M phases of the cell cycle and the mean values of γ H2AX IF for cells in each of these cell cycle phases were calculated. The numerical figures show the percent reduction in mean values of γ H2AX IF of the metformin-treated cells with respect to the mean values of the untreated cells (Ctrl) in the respective phases of the cell cycle.

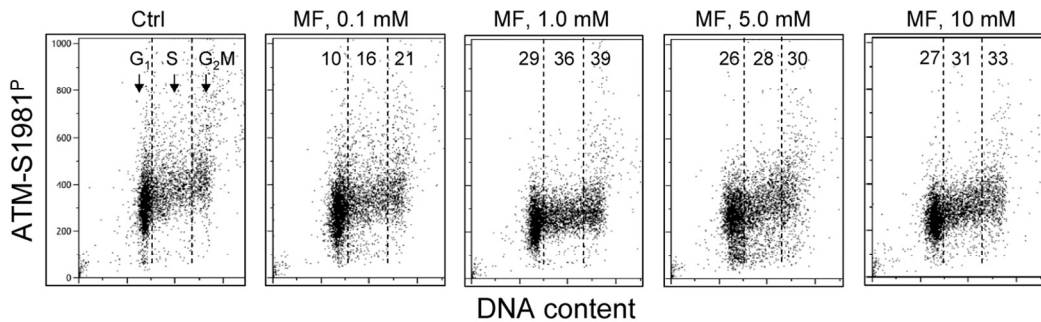


Figure 4. Effect of metformin on the level of constitutive expression of ATM-S1981^P. Exponentially growing TK6 cells were untreated (Ctrl) or were grown in the presence of 0.1, 1.0, 5.0 and 10 mM metformin (MF) for 48 h. The expression of ATM-S1981^P was detected with phospho-specific Ab. As in Fig. 3, the cells were gated in G₁, S and G₂M phases of the cell cycle and the mean values of ATM-S1981^P for cells in each of these cell cycle phases were estimated. The figures show the percent reduction in mean values of ATM-S1981^P IF of the metformin-treated cells with respect to the mean values of the untreated cells (Ctrl) in the respective phases of the cell cycle.

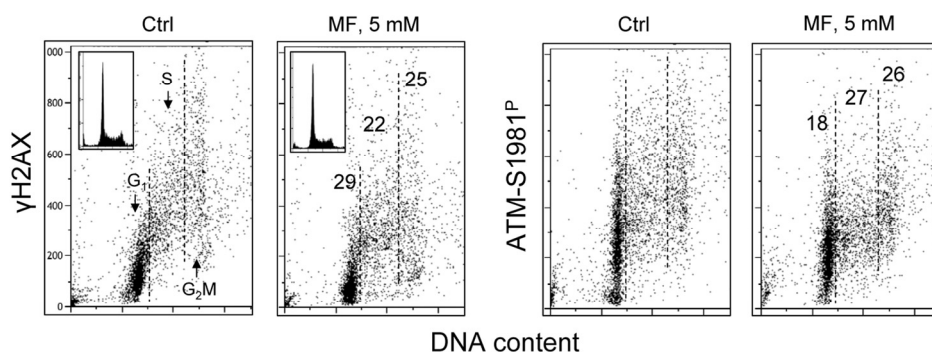


Figure 5. Effect of metformin on constitutive expression γ H2AX and ATM-S1981^P in normal human proliferating lymphocytes. Peripheral blood lymphocytes were mitogenically stimulated by phytohemagglutinin for 48 h and then were grown in the absence (Ctrl) or presence of 5 mM metformin (MF) for additional 24 h. The expression of γ H2AX and ATM-S1981^P was detected with phospho-specific Abs and cell fluorescence we as measured by flow cytometry. The numerical figures show the percent reduction in expression of γ H2AX and ATM-S1981^P of cells treated with metformin with respect to Ctrl, in the respective phases of the cell cycle.

Figure 5 illustrates the effect of metformin on proliferating human lymphocytes. The peripheral blood lymphocytes were stimulated to proliferate by the polyvalent mitogen phytohemagglutinin for 48 h and subsequently were grown in the absence or presence of 5 mM metformin for 24 h. The data show that, as was the case with the tumor cell lines A549 and TK6, growth of lymphocytes in the presence of 5mM metformin distinctly reduced both the level of constitutive expression of γ H2AX as well as of ATM-S1981^P.

As mentioned in the Introduction, the decline in the level of constitutive expression of γ H2AX and phosphorylation of ATM was observed in cells treated with agents that decrease the level of endogenous oxidants such as ROS scavengers or antioxidants [39-45,58]. Therefore, we assessed the effect of metformin on the abundance of reactive oxidants in human leukemic TK6 cells in the same cultures in which we observed the decline in expression of γ H2AX (Figure 3) and ATM-S1981^P (Figure 4). As is quite evident from the data shown in Figure 6, the growth of TK6 cells for 48 h in the presence of metformin led to a decrease in the level of ROS that were detected by their ability to oxidize 2',7'-dihydro-dichlorofluorescein diacetate (H2DCF-DA); following oxidation by ROS the non-fluorescent substrate H2DCF-DA is converted to the highly fluorescent product DCF [59]. The effect was concentration dependent and the oxidation of H2DCF-DA was reduced by nearly two orders of magnitude at a 10 mM concentration of metformin compared to untreated cells (Figure 6).

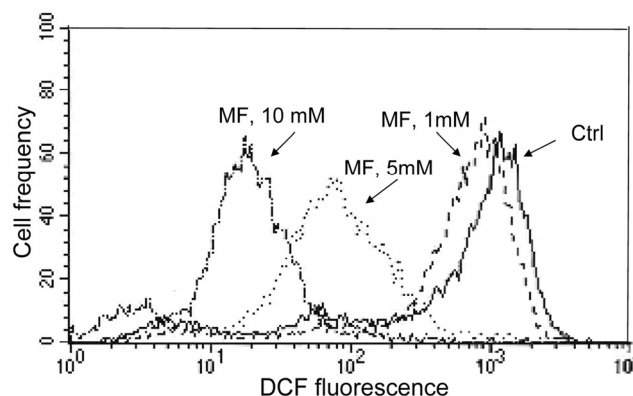


Figure 6. Effect of metformin on ability of TK6 cells to oxidize 2',7'-dihydro-dichlorofluorescein diacetate (H2DCF-DA). TK6 cells were untreated (Ctrl) or treated with 1, 5 or 10 mM metformin (MF) for 48 h. The cells were then incubated for 30 min with 10 μ M H2DCF-DA and their fluorescence was measured by flow cytometry. While H2DCF-DA is not fluorescent, the product of its oxidation (DCF) by intracellular ROS shows strong green fluorescence. Note dramatic decline in fluorescence intensity of cells treated with 5 or 10 mM metformin.

DISCUSSION

The present data demonstrate that exposure of either normal, mitogenically activated lymphocytes, or tumor cell lines (A549, TK6) to metformin leads to a decrease in the level of constitutive phosphorylation of H2AX on Ser139 and constitutive activation of ATM. The

observed decrease was evident even at a concentration as low as 0.1 mM metformin (Figures 3 and 4). Pharmacokinetic data indicate that this concentration of metformin is of pharmacological relevance [60]. Since the level of constitutive expression of γ H2AX and ATM-S1981^P to a large extent reports DNA damage signaling in response to DNA damage by endogenous oxidants generated during aerobic respiration [39-45,58], the present findings would be consistent with a notion that metformin exerts protective effect on nuclear DNA against oxidative damage. These findings are consistent with the observation that exposure of cells to metformin lowered the extent of reactive oxidants that were able to oxidize the H2DCF-DA substrate (Figure 5). They are also in accordance with numerous studies in which a decrease in the level of ROS in cells treated with metformin has been observed [55,61-65]. It appears that the mechanisms activated by metformin for neutralizing ROS such as upregulation of the antioxidant thioredoxin [55], and/or suppression of NAD(P)H oxidase activity [61] may prevail over the ROS-generating inhibitory effect on mitochondrial respiratory complex I or catabolic processes activated by AMPK [66,67].

It should be noted that DNA damage signaling such as reported by H2AX phosphorylation and ATM activation do not necessarily indicate the actual DNA damage that involves formation of DNA strand breaks [68]. While some breaks may be formed during replication of DNA sections containing the primary oxidative lesions (e.g. oxo8dG) the presence of such lesions by themselves can induce persistent replication stress. The persistent replication stress combined with activation of mTOR pathways is considered to be the main mechanism contributing to aging and senescence [22-27,69,70]. Induction of replication stress by arrest in the cell cycle e.g. by upregulation of the CKI p21, with no evidence of actual DNA damage, elevates the level of constitutive DNA damage signaling (“pseudo-DNA damage response”) whereas attenuation of this “pseudo-DNA damage response” can be achieved by reduction in mTOR-signaling [29]. Likewise, the cell senescence induced by the replication stress triggered by low doses (1 – 2 nM) of the DNA damaging agent mitoxantrone, that is also accompanied by elevated levels of DNA damage signaling, was shown to be attenuated by the caloric restriction-mimicking drug 2-deoxy-D-glucose [71]. All this evidence collectively indicates that the observed constitutive DNA damage signaling occurs as a response to persistent DNA replication stress. Thus, by reducing the level of DNA damage signaling, as we presently see, metformin appears to alleviate the extent of the persistent DNA replication stress. Since metformin inhibits mTOR pathways, the reduction of

replication stress by metformin may not only be mediated by attenuation of the oxidative stress through reduction of ROS, but also may be mediated by its direct inhibitory effect on mTOR [50-53].

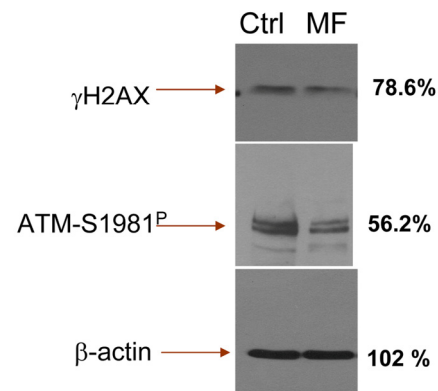


Figure 7. Detection of γ H2AX and ATM-S1981^P in TK6 cells untreated (Ctrl) and treated with 5 mM metformin (MF) for 48 h, by immunoblotting. The figures on right side of the blot represent the percent intensity of the scanned protein bands of the metformin-treated cells (UN-SCAN-IT gel 6.1) as that of the intensity of the respective protein bands of the untreated (Ctrl) cells.

Our observation that cells exposure to metformin reduces expression of γ H2AX and ATM-S1981^P remains in contrast to recent data by Vazquez-Martin et al., that show the opposite, namely an activation of ATM and phosphorylation of H2AX in cells treated with metformin [72]. This report prompted us to repeat our experiments numerous times, using a variety of positive and negative controls. Yet in each experiment we observed that treatment of proliferating lymphocytes, TK6 or A549 cells led to a *decline* in expression of γ H2AX and ATM-S1981^P. We have also tested the A431 epidermoid carcinoma cells used by these authors [72]. The data show that treatment of A431 with metformin *decreased* the level of H2AX and ATM phosphorylation (Supplemental data, Figure 1). To exclude the possibility of bias resulting from different methodologies we also assessed the effect of metformin on expression of γ H2AX and ATM-S1981^P in TK6 cells using immunoblotting, the methodology used by the authors [72]. The results obtained by immunoblotting (Figure 7) confirm all our immunocytochemical data (Figs. 1-5) by showing a distinct reduction of γ H2AX and ATM-S1981^P in cells treated with metformin. In fact, the reduction in expression of ATM-S1981^P was nearly 45% related to the control. We have also observed that constitutive

H2AX phosphorylation and ATM activation in quiescent A549 cells, maintained for 5 days at high cells density ($>10^6$ cells/ml) with no medium change also was reduced by treatment with metformin (Supplemental data Figure 2). The effect of metformin, thus, was unrelated as to whether the cells were in exponential- or stationary- phase of growth. Our data also concur with the findings of Nilsson et al., who did not detect any induction of γ H2AX in U2OS or HT1080 cells treated with 40 mM metformin [73]. Actually, careful inspection of their data provides some evidence of a decline in expression of γ H2AX upon treatment with metformin [73]. At present we see no explanation for the apparent discrepancy of our results (and the data of Nilsson et al., [73]) versus the data presented by Vazquez-Martin et al., [72].

As mentioned, cell aging and senescence appear to be driven by persistent mTOR activation in conjunction with DNA replication stress; the latter can be induced by ROS as well as by inhibition of cell cycle progression, such as activation of CKIs. DNA replication stress and mTOR activation are being reported by the elevated level of constitutive DNA damage signaling (“pseudo-DNA damage response”) [29,71]. As shown in the present study, the effectiveness of potential anti-aging factors such as metformin may be tested by monitoring their effect on constitutive DNA damage signaling. This approach offers novel means to assess the anti-aging or aging-promoting properties of different factors suspected of such activities. Assessment of DNA damage signaling may serve to detect both genotoxicity [38,74] as well as genome-protective mechanisms related to attenuation of DNA replication stress.

MATERIALS AND METHODS

Cells, cell treatment. Human lung carcinoma A549 cells, epidermoid carcinoma A431 and lymphoblastoid TK6 cells were obtained from American Type Culture Collection (ATCC CCL-185, Manassas, VA). Human peripheral blood lymphocytes were obtained by venipuncture from healthy volunteers and isolated by density gradient centrifugation. A549 cells were cultured in Ham’s F12K, TK6 and lymphocytes were cultured in RPMI 1640 and A431 cells in Dulbecco modified Eagle medium, with 2 mM L-glutamine adjusted to contain 1.5 g/L sodium bicarbonate supplemented with 10% fetal bovine serum (GIBCO/Invitrogen, Carlsbad, CA). Adherent A549 and A431 cells were grown in dual-chambered slides (Nunc Lab-Tek II), seeded with 10^5 cells/ml suspended in 2 ml medium per chamber. TK6 cells and lymphocytes were grown in suspension; lymphocyte cultures were treated

with the polyvalent mitogen phytohemagglutinin (Sigma/Aldrich; St Louis, MO) as described [75]. During treatment with metformin (1,1-dimethylbiguanide; Calbiochem, La Jolla, CA) the cells were in exponential phase of growth unless indicated otherwise. After exposure to metformin at various concentrations and for specified periods of time (as shown in figure legends) the cells were rinsed with phosphate buffered salt solution (PBS) and fixed in 1% methanol-free formaldehyde (Polysciences, Warrington, PA) for 15 min on ice. The cells were then transferred to 70% ethanol and stored at -20 °C for up to 3 days until staining.

Detection of H2AX phosphorylation and ATM activation. The cells were washed twice in PBS and with 0.1% Triton X-100 (Sigma) in PBS for 15 min and with a 1% (w/v) solution of bovine serum albumin (BSA; Sigma) in PBS for 30 min to suppress nonspecific antibody (Ab) binding. The cells were then incubated in 1% BSA containing a 1:300 dilution of phospho-specific (Ser139) γ H2AX mAb (Biolegend, San Diego, CA or with a 1:100 dilution of phospho-specific (Ser1981) ATM mAb (Millipore, Tamecula, CA). The secondary Ab was tagged with AlexaFluor 488 fluorochrome (Invitrogen/Molecular Probes, used at 1:200 dilution). Cellular DNA was counterstained with 2.8 μ g/ml 4,6-diamidino-2-phenylindole (DAPI; Sigma). Each experiment was performed with an IgG control in which cells were labeled only with the secondary AlexaFluor 488 Ab, without primary Ab incubation to estimate the extent of nonspecific adherence of the secondary Ab to the cells. The fixation, rinsing and labeling of A549 or A431 cell was carried out on slides, and lymphocytes and TK6 cells in suspension. Other details have been previously described [38-40].

Analysis of cellular fluorescence. *A549 and A431 cells:* Cellular immunofluorescence representing the binding of the respective phospho-specific Abs as well as the blue emission of DAPI stained DNA was measured with an LSC (iCys; CompuCyte, Westwood, MA) utilizing standard filter settings; fluorescence was excited with 488-nm argon, helium-neon (633 nm) and violet (405 nm) lasers [76]. The intensities of maximal pixel and integrated fluorescence were measured and recorded for each cell. At least 3,000 cells were measured per sample. Gating analysis was carried out as described in Figure legends. *TK6 cells and lymphocytes:* Cellular fluorescence was measured by using a MoFlo XDP (Beckman-Coulter, Brea, CA) high speed flow cytometer/sorter. DAPI fluorescence was excited with the UV laser (355-nm) and AlexaFluor 488 with the argon ion (488-nm) laser.

Protein immunoblotting. Nitrocellulose membrane was blocked with 5% w/v nonfat dry milk in TBST (20 mM TrisHCl, pH 7.4, 150 mM NaCl, 0.05% Tween 20) for 1h at room temperature. The blot was then incubated with the primary antibody either phospho-specific (Ser139) γ H2AX mAb (Biolegend) or a phospho-specific (Ser1981) ATM mAb (Millipore) at 1:500 dilution overnight at 4 °C. After three washes in TBST, the blot was incubated with HRP-conjugated goat anti-mouse IgG (Pierce, Rockford, IL) for 1h at room temperature and washed with TBST three times. SuperSignal West Pico chemiluminescence substrate (Pierce) was used for signal production.

CONFLICT OF INTERESTS STATEMENT

The authors of this manuscript have no conflict of interest to declare.

REFERENCES

1. Barzilai A and Yamamoto K: DNA damage responses to oxidative stress. *DNA repair (Amst)* 2004;3:1109-1115.
2. Nohl H. Generation of superoxide radicals as byproducts of cellular respiration. *Ann Biol Clin* 1994;52:199-204.
3. Moller P and Loft S. Interventions with antioxidants and nutrients in relation to oxidative DNA damage and repair. *Mutat Res* 2004;551:79-89.
4. Beckman KB and Ames BN. Oxidative decay of DNA. *J Biol Chem* 1997;272: 13300-13305.
5. Dianov GL, Parsons JL. Co-ordination of DNA single strand break repair. *DNA repair (Amst)* 2007;6:454-460.
6. Vilenchik MM and Knudson AG. Endogenous DNA double-strand breaks: Production, fidelity of repair, and induction of cancer. *Proc Natl Acad Sci USA* 2003;100:12871-12876.
7. Taioli E, Sram RJ, Garte BM, Kalina I, Popov TA and Farmer PB. Effects of polycyclic aromatic hydrocarbons (PAHs) in environmental pollution on exogenous and oxidative DNA damage (EXPAH project): description of the population under study. *Mutat Res* 2007;620:1-6.
8. Tanaka T, Halicka HD, Traganos F and Darzynkiewicz Z. Phosphorylation of histone H2AX on Ser 139 and activation of ATM during oxidative burst in phorbol ester-treated human leukocytes. *Cell Cycle* 2006;5:2671-2675.
9. Shacter E, Beecham EJ, Covey JM, Kohn KW and Potter M. Activated neutrophils induce prolonged DNA damage in neighboring cells. *Carcinogenesis* 1988;9:2297-2304.
10. Chong YC, Heppner GH, Paul LA and Fulton AM. Macrophage-mediated induction of DNA strand breaks in target tumor cells. *Cancer Res* 1989;49:6652-6657.
11. Demirbag R, Yilmaz R, Kocyigit A and Guzel S. Effect of coronary angiography on oxidative DNA damage observed in circulating lymphocytes. *Angiology* 2007;58:141-147.
12. Altman SA, Zastawny TH, Randers-Eichorn L, Caciuttolo MA, Akman SA, Disdaroglu M and Rao G. Formation of DNA-protein cross-links in cultured mammalian cells upon treatment with iron ions. *Free Radic Biol Med* 1995;19:897-902.
13. Cadet J, Delatour T, Douki T, Gasparutto D, Pouget JP, Ravanat JL and Sauvaigo S. Hydroxyl radicals and DNA base damage. *Mutat Res* 1999;424:9-21.
14. Marnett LJ. Oxy radicals, lipid peroxidation and DNA damage. *Toxicology* 2002; 219:181-182.
15. Pastwa E and Blasiak J. Non-homologous DNA end joining. *Acta Biochim Pol* 2003;50:891-908.
16. Jeggo PA and Lobrich M. Artemis links ATM to double strand end rejoining. *Cell Cycle* 2005;4:359-362.
17. Kryston TB, Georgiev AB, Pissis P, Georgakilas AG. Role of oxidative stress and DNA damage in human carcinogenesis. *Mutat Res* 2011; Jan7 (Epub)
18. Gorbunova V, Seluanov A. Making ends meet in old age: DSB repair and aging. *Mech Ageing Dev* 2005;126:621-628.
19. Espejel S, Franco S, Rodriguez-Perales S, Bouffler SD, Cigudosa JC, Blasco MA. Mammalian Ku86 mediates chromosomal fusions and apoptosis caused by critically short telomeres. *EMBO J* 2002;21:2207-2219.
20. Karanjawala ZE, Lieber MR. DNA damage and aging. *Mech Ageing Dev* 2004; 125:405-416.
21. Blagosklonny MV. Aging: ROS or TOR. *Cell Cycle* 2008;7:3344-3354.
22. Blagosklonny MV, Campisi J. Cancer and aging: more puzzles, more promises? *Cell Cycle* 2008;7:2615-2618.
23. Demidenko ZN, Zubova SG, Bukreeva EI, Pospelov VA, Pospelova TV, Blagosklonny MV. Rapamycin decelerates cellular senescence. *Cell Cycle*. 2009; 8:1888-1895.
24. Blagosklonny MV. Increasing healthy lifespan by suppressing aging in our lifetime: Preliminary proposal. *Cell Cycle* 2010;9:4788-4794.
25. Blagosklonny MV. Revisiting the antagonistic pleiotropy theory of aging: TOR-driven program and quasi-program. *Cell Cycle*. 2010;9:3151-6.
26. Blagosklonny MV. Why human lifespan is rapidly increasing: solving "longevity riddle" with "revealed-slow-aging" hypothesis. *Aging*. 2010;2:177-182.
27. Blagosklonny MV. Validation of anti-aging drugs by treating age-related diseases. *Aging* 2009;1:281-288.
28. Pospelova TV, Demidenko ZN, Bukreeva EI, Gudkov VA, Blagosklonny MV. Cell Pseudo-DNA damage response in senescent cells. *Cycle* 2009;8:4112-4118.
29. Olive PL, Durand RE, Banath JP, Johnston PJ. Analysis of DNA damage in individual cells. *Methods Cell Biol* 2001;64:235-249.
30. Gorczyca W, Gong J, Darzynkiewicz Z. Detection of DNA strand breaks in individual apoptotic cells by the *in situ* terminal deoxynucleotidyl transferase and nick translation assays. *Cancer Res* 1993;53:1945-1951.
31. Huang X, Halicka HD, Traganos F, Tanaka T, Kurose A, Darzynkiewicz Z. Cytometric assessment of DNA damage in relation to cell cycle phase and apoptosis. *Cell Prolif* 2005;38:223-243.
32. Kitagawa R, Kastan MB. The ATM-dependent DNA damage signaling pathway. *Cold Spring Harb Symp Quant Biol* 2005;70:99-109.
33. Rogakou EP, Pilch DR, Orr AH, Ivanova VS, Bonner WM. DNA double-stranded breaks induce histone H2AX phosphorylation on serine 139. *J Biol Chem* 1998;273:5858-5868.
34. Bartkova J, Bakkenist CJ, Rajpert-De Meyts E, Skakkebaek NE, Sehested M, Lukas J, Kastan MB, Bartek J. ATM activation in

- normal human tissues and testicular cancer. *Cell Cycle* 2005;4:838-845.
35. Sedelnikova OA, Rogakou EP, Panuytin IG, Bonner W. Quantitative detection of ¹²⁵IUdr-induced DNA double-strand breaks with γ -H2AX antibody. *Radiation Res* 2002;158:486-492.
 36. Huang X, Traganos F, Darzynkiewicz Z. DNA damage induced by DNA topoisomerase I- and topoisomerase II- inhibitors detected by histone H2AX phosphorylation in relation to the cell cycle phase and apoptosis. *Cell Cycle* 2003; 2:614-619.
 37. Banath JP, Olive PL. Expression of phosphorylated histone H2AX as a surrogate of cell killing by drugs that create DNA double-strand breaks. *Cancer Res* 2003; 63:4347-4350.
 38. Tanaka T, Huang X, Halicka HD, Zhao H, Traganos F, Albino AP, Dai W, Darzynkiewicz Z. Cytometry of ATM activation and histone H2AX phosphorylation to estimate extent of DNA damage induced by exogenous agents. *Cytometry A* 2007; 71A:648-661.
 39. Tanaka T, Halicka HD, Huang X, Traganos F, Darzynkiewicz Z. Constitutive histone H2AX phosphorylation and ATM activation, the reporters of DNA damage by endogenous oxidants. *Cell Cycle* 2006;5:1940-1945.
 40. Zhao H, Tanaka T, Halicka HD, Traganos F, Zarebski M, Dobrucki J, Darzynkiewicz Z. Cytometric assessment of DNA damage by exogenous and endogenous oxidants reports the aging-related processes. *Cytometry A* 2007;71A:905-914.
 41. Tanaka T, Kajstura M, Halicka HD, Traganos F, Darzynkiewicz Z. Constitutive histone H2AX phosphorylation and ATM activation are strongly amplified during mitogenic stimulation of lymphocytes. *Cell Prolif* 2007;40:1-13.
 42. Tanaka T, Kurose A, Halicka HD, Traganos F, Darzynkiewicz Z. 2-Deoxy-D-glucose reduces the level of constitutive activation of ATM and phosphorylation of histone H2AX. *Cell Cycle* 2006; 5:878-882.
 43. Zhao H, Tanaka T, Mitlitski V, Heeter J, Balazs EA, Darzynkiewicz Z. Protective effect of hyaluronate on oxidative DNA damage in WI-38 and A549 cells. *Int J Oncol* 2008;32:1159-1169.
 44. Halicka HD, Darzynkiewicz Z, Teodori L. Attenuation of constitutive ATM activation and H2AX phosphorylation in human leukemic TK6 cells by their exposure to static magnetic field. *Cell Cycle*, 2009;8:3236-3238.
 45. Halicka HD, Ita M, Tanaka T, Kurose A, Darzynkiewicz Z. The biscoclaurine alkaloid cepharanthine protects DNA in TK6 lymphoblastoid cells from constitutive oxidative damage. *Pharmacol Rep* 2008;60:93-100.
 46. Towler MC, Hardie DG. AMP-activated protein kinase in metabolic control and insulin signaling. *Circ Res* 2007;100:328-341.
 47. Hardie DG. AMP-activated protein kinase: a cellular energy sensor with a key role in metabolic disorders and in cancer. *Biochem Soc Trans* 2011; 39:1-13.
 48. Viollet B, Andreelli F. AMP-activated protein kinase and metabolic control. *Handb Exp Pharmacol*. 2011; 203:303-330.
 49. Carling D, Mayer FV, Sanders MJ, Gamblin SJ. AMP-activated protein kinase: nature's energy sensor. *Nat Chem Biol* 2011; 7:512-518.
 50. Anisimov VN. Metformin for aging and cancer prevention. *Aging* 2010;2:760-74.
 51. Xie Y, Wang Y, Yu L, Hu Q, Ji L, Zhang Y, Liao Q. Metformin promotes progesterone receptor expression via inhibition of mammalian target or rapamycin (mTOR) in endometrial cancer cells. *J Ster Biochem Mol Biol* 2010; Dec 17 Epub.
 52. Shaw RJ, Lamia KA, Vasquez D, Koo SH, Bardeesy N, Depinho RA, Montminy M, Cantley LC. The kinase LKB1 mediates glucose homeostasis in liver and therapeutic effects of metformin. *Science* 2005;310:1642-1646.
 53. Jalving M, Gietema JA, Lefrandt JD, De Jong S, Reyners AKL, Gans ROB, de Vries EGE. Metformin: taking away the candy for cancer? *Eur J Cancer* 2010; 46:2369-2380.
 54. Ouyang J, Parakhia RA, Ochs RS. Metformin activates AMP kinase through inhibition of AMP deaminase. *J Biol Chem* 2011;286:1-11.
 55. Hou X, Song J, Li X-N, Zhang L, Wang XL, Chen L, Shen YH. Metformin reduces intracellular reactive oxygen species levels by upregulating expression of the antioxidant thioredoxin via the AMPK-FOXO3 pathway. *Biochem Biophys Res Commun* 2010;396:199-205.
 56. Anisimov VN, Egormin PA, Piskunova TS, Popovich IG, Tyndyk ML, Yurova MN, Zabezhinski MA, Anikin IV, Karkach AS, Romanyukha AA. Metformin extends life span of HER-2/neu transgenic mice and in combination with melatonin inhibits growth of transplantable tumors. *Cell Cycle* 2010;9:188-197.
 57. Darzynkiewicz Z, Traganos F, Zhao H, Halicka HD, Skommer J, Wlodkovic D. Analysis of individual molecular events of DNA damage response by flow and image-assisted cytometry. *Methods Cell Biol* 2011;103:115-148.
 58. Huang X, Tanaka T, Kurose A, Traganos F, Darzynkiewicz Z. Constitutive histone H2AX phosphorylation on Ser-139 in cells untreated by genotoxic agents is cell-cycle phase specific and attenuated by scavenging reactive oxygen species. *Int J Oncol* 2006;29:495-501.
 59. Rothe G, Klouche M. Phagocyte functions. *Methods Cell Biol* 2004;75:679-708.
 60. Graham GG, Punt J, Arora M, Day RO, Doogue MP, Duong JK, Furlong JR, Greenfield JR, Greenup LC, Kirkpatrick CM, Ray JE, Timmins P, Williams KM. Clinical pharmacokinetics of metformin. *Clin Pharmacokinet* 2011;50:81-98.
 61. Piwkowska A, Rogacka D, Jankowski M, Dominiczak MH, Stepinski JK, Angielski S. Metformin induces suppression of NAD(P)H oxidase activity in podocytes. *Biochem Biophys Res Commun* 2010; 393:268-273.
 62. Ouslimani, N.; Peynet, J.; Bonnefont-Rousselot, D.; Therond, P.; Legrand, A.; Beaudoux, J. L. Metformin decreases intracellular production of reactive oxygen species in aortic endothelial cells. *Metabolism* 2005;54:829-834.
 63. Kane DA, Andersen EJ, Price III JW, Woodlief TL, Lin C-T, Bikman BT, Cortright RN, Neuffer PD. Metformin selectively attenuates mitochondrial H₂O₂ emission without affecting respiratory capacity in skeletal muscle of obese rats. *Free Radical Biol Med* 2010;49:1082-1087.
 64. Piro S, Rabuazzo AM, Renis M, Purello F. Effects of metformin on oxidative stress, adenine nucleotides balance and glucose-induced insulin release impaired by chronic FFA exposure in rat pancreatic islets. *J Endocrinol Invest* 2011 Jul 12 (Epub).
 65. Bellin, C, de Wiza DH, Wiernsperger NF, Rosen P. Generation of reactive oxygen species by endothelial and smooth muscle cells: Influence of hyperglycemia and metformin. *Horm Metab Res* 2006;38:732-739.

66. Brunmair B, Staniek K, Gras F, Scharf N, Althaym A, Clara R, Roden M, Gnaiger E, Hohl H, Waldhansl W, Furnassin C. Thiazolidinediones, like metformin, inhibit respiratory complex I. A common mechanism contributing to their antidiabetic action. *Diabetes* 2004;53:1052-1059.

67. Drose S, Hanley PJ, Brandt U. Ambivalent effects of diazoxide on mitochondrial ROS production at respiratory chain complexes I and II. *Biochim Biophys Acta* 2009;1790:558-565.

68. Cleaver JA, Feeney L, Revet I. Phosphorylated H2Ax is not an unambiguous marker of DNA double strand breaks. *Cell Cycle* 2011;10:3223-3224.

69. Burhans WC, Weinberger M. DNA replication stress, genome instability and aging. *Nucleic Acids Res* 2007;33:7545-7556.

70. Bartkova J, Hamerlik P, Stockhausen MT, Ehrman J, Hlobikova A, Laursen H, Kalita O, Kolar Z, Paulsen HS, Broholm H, Lukas J, Bartek J. Replication stress and oxidative damage contributes to aberrant constitutive activation of DNA damage signaling in human gliomas. *Oncogene* 2010;29:5095-5102.

71. Zhao H, Halicka HD, Jorgensen E, Traganos F, Darzynkiewicz Z. New biomarkers probing the depth of cell senescence assessed by laser scanning cytometry. *Cytometry A*, 2010, 77A, 999-1007.

72. Vazquez-Martin A, Oliveras-Ferraros C, Cufi S, Martin-Castillo B, Menendez Ja. Metformin activates an Ataxia Telangiectasia Mutated (ATM)/Chk2-regulated DNA damage-like response. *Cell Cycle* 2011;10:1499-1501.

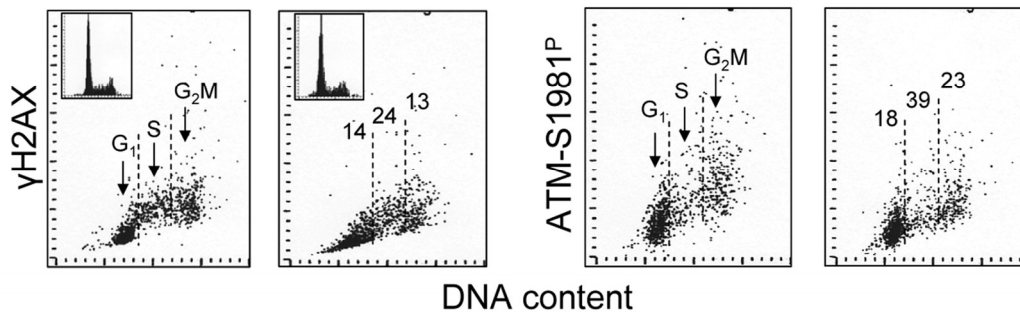
73. Nilsson S, Huelsenbeck J, Fritz G. Mevalonate pathway inhibitors affect anticancer drug-induced cell death and DNA damage response of human sarcoma cells. *Cancer Lett* 2011;304:60-69.

74. Smart DJ, Ahmedi KP, Harvey JS, Lynch AM. Genotoxicity screening via the γ H2AX by flow assay. *Mutat Res* 2011;71:21-31.

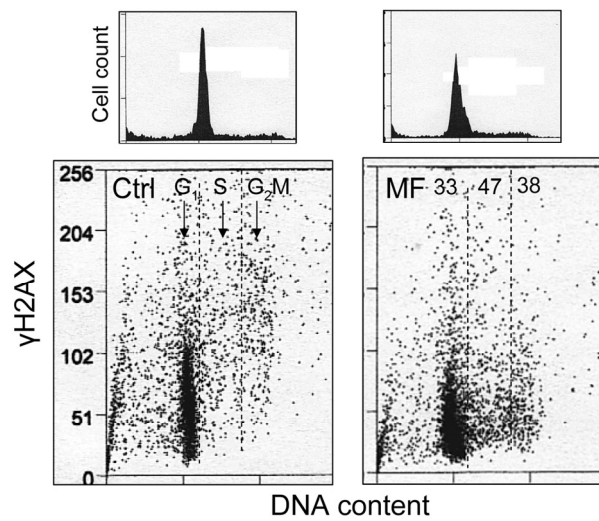
75. Kajstura M, Halicka HD, Pryjma J, Darzynkiewicz Z. Discontinuous fragmentation of nuclear DNA during apoptosis revealed by discrete "sub-G₁" peaks on DNA content histograms. *Cytometry A* 2007; 71A:125-131.

76. Pozarowski P, Holden E, Darzynkiewicz Z. Laser scanning cytometry: Principles and applications. *Meth Molec Biol*. 2006; 319:165-192.

SUPPLEMENTARY FIGURES



Supplemental Figure 1. Effect of metformin (MF) on the level of constitutive expression of γ H2AX and ATM-S1981P in A431 cells. Exponentially growing A431 cells were left untreated (Ctrl) or treated with 5 mM metformin for 48 h. γ H2AX and ATM-S1981 immunofluorescence (IF) was detected with the phospho-specific Abs and cells fluorescence was measured by laser scanning cytometry.⁷⁵ Based on differences in DNA content the cells were gated in G₁, S and G₂M phases of the cell cycle and the mean values of γ H2AX and ATM-S1981^P IF for cells in each of these cell cycle phases by were obtained gating analysis. The percent reduction of these mean values of the metformin-treated related to the untreated (Ctrl) cells is shown in the respective panels (the means of the three separate bands per each protein). The insets show DNA content frequency histograms in the untreated and metformin-treated cultures.



Supplemental Figure 2. Effect of metformin (MF) on the level of expression of γ H2AX in TK6 cells in stationary cultures. TK6 cells were maintained at high cell density ($>10^6$ cells/ml) with no medium change for 5 days, then cells were left untreated (Ctrl) or treated with 5 mM metformin for 24 h (MF). The percent decline in mean values of γ H2AX IF of cells in G₁, S, and G₂M phases of the cycle in the metformin-treated culture is shown in the MF panel.

Roles of the Raf/MEK/ERK and PI3K/PTEN/Akt/mTOR pathways in controlling growth and sensitivity to therapy-implications for cancer and aging

Linda S. Steelman^{1,2}, William H. Chappell¹, Stephen L. Abrams¹, C. Ruth Kempf², Jacquelyn Long², Piotr Laidler³, Sanja Mijatovic⁴, Danijela Maksimovic-Ivanic⁴, Franca Stivala⁵, Maria C. Mazarino⁵, Marco Donia⁵, Paolo Fagone⁵, Graziella Malaponte⁵, Ferdinando Nicoletti⁵, Massimo Libra⁵, Michele Milella⁶, Agostino Tafuri⁷, Antonio Bonati⁸, Jörg Bäsecke⁹, Lucio Cocco¹⁰, Camilla Evangelisti¹⁰, Alberto M. Martelli^{10,11}, Giuseppe Montalto¹², Melchiorre Cervello¹³ and James A. McCubrey¹

¹Department of Microbiology and Immunology, ²Department of Physics, East Carolina University, Greenville, NC 27858, USA

³Department of Medical Biochemistry, Jagiellonian University Medical College, Krakow, Poland

⁴Department of Immunology, Institute for Biological Research "Sinisa Stankovic", University of Belgrade, Belgrade, Serbia

⁵Department of Biomedical Sciences, University of Catania, Catania, Italy

⁶Regina Elena Cancer Center, Rome 00144, Italy

⁷University of Rome, La Sapienza, Department of Hematology-Oncology, Rome 99161, Italy

⁸University Hospital of Parma, Unit of Hematology and Bone-Marrow Transplantation, Via Gramsci n.14, Parma 43100, Italy

⁹Department of Medicine, University of Göttingen, Göttingen, Germany

¹⁰Dipartimento di Scienze Anatomiche Umane e Fisiopatologia dell'Apparato Locomotore, Università di Bologna, Bologna, Italy

¹¹IGM-CNR, Sezione di Bologna, C/o IOR, Bologna, Italy

¹²Department of Internal Medicine and Specialties, University of Palermo, Palermo, Italy

¹³Consiglio Nazionale delle Ricerche, Istituto di Biomedicina e Immunologia, Molecolare "Alberto Monroy", Palermo, Italy

Key words: Raf, MEK, PI3K, mTOR, cancer, kinases, protein phosphorylation, signal transduction, apoptosis

Received: 2/25/11; **Accepted:** 3/10/11; **Published:** 3/10/11

Corresponding author: James A. McCubrey, PhD; **Email:** mccubreyj@ecu.edu

© Steelman et al. This is an open-access article distributed under the terms of the Creative Commons Attribution License, which permits unrestricted use, distribution, and reproduction in any medium, provided the original author and source are credited.

Abstract: Dysregulated signaling through the Ras/Raf/MEK/ERK and PI3K/PTEN/Akt/mTOR pathways is often the result of genetic alterations in critical components in these pathways or upstream activators. Unrestricted cellular proliferation and decreased sensitivity to apoptotic-inducing agents are typically associated with activation of these pro-survival pathways. This review discusses the functions these pathways have in normal and neoplastic tissue growth and how they contribute to resistance to apoptotic stimuli. Crosstalk and commonly identified mutations that occur within these pathways that contribute to abnormal activation and cancer growth will also be addressed. Finally the recently described roles of these pathways in cancer stem cells, cellular senescence and aging will be evaluated. Controlling the expression of these pathways could ameliorate human health.

INTRODUCTION

The Ras/Raf/MEK/ERK and Ras/PI3K/PTEN/Akt/mTOR signaling pathways have been shown over the past 25 years to play key roles in the transmission of proliferative signals from membrane bound receptors. Mutations can occur in the genes encoding pathway constituents (e.g., *RAS*, *RAF*, *PIK3CA*, *PTEN*, *AKT*, *TSC1*, *TSC2*) or in upstream receptors which activate these pathways. These pathways relay this information through interactions with various other proteins to the nucleus to control gene expression [1-13]. This review will discuss how these pathways may be aberrantly regulated by either upstream mutations/amplification or by intrinsic mutations of key components of these signaling pathways. Elevated levels of activated components of these pathways are often associated with poor prognosis in cancer patients or premature aging [2-5, 7]. Increased expression of signaling pathways can also be correlated with altered sensitivity to targeted therapy compared to patients that do not exhibit elevated expression [2-4]. Inhibition of Raf, MEK, PI3K, Akt and mTOR may prove useful in cancer treatment as well as in preventing or suppressing cellular aging. These observations have propelled the pharmaceutical industry to develop inhibitors that target key components of these pathways.

The Ras/Raf/MEK/ERK and Ras/PI3K/PTEN/Akt/mTOR signaling pathways consist of kinases cascades that are regulated by phosphorylation and dephosphorylation by specific kinases, phosphatases as well as GTP/GDP exchange proteins, adaptor proteins and scaffolding proteins. The regulation of these cascades can be much like the axiom of real estate, "location-location-location", as the membrane localization of these components is often critical for their activity, even though some members of these pathways can function in other cellular regions (e.g., mitochondrion, nucleus). Indeed, one emerging observation in both extracellular signal-regulated kinase 1 and 2 (ERK1/2) and mammalian target of rapamycin (mTOR) signaling is the realization that pathways generate specific biological responses dependent upon where in the cell the signal originates [12]. For example, phosphorylation of both epidermal growth factor receptor (EGFR) and cytosolic phospholipase A(2) [cPLA(2)] is most prominent when ERK1/2 is activated from lipid rafts, whereas p90 Ribosomal S6 kinase-1 (p90^{Rsk-1}) is mainly activated by Ras signals emanating from disordered membranes. This substrate selectivity is governed by the participation of different scaffold proteins that distinctively couple ERK1/2, activated at defined subcellular domains, to specific substrates. Ras subcellular localization can determine

substrate specificity through distinct utilization of scaffold proteins [1,6,12]. Clearly the subcellular localization of pathway components and the presence of various adaptor and scaffolding molecules are critical for the activity of these pathways. The regulation and function of these two pathways will be concisely reviewed as well as the effects of genetic mutations that are important in human cancer.

The Ras/Raf/MEK/ERK Pathway

An introductory overview of the Ras/Raf/MEK/ERK pathway is presented in Figure 1. Also outlined in this figure are common sites of intervention with signal transduction inhibitors. Many of these inhibitors have been evaluated in various clinical trials and some are currently being used to treat patients with specific cancers. Extensive reviews of many inhibitors targeting these pathways have been recently published [2-4]. This figure serves as a starting reference point for understanding the flow of information through the Ras/Raf/MEK/ERK pathway from a growth factor to a specific receptor to phosphorylation of appropriate transcription factors in the nucleus, which modulate the expression of key genes [7-11]. The effects of this pathway on the translational apparatus are also diagrammed. Often mRNAs encoding growth factors are entitled "weak" mRNAs and require the effects of the Ras/Raf/MEK/ERK and Ras/PI3K/PTEN/Akt/mTOR pathways for efficient translation [2,4,11]. As an example, we present the autocrine production of a growth factor. Importantly, many components and interacting members of this pathway are also present as mutated forms in the genomes of retroviruses that induced cancer in experimental animals. Thus there have always been direct pivotal links of this pathway with malignancy.

After growth factor/cytokine/mitogen stimulation of the appropriate (cognate) receptor, a Src homology 2 domain containing protein (Shc) adaptor protein becomes associated with the C-terminus of the specific activated growth factor receptor (e.g., vascular endothelial growth factor receptor [VEGFR], epidermal growth factor receptor [EGFR], insulin like growth factor-1 receptor [IGF-1R] and many others) [2-4]. Shc recruits the Grb2 protein and the son of sevenless (SOS) homolog protein, resulting in the loading of membrane-bound Ras with GTP [7]. Ras can also be activated by growth factor receptor tyrosine kinases [GFRTK], such as insulin receptor (IR), via intermediates like insulin receptor substrate (IRS) proteins that bind growth factor receptor-bound protein 2 [7,8]. Ras:GTP then recruits Raf to the membrane where it becomes activated, likely via a Src-family tyrosine (Y) kinase [9]. At this point

we will be somewhat generic, although it should be pointed out that both Ras and Raf are members of multi-gene families and there are three Ras members (Ki-Ras, N-Ras and Ha-Ras) [7] and three Raf members (B-Raf, Raf-1 [*a.k.a* c-Raf] and A-Raf) [9]. Raf is responsible for serine/threonine (S/T) phosphorylation of mitogen-activated protein kinase kinase-1 (MEK1) [2,3,7]. MEK1 phosphorylates ERK1 and 2 at specific T and Y residues [10]. Activated ERK1 and ERK2 serine S/T kinases phosphorylate and activate a variety of substrates, including p90^{Rsk1} [2,3,7,10]. ERK1/2 has many downstream and even upstream substrates (see below). p90^{Rsk1} can activate the cAMP response element binding protein (CREB) transcription factor [13].

The number of ERK1/2 targets is easily in the hundreds (>600). Thus suppression of MEK and ERK activities will have profound effects on cell growth and aging. Activated ERK can also phosphorylate B-Raf, Raf-1 and MEK1 which alter their activity (Figure 1). Depending upon the site phosphorylated on Raf-1, ERK phosphorylation can either enhance [14] or inhibit [15] Raf-1 activity. In contrast, when B-Raf [16] or MEK1 [17] are phosphorylated by ERK, their activity decreases. These phosphorylation events serve to alter the stability and/or activities of the proteins. This is the first discussion of feed-back loops which will become important in consideration of whether to just target MEK or to target both Raf and MEK in various cancers. It is important that the reader realize that certain phosphorylation events can either inhibit or repress the activity of the affected protein. This often depends on the particular residue phosphorylated on the protein which can confer a different configuration to the protein or target the protein to a different subcellular localization that may result in proteasomal degradation. Furthermore, as previously mentioned, certain phosphorylation events will actually serve to shut off or slow down the pathway. Thus protein phosphorylation by the Ras/Raf/MEK/ERK pathway is a very intricate process which serves to fine tune the signal often originating from a growth factor or mitogens.

Activated ERK can translocate to the nucleus and phosphorylate additional transcription factors, such as Elk-1, CREB, Fos and globin transcription factor 1 (Gata-1) and others [2-4, 14,18], that bind promoters of many genes, including growth factor and cytokine genes that are important in promoting growth and preventing apoptosis of multiple cell types. Under certain circumstances, aberrant regulation of this pathway can contribute to abnormal cellular proliferation which may lead to many abnormalities including; autocrine transformation, drug resistance, senescence or premature aging [2,4,5,19].

The Ras/PI3K/PTEN/Akt/mTOR Pathway

An introductory overview of the Ras/PI3K/PTEN/Akt/mTOR pathway is presented in Figure 2. Also outlined in this diagram are common sites of intervention with signal transduction inhibitors. Many of these inhibitors have been evaluated in various clinical trials and some are currently being used to treat patients with specific cancers. Extensive reviews of many inhibitors targeting these pathways have been recently published [2,4,19,20]. Phosphatidylinositol-3-kinase (PI3K) is a heterodimeric protein with an 85-kDa regulatory subunit and a 110-kDa catalytic subunit (*PIK3CA*) [20,21]. PI3K serves to phosphorylate a series of membrane phospholipids including phosphatidylinositol 4-phosphate (PtdIns(4)P) and phosphatidylinositol 4,5-bisphosphate (PtdIns(4,5)P₂), catalyzing the transfer of ATP-derived phosphate to the D-3 position of the inositol ring of membrane phosphoinositides, thereby forming the second messenger lipids phosphatidylinositol 3,4-bisphosphate (PtdIns(3,4)P₂) and phosphatidylinositol 3,4,5-trisphosphate (PtdIns(3,4,5)P₃) [4,19,20]. Most often, PI3K is activated via the binding of a ligand to its cognate receptor, whereby p85 associates with phosphorylated tyrosine residues on the receptor via a Src-homology 2 (SH2) domain. After association with the receptor, the p110 catalytic subunit then transfers phosphate groups to the aforementioned membrane phospholipids [4,19,20]. It is these lipids, specifically PtdIns(3,4,5)P₃, that attract a series of kinases to the plasma membrane thereby initiating the signaling cascade [4,19,20].

Downstream of PI3K is the primary effector molecule of the PI3K signaling cascade, Akt/ protein kinase B (PKB). Akt was originally discovered as the cellular homologue of the transforming retrovirus AKT8 and as a kinase with properties similar to protein kinases A and C [4,19,21,22]. Akt contains an amino-terminal pleckstrin homology (PH) domain that serves to target the protein to the membrane for activation [21,22]. Within its central region, Akt has a large kinase domain and is flanked on the carboxy-terminus by hydrophobic and proline-rich regions [22]. Akt is activated via phosphorylation of two residues: T308 and S473.

The phosphatidylinositide-dependent kinases (PDKs) are responsible for activation of Akt. PDK1 is the kinase responsible for phosphorylation of T308 [23]. Akt is also phosphorylated by the mammalian target of Rapamycin (mTOR) complex referred to as (Rapamycin-insensitive companion of mTOR/mLST8 complex) mTORC2 [4,19] (See Figures 2 & 3). Before its discovery, the activity responsible for this

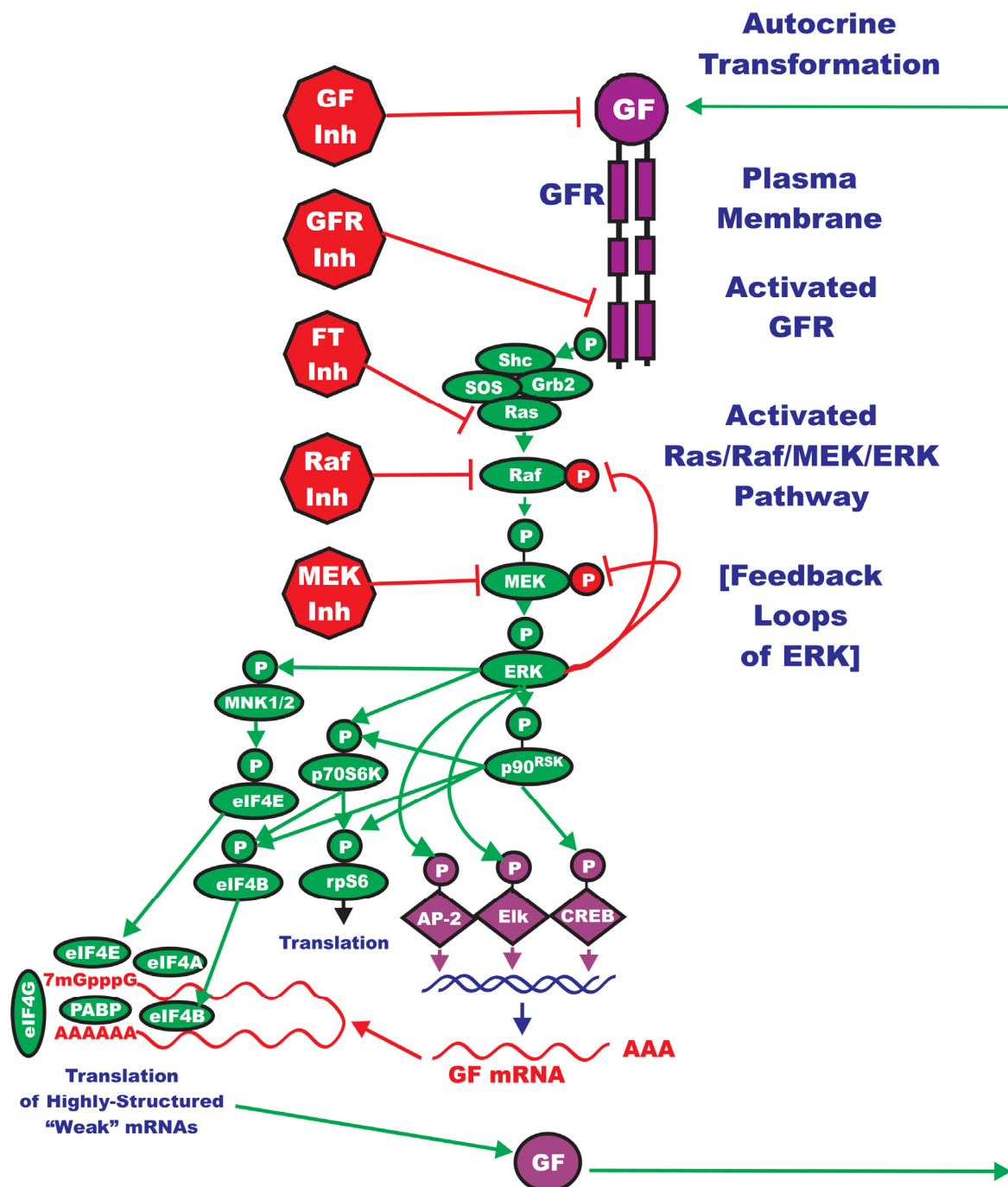


Figure 1. Overview of the Ras/Raf/MEK/ERK Pathway and Potential Sites of Therapeutic Intervention with Small Molecule Membrane-Permeable Inhibitors. The Ras/Raf/MEK/ERK pathway is regulated by Ras (indicated in green ovals), as well as various upstream growth factor receptors (indicated in purple) and non-receptor kinases. Sites where various small molecule inhibitors suppress this pathway are indicated by red octagons. The downstream transcription factors regulated by this pathway are indicated in purple diamond shaped outlines. The Ras/Raf/MEK/ERK pathway also interacts with key proteins involved in protein translation (indicated in green ovals). The Ras/Raf/MEK/ERK pathway aids in the assembly of the protein translation complex responsible for the translation of “weak” mRNAs (indicated in a red line folding over on itself) important in the prevention of apoptosis. This drawing depicts a relative common, yet frequently overlooked phenomenon in human cancer, autocrine transformation. GF = growth factor, GFR = growth factor receptor.

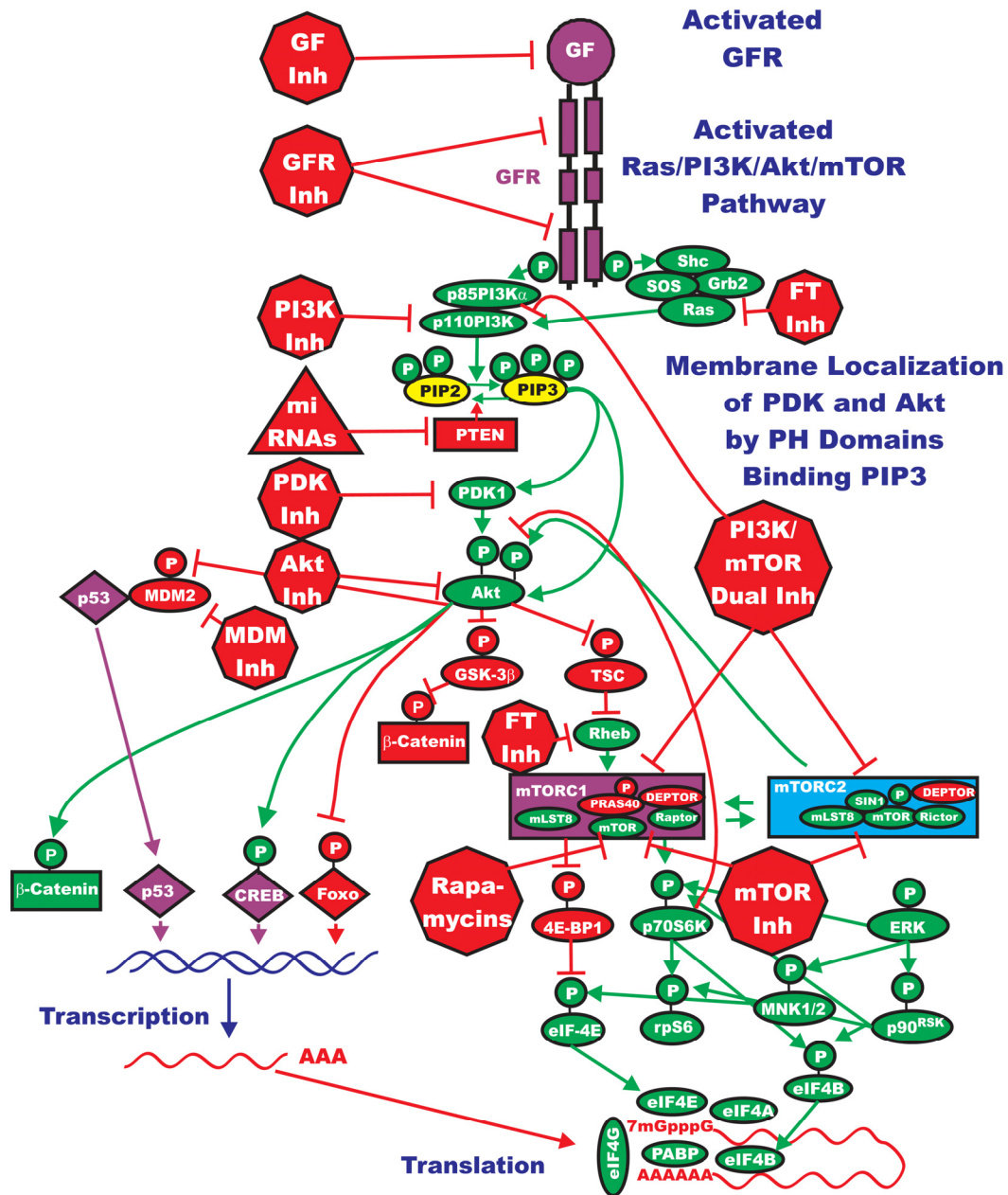


Figure 2. Overview of the Ras/PI3K/PDEN/Akt/mTOR Pathway and Potential Sites of Therapeutic Intervention. The Ras/PI3K/PDEN/mTOR pathway is regulated by Ras (indicted in green ovals), as well as various upstream growth factor receptors (indicated in purple). Sites where various small molecule inhibitors suppress this pathway are indicated by red octagons. Naturally occurring miRNAs have been discovered to certain components of this pathway (e.g., PTEN) and are indicated in a red triangle; other miRNAs to other components, especially tumor suppressor genes will likely be discovered. The downstream transcription factors regulated by this pathway are indicated in diamond shaped purple (active) or red (inactivated) outlines. This drawing depicts some of the complicated regulations of this pathway by both positive and negative phosphorylation events which serve to fine tune this pathway. Phosphorylation of some molecules by certain kinases (e.g., phosphorylation of β -catenin by glycogen synthase kinase-3 β [GSK-3 β], indicated in red oval) results in their proteosomal degradation (indicated in red box), while phosphorylation of some molecules by certain kinases (e.g., β -catenin by Akt) results in their activation (nuclear translocation, indicated in green box). The Ras/PI3K/PDEN/Akt/mTOR pathway plays a key role in regulating p53 activity (indicated in purple diamond) by phosphorylating MDM2 (indicated in red oval) which controls the stability of p53 by ubiquitination. The Ras/PI3K/PDEN/Akt/mTOR pathway plays a key role in regulating critical proteins involved in protein translation (indicated in green ovals), especially those necessary for the translation of "weak" mRNAs (mTORC1, grouped together a purple box). This pathway also indicates that Akt can result in the activation of downstream mTOR which can subsequently serve as either a negative feed back to inactivate Akt by p70S6K or activate Akt by mTORC2 (grouped together in a blue box). GF = growth factor, GFR = growth factor receptor.

phosphorylation event was referred to as PDK2. Therefore, phosphorylation of Akt is somewhat complicated as it is phosphorylated by a complex that lies downstream of activated Akt itself [4,19]. Thus, as with the Ras/Raf/MEK/ERK pathway, there are feedback loops that serve to regulate the Ras/PI3K/PTEN/Akt/mTOR pathway. Once activated, Akt leaves the cell membrane to phosphorylate intracellular substrates.

After activation, Akt is able to translocate to the nucleus [4,19,24] where it affects the activity of a number of transcriptional regulators. CREB [25], E2F [26], nuclear factor κ B from B cells (NF- κ B) via inhibitor κ B protein kinase (Ik-K) [27], the forkhead transcription factors [28] and murine double minute 2 (MDM2) which regulates p53 activity. These are all either direct or indirect substrates of Akt and each can regulate cellular proliferation, survival and epithelial mesenchymal transition (EMT) [4,11,19,28-31]. Aside from transcription factors, Akt is able to target a number of other molecules to affect the survival state of the cell including: the pro-apoptotic molecule Bcl-2-associated death promoter (BAD) [29], and glycogen-synthase kinase-3 β (GSK-3 β) [30]. GSK-3 β regulates β -catenin protein stability. Hence the PI3K/PTEN/Akt/mTOR pathway is connected to the Wnt/ β -catenin, p53 and many additional pathways (Figure 3).

Negative regulation of the PI3K pathway is primarily accomplished through the action of the phosphatase and tensin homologue deleted on chromosome ten (PTEN) tumor suppressor proteins. *PTEN* encodes a lipid and protein phosphatase whose primary lipid substrate is PtdIns(3,4,5)P₃ [31-39]. The purported protein substrate(s) of *PTEN* are more varied, including focal adhesion kinase (FAK), the Shc exchange protein and the transcriptional regulators ETS-2 and Sp1 and the platelet-derived growth factor receptor (PDGFR) [31-33].

PTEN has four primary structural domains. On the amino terminus is the lipid and protein phosphatase domain, which is flanked adjacent to the C2 domain that is responsible for lipid binding and membrane localization. Next are two protein sequences rich in proline (P), glutamic acid (E), serine (S), and threonine (T) (PEST) domains that regulate protein stability. Lastly, PTEN has a PDZ domain, which helps facilitate protein-protein interactions. Mutations within the phosphatase domain have been reported to nullify the endogenous function of PTEN [31, 35]. Thus PTEN is an enticing therapeutic target for activation since it is frequently inactivated in many human cancers through point mutations as well as other means (e.g., promoter

hypermethylation, gene deletion) and its inactivation results in elevated Akt activity and abnormal growth regulation [31, 35]. Moreover, PTEN can be inactivated by phosphorylation and oxidation in human cancer and which results in elevated Akt activity and abnormal growth regulation [31,35,36]. Thus, drugs reactivating PTEN could potentially be very useful in some types of tumors driven by PTEN inactivation.

Another negative regulator of the PI3K pathway is the PH domain leucine-rich repeat protein phosphatase (PHLPP). PHLPP dephosphorylates S473 on Akt which induces apoptosis and inhibits tumor growth [37]. Two other phosphatases, SH2 domain-containing inositol 5'phosphatase (SHIP)-1 and SHIP-2, remove the 5-phosphate from PtdIns(3,4,5)P₃ to produce PtdIns(3,4)P₂ [38-41]. Mutations in these phosphatases, which eliminate their activity, can lead to tumor progression. Consequently, the genes encoding these phosphatases are referred to as anti-oncogenes or tumor suppressor genes.

Next we discuss some of the key downstream targets of Akt that can also contribute to abnormal cellular growth and are key therapeutic targets [4,19,35,42-47]. Akt-mediated regulation of mTOR activity is a complex multi-step phenomenon. Some of these targets and how they interact with the Ras/PI3K/PTEN/Akt/mTOR and Ras/Raf/MEK/ERK pathways are indicated in Figure 3. Akt inhibits tuberous sclerosis 2 (TSC2 or hamartin) function through direct phosphorylation [4,19,35,42]. TSC2 is a GTPase-activating protein (GAP) that functions in association with the putative tuberous sclerosis 1 (TSC1 or tuberin) to inactivate the small G protein Rheb [4,19,35,43,44]. TSC2 phosphorylation by Akt represses GAP activity of the TSC1/TSC2 complex, allowing Rheb to accumulate in a GTP-bound state. Rheb-GTP then activates, through a mechanism not yet fully elucidated, the protein kinase activity of mTOR when complexes with the Raptor (Regulatory associated protein of mTOR) adaptor protein, DEPTOR and mLST8, a member of the Lethal-with-Sc-Thirteen gene family, first identified in yeast [4,19]. The mTOR/Raptor/mLST8 complex (mTORC1) is sensitive to rapamycin and, importantly, inhibits Akt via a negative feedback loop which involves, at least in part, p70S6K [44]. This is due to the negative effects that p70^{S6K} has on IRS1 [43] (see Figure 3).

The mechanism by which Rheb-GTP activates mTORC1 has not been fully elucidated yet, however it requires Rheb farnesylation and can be blocked by farnesyl transferase (FT) inhibitors. It has been proposed that Rheb-GTP would relieve the inhibitory function of FKBP38 (another component of mTORC1)

on mTOR, thus leading to mTORC1 activation [44]. However, more recent investigations did not confirm these findings [45].

Nevertheless, Akt also phosphorylates proline-rich Akt-substrate-40 (PRAS40), an inhibitor of mTORC1, and by doing so, it prevents the ability of PRAS40 to suppress mTORC1 signalling (recently reviewed in [4,19,44]). Thus, this could be yet another mechanism by which Akt activates mTORC1. Moreover, PRAS40 is a substrate of mTORC1 itself, and it has been demonstrated that mTORC1-mediated phosphorylation of PRAS40 facilitates the removal of its inhibition on downstream signaling of mTORC1 [4,19,44]. Also Ras/Raf/MEK/ERK signaling positively impinges on mTORC1. Indeed, both p90^{Rsk-1} and ERK 1/2 phosphorylate TSC2, thus suppressing its inhibitory function [4,19,44] (See Figure 3). Moreover, recent evidence has highlighted that, in solid tumors, mTORC1 inhibition resulted in ERK 1/2 activation, through p70^{S6K}/PI3K/Ras/Raf/MEK [46].

The relationship between Akt and mTOR is further complicated by the existence of the mTOR/Rictor complex (mTORC2), which, in some cell types, displays rapamycin-insensitive activity. mTORC2 has been found to directly phosphorylate Akt on S473 *in vitro* and to facilitate T308 phosphorylation. Thus, mTORC2 can function as the elusive PDK-2 which phosphorylates Akt on S473 in response to growth factor stimulation [47]. Akt and mTOR are linked to each other via positive and negative regulatory circuits, which restrain their simultaneous hyperactivation through a mechanism involving p70^{S6K} and PI3K [4,19,35,44,48-55]. Assuming that equilibrium exists between these two complexes, when the mTORC1 complex is formed, it could antagonize the formation of the mTORC2 complex and reduce Akt activity [44-46]. Thus, at least in principle, inhibition of the mTORC1 complex could result in Akt hyperactivation. This is one problem associated with therapeutic approaches using rapamycin that block some actions of mTOR but not all.

mTOR is a 289-kDa S/T kinase. It regulates translation in response to nutrients and growth factors by phosphorylating components of the protein synthesis machinery, including p70^{S6K} and eukaryotic initiation factor (eIF)-4E binding protein-1 (4EBP-1), the latter resulting in release of the eukaryotic initiation factor-4E eIF-4E, allowing eIF-4E to participate in the assembly of a translational initiation complex [4,19,35,44]. p70S6K phosphorylates the 40S ribosomal protein S6, (rpS6), leading to active translation of mRNAs [4,19,35,44]. Integration of a variety of signals (mitogens, growth factors, hormones) by mTOR assures

cell cycle entry only if nutrients and energy are sufficient for cell duplication [4, 48-52]. Therefore, mTOR controls multiple steps involved in protein synthesis, but importantly enhances production of key molecules such as c-Myc, cyclin D1, p27^{Kip1}, and retinoblastoma protein (pRb) [35].

mTOR also controls the translation of hypoxia-inducible transcription factor-1 α (HIF-1 α) mRNA [51,52]. HIF-1 α upregulation leads to increased expression of angiogenic factors such as vascular endothelial growth factor (VEGF) and PDGF [4]. Moreover, HIF-1 α regulates the glycolytic pathway by controlling the expression of glucose-sensing molecules including glucose transporter (Glut) 1 and Glut3 [51]. By regulating protein synthesis, p70S6K and 4E-BP1 also control cell growth and hypertrophy, which are important processes for neoplastic progression. Hence targeting the mTOR pathway could have many effects on the regulation of cellular growth.

Many of the mRNAs encoding the previously mentioned genes contain 5' untranslated regions which are G+C rich and difficult to translate and referred to as weak mRNAs [35]. 4EP-B1 forms a complex with these mRNAs and other binding factors allowing the translation of these weak mRNAs [35,53-58]. Rapamycin and mTOR kinase inhibitors suppress the translation of these critical mRNAs involved in cell survival and growth.

Control of Apoptotic Regulatory Molecules by the Ras/Raf/MEK/ERK and Ras/PI3K/Akt/mTOR Pathways

These two pathways regulate the activity of many proteins involved in apoptosis. In the following section, we will mainly discuss the effects of these pathways elicited by post-translational mechanisms [2, 3, 58-62], although it should be noted that both ERK and Akt also phosphorylate transcription factors that influence the transcription of the Bcl-2 family of genes as well as other important genes involved in the regulation of apoptosis [2, 4, 35, 60-62]. Many of the effects of the Ras/Raf/MEK/ERK and Ras/PI3K/Akt/mTOR pathways on apoptosis are mediated by ERK or Akt phosphorylation of key apoptotic effector molecules (e.g., Bcl-2, Mcl-1, Bad, Bim, CREB, Foxo, Caspase-9 and many others) [2, 4, 35, 59-62]. In addition, both pathways regulate the translation of weak mRNAs. ERK, p90^{Rsk-1}, MNK1/2 and p70S6K regulate the phosphorylation of many of the proteins involved in the key complex required for the translation of the weak mRNAs [35,44,56,57]. In some cases, members of the two pathways (e.g., p90^{Rsk-1} and p70^{S6K}) will phosphor-

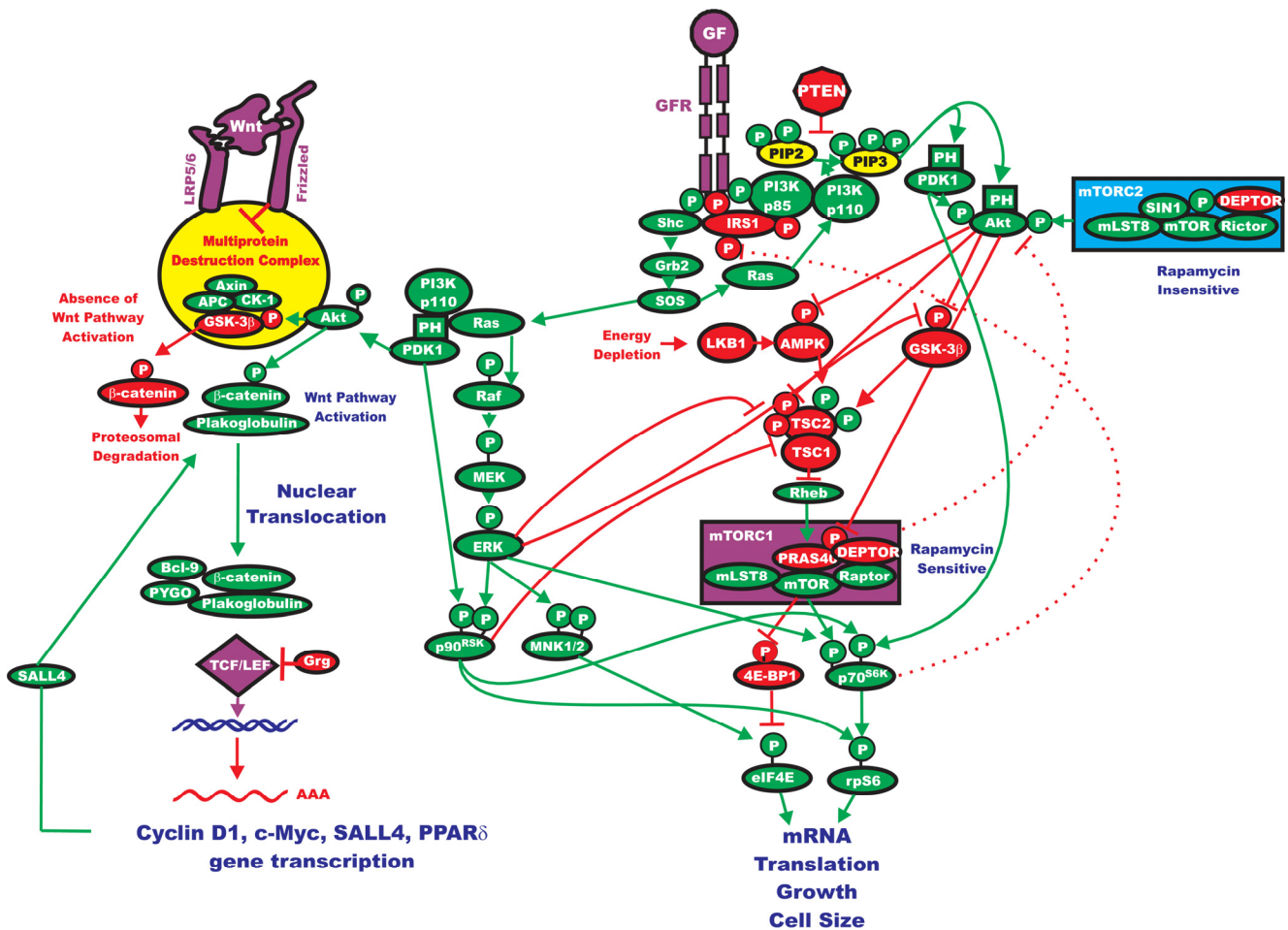


Figure 3. Interactions between the Ras/Raf/MEK/ERK, Ras/PI3K/PTEN/mTOR and Wnt/β-Catenin Pathways that Result in the Regulation of Protein Translation and Gene Transcription. The Ras/Raf/MEK/ERK and Ras/PI3K/PTEN/Akt/mTOR pathways can affect protein translation by complex interactions regulating the mTORC1 (grouped together in a purple box) and mTORC2 (grouped together in a blue box) complexes. GF stimulation results in GFR activation which can activate both the Ras/Raf/MEK/ERK and Ras/PI3K/PTEN/Akt/mTOR pathways. Akt can phosphorylate and inhibit the effects of GSK-3β, TSC2 and PRAS-40 (indicated in red ovals), which result in mTORC1 activation. ERK and PDK1 can phosphorylate p90^{Rsk1} (indicated in green ovals), which in turn can phosphorylate and inhibit TSC2 (indicated in red oval). Akt-mediated phosphorylation of GSK-3β also affects the Wnt/β-catenin pathway and EMT. Rapamycin targets mTORC1 and inhibits its activity and also results in inhibition of downstream p70S6K. The effects of rapamycin are complex as long term administration of rapamycin may prevent mTOR from associating with mTORC2 and hence full activation of Akt is prevented. However, rapamycin treatment may result in activation of PI3K, by inhibiting the effects of p70S6K on IRS-1 phosphorylation which results in PI3K and Akt activation. Also rapamycin treatment may result in the activation of ERK in some cells, presumably by inhibition of the p70S6K mediated inhibition of IRS1. These later two effects of rapamycin could have positive effects on cell growth. Energy deprivation will result in the activation of serine/threonine kinase 11 (STK11 a.k.a LKB1) and AMP kinase (AMPK) which can result in TSC2 activation (indicated in red ovals) and subsequent suppression of mTORC1. In contrast Akt can phosphorylate and inhibit the activity of AMPK. Inhibition of PDK-1 activity can also result in activation of mTORC1, presumably by suppression of p70S6K and hence inhibition of IRS1 (indicated in red oval) effects on PI3K activity. The PTEN, TSC1, TSC2 and LKB1 tumor suppressor genes all converge on the mTORC1 complex to regulate protein translation. Thus the Ras/Raf/MEK/ERK and Ras/PI3K/PTEN/Akt/mTOR pathways can finely tune protein translation and cell growth by regulating mTORC1. Rapamycin can have diverse effects on these processes. Also these pathways can interact with the Wnt/β-catenin pathway which is important in developmental processes, EMT and CICs. Upon activation of the Wnt pathway, β-catenin forms a complex with Bcl-9, PYGO, plakoglobin and TCF/LEF which result in the transcription of critical genes including cyclin D1, c-Myc, SALL4 and PPARδ.

ylate the same molecule in the translation complex at the same site *e.g.* ribosomal protein S6 (rpS6) [57, 58]. However, the kinetics of phosphorylation of rpS6 by the two kinases differs. Thus these two pathways regulate the activity of this translation complex which is responsible for the translation of certain weak mRNAs involved in regulation of apoptosis. Mcl-1 is an example of a weak mRNA and it plays key roles in the regulation of apoptosis.

Aberrant regulation of apoptosis is critically implicated in cancer as well as many other diseases (*e.g.*, inflammation, auto-immune diseases). Therefore controlling the activity of the Ras/Raf/MEK/ERK and Ras/PI3K/PTEN/Akt/mTOR pathways have been keen pharmaceutical objectives for many years. The activity of many key components in apoptotic cascades is sensitive to inhibitors that target these pathways.

Akt regulates the apoptotic response to a variety of stimuli via its ability to interact with a number of key players in the apoptotic process [2,4,61,62]. Akt can directly phosphorylate BAD on S136, causing its inactivation preventing it from interacting with anti-apoptotic members of the Bcl-2 family of proteins (Bcl-2, Bcl-X_L) [29,62]. Activated Akt can inhibit the release of cytochrome c from the mitochondria, which is a potent activator of the apoptotic caspase cascade [59]. The Akt target, Foxo-3 is capable of upregulating Fas ligand (Fas-L) and Bim, two very important molecules that are potent inducers of apoptosis; however, when inactivated by Akt, Foxo-3 is localized to the cytosol where it is unable to augment expression of these genes [28,60]. Akt can also phosphorylate Bim which inhibits its proapoptotic activity [61]. In concert, these events caused by Akt activation affect the survival status of the cell.

Frequent Oncogenic Mutations at Members of these Pathways Result in Activation: Rationale for Therapeutic Targeting of these Pathways

Effective targeting of signal transduction pathways activated by mutations and gene amplification may be an appropriate approach to limit cancer growth, metastasis, drug resistance as well as aging. The Ras/Raf/MEK/ERK and Ras/PI3K/PTEN/Akt/mTOR pathways can be activated by mutations/amplifications of upstream growth factor receptors. The abnormal production of growth factors can result in receptor activation which in turns mobilizes the Ras/Raf/MEK/ERK and Ras/PI3K/PTEN/Akt/mTOR cascades. An illustration of some of the receptors, exchange factors, kinases and phosphatases that are mutated/amplified in human cancer and how they may

impact the Ras/Raf/MEK/ERK and Ras/PI3K/PTEN/Akt/mTOR cascades is presented in Figure 4.

Perhaps one of the biggest advances in medical science in the 1980's was the confirmation of the proto-oncogene hypothesis, that predicted that the human genome contains genes related to viral oncogenes which when mutated could cause human cancer [4,7,19,35,62-84]. Key genetic members of the Ras/Raf/MEK/ERK pathway [*e.g.*, *RAS*, *RAF*), *MEK* (rarely) [81-84], the downstream transcription factor (*ETS*) the Ras/PI3K/PTEN/Akt/mTOR (*e.g.*, *PIK3CA*, *AKT*, *PTEN*) pathway and upstream receptors (*e.g.*, *ERBB1* (EGF-R), *ERBB2* (HER2), *PDGFR*, *KIT*, *FLT3*, *FMS*) were shown to fulfill this hypothesis as they were sometimes mutated/amplified/deleted in specific human cancers. The *RAS*, *RAF*, *PIK3CA*, *AKT*, *ERBB1*, *KIT*, *FMS* and *ETS* oncogenes are also contained as viral oncogenes in the genomes of certain retroviruses that cause cancer in animals [2,7,35,62]. Furthermore, genetic mutations at these cellular oncogenes often alter sensitivity to specific targeted therapeutic approaches. Thus many of the genes in these two signal transduction pathway can cause cancer under the appropriate conditions.

Mutation of Upstream Receptors that Activate the Ras/Raf/MEK/ERK and Ras/PI3K/Akt/mTOR Pathways in Human Cancer

Amplification/overexpression of HER2 [human epidermal growth factor receptor, *a.k.a.*, c-ErbB-2, (*ERBB2*)] is an important cause of sporadic breast cancer that occurs in approximately 30% of breast cancer. HER2 is a receptor tyrosine kinase (RTK) [85]. HER2 can heterodimerize with c-ErbB-3 which has six docking sites for PI3K. While a normal breast cell possesses 20,000 to 50,000 HER2 molecules, amplification of this gene in HER2+ cancers can increase levels of HER2 up to 2,000,000 molecules per cell [85]. Overexpression of HER2 is linked to comedo forms of ductal carcinoma in situ (DCIS) and occurs in approximately 90% of these cases. HER2 overexpression will lead to increased expression of both the Ras/PI3K/Akt/PTEN/mTOR and Ras/Raf/MEK/ERK pathways. Association of genes that regulate signal transduction pathways with breast cancer implies an important role of these pathways in neoplasia.

In acute myeloid leukemia (AML), activation of the Ras/Raf/MEK/ERK and Ras/PI3K/Akt/mTOR pathway can result from mutated upstream targets such as class III RTKs. These include point mutations such as FLT3-internal tandem duplications (FLT3-ITD) and mutated c-KIT, which are present in 35-40% of all AML

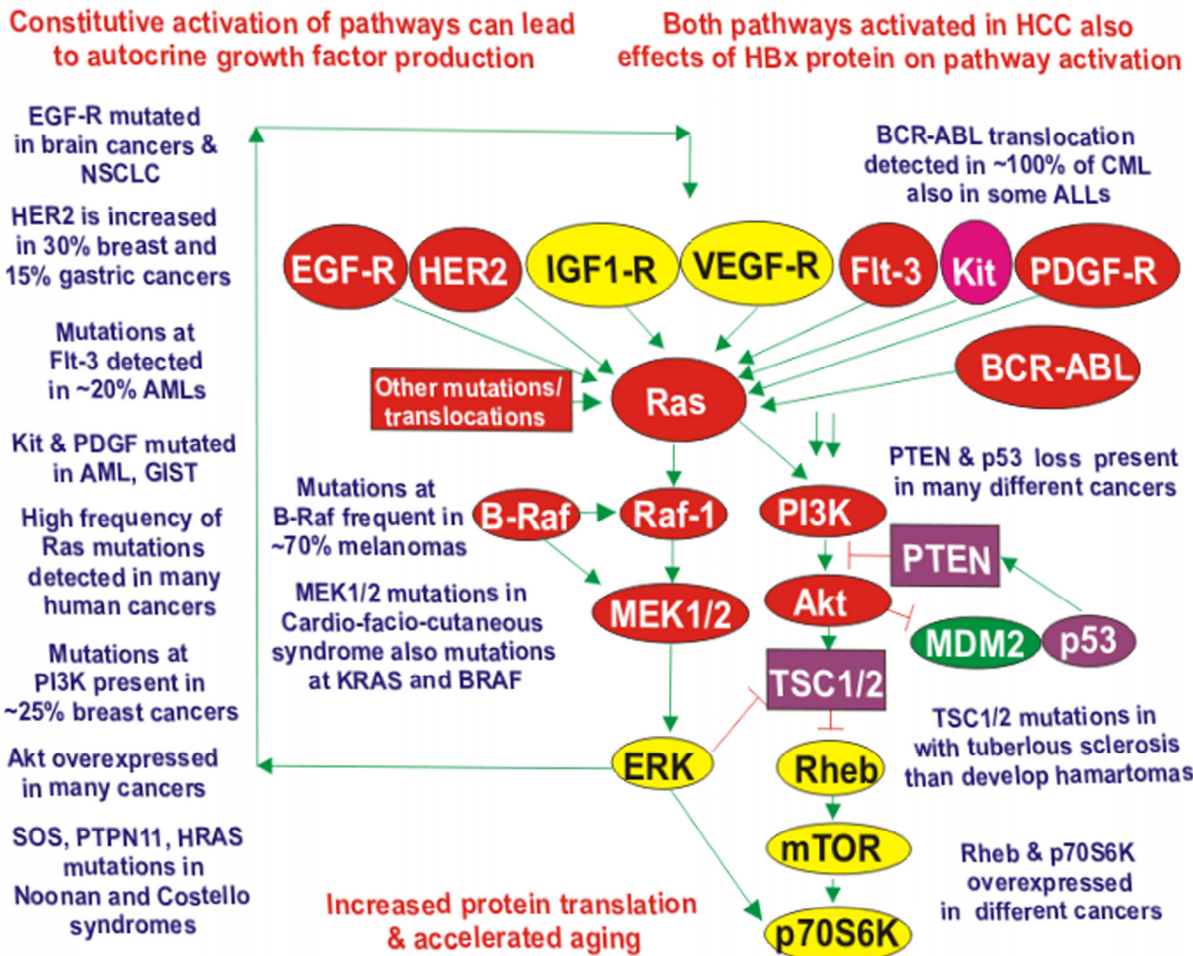


Figure 4. Dysregulated Expression of Upstream Receptors and Kinases Can Result in Activation of the Ras/Raf/MEK/ERK and Ras/PI3K/PTEN/Akt/mTOR Pathways. Sometimes dysregulated expression of growth factor receptors occurs by either increased expression or genomic amplifications (e.g., *VEGFR*, *EGFR*, *HER2*, *IGF1R*). Mutations have been detected in *EGFR*, *FLT3*, *KIT*, *PDGFR*, *PIK3CA*, *RAS*, *BRAF*, *MEK1/MEK2*, *SOS*, *PTPN11* (indicated in red ovals), and *PTEN* (indicated in a purple square). Akt and Rheb are overexpressed in certain cancers. Other signaling molecules which may be overexpressed (e.g., IGF-1R, VEGF-R, ERK, mTOR, p70S6K) but not necessarily mutated or amplified are indicated in yellow ovals. The MDM2 ubiquitin ligase is indicated in a green oval. The p53 tumor suppressor is one of the most frequently inactivated genes in human cancer and has multiple effects on these pathways and is indicated in a purple oval. Amplifications of *HER2* and *EGFR* are detected in certain cancer types. The *BCRABL* chromosomal translocation is present in virtually all chronic myeloid leukemias (CMLs) and some acute lymphatic leukemias (ALLs). Many of these mutations and chromosomal translocations result in the activation of the Ras/Raf/MEK/ERK and Ras/PI3K/PTEN/Akt/mTOR cascades. These pathways can also be activated by autocrine growth stimulation, the genetic basis of which is frequently unknown. Deregulated expression of these pathways can result in cancer as well as premature aging.

[2,4,35,62]. Mutations in upstream signaling molecules such as *KIT* and *FLT3* are believed to activate the downstream signal transduction cascades, such as Ras/Raf/MEK/ERK and Ras/PI3K/Akt/mTOR pathways.

Mutations at *RAS* in Human Cancer

Mutations that lead to expression of constitutively-active Ras proteins have been observed in approximate-

ly 20 to 30% of human cancers [7,63-69]. The frequency of *RAS* mutations and other key genes in the Ras/Raf/MEK/ERK and Ras/PI3K/PTEN/Akt/mTOR pathways in various types of cancers is presented in Table 1. Often point mutations are detected in *RAS* genes in cancer cells from patients which enhance Ras activity. Genome *RAS* amplification or overexpression of Ras, perhaps due to altered methylation of its promoter region, are also detected in some tumors [7,63-69]. In cholangiocarcinoma, *KRAS* gene mutations have been identified in 45% of examined tumors [7]. Ras mutations are present in up to 20% of AML [67] and are another major cause of activation of this cascade. The frequency of *KRAS* mutations is very high (~80%) in advanced pancreatic cancers [7,63]. Mutations that result in increased Ras activity often perturb the Raf/MEK/ERK and also the PI3K/PTEN/Akt/mTOR cascades [7].

A key event in the activation of the Ras protein is farnesylation. Inhibitors that target the enzyme farnesyl transferase (FT) have been developed with the goal of targeting Ras [2]. Clinical testing of FT inhibitors (FTIs) unfortunately has yielded disappointing results. The lack of usefulness of FTIs may be due to multiple reasons. First, there are many proteins that are regulated by FT. Second, although H-Ras is exclusively modified by FT and K-Ras to a lesser extent, N-Ras can also be modified by geranylgeranyltransferase (GGT). This modified N-Ras is still able to support the biological requirement of Ras in the cancer cell. Geranylgeranylation of K-Ras and N-Ras become critical only when farnesylation is inhibited. The majority of *RAS* mutations in humans occur in *KRAS*, which is followed by *NRAS* [7,67]. The mutation rate at *HRAS* is a distant third [7]. Hence, it is very possible that the effects that FTIs had in initial clinical trials were not due to inhibition of mutant *RAS* genes present in the cell, but in fact resulted from non-specific effects which are related to the first point mentioned. Another important target of FTIs is the Rheb protein (Ras homologue enriched in brain) (See Figure 2). Rheb, another GTP binding/exchange protein, plays key roles in regulating mTORC1 and controlling the efficiency of protein translation [4,19,35].

Mutations at *RAF* in Human Cancer

Prior to 2003, it was believed that the *RAF* oncogenes were not frequently mutated in human cancer. There are three *RAF* genes in humans, (*ARAF*, *BRAF* and *CRAF* (a.k.a. Raf-1) encoding three distinct proteins with diverse and common functions. With the advent of improved methods of DNA sequencing, it was demonstrated that *BRAF* is frequently mutated in

melanoma (27 to 70%), papillary thyroid cancer (36 to 53%), colorectal cancer (5 to 22%), cholangiocarcinoma (22%), ovarian cancer (30%), and a small minority of lung cancer patients (1-3%) [70-75]. *BRAF* mutation occurs in approximately 7% of all cancers [70-73]. In contrast, *CRAF* and *ARAF* are not believed to be frequently mutated in human cancer [80-81].

It was proposed that the structures of B-Raf, Raf-1 and A-Raf kinases may dictate the ability of activating mutations to occur at, and be selected in, the genes encoding these proteins, which can permit the selection of oncogenic forms [75]. These predictions have arisen from the solved structure of B-Raf [75]. Like many enzymes, B-Raf is proposed to have small and large lobes, which are separated by a catalytic cleft. The structural and catalytic domains of B-Raf and the importance of the size and positioning of the small lobe may be critical in its ability to be stabilized by certain activating mutations. In contrast, the functionally similar mutations in *ARAF* and *CRAF* are not predicted to result in small lobe stabilization, this may prevent or hinder the selection of mutations at *ARAF* and *CRAF*, which would result in activated oncogenes [75].

The most frequent mutation detected at the *BRAF* gene is a change at amino acid 600, which converts a Val to Glu (Val600→Glu, V600E) [72]. This *BRAF* mutation accounts for > 90% of the *BRAF* mutations found in melanoma and thyroid cancer. *BRAF* mutations may arise in certain cells that express high levels of B-Raf as a result of hormonal stimulation. Certain hormonal signaling events will elevate intracellular cAMP levels, which result in B-Raf activation, leading to proliferation. Melanocytes and thyrocytes are two such cell types that have elevated B-Raf expression, as they are often stimulated by the appropriate hormones [76]. Moreover, it is thought that B-Raf is the most important kinase in the Ras/Raf/MEK/ERK cascade [75]. In some models, wild-type (WT) and mutant B-Raf are proposed to activate Raf-1, which then activates MEK and ERK [77,78]. A number of pharmaceutical and biotechnological companies have developed inhibitors that specifically target mutant B-Raf alleles (mutant-allele specific inhibitors), which do not inhibit WT B-Raf [3].

In many cancers with *BRAF* mutations, the mutations are believed to be initiating events and also the driver mutations, but are not sufficient for complete neoplastic transformation [35,65,66,72-75]. Mutations at other genes (*e.g.*, in components of the Ras/PI3K/PTEN/Akt/mTOR pathway) have been hypothesized to be also necessary for malignant transformation in some cancers. Moreover, there may

Table 1			
Mutations of the Ras/Raf/MEK/ERK and PI3K/PTEN/Akt/mTOR Pathways in Human Cancer			
Gene	Cancer Mutated At	Approximate Reported Frequency	Reference
<i>RAS</i> genes can be activated by point mutations, gene amplifications and other mechanisms.			
<i>RAS</i>	Many different types including pancreatic, acute myeloid leukemia, endometrial, lung, colorectal	20-25% all human cancers, <i>KRAS</i> mutations account for about 85%, <i>NRAS</i> for about 15%, <i>HRAS</i> for <1%.	7
<i>KRAS</i>	Pancreatic	90%	7
<i>HRAS, KRAS, NRAS</i>	Thyroid (papillary)	60%	7
<i>HRAS, KRAS, NRAS</i>	Thyroid (follicular)	55%	7
<i>KRAS</i>	Colorectal	45%	7
<i>KRAS, NRAS</i>	Seminoma	45%	7
<i>NRAS, KRAS</i>	Myelodysplastic syndrome	40%	7
<i>KRAS</i>	Non Small Cell Lung Carcinoma	35%	7
<i>NRAS</i>	Acute myelogenous leukemia	30%	7
<i>NRAS</i>	Liver	30%	7
<i>KRAS</i>	Endometrial	20%	7
<i>NRAS</i>	Melanoma	15%	7
<i>HRAS</i>	Bladder	10%	7
<i>HRAS</i>	Kidney	10%	7
<i>BRAF</i> is activated in approximately 7% all cancers, highest in melanoma, often activated by point mutations.			
<i>BRAF</i>	Melanoma	27-70%	72
<i>BRAF</i>	Papillary Thyroid	36-53%	72
<i>BRAF</i>	Serous Ovarian	30%	72
<i>BRAF</i>	Colorectal	5-22%	72
<i>PIK3CA</i> is often activated by point mutations, also by gene amplification.			
<i>PIK3CA</i>	One of the most frequently mutated kinases in human cancer	>30% solid cancers	106, 110
<i>PIK3CA</i>	Breast	8-40%	106, 108, 110
<i>PIK3CA</i>	Endometrial	23-36%	106, 110
<i>PIK3CA</i>	Hepatocellular	36%	106, 108, 110
<i>PIK3CA</i>	Colon	19-32%	110
<i>PIK3CA</i>	Prostate	29%	31
<i>PIK3CA</i>	Glioblastoma	5-27%	106, 110
<i>PIK3CA</i>	Head/Neck Squamous Cell	33%	106, 110

<i>PIK3CA</i>	Gastric	25%	106, 110
<i>PIK3CA</i>	Urinary Track	17%	31
<i>PIK3CA</i>	Anaplastic Oligodendroglioma	14%	106, 110
<i>PIK3CA</i>	Ovarian	6-12%	110
<i>PIK3CA</i>	Intraductal Papillary Mucinous Neoplasm Carcinoma of the pancreas	11%	110
<i>PIK3CA</i>	Upper Digestive Track	10%	31
<i>PIK3CA</i>	Stomach	8%	31
<i>PIK3CA</i>	Esophagus	7%	31
<i>PIK3CA</i>	Oral Squamous Cell	7%	110
<i>PIK3CA</i>	Pancreas	6%	31
<i>PIK3CA</i>	Medulloblastoma	5%	110
<i>PIK3CA</i>	Lung	4%	110
<i>PIK3CA</i>	Hematopoietic & Lymphoid	4%	31
<i>PIK3CA</i>	Skin	3%	31
<i>PIK3CA</i>	Anaplastic Astrocytoma	3%	110
<i>PIK3CA</i>	Thyroid	2%	31
<i>PTEN</i> often inactivated by deletion, gene methylation, protein stability and other genetic mechanisms.			
<i>PTEN</i>	Endometrial	38%	31
<i>PTEN</i>	Central nervous system	20%	31
<i>PTEN</i>	Skin	17%	31
<i>PTEN</i>	Prostate	14%	31
<i>PTEN</i>	Colon	9%	31
<i>PTEN</i>	Urinary track	9%	31
<i>PTEN</i>	Lung	8%	31
<i>PTEN</i>	Ovary	8%	31
<i>PTEN</i>	Breast	6%	31
<i>PTEN</i>	Hematopoietic & Lymphoid	6%	31
<i>PTEN</i>	Thyroid	5%	31
<i>PTEN</i>	Stomach	5%	31
<i>PTEN</i>	Liver	5%	31
<i>PTEN</i>	Upper aerodigestive track	4%	31
<i>PTEN</i>	Esophagus	1%	31
<i>PTEN</i>	Pancreas	1%	31
<i>AKT</i> is infrequently mutated in human cancer but <i>AKT2</i> gene can undergo amplification in certain cancers.			
<i>AKT1</i>	Thyroid	5%	www.sanger.ac.uk/perl.genetics/CGP/cosmic
<i>AKT1</i>	Breast	3%	www.sanger.ac.uk/perl.genetics/CGP/cosmic
<i>AKT1</i>	Endometrial	3%	www.sanger.ac.uk/perl.genetics/CGP/cosmic

<i>AKT1</i>	Ovary	1%	www.sanger.ac.uk/perl.genetics/CGP/cosmic
<i>AKT1</i>	Urinary track	1%	www.sanger.ac.uk/perl.genetics/CGP/cosmic
<i>AKT1</i>	Prostate	1%	www.sanger.ac.uk/perl.genetics/CGP/cosmic
<i>AKT1</i>	Large Intestine	1%	www.sanger.ac.uk/perl.genetics/CGP/cosmic
<i>AKT1</i>	Hematopoietic & Lymphoid tissue	1%	www.sanger.ac.uk/perl.genetics/CGP/cosmic
<i>AKT2</i>	Head and Neck squamous cell carcinomas	30% amplified	31
<i>AKT2</i>	Pancreatic	20% amplified	31
<i>AKT2</i>	Ovarian	12% amplified	31
<i>AKT2</i>	Breast	3% amplified	31
<i>TSC1/TSC2</i> is inactivated by point mutations, deletion and other genetic mechanisms. Only <i>TSC1</i> is associated with some human cancers.			
<i>TSC1</i>	Urothelial Carcinoma	15%	159

be certain situations where certain potent *BRAF* mutations (Val⁶⁰⁰→Glu) and *RAS* mutations are not permitted in the same cell, as they might result in hyperactivation of Ras/Raf/MEK/ERK signaling and expression, which could lead to cell cycle arrest [75]. In contrast, there are other cases that require both *BRAF* and *RAS* mutations for transformation. The *BRAF* mutations in these cases may result in weaker levels of B-Raf activity which is insufficient for abnormal proliferation [65,66,75,77,78]. It should be pointed out that *RAS* mutations may also result in activation of the Ras/PI3K/Akt/mTOR pathway.

Different *BRAF* mutations have been mapped to various regions of the B-Raf protein. Mutations at *BRAF* that result in low kinase activity may signal through Raf-1 [75,77,78]. Heterodimerization between B-Raf and Raf-1 proteins may allow the impaired B-Raf to activate Raf-1. Other mutations, such as Asp⁵⁹³→Val, may activate alternative signal transduction pathways [75].

One study has observed that mutated alleles of *CRAF* are present in therapy-induced acute myelogenous leukemia (t-AML) [80]. This t-AML arose after chemotherapeutic drug treatment of breast cancer patients. The mutated *CRAF* genes were transmitted in the germ line, thus, they were not spontaneous mutations in the leukemia, but they may be associated with the susceptibility to induction of t-AML in the

breast cancer patients studied. Subsequent studies demonstrated that blast cells from patients with the *CRAF* germline mutations also had loss of the tumor and metastasis suppressor Raf kinase inhibitor protein (RKIP) [81]. The importance of RKIP was determined by transfection experiments with either siRNA directed against RKIP or expression vectors overexpressing RKIP [81]. The levels of RKIP were determined to influence the levels of *CRAF*-mediated transformation as high levels of RKIP suppressed *CRAF*-mediated transformation, while low levels enhanced *CRAF*-mediated transformation [81]. Decreased RKIP expression has also been observed in some cutaneous squamous cell carcinomas which also displayed decreased BRAF expression [79]. Thus mutation at both *BRAF* and *CRAF* have been detected in certain cancer patients and other studies have shown that the levels of mutant and WT B-Raf, Raf-1 and RKIP will influence the levels of transformation observed, hence there is a strong basis for the development of Raf inhibitors [3].

Mutations downstream of Raf in the Ras/Raf/MEK/ERK cascade have not been frequently detected in human cancer although there are some rare germline mutations detected at *MEK1* and *MEK2* in cardiofaciocardiac syndrome (CFC) [82]. There are also mutations at other components of the Ras/Raf/MEK/ERK pathway including *KRAS* and *BRAF* in CFC. There are mutations at components of

the Ras/Raf/MEK/ERK pathway in the related Costello and Noonan syndromes, including: *SOS*, and *PTPN11* (Shp2) in Noonan syndrome and *HRAS* mutations in Costello syndrome [83]. These germline mutations confer sensitivity to MEK inhibitors. *MEK1* but not *ERK2* mutations have been observed in some melanomas and colon carcinomas [84].

Activation of the Ras/Raf/MEK/ERK Cascade in the Absence of Mutations in the Pathway

Hepatocellular carcinoma (HCC) is the fifth most common cancer worldwide and the third most prevalent cause of cancer mortality, accounting for approximately 6% of all human cancers and more than 600,000 deaths annually worldwide [85,86]. Although the clinical diagnosis and management of early-stage HCC has improved significantly, HCC prognosis is still extremely poor. Therefore, investigating HCC pathogenesis and finding new diagnostic and treatment strategies is important.

Signaling via the Ras/Raf/MEK/ERK cascade plays a critical role in liver carcinogenesis [86-91]. Although mutations of Ras and Raf occur infrequently in HCC, a recent study demonstrated that activation of Ras pathway occurred in 100% of HCC specimens analyzed when compared with non-neoplastic surrounding tissues and normal livers [91].

In addition, activation of Ras/Raf/MEK/ERK pathway in HCC may be due to down-regulation of Ras inhibitors Sprouty and the Sprouty-related protein with Ena/vasodilator-stimulated phosphoprotein homology-1 domain (Spred-1) and Spred-2 proteins [92,93]. It has been shown that the expression of Spred-1 and -2 in human HCC tissues is frequently decreased, in comparison to adjacent non-tumorous tissues. This decreased expression inversely correlated with the incidences of tumor invasion and metastasis [92]. Moreover, ectopic Spred expression inhibited HCC cell proliferation both *in vitro* and *in vivo*, which was associated with reduced ERK activation, suggesting that Spred could be both a novel prognostic factor and a new therapeutic target for human HCC [93].

Down-regulation of RKIP expression is a major factor in activation of the Ras/Raf/MEK/ERK pathway during human hepatocarcinogenesis [94]. These studies indicate the complex interplay of various genes that serve to regulate the Ras/Raf/MEK/ERK pathway. Deregulation of their expression by various mechanisms (*e.g.*, promoter methylation, point mutations, post-translational mechanisms) may result in

Ras/Raf/MEK/ERK pathway activation in the absence of detectable mutations at either *RAF* or *MEK*. Hence, the Ras/Raf/MEK/ERK cascade is a therapeutic target in HCC [3,95,96].

Obesity is another important contributing factor for the development of HCC [97]. The important role of Ras/Raf/MEK/ERK signaling has also been suggested for HCC progression in obese patients. A possible explanation for risk associated between obesity and HCC comes from the study of Saxena *et al.*, which for the first time demonstrated that leptin, a key molecule involved in the regulation of energy balance and body weight control, promotes HCC growth and invasiveness through activation of Ras/Raf/MEK/ERK signaling [98].

Other well known risk factors for HCC such as hepatitis B and C viruses (HBV and HCV) also utilize the Ras/Raf/MEK/ERK pathway for the control of hepatocyte survival and viral replication [99]. Among the four proteins encoded by HBV genome, HBx is involved in hepatocarcinogenesis. HBx activates Ras/Raf/MEK/ERK signaling cascade [100]. Among HCV components, the core protein has been reported to activate the Ras/Raf/MEK/ERK pathway and thereby might contribute to HCC carcinogenesis [101, 102]. Therefore, these studies suggest that the Ras/Raf/MEK/ERK pathway is a novel therapeutic target that could be exploited for the treatment of HCC resulting from HBV and HCV infection. microRNAs (miRNAs) may play a key role in regulating HCV translation [103]. Protein translation is regulated by the Ras/Raf/MEK/ERK and Ras/PI3K/PTEN/Akt/mTOR pathways and may be a therapeutic target for HCC [104]. The interacting Wnt/ β -catenin pathway also has effects on HCC [105].

Mutations at *PIK3CA* in Human Cancer

The PI3K p110 α catalytic subunit (*PIK3CA*) gene is currently the most frequently mutated kinase in human cancer. *PIK3CA* is mutated in approximately 25% of breast, 32% of colorectal, 30% of endometrial, 27% of brain, 25% of gastric, 4% of lung cancers [106-110] (Table 1). These mutations are clustered in small hot-spot regions within the helical (E542, E545) and kinase (H1047) domains [106-110]. The locations of these mutations have been recently critically evaluated [110]. These mutations frequently result in activation of its kinase activity [110]. Furthermore increased expression of the Ras/PI3K/Akt/mTOR pathway also occurs frequently in some cancers as the *PIK3CA* gene is amplified in approximately 40% of ovarian cancers [109].

Activation of PI3K/PTEN/Akt/mTOR signaling through mutation, inactivation or silencing of pathway components occurs in various malignancies, including liver cancer [111]. Deregulation of this pathway has clinical importance in HCC. For example, recent data from genomic sequence of HCC samples identified mutations in *PIK3CA* in 50% of patients with poor prognosis, survival length < 3 years following partial liver resection, and only 10% of the HCC patients with a good prognosis had mutation in *PIK3CA* [111]. The identified mutations were restricted to residues H1047 in 61.1%, to E545 in 33.3%, and to E542 in 5.5% of cases, and as a consequence this result in gain of enzymatic function and consequently in oncogenic activity of PI3K [111].

Mutations at *PTEN* in Human Cancer

Germline *PTEN* mutations are present in approximately 80% of patients with Cowden syndrome [112]. This disease, which is also known as multiple hamartoma syndrome, is another familial syndrome that includes many different types of cancer conditions including early onset breast cancer. Mutations have been reported to occur at *PTEN* in breast cancer in varying frequencies (5-21%) [113,114]. Loss of heterozygosity (LOH) is probably more common (30%) [114]. Mutations at certain residues of *PTEN*, that are associated with Cowden's disease, affect the ubiquitination of *PTEN* and prevent nuclear translocation. These mutations leave the phosphatase activity intact [115]. Inhibition of *PTEN* activity leads to centromere breakage and chromosome instability [34]. Thus *PTEN* has diverse activities.

Akt and mTOR phosphorylation are frequently detected in ovarian and endometrial cancers. An early occurrence in endometrial cancer is the loss of functional *PTEN* activity by mutation or other mechanisms, this occurs in approximately 40-80% of patients [116]. Since the loss of *PTEN* results in activation of Akt, that in turn up-regulates mTOR activity, cancer cells deficient in *PTEN* are thought to be major targets of mTOR inhibitors.

The best evidence that strongly supports the connection between *PTEN*-suppression and liver carcinogenesis comes from genetic studies. All mice with *PTEN*-deficient hepatocytes exhibited liver adenomas and 66% of them developed HCC [117]. In these mice, hepatocytes were hyperproliferative and displayed an abnormal activation of Akt [117]. Furthermore, although mutations in the *PTEN* gene rarely occur in HCC, frequent loss of heterozygosity of *PTEN* allele has been identified in 20-30% of HCC patients [118-121]. In addition, down-regulation of *PTEN* expression may be partly due to *PTEN* promoter methylation [122].

PTEN expression plays a critical role in HCC progression and patient's outcome. Patients with high expression of *PTEN* had a significantly better overall survival than patients with low *PTEN* expression [123]. As mentioned above, hepatitis viruses protect hepatocytes from apoptotic cell death by promoting the activation of Ras/PI3K/Akt/mTOR survival pathway [124,125]. Among the four proteins encoded by HBV genome, HBx has been reported to be involved in hepatocarcinogenesis. It has been reported that HBx expression downregulated *PTEN* expression in hepatocytes [125,125]. In contrast, *PTEN* expression in liver cells downregulated HBx-induced PI3K and Akt activities [126]. Therefore, these studies suggest the possible use of *PTEN* as a target in therapeutic approaches for the treatment of at least those HCC caused by HBV infection.

In some cancer settings, *PTEN* and *BRAF* mutations appear to interact. Two recent papers have highlighted the hypothesis of mutant *BRAF*- and *PTEN*-loss-driven carcinogenesis in mouse models. In a study by Dhomen *et al.*, inducible expression of B-Raf^{V600E} was sufficient to induce multiple melanocytic lesions including skin hyperpigmentation, dysplastic nevi and melanoma [127]. Tumor cells from these B-Raf^{V600E} mice displayed both melanoma growth and melanocyte senescence in this system. Approximately 70% of these mice developed melanomas that exhibited histological and molecular characteristics similar to that of human melanoma and were able to colonize the lungs in nude mice [127]. In contrast, another group of researchers generated mice that conditionally-expressed melanocyte-specific B-Raf^{V600E} that were only able to induce benign melanocytic hyperplasias and were unable to progress any further over a 15-20 month period [128]. However, B-Raf^{V600E} expression in a *PTEN* gene-silenced background led to the production of melanoma with 100% establishment, short latency and metastasis to lymph nodes and lungs. This development was prevented by the treatment of mice with either the mTOR inhibitor rapamycin or the MEK1/2 inhibitor (PD0325901). Moreover, while combination treatment with rapamycin or PD0325901 led to the reduction of established tumors, upon termination of drug treatment the melanomas reappeared the presence of drug resistant melanoma-initiating cells in these mice. Overall, these two papers further validated the mutant B-Raf/MEK/ERK and the PI3K/Akt/mTOR pathways, as promising therapeutic targets in melanoma.

Mutations and hemizygous deletions of *PTEN* have been detected in AML and non Hodgkin's lymphoma (NHL) and other cancers [129,130]. Thus the *PTEN*

gene is a critical tumor suppression gene, frequently mutated in human cancer.

Alterations of PTEN Expression in Human Cancer

Phosphorylation (inactivation) of PTEN has been associated with increased Akt-activity. Although many groups have investigated the PTEN-phosphorylation status in leukemia and lymphoma, its relevance concerning Akt-activation is still not clear [129-133]. PTEN phosphorylation as well as low or absent PTEN expression has been observed in AML.

Furthermore, the level of PTEN expression does not always correlate with the degree of phosphorylation of Akt [129]. Although the picture concerning PTEN-inactivation and corresponding Akt-activation is not clear, *in vivo* studies indicate, that PTEN dysregulation promotes leukemogenesis. *PTEN*-deficient hematopoietic stem cells display dysregulated cell cycle progression, and the mice develop a myeloproliferative disease which leads to leukemic transformation [131]. In T-acute lymphoblastic leukemia (T-ALL), PTEN-downregulation is also closely correlated with Akt-activation [132,133]. To discern the role of PTEN for Akt-activation, it may be useful to exclude concomitant causes for Akt-activation such as mutant upstream targets and to include the investigation of regulators of PTEN such as c-Myc and Notch/Hes1 [132,133].

PTEN promoter methylation leads to low PTEN expression [134]. In one study, 26% of primary breast cancers had low PTEN levels that correlated with lymph node metastases and poor prognoses [135].

Other mechanisms important in the regulation of PTEN are miRNAs. Certain miRNAs have been shown to regulate PTEN protein expression. mi-214 induces cell survival and may contribute to oncogenesis and drug resistance (see below) by binding the 3' untranslated region (3'UTR) of PTEN which prevents PTEN mRNA translation and leads of overexpression of downstream Akt [136].

Mutations at SHIP Phosphatase in Human Cancer

The SHIP-1 phosphatase has been implicated as a suppressor of hematopoietic transformation as it basically can prevent Akt-activation [137]. SHIP-1-deficient mice develop a myeloproliferative disease [138] and an inactivating point mutation (*SHIP V684E*) has been observed in approximately one of thirty AML cases [137]. Also another mutation, *SHIP Q1154L*, has

been observed in AML, but was even less frequent (1 of 192 cases) [138]. Though some studies confirmed, that SHIP-1 is a leukemia suppressor [137,138] it is unlikely that *SHIP1* mutations are a frequent cause of Akt-activation in AML. Disruption of *PTEN* or *SHIP* activity by various genetic mechanisms could have vast effects on different processes affecting the sensitivity of different cancers to various therapeutic approaches.

Mutations of AKT in Human Cancer

The roles that Akt plays in cancer are complex. Akt can be activated by genetic mutations, genome amplifications and more commonly by mutations in upstream signaling components. Amplification of Akt-2 was observed in human ovarian carcinomas [139]. Increased levels of Akt are detected in carcinomas of the breast, ovary and prostate and are associated with a poorer prognosis in comparison with tumors that do not display increased levels of expression. Akt is a member of a multi-gene family that consists of *AKT1*, *AKT2* and *AKT3*. *AKT1* has been reported to be mutated in some breast, colorectal, melanoma and ovarian cancers [140-142] (see below). *AKT2* is not mutated frequently in human cancer. *AKT2* is amplified in certain cancers (e.g., 12.1% ovarian and 2.8% breast carcinomas) [142]. A recent report documents the mutation of *AKT3* in some melanoma samples [143].

AKT1 is mutated in 2 to 8% of breast, 6% of colorectal and 2% of ovarian cancers samples examined in one study [140]. This study documented an Akt mutation that results in a glutamic acid (E) for a lysine (K) substitution at amino acid 17 (E17K) in the PH domain. Cells with this *AKT1* mutation have not been observed to have mutations at *PIK3CA*; a similar scenario is also frequently observed with *RAS* and *BRAF* mutations [144]. This *AKT1* mutation alters the electrostatic interactions of Akt-1 which allows it to form new hydrogen bonds with the natural PtdIns ligand [140]. The PH domain mutation confers many different properties to the *AKT1* gene. Namely the mutant *AKT1* gene has: 1) an altered PH domain conformation, 2) is constitutively-active, 3) has an altered cellular distribution as it is constitutively-associated with the cell membrane, 4) morphologically transforms Rat-1 tissue culture cells and 5) interacts with c-Myc to induce leukemia in E μ -Myc mice (E μ = Enhancer of immunoglobulin μ gene, Myc = Myc oncogene originally isolated in avian myelocytomatosis virus) [140]. This PH domain mutated *AKT1* gene does not alter its sensitivity to ATP competitive inhibitors, but does alter its sensitivity to allosteric kinase inhibitors [140]. These results demonstrate that targeting the

kinase domain of Akt may not be sufficient to suppress the activity of various *AKT* genes that have mutations in the PH domain.

Alterations of Akt Expression in Human Cancer

Akt is often upregulated in cancer cells and its overexpression is associated with a poor prognosis. Increased expression of Akt can result from activating *PIK3CA* mutations or elimination or decrease in PTEN activity. Elevated Akt expression has also been associated with the pathology of pancreatic, glioma and prostate cancers [145-148].

Pancreatic cancer cells have elevated IGF-1R expression and it is well known that Akt regulates IGF-1R expression [149]. This Akt effect on IGF-1R has been suggested to be responsible for the invasiveness of pancreatic cancer cells. Active Src can also activate Akt, and both Src and Akt up-regulate IGF-1R expression in this cancer. It has been demonstrated that IGF-1 is expressed in the surrounding stromal cells but not in the cancer cells. This IGF-1 expression may serve as a paracrine growth factor to activate the IGF-1R pathway and the downstream Ras/PI3K/Akt/mTOR pathway in pancreatic cells.

Cyclooxygenase-2 (COX-2) is expressed at high levels in some primary endometrial tumors and is associated with an aggressive phenotype [150]. Akt is elevated and PTEN is often mutated in these cancers. Recently, NF- κ B activation has been shown to have oncogenic effects important in the control of apoptosis, cell cycle, differentiation and cell migration. Akt may exert its effects through the NF- κ B pathway and COX-2 is the regulator of this pathway. Akt regulates *COX2* gene and protein expression in endometrial cancers. This study was undertaken to examine the involvement of Akt in the regulation of NF- κ B and COX-2 [150]. The expression of both inhibitor of NF- κ B (I κ B) and phosphorylated I κ B were increased in the cells containing mutant *PTEN* genes. In contrast, there was no difference in NF- κ B protein abundance between the cell lines, which differed in PTEN gene status. I κ B phosphorylation by the PI3K pathway was inhibited by the PI3K inhibitors Wortmannin and LY294002. There was less NF- κ B nuclear activity, less COX-2 expression and more apoptosis after inhibition of the PI3K pathway. Dominant negative (DN) Akt blocked I κ B phosphorylation and decreased COX-2 expression. In contrast, introduction of constitutively-active Akt induced I κ B phosphorylation and up-regulated COX-2 expression.

When *PTEN* is mutated, Akt signals via the NF- κ B/I κ B pathway to induce COX-2 expression in endometrial cancer cells. COX-2 can inhibit apoptosis, increase angiogenesis, and promote invasiveness. COX-2 also promotes inflammation/immunosuppression and conversion of procarcinogens into carcinogens that contribute to tumorigenesis and a malignant phenotype. This study demonstrated that Akt signals via the NF- κ B/I κ B pathway to induce *COX2* gene and protein expression in endometrial cancer [150].

Elevated Akt activity can also result in increased phosphorylation of mTOR. mTOR was found to be phosphorylated in AML blasts, along with its two downstream substrates, p70^{S6K} and 4EBP-1, in a PI3K/Akt-dependent fashion [151]. Nevertheless, others failed to detect any relationship between PI3K/Akt signalling upregulation and p70^{S6K} phosphorylation in AML primary cells [152]. This might occur via the Ras/Raf/MEK/ERK pathway activating mTOR via ERK phosphorylation [152]. The Ras/Raf/MEK/ERK pathway is frequently activated in AML [153]. Thus treatment of AMLs with Raf and MEK inhibitors is being activated investigated [3,154,155].

Akt is activated in HCC, which results in enhanced resistance to apoptosis through multiple mechanisms [101,156-158]. As an example, activation of the Akt pathway suppresses transforming growth factor- β (TGF- β) induced apoptosis and growth-inhibitory activity of CCAAT/enhancer binding protein alpha (CEBP- α). Activation of Akt is a risk factor for early disease recurrence and poor prognosis in patients with HCC [156]. Several mechanisms may be responsible for the activation of Akt. The high frequency of *PIK3CA* mutations and/or its upregulation in patients with shorter survival might be responsible for the Akt hyperactivation found in HCC with poor prognosis [118-124]. Selective epigenetic silencing of multiple inhibitors of the Ras pathway seems also to be responsible for the activation of Akt found in HCC [111]. Moreover, impaired expression of PTEN is involved in the regulation of Akt activity. Activation of Akt signaling and reduced expression of PTEN has been reported in 40%–60% of human HCC cases [111,118-124]. Some well known risk factors, HBV and HCV seem to utilize the Ras/PI3K/PTEN/Akt/mTOR pathway for the control of hepatocytes survival and viral replication [157,158]. Taken together, these data suggest that Ras/PI3K/Akt/mTOR pathway may represent an important therapeutic target for the treatment of HCC among patients with differing etiologies that lead to the development of this aggressive tumor.

Mutations of *TSC1/TSC2* Genes in Human Cancer

Mutations in the tumor suppressor genes *TSC1* and *TSC2* are associated with a dominant genetic disorder, tuberous sclerosis [42,159]. Patients with mutant *TSC* genes develop benign tumors (hamartomas). In contrast to Cowden's patients who have germline mutations at *PTEN* and the patients have a high propensity to develop multiple malignancies, TSC patients rarely develop multiple malignant cancers, and if they do develop malignant cancers they are usually either renal cell carcinomas (RCCs) or angiomyolipomas [159]. This has been hypothesized to result from a lack of activation of Akt in cells that have mutant *TSC1* or *TSC2* as mTOR activity is expressed at higher levels which results in inhibition of Akt, perhaps via the effects of p70S6K on insulin regulated substrate-1 (IRS1) (Figure 3). *TSC1* has been shown to be mutated in approximately 15% of urothelial carcinomas (bladder cancers) [159].

Altered Expression of Components Downstream of mTOR in Human Cancer

mTOR regulates translation by phosphorylating components of the protein synthesis machinery, including p70S6K and 4E-BP1 (eukaryotic initiation factor 4E-binding protein 1) [160,161]. p70S6K phosphorylates the 40S ribosomal protein, rpS6, leading to active translation of mRNAs [4]. In contrast, 4E-BP1 phosphorylation by mTORC1 on several amino acid residues (S37; T46; S65; T70) results in the release of the eukaryotic initiation factor 4E (eIF4E) [5]. mRNAs differ in their ability to be translated; the length and sequence of the 5' UTR largely dictates the efficiency with which an mRNA transcript will be translated. Most mRNAs contain short, unstructured GC-poor 5' UTRs and are efficiently translated. In contrast, long, GC-rich sequences in the 5' UTR often hinder the ability of the eIF-4E complex to efficiently scan and initiate translation at the start codon [4,19,35]. These are called weak mRNAs as previously discussed. Consequently, under normal circumstances these mRNAs are not efficiently translated, and are considered "weak" mRNAs [4,19,35]. However, upon Akt-mediated activation of mTOR, these latter mRNAs are highly and disproportionately translated. Interestingly, many of these weak mRNA molecules encode oncogenic proteins involved in cell proliferation or survival (e.g., c-Myc, Mcl-1, cyclin-D, VEGF and survivin). These oncogenic mRNAs are therefore tightly regulated at the translation level and their accumulation in cancer cells strongly contributes to the malignant phenotype.

Several key proteins that are overexpressed as a consequence of mTOR activation include: c-Myc [162-

164], cyclin D1 [164], and VEGF [165] and others. Cyclin D1 has been reported to be overexpressed in prostate cancer xenografts and metastases [166], while early stage prostatic lesions possess much lower levels of the protein [167]. A number of reports support the notion that mTOR signaling is a prominent feature of cancer progression and aging, as recurrent tumors have altered expression of a number of molecular targets of rapamycin including the above mentioned genes which encode "weak" mRNAs [168-171]. Hence mTOR inhibitors such as rapamycin may be effective in cancer therapy.

One central molecule involved in cell growth is p70S6K which is regulated by both the Ras/PI3K/PTEN/Akt/mTOR and Ras/Raf/MEK/ERK pathways [4]. The p70S6K gene is amplified in approximately 9% of primary breast cancers and elevated levels of its mRNA transcripts are found in about 41% of the tumors [173,174]. It is known that some PTEN-deficient cells and tumors that are purported to grow in response to activated Akt are hypersensitive to mTOR inhibitors. p70S6K activity is reduced by mTOR inhibitors in PTEN-deficient cells and transgenic PTEN^{+/-} mice [175,176].

Involvement of the Ras/Raf/MEK/ERK and Ras/PI3K/PTEN/Akt/mTOR Pathways in Hormone-Independent Prostate Cancer

The progression of prostate cancer from androgen-dependent to androgen-independent tumors involves the alteration of the androgen receptor and/or the activation of pro-survival pathways, namely those of the Ras/Raf/MEK/ERK and Ras/PI3K/PTEN/Akt/mTOR signaling cascades [177,178]. Research has shown that inhibition of one or both of these pathways has a more profound effect on tumor cell development and death making them very attractive as combinational targets in prostate cancer therapy. In the study by Wu *et al.*, cells from the androgen-dependent cell line LNCaP were able to differentiate into neuroendocrine type cells upon androgen withdrawal from the culture media [177]. This differentiation was marked by a change in cellular morphology and expression of the chromogranin and neuron-specific enolase (NSE), as well as an increase in phosphorylated ERK and Akt. Inhibition of the Ras/PI3K/PTEN/Akt/mTOR pathway with the PI3K inhibitor LY294002 and the mTOR inhibitor Rapamycin reduced the expression of these neuroendocrine specific cell markers however the use of the MEK inhibitor U0126 appeared to have no effect [177]. In another study, *Nkx3.1;Pten* mutant mice were used as a preclinical model for the effects that inhibition of both Ras/Raf/MEK/ERK and

Ras/PI3K/PTEN/Akt/mTOR pathways would have on hormone-dependent and -independent prostate cancer growth [178]. The *Nkx3.1;Pten* mutant mouse model resembles that of human prostate cancer progression in which spontaneous PIN lesions form and progress to adenocarcinomas and eventually hormone refractory tumors upon androgen deprivation. Treatment of tumors from these mice both *in vivo* and *in vitro* with rapamycin and the MEK inhibitor PD0325901 were able to synergistically decrease their respective target pathway's activation more effectively and at a lower IC₅₀ compared to treatment with each agent alone [179]. Interestingly, although combination inhibitor therapy was somewhat effective at reducing tumor size and proliferation in the androgen-intact mouse model, the highest reduction in tumor growth from therapy was observed in the androgen-deficient mice [178]. In addition to the mouse study these authors were able to show, using human patient tissue microarrays, that aberrant activation of some of the Ras/PI3K/PTEN/Akt/mTOR pathway components (Akt, mTOR, p70S6K) are frequent in progressed human prostate tumors. In addition, activation of the Ras/Raf/MEK/ERK pathway coincides with a high percentage of these tumors as well, suggesting that combination inhibitor treatment along with hormone ablation could prove useful in human prostate cancer therapies [178].

Interactions of p53 and the Ras/Raf/MEK/ERK and PI3K/PTEN/Akt/mTOR pathways

Ras/Raf/MEK/ERK and Ras/PI3K/PTEN/Akt/mTOR pathways are often regulated by the tumor suppressor p53. Furthermore p53 activity is likewise regulated by the Ras/Raf/MEK/ERK and Ras/PI3K/PTEN/Akt/mTOR pathways. p53 is a critical tumor suppressor gene which encodes a transcription factor that is frequently mutated in human cancer [179-195]. P53 regulates the transcription of many genes whose protein products play critical roles in cell cycle progression, apoptosis, senescence, quiescence and aging. p53 is often activated after chemotherapeutic drug treatment and DNA damage [182,183,193-195]. There are complex interactions between p53, DNA damage responses and these two signaling pathways [180-195]. Akt can phosphorylate MDM-2 which leads to its proteasomal degradation and prevents its ability to interact with and destabilize p53 [4]. The p53 and MDM families of genes are critically involved in the response to DNA damage [183-185], apoptosis [185], senescence [186], metastasis [188], autophagy [190], chemosensitivity [191,195] and cellular aging [179,181,182]. Thus the ability to fine tune these pathways could significantly advance human health.

MDM-2 inhibitors such as Nutlin-3A increase p53 stability [179]. p53 can affect the transcription of the PTEN and other important gene involved in cell cycle regulation (*e.g.*, p21^{Cip-1}), apoptosis (*e.g.*, Bax, Noxa, Puma) and cellular senescence [*e.g.*, Yippee-like-3 (YPEL3)], [180,184-186,192]. Thus reactivation of p53 expression could enhance PTEN gene expression and hinder activation of Akt.

The Ras/Raf/MEK/ERK pathway can regulate p53 activity and p53 can also induce the activity of key components of this pathway [196-198]. ERK can phosphorylate p53 and alter its activity. Moreover, chemotherapeutic drugs such as doxorubicin can induce the p53 activity that in turn can activate the expression of the discoidin domain receptor (DDR) which can induce Ras and the downstream Ras/Raf/MEK/ERK and Ras/PI3K/PTEN/Akt/mTOR pathways [196-198].

In certain scenarios, increased p53 expression after chemotherapeutic drug treatment may lead to increased Ras/Raf/MEK/ERK and Ras/PI3K/PTEN/Akt/mTOR pathways activation, resulting in an undesired pro-proliferative effect [195]. This may occur in certain cancer initiating cells (CICs) and be a component of their inherent drug resistance. In addition, Akt has critical roles in regulation of cell cycle progression [199-202]. Thus in those therapeutic scenarios where increased p53 activity is desired, it may also be prudent to also consider treatment with either a Raf or MEK inhibitor to decrease the activation of this pro-proliferative pathway.

Novel Roles of the Ras/Raf/MEK/ERK and Ras/PI3K/PTEN/Akt/mTOR Pathways in Cancer and Aging

In the previous sections, we have discussed the mechanisms of activation of the Ras/Raf/MEK/ERK and Ras/PI3K/PTEN/Akt/mTOR pathways in human cancers, predominantly by mutational based mechanisms. Recently the Ras/Raf/MEK/ERK and Ras/PI3K/PTEN/Akt/mTOR pathways have been shown to have roles in cancer stem cells, senescence, aging and sensitivity to targeted therapy [203-245]. These additional functions of these pathways expand their important in human health.

An area of intense interest in cancer biology is the cancer stem cell, more appropriately referred to as the cancer initiating cell (CIC) [203-211]. The concept that the Ras/Raf/MEK/ERK and Ras/PI3K/PTEN/Akt/mTOR pathways serve as key pathways in regulating CIC survival is beginning to emerge. CICs have unique properties as they can be

both quiescent and also resistant to chemotherapeutic and hormonal based drugs [203]. However, under certain conditions, they resume proliferation and hence should be potentially susceptible to Ras, Raf, MEK, PI3K, Akt or mTOR inhibitors.

The *PTEN* gene has been shown to exert effects on CICs, especially in hematopoietic and breast cells [204-209]. In conditional *PTEN* knock-out mice, upon inactivation of *PTEN*, there is a transient increase in hematopoietic CICs and a myeloproliferative disease develops and the mice subsequently develop leukemia after 4-6 weeks [204]. If the mice are treated with rapamycin, the myeloproliferative disorder and leukemia are prevented. The initial leukemic CICs that arise after conditional *PTEN* deletion by themselves are not able to induce leukemia upon transfer into severe combined immunodeficiency (SCID)-recipient mice, but if the leukemic CICs were derived from the *PTEN*-conditional mice that had developed leukemia, they were able to transfer leukemia to the SCID-recipient mice, which could be prevented by rapamycin treatment [204]. Also the normal hematopoietic stem cells from the *PTEN*-conditional knock-out mice could repopulate the hematopoietic cell component of irradiated mice treated with rapamycin indicating that it is possible to selectively eliminate leukemic CICs.

PTEN also plays important roles in breast CICs [205,206]. If *PTEN* is mutated, Akt phosphorylates and inactivates glycogen synthetase kinase 3 β (GSK-3 β) which in turn regulates the activity of the Wnt/ β -catenin pathway [Figure 3], as β -catenin is not phosphorylated by GSK-3 β and not degraded. β -catenin can localize to the nucleus, perhaps due to Akt-mediated phosphorylation at S552 and exert its effects. β -catenin can then promote the expression of many genes such as cyclin D, c-Myc, SALL4 and peroxisome proliferator-activated receptor- δ (PPAR δ) which are important in cell survival and EMT. The Ras/PI3K/*PTEN*/Akt/mTOR pathway performs key roles in the regulation of the size of the Aldefluor-positive cell population that are enriched in breast CICs. Treatment with the Akt inhibitor perifosine was able to target these cells both in *in vitro* and xenograft models [206]. In contrast, the chemotherapeutic drug docetaxel was unable to target the Aldefluor-positive cells and these cells were not sensitive to mTOR inhibitors, suggesting that the mTOR pathway was not involved in these breast CIC. The studies by Korkaya *et al.* [206] indicate that targeting some breast CICs with perifosine may eliminate these cells that are responsible for tumor reappearance. Other studies have shown that breast CICs are resistant to chemotherapeutic drugs [212-214].

We have observed that some drug resistant breast cells that express properties similar to CICs display elevated activation of the Ras/Raf/MEK/ERK and Ras/PI3K/*PTEN*/Akt/mTOR signaling cascades and that CICs can be isolated from these cell populations [215-217]. Our recent data suggests these CICs are more sensitive to MEK and mTOR inhibitors than either the parental or drug resistant cells from which they were derived [215]. Targeting the Ras/Raf/MEK/ERK and Ras/PI3K/*PTEN*/mTOR pathways could be very important in terms of CIC elimination.

Involvement of the Ras/Raf/MEK/ERK and PI3K/*PTEN*/Akt/mTOR Pathways in Suppression Cellular Senescence and Premature Aging

The Ras/Raf/MEK/ERK and PI3K/*PTEN*/Akt/mTOR pathways play key roles in regulation of diverse processes ranging from: autophagy DNA damage responses, cellular senescence and aging [217-237]. Treatment of cells induced to undergo senescence with MEK, PI3K and mTOR inhibitors will prevent the induction of cellular senescence and aging [219-221]. These experiments have led to innovative hypothesis that cellular senescence results from the hyper-activation of proliferative pathways. Drugs used to treat diabetes (*e.g.*, Metformin) or inhibit signal transduction pathways (*e.g.*, Raf, MEK, PI3K, mTOR inhibitors) can inhibit cellular proliferation and cellular aging [229-234]. Similar effects on the prevention of cellular senescence were observed with Resveratrol, the active component contained in the skins of red grapes which was shown to also inhibit mTOR and cellular senescence [229,230]. Additional studies have shown that the commonly-prescribed diabetes drug Metformin will also inhibit mTOR and prevent cellular aging [234]. Since both the Raf/MEK/ERK and PI3K/*PTEN*/Akt/mTOR pathways interact to regulate the activity of mTOR and downstream components of this pathway which are critical for both mRNA stability and protein translation, it is believed that by inhibiting some of these key pathways, it may be possible to prevent cellular aging (See Figures 1-3).

CONCLUSIONS

Over the past 25 years, there has been significant progress in elucidating the involvement of the Ras/Raf/MEK/ERK and Ras/PI3K/*PTEN*/Akt/mTOR cascades in promoting cell growth, regulating apoptosis, chemotherapeutic drug resistance and more recently, cellular senescence and aging. Initial seminal studies performed in the late 70's and early 80's elucidated that oncogenes were present in the genomes of avian and

murine retroviruses. Many of the viral oncogenes: *ErbB*, *Fms*, *Ras*, *PI3K*, *Akt*, *Src*, *Abl*, *Raf*, *Fos*, *Jun*, *Ets* and *NF- κ B* (*Rel*) were subsequently identified as cellular genes which in some cases were captured by retroviruses. Now we know that these cellular genes are frequently abnormally regulated in human cancer. Furthermore mutations in human cancer often occur in upstream receptor genes such as *EGFR*, *HER2*, *Flt-2*, *PDGFR*, *FMS*, as well as chromosomal translocations (e.g., *BCR-ABL*, *TEL-PDGFR*) that serve to activate the Ras/Raf/MEK/ERK and Ras/PI3K/PTEN/Akt/mTOR pathways which have been discussed as playing critical roles in cellular proliferation in this review. Hence the Ras/Raf/MEK/ERK and Ras/PI3K/Akt/mTOR pathways are important therapeutic targets. Both of these pathways also interact with the p53 and Wnt pathways, which also play critical roles in regulation of cell growth, aging, CICs and metastasis. Specific Raf, MEK, PI3K, Akt, mTOR and Mdm-2 inhibitors have been developed and represent promising therapies for cancer and other proliferative diseases including premature aging.

Scientists and clinicians often have an intentionally narrow view of a particular topic. For example, cancer researchers predominately consider that Raf, MEK, PI3K, Akt and mTOR inhibitors will suppress the growth of malignant cancer cells. Yet MEK and mTOR and other inhibitors may also be useful in the treatment of diseases and disorders where there is abnormal cellular proliferation. Recent reports have also demonstrated that the suppression of the Ras/Raf/MEK/ERK and Ras/PI3K/PTEN/Akt/mTOR pathways may prevent the induction of cellular senescence and aging. Clearly, this later topic, aging, greatly enhances the potential clinical uses of these targeted therapeutic drugs. In conclusion, the Ras/Raf/MEK/ERK and Ras/ PI3K/PTEN/Akt/mTOR pathways are prime therapeutic targets for diverse human diseases as well as aging.

Cancer therapy is often complex as there are relatively few cancers which proliferate in response to a single mutation preventing them from being treated with a mono-specific drug. One exception is the use of the drug Gleevec (Imatinib) for the treatment of chronic myeloid leukemia (CML). Although even with this therapeutic approach, resistance develops. Scientists and clinicians have developed newer BCR-ABL inhibitors (e.g., Dasatinib, Nilotinib, Bosutinib) which can reduce resistance which has also resulted in more through analysis and understanding of how the BCR-ABL kinase functions and resistance can arise by additional genetic mutations. These studies on BCR-ABL inhibitors have also paved the way for

development of more effective inhibitors for other oncogenes.

It is possible that activation of the Ras/Raf/MEK/ERK and Ras/PI3K/PTEN/Akt/mTOR survival pathways by additional mutations in upstream oncogenes may replace the tumor's initial oncogene addition. This may complicate therapy as the tumor may no longer be responsive to treatment with a single inhibitor which targets the original oncogene responsible for malignant transformation as the cells now have additional downstream signalling pathways activated. In addition, the tumor cells may acquire subsequent mutations which make them resistant to inhibitors that target the original activated oncogene. Such mutations may occur in the original activated oncogene or in additional genes which are critical in anti-apoptotic survival cascades. These observations document the need for further elucidation of mechanisms of inhibitor resistance as well as the development of additional inhibitors which target either the mutated oncogene or other genes activated in the resistant cells.

The activation of multiple signalling pathways by many oncogenes illustrates the need for the targeting of more than one signalling pathway. Although one inhibitor which targets one molecule in one pathway may initially appear to be effective in inhibiting tumor cell growth, the cell may adapt and be able to survive due to the activation of an additional signalling pathway. Although the Ras/Raf/MEK/ERK and Ras/PI3K/PTEN/Akt/mTOR pathways have distinct effects on cell proliferation, they have many common downstream targets that may be able to function in promoting survival in the absence of the corresponding functional pathway. In some cases resistance to small molecule inhibitors may be due to the activation of an additional pathway that also serves to promote survival (e.g., *PIK3CA* and *HRAS* mutations can confer resistance to MEK inhibitors and other targeted therapeutics such as Erbitux and others) [238-245].

Most cancers are more complex and often the genes and events involved are either not known or difficult to counterbalance. Chemotherapy and radiotherapy can be effective in the treatment of certain tumors, however, often cancers become resistant to these approaches, perhaps due to the emergence of CICs [203,215-217]. Thus scientists and clinicians have endeavored to develop more specific therapies that target key pathways involved in cancer growth. In this respect, the Ras/Raf/MEK/ERK and Ras/PI3K/PTEN/mTOR/Akt pathways represent key therapeutic targets as they are often dysregulated by various mutations in cancer and these cascades control the activities of many proteins

critical for cell growth and metastasis. In fact, these pathways are already being targeted in certain cancer patients. However, usually the cancer patients being treated with inhibitors that target these cascades have diseases that often have poor prognoses. That being said, what are the pros and cons of targeting these pathways? Let us first consider the positive aspects of targeting these pathways. First, these pathways are frequently activated in human cancer, thus in many cases, targeting the cascades will suppress cell growth, in the absence of knowing the precise mutation(s) responsible for the cancer. Second, although the biochemical interactions of these pathways are quite complex, there is quite a bit of knowledge of how these pathways function. Third, some inhibitors which target key components in this pathway (e.g., rapamycin which targets mTOR) have undergone extensive evaluation in humans as they have been used to prevent allograft rejection in kidney and other transplant patients for many years. Fourth, targeting these pathways may prevent aging and cellular senescence.

Now, let us summarize some of the cons of targeting these pathways. First, an obvious problem results from these pathways controlling the expression of many downstream targets (easily in the 1000's), thus inhibiting these pathways will be detrimental in certain cells, unless it is possible to deliver the inhibitor to specifically the cancer cell. Second, the Ras/Raf/MEK/ERK and Ras/PI3K/PTEN/Akt/mTOR pathways cross regulate each other and other pathways including the Wnt/ β -catenin pathway which is critical for many aspects of cellular growth and differentiation including the EMT. The Ras/Raf/MEK/ERK and Ras/PI3K/PTEN/Akt/mTOR pathways also regulate other pathways which have not been discussed in this manuscript. These other pathways include: the Jak/STAT, NF- κ B and transforming growth factor- β (TGF- β) pathways which can be directly and indirectly regulated by ERK and Akt phosphorylation [62]. In this regard there will be a Ying-Yang effect, when one cascade is inhibited, components of the other pathway could be deregulated. Third, inhibitors that target these pathways are often cytostatic and not cytotoxic, that is somewhat logical as if these inhibitors were cytotoxic, there would be massive toxicity problems. To get around this problem, inhibitors targeting these pathways could be combined with cytotoxic chemotherapeutic drugs or radiation therapy that affects the rapidly growing cancer cell. In summary, the Ras/Raf/MEK/ERK and Ras/PI3K/PTEN/Akt/mTOR cascades are complex, interacting pathways playing key roles in normal and malignant cell growth. These pathways are frequently activated by mutations in human cancer. They represent key therapeutic targets for cancer and

various other diseases as well as the prevention of aging.

ACKNOWLEDGEMENTS

This work was supported in part by grants from: Fondazione del Monte di Bologna e Ravenna, MinSan 2008 "Molecular therapy in pediatric sarcomas and leukemias against IGF-1 receptor system", PRIN 2008 and FIRB 2010 (RBAP10447J) to AMM.

REFERENCES

1. Casar B, Pinto A, Crespo P. ERK dimmers and scaffold proteins: unexpected partners for a forgotten task. *Cell Cycle*. 2009; 8:1007-1013.
2. McCubrey JA, Steelman LS, Abrams SL, Bertrand FE, Ludwig DE, Basecke J, et al. Targeting Survival Cascades Induced by Activation of Raf/Raf/MEK/ERK, PI3K/PTEN/Akt/mTOR and Jak/STAT pathways for effective leukemia therapy. *Leukemia*. 2008;22:708-722.
3. McCubrey JA, Steelman LS, Abrams SL, Chappell WH, Russo S, Ove R et al. Emerging Raf Inhibitors. *Exp Opin Emerging Drugs* 2009;14:633-648.
4. Martelli AM, Evangelisti C, Chiarini F, Grimaldi C, Cappellini A, Ognibene A, McCubrey JA. The emerging role of the phosphatidylinositol 3-kinase/Akt/mammalian target of rapamycin signaling network in normal myelopoiesis and leukemogenesis. *Biochim Biophys Acta*. 2010;1803:991-1002.
5. Korotchkina LG, Leontieva OV, Bukreeva EI, Demidenko ZN, Gudkov AV, Blagosklonny MV. The choice between p53-induced senescence and quiescence is determined in part by the mTOR pathway. *Aging*. 2010; 2:344-352.
6. Safina AF, Varga AE, Bianchi A, Zheng Q, Kunnev D, Liang P, Bakin AV. Ras alters epithelial-mesenchymal transition in response to TGFbeta by reducing actin fibers and cell-matrix adhesion. *Cell Cycle*. 2009;8:284-298.
7. Downward J. Targeting Ras signaling pathways in cancer therapy. *Nature Reviews Cancer*. 2003;3:11-22.
8. Hayashi K, Shibata K, Morita T, Iwasaki K, Watanabe M, Sobue K. Insulin receptor substrate-1/SHP-2 interaction, a phenotype-dependent switching machinery of insulin-like growth factor-I signaling in vascular smooth muscle cells. *J Biol Chem*. 2004; 279:40807-40818.
9. Marais R, Light Y, Paterson HF, Marshall CJ. Ras recruits Raf-1 to the plasma membrane for activation by tyrosine phosphorylation. *EMBO J*. 1995;14:3136-145.
10. Lefloch R, Pouyssegur J, Lenormand P. Total ERK1/2 activity regulates cell proliferation. *Cell Cycle*. 2009;8:705-711.
11. Knizetova P, Ehrmann J, Hlobilkova A, Vancova I, Kalita O, Kolar Z, Bartek J. Autocrine regulation of glioblastoma cell cycle progression, viability and radioresistance through the VEGF-VEGFR2 (KDR) interplay. *Cell Cycle*. 2008;7:2553-2561.
12. Mebratu Y, Tesfaigzi Y. How ERK1/2 activation controls cell proliferation and cell death: Is subcellular localization the answer? *Cell Cycle*. 2009; 8:1168-1175.
13. Xing J, Ginty DD, Greenberg ME. Coupling of the Ras-MAPK pathway to gene activation by Rsk2, a growth factor regulated CREB kinase. *Science*. 1996;273:959-963.

14. Balan V, Leicht DT, Zhu J, Balan K, Kaplun A, Singh-Gupta V, Qin J, Ruan H, Comb MJ, Tzivion G. Identification of novel in vivo Raf-1 phosphorylation sites mediating positive feedback Raf-1 regulation by extracellular signal-regulated kinase. *Mol Biol Cell*. 2006;17:1141-1153.
15. Dougherty MK, Muller J, Ritt DA, Zhou M, Zhou XZ, Copeland TD, Conrads TP, Veenstra TD, Lu KP, Morrison DK. Regulation of Raf-1 by direct feedback phosphorylation. *Mol Cell*. 2005;17:215-224.
16. Brummer T, Naegele H, Reth M, Misawa Y. Identification of novel ERK-mediated feedback phosphorylation sites at the C-terminus of B-Raf. *Oncogene*. 2003;22:8823-8834.
17. Catalanotti, F, Reyes G, Jesenberger V Galabova-Kovacs G, de Matos Simoes R, Carugo O, Baccharini M. A Mek1-Mek2 heterodimer determines the strength and duration of the Erk signal. *Nat Struct Mol Biol*. 2009;16:294-303.
18. Davis RJ. Transcriptional regulation by MAP kinases. *Mol Reprod Dev*. 1995;42:459-467.
19. Martelli AM, Evangelisti C, Chiarini F, McCubrey JA. The phosphatidylinositol 3-kinase/Akt/mTOR signaling network as a therapeutic target in acute myelogenous leukemia patients. *Oncotarget*. 2010;1:89-103.
20. Zhao L, Vogt PK. Hot-spot mutations in p110alpha of phosphatidylinositol 3-kinase (pi3K): differential interactions with the regulatory subunit p85 and with RAS. *Cell Cycle*. 2010;9:596-600.
21. Franke TF, Kaplan DR, Cantley LC, Toker A. Direct regulation of the Akt proto-oncogene product by phosphatidylinositol-3,4-bisphosphate. *Science*. 1997;275:665-668.
22. Coffey PJ, Woodgett JR. Molecular cloning and characterisation of a novel putative protein-serine kinase related to the cAMP-dependent and protein kinase C families. *Eur J Biochem*. 1991;201:475-481.
23. Alessi DR, James SR, Downes CP, Holmes AB, Gaffney PR, Reese CB, Cohen P. Characterization of a 3-phosphoinositide-dependent protein kinase which phosphorylates and activates protein kinase Balpha. *Curr Biol*. 1997;7:261-269.
24. Lee JT, Steelman LS, Chappell WH, McCubrey JA. Akt inactivates ERK causing decreased response to chemotherapeutic drugs in advanced CaP cells. *Cell Cycle*. 2008;7:631-636.
25. Du K, Montminy M. CREB is a regulatory target for the protein kinase Akt/PKB. *J Biol Chem*. 1998;273:32377-32379.
26. Brennan P, Babbage JW, Burgering BM, Groner B, Reif K, Cantrell DA. Phosphatidylinositol 3-kinase couples the interleukin-2 receptor to the cell cycle regulator E2F. *Immunity*. 1997;7:679-689.
27. Kane LP, Shapiro VS, Stokoe D, Weiss A. Induction of NF-kappaB by the Akt/PKB kinase. *Curr Biol*. 1999;9:601-604.
28. Buitenhuis M, Coffey PJ. The role of the PI3K-PKB signaling module in regulation of hematopoiesis. *Cell Cycle*. 2009;8:560-566.
29. del Peso L, Gonzalez-Garcia M, Page C, Herrera R, Nuñez G. Interleukin-3-induced phosphorylation of BAD through the protein kinase Akt. *Science*. 1997;278:687-689.
30. Cross DA, Alessi DR, Cohen P, Andjelkovich M, Hemmings BA. Inhibition of glycogen synthase kinase-3 by insulin mediated by protein kinase B. *Nature*. 1995;378:785-789.
31. Chalhoub N, Baker SJ. PTEN and the PI3-kinase pathway in cancer. *Ann Rev Pathol Mech Dis*. 2009;4:127-150.
32. Diaz-Meco MT, Abu-Baker S. The Par-4/PTEN connection in tumor suppression. *Cell Cycle*. 2009;8:2518-2522.
33. Mahimainathan L, Choudhury GG. Inactivation of platelet-derived growth factor receptor by the tumor suppressor PTEN provides a novel mechanism of action of the phosphatase. *J Biol Chem*. 2004;279:15258-15268.
34. Gupta A, Yang Q, Pandita RK, Hunt CR, Xiang T, Misri S, Zeng S, Pagan J, Jeffery J, Puc J, Kumar R, Feng Z, et al. Cell cycle checkpoint defects contribute to genomic instability in PTEN deficient cells independent of DNA DSB repair. *Cell Cycle*. 2009;8:2198-2210.
35. McCubrey JA, Steelman LS, Kempf CR, Chappell WH, Abrams SL, Stivala F, Malaponte G, Nicoletti F, Libra M, Bäsecke J, Maksimovic-Ivanic D, Mijatovic S, et al. Therapeutic resistance resulting from mutations in Raf/MEK/ERK and PI3K/PTEN/Akt/mTOR signaling pathways. *J Cell Physiol*. 2011; In Press.
36. Silva A, Yunes JA, Cardoso BA, Martins LR, Jotta PY, Abecasis M, Nowill AE, Leslie NR, Cardoso AA, Barata JT. PTEN posttranslational inactivation and hyperactivation of the PI3K/Akt pathway sustain primary T cell leukemia viability. *J Clin Invest*. 2008;118:3762-3774.
37. Gao T, Furnari F, Newton AC. PHLPP: a phosphatase that directly dephosphorylates Akt, promotes apoptosis, and suppresses tumor growth. *Mol Cell*. 2005;18:13-24.
38. Damen JE, Liu L, Rosten P, Humphries RK, Jefferson AB, Majerus PW, Krystal G. The 145-kDa protein induced to associate with Shc by multiple cytokines is an inositol tetrakisphosphate and phosphatidylinositol 3,4,5-trisphosphate 5-phosphatase. *Proc Natl Acad Sci USA*. 1996;93:1689-1693.
39. Lioubin MN, Algate PA, Tsai S, Carlberg K, Aebersold A, Rohrschneider LR. p150Ship, a signal transduction molecule with inositol polyphosphate-5-phosphatase activity. *Genes & Dev*. 1996;10:1084-1095.
40. Muraille E, Pesesse X, Kuntz C, Erneux C. Distribution of the src-homology-2-domain-containing inositol 5-phosphatase SHIP-2 in both non-haemopoietic and haemopoietic cells and possible involvement in SHIP-2 in negative signaling of B-cells. *Biochem J*. 1999;342:697-705.
41. Taylor V, Wong M, Brandts C, Reilly L, Dean NM, Cowser LM, Moodie S, Stokoe D. 5'phospholipid phosphatase SHIP-2 causes protein kinase B inactivation and cell cycle arrest in glioblastoma cells. *Mol Cell Biol*. 2000;20:6860-6871.
42. Krymskaya VP, Goncharova EA. PI3K/mTORC1 activation in hamartoma syndromes: therapeutic prospects. *Cell Cycle*. 2009;8:403-413.
43. Vazquez-Martin A, Oliveras-Ferraro C, Lopez-Bonet E, Menendez JA. AMPK: Evidence for an energy-sensing cytotoxic tumor suppressor. *Cell Cycle*. 2009;8:3679-3683.
44. Tamburini J, Green AS, Chapuis N, Bardet V, Lacombe C, Mayeux P, Bouscary D. Targeting translation in acute myeloid leukemia: a new paradigm for therapy? *Cell Cycle*. 2009;8:3893-3899.
45. Sato T, Nakashima A, Guo L, Tamanoi F. Specific activation of mTORC1 by Rheb G-protein in vitro involves enhanced recruitment of its substrate protein. *J Biol Chem*. 2009;284:12783-12791.
46. Carracedo A, Ma L, Teruya-Feldstein J, Rojo F, Salmena L, Alimonti A, Egia A, Sasaki AT, Thomas G, Kozma SC, Papa A,

- Nardella C, *et al.* Inhibition of mTORC1 leads to MAPK pathway activation through a PI3K-dependent feedback loop in human cancer. *J Clin Invest.* 2008;118:3065-3074.
47. Hresko RC, Mueckler M. mTOR.RICTOR is the Ser473 kinase for Akt/protein kinase B in 3T3-L1 adipocytes. *J Biol Chem.* 2005;280:40406-40416.
48. Gonzalez E, McGraw TE. The Akt kinases: isoform specificity in metabolism and cancer. *Cell Cycle.* 2009;8:2502-2508.
49. Narasimhan SD, Mukhopadhyay A, Tissenbaum HA. InAKTivation of insulin/IGF-1 signaling by dephosphorylation. *Cell Cycle.* 2009;8:3878-3884.
50. Larrea MD, Wander SA, Slingerland JM. p27 as Jekyll and Hyde: regulation of cell cycle and cell motility. *Cell Cycle.* 2009;8:3455-3461.
51. Mobasheri A, Richardson S, Mobasheri R, Shakibaei M, Hoyland JA. Hypoxia inducible factor-1 and facilitative glucose transporters GLUT1 and GLUT3: putative molecular components of the oxygen and glucose sensing apparatus in articular chondrocytes. *Histol Histopathol.* 2005;20:1327-1338.
52. Eitel JA, Bijangi-Vishehsaraei K, Saadatzadeh MR, Bhavsar JR, Murphy MP, Pollok KE, Mayo LD. PTEN and p53 are required for hypoxia induced expression of maspin in glioblastoma cells. *Cell Cycle.* 2009;8:896-901.
53. Domina AM, Vrana JA, Gregory MA, Hann SR, Craig RW. MCL1 is phosphorylated in the PEST region and stabilized upon ERK activation in viable cells, and at additional sites with cytotoxic okadaic acid or taxol. *Oncogene.* 2004;23:5301-5315.
54. Wang JM, Chao JR, Chen W, Kuo ML, Yen JJ, Yang-Yen HF. The antiapoptotic gene Mcl-1 is upregulated by the phosphatidylinositol 3-kinase/Akt signaling pathway through a transcription factor complex containing CREB. *Mol Cell Biol.* 1999;19:6195-6206.
55. Pugazhenthii S, Nesterova A, Sable C, Heidenreich KA, Boxer LM, Heasley LE, Reusch JE. Akt/protein kinase B up-regulates Bcl-2 expression through cAMP-response element-binding protein. *J Biol Chem.* 2000;275:10761-10766.
56. Roux PP, Shahbazian D, Vu H, Holz MK, Cohen MS, Taunton J, Sonenberg N, Blenis J. RAS/ERK signaling promotes site-specific ribosomal protein S6 phosphorylation via RSK and stimulates Cap-dependent translation. *J Biol Chem.* 2007;282:14056-14064.
57. Shahbazian D, Roux PP, Mieulet V, Cohen MS, Raught B, Taunton J, Hershey JW, Blenis J, Pende M, Sonenberg N. The mTOR/PI3K and MAPK pathways converge on eIF4B to control its phosphorylation and activity. *EMBO J.* 2006;25:2781-2791.
58. Datta SR, Dudek H, Tao X, Masters S, Fu H, Gotoh Y, Greenberg ME. Akt phosphorylation of BAD couples survival signals to the cell-intrinsic death machinery. *Cell.* 1997; 91:231-241.
59. Fletcher JI, Huang DC. Controlling the cell death mediators Bax and Bak: puzzles and conundrums. *Cell Cycle.* 2008;7:39-44.
60. Dijkers PF, Medema RH, Lammers JW, Koenderman L, Coffey PJ. Expression of the pro-apoptotic Bcl-2 family member Bim is regulated by the forkhead transcription factor FKHR-L1. *Curr Biol.* 2000;10:1201-1204.
61. Qi XJ, Wildey GM, Howe PH. Evidence that Ser87 of BimEL is phosphorylated by Akt and regulates BimEL apoptotic function. *J Biol Chem.* 2006; 281:813-823.
62. Steelman LS, Abrams SL, Whelan J, Bertrand FE, Ludwig DE, Basecke J, Libra M, Stivala F, Milella M, Tafuri A, Lunghi P, Bonati A, *et al.* Contributions of the Raf/MEK/ERK, PI3K/PTEN/Akt/mTOR and JAK/STAT pathways to leukemia. *Leukemia.* 2008;22:686-707.
63. De La O JP, Murtaugh LC. Notch and Kras in pancreatic cancer: at the crossroads of mutation, differentiation and signaling. *Cell Cycle.* 2009;8:1860-1864.
64. Liu Y, Dean DC. Tumor initiation via loss of cell contact inhibition versus Ras mutation: do all roads lead to EMT? *Cell Cycle.* 2010;9:897-900.
65. Goel VK, Lazar AJ, Warneke CL, Redston MS, Haluska FG. Examination of mutations in BRAF, NRAS and PTEN in primary cutaneous melanoma. *J Inv Dermatol.* 2006;126:154-160.
66. Dahl C, Guidberg P. The genome and epigenome of malignant melanoma. *APMIS.* 2007;115:1161-1176.
67. Bacher U, Haferlach T, Schoch C, Kern W, Schnittger S. Implications of NRAS mutations in AML: a study of 2502 patients. *Blood.* 2006;107:3847-3853.
68. Wang S, Koromilas AE. Stat1 is an inhibitor of Ras-MAPK signaling and Rho small GTPase expression with implications in the transcriptional signature of Ras transformed cells. *Cell Cycle.* 2009;8:2070-2079.
69. Kiyoi H, Naoe T, Nakano Y, Yokota S, Minami S, Miyawaki S, Asou N, Kuriyama K, Jinnai I, Shimazaki C, Akiyama H, Saito K, *et al.* Prognostic implication of FLT3 and N-RAS gene mutations in acute myeloid leukemia. *Blood.* 1999;93:3074-3080.
70. Tannapfel A, Sommerer F, Benicke M, Katalinic A, Uhlmann D, Witzigmann H, Hauss J, Wittekind C. Mutations of the BRAF gene in cholangiocarcinoma but not in hepatocellular carcinoma. *Gut.* 2003;52:706-712.
71. Shan W, Liu J. Epithelial ovarian cancer: focus on genetics and animal models. *Cell Cycle.* 2009;8:731-735.
72. Davies H, Bignell GR, Cox C, Stephens P, Edkins S, Clegg S, Teague J, Woffendin H, Garnett MJ, Bottomley W, Davis N, Dicks E, *et al.* Mutations of the BRAF gene in human cancer. *Nature.* 2002;417:949-954.
73. Libra L, Malaponte G, Navolanic PM, Gangemi P, Bevelacqua V, Proietti L, Bruni B, Stivala F, Mazzarino MC, Travali S, McCubrey JA. *al.* Analysis of BRAF mutation in primary and metastatic melanoma. *Cell Cycle.* 2005;4:1382-1384.
74. Fransén K, Klinton M, Osterström A, Dimberg J, Monstein HJ, Söderkvist P. Mutation analysis of the BRAF, ARAF and RAF-1 genes in human colorectal adenocarcinomas. *Carcinogenesis.* 2004;25:527-533.
75. Wan PT, Garnett MJ, Roe SM, Lee S, Niculescu-Duvaz D, Good VM, Jones CM, Marshall CJ, Springer CJ, Barford D, Marais R; Cancer Genome Project. Mechanism of activation of the RAF-ERK signaling pathway by oncogenic mutations of B-RAF. *Cell.* 2004;116:855-867.
76. Buscà R, Abbe P, Mantoux F, Aberdam E, Peyssonnaud C, Eychène A, Ortonne JP, Ballotti R. Ras mediates the cAMP-dependent activation of extracellular signal-regulated kinases (ERKs) in melanocytes. *EMBO J.* 2000;19:2900-2910.
77. Rushworth LK, Hindley AD, O'Neill E, Kolch W. Regulation and role of Raf-1/B-Raf heterodimerization. *Mol Cell Biol.* 2006;26:2262-2272.
78. Garnett MJ, Rana S, Paterson H, Barford D, Marais R. Wild-type and mutant B-RAF activate C-RAF through distinct mechanisms involving heterodimerization. *Mol Cell.* 2005;20:963-969.
79. Zaravinos A, Kanellou P, Baritaki S, Bonavida B, Spandidos

- DA. BRAF and RKIP are significantly decreased in cutaneous squamous cell carcinoma. *Cell Cycle*. 2009;8:1402-1408.
80. Zebisch A, Staber PB, Delavar A, Bodner C, Hiden K, Fischereeder K, Janakiraman M, Linkesch W, Auner HW, Emberger W, Windpassinger C, Schimek MG, **et al.** Two transforming C-RAF germ-line mutations identified in patients with therapy-related acute myeloid leukemia. *Cancer Res*. 2006;166:3401-3408.
81. Zebisch A, Haller M, Hiden K, Goebel T, Hoefler G, Troppmair J, Sill H. Loss of Raf kinase inhibitor protein is a somatic event in the pathogenesis of therapy-related acute myeloid leukemias with c-RAF germline mutations. *Leukemia*. 2009;23:1049-1053.
82. Rodriguez-Viciana P, Tetsu O, Tidyman WE, Estep AL, Conger BA, Cruz MS, McCormick F, Rauen KA. Germline mutations in genes within the MAPK pathway cause cardio-facio-cutaneous syndrome. *Science*. 2006;311:1287-1290.
83. Nystrom A-M, Ekvall S, Berglund E, Bjorkqvist M, Braaten G, Duchon K, Enell H, Holmberg E, Holmund U, Olsson-Engman M, Anneren G, Bondeson M-L. Noonan and cardio-facio-cutaneous syndromes: two clinically and genetically overlapping disorders. *J Med Genet*. 2008;45:500-506.
84. Murugan AK, Dong J, Xie J, Xing M. MEK1 mutations, but not ERK2 mutations, occur in melanomas and colon carcinomas, but none in thyroid carcinomas. *Cell Cycle*. 2009;8:2122-2124.
85. El-Serag HB, Rudolph KL. Hepatocellular carcinoma: epidemiology and molecular carcinogenesis. *Gastroenterology*. 2007;132:2557-2576.
86. Montalto G, Cervello M, Giannitrapani L, Dantona F, Terranova A, Castagnetta LA. Epidemiology, risk factors, and natural history of hepatocellular carcinoma. *Ann N Y Acad Sci*. 2002;963:13-20.
87. Huynh H, Nguyen TT, Chow KH, Tan PH, Soo KC, Tran E. Overexpression of the mitogen-activated protein kinase (MAPK) kinase (MEK)-MAPK in hepatocellular carcinoma: its role in tumor progression and apoptosis. *BMC Gastroenterol*. 2003;3:19.
88. Ito Y, Sasaki Y, Horimoto M, Wada S, Tanaka Y, Kasahara A, Ueki T, Hirano T, Yamamoto H, Fujimoto J, Okamoto E, Hayashi N, **et al.** Activation of mitogen-activated protein kinases/extracellular signal-regulated kinases in human hepatocellular carcinoma. *Hepatology*. 1998;27:951-958.
89. Tanimura S, Chatani Y, Hoshino R, Sato M, Watanabe S, Kataoka T, Nakamura T, Kohno M. Activation of the 41/43 kDa mitogen-activated protein kinase signaling pathway is required for hepatocyte growth factor-induced cell scattering. *Oncogene*. 1998;17:57-65.
90. Tsuboi Y, Ichida T, Sugitani S, Genda T, Inayoshi J, Takamura M, Matsuda Y, Nomoto M, Aoyagi Y. Overexpression of extracellular signal-regulated protein kinase and its correlation with proliferation in human hepatocellular carcinoma. *Liver Int*. 2004;24:432-436.
91. Calvisi DF, Ladu S, Gorden A, Farina M, Conner EA, Lee JS, Factor VM, Thorgeirsson SS. Ubiquitous activation of Ras and Jak/Stat pathways in human HCC. *Gastroenterology*. 2006;130:1117-1128.
92. Fong CW, Chua MS, McKie AB, Ling SH, Mason V, Li R, Yusoff P, Lo TL, Leung HY, So SK, Guy GR. Sprouty 2, an inhibitor of mitogen-activated protein kinase signaling, is down-regulated in hepatocellular carcinoma. *Cancer Res*. 2006;66:2048-2058.
93. Yoshida T, Hisamoto T, Akiba J, Koga H, Nakamura K, Tokunaga Y, Hanada S, Kumemura H, Maeyama M, Harada M, Ogata H, Yano H, **et al.** Spreds, inhibitors of the Ras/ERK signal transduction, are dysregulated in human hepatocellular carcinoma and linked to the malignant phenotype of tumors. *Oncogene*. 2006;25:6056-6066.
94. Lee HC, Tian B, Sedivy JM, Wands JR, Kim M. Loss of Raf kinase inhibitor protein promotes cell proliferation and migration of human hepatoma cells. *Gastroenterology*. 2006;131:1208-1217.
95. Klein PJ, Schmidt CM, Wiesenauer CA, Choi JN, Gage EA, Yip-Schneider MT, Wiebke EA, Wang Y, Omer C, Sebolt-Leopold JS. The effects of a novel MEK inhibitor PD184161 on MEK-ERK signaling and growth in human liver cancer. *Neoplasia*. 2006;8:1-8.
96. Galle PR. Sorafenib in advanced hepatocellular carcinoma.-we have won a battle but not the war. *J Hepatology*. 2008;49:871-873.
97. Regimbeau JM, Colombat M, Mognol P, Durand F, Abdalla E, Degott C, Degos F, Farges O, Belghiti J. Obesity and diabetes as a risk factor for hepatocellular carcinoma. *Liver Transpl*. 2004;10:S69-S73.
98. Saxena NK, Sharma D, Ding X, Lin S, Marra F, Merlin D, Anania FA. Concomitant activation of the JAK/STAT, PI3K/AKT, and ERK signaling is involved in leptin-mediated promotion of invasion and migration of hepatocellular carcinoma cells. *Cancer Res*. 2007;67:2497-2507.
99. Schmitz KJ, Wohlschlaeger J, Lang H, Sotiropoulos GC, Malago M, Steveling K, Reis H, Ciccinnati VR, Schmid KW, Baba HA. Activation of the ERK and AKT signalling pathway predicts poor prognosis in hepatocellular carcinoma and ERK activation in cancer tissue is associated with hepatitis C virus infection. *J Hepatol*. 2008;48:83-90.
100. Benn J, Schneider, RJ. Hepatitis B virus HBx protein activates Ras-GTP complex formation and establishes a Ras, Raf, MAP kinase signaling cascade. *Proc Natl Acad Sci USA*. 1994;91:10350-10354.
101. Yun C, Cho H, Kim SJ, Lee JH, Park SY, Chan GK, Cho H. Mitotic aberration coupled with centrosome amplification is induced by hepatitis B virus X oncoprotein via the Ras-mitogen-activated protein/extracellular signal-regulated kinase-mitogen-activated protein pathway. *Mol Cancer Res*. 2004;2:159-169.
102. Chung TW, Lee YC, Kim CH. Hepatitis B viral HBx induces matrix metalloproteinase-9 gene expression through activation of ERK and PI-3K/AKT pathways: involvement of invasive potential. *FASEB J*. 2004;18:1123-1125.
103. Niepmann M. Activation of hepatitis C virus translation by a liver-specific microRNA. *Cell Cycle*. 2009;8:1473-1477, 2009.
104. Shor B, Gibbons JJ, Abraham RT, Yu K. Targeting mTOR globally in cancer: thinking beyond rapamycin. *Cell Cycle*. 2009;8:3831-3837.
105. Wang X, Meng X, Sun X, Liu M, Gao S, Zhao J, Pei F, Yu H. Wnt/beta-catenin signaling pathway may regulate cell cycle and expression of cyclin A and cyclin E protein in hepatocellular carcinoma cells. *Cell Cycle*. 2009;8:1567-1570.
106. Samuels Y, Wang Z, Bardelli A, Silliman N, Ptak J, Szabo S, Yan H, Gazdar A, Powell SM, Riggins GJ, Willson JK, Markowitz S, **et al.** High frequency of mutations of the PIK3CA gene in human cancers. *Science*. 2004;304:554.
107. Huang CH, Mandelker D, Gabelli SB, Amzel LM. Insights into the oncogenic effects of PIK3CA mutations from the structure of p110alpha/p85alpha. *Cell Cycle*. 2008;7:1151-1156.
108. Lee JW, Soung YH, Kim SY, Lee HW, Park WS, Nam SW, Kim SH, Lee JY, Yoo NJ, Lee SH. PIK3CA gene is frequently mutated in breast carcinomas and hepatocellular carcinomas. *Oncogene*. 2005;24:1477-1480.
109. Shatysteh L, Lu Y, Kuo WL, Baldocchi R, Godfrey T, Collins C,

- Pinkel D, Powell B, Mills GB, Gray JW. PIK3CA is implicated as an oncogene in ovarian cancer. *Nat Genet.* 1999;21:99-102.
- 110.** Ligresti G, Militello L, Steelman LS, Cavallaro A, Basile F, Nicoletti F, Stivala F, McCubrey JA, Libra M. PIK3CA mutations in human solid tumors. *Cell Cycle.* 2009;8:1352-1358.
- 111.** Calvisi DF, Ladu S, Gorden A, Farina M, Lee JS, Conner EA, Schroeder I, Factor VM, Thorgeirsson SS. Mechanistic and prognostic significance of aberrant methylation in the molecular pathogenesis of human hepatocellular carcinoma. *J Clin Invest.* 2007;117:2713-2722.
- 112.** Steelman LS, Bertrand FE, McCubrey JA. The complexity of PTEN: mutation, marker and potential target for therapeutic intervention. *Expert Opin Ther Targets.* 2004;8:537-550.
- 113.** Rhei E, Kang L, Bogomolny F, Federici MG, Borgen PI, Boyd J. Mutation analysis of the putative tumor suppressor gene PTEN/MMAC1 in primary breast carcinomas. *Cancer Res.* 1997;57:3657-3659.
- 114.** Singh B, Ittmann MM, Krolewski JJ. Sporadic breast cancers exhibit loss of heterozygosity on chromosome segment 10q23 close to the Cowden disease locus. *Genes Chromosome Can.* 1998;21:166-171.
- 115.** Trotman LC, Wang X, Alimonti A, Chen Z, Teruya-Feldstein J, Yang H, Pavletich NP, Carver BS, Cordon-Cardo C, Erdjument-Bromage H, Tempst P, Chi SG, **et al.** Ubiquitination regulates PTEN nuclear import and tumor suppression. *Cell.* 2007;128:141-156.
- 116.** Kappes H, Goemann C, Bamberger AM, Löning T, Milde-Langosch K. PTEN expression in breast and endometrial cancer: correlation with steroid hormone receptor status. *Pathobiology.* 2001;69:136-142.
- 117.** Suzuki A, Nakano T, Mak TW, Sasaki T. Portrait of PTEN: messages from mutant mice. *Cancer Sci.* 2008;99:209-213.
- 118.** Yao YJ, Ping XL, Zhang H, Chen FF, Lee PK, Ahsan H, Chen CJ, Lee PH, Peacocke M, Santella RM, Tsou HC. PTEN/MMAC1 mutations in hepatocellular carcinomas. *Oncogene.* 1999;18:3181-3185.
- 119.** Yeh KT, Chang JG, Chen YJ, Chen ST, Yu SY, Shih MC, Perng LI, Wang JC, Tsai M, Chang CP. Mutation analysis of the putative tumor suppressor gene PTEN/MMAC1 in hepatocellular carcinoma. *Cancer Invest.* 2000;18:123-129.
- 120.** Kawamura N, Nagai H, Bando K, Koyama M, Matsumoto S, Tajiri T, Onda M, Fujimoto J, Ueki T, Konishi N, Shiba T, Emi M. PTEN/MMAC1 mutations in hepatocellular carcinomas: somatic inactivation of both alleles in tumors. *Jpn J Cancer Res.* 1999;90:413-418.
- 121.** Fujiwara Y, Hoon DS, Yamada T, Umeshita K, Gotoh M, Sakon M, Nishisho I, Monden M. PTEN/MMAC1 mutation and frequent loss of heterozygosity identified in chromosome 10q in a subset of hepatocellular carcinomas. *Jpn J Cancer Res.* 2000;91:287-292.
- 122.** Wang L, Wang WL, Zhang Y, Guo SP, Zhang J, Li QL. Epigenetic and genetic alterations of PTEN in hepatocellular carcinoma. *Hepatol Res.* 2007;37:389-396.
- 123.** Rahman MA, Kyriazanos ID, Ono T, Yamanoi A, Kohno H, Tsuchiya M, Nagasue N. Impact of PTEN expression on the outcome of hepatitis C virus-positive cirrhotic hepatocellular carcinoma patients: possible relationship with COX II and inducible nitric oxide synthase. *Int J Cancer.* 2002;100:152-157.
- 124.** Hu TH, Wang CC, Huang CC, Chen CL, Hung CH, Chen CH, Wang JH, Lu SN, Lee CM, Changchien CS, Tai MH. Down-regulation of tumor suppressor gene PTEN, overexpression of p53, plus high proliferating cell nuclear antigen index predict poor patient outcome of hepatocellular carcinoma after resection. *Oncol Rep.* 2007;18:1417-1426.
- 125.** Chung TW, Lee YC, Ko JH, Kim CH. Hepatitis B Virus X protein modulates the expression of PTEN by inhibiting the function of p53, a transcriptional activator in liver cells. *Cancer Res.* 2003;63:3453-3458.
- 126.** Kang-Park S, Im JH, Lee JH, Lee YI. PTEN modulates hepatitis B virus-X protein induced survival signaling in Chang liver cells. *Virus Res.* 2006;122:53-60.
- 127.** Dhomen N, Reis-Filho JS, da Rocha Dias S, Hayward R, Savage K, Delmas V, Larue L, Pritchard C, Marais R. Oncogenic Braf induces melanocyte senescence and melanoma in mice. *Cancer Cell.* 2009;15:294-303.
- 128.** Dankort D, Curley DP, Cartlidge RA, Nelson B, Karnezis AN, Damsky WE Jr, You MJ, DePinho RA, McMahon M, Bosenberg M. Braf(V600E) cooperates with PTEN loss to induce metastatic melanoma. *Nat Genet.* 2009;41:544-552.
- 129.** Butler MP, Wang SI, Chaganti RS, Parsons R, Dalla-Favera R. Analysis of PTEN mutations and deletions in B-cell non-Hodgkin's lymphomas. *Genes Chromosomes Cancer.* 1999;24:322-327.
- 130.** Sakai A, Thieblemont C, Wellmann A, Jaffe ES, Raffeld M. PTEN gene alterations in lymphoid neoplasms. *Blood.* 1998;92:3410-3415.
- 131.** Uddin S, Hussain A, Al Hussein K, Platanius LC, Bhatia KG. Inhibition of phosphatidylinositol 3'-kinase induces preferentially killing of PTEN-null T leukemias through AKT pathway. *Biochem Biophys Res Commun.* 2004;320:932-938.
- 132.** Palomero T, Sulis ML, Cortina M, Real PJ, Barnes K, Ciofani M, Caparros E, Buteau J, Brown K, Perkins SL, Bhagat G, Agarwal AM, **et al.** Mutational loss of PTEN induces resistance to NOTCH1 inhibition in T-cell leukemia. *Nat Med.* 2007;13:1203-1210.
- 133.** Palomero T, Dominguez M, Ferrando AA. The role of the PTEN/AKT Pathway in NOTCH1-induced leukemia. *Cell Cycle.* 2008;7:965-970.
- 134.** Garcia JM, Silva J, Pena C, Garcia V, Rodríguez R, Cruz MA, Cantos B, Provencio M, España P, Bonilla F. Promoter methylation of the PTEN gene is a common molecular change in breast cancer. *Genes Chromosomes Cancer.* 2004;41:117-124.
- 135.** Tsutsui S, Inoue H, Yasuda K, Suzuki K, Higashi H, Era S, Mori M. Reduced expression of PTEN protein and its prognostic implications in invasive ductal carcinoma of the breast. *Oncology.* 2005;68:398-404.
- 136.** Yang H, Kong W, Zhao JJ, O'Donnell JD, Wang J. MicroRNA expression profiling in human ovarian cancer: miR-274 induces cell survival and cisplatin resistance by targeting PTEN. *Cancer Res.* 2008;68:425-433.
- 137.** Luo JM, Yoshida H, Komura S, Ohishi N, Pan L, Shigeno K, Hanamura I, Miura K, Iida S, Ueda R, Naoe T, Akao Y, **et al.** Possible dominant-negative mutation of the SHIP gene in acute myeloid leukemia. *Leukemia.* 2003;17:1-8.
- 138.** Metzner A, Horstmann MA, Fehse B, Ortmeier G, Niemeyer CM, Stocking C, Mayr GW, Jücker M. Gene transfer of SHIP-1 inhibits proliferation of juvenile myelomonocytic leukemia cells carrying KRAS2 or PTPN11 mutations. *Gene Ther.* 2007;14:699-703.
- 139.** Cheng JQ, Godwin AK, Bellacosa A, Taguchi T, Franke TF, Hamilton TC, Tschlis PN, Testa JR. AKT2, a putative oncogene encoding a member of a subfamily of protein-serine/threonine kinases, is amplified in human ovarian carcinomas. *Proc Natl Acad Sci USA.* 1992;89:9267-9271.
- 140.** Carpten JD, Faber AL, Horn C, Donoho GP, Briggs SL, Robbins

- CM, Hostetter G, Boguslawski S, Moses TY, Savage S, Uhlik M, Lin A, [et al.](#) A transforming mutation in the pleckstrin homology domain of AKT1 in cancer. *Nature*. 2007;448:439-444.
- 141.** Stemke-Hale K, Gonzalez-Angelo M, Lhuch A, Neve RM, Kuo WL, Davies M, Carey M, Hu Z, Guan Y, Sahin A, Symmans WF, Puzstai L, [et al.](#) An integrative genomic and proteomic analysis of PIK3CA, PTEN and Akt mutations in breast cancer. *Cancer Res*. 2008;68:6084-6091.
- 142.** Bellacosa A, DeFeo D, Godwin AK, Bell DW, Cheng JQ, Altomare DA, Wan M, Dubeau L, Scambia G, Masciullo V, Ferrandina G, Benedetti Panici P, [et al.](#) Molecular alterations of the Akt oncogene in breast cancer. *Int J Cancer*. 1995;64:280-285.
- 143.** Davies MA, Stemke-Hale K, Tellez C, Calderone TL, Deng W, Prieto VG, Lazar AJ, Gershenwald JE, Mills GB. A novel Akt3 mutation in melanoma tumours and cell lines. *Brit J Cancer*. 2008;99:1265-1268.
- 144.** Greenman C, Stephens P, Smith R, Dalglish GL, Hunter C, Bignell G, Davies H, Teague J, Butler A, Stevens C, Edkins S, O'Meara S, [et al.](#) Patterns of somatic mutation in human cancer genomes. *Nature*. 2007;446:153-158.
- 145.** Karst AM, Dai DL, Cheng JQ, Li G. Role of p53 up-regulated modulator of apoptosis and phosphorylated Akt in melanoma cell growth, apoptosis and patient survival. *Cancer Res*. 2006;66:9221-9226.
- 146.** Slipicevic A, Holm R, Nguyen MTP, Bøhler PJ, Davidson B, Flørenes VA. Expression of activated Akt and PTEN in malignant melanomas: Relationship with clinical outcome. *Am J Clin Pathol*. 2005;124:528-536.
- 147.** Balsara BR, Pei J, Mitsuuchi Y, Page R, Klein-Szanto A, Wang H, Unger M, Testa JR. Frequent activation of AKT in non-small cell lung carcinomas and preneoplastic bronchial lesions. *Carcinogenesis*. 2004;25:2053-2059.
- 148.** Shah A, Swain WA, Richardson D, Edwards J, Stewart DJ, Richardson CM, Swinson DE, Patel D, Jones JL, O'Byrne KJ. Phospho-Akt expression is associated with a favorable outcome in non-small cell lung cancer. *Clin Cancer Res*. 2005;11:2930-2936.
- 149.** Tanno S, Tanno S, Mitsuuchi Y, Altomare DA, Xiao GH, Testa JR. AKT activation up-regulates insulin-like growth factor I receptor expression and promotes invasiveness of human pancreatic cancer cells. *Cancer Res*. 2001;61:589-593.
- 150.** St-Germain ME, Gagnon V, Parent S, Asselin E. Regulation of COX-2 protein expression by Akt in endometrial cancer cells is mediated through NF- κ B pathway. *Mol Cancer*. 2004;3:7.
- 151.** Chow S, Minden MD, Hedley DW. Constitutive phosphorylation of the S6 ribosomal protein via mTOR and ERK signaling in the peripheral blasts of acute leukemia patients. *Exp Hematol*. 2006;34:1183-1191.
- 152.** Grandage VL, Gale RE, Linch DC, Khwaja A. PI3-kinase/Akt is constitutively active in primary acute myeloid leukaemia cells and regulates survival and chemoresistance via NF-kappaB, Mapkinase and p53 pathways. *Leukemia*. 2005;19:586-594.
- 153.** Ricciardi MR, McQueen T, Chism D, Milella M, Estey E, Kaldjian E, Sebolt-Leopold J, Konopleva M, Andreeff M. Quantitative single cell determination of ERK phosphorylation and regulation in relapsed and refractory primary acute myeloid leukemia. *Leukemia*. 2005;19:1543-1549.
- 154.** McCubrey JA, Milella M, Tafuri A, Martelli AM, Lunghi P, Bonati A, Bonati A, Cervello M, Lee JT, Steelman LS. Targeting the Raf/MEK/ERK pathway with small molecule inhibitors. *Current Opinion Investigational Drugs*. 2008;9:614-630.
- 155.** McCubrey JA, Steelman LS, Abrams SL, Chappell WH, Russo S, Ove R, Milella M, Tafuri A, Lunghi P, Bonati A, Stivala F, Nicoletti F, [et al.](#) Emerging MEK Inhibitors. *Exp Opin Emerging Drugs*. 2010; 15:203-223.
- 156.** Hu TH, Huang CC, Lin PR, Chang HW, Ger LP, Lin YW, Changchien CS, Lee CM, Tai MH. Expression and prognostic role of tumor suppressor gene PTEN/MMAC1/TEP1 in hepatocellular carcinoma. *Cancer*. 2003;97:1929-1940.
- 157.** Lee YI, Kang-Park S, Do SI, Lee YI. The hepatitis B virus-X protein activates a phosphatidylinositol 3-kinase-dependent survival signaling cascade. *J Biol Chem*. 2001;276:16969-16977.
- 158.** Mannová P, Beretta L. Activation of the N-Ras-PI3K-Akt-mTOR pathway by hepatitis C virus: control of cell survival and viral replication. *J Virol*. 2005;79:8742-8749.
- 159.** Knowles MA, Platt FM, Ross RL, Hurst CD. Phosphatidylinositol 3-kinase (PI3K) pathway activation in bladder cancer. *Cancer Metastasis Rev*. 2009;28:305-316.
- 160.** Graff JR, Zimmer SG. Translational control and metastatic progression: enhanced activity of the mRNA cap-binding protein eIF-4E selectively enhances translation of metastasis-related mRNAs. *Clin Exp Metastasis*. 2003;20:265-273.
- 161.** Zimmer SG, DeBenedetti A, Graff JR. Translational control of malignancy: the mRNA cap-binding protein, eIF-4E, as a central regulator of tumor formation, growth, invasion and metastasis. *Anticancer Res*. 2000;20:1343-1351.
- 162.** Galmozzi E, Casalini P, Iorio MV, Casati B, Olgiati C, Menard S. HER2 signaling enhances 5'UTR-mediated translation of c-Myc mRNA. *J Cell Physiol*. 2004;200:82-88.
- 163.** Podar K, Anderson KC. A therapeutic role for targeting c-Myc/Hif-1-dependent signaling pathways. *Cell Cycle*. 2010;9:1722-1728.
- 164.** Gera JF, Mellinghoff IK, Shi Y, Rettig MB, Tran C, Hsu JH, Sawyers CL, Lichtenstein AK. AKT activity determines sensitivity to mammalian target of rapamycin (mTOR) inhibitors by regulating cyclin D1 and c-myc expression. *J Biol Chem*. 2004;279:2737-2746.
- 165.** Chung J, Bachelder RE, Lipscomb EA, Shaw LM, Mercurio AM. Integrin (alpha 6 beta 4) regulation of eIF-4E activity and VEGF translation: a survival mechanism for carcinoma cells. *J Cell Biol*. 2002;158:165-174.
- 166.** Drobnyak M, Osman I, Scher HI, Fazzari M, Cordon-Cardo C. Overexpression of cyclin D1 is associated with metastatic prostate cancer to bone. *Clin Cancer Res*. 2000;6:1891-1895.
- 167.** Dunsmuir WD, Gillett CE, Meyer LC, Young MP, Corbishley C, Eeles RA, Kirby RS. Molecular markers for predicting prostate cancer stage and survival. *BJU Int*. 2000;6:869-878.
- 168.** Gallant P, Steiger D. Myc's secret life without Max. *Cell Cycle*. 2009;8:3848-3853.
- 169.** Hydrbring P, Larsson LG. Cdk2: a key regulator of the senescence control function of Myc. *Aging*. 2010;2:244-250.
- 170.** Jin J, Wang GL, Timchenko L, Timchenko NA. GSK3beta and aging liver. *Aging*. 2009;1:582-585.
- 171.** Gan B, DePinho RA. mTORC1 signaling governs hematopoietic stem cell quiescence. *Cell Cycle*. 2009;8:1003-1006.
- 172.** Lluís F, Cosma MP. Somatic cell reprogramming control: signaling pathway modulation versus transcription factor activities. *Cell Cycle*. 2009;8:1138-1144.
- 173.** Wu GJ, Sinclair CS, Paape J, Ingle JN, Roche PC, James CD, Couch FJ. 17q23 amplifications in breast cancer involve the PAT1, RAD51C, PS6K and SIGMA1B genes. *Cancer Res*. 2000;60:5371-5375

- 174.** Barlund M, Forozan F, Kononen J, Bubendorf L, Chen Y, Bittner ML, Torhorst J, Haas P, Bucher C, Sauter G, Kallioniemi OP, Kallioniemi A. Detecting activation of ribosomal protein S6 kinase by complementary DNA and tissue microarray analysis. *J Natl Cancer Inst.* 2000;92:1252-1259.
- 175.** Neshat MS, Mellinghoff IK, Tran C, Stiles B, Thomas G, Petersen R, Frost P, Gibbons JJ, Wu H, Sawyers CL. Enhanced sensitivity of PTEN-deficient tumors to inhibition of FRAP/mTOR. *Proc Natl Acad Sci USA.* 2001;98:10314-10319.
- 176.** Podsypanina K, Lee RT, Politis C, Hennessy I, Crane A, Puc J, Neshat M, Wang H, Yang L, Gibbons J, Frost P, Dreisbach V, **et al.** An inhibitor of mTOR reduces neoplasia and normalizes p70/S6 kinase activity in PTEN^{+/−} mice. *Proc Natl Acad Sci USA.* 2001;98:10320-10325.
- 177.** Wu C, Huang J. Phosphatidylinositol 3-kinase-AKT-mammalian target of rapamycin pathway is essential for neuroendocrine differentiation of prostate cancer. *J Biol Chem.* 2007;282:3571-3583.
- 178.** Kinkade CW, Castillo-Martin M, Puzio-Kuter A, Yan J, Foster TH, Gao H, Sun Y, Ouyang X, Gerald WL, Cordon-Cardo C, Abate-Shen C. Targeting AKT/mTOR and ERK MAPK signaling inhibits hormone-refractory prostate cancer in a preclinical mouse model. *J Clin Invest.* 2008;118:3051-3064.
- 179.** Demidenko ZN, Korotchkina LG, Gudkov AV, Blagosklonny MV. Paradoxical suppression of cellular senescence by p53. *Proc Natl Acad Sci USA.* 2010;107:9660-9664.
- 180.** Liu Y, Elf SE, Asai T, Miyata Y, Liu Y, Sashida G, Huang G, Di Giandomenico S, Koff A, Nimer SD. The p53 tumor suppressor protein is a critical regulator of hematopoietic stem cell behavior. *Cell Cycle.* 2009;8:3120-3124.
- 181.** Jung-Hynes B, Ahmad N. Role of p53 in the anti-proliferative effects of Sirt1 inhibition in prostate cancer cells. *Cell Cycle.* 2009;8:1478-1483.
- 182.** Yamakuchi M, Lowenstein CJ. MiR-34, SIRT1 and p53: the feed back loop. *Cell Cycle.* 2009;8:712-715.
- 183.** Cheng Q, Chen J. Mechanism of p53 stabilization by ATM after DNA damage. *Cell Cycle.* 2010;9:472-478.
- 184.** Wang B, Xiao Z, Ko HL, Ren EC. The p53 response element and transcriptional repression. *Cell Cycle.* 2010;9:870-879.
- 185.** O'Prey J, Crighton D, Martin AG, Vousden KH, Fearhead HO, Ryan KM. p53-mediated induction of Noxa and p53AIP1 requires NFκB. *Cell Cycle.* 2010;9:947-952.
- 186.** Kelley KD, Miller KR, Todd A, Kelley AR, Tuttle R, Berberich SJ. YPEL3, a p53-regulated gene that induces cellular senescence. *Cancer Res.* 2010;70:3566-575.
- 187.** Lane DP, Cheok CF, Brown C, Madhumalar A, Ghadessy FJ, Verma C. Mdm2 and p53 are highly conserved from placozoans to man. *Cell Cycle.* 2010;9:540-547.
- 188.** Ho L, Alman B. Protecting the hedgerow: p53 and hedgehog pathway interactions. *Cell Cycle.* 2010;9:506-511.
- 189.** Zawacka-Pankau J, Kostecka A, Sznarkowska A, Hedstrom E, Kawiak A. p73 tumor suppressor protein: a close relative of p53 not only in structure but also in anti-cancer approach? *Cell Cycle.* 2010;9:720-728.
- 190.** Galluzzi L, Morselli E, Kepp O, Maiuri MC, Kroemer G. Defective autophagy control by the p53 rheostat in cancer. *Cell Cycle.* 2010;9:250-255.
- 191.** Matthew EM, Hart LS, Astrinidis A, Navaraj A, Dolloff NG, Dicker DT, Henske EP, El-Deiry WS. The p53 target Plk2 interacts with TSC proteins impacting mTOR signaling, tumor growth and chemosensitivity under hypoxic conditions. *Cell Cycle.* 2009;8:4168-4175.
- 192.** Mancini F, Moretti F. Mitochondrial MDM4 (MDMX): an unpredicted role in the p53-mediated intrinsic apoptotic pathway. *Cell Cycle.* 2009;8:3854-3849.
- 193.** Kim DH, Rho K, Kim S. A theoretical model for p53 dynamics: identifying optimal therapeutic strategy for its activation and stabilization. *Cell Cycle.* 2009;8:3707-3716.
- 194.** Jain AK, Barton MC. Regulation of p53: TRIM24 enters the RING. *Cell Cycle.* 2009;8:3668-3674.
- 195.** McCubrey JA, Abrams SL, Ligresti G, Misaghian N, Wong ET, Basecke J, Troppmair J, Libra N, Nicoletti F, Molton S, McMahon M, Evangelisti C, **et al.** Involvement of p53 and Raf/MEK/ERK pathways in hematopoietic drug resistance. *Leukemia.* 2008;2:2080-2090.
- 196.** McCubrey JA, Steelman LS, Chappell WH, Abrams SL, Wong EW, Chang F, Lehmann B, Terrian DM, Milella M, Tafuri A, Stivala F, Libra M, **et al.** Roles of the Raf/MEK/ERK pathway in cell growth, malignant transformation and drug resistance. *Biochim Biophys Acta.* 2007;1773:1263-1284.
- 197.** McCubrey J, LaHair M, Franklin RA. Reactive oxygen species-induced activation of the MAP kinase signaling pathway. *Antioxidants & Redox Signaling.* 2006;8:1745-1748.
- 198.** Franklin R, Rodriguez-Mora O, La Hair M, McCubrey JA. Activation of the calcium/calmodulin-dependent protein kinases as a consequence of oxidative stress. *Antioxidants & Redox Signaling.* 2006;8:1807-1817.
- 199.** Brauer PM, Tyner AL. RAKing in AKT: a tumor suppressor function for the intracellular tyrosine kinase FRK. *Cell Cycle.* 2009;8:2728-2732.
- 200.** Yang WL, Wu CY, Wu J, Lin HK. Regulation of Akt signaling activation by ubiquitination. *Cell Cycle.* 2010;9:487-497.
- 201.** Lal MA, Bae D, Camilli TC, Patierno SR, Ceryak S. AKT1 mediates bypass of the G1/S checkpoint after genotoxic stress in normal human cells. *Cell Cycle.* 2009;8:1589-1602.
- 202.** Zhang H. Skip the nucleus, AKT drives Skp2 and FOXO1 to the same place? *Cell Cycle.* 2010;9:868-869.
- 203.** Misaghian N, Ligresti G, Steelman LS, Bertrand FE, Basecke J, Libra M, Nicoletti F, Stivala F, Milella M, Tafuri A, Cervello M, Martelli AM, McCubrey JA. Targeting the leukemic stem cell – the holy grail of leukemia therapy. *Leukemia.* 2009;23:25-42.
- 204.** Yilmaz NH, Valdez R, Theisen BK, Guo W, Ferguson DO, Wu H, Morrison SJ. PTEN-dependence distinguishes haematopoietic stem cells from leukemia-initiating cells. *Nature.* 2006;441:475-478.
- 205.** Zhou J, Wulkuhle, H, Zhang H, Gu P, Yang Y, Deng J, Margolick JB, Liotta LA, Petricoin E 3rd, Zhang Y. Activation of the PTEN/mTOR/STAT3 pathway in breast cancer stem-like cells is required for viability and maintenance. *Proc Natl Acad Sci USA.* 2007;104:16158-16163.
- 206.** Korkaya H, Paulson A, Charafe-Jauffret E, Ginestier C, Brown M, Dutcher J, Clouthier SG, Wicha MS. Regulation of mammary stem/progenitor cells by PTEN/Akt/β-catenin signaling. *PLOS Biology.* 2009;7: e1000121.
- 207.** Yim EK, Siwko S, Lin SY. Exploring Rak tyrosine kinase function in breast cancer. *Cell Cycle.* 2009;8:2360-2364.
- 208.** Shan W, Liu J. Epithelial ovarian cancer: focus on genetics and animal models. *Cell Cycle.* 2009;8:731-735.
- 209.** Saudemont A, Colucci F. PI3K signaling in lymphocyte migration. *Cell Cycle.* 2009;8:3307-3310.

- 210.** Sabisz M, Skladonowski A. Cancer stem cells and escape from drug-induced premature senescence in human lung tumor cells: implications for drug resistance and in vitro drug screening models. *Cell Cycle*. 2009;8:3208-3217.
- 211.** Shafee N, Smith CR, Wei S, Kim Y, Mills GB, Hortobagyi GN, Stanbridge EJ, Lee EY. Cancer stem cells contribute to cisplatin resistance in Brca1/p53-mediated mouse mammary tumors. *Cancer Res*. 2008;68:3243-3250.
- 212.** Heddleston JM, Li Z, McLendon RE, Hjelmeland AB, Rich JN. The hypoxic microenvironment maintains glioblastoma stem cells and promotes reprogramming towards a cancer stem cell phenotype. *Cell Cycle*. 2009;8:3274-3284.
- 213.** Ma S, Lee TK, Zheng BJ, Chan KW, Guan XY. CD133+ cancer stem cells confer chemoresistance by preferential expression of the Akt/PKB survival pathway. *Oncogene*. 2008;27:1749-1758.
- 214.** Li X, Lewis MT, Huang J, Gutierrez C, Osborne CK, Wu MF, Hilsenbeck SG, Pavlick A, Zhang X, Chamness GC, Wong H, Rosen J, **et al.** Intrinsic resistance of tumorigenic breast cancer cells to chemotherapy. *J Natl Cancer Inst*. 2008;100:672-679.
- 215.** McCubrey JA, Abrams SL, Stadelman K, Chappell WH, Lahair M, Ferland RA, Steelman LS. Targeting signal transduction pathways to eliminate chemotherapeutic drug resistance and cancer stem cells. *Advances in Enzyme Regulation*. 2010;50:285-307.
- 216.** McCubrey JA, Chappell WH, Abrams SL, Franklin RA, Long JM, Sattler JA, Kempf CR, Laidler P, Steelman LS. Targeting the cancer initiating cells: the Achilles' heel of cancer. *Advances in Enzyme Regulation*. 2011;51: In Press.
- 217.** Kandouz M, Haidara K, Zhao J, Brisson ML, Batist G. The EphB2 tumor suppressor induces autophagic cell death via concomitant activation of the ERK1/2 and PI3K pathways. *Cell Cycle*. 2010;9:398-407.
- 218.** Garinis GA, Schumacher B. Transcription-blocking DNA damage in aging and longevity. *Cell Cycle*. 2009;8:2134-2135.
- 219.** Bazarov AV, Hines WC, Mukhopadhyay R, Beliveau A, Meldoyev S, Zaslavsky Y, Yaswen P. Telomerase activation by c-Myc in human mammary epithelial cells requires additional genomic changes. *Cell Cycle*. 2009;8:3373-3378.
- 220.** Mele DA, Bista P, Baez DV, Huber BT. Dipeptidyl-peptidase 2 is an essential survival factor in the regulation of cell quiescence. *Cell Cycle*. 2009;8:2425-2434.
- 221.** Acquaviva C, Chevrier V, Chauvin JP, Fournier G, Birnbaum D, Rosnet O. The centrosomal FOP protein is required for cell cycle progression and survival. *Cell Cycle*. 2009;8:1217-1227.
- 222.** Jin J, Wang GL, Salisbury E, Timchenko L, Timchenko NA. GSK3beta-cyclin D3-CUGBP1-eIF2 pathway in aging and in myotonic dystrophy. *Cell Cycle*. 2009;8:2356-2359.
- 223.** Gems D, Doonan R. Antioxidant defense and aging in *C. elegans*: is the oxidative damage theory of aging wrong? *Cell Cycle*. 2009;8:1681-1687.
- 224.** Perucca P, Cazzalini O, Madine M, Savio M, Laskey RA, Vannini V, Prosperi E, Stivala LA. Loss of p21 CDKN1A impairs entry to quiescence and activates a DNA damage response in normal fibroblasts induced to quiescence. *Cell Cycle*. 2009;8:105-114.
- 225.** Riffell JL, Zimmerman C, Knong A, McHardy LM, Roberg M. Effects of chemical manipulation of mitotic arrest and slippage on cancer cell survival and proliferation. *Cell Cycle*. 2009;8:3025-3038.
- 226.** Shan W, Liu J. Epithelial ovarian cancer: focus on genetics and animal models. *Cell Cycle*. 2009;8:731-735.
- 227.** Zuin A, Castellano-Esteve D, Ayte J, Hidalgo E. Living on the edge: stress and activation of stress responses promote lifespan extension. *Aging*. 2010;2:231-237.
- 228.** Blagosklonny MV. Revisiting the antagonistic pleiotropy theory of aging: TOR-driven program and quasi-program. *Cell Cycle*. 2010 Aug 15;9(16):3151-3156.
- 229.** Harikumar KB, Aggarwal BB. Resveratrol: a multitargeted agent for age-associated chronic diseases. *Cell Cycle*. 2008;7:1020-1035.
- 230.** Demidenko ZN, Blagosklonny MV. At concentrations that inhibit mTOR, resveratrol suppresses cellular senescence. *Cell Cycle*. 2009;8:1901-1904.
- 231.** Demidenko ZN, Shtutman M, Blagosklonny MV. Pharmacologic inhibition of MEK and PI-3K converges on the mTOR/S6 pathway to decelerate cellular senescence. *Cell Cycle*. 2009;8:1896-1900.
- 232.** Demidenko ZN, Zubova SG, Bukreeva EI, Pospelov VA, Pospelova TV, Blagosklonny MV. Rapamycin decelerates cellular senescence. *Cell Cycle*. 2009;8:1888-1895.
- 233.** Blagosklonny MV. Aging-suppressants: Cellular senescence (hyperactivation) and its pharmacologic deceleration. *Cell Cycle*. 2009;8:1883-1887.
- 234.** Alimova IN, Liu B, Fan Z, Edgerton SM, Dillon T, Lind SE, Thor AD. Metformin inhibits breast cancer cell growth, colony formation and induces cell cycle arrest in vitro. *Cell Cycle*. 2009;8:909-915.
- 235.** Guenther GG, Gdinger AL. A new take on ceramide: starve cells by cutting off the nutrient supply. *Cell Cycle*. 2009;8:1122-1126.
- 236.** Korotchkina LG, Demidenko ZN, Gudkov AV, Blagosklonny MV. Cellular quiescence caused by the Mdm-2 inhibitor nutlin-3A. *Cell Cycle*. 2009;8:3777-3781.
- 237.** Shen J, Curtis C, Tavares S, Tower J. A screen of apoptosis and senescence regulatory genes for life span effects when overexpressed in *Drosophila*. *Aging*. 2009;1:191-211.
- 238.** Wee S, Jagani Z, Xiang KX, Loo A, Dorsch M, Yao YM, Sellers WR, Lengauer C, Stegmeier F. PI3K pathway activation mediates resistance to MEK inhibitors in KRAS mutant cancers. *Cancer Res*. 2009; 69: 4286-4293.
- 239.** Hoeflich KP, O'Brien C, Boyd Z, Cavet G, Guerrero S, Jung K, Januario T, Savage H, Punnoose E, Truong T, Zhou W, Berry L, **et al.** In vivo antitumor activity of MEK and phosphatidylinositol 3-kinase in basal-like breast cancer models. *Clin Cancer Res*. 2009; 15: 4649-4664.
- 240.** Laurent-Puig P, Cayre A, Manceau G, Buc E, Bachet JB, Lecomte T, Rougier P, Lievre A, Landi B, Boige V, Ducreux M, Ychou M, **et al.** Analysis of PTEN, BRAF, and EGFR status in determining benefit from cetuximab therapy in wild-type KRAS metastatic colon cancer. *J Clin Oncol*. 2009; 27:5924-5930.
- 241.** Laurent-Puig P, Lievre A, Blons H. Mutations and response to epidermal growth factor receptor inhibitors. *Clin Cancer Res*. 2009; 15:1133-1139.
- 242.** Lièvre A, Bachet JB, Le Corre D, Boige V, Landi B, Emile JF, Côté JF, Tomicic G, Penna C, Ducreux M, Rougier P, Penault-Llorca F, Laurent-Puig P. KRAS mutation status is predictive of response to cetuximab therapy in colorectal cancer. *Cancer Res*. 2006; 66:3992-3995.

- 243.** Lièvre A, Blons H, Laurent-Puig P. Oncogenic mutations as predictive factors in colorectal cancer. *Oncogene*. 2010; 29:3033-3043.
- 244.** Pratilas CA, Hanrahan AJ, Halilovic E, Persaud Y, Soh J, Chitale D, Shigematsu H, Yamamoto H, Sawai A, Janakiraman M, Taylor BS, Pao W, **et al.** Genetic predictors of MEK dependence in non-small cell lung cancer. *Cancer Res*. 2008; 68:9375-9383.
- 245.** Pratilas CA, Solit DB. Targeting the mitogen-activated protein kinase pathway: physiological feedback and drug response. *Clin Cancer Res*. 2010; 16:3329-3334

Potential of mTOR inhibitors for the treatment of subependymal giant cell astrocytomas in tuberous sclerosis complex

Philippe Major

Department of Pediatrics, Neurology Service, Centre Hospitalier Universitaire Sainte-Justine, Université de Montréal, Montréal, Québec, Canada

Key words: Rapamycin, mTOR, tuberous sclerosis complex, subependymal giant cell astrocytoma

Received: 3/3/11; **Accepted:** 3/12/11; **Published:** 3/12/11

Correspondence: philippe.major@umontreal.ca

© Major. This is an open-access article distributed under the terms of the Creative Commons Attribution License, which permits unrestricted use, distribution, and reproduction in any medium, provided the original author and source are credited.

Abstract: Rapamycin inhibits the mTOR (target of rapamycin) pathway and extends lifespan in multiple species. The tuberous sclerosis complex (TSC) protein is a negative regulator of mTOR. In humans, loss of the TSC protein results in a disorder characterized clinically by the growth of benign tumors in multiple organs, due to overactivation of mTOR inhibition. Subependymal giant cell astrocytomas (SEGAs) are benign brain tumors associated with TSC that have traditionally been treated by surgery, but for which mTOR inhibitors have recently been suggested as potential alternative treatments. The duration of mTOR treatment for SEGAs might have to be prolonged, probably lifelong, because SEGAs usually grow back after treatment is stopped. This cohort of patients who will experience prolonged exposure to mTOR inhibitors should be carefully followed longitudinally to better document long term side effects, but also to compare their longevity with the one of similar patients with TSC. These patients represent a unique opportunity to study the potential anti-aging properties of mTOR inhibitors in humans.

Rapamycin (also called sirolimus) is an immunosuppressive drug that has recently been shown to extend lifespan in multiple species including mammals [1]. This anti-aging property is presumably related to the mTOR (mammalian target of rapamycin) inhibition properties of rapamycin. The mTOR pathway is crucial for the coordination of growth in response to energy status, stress, and nutrient availability [2,3].

The potential anti-aging properties of rapamycin and of other mTOR inhibitors, such as RAD001 (everolimus), and CCI-779 (temsirolimus) are of great interest. Unfortunately, the side effects related to these drugs preclude the undertaking of research trials about their impacts on aging in healthy individuals. Considering this obstacle, experts in the field of aging have suggested that the potential anti-aging drugs should be introduced to the clinical trials for therapy of particular diseases and then be approved for prevention of all age-related diseases in healthy individuals [4]. In this context, tuberous sclerosis complex (TSC) seems to be an ideal disease model where the potential of mTOR inhibitors can be assessed because these drugs are

increasingly being tested and used clinically to treat certain aspects of this condition [5].

TSC is an autosomal dominant disorder caused by the inactivation in one of two tumor suppressor genes, hamartin (TSC1) or tuberin (TSC2). In the normal state, the hamartin-tuberin complex activates the protein Rheb, which inhibits mTOR. If a TSC mutation is present, mTOR is constitutively activated, leading to abnormal cellular proliferation, ribosome biogenesis, and mRNA translation (see [2] for complete review of the mTOR molecular pathway). In consequence, TSC is characterized clinically by the growth of benign tumors in multiple organs, including the brain, the heart, the kidneys, the lungs, and the skin [6]. Its incidence is estimated at 1 in 6000 live births [7]. The severity of the disease is highly variable, ranging from mild skin manifestations to intractable epilepsy, mental retardation, and autism [8].

The only report studying specifically the causes of death in TSC was performed at the Mayo clinic [9]. Overall, the survival curves showed a decreased survival for

patients with TSC compared with the general population. Of the 355 patients with TSC followed, 40 died of causes related to TSC, with renal disease being the most common cause of death (11/40). Ten patients died as a consequence of brain tumors and four patients died of lymphangiomyomatosis (LAM). Thirteen patients with severe mental impairment passed away due to status epilepticus or bronchopneumonia. One baby died of cardiac failure and one child died of rupture of an aneurysm of the thoracic aorta.

The main current clinical complication related to TSC for which treatment with mTOR inhibitors is indicated are subependymal giant cell astrocytomas (SEGA). This complication affects approximately 15% of patients with TSC and it occurs in the pediatric age group [10]. SEGAs tend to lose their propensity to grow in the early twenties. They are slow-growing benign tumors of mixed glioneuronal lineage that arise from the growth of pre-existing subependymal nodules, which are asymptomatic lesions that protrude from the walls of the ventricles [10]. SEGAs most commonly grow near the foramen of Monro. This can lead to obstruction of the normal cerebrospinal fluid circulation and subsequent intracranial hypertension that can be fatal if left untreated. The distinction between a SEGA and a subependymal nodule is still debated. Generally, a clinical diagnosis of SEGA is made when there are symptoms of intracranial hypertension, papilledema, or radiological evidence of hydrocephalus or interval growth.

The traditional management approach is to monitor SEGAs with periodic neuroimaging and to resect those that exhibit growth and/or cause clinical signs of intracranial hypertension. This approach is being challenged by recent observations that suggest that mTOR inhibitors, such as rapamycin (sirolimus) and RAD001 (everolimus), can induce partial regression of SEGAs [11,12,13]. The first report showing clear regression of SEGAs in five patients with the use of rapamycin was published in 2006 [11]. Recently, a phase II trial [13] using everolimus to treat SEGAs in 28 patients with TSC showed SEGA reduction of at least 30% in 21 patients (75%) and at least 50% in 9 patients (32%). Everolimus was well tolerated as only single cases of grade 3 treatment-related sinusitis, pneumonia, viral bronchitis, tooth infection, stomatitis, and leukopenia were reported.

These observations suggest that mTOR inhibitors could serve as an acceptable alternative treatment to SEGA surgery. Renal angiomyolipomas and lymphangiomyomatosis (LAM) are other TSC manifestations for which mTOR inhibitors have proven potential efficacy

[14]. In addition, animal models of TSC have suggested that mTOR inhibitors could have beneficial effects on cognitive deficits [15] and on epileptogenesis [16]. Whether similar benefits would be observed in humans with TSC is still unknown. Research trials are ongoing and should soon provide answers to these questions.

Other important questions remain regarding the use of mTOR inhibitors for the treatment of SEGA in TSC. Side effects, especially long term side effects, and optimal duration of treatment are still under investigation. The short-term side effects related to rapamycin are generally considered acceptable. The most common side effects are oral ulcers, acneiform rash, thrombocytopenia, hyperlipidemia, impaired wound healing, and immunosuppression [14]. Long term side effects are less known. For example, reports from the literature related to the use of rapamycin for kidney transplant prevention suggested that rapamycin might be associated with impaired spermatogenesis and, as a corollary, may reduce male fertility [17]. This observation might not be applicable to other patients populations, but requires further investigation.

The duration of treatment might be prolonged, probably lifelong. There is clear evidence that SEGAs grow back after the mTOR inhibitor is stopped [11]. Most experts currently recommend continuation of mTOR inhibitors at the lowest efficacious dose. This cohort of patients who will experience prolonged exposure to mTOR inhibitors should be carefully followed longitudinally to better document long term side effects, but also to compare their longevity with the one of similar patients with TSC. These patients represent a unique opportunity to study the potential anti-aging properties of mTOR inhibitors in humans.

In conclusion, a new treatment era has begun in the field of TSC since the discovery of the potential beneficial effects of mTOR inhibitors. Although the use of mTOR inhibitors is becoming increasingly accepted, especially for the treatment of SEGAs in TSC, questions now remain about the duration of treatment and long term side effects. Whether mTOR inhibitors will have a significant impact on longevity in TSC is unknown, but warrants attention as mTOR inhibitors are increasingly recognized as anti-aging drugs in animal models. Long-term prospective studies in patients with TSC might provide evidence about the potential anti-aging properties of mTOR inhibitors in humans.

ACKNOWLEDGEMENTS

This work was not funded by any sources.

CONFLICT OF INTERESTS STATEMENT

The author of this manuscript has no conflict of interests to declare.

REFERENCES

1. Harrison DE, Strong R, Sharp ZD, Nelson JF, Astle CM, Flurkey K, Nadon NL, Wilkinson JE, Frenkel K, Carter CS, Pahor M, Javors MA, Fernandez E, Miller RA. Rapamycin fed late in life extends lifespan in genetically heterogeneous mice. *Nature*. 2009; 460(7253): 392-395.
2. Orlova KA, Crino PB. The tuberous sclerosis complex. *Ann N Y Acad Sci*. 2010; 1184: 87-105.
3. Reiling JH, Sabatini DM. Stress and mTOR signaling. *Oncogene*. 2006; 25: 6373-6383.
4. Blagosklonny MV. Validation of anti-aging drugs by treating age-related diseases. *Aging*. 2009; 1(3): 281-288.
5. Franz DN, Bissler JJ, McCormack FX. Tuberous sclerosis complex: neurological, renal and pulmonary manifestations. *Neuropediatrics*. 2010; 41: 199-208.
6. Crino PB, Nathanson KL, Henske EP. The Tuberous Sclerosis Complex. *N Engl J Med*. 2006; 355: 1345-1356.
7. Osborne JP, Fryer A, Webb D. Epidemiology of tuberous sclerosis. *Ann NY Acad Sci*. 1991; 615: 125-127.
8. Lyczkowski DA, Conant KD, Pulsifer MB, Jarrett DY, Grant PE, Kwiatkowski DJ, Thiele EA: Intrafamilial phenotypic variability in tuberous sclerosis complex. *J Child Neurol*. 2007; 22(12):1348-1355.
9. Shepherd CW, Gomez MR, Lie JT, Crowson BA. Causes of death in patients with tuberous sclerosis. *Mayo Clin Proc*. 1991; 66: 792-796.
10. Goh S, Butler W, Thiele EA. Subependymal giant cell tumors in tuberous sclerosis complex. *Neurology*. 2004; 63: 1457-1461.
11. Franz DN, Leonard J, Tudor C, Chuck G, Care M, Sethuraman G, Dinopoulos A, Thomas G, Crone KR. Rapamycin causes regression of astrocytomas in tuberous sclerosis complex. *Ann Neurol*. 2006; 59: 490-498.
12. Birca A, Mercier C, Major P. Rapamycin as an alternative to surgical treatment of subependymal giant cell astrocytomas in a patient with tuberous sclerosis complex. *J Neurosurg Pediatrics*. 2010; 6: 381-384.
13. Krueger DA, Care MM, Holland KM, Agricola K, Tudor C, Mangeshkar P, Wilson KA, Byars A, Sahmoud T, Franz DN. Everolimus for Subependymal Giant-Cell Astrocytomas in Tuberous Sclerosis. *N Engl J Med*. 2010; 363:1801-1811.
14. Bissler JJ, McCormack FX, Young LR, Elwing JM, Chuck G, Leonard JM, Schmithorst VJ, Laor T, Brody AS, Bean J, Salisbury S, Franz DN. Sirolimus for angiomyolipoma in tuberous sclerosis complex or lymphangiomyomatosis. *N Engl J Med*. 2008; 358: 140-151.
15. Ehninger D, Han S, Shilyansky C, Zhou Y, Li W, Kwiatkowski DJ, Ramesh V, Silva AJ. Reversal of learning deficits in a Tsc2+/- mouse model of tuberous sclerosis. *Nat Med*. 2008; 14: 843-848.
16. Wong M. Mammalian target of rapamycin (mTOR) inhibition as a potential antiepileptogenic therapy: From tuberous sclerosis to common acquired epilepsies. *Epilepsia*. 2010; 51: 27-36.
17. Boobes Y, Bernieh B, Saadi H, Raafat Al Hakim M, Abouchacra S. Gonadal dysfunction and infertility in kidney transplant patients receiving sirolimus. *Int Urol Nephrol*. 2010; 42(2): 493-498.

Phospho- Δ Np63 α /Rpn13-dependent regulation of LKB1 degradation modulates autophagy in cancer cells

Yiping Huang and Edward A. Ratovitski

Department of Dermatology, Johns Hopkins University School of Medicine, Baltimore, MD 21231, USA

Key words: p63, LKB1, oncogene, tumor suppressor, protein degradation, autophagy, chemoresistance

Received: 11/15/10; **Accepted:** 12/18/10; **Published:** 12/20/10

Corresponding author: Edward A. Ratovitski, PhD; **E-mail:** eratovi1@jhmi.edu

Copyright: © Huang and Ratovitski. This is an open-access article distributed under the terms of the Creative Commons Attribution License, which permits unrestricted use, distribution, and reproduction in any medium, provided the original author and source are credited

Abstract: Oxidative stress was shown to promote the translocation of Ataxia-telangiectasia mutated (ATM) to cytoplasm and trigger the LKB1-AMPK-tuberin pathway leading to a down-regulation of mTOR and subsequently inducing the programmed cell death II (autophagy). Cisplatin was previously found to induce the ATM-dependent phosphorylation of Δ Np63 α in squamous cell carcinoma (SCC) cells. In this study, phosphorylated (p)- Δ Np63 α was shown to bind the ATM promoter, to increase the ATM promoter activity and to enhance the ATM cytoplasmic accumulation. P- Δ Np63 α protein was further shown to interact with the Rpn13 protein leading to a proteasome-dependent degradation of p- Δ Np63 α and thereby protecting LKB1 from the degradation. In SCC cells (with an altered ability to support the ATM-dependent Δ Np63 α phosphorylation), the non-phosphorylated Δ Np63 α protein failed to form protein complexes with the Rpn13 protein and thereby allowing the latter to bind and target LKB1 into a proteasome-dependent degradation pathway thereby modulating a cisplatin-induced autophagy. We thus suggest that SCC cells sensitive to cisplatin-induced cell death are likely to display a greater ratio of p- Δ Np63 α /non-phosphorylated Δ Np63 α than cells with the innate resistant/impaired response to a cisplatin-induced cell death. Our data also suggest that the choice made by Rpn13 between p- Δ Np63 α or LKB1 to be targeted for degradation is critical for cell death decision made by cancer cells in response to chemotherapy.

INTRODUCTION

Cisplatin is the most applicable drug for treating various human cancers, however, its efficiency is limited due to development of drug resistance by tumor cells [1-3]. Cisplatin-induced programmed cell death is associated with expression of specific “cell death” genes and down regulation of “survival” genes [1-3]. Failure of cancer cells to maintain expression of the former genes may be an important factor in cisplatin resistance [1-3]. Previous reports from our research team emphasized the intriguing link between p63 regulatory roles in gene transcription and protein stability, and resistance of tumor cells to cisplatin chemotherapy [3-5]. *P53* homolog *p63* is a novel transcription factor implicated in regulation of genes involved in DNA damage response and chemotherapeutic stress in tumor cells [3-6]. Due to the two independent promoters, *p63* gene encodes two types of protein isoforms, with the long transactivation (TA)-domain and with the short TA-

domain [3, 6]. The latter is designated as Δ Np63 α . Due to several alternative-splicing events p63 produces three isoforms with the various length of the carboxyl terminus (α , β and γ). Δ Np63 α is the longest and is the most predominant isoform expressed in squamous cell carcinoma (SCC) cells [3-5].

Δ Np63 α is phosphorylated by the Ataxia-telangiectasia mutated (ATM)-dependent mechanism following cisplatin treatment, functioning as a pro-survival factor in SCC cells [4, 5]. From the other hand, the Δ Np63 α ability to activate ATM transcription thereby supports a feedback-regulatory mechanism [7]. However, whether this transcription factor needs to undergo phosphorylation in order to activate ATM transcription remains unclear. Moreover, ATM was shown to translocate to cytoplasm where it phosphorylates LKB1 kinase [8, 9] subsequently leading to an autophagic process through an AMPK/mTOR signaling pathway [10-12]. Finally,

cisplatin was shown to induce the phospho (p)- Δ Np63 α -dependent regulation of the regulatory particle non-ATPase subunit (Rpn)-13 gene transcription thereby contributing to cell death pathway of tumor cells [13]. Here, we report that upon cisplatin exposure, SCC cells display protein complex formations between Rpn13, Δ Np63 α or LKB1 leading to a proteasome-dependent degradation of p- Δ Np63 α or LKB1 by binding to Rpn13 in turn leading to autophagic-related chemosensitivity or chemoresistance.

RESULTS

P- Δ Np63 α regulates the ATM transcription

Δ Np63 α was previously found to activate the ATM transcription in human keratinocytes [7]. This transcription factor was shown to induce the ATM transcription through the CCAAT element found in the human ATM promoter (Fig. 1). As shown in Figure 1, the ATM promoter contains a few p63 responsive elements (RE) along with E2F and NF-Y cognate sequences, where latter one specifically binds to the CCAAT element playing a critical role for p- Δ Np63 α dependent regulation of transcription [5]. Although, previous report supports the ability of Δ Np63 α to induce ATM transcription [7], it is unclear whether the Δ Np63 α phosphorylation is needed for ATM transcriptional regulation. To access the role for p- Δ Np63 α in the regulation of ATM expression under DNA damage, we employed the cellular model, isogenic SCC clones, which contain the genomic copy of wild type Δ Np63 α or Δ Np63 α -S385G. The latter protein displays an altered ability to be phosphorylated by ATM kinase upon cellular response to cisplatin treatment [4, 5]. These clones were used as tools to examine the role for phosphorylation of Δ Np63 α in transcriptional regulation of gene expression and in the cellular response to chemotherapeutic treatment allowing us to define novel gene targets involved in cisplatin-mediated resistance [4, 5].

Using ChIP analysis with antibodies to Δ Np63 and p- Δ Np63 α , we found that cisplatin exposure led to an increase of the p- Δ Np63 α binding to the ATM promoter in wild type Δ Np63 α cells, while there is no such binding found in Δ Np63 α -S385G cells (Fig. 2A). Furthermore, p- Δ Np63 α binding was associated with the specific region of the ATM promoter containing NF-Y/ CCAAT element (Fig. 2A). There is no Δ Np63 α binding was found in the non-specific region of the ATM promoter (Fig. 2A). The quantitative analysis of p- Δ Np63 α binding by qPCR showed that the cisplatin treatment dramatically induced p- Δ Np63 α binding to the ATM promoter (by $\sim 14.5 \pm 1.3$ fold) in wild type Δ Np63 α cells only (Suppl. Fig. S1).

We further tested whether the Δ Np63 α phosphorylation affects the ability of Δ Np63 α to induce the ATM promoter-driven luciferase reporter. Wild type Δ Np63 α cells and Δ Np63 α -S385G cells were transfected with the promoter-less pGL3-Luc and pGL3-ATM (1259)-Luc plasmids followed by the exposure of cells to a control medium or 10 μ g/ml cisplatin for 24h. We showed

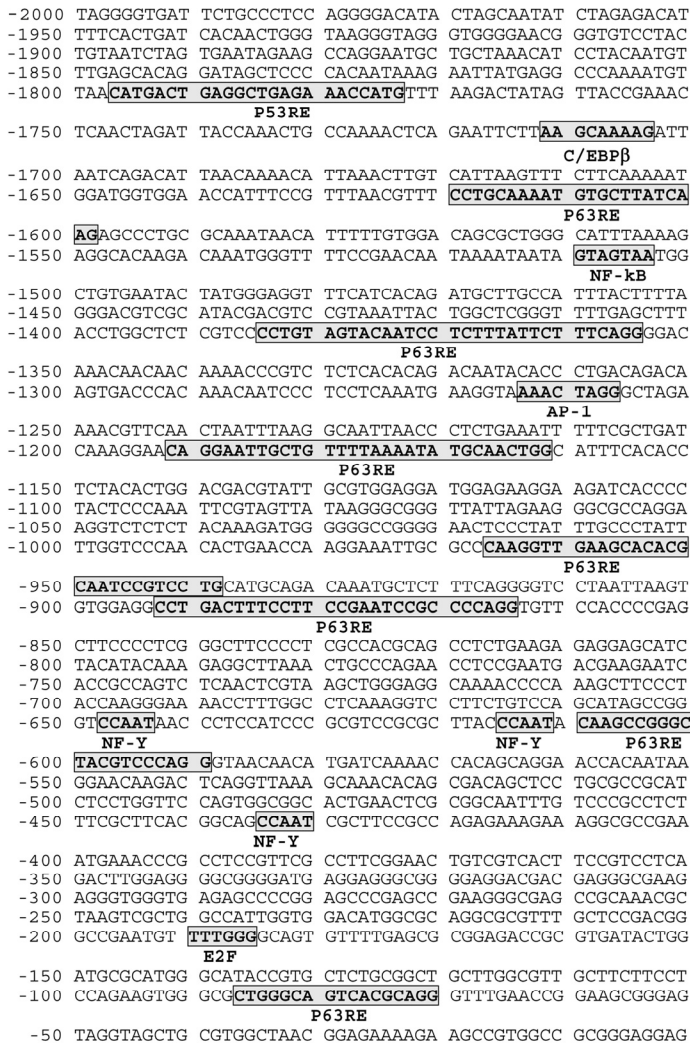


Figure 1. Schematic representation of ATM (2000 bp) promoter. Putative cognate sequences for transcription factors are bolded, bordered and shadowed. Several p63 responsive elements (RE) were found in the ATM promoter sequence.

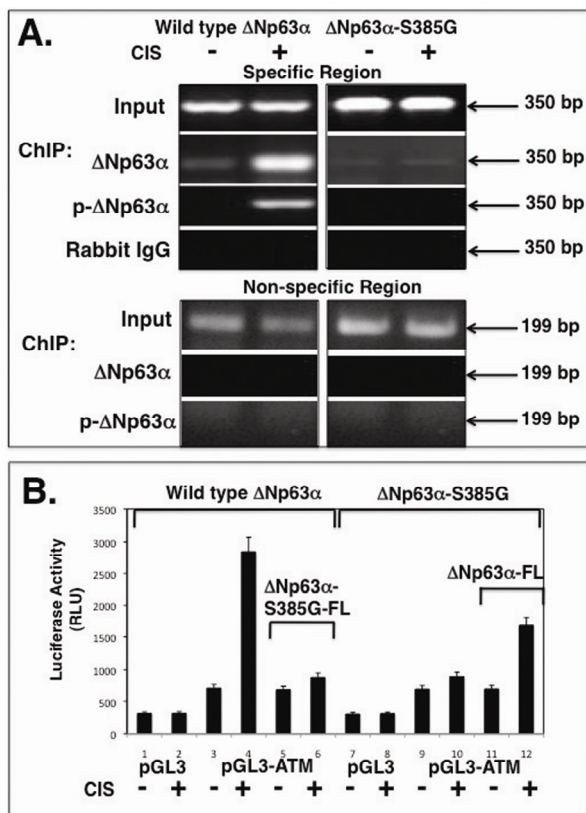


Figure 2. Binding of the p-ΔNp63α protein to the ATM promoter in vivo. Wild type ΔNp63α cells (left panels) and ΔNp63α-S385G cells (right panels) were exposed to a control medium and 10 μg/ml cisplatin for 24h. (A) ChIP assay of a specific region of the ATM promoter with anti-p-ΔNp63a antibody and anti-ΔNp63 antibody. As negative controls, we used ChIP of the ATM promoter specific region with rabbit immunoglobulins (IgG) and ChIP of the ATM promoter non-specific region with anti-p-ΔNp63α antibody as indicated. (B) Luciferase reporter assay. Both types of cells were transfected with 100 ng of the promoter-less pGL3 plasmid or pGL3-ATM (1259bp) promoter plasmid along with 1 ng of the pRL-SV40 plasmid for 24h. Cells were also transfected with 100 ng of the ΔNp63α-FL (Flag) or ΔNp63α-S385G-FL expression cassettes, as indicated. Cells were exposed to control medium (Con) and 10 μg/ml cisplatin (CIS) for 24h. Luciferase reporter assays were conducted in triplicate (±SD are indicated, p<0.05) as described in the Materials and methods. Firefly luciferase activity values were normalized by Renilla luciferase values.

that the cisplatin treatment significantly increased the ATM promoter-driven luciferase activity in wild type ΔNp63α cells (by ~4.01±0.34 fold), while no such effect (by ~1.06±0.12) was observed in ΔNp63α-S385G cells upon cisplatin exposure (Fig. 2B). In addition, 100

ng of the ΔNp63α-FL expression construct and ΔNp63α-S385G-FL construct was introduced into ΔNp63α-S385G cells and wild type ΔNp63α cells, respectively (Fig. 2B). We observed that ΔNp63α-S385G-FL markedly attenuated the cisplatin-mediated activation of the luciferase activity (by ~1.28±0.12 fold) in wild type ΔNp63α cells, while ΔNp63α-FL increased this activity (by ~2.39±0.21) in ΔNp63α-S385G cells (Fig. 2B).

P-ΔNp63α induces ATM-mediated LKB1-mTOR pathway

Recent seminal report by Dr. Cheryl Walker's group clearly demonstrated the stress-dependent export of ATM from nucleus to cytoplasm subsequently leading to the LKB1 phosphorylation followed by tuberin (TSC2) activation and down-regulation of mTOR [8, 9]. Since ΔNp63α induces ATM expression [7], we suggested the potential role for p-ΔNp63α in ATM regulation, ATM translocation to cytoplasm and ATM-dependent triggering of the LKB1-TSC2-mTOR pathway. We treated wild type ΔNp63α cells and ΔNp63α-S385G cells with a control medium and 10 μg/ml cisplatin for 24h. We then found that the cisplatin exposure induced the ΔNp63α phosphorylation leading to reduction of ΔNp63α protein levels (Fig. 3A). At the same, the levels of cytoplasmic ATM and activated TSC2 were significantly increased, while mTOR protein levels were decreased in wild type ΔNp63α cells upon cisplatin exposure (Fig. 3A, left panel). No such changes were observed in ΔNp63α-S385G cells (Fig. 3A, right panel). However, we showed that the LKB1 levels were decreased in ΔNp63α-S385G cells after cisplatin treatment suggesting the possibility for LKB1 to be degraded (Fig. 3A, right panel). To further examine this hypothesis, we exposed cells to lactacystin, the 26S proteasome inhibitor [13]. We thus found that the lactacystin treatment (25 mM for 12h) rescued ΔNp63α degradation in wild type ΔNp63α cells, and LKB1 degradation in ΔNp63α-S385G cells (Fig. 3B) suggesting the critical involvement of the 26S proteasome machinery.

Rpn13 binding promotes a proteasome-dependent degradation of either p-ΔNp63α or LKB1

A regulatory particle non-ATPase subunit (Rpn)-13 was shown to function as a 19S proteasome cap-associated protein, acting as an ubiquitin receptor recruiting the deubiquitinating enzyme UCH37 to the 26S proteasome [13-18]. We previously found that the cisplatin treatment induced Rpn13 transcription by p-ΔNp63α

and subsequently increased the physical interaction of Rpn13, UCH37 and NOS2 proteins leading to an essential degradation of the latter through a proteasome-dependent mechanism in SCC cells [13].

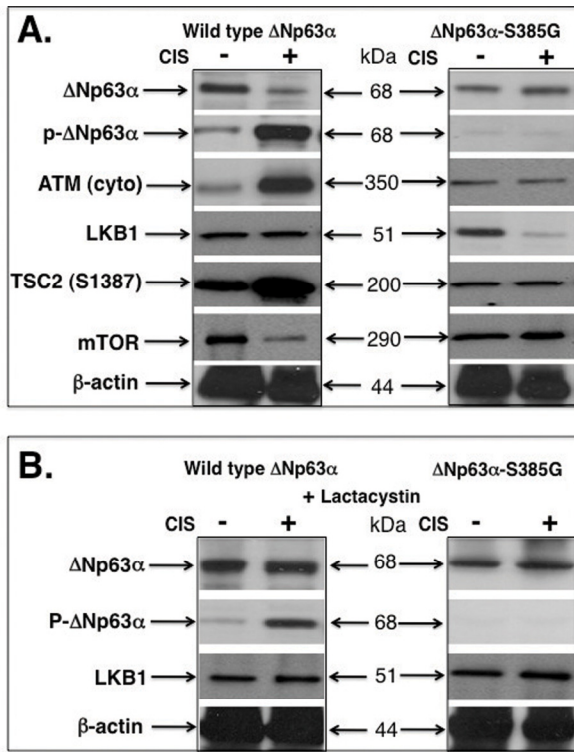


Figure 3. Cisplatin induces the p- $\Delta Np63\alpha$ and LKB1 protein levels in SCC cells. Wild type $\Delta Np63\alpha$ cells and $\Delta Np63\alpha$ -S385G cells were exposed to control media and 10 μ g/ml cisplatin for 24h. Protein levels were tested with indicated antibodies. Cytoplasmic (cyto) protein levels were tested with the anti- β -actin antibody. (A) No lactacystin treatment. (B) With lactacystin treatment.

In this study, we examined whether the Rpn13-dependent mechanism is implicated in down-regulation of the $\Delta Np63\alpha$ protein or LKB1 protein in SCC cells upon cisplatin exposure. First, we showed that the cisplatin treatment reduced the $\Delta Np63\alpha$ protein level, while induced the $\Delta Np63\alpha$ phosphorylation level in wild type $\Delta Np63\alpha$ cells (Fig. 4A, left panel). At the same time, cisplatin up-regulated Rpn13 protein level in wild type $\Delta Np63\alpha$ cells (Fig. 4A, left panel). However, $\Delta Np63\alpha$ and Rpn13 levels were not changed in $\Delta Np63\alpha$ -S385G cells after cisplatin exposure, while no p- $\Delta Np63\alpha$ was detected (Fig. 4A, right panel). We

further showed that the cisplatin exposure induced a complex formation between Rpn13, UCH13 and p- $\Delta Np63\alpha$ proteins in wild type $\Delta Np63\alpha$ cells (Fig. 4B, left panel), while no such complexes were observed in $\Delta Np63\alpha$ -S385G cells (Fig. 4B, right panel). We next found that the cisplatin treatment led to a physical association between Rpn13, UCH37 and LKB1 proteins in $\Delta Np63\alpha$ -S385G cells (Fig. 4C, right panel), while no similar protein complexes were detected in wild type $\Delta Np63\alpha$ cells (Fig. 4C, left panel).

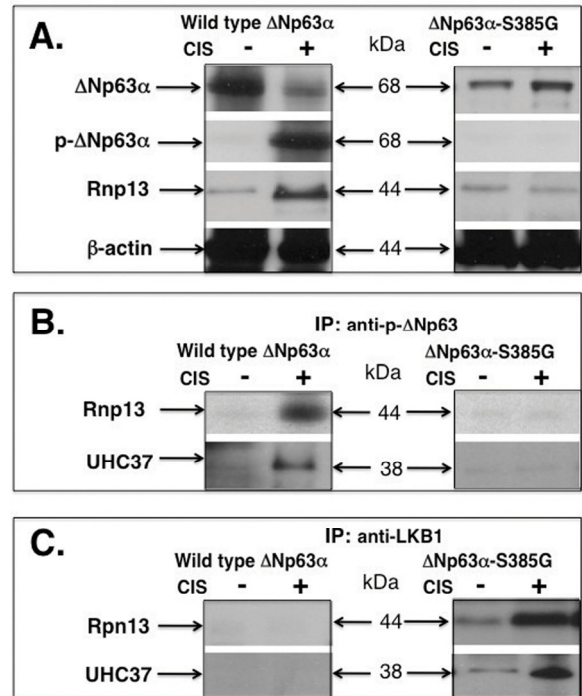


Figure 4. Cisplatin induces a protein complex formation between p- $\Delta Np63\alpha$ and Rpn13 in wild type $\Delta Np63\alpha$ cells and between Rpn13 and LKB1 in $\Delta Np63\alpha$ -S385G cells. Wild type $\Delta Np63\alpha$ cells and $\Delta Np63\alpha$ -S385G cells were exposed to control media and 10 μ g/ml cisplatin for 24h. Immunoprecipitation (IP) was performed with indicated antibodies and the protein levels were tested with indicated antibodies. (A) Immunoblotting. (B) and (C) Immunoprecipitation.

P- $\Delta Np63\alpha$ enhances the autophagic process in SCC through a LKB1-dependent pathway

Accumulating evidence supports the notion that stress induces autophagic-related characteristics through the LKB1-AMPK-TSC-mTOR pathway [10-12]. We thus

examined whether cisplatin treatment promotes the autophagy, and whether LKB1- or Rpn13- dependent mechanisms play any role in it. Microtubule-associated protein light chain 3 (LC3B), a mammalian homolog of yeast Atg8, has been used as a specific marker to monitor autophagy [19]. Upon induction of autophagy, the cytosolic form LC3B (LC3B-I) is conjugated to phosphatidylethanolamine (conversion into LC3B-II) and targeted to autophagic membranes.

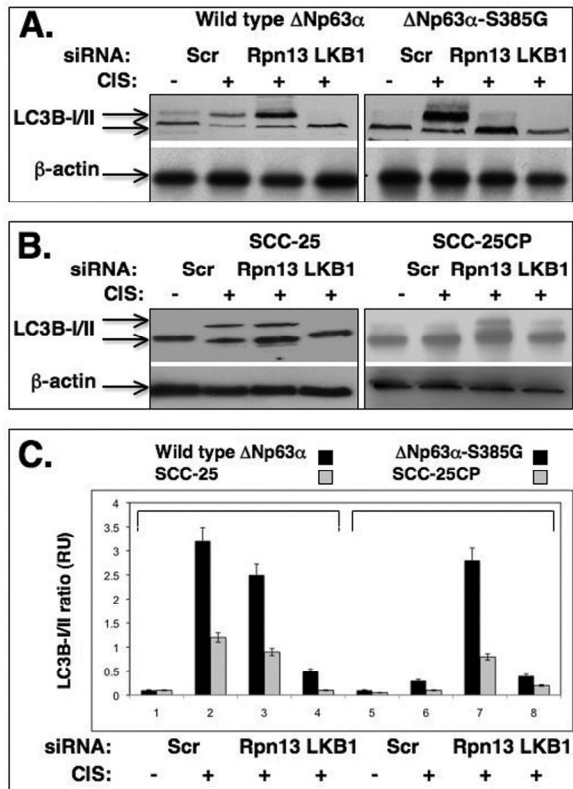


Figure 5. Cisplatin induces the autophagic process through a LKB1 up-regulation. (A) Wild type $\Delta Np63\alpha$ cells and $\Delta Np63\alpha$ -S385G cells and (B) Sensitive (SCC-25) and resistant (SCC-25CP) squamous carcinoma cells were exposed to control media and 10 μ g/ml cisplatin for 24h. Cells were transiently transfected with scrambled siRNA, siRNA against Rpn13 or LKB1. Cells were grown up in the presence of lysosomal protease inhibitors (10 μ g/ml of both E64d and pepstatin A). Protein levels of autophagic markers were analyzed by immunoblotting with indicated antibodies. β -actin expression was used as a loading control. (C). Quantitative analysis of LC3B -I/II ratio. Immunoblots were scanned using PhosphorImager (Molecular Dynamics) and quantified by Image-Quant software version 3.3 (Molecular Dynamics). Values of LC3B-II were expressed as a portion of LC3B-I values defined as 1. The LC3B-II/LC3B-I ratios were plotted as bars using the Microsoft Excel software with standard deviations (\pm SD, $p > 0.05$) resulting from three independent experiments and three individual measurements of each experiment. Black bars represent the set of wild type $\Delta Np63\alpha$ / $\Delta Np63\alpha$ -S385G cells, while grey bars represent a set of SCC-25/SCC-25CP cells.

$\Delta Np63\alpha$ to be phosphorylated by ATM in SCC cells upon cisplatin treatment is a superficial tool providing a suitable model system to investigate a potential relationship between $\Delta Np63\alpha$ and ATM-dependent phosphorylation. Thus, we used this model to assess a role for ATM-dependent phosphorylation of the $\Delta Np63\alpha$ in cisplatin chemoresistance of SCC cells. Wild type $\Delta Np63\alpha$ cells and $\Delta Np63\alpha$ -S385G cells were transiently transfected with scrambled siRNA, siRNA against Rpn13 or LKB1 for 24h and then exposed to control media or 10 μ g/ml cisplatin for 24h in the presence of 10 μ g/ml of lysosomal protease inhibitors, E64d and pepstatin A, as recommended elsewhere [19]. By immunoblotting with an antibody against an autophagosome marker, LC3B-I (16 kDa) and its conversion variant LC3B-II (14 kDa), we observed the cisplatin-induced autophagy-related changes of LC3B expression in SCC cells (Fig. 5). We found that wild type $\Delta Np63\alpha$ cells (which support the $\Delta Np63\alpha$ phosphorylation in response to cisplatin) displayed a marked expression of LC3B-II, while siRNA against LKB1 dramatically reduced this effect. Interestingly, siRNA against Rpn13 had a minimal effect on the cisplatin-induced LC3B-II activation (Fig. 5A, left panel). From the other hand, cisplatin treatment failed to induce autophagic changes in LC3B expression in $\Delta Np63\alpha$ -S385G cells (Fig. 5A, right panel). Intriguingly, siRNA against Rpn13 markedly increased the level of the LC3B-II autophagic marker in $\Delta Np63\alpha$ -S385G cells (Fig. 5A, right panel) suggesting the Rpn13-dependent regulation of LKB1 protein levels in these cells.

We also employed a set of SCC cells displaying sensitivity or resistance to cisplatin (SCC-25 and SCC-25CP, respectively) as reported elsewhere [20]. We first examined whether SCC-25 and SCC-25CP cells expressed $\Delta Np63\alpha$ or p- $\Delta Np63\alpha$ in response to cisplatin treatment. We found that after cisplatin exposure, resistant SCC-25CP cells, indeed, express far less of the p- $\Delta Np63\alpha$ protein than their sensitive counterpart, SCC-25 (Suppl. Fig. S2). We further found that, in contrast to SCC-25 cells, cisplatin reduced the LKB1 protein levels in SCC-25CP cells (Suppl. Fig. S2) suggesting that the greater ratio between non-phosphorylated $\Delta Np63\alpha$ and p- $\Delta Np63\alpha$ might be an important factor contributing to LKB1 reduction and is likely to play a role in cisplatin resistance displayed by SCC-25CP cells.

We further found that cisplatin induced the LC3B-II expression in sensitive SCC-25 cells, while siRNA against LKB1 significantly inhibited this expression, and siRNA against Rpn13 had only a minimal effect on

the LC3B-II level reduction (Fig. 5B, left panel). In the case of resistant SCC-25CP cells, one could see no cisplatin-induced LC3B-II up-regulation, however siRNA against Rpn13 promoted a significant increase of this autophagic marker (Fig. 5B, right panel). The quantitative analysis of the LC3B-I/LC3B-II ratio (Fig. 5C) led us to the same conclusion. Using immunofluorescence analysis, we further examined the expression of LC3B-II isotype in SCC upon cisplatin exposure and observed the clustering (“punctuated appearance”) of the membrane-associated protein, MAP LC3 α/β (LC3B), as previously described elsewhere [19, 21]. We also observed that cisplatin-resistant cells showed much lesser autophagic-related levels of LC3B-II expression than cisplatin-sensitive cells (Fig. 6) suggesting the critical role for autophagy in tumor response to a chemotherapeutic treatment.

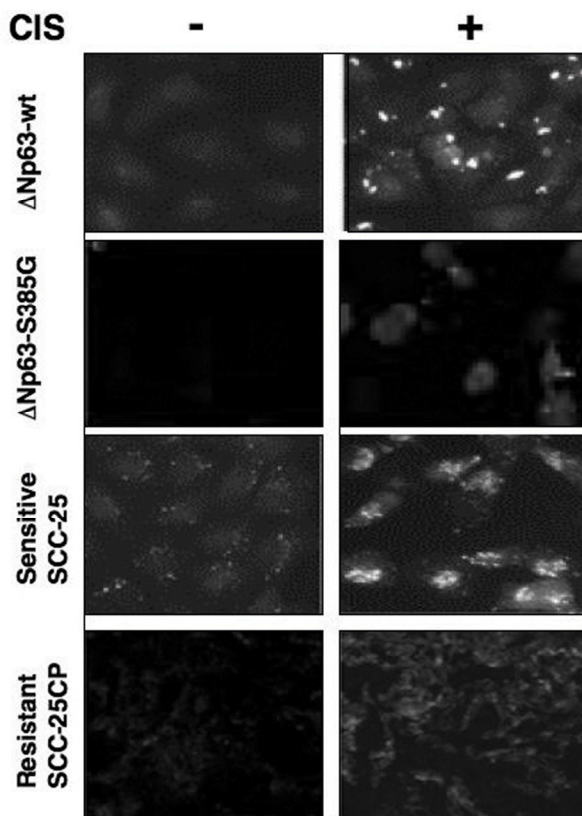


Figure 6. Immunofluorescence staining of LC3B expression in squamous carcinoma cells upon cisplatin exposure. Sets of wild type $\Delta Np63\alpha/\Delta Np63\alpha$ -S385G cells and SCC-25/SCC-25CP cells were exposed to control media and 10 μ g/ml cisplatin for 24h. Cells were stained with a polyclonal antibody against MAP LC3 α/β (1:100), and then photographed under fluorescent microscope.

An optimal cellular response to DNA damage/stress (ionizing radiation, oxidative stress, chemotherapeutic drugs, UV radiation, nutrient deprivation, and hypoxia) requires repair of damage and coordination of critical cellular processes such as transcription, translation, metabolism, and control of cell survival through an apoptosis or autophagy [22-26].

Emerging evidence supports the notion that the cisplatin-induced autophagy plays a central role in tumor cell resistance to platinum-based therapy [27-29]. A dose- and time-dependent induction of autophagy observed in tumor cells following cisplatin treatment is evidenced by up-regulation Beclin-1 and cisplatin-triggered activation of AMPK pathway leading to a subsequent suppression of mTOR activity [28]. Autophagy is also shown to delay apoptosis in renal tubular epithelial cells exposed to cisplatin cytotoxicity [30, 31]. The switch from autophagy to apoptosis suggests that autophagy induction mediates a pre-apoptotic lag phase observed in renal tubular cells exposed to cisplatin supporting the idea that autophagy mounts an adaptive cell response that delays apoptosis and might contribute to a cisplatin resistance in other cellular systems including cancer [30, 31].

A few oncogenes (e.g. phosphatidylinositol 3-kinase, activated AKT1) inhibit autophagy, while numerous tumor suppressors (e.g. BH3-only proteins, death-associated protein kinase-1, PTEN, tuberous sclerosis complex 1 and 2, TSC1 and TSC2 and LKB1/STK11) induce autophagy [32]. As known guardians of genome integrity, p53 and p73, were shown to be involved in autophagic processes [24, 25, 33-37]. However, to date no evidences were reported that p63 plays a role in autophagic pathway.

ATM is a biosensor that coordinates cellular response to various damaging signals to preserve genomic integrity [8, 9, 22, 23]. ATM has been recently implicated in cellular response to elevated reactive oxygen species (ROS) and therefore involved in redox homeostasis [8, 9, 22]. The key reports of the Cheryl Walker’ research team showed that the ATM import to cytoplasm activates the specific phosphorylation of LKB1 at the Threonine-366 position leading to subsequent TSC2 activation via the LKB1/AMPK metabolic pathway, and reduction of mTOR level, in turn promoting autophagy [8, 9].

Our previous observations showed that the cisplatin exposure induced the ATM-dependent phosphorylation of $\Delta Np63\alpha$ resulting in the p(S385)- $\Delta Np63\alpha$ modification and subsequently leading to a proteasome-dependent degradation of $\Delta Np63\alpha$ in SCC cells [4].

Our later studies emphasized the p- Δ Np63 α role in transcriptional regulation of numerous gene targets involved in tumor cell response to cisplatin, some of them with pro-apoptotic functions and some – with cell survival functions [5]. The complex response of the p- Δ Np63 α dependent gene targets to cisplatin prompted us to continue the quest for the signaling pathways leading to cisplatin sensitivity or cisplatin resistance displayed by tumor cells [3-5]. Recent observations by the research groups of Ted Hupp and Borivoj Vojtesek defined Δ Np63 α as a novel regulator of p53 activation through the ATM kinase transcription [7]. They further reported that the Δ Np63 α protein interacts with the ATM promoter-derived CCAAT sequence [38], previously shown to be critical for the p- Δ Np63 α transcription function in SCC upon cisplatin exposure [5]. Intriguingly, these investigators showed that Δ Np63 α activates the ATM gene transcription, whereas TAp63 α does not, highlighting an essential role for the TA2 domain in mediating Δ Np63 α function [7].

In this study, we found that p- Δ Np63 α binds the ATM promoter, induces the ATM promoter activity and activates the ATM cytoplasmic accumulation. We further found that the p- Δ Np63 α protein interacts with the Rpn13 protein leading to a proteasome-dependent degradation of p- Δ Np63 α . Next, we observed that ATM triggers the LKB1-AMPK-tuberin pathway leading to a down-regulation of mTOR subsequently enhancing the cisplatin-dependent autophagy in wild type Δ Np63 α cells upon cisplatin exposure. Using the SCC cells with an altered ability to support the ATM-dependent Δ Np63 α phosphorylation, non-phosphorylated Δ Np63 α failed forming protein complexes with Rpn13 and allowing the latter to bind and target LKB1 into a proteasome-dependent degradation pathway thereby modulating a cisplatin-induced autophagy. SCC cells with the innate resistant/impaired response to a cisplatin-induced cell death displayed a greater ratio of non-phosphorylated Δ Np63 α /p- Δ Np63 α than cells that are sensitive to cisplatin-induced cell death. Based on our findings so far, we suggest that the choice made by Rpn13 between p- Δ Np63 α or LKB1 to be targeted for degradation is critical for cell death decision made by cancer cells in response to chemotherapy. The discovery that the Δ Np63 promoter is subject to both p53-mediated activation and repression by Δ Np63 α [39], and that ATM-dependent phosphorylation mediates Δ Np63 α degradation [4, 5] suggests that activity of the damage-response Δ Np63 α -ATM-p53 pathway is finely modulated by complex feedback mechanisms [7]. Further dissection of this pathway should provide molecular targets for combating cancer and ageing [7, 9, 40-44].

METHODS

Cells and reagents. We have used the head and neck squamous carcinoma (SCC) stable cell lines expressing wild type Δ Np63 α or Δ Np63 α -S385G (with an altered ability to be phosphorylated by ATM kinase) as previously described [4, 5]. We also used cisplatin-sensitive (SCC-25) and resistant (SCC-25CP) squamous carcinoma cell lines obtained from Dr. J.S. Lazo (Department of Pharmacology, University of Pittsburgh School of Medicine) as a result of the Material Transfer Agreement [20]. Cells were maintained in RPMI medium 1640, 10% fetal bovine serum. Cells were incubated with 10 μ g/ml cisplatin, 25 μ M of lactacystin β -lactone (Calbiochem) for indicated periods of time, as described elsewhere [13]. Cells were lysed in 50 mM Tris, pH 7.5, 100 mM NaCl, 2mM EDTA, 0.5% Triton X-100, 0.5% Brij-50, 1 mM PMSF, 0.5 mM NaF, 0.1 mM Na₃VO₄, 2X protease inhibitor cocktail, sonicated for 10 sec time intervals, and clarified for 30min at 15,000xg. Supernatants (total lysates) were used for immunoprecipitation and immunoblotting [4, 5, 13]. Control (scrambled) siRNA and Rpn13 siRNA (sc-72453) were obtained from Santa Cruz Biotechnology, while siRNA against LKB1 was purchased from Dharmacon [45]. SiRNAs (200 pmol/six-well plate) were transiently transfected into cells using FuGENE 6 (4 μ L, Roche) for 24h and then after the 24h treatment with control media or 10 μ g/ml cisplatin.

Isolation of cytoplasmic fraction. 1–2 \times 10⁶ cells were resuspended in a hypotonic lysis buffer (10 mM HEPES pH 7.9, 10 mM KCl, 0.1 mM EDTA, 0.1 mM EGTA) with protease inhibitors (Sigma), Triton X-100 (0.6% final concentration) was then added and the nuclei were pelleted at 2,500-3,000xg for 10 min at 4°C. Supernatants served as cytoplasmic fractions [13].

Antibodies. We used a rabbit polyclonal antibody against Δ Np63 α (Ab-1, EMD Chemicals), a mouse monoclonal antibody against β -actin (Sigma), and rabbit polyclonal antibodies against UCH3 (ab38528), mTOR (ab2833) and Rpn13 (ab91567), and a mouse monoclonal antibody against ATM (2C11A1, ab78) were purchased from Abcam. We also obtained a mouse monoclonal antibody against Rpn13 (M01, clone 3C6, Abnova). A mouse monoclonal anti-LKB1 antibody (clone 27D10, ab3050) was obtained from Cell Signaling Technology. A custom rabbit polyclonal antibody against p Δ Np63 α (ATM motif, residues 379-392) was previously described [4]. A polyclonal rabbit anti-phospho-tuberin antibody (TSC2-S1387, AP3338a; which represents the AMPK-dependent phosphorylation) was obtained from Abgent.

Chromatin immunoprecipitation (ChIP). First, 5×10^6 cell equivalents of chromatin (2–2.5 kb in size) were immunoprecipitated (IP) with 10 μg of anti-p $\Delta\text{Np63}\alpha$ antibody as described elsewhere [5, 13]. After reversal of formaldehyde crosslinking, RNAase A and proteinase K treatments, IP-enriched DNAs were used for PCR amplification. PCR consisted of 40 cycles of 94°C for 30 s, 60°C for 30 s, and 72°C for 30 s using Taq DNA polymerase (Invitrogen). The following PCR primers were used for amplification of the ATM promoter: for the specific region, sense, (-920) 5'-TTCAGGGGTCCTAATTAAGT -3'(901), and antisense, (-570) 5'-TGATCAAACACAGCAGG-3' (-551) yielding the 350 bp PCR product, and for the non-specific region, sense, (-2000) 5'-TAGGGGTGATTCTGCCCTCC-3' (-1880) and antisense, (-1821) 5'-AATTATGAGGCCCAAATG-3' (-1802) yielding the 199 bp PCR product. Binding of the endogenous p- $\Delta\text{Np63}\alpha$ protein to the ATM promoter was also assessed by qPCR using the above-mentioned primers for the specific region of the ATM promoter as previously described [13]. ChIP-PCR values (relative units, RU) were normalized by the GAPDH values and those obtained from the control samples (cells treated with control medium) were designated as 1. Experiments were performed in triplicate.

Luciferase reporter assay. We used the pGL3-ATM (S118526, SwitchGear Genomics) promoter-luciferase reporter plasmid (encompassing -1259 bp to +1 bp of the ATM promoter). A total of 5×10^4 cells/well in a 24-well plate were transfected with 100 ng of the pGL3 luciferase reporter constructs plus 1 ng of the Renilla luciferase plasmid pRL-SV40 (Promega) using FuGENE 6 (Roche) as previously described [3, 13]. At 24h, cells were also treated with 10 $\mu\text{g}/\text{ml}$ cisplatin or control medium and then after an additional 24h, luciferase assays were performed using the Dual luciferase reporter assay kit (Promega). For each experiment, the wells were transfected in triplicate and each well was assayed in triplicate by measuring the Firefly luciferase activity in a luminometer. Renilla luciferase activity was measured in the same tube [3,13]. The values for Firefly luciferase activity were normalized against the Renilla luciferase activity values for each transfected well. Resulting data were presented as relative luciferase units (RLU).

Autophagy assay. Cells were transiently transfected with scrambled siRNA, siRNA against Rpn13 or LKB1. Cells were exposed to control medium or 10 $\mu\text{g}/\text{ml}$ cisplatin for 24h in the presence of lysosomal protease inhibitors (10 $\mu\text{g}/\text{ml}$ of both E64d and pepstatin A purchased from Sigma) as previously described [19].

Protein levels of LC3B-I and LC3B-II were tested with a rabbit polyclonal antibody against MAP LC3 α/β (LC3B, L7453, Sigma Aldrich Co). Immunoblots were scanned using PhosphorImager (Molecular Dynamics) and quantified by ImageQuant software version 3.3 (Molecular Dynamics). Values of LC3B-II were expressed as a portion of LC3B-I values defined as 1. The LC3B-II/LC3B-I ratios were plotted as bars using the Microsoft Excel software with standard deviations ($\pm\text{SD}$) resulting from three independent experiments and three individual measurements of each experiment.

Immunofluorescence microscopy. Cells were washed with ice-cold phosphate-buffered saline and after fixation with 4% paraformaldehyde for 10 min at room temperature, they were permeabilized with 50 $\mu\text{g}/\text{ml}$ digitonin for 5 min. Cells were then quenched in 0.1% sodium borohydride for 5 min, and blocked with 10% goat serum, 1% bovine serum albumin (BSA, Amersham Biosciences) at room temperature for 60 min. Cells were incubated overnight with the primary antibody against MAPLC3 α/β diluted in 1% BSA at 4 °C. After washing, the cells were incubated with the Cy3-conjugated anti-rabbit antibody (1:500, Jackson ImmunoResearch Laboratories Inc) diluted in 1% BSA for 1h. Finally, images were obtained using a Leica TCS-NT laser scanning microscope system and processed with Adobe Photoshop software [29-31].

Statistical analysis. The data represent mean \pm SD from three independent experiments and the statistical analysis was performed by Student's t test at a significance level of $p < 0.05$ to < 0.001 .

CONFLICT OF INTERESTS STATEMENT

The authors of this manuscript have no conflict of interests to declare.

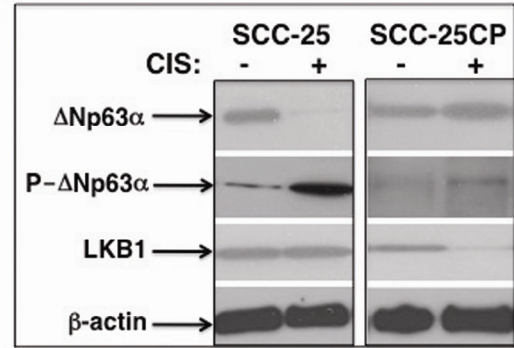
REFERENCES

1. Kelland, L. The resurgence of platinum-based cancer chemotherapy. *Nat Rev Cancer* 2007; 7: 573-584.
2. Helmbach H, Kern MA, Rossmann E, Renz K, Kissel C, et al. Drug resistance towards etoposide and cisplatin in human melanoma cells is associated with drug-dependent apoptosis deficiency. *J Invest Dermatol* 2002; 118: 923-932.
3. Sen T, Sen N, Brait M, Begum S, Chatterjee A, et al. DNp63a confers tumor cell resistance to cisplatin treatment through the transcriptional regulation of AKT. *Cancer Res*. 2010, In Press.
4. Huang Y, Sen T, Nagpal J, Upadhyay S, Trink B, et al. ATM kinase is a master switch for the DNp63a phosphorylation/ degradation in human head and neck squamous cell carcinoma cells upon DNA damage. *Cell Cycle* 2008; 7: 2846-2855.

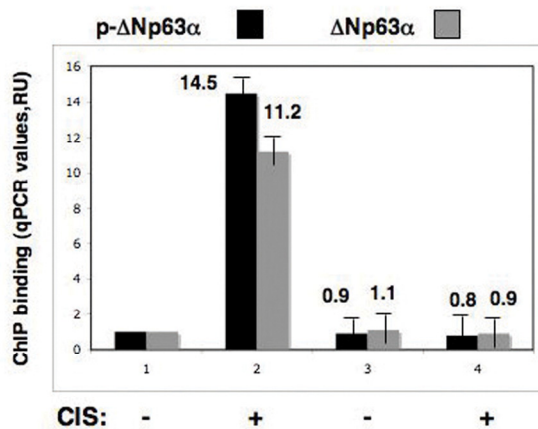
5. Huang, Y., Chuang, A. Y., Romano, R. A., Liegeois, N. J., Sinha, S., et al. Phospho- Dnp63a /NF-Y protein complex transcriptionally regulates DDIT3 expression in squamous cell carcinoma cells upon cisplatin exposure. *Cell Cycle* 2010; 9: 328-338.
6. Keyes WM, Wu Y, Vogel H, Guo X, Lowe SW, Mills AA. p63 deficiency activates a program of cellular senescence and leads to accelerated aging. *Genes Dev* 2005; 19:1986- 1999.
7. Craig AL, Holcakova J, Finlan LE, Nekulova M, Hrstka R, et al. Dnp63 transcriptionally regulates ATM to control p53 Serine-15 phosphorylation. *Mol Cancer*. 2010; 9: 195-201.
8. Alexander A, Walker CL. Differential localization of ATM is correlated with activation of distinct downstream signaling pathways. *Cell Cycle*. 2010; 9:3685-3686.
9. Alexander A, Cai SL, Kim J, Nanez A, Sahin M, et al. ATM signals to TSC2 in the cytoplasm to regulate mTORC1 in response to ROS. *Proc Natl Acad Sci USA*. 2010; 107: 4153-4158.
10. Herrero-Martín G, Høyer-Hansen M, García-García C, Fumarola C, Farkas T, et al. TAK1 activates AMPK-dependent cytoprotective autophagy in TRAIL-treated epithelial cells. *EMBO J*. 2009; 28: 677-685.
11. Høyer-Hansen M, Jäättelä M. AMP-activated protein kinase: a universal regulator of autophagy? *Autophagy*. 2007; 3: 381-383.
12. Liang J, Shao SH, Xu ZX, Hennessy B, Ding Z, et al. The energy sensing LKB1-AMPK pathway regulates p27(kip1) phosphorylation mediating the decision to enter autophagy or apoptosis. *Nat Cell Biol*. 2007; 9: 218-224.
13. Huang YP, Ratovitski EA. Phosphorylated p63 induces transcription of regulatory particle non ATP-ase subunit (Rpn)-13 leading to a nitric oxide synthase-2 protein degradation. *J Biol Chem*. 2010; In Press.
14. Chen X, Lee BH, Finley D, Walters KJ. Structure of proteasome ubiquitin receptor hRpn13 and its activation by the scaffolding protein hRpn2. *Mol Cell*. 2010; 38: 404-415.
15. Schreiner P, Chen X, Husnjak K, Randles L, Zhang N, Elsasser S, Finley D, Dikic I, Walters KJ, Groll M. Ubiquitin docking at the proteasome through a novel pleckstrin-homology domain interaction. *Nature*. 2008; 453: 548-552.
16. Husnjak K, Elsasser S, Zhang N, Chen X, Randles L, Shi Y, Hofmann K, Walters KJ, Finley D, Dikic I. Proteasome subunit Rpn13 is a novel ubiquitin receptor. *Nature*. 2008; 453: 481-488.
17. Hamazaki J, Iemura S, Natsume T, Yashiroda H, Tanaka K, Murata S. A novel proteasome interacting protein recruits the deubiquitinating enzyme UCH37 to 26S proteasomes. *EMBO J*. 2006; 25: 4524-4536.
18. Yao T, Song L, Xu W, DeMartino GN, Florens L, Swanson SK, Washburn MP, Conaway RC, Conaway JW, Cohen RE. Proteasome recruitment and activation of the Uch37 deubiquitinating enzyme by Adrm1. *Nat Cell Biol*. 2006; 8: 994-1002.
19. Mizushima N, Yoshimori T. How to interpret LC3 immunoblotting. *Autophagy*. 2007; 3: 542-545.
20. Yang YY, Robbins PD, Lazo JS. Differential transactivation of human metallothionein-IIa in cisplatin-resistant and -sensitive cells. *Oncol Res*. 1998; 10: 85-98.
21. Mathew R, Kongara S, Beaudoin B, Karp CM, Bray K, Degenhardt K, Chen G, Jin S, White E. Autophagy suppresses tumor progression by limiting chromosomal instability. *Genes Dev*. 2007; 21:1367-1381.
22. Kurz EU, Douglas P, Lees-Miller SP. Doxorubicin activates ATM-dependent phosphorylation of multiple downstream targets in part through the generation of reactive oxygen species. *J Biol Chem* 2004; 279:53272-53281.
23. Stiff T, Walker SA, Cerosaletti K, Goodarzi AA, Petermann E, et al. ATR-dependent phosphorylation and activation of ATM in response to UV treatment or replication fork stalling. *EMBO J* 2006; 25:5775-5782.
24. Bitomsky N, Hofmann TG. Apoptosis and autophagy: Regulation of apoptosis by DNA damage signalling - roles of p53, p73 and HIPK2. *FEBS J*. 2009; 276: 6074-6083.
25. Rosenbluth JM, Pietenpol JA. mTOR regulates autophagy-associated genes downstream of p73. *Autophagy*. 2009; 5:114-116.
26. Scherz-Shouval R, Weidberg H, Gonen C, Wilder S, Elazar Z, Oren M. p53-Dependent regulation of autophagy protein LC3 supports cancer cell survival under prolonged starvation. *Proc Natl Acad Sci U S A*. 2010; 107: 18511-18516.
27. Chen S, Rehman SK, Zhang W, Wen A, Yao L, Zhang J. Autophagy is a therapeutic target in anticancer drug resistance. *Biochim Biophys Acta*. 2010, In Press.
28. Harhaji-Trajkovic L, Vilimanovich U, Kravic-Stevovic T, Bumbasirevic V, Trajkovic V. AMPK-mediated autophagy inhibits apoptosis in cisplatin-treated tumour cells. *J Cell Mol Med*. 2009; 13: 3644-3654.
29. Ren JH, He WS, Nong L, Zhu QY, Hu K, Zhang RG, Huang LL, Zhu F, Wu G. Acquired cisplatin resistance in human lung adenocarcinoma cells is associated with enhanced autophagy. *Cancer Biother Radiopharm*. 2010; 25: 75-80.
30. Inoue K, Kuwana H, Shimamura Y, Ogata K, Taniguchi Y, et al. Cisplatin-induced macroautophagy occurs prior to apoptosis in proximal tubules in vivo. *Clin Exp Nephrol*. 2010; 14: 112-122.
31. Kaushal GP, Kaushal V, Herzog C, Yang C. Autophagy delays apoptosis in renal tubular epithelial cells in cisplatin cytotoxicity. *Autophagy*. 2008; 4: 710-712.
32. Maiuri MC, Tasdemir E, Criollo A, Morselli E, Vicencio JM, et al. Control of autophagy by oncogenes and tumor suppressor genes. *Cell Death Differ*. 2009; 16: 87-93.
33. Maiuri MC, Galluzzi L, Morselli E, Kepp O, Malik SA, Kroemer G. Autophagy regulation by p53. *Curr Opin Cell Biol*. 2010; 22: 181-185.
34. Vousden KH, Ryan KM. p53 and metabolism. *Nat Rev Cancer*. 2009; 9: 691-700.
35. Green DR, Kroemer G. Cytoplasmic functions of the tumour suppressor p53. *Nature*. 2009; 458: 1127-1130.
36. Tasdemir E, Chiara Maiuri M, Morselli E, Criollo A, D'Amelio M, et al. A dual role of p53 in the control of autophagy. *Autophagy*. 2008; 4: 810-814.
37. Tasdemir E, Maiuri MC, Galluzzi L, Vitale I, Djavaheri-Mergny M, et al. Regulation of autophagy by cytoplasmic p53. *Nat Cell Biol*. 2008; 10: 676-687.
38. Testoni B, Mantovani R. Mechanisms of transcriptional repression of cell-cycle G2/M promoters by p63. *Nucleic Acids Res* 2006; 34:928-938.

39. Harnes DC, Bresnick E, Lubin EA, Watson JK, Heim KE, Curtin JC, Suskind AM, Lamb J, DiRenzo J: Positive and negative regulation of DNp63 promoter activity by p53 and DNp63a contributes to differential regulation of p53 target genes. *Oncogene* 2003; 22: 7607-7616.
40. Marino G, Ugalde AP, Salvador-Montoliu N, Varela I, Quirpos PM, et al. Premature aging in mice activates a systemic metabolic response involving autophagy induction. *Hum Mol Genet.* 2008; 17: 2196-2211.
41. Madeo F, Tavernarakis N, Kroemer G. Can autophagy promote longevity? *Nat Cell Biol.* 2010; 12: 842-846.
42. Salminen A, Kaarniranta K. Regulation of the aging process by autophagy. *Trends Mol Med.* 2009; 15: 217-224.
43. Eisenberg-Lerner A, Bialik S, Simon HU, Kimchi A. Life and death partners: apoptosis, autophagy and the cross-talk between them. *Cell Death Differ.* 2009; 16: 966-975.
44. Tavernarakis N, Pasparaki A, Tasdemir E, Maiuri MC, Kroemer G. The effects of p53 on whole organism longevity are mediated by autophagy. *Autophagy.* 2008; 4: 870-873.
45. Upadhyay S, Liu C, Chatterjee A, Hoque MO, Kim MS, Engles J, Westra W, Trink B, Ratovitski E, Sidransky D. LKB1/STK11 suppresses cyclooxygenase-2 induction and cellular invasion through PEA3 in lung cancer. *Cancer Res.* 2006; 66: 7870-7879.

SUPPLEMENTAL FIGURES



Supplemental Figure S2. Expression levels for $\Delta Np63\alpha$, p- $\Delta Np63\alpha$ and LKB1 in SCC-25 cells and SCC-25CP cells upon cisplatin exposure. Cells were treated with the control medium (CIS, -) or 10 μ g/ml cisplatin (CIS, +) for 24h. Immunoblotting of total lysates was performed with indicated antibodies and loading level was monitored by the β -actin level.



Supplemental Figure S1. Quantitative PCR analysis of the ChIP binding. Wild type $\Delta Np63\alpha$ cells and $\Delta Np63\alpha$ -S385G cells were treated with the control medium (CIS, -) or 10 μ g/ml cisplatin (CIS, +) for 24h. ChIP assay of ATM promoter was performed with antibodies against p- $\Delta Np63\alpha$ (black) and $\Delta Np63\alpha$ (grey). The quantitation of binding was monitored by qPCR using the following specific ATM promoter primers: sense, (-920) 5'- TTCAGGGTCTTA-ATTAAGT - 3'(901), and antisense, (-570) 5'- TGATCAAACCACAGCAGG-3' (-551) yielding the 350 bp PCR product. ChIP-PCR values (relative units, RU) were normalized by the GAPDH values and those obtained from the control conditions (cells treated with control medium) were designated as 1. Experiments were performed in triplicate. Numerical values indicate the fold differences between control conditions and cisplatin treatment conditions.

Age-related mTOR in gynaecological cancers

Preety Bajwa, Subhransu S. Sahoo, Pradeep S. Tanwar

Aging is an uninvited sequel of organismal growth and the ultimacy of which is death. At the molecular level, organismal aging is a conversion from cellular quiescence to senescence state. Age is a major risk factor for many diseases including diabetes, obesity, neurodegenerative disorders, and cancer. Other consequences of aging are not defined by diseases, but rather considered 'stages of life', because they normally occur in everyone, such as menopause in females. However, deregulated female reproductive cycles (early menarche and/or late menopause) lead to hormonal imbalance and cancer at later stages of life. Endometrial and ovarian cancers are the most frequently diagnosed cancers in aged women and account for significant mortality. The incidence of both these cancer increases with advancing age, peaking around 60 to 70 years of age [1, 2]. Up to 80% of such patients are found to have genetic aberrations in the members of the PI3K-mTOR (phosphoinositide 3-kinase-mammalian target of rapamycin) pathway [3, 4]. mTOR signaling is important in regulating the cell cycle of the majority of proliferating cells, where homeostasis is maintained by either cell division or quiescence [5]. In contrast, hyperactive mTOR signaling causes cellular hypertrophy, which alters homeostasis, leading to cellular senescence, cancer and age-related diseases [5].

Recently, we demonstrated that with advancing age, female mice and humans develop endometrial and ovarian surface epithelial (OSE) cell hyperplasia, papillary growth and inclusion cysts [4, 6]. Histopathological examination of these abnormal growths revealed expression of bonafide markers of human ovarian cancer precursor lesions, Pax8 and Stathmin 1, and concurrent elevated expression of pS6 protein (a downstream target of the mTOR pathway) compared to young mice and humans [6]. Genetic deletion or overexpression of *PTEN* (a negative regulator of mTOR signaling) significantly altered the age-associated changes in female mice and human reproductive tract organs [4]. Furthermore, pharmacological suppression of the mTOR pathway using rapamycin treatment significantly reduced both endometrial and OSE hyperplasia in aged mice [4, 6]. Taken together, these observations established that the age-associated pathological changes in the female

reproductive tract organs are driven by aberrant mTOR signaling.

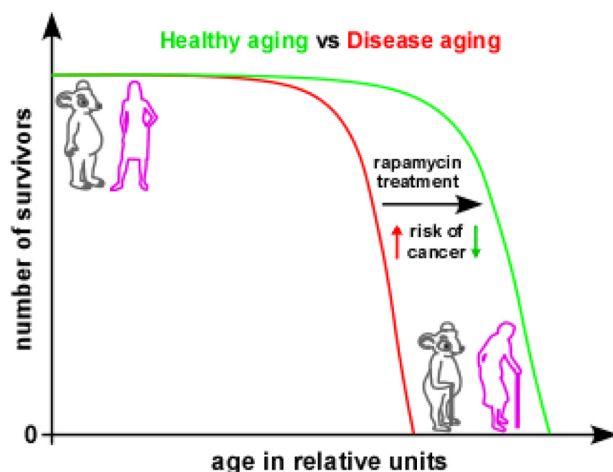


Figure 1. Hypothetical model of mTOR-driven cancer in aged women. A potential therapeutic opportunity for the treatment of gynaecologic cancers is outlined. In post-menopausal aged women, rapamycin treatment can suppress hyperactive mTOR signalling in ovarian and uterine epithelium, potentially promoting healthy aging.

Cancer is an age-related disease and any lifestyle changes or interventions that slow aging also delay cancer [7]. Many independent studies have already demonstrated the effectiveness of an anti-aging drug, rapamycin, in many species. In model organisms, rapamycin prolongs lifespan and delays cancer, even when calorie restriction does not. The TOR signaling is a major evolutionarily conserved player in longevity regulation as pharmacological modulation of this pathway extends lifespan in flies, worms, yeast and mice. Under these circumstances, our study provides evidence that rapamycin treatment inhibits mTOR-driven precancerous lesions in the female reproductive tract organs and may also extend lifespan or promote healthy aging in post-menopausal women. Our study highlights that even rapamycin treatment in genetically heterogeneous, 9 months-old mice (equivalent to ~50 years age of human) significantly suppresses mTOR activity and gynaecologic cancer lesions. Thus, if

rapamycin can rescue aging phenotypes in cancer-prone transgenic mice, it is predictable that rapamycin intervention in post-menopausal women should delay age-related cancers and promote a healthy life. Nevertheless, many questions remain to be answered. In aged mice and women, why is overactive mTOR specific to a few cell types of the reproductive tract organs? Is there any link between unopposed estrogen signaling and the mTOR pathway that leads to hyperplastic epithelium of the uterus and ovary? Moreover, how can we use this knowledge to treat cancer? Our studies, therefore, open up an avenue to explore the mTOR pathway as a target for prevention and/or treatment of gynaecological cancers.

REFERENCES

1. Damle RP, et al. J Clin Diagn Res. 2013; 7:2774-76. doi: 10.7860/JCDR/2013/6291.3755
2. Lambrou NC and Bristow RE. 2003; 17:1075-81; discussion 1081, 1085-6, 1091.
3. Tanwar PS, et al. Carcinogenesis. 2014; 35:546-53. doi: 10.1093/carcin/bgt357
4. Bajwa P, et al. Oncotarget. 2017; 8:7265-75. doi: 10.18632/oncotarget.13919
5. Serrano M. Cell Cycle. 2012; 11:2231-32. doi: 10.4161/cc.21065
6. Bajwa P, et al. Oncotarget. 2016; 7:19214-27. doi: 10.18632/oncotarget.8468
7. Blagosklonny MV. Cancer Biol Ther. 2012; 13:1349-54. doi: 10.4161/cbt.22859

Pradeep Tanwar: Gynaecology Oncology Group, School of Biomedical Sciences and Pharmacy, University of Newcastle, Callaghan, New South Wales, Australia

Correspondence: Pradeep Tanwar

Email: pradeep.tanwar@newcastle.edu.au

Keywords: aging, mTOR, cancer

Received: February 20, 2017

Published: February 28, 2017

Gerosuppression by pan-mTOR inhibitors

Olga V. Leontieva¹ and Mikhail V. Blagosklonny¹

¹Department of Cell Stress Biology, Roswell Park Cancer Institute, Buffalo, NY 14263, USA

Correspondence to: Mikhail V. Blagosklonny; email: Mikhail.blagosklonny@roswellpark.org

Keywords: dual mTORC1/C2 inhibitors, rapalogs, sirolimus, aging, cancer, senescence

Received: August 12, 2016

Accepted: November 15, 2016

Published: December 30, 2016

ABSTRACT

Rapamycin slows organismal aging and delays age-related diseases, extending lifespan in numerous species. In cells, rapamycin and other rapalogs such as everolimus suppress geroconversion from quiescence to senescence. Rapamycin inhibits some, but not all, activities of mTOR. Recently we and others demonstrated that pan-mTOR inhibitors, known also as dual mTORC1/C2 inhibitors, suppress senescent phenotype. As a continuation of these studies, here we investigated in detail a panel of pan-mTOR inhibitors, to determine their optimal gerosuppressive concentrations. During geroconversion, cells become hypertrophic and flat, accumulate lysosomes (SA-beta-Gal staining) and lipids (Oil Red staining) and lose their re-proliferative potential (RPP). We determined optimal gerosuppressive concentrations: Torin1 (30 nM), Torin 2 (30 nM), AZD8055 (100 nM), PP242 (300 nM), both KU-006379 and GSK1059615 (1000 nM). These agents decreased senescence-associated hypertrophy with IC50s: 20, 18, 15, 200 and 400 nM, respectively. Preservation of RPP by pan-mTOR inhibitors was associated with inhibition of the pS6K/pS6 axis. Inhibition of rapamycin-insensitive functions of mTOR further contributed to anti-hypertrophic and cytostatic effects. Torin 1 and PP242 were more “rapamycin-like” than Torin 2 and AZD8055. Pan-mTOR inhibitors were superior to rapamycin in suppressing hypertrophy, senescent morphology, Oil Red O staining and in increasing so-called “chronological life span (CLS)”. We suggest that, at doses lower than anti-cancer concentrations, pan-mTOR inhibitors can be developed as anti-aging drugs.

INTRODUCTION

Rapamycin slows down aging in yeast [1, 2], *Drosophila* [3-7], worm [8] and mice [9-30]. It also delays age-related diseases in a variety of species including humans [31-46]. Numerous studies have demonstrated life extension by rapamycin in rodent models of human diseases [9-48]. The maximal lifespan extension is dose-dependent [26, 42, 49]. One explanation is trivial: the higher the doses, the stronger inhibition of mTOR. There is another explanation: mTOR complex 1 (mTORC1) has different affinity for its substrates. For example, inhibition of phosphorylation of S6K is achieved at low concentrations of rapamycin, whereas phosphorylation of 4EBP1 at T37/46 sites is insensitive to pharmacological concentrations of rapamycin [50-61]. Unlike rapalogs, ATP-competitive kinase inhibitors, also known as dual mTORC1/C2 or pan-mTOR inhibitors, directly inhibit

the mTOR kinase in both mTORC1 and mTORC2 complexes [56, 59, 62-65].

In cell culture, induction of senescence requires two events: cell cycle arrest and mTOR-dependent geroconversion from arrest to senescence [66-75]. In proliferating cells, mTOR is highly active, driving cellular mass growth. When the cell cycle gets arrested, then still active mTOR drives geroconversion: growth without division (hypertrophy) and a compensatory lysosomal hyperfunction (beta-Gal staining) [76]. So senescence can be caused by forced arrest in the presence of an active mTOR [76]. Senescent cells lose re-proliferative potential (RPP): the ability to regenerate cell culture after cell cycle arrest is lifted. Quiescence or reversible arrest, in contrast, is caused by deactivation of mTOR. When arrest is released, quiescent cells re-proliferate [66, 67].

In one cellular model of senescence (cells with IPTG-inducible p21), IPTG forces cell cycle arrest without affecting mTOR. During IPTG-induced arrest, the cells become hypertrophic, flat, SA-beta-Gal positive and lose RPP. When IPTG is washed out, such cells cannot resume proliferation. Loss of RPP is a simple quantitative test of geroconversion. Treatment with rapamycin during IPTG-induced arrest preserves RPP. When IPTG and rapamycin are washed out, cells re-proliferate [68-73, 77]. Recently, we have shown that Torin 1 and PP242 suppresses geroconversion, preventing senescent morphology and loss of RPP [78, 79]. In agreement, reversal of senescent phenotype was shown by another pan-mTOR inhibitor, AZD8085 [80].

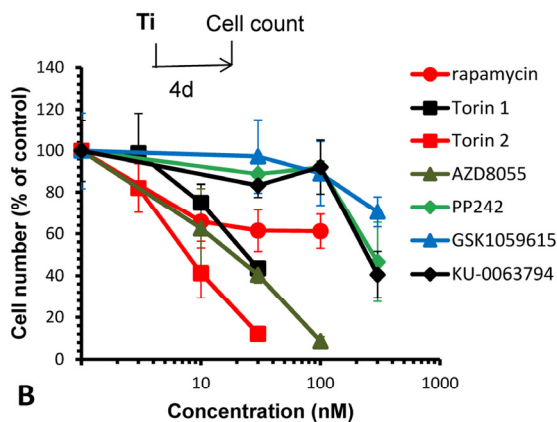
Pan-mTOR inhibitors have been developed as cytostatics to inhibit cancer cell proliferation. Cytostatic side effects in normal cells are generally acceptable for anti-cancer drugs. However, cytostatic side effects may not be acceptable for anti-aging drugs. Gerosuppressive

(anti-aging) effects at drug concentrations that only mildly cytostatic are desirable. Pan-mTOR inhibitors differ by their affinity for mTOR complexes and other kinases. Here we studied 6 pan-mTOR inhibitors (in comparison with rapamycin) and investigated effects of 6 pan-mTOR inhibitors on rapamycin-sensitive and -insensitive activities of mTOR, cell proliferation and geroconversion.

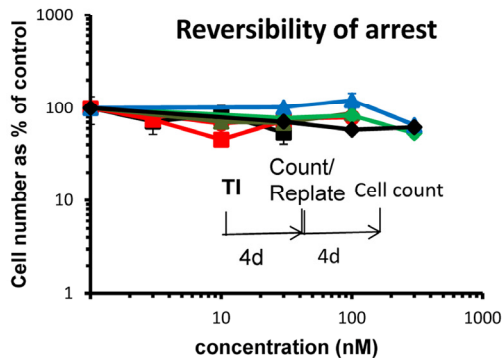
RESULTS

First we investigated the relationship between cytostatic and gerosuppressive activities of 6 pan-mTOR inhibitors: Torin1, Torin 2, AZD8055, PP242, KU-006379 and GSK1059615. All inhibitors inhibited proliferation in a dose-dependent manner (Fig. 1A). Inhibitory concentrations 50 (IC₅₀) varied: Torin1 (22 nM), Torin 2 (8 nM), AZD8055 (20 nM), PP242 (285 nM), KU-006379 (230 nM) and GSK1059615 (>300 nM). At IC₅₀, no cell death was observed. The inhibitory

A Cytostatic effect



B



C

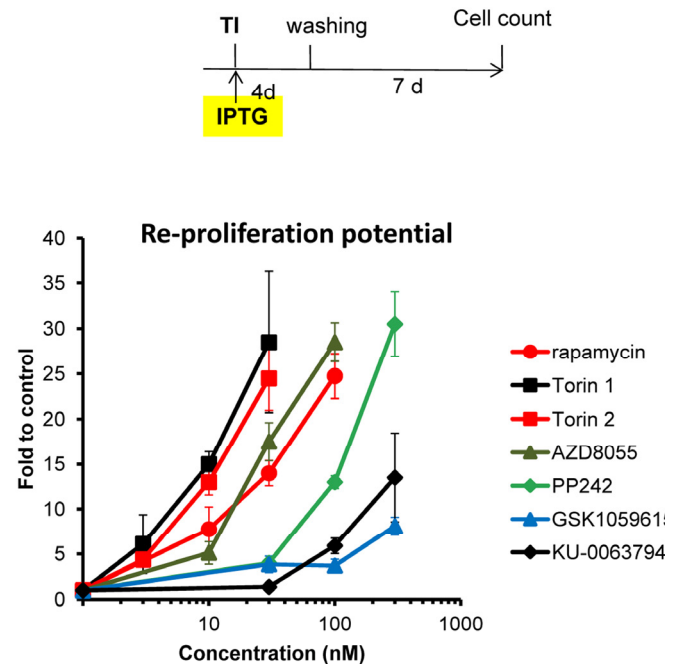


Figure 1. (A) Cytostatic effect. Effect of TOR inhibitors (Ti) on proliferation. HT-p21 cells were treated with serial dilutions of indicated Ti for 4 days and counted in triplicates. Data presented as mean \pm SD. (B) Reversibility. Cells were treated as in A. After 4 day-treatment cells were counted and re-plated at 1000/well in 6-well plates in drug-free medium. Cells were allowed to re-proliferate for 4 days and counted. Cytostatic arrest was fully reversible. (C) Gerosuppression. Effect of TOR inhibitors on re-proliferative potential. HT-p21 cells were treated with IPTG in the presence of different concentrations of indicated Ti in triplicates. After 4 day-treatment, cells were washed off the drugs and allowed to regrow in drug-free medium for 7 days and counted. Data presented as mean \pm SD.

effect was cytostatic rather than cytotoxic and, furthermore, reversible (Fig. 1B). When cells were treated with pan-mTOR inhibitors for 4 days and then re-plated and incubated in drug-free medium, the cells re-proliferated as efficiently as untreated control cells (Fig. 1B).

In the same cell line, HT-p21, we also measured gerosuppressive activities of mTOR inhibitors, by measuring re-proliferative potential (RPP) after induction of senescence with IPTG (Fig. 1C and Suppl. Fig. S1). In HT-p21 cells, IPTG induces p21, which in turn causes cell cycle arrest [76]. During cell cycle arrest, mTOR drives geroconversion to senescence, characterized by loss of RPP [68-73, 77]. Loss of RPP becomes evident after washing IPTG out. Although cells re-enter cell cycle, they cannot proliferate [81].

Inhibitors of mTOR preserved RPP in IPTG-treated cells. When IPTG and inhibitors of mTOR were washed out, the cells re-proliferated. By counting cell numbers after IPTG is washed out, we can measure gerosuppressive effects of mTOR inhibitors.

As shown in figure 1C and S1, all TOR inhibitors demonstrated equal maximal gerosuppressive activity, however, at different concentrations. Therefore, they have equal efficacy and different potency. (Note: Efficacy: maximum effect that mTOR inhibitor can cause regardless of concentration. Potency: concentration that is needed to cause this effect.) When we compared cytostatic versus gerosuppressive effects for each compound (Fig S2), we noticed that the gerosuppressive effect mirrored the cytostatic effect.

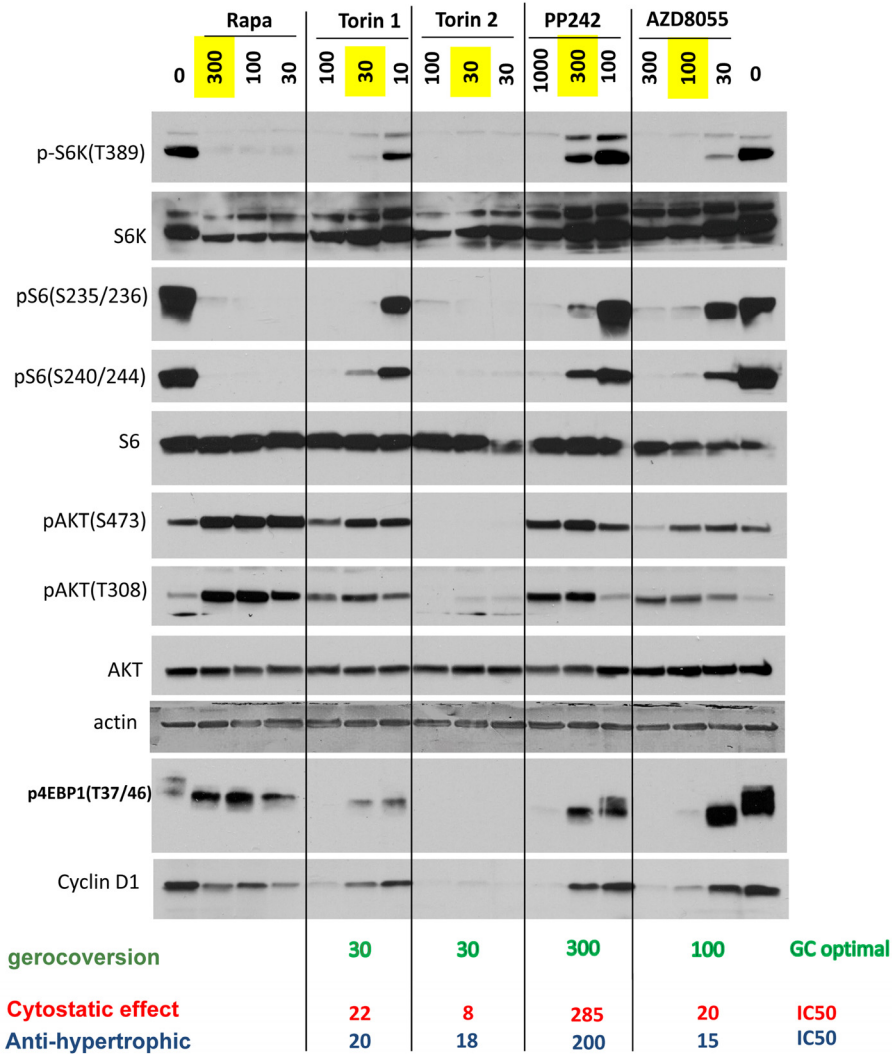


Figure 2. Effect of TOR inhibitors on mTOR-pathway in HT-p21 cells. Cells were treated with IPTG and different concentrations of indicated inhibitors for 24h and lysed. Immunoblotting was performed with indicated antibodies. Maximal optimal gerosuppressive concentrations are highlighted in yellow.

The lower concentration was required to inhibit proliferation, the lower concentration was required to suppress geroconversion (Suppl. Fig. S2). We estimated concentration at which compounds exerted maximum gerosuppressive effect (Fig. 1C and Suppl. Fig. S1). Torins 1 and 2 turned out to be the most potent and GSK1059615 was the least potent. Torin 1 and 2 showed the same maximal effect in suppressing geroconversion at 30 nM (Fig. 1C and Suppl. Fig. S1). Maximal gerosuppressive effect was achieved by GSK1059615 and KU-0063794 at 1000 nM (Suppl. Fig. S1). AZD8055 displayed maximum gerosuppressive effect at 100 nM. As seen in figure S1, gerosuppressive effects reached the plateau and then decreased at higher concentrations, due to toxicity.

Preservation of RPP correlated with inhibition of mTORC1

MTOR complex 1 (mTORC1) phosphorylates S6 kinase (S6K) at T389, which in turn phosphorylates S6 at S235/236 and S240/244. This S6K/S6 axis is rapamycin-sensitive. Phosphorylation of 4EBP1 at T37/46 is rapamycin-insensitive. Function of mTORC2, which is rapamycin-insensitive, can be measured by phospho-AKT (S473), albeit it is not the only kinase that phosphorylates Akt at that site.

At optimal gerosuppressive concentrations, pan-mTOR inhibitors decreased phosphorylation of S6K at T389 (target of mTORC1) and its downstream targets S6 (S235/236) and (S240/244) (Fig. 2 and Suppl. Fig. S3). At optimal concentration (30 nM), Torin 2 inhibited phosphorylation of AKT at S473 and T308. Other inhibitors, at optimal gerosuppressive concentrations, did not decrease phosphorylation of AKT or even caused an increase in level of pAKT(S473) and/or

pAKT(T308) similar to the effect of rapamycin, which induces phosphorylation of AKT in HT-p21 cells (Fig. 2). We conclude that mTORC2 and/or AKT in particular are not essential for geroconversion, as measured by RPP, in HT-p21 cells. Phosphorylation status of 4EBP1, a substrate of TORC1, was revealing. Rapamycin caused mobility shift but did not inhibit phosphorylation at the particular T37/46 sites. Torin 2 inhibited 4EBP1 phosphorylation at T37/46 sites. At optimal gerosuppressive concentrations, all other pan-mTOR inhibitors caused mobility shift and only marginally decreased T37/46 phosphorylation, which however was inhibited at higher concentrations (Fig. 2 and Suppl. Fig. S3).

Pan-mTOR inhibitors prevent cellular hypertrophy

We next determined effects of mTOR inhibitors on senescence-associated hypertrophy in IPTG-arrested HT-p21 cells. Hypertrophy can be measured as protein per cell [82]. IPTG induces cell cycle arrest, so that cells do not proliferate and the number of plated cells stays the same throughout the treatment [82]. Therefore, hypertrophy can be easily determined by measuring protein per well. We treated cells with IPTG and its combination with mTOR inhibitors. After a 4 day-treatment, cells were lysed and protein was measured. Pan-mTOR inhibitors decreased cellular hypertrophy in a dose-dependent manner. Rapamycin was an exception, i.e. its inhibitory effect on cellular hypertrophy was moderate and reached a plateau. IC50 values were as follows: 20, 18, 15, 200 and 400 nM for Torin 1, Torin 2, AZD8085, PP242 and GSK1059615, respectively (Fig. 3). All inhibitors reduced amount of protein by more than 50% at concentrations corresponding to their optimal gerosuppressive concentrations measured by RPP.

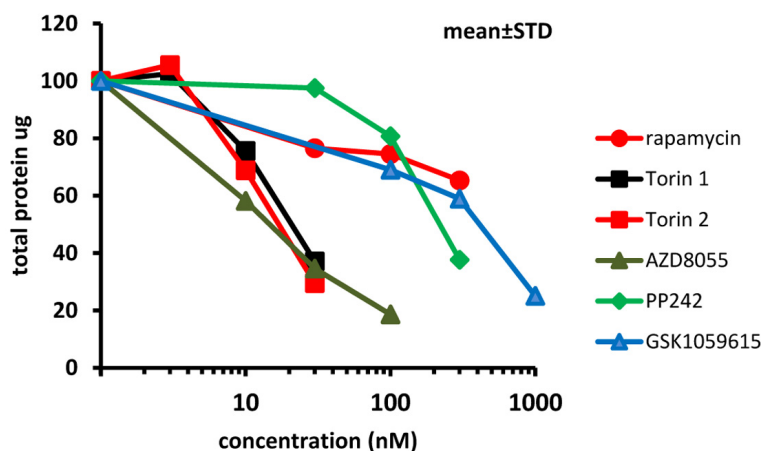


Figure 3. Effect of TORINs on protein level in senescent HT-p21 cells. Cells were treated with IPTG and different concentrations of TORINs for 4 days and protein amounts were measured. Data are mean \pm SD.

We next employed additional method of measuring cellular hypertrophy by measuring GFP under CMV-constitutive promoter in HT-p21 cells. (HT-p21 cells are stably transfected with GFP-CMV). It was previously shown that GFP accumulation is a marker of hypertrophy [82]. Torin 2 was more potent anti-hypertrophic agent than Torin 1 (Fig. 4A). IC₅₀ values were 3 nM and 10 nM for torin 1 and 2, respectively (Fig. 4A). At 30 nM, both Torins were more anti-hypertrophic than rapamycin (Fig. 4A, rapamycin was used at 500 nM). Anti-hypertrophic effect of Torins was independent of the nature of senescence-inducing agent, i.e. IPTG-inducible ectopic p21 or inhibitor of CDK4/6 PD0332991 (Fig. 4B, C). We conclude that Torins blocked senescence-associated hypertrophy more effectively compared with rapamycin. Furthermore, Torin 1, which is more rapamycin-like than Torin 2, was less potent as anti-hypertrophic agent than Torin 2.

Torins 1 and 2 decrease lipid accumulation in senescing cells

One of the features of senescent HT-p21 cells is accumulation of lipids, which is detected as positive Oil Red O staining in perinuclear region (Fig. 5, IPTG). When these cells were co-treated with IPTG and Torins 1 or 2, cells remained small and Oil Red O negative (Fig. 5). As in the case of SA-beta-Gal staining, rapamycin was less effective than Torins in decreasing this marker of senescent HT-p21 cells.

Pan-mTOR inhibitors prolongs CLS in HT-p21 cells

The yeast is commonly used as a model of aging. In particular, rapamycin extends chronological lifespan (CLS) [2]. In stationary culture, yeast cells lose viability measured as re-proliferative potential in fresh culture [1-7]. It is erroneously believed that “chronological

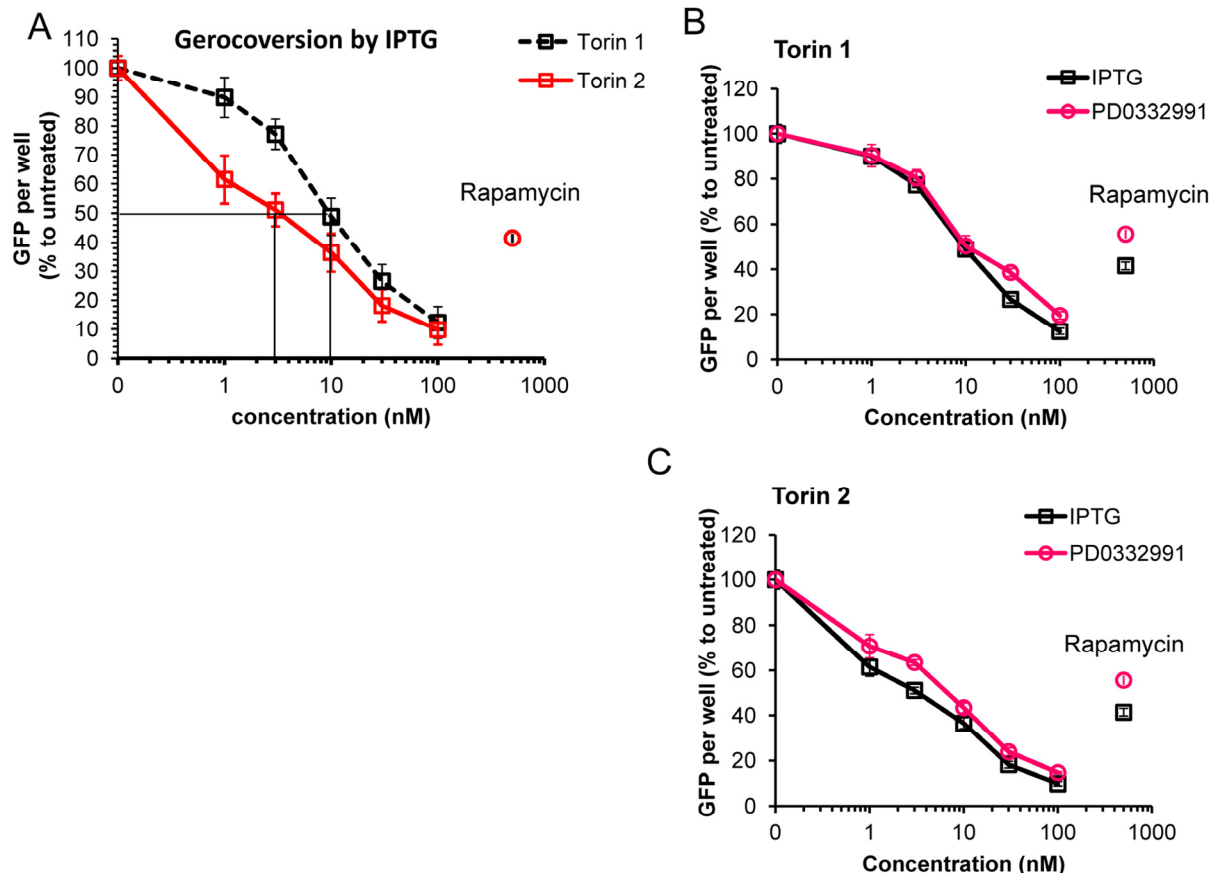


Figure 4. Effect of torins 1 and 2 on hypertrophy of senescent HT-p21 cells measured by constitutive GFP fluorescence of these cells. (A) HT-p21 cells were treated with IPTG and concentration range of torin1 or torin 2, rapamycin (500 nM) was included for comparison as additional control. After 4 day-treatment GFP fluorescence was quantified using Typhoon scanner (Amersham Biosciences variable mode imager) and ImageQuantTL software. (B) and (C) HT-p21 cells were induce to senesce by treatment with either IPTG (3 days) or PD0332991 (0.5 μ M, for 4 days) and concentration range of torin 1 (B) or torin 2 (C). Effect of torins on hypertrophy was assessed by measuring GFP fluorescence as described in (A). GFP per well is presented as % to IPTG or PD0332991 only treated cells for each set. Data are means \pm SE of 8 replicates from one out of three independent experiments.

aging” is an equivalent of aging of post-mitotic cells in multicellular organism. In reality, this phenomenon is an equivalent of lose of cancer cell viability in overcrowded culture [83]. Both yeast and cancer cells acidify the culture medium and lose viability, as measured for example by re-proliferation in fresh low-density culture. When plated at very high cell density, HT-p21 cells produce high levels of lactic acid, acidifying medium (“yellow color”). This causes loss of re-proliferative potential [83]. Rapamycin extends CLS by decreasing lactate production [83]. Here we tested whether pan-mTOR inhibitors can extend CLS of HT-p21 cells. After 3 days in a high-density culture, HT-p21 cells remained alive, but could not re-proliferate and form colonies when re-plated in fresh medium (Fig. 6, control). When high-density cultures were treated with mTOR inhibitors, these cells produced less lactic acid as seen by the color of the medium (Fig. 6; yellow indicates low pH and high levels of lactic acid) [84]. They maintained re-proliferative potential and formed colonies when re-plated in fresh medium in low density (Fig. 6). Rapamycin was less effective than pan-mTOR inhibitors. At equipotent (optimal) concentrations, all pan-mTOR inhibitors showed similar efficacy in prolonging chronological life span.

Pan-mTOR inhibitors suppress senescent morphology of SKBR3 and MEL10 cells

We next investigated gerosuppressive effects of mTOR inhibitors in SKBR3 and MEL10 cells undergoing geroconversion after treatment with CDK4/6 inhibitor PD0332991 and nutlin-3a, respectively [72]. As shown in Fig 7, treatment with PD0332991 caused senescent morphology in SKBR3 cells. Co-treatment with pan-mTOR inhibitors prevented senescent morphology and hypertrophy (Fig.7 and Suppl. Fig. S4A). Pan-mTOR inhibitors also prevented senescent morphology of MEL10 cells induced to senesce by treatment with low concentration of nutlin-3a (Fig. 8 and Suppl. Fig. S4B).

DISCUSSION

As predicted by theory of TOR-driven aging [29, 85-97], rapamycin extends life span and prevents age-related diseases (see Introduction). Yet, rapamycin (and other rapalogs such as everolimus) does not inhibit all functions of mTOR. Inhibition of both rapamycin-sensitive and --insensitive functions of mTOR may be translated in superior anti-aging effects. However, potential benefits may be limited by undesirable effects

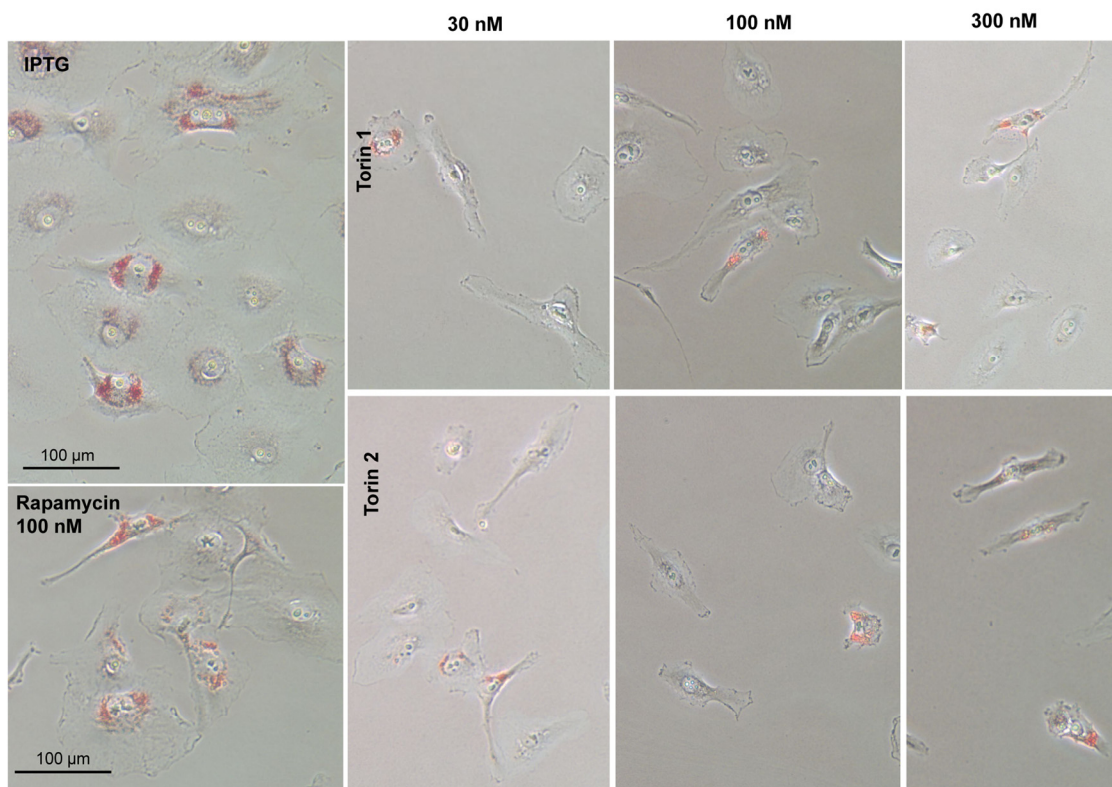


Figure 5. Effect of torin analogs on lipid accumulation in senescent HT-p21 cells. Cells were treated with IPTG and concentrations range of torin 1or torin 2 for 4 days and stained with Oil Red O. Bar – 100 μm.

such as inhibition of cell proliferation (cytostatic effect) and cell death (cytotoxic effect). In fact, pan-mTOR inhibitors have been developed to treat cancer, so they are cytostatic and cytotoxic at intended anti-cancer concentrations. Yet, the window between gerosuppressive and cytotoxic effects exists. At optimal gerosuppressive concentrations, pan-mTOR inhibitors caused only mild cytostatic effect. For Torin 1 and PP242, the ratio of gerosuppressive (measured by RPP) to cytostatic concentrations was the most favorable. The ratio of anti-hypertrophic to cytostatic concentration was similar for all pan-mTOR inhibitors.

Gerosuppressive effect of pan-mTOR inhibitors (as measured by RPP) was equal to that of rapamycin because it is mostly associated with inhibition of the S6K/S6 axis. Yet anti-hypertrophic effect as well as prevention of SA-beta-Gal staining and large cell morphology was more pronounced with pan-mTOR inhibitors than with rapamycin. Also, at optimal concentrations, all pan-mTOR inhibitors extended loss of re-proliferative potential in stationary cell culture more potently than rapamycin. This test determines

hyper-metabolism and lactic acid production and is an equivalent of “yeast CLS” (see [83]). One conclusion is that pan-mTOR inhibitors may be superior to rapamycin.

At low concentrations, pan-mTOR inhibitors acted like rapamycin, inhibiting the S6K/S6 axis and causing mobility shift of 4EBP1 (Fig. 2). With increasing concentrations, these drugs inhibited phospho-4EBP1 (T37/46) followed by inhibition of phospho-AKT (S473) (Fig. 2) and thereby further contributed to anti-hypertrophic effects (and cytostatic effect), prevention of senescent morphology as well as inhibition of CLS. Importantly, effects of pan-mTOR inhibitors varied in their resemblance to rapamycin effects. In particular, Torin 1 and PP242 were rapamycin-like. The window between inhibition of pS6K/S6 versus p4EBP1 and AKT was narrower for Torin 2 and AZD8085 than for other 4 pan-mTOR inhibitors. In general, maximal gerosuppression (as measured by RPP) was achieved at concentrations that inhibited phosphorylation of S6K and S6 and only partially inhibited rapamycin-insensitive functions of mTOR. Rapamycin-like effects achieved at lower concentrations of pan-mTOR inhi-

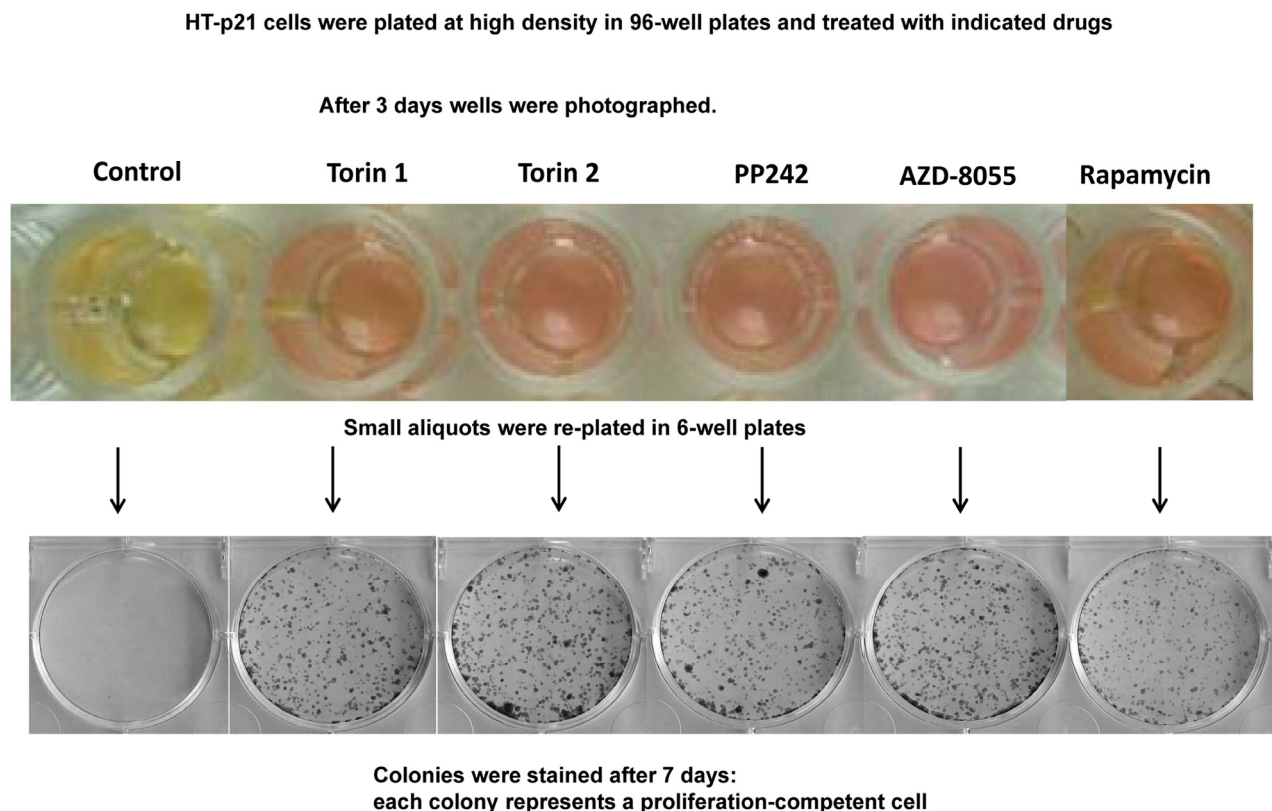


Figure 6. Effect of TOR inhibitors on chronological senescence of cancer HT-p21 cells. Cells were plated at high density in 96-well plates and treated with TOR inhibitors or rapamycin at selected optimal concentrations. After 3 days in culture cells were photographed (color manifests pH of medium), trypsinized and small aliquots were re-plated in 6-well plates. Formed colonies were stained after 7 days in culture with Crystal Violet.

bitors than rapamycin—unlike effects. Preservation of RPP depends on rapamycin-sensitive functions. Inhibition of senescent morphology (SA - beta - Gal

staining, hypertrophy, flat morphology) and CLS depends on both rapamycin-sensitive and -insensitive functions of mTOR.

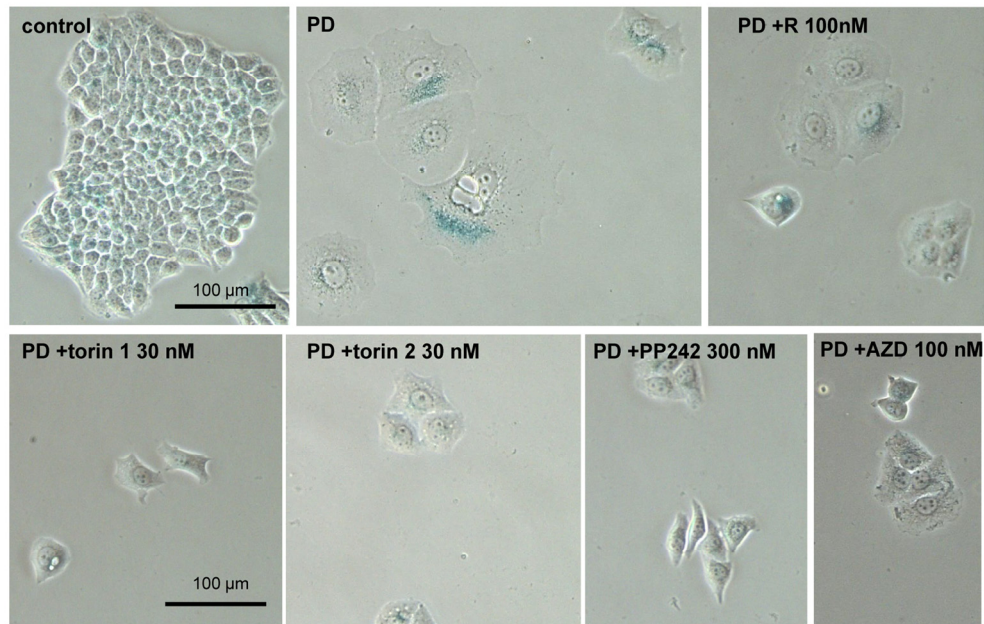


Figure 7. Effect of TORINs on senescent morphology of SKBR3 cells induced to senesce by treatment with PD0332991. Cells were treated with selected concentrations of TORINs and 10 μM PD0332991 (PD). After 4-day treatment drugs were washed out and cells were incubated in drug free medium for 2 days and stained for SA-beta-gal. Bar – 100 μm.

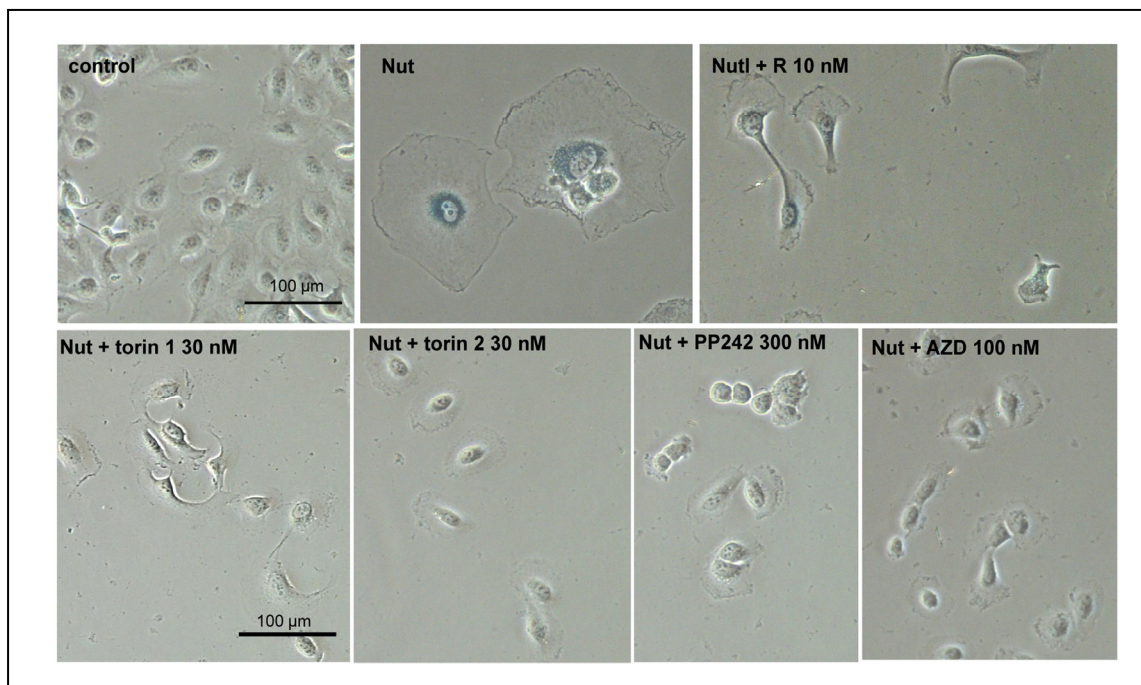


Figure 8. Effect of TORINs on senescent morphology of MEL10 cells undergoing senescence by treatment with nutlin 3a. Cells were treated with nutlin 3a (2.5 μM) and TORINs at selected concentrations or rapamycin (R). After 4-day treatment drugs were washed out and cells were incubated in drug-free medium for another 2 days and stained for SA-beta-gal. Bar – 100 μm. Nut – nutlin 3a; AZD – AZD8085.

At gerosuppressive concentrations, pan-mTOR inhibitors should be tested as anti-aging drugs. Life-long administration of pan-mTOR inhibitors to mice will take several years. Yet, administration of pan-mTOR inhibitors can be started late in life, thus shortening the experiment. In fact, rapamycin is effective when started late in life in mice [9]. Optimal doses and schedules of administration could be selected by administration of pan-mTOR inhibitors to prevent obesity in mice on high fat diet (HFD). It was shown that high doses of rapamycin prevented obesity in mice on HFD even when administered intermittently [21, 98-100]. Testing anti-obesity effects of pan-mTOR inhibitors will allow investigators to determine their effective doses and schedules within several months. It would be important to test both rapamycin-like agents such as Torin 1 and rapamycin-unlike agent such as Torin 2 or AZD8085. Selected doses and schedules can then be used to extend life-span in both short-lived mice, normal and heterogeneous mice as well as mice on high fat diet. These experiments will address questions of theoretical and practical importance: (a) role of rapamycin-insensitive functions of mTOR in aging. We would learn more about aging and age-related diseases. (b) can pan-mTOR inhibitors extend life span beyond the limits achievable by rapamycin. If successful, such experiments may reveal new causes of death in the absence of mTOR-driven aging, a post-aging syndrome, as mentioned previously [101]. Given that pan-mTOR inhibitors are already undergoing clinical trials for cancer therapy, one can envision their fast application for prevention of age-related diseases by slowing down aging.

MATERIALS AND METHODS

Cell lines and reagents

HT-p21 cells, derived from human fibrosarcoma HT1080, were described previously [69, 76, 81, 102, 103]. In HT-p21 cells, p21 expression can be turned on and off using IPTG (isopropyl-thio-galactosidase). These cells express GFP under CMV promoter. HT-p21 cells were cultured in DMEM/10% FC2 serum (HyClone FetaClone II; Thermo Scientific). Melanoma cell line MEL10 and breast adenocarcinoma SKBR3 (ATCC, Manassas, VA) were maintained in DMEM/10% FBS.

Rapamycin was purchased from LC Laboratories (Woburn, MA). Pan-mTOR inhibitors (torin 1, torin 2, PP242, AZD8085, KU-0063794, GSK1059615) and PD0332991 were from Selleckchem (Houston, TX). Stock solutions were prepared in DMSO.

Re-proliferative potential (RPP)

HT-p21 cells were plated at low densities and treated with IPTG alone or in combination with mTOR inhibitors as described in figure legends. After 3-4 days, IPTG and drugs were washed out and cells were allowed to re-proliferate in drug free medium for 7 days and counted in triplicates.

Immunoblot analysis

Cells were lysed using boiling lysis buffer (1% SDS, 10 mM Tris.HCl, pH7.4). Protein concentrations were measured using BCA protein reagent (Thermo Scientific) and equal amounts of protein were separated on 10% or gradient polyacrylamide gels and transferred onto PVDF membranes [69, 81]. The following antibodies were used: rabbit antibodies against phospho-pS6K(T389), phospho-S6(S235/236) and phospho-S6(S240/244), S6K, phospho-4EBP1(T37/46), phospho-AKT(S473) and phospho-AKT(T308), AKT and mouse anti-S6 – from Cell Signaling Technology (Danvers, MA); mouse monoclonal antibodies against cyclin D1 and rabbit anti-actin were from Santa Cruz Biotechnology (Paso Robles, CA) and Sigma-Aldrich (St. Louis, MO), respectively.

SA- β -galactosidase staining

β -gal staining was performed using Senescence-galactosidase staining kit from Cell Signaling Technology according to manufacturer's protocol. Cells were microphotographed under light microscope [69, 73].

CLS in mammalian cells

Cells were plated at high density in 96-well plates. After 3 days, cells were trypsinized and a small aliquot of attached cells was re-plated at low density in 6-well plates in fresh medium. After 7 days in culture colonies were stained with 1% Crystal Violet (Sigma-Aldrich) [83].

Oil Red O staining

0.35% Oil Red O (Sigma-Aldrich) stock was prepared in isopropanol. Working solution was prepared fresh before use by mixing 3 parts of Oil Red O stock with 2 parts of water and incubating it at RT for 20 min followed by filtering through 0.2 μ m filter. Cells were washed with PBS and incubated in 10% formalin at RT for 10 min and then with refreshed formalin for another 1 h followed by two washes in ddH₂O. Fixed cells were incubated in 60% isopropanol for 5 min at RT followed

by incubation with working solution of Oil Red O for 20 min. After extensive washes in ddH₂O, cells were microphotographed under light microscope.

CONFLICTS OF INTEREST

The authors have no conflict of interests to declare.

FUNDING

This work was supported by Roswell Park Cancer Institute fund.

REFERENCES

1. Kaeberlein M, Powers RW 3rd, Steffen KK, Westman EA, Hu D, Dang N, Kerr EO, Kirkland KT, Fields S, Kennedy BK. Regulation of yeast replicative life span by TOR and Sch9 in response to nutrients. *Science*. 2005; 310:1193–96. doi: 10.1126/science.1115535
2. Powers RW 3rd, Kaeberlein M, Caldwell SD, Kennedy BK, Fields S. Extension of chronological life span in yeast by decreased TOR pathway signaling. *Genes Dev*. 2006; 20:174–84. doi: 10.1101/gad.1381406
3. Kapahi P, Zid BM, Harper T, Koslover D, Sapin V, Benzer S. Regulation of lifespan in *Drosophila* by modulation of genes in the TOR signaling pathway. *Curr Biol*. 2004; 14:885–90. doi: 10.1016/j.cub.2004.03.059
4. Scialò F, Sriram A, Naudí A, Ayala V, Jové M, Pamplona R, Sanz A. Target of rapamycin activation predicts lifespan in fruit flies. *Cell Cycle*. 2015; 14:2949–58. doi: 10.1080/15384101.2015.1071745
5. Moskalev AA, Shaposhnikov MV. Pharmacological inhibition of phosphoinositide 3 and TOR kinases improves survival of *Drosophila melanogaster*. *Rejuvenation Res*. 2010; 13:246–47. doi: 10.1089/rej.2009.0903
6. Bjedov I, Toivonen JM, Kerr F, Slack C, Jacobson J, Foley A, Partridge L. Mechanisms of life span extension by rapamycin in the fruit fly *Drosophila melanogaster*. *Cell Metab*. 2010; 11:35–46. doi: 10.1016/j.cmet.2009.11.010
7. Danilov A, Shaposhnikov M, Plyusnina E, Kogan V, Fedichev P, Moskalev A. Selective anticancer agents suppress aging in *Drosophila*. *Oncotarget*. 2013; 4:1507–26. doi: 10.18632/oncotarget.1272
8. Robida-Stubbs S, Glover-Cutter K, Lamming DW, Mizunuma M, Narasimhan SD, Neumann-Haefelin E, Sabatini DM, Blackwell TK. TOR signaling and rapamycin influence longevity by regulating SKN-1/Nrf and DAF-16/FoxO. *Cell Metab*. 2012; 15:713–24. doi: 10.1016/j.cmet.2012.04.007
9. Harrison DE, Strong R, Sharp ZD, Nelson JF, Astle CM, Flurkey K, Nadon NL, Wilkinson JE, Frenkel K, Carter CS, Pahor M, Javors MA, Fernandez E, Miller RA. Rapamycin fed late in life extends lifespan in genetically heterogeneous mice. *Nature*. 2009; 460:392–95. doi: 10.1038/nature08221
10. Anisimov VN, Zabezhinski MA, Popovich IG, Piskunova TS, Semenchenko AV, Tyndyk ML, Yurova MN, Antoch MP, Blagosklonny MV. Rapamycin extends maximal lifespan in cancer-prone mice. *Am J Pathol*. 2010; 176:2092–97. doi: 10.2353/ajpath.2010.091050
11. Anisimov VN, Zabezhinski MA, Popovich IG, Piskunova TS, Semenchenko AV, Tyndyk ML, Yurova MN, Rosenfeld SV, Blagosklonny MV. Rapamycin increases lifespan and inhibits spontaneous tumorigenesis in inbred female mice. *Cell Cycle*. 2011; 10:4230–36. doi: 10.4161/cc.10.24.18486
12. Wilkinson JE, Burmeister L, Brooks SV, Chan CC, Friedline S, Harrison DE, Hejtmancik JF, Nadon N, Strong R, Wood LK, Woodward MA, Miller RA. Rapamycin slows aging in mice. *Aging Cell*. 2012; 11:675–82. doi: 10.1111/j.1474-9726.2012.00832.x
13. Comas M, Toshkov I, Kuropatwinski KK, Chernova OB, Polinsky A, Blagosklonny MV, Gudkov AV, Antoch MP. New nanoformulation of rapamycin Rapatar extends lifespan in homozygous p53^{-/-} mice by delaying carcinogenesis. *Aging (Albany NY)*. 2012; 4:715–22. doi: 10.18632/aging.100496
14. Komarova EA, Antoch MP, Novototskaya LR, Chernova OB, Paszkiewicz G, Leontieva OV, Blagosklonny MV, Gudkov AV. Rapamycin extends lifespan and delays tumorigenesis in heterozygous p53^{+/-} mice. *Aging (Albany NY)*. 2012; 4:709–14. doi: 10.18632/aging.100498
15. Ramos FJ, Chen SC, Garelick MG, Dai DF, Liao CY, Schreiber KH, MacKay VL, An EH, Strong R, Ladiges WC, Rabinovitch PS, Kaeberlein M, Kennedy BK. Rapamycin reverses elevated mTORC1 signaling in lamin A/C-deficient mice, rescues cardiac and skeletal muscle function, and extends survival. *Sci Transl Med*. 2012; 4:144ra103. doi: 10.1126/scitranslmed.3003802
16. Livi CB, Hardman RL, Christy BA, Dodds SG, Jones D, Williams C, Strong R, Bokov A, Javors MA, Ikeno Y, Hubbard G, Hasty P, Sharp ZD. Rapamycin extends life span of Rb1^{+/-} mice by inhibiting neuroendocrine tumors. *Aging (Albany NY)*. 2013; 5:100–10. doi: 10.18632/aging.100533
17. Miller RA, Harrison DE, Astle CM, Fernandez E, Flurkey K, Han M, Javors MA, Li X, Nadon NL, Nelson JF, Pletcher S, Salmon AB, Sharp ZD, et al. Rapamycin-

- mediated lifespan increase in mice is dose and sex dependent and metabolically distinct from dietary restriction. *Aging Cell*. 2014; 13:468–77. doi: 10.1111/accel.12194
18. Popovich IG, Anisimov VN, Zabezhinski MA, Semenchenko AV, Tyndyk ML, Yurova MN, Blagosklonny MV. Lifespan extension and cancer prevention in HER-2/neu transgenic mice treated with low intermittent doses of rapamycin. *Cancer Biol Ther*. 2014; 15:586–92. doi: 10.4161/cbt.28164
 19. Zhang Y, Bokov A, Gelfond J, Soto V, Ikeno Y, Hubbard G, Diaz V, Sloane L, Maslin K, Treaster S, Réndon S, van Remmen H, Ward W, et al. Rapamycin extends life and health in C57BL/6 mice. *J Gerontol A Biol Sci Med Sci*. 2014; 69:119–30. doi: 10.1093/gerona/glt056
 20. Fok WC, Chen Y, Bokov A, Zhang Y, Salmon AB, Diaz V, Javors M, Wood WH 3rd, Zhang Y, Becker KG, Pérez VI, Richardson A. Mice fed rapamycin have an increase in lifespan associated with major changes in the liver transcriptome. *PLoS One*. 2014; 9:e83988. doi: 10.1371/journal.pone.0083988
 21. Leontieva OV, Paszkiewicz GM, Blagosklonny MV. Weekly administration of rapamycin improves survival and biomarkers in obese male mice on high-fat diet. *Aging Cell*. 2014; 13:616–22. doi: 10.1111/accel.12211
 22. Hasty P, Livi CB, Dodds SG, Jones D, Strong R, Javors M, Fischer KE, Sloane L, Murthy K, Hubbard G, Sun L, Hurez V, Curiel TJ, Sharp ZD. eRapa restores a normal life span in a FAP mouse model. *Cancer Prev Res (Phila)*. 2014; 7:169–78. doi: 10.1158/1940-6207.CAPR-13-0299
 23. Fischer KE, Gelfond JA, Soto VY, Han C, Someya S, Richardson A, Austad SN. Health Effects of Long-Term Rapamycin Treatment: The Impact on Mouse Health of Enteric Rapamycin Treatment from Four Months of Age throughout Life. *PLoS One*. 2015; 10:e0126644. doi: 10.1371/journal.pone.0126644
 24. Ye L, Widlund AL, Sims CA, Lamming DW, Guan Y, Davis JG, Sabatini DM, Harrison DE, Vang O, Baur JA. Rapamycin doses sufficient to extend lifespan do not compromise muscle mitochondrial content or endurance. *Aging (Albany NY)*. 2013; 5:539–50. doi: 10.18632/aging.100576
 25. Johnson SC, Rabinovitch PS, Kaeberlein M. mTOR is a key modulator of ageing and age-related disease. *Nature*. 2013; 493:338–45. doi: 10.1038/nature11861
 26. Johnson SC, Yanos ME, Kayser EB, Quintana A, Sangesland M, Castanza A, Uhde L, Hui J, Wall VZ, Gagnidze A, Oh K, Wasko BM, Ramos FJ, et al. mTOR inhibition alleviates mitochondrial disease in a mouse model of Leigh syndrome. *Science*. 2013; 342:1524–28. doi: 10.1126/science.1244360
 27. Fang Y, Bartke A. Prolonged rapamycin treatment led to beneficial metabolic switch. *Aging (Albany NY)*. 2013; 5:328–29. doi: 10.18632/aging.100554
 28. Spong A, Bartke A. Rapamycin slows aging in mice. *Cell Cycle*. 2012; 11:845. doi: 10.4161/cc.11.5.19607
 29. Blagosklonny MV. Rapamycin extends life- and health span because it slows aging. *Aging (Albany NY)*. 2013; 5:592–98. doi: 10.18632/aging.100591
 30. Hurez V, Dao V, Liu A, Pandeswara S, Gelfond J, Sun L, Bergman M, Orihuela CJ, Galvan V, Padrón Á, Drerup J, Liu Y, Hasty P, et al. Chronic mTOR inhibition in mice with rapamycin alters T, B, myeloid, and innate lymphoid cells and gut flora and prolongs life of immune-deficient mice. *Aging Cell*. 2015; 14:945–56. doi: 10.1111/accel.12380
 31. Verlingue L, Dugourd A, Stoll G, Barillot E, Calzone L, Londoño-Vallejo A. A comprehensive approach to the molecular determinants of lifespan using a Boolean model of geroconversion. *Aging Cell*. 2016; 15:1018–26. doi: 10.1111/accel.12504
 32. Stanfel MN, Shamieh LS, Kaeberlein M, Kennedy BK. The TOR pathway comes of age. *Biochim Biophys Acta*. 2009; 1790:1067–74. doi: 10.1016/j.bbagen.2009.06.007
 33. Campistol JM, Eris J, Oberbauer R, Friend P, Hutchison B, Morales JM, Claesson K, Stallone G, Russ G, Rostaing L, Kreis H, Burke JT, Braut Y, et al. Sirolimus therapy after early cyclosporine withdrawal reduces the risk for cancer in adult renal transplantation. *J Am Soc Nephrol*. 2006; 17:581–89. doi: 10.1681/ASN.2005090993
 34. Kauffman HM, Cherikh WS, Cheng Y, Hanto DW, Kahan BD. Maintenance immunosuppression with target-of-rapamycin inhibitors is associated with a reduced incidence of de novo malignancies. *Transplantation*. 2005; 80:883–89. doi: 10.1097/01.TP.0000184006.43152.8D
 35. Euvrard S, Morelon E, Rostaing L, Goffin E, Brocard A, Tromme I, Broeders N, del Marmol V, Chatelet V, Domp Martin A, Kessler M, Serra AL, Hofbauer GF, et al, and TUMORAPA Study Group. Sirolimus and secondary skin-cancer prevention in kidney transplantation. *N Engl J Med*. 2012; 367:329–39. doi: 10.1056/NEJMoa1204166
 36. Bravo-San Pedro JM, Senovilla L. Immunostimulatory activity of lifespan-extending agents. *Aging (Albany NY)*. 2013; 5:793–801. doi: 10.18632/aging.100619
 37. Mannick JB, Del Giudice G, Lattanzi M, Valiante NM,

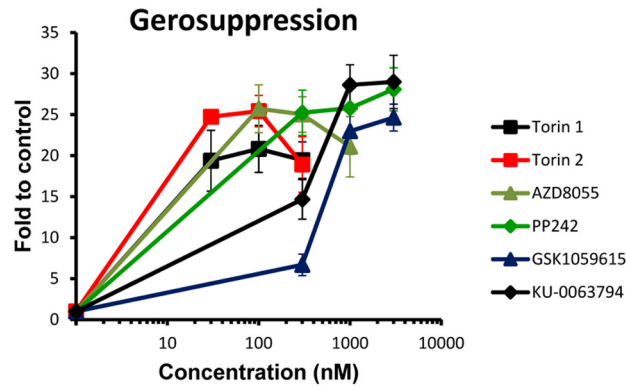
- Praestgaard J, Huang B, Lonetto MA, Maecker HT, Kovarik J, Carson S, Glass DJ, Klickstein LB. mTOR inhibition improves immune function in the elderly. *Sci Transl Med.* 2014; 6:268ra179. doi: 10.1126/scitranslmed.3009892
38. Kennedy BK, Pennington JK. Aging interventions get human. *Oncotarget.* 2015; 6:590–91. doi: 10.18632/oncotarget.3173
39. Blagosklonny MV. Rejuvenating immunity: “anti-aging drug today” eight years later. *Oncotarget.* 2015; 6:19405–12. doi: 10.18632/oncotarget.3740
40. Ross C, Salmon A, Strong R, Fernandez E, Javors M, Richardson A, Tardif S. Metabolic consequences of long-term rapamycin exposure on common marmoset monkeys (*Callithrix jacchus*). *Aging (Albany NY).* 2015; 7:964–73. doi: 10.18632/aging.100843
41. Fan X, Liang Q, Lian T, Wu Q, Gaur U, Li D, Yang D, Mao X, Jin Z, Li Y, Yang M. Rapamycin preserves gut homeostasis during *Drosophila* aging. *Oncotarget.* 2015; 6:35274–83.
42. Johnson SC, Yanos ME, Bitto A, Castanza A, Gagnidze A, Gonzalez B, Gupta K, Hui J, Jarvie C, Johnson BM, Letexier N, McCanta L, Sangesland M, et al. Dose-dependent effects of mTOR inhibition on weight and mitochondrial disease in mice. *Front Genet.* 2015; 6:247. doi: 10.3389/fgene.2015.00247
43. Zaseck LW, Miller RA, Brooks SV. Rapamycin Attenuates Age-associated Changes in Tibialis Anterior Tendon Viscoelastic Properties. *J Gerontol A Biol Sci Med Sci.* 2016; 71:858–65. doi: 10.1093/gerona/glv307
44. Xue QL, Yang H, Li HF, Abadir PM, Burks TN, Koch LG, Britton SL, Carlson J, Chen L, Walston JD, Leng SX. Rapamycin increases grip strength and attenuates age-related decline in maximal running distance in old low capacity runner rats. *Aging (Albany NY).* 2016; 8:769–76. doi: 10.18632/aging.100929
45. Bitto A, Ito TK, Pineda VV, LeTexier NJ, Huang HZ, Sutlief E, Tung H, Vizzini N, Chen B, Smith K, Meza D, Yajima M, Beyer RP, et al. Transient rapamycin treatment can increase lifespan and healthspan in middle-aged mice. *eLife.* 2016; 5:e16351. doi: 10.7554/eLife.16351
46. Lelegren M, Liu Y, Ross C, Tardif S, Salmon AB. Pharmaceutical inhibition of mTOR in the common marmoset: effect of rapamycin on regulators of proteostasis in a non-human primate. *Pathobiol Aging Age Relat Dis.* 2016; 6:31793. doi: 10.3402/pba.v6.31793
47. Halloran J, Hussong SA, Burbank R, Podlitskaya N, Fischer KE, Sloane LB, Austad SN, Strong R, Richardson A, Hart MJ, Galvan V. Chronic inhibition of mammalian target of rapamycin by rapamycin modulates cognitive and non-cognitive components of behavior throughout lifespan in mice. *Neuroscience.* 2012; 223:102–13. doi: 10.1016/j.neuroscience.2012.06.054
48. Lesovaya EA, Kirsanov KI, Antoshina EE, Trukhanova LS, Gorkova TG, Shipaeva EV, Salimov RM, Belitsky GA, Blagosklonny MV, Yakubovskaya MG, Chernova OB. Rapatar, a nanoformulation of rapamycin, decreases chemically-induced benign prostate hyperplasia in rats. *Oncotarget.* 2015; 6:9718–27. doi: 10.18632/oncotarget.3929
49. Kaeberlein M. Rapamycin and ageing: when, for how long, and how much? *J Genet Genomics.* 2014; 41:459–63. doi: 10.1016/j.jgg.2014.06.009
50. Tuháčková Z, Sovová V, Sloncová E, Proud CG. Rapamycin-resistant phosphorylation of the initiation factor-4E-binding protein (4E-BP1) in v-SRC-transformed hamster fibroblasts. *Int J Cancer.* 1999; 81:963–69. doi: 10.1002/(SICI)1097-0215(19990611)81:6<963::AID-IJC20>3.0.CO;2-C
51. Diggle TA, Moule SK, Avison MB, Flynn A, Foulstone EJ, Proud CG, Denton RM. Both rapamycin-sensitive and -insensitive pathways are involved in the phosphorylation of the initiation factor-4E-binding protein (4E-BP1) in response to insulin in rat epididymal fat-cells. *Biochem J.* 1996; 316:447–53. doi: 10.1042/bj3160447
52. Choo AY, Yoon SO, Kim SG, Roux PP, Blenis J. Rapamycin differentially inhibits S6Ks and 4E-BP1 to mediate cell-type-specific repression of mRNA translation. *Proc Natl Acad Sci USA.* 2008; 105:17414–19. doi: 10.1073/pnas.0809136105
53. Choo AY, Blenis J. Not all substrates are treated equally: implications for mTOR, rapamycin-resistance and cancer therapy. *Cell Cycle.* 2009; 8:567–72. doi: 10.4161/cc.8.4.7659
54. Kang SA, Pacold ME, Cervantes CL, Lim D, Lou HJ, Ottina K, Gray NS, Turk BE, Yaffe MB, Sabatini DM. mTORC1 phosphorylation sites encode their sensitivity to starvation and rapamycin. *Science.* 2013; 341:1236566. doi: 10.1126/science.1236566
55. Liu Y, Vertommen D, Rider MH, Lai YC. Mammalian target of rapamycin-independent S6K1 and 4E-BP1 phosphorylation during contraction in rat skeletal muscle. *Cell Signal.* 2013; 25:1877–86. doi: 10.1016/j.cellsig.2013.05.005
56. Thoreen CC, Kang SA, Chang JW, Liu Q, Zhang J, Gao Y, Reichling LJ, Sim T, Sabatini DM, Gray NS. An ATP-competitive mammalian target of rapamycin inhibitor

- reveals rapamycin-resistant functions of mTORC1. *J Biol Chem.* 2009; 284:8023–32. doi: 10.1074/jbc.M900301200
57. Yellen P, Saqcena M, Salloum D, Feng J, Preda A, Xu L, Rodrik-Outmezguine V, Foster DA. High-dose rapamycin induces apoptosis in human cancer cells by dissociating mTOR complex 1 and suppressing phosphorylation of 4E-BP1. *Cell Cycle.* 2011; 10:3948–56. doi: 10.4161/cc.10.22.18124
58. Jiang YP, Ballou LM, Lin RZ. Rapamycin-insensitive regulation of 4e-BP1 in regenerating rat liver. *J Biol Chem.* 2001; 276:10943–51. doi: 10.1074/jbc.M007758200
59. Benjamin D, Colombi M, Moroni C, Hall MN. Rapamycin passes the torch: a new generation of mTOR inhibitors. *Nat Rev Drug Discov.* 2011; 10:868–80. doi: 10.1038/nrd3531
60. Hassan B, Akcakanat A, Sangai T, Evans KW, Adkins F, Eterovic AK, Zhao H, Chen K, Chen H, Do KA, Xie SM, Holder AM, Naing A, et al. Catalytic mTOR inhibitors can overcome intrinsic and acquired resistance to allosteric mTOR inhibitors. *Oncotarget.* 2014; 5:8544–57. doi: 10.18632/oncotarget.2337
61. Jacinto E, Loewith R, Schmidt A, Lin S, Ruegg MA, Hall A, Hall MN. Mammalian TOR complex 2 controls the actin cytoskeleton and is rapamycin insensitive. *Nat Cell Biol.* 2004; 6:1122–28. doi: 10.1038/ncb1183
62. Markman B, Dienstmann R, Tabernero J. Targeting the PI3K/Akt/mTOR pathway--beyond rapalogs. *Oncotarget.* 2010; 1:530–43. doi: 10.18632/oncotarget.188
63. Chresta CM, Davies BR, Hickson I, Harding T, Cosulich S, Critchlow SE, Vincent JP, Ellston R, Jones D, Sini P, James D, Howard Z, Dudley P, et al. AZD8055 is a potent, selective, and orally bioavailable ATP-competitive mammalian target of rapamycin kinase inhibitor with in vitro and in vivo antitumor activity. *Cancer Res.* 2010; 70:288–98. doi: 10.1158/0008-5472.CAN-09-1751
64. Guo Y, Kwiatkowski DJ. Equivalent benefit of rapamycin and a potent mTOR ATP-competitive inhibitor, MLN0128 (INK128), in a mouse model of tuberous sclerosis. *Mol Cancer Res.* 2013; 11:467–73. doi: 10.1158/1541-7786.MCR-12-0605
65. Yu K, Toral-Barza L, Shi C, Zhang WG, Lucas J, Shor B, Kim J, Verheijen J, Curran K, Malwitz DJ, Cole DC, Ellingboe J, Ayril-Kaloustian S, et al. Biochemical, cellular, and in vivo activity of novel ATP-competitive and selective inhibitors of the mammalian target of rapamycin. *Cancer Res.* 2009; 69:6232–40. doi: 10.1158/0008-5472.CAN-09-0299
66. Blagosklonny MV. Cell cycle arrest is not yet senescence, which is not just cell cycle arrest: terminology for TOR-driven aging. *Aging (Albany NY).* 2012; 4:159–65. doi: 10.18632/aging.100443
67. Blagosklonny MV. Geroconversion: irreversible step to cellular senescence. *Cell Cycle.* 2014; 13:3628–35. doi: 10.4161/15384101.2014.985507
68. Demidenko ZN, Korotchkina LG, Gudkov AV, Blagosklonny MV. Paradoxical suppression of cellular senescence by p53. *Proc Natl Acad Sci USA.* 2010; 107:9660–64. doi: 10.1073/pnas.1002298107
69. Leontieva OV, Natarajan V, Demidenko ZN, Burdelya LG, Gudkov AV, Blagosklonny MV. Hypoxia suppresses conversion from proliferative arrest to cellular senescence. *Proc Natl Acad Sci USA.* 2012; 109:13314–18. doi: 10.1073/pnas.1205690109
70. Leontieva OV, Demidenko ZN, Blagosklonny MV. S6K in geroconversion. *Cell Cycle.* 2013; 12:3249–52. doi: 10.4161/cc.26248
71. Leontieva OV, Blagosklonny MV. CDK4/6-inhibiting drug substitutes for p21 and p16 in senescence: duration of cell cycle arrest and MTOR activity determine geroconversion. *Cell Cycle.* 2013; 12:3063–69. doi: 10.4161/cc.26130
72. Leontieva OV, Blagosklonny MV. Tumor promoter-induced cellular senescence: cell cycle arrest followed by geroconversion. *Oncotarget.* 2014; 5:12715–27. doi: 10.18632/oncotarget.3011
73. Leontieva OV, Demidenko ZN, Blagosklonny MV. Contact inhibition and high cell density deactivate the mammalian target of rapamycin pathway, thus suppressing the senescence program. *Proc Natl Acad Sci USA.* 2014; 111:8832–37. doi: 10.1073/pnas.1405723111
74. Zhao H, Halicka HD, Li J, Darzynkiewicz Z. Berberine suppresses gero-conversion from cell cycle arrest to senescence. *Aging (Albany NY).* 2013; 5:623–36. doi: 10.18632/aging.100593
75. Sousa-Victor P, Gutarra S, García-Prat L, Rodríguez-Ubrea J, Ortet L, Ruiz-Bonilla V, Jardí M, Ballestar E, González S, Serrano AL, Perdiguero E, Muñoz-Cánoves P. Geriatric muscle stem cells switch reversible quiescence into senescence. *Nature.* 2014; 506:316–21. doi: 10.1038/nature13013
76. Demidenko ZN, Blagosklonny MV. Growth stimulation leads to cellular senescence when the cell cycle is blocked. *Cell Cycle.* 2008; 7:3355–61. doi: 10.4161/cc.7.21.6919
77. Demidenko ZN, Zubova SG, Bukreeva EI, Pospelov VA, Pospelova TV, Blagosklonny MV. Rapamycin

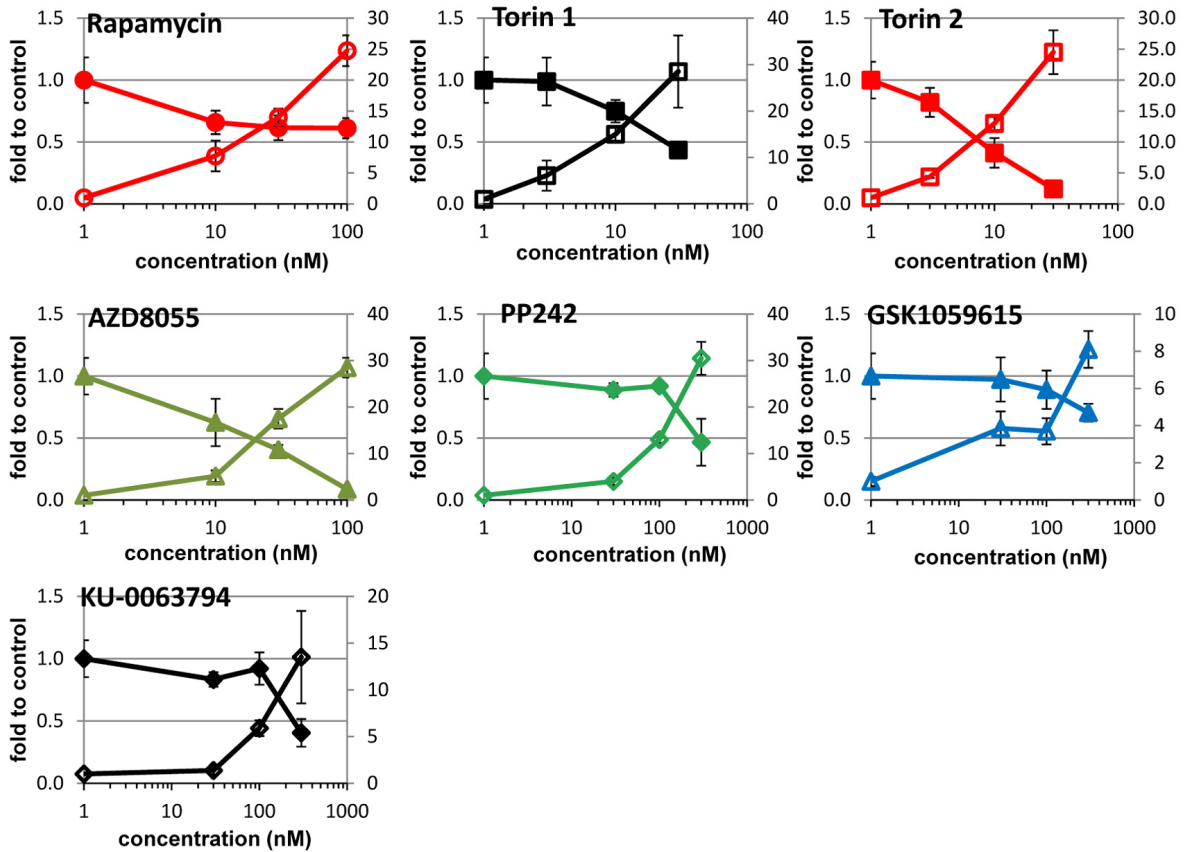
- decelerates cellular senescence. *Cell Cycle*. 2009; 8:1888–95. doi: 10.4161/cc.8.12.8606
78. Leontieva OV, Demidenko ZN, Blagosklonny MV. Dual mTORC1/C2 inhibitors suppress cellular geroconversion (a senescence program). *Oncotarget*. 2015; 6:23238–48. doi: 10.18632/oncotarget.4836
79. Sousa-Victor P, García-Prat L, Muñoz-Cánoves P. Dual mTORC1/C2 inhibitors: gerosuppressors with potential anti-aging effect. *Oncotarget*. 2015; 6:23052–54. doi: 10.18632/oncotarget.5563
80. Walters HE, Deneka-Hannemann S, Cox LS. Reversal of phenotypes of cellular senescence by pan-mTOR inhibition. *Aging (Albany NY)*. 2016; 8:231–44. doi: 10.18632/aging.100872
81. Leontieva OV, Lenzo F, Demidenko ZN, Blagosklonny MV. Hyper-mitogenic drive coexists with mitotic incompetence in senescent cells. *Cell Cycle*. 2012; 11:4642–49. doi: 10.4161/cc.22937
82. Demidenko ZN, Blagosklonny MV. Quantifying pharmacologic suppression of cellular senescence: prevention of cellular hypertrophy versus preservation of proliferative potential. *Aging (Albany NY)*. 2009; 1:1008–16. doi: 10.18632/aging.100115
83. Leontieva OV, Blagosklonny MV. Yeast-like chronological senescence in mammalian cells: phenomenon, mechanism and pharmacological suppression. *Aging (Albany NY)*. 2011; 3:1078–91. doi: 10.18632/aging.100402
84. Leontieva OV, Blagosklonny MV. M(o)TOR of pseudo-hypoxic state in aging: rapamycin to the rescue. *Cell Cycle*. 2014; 13:509–15. doi: 10.4161/cc.27973
85. Blagosklonny MV. Aging and immortality: quasi-programmed senescence and its pharmacologic inhibition. *Cell Cycle*. 2006; 5:2087–102. doi: 10.4161/cc.5.18.3288
86. Blagosklonny MV. An anti-aging drug today: from senescence-promoting genes to anti-aging pill. *Drug Discov Today*. 2007; 12:218–24. doi: 10.1016/j.drudis.2007.01.004
87. Blagosklonny MV. Paradoxes of aging. *Cell Cycle*. 2007; 6:2997–3003. doi: 10.4161/cc.6.24.5124
88. Blagosklonny MV. Aging: ROS or TOR. *Cell Cycle*. 2008; 7:3344–54. doi: 10.4161/cc.7.21.6965
89. Blagosklonny MV. Validation of anti-aging drugs by treating age-related diseases. *Aging (Albany NY)*. 2009; 1:281–88. doi: 10.18632/aging.100034
90. Blagosklonny MV, Hall MN. Growth and aging: a common molecular mechanism. *Aging (Albany NY)*. 2009; 1:357–62. doi: 10.18632/aging.100040
91. Blagosklonny MV. Calorie restriction: decelerating mTOR-driven aging from cells to organisms (including humans). *Cell Cycle*. 2010; 9:683–88. doi: 10.4161/cc.9.4.10766
92. Blagosklonny MV. Rapamycin and quasi-programmed aging: four years later. *Cell Cycle*. 2010; 9:1859–62. doi: 10.4161/cc.9.10.11872
93. Blagosklonny MV. Answering the ultimate question “what is the proximal cause of aging?”. *Aging (Albany NY)*. 2012; 4:861–77. doi: 10.18632/aging.100525
94. Blagosklonny MV. Aging is not programmed: genetic pseudo-program is a shadow of developmental growth. *Cell Cycle*. 2013; 12:3736–42. doi: 10.4161/cc.27188
95. Gems D, de la Guardia Y. Alternative Perspectives on Aging in *Caenorhabditis elegans*: Reactive Oxygen Species or Hyperfunction? *Antioxid Redox Signal*. 2013; 19:321–29. doi: 10.1089/ars.2012.4840
96. Gems D, Partridge L. Genetics of longevity in model organisms: debates and paradigm shifts. *Annu Rev Physiol*. 2013; 75:621–44. doi: 10.1146/annurev-physiol-030212-183712
97. Stipp D. A new path to longevity. *Sci Am*. 2012; 306:32–39. doi: 10.1038/scientificamerican0112-32
98. Chang GR, Chiu YS, Wu YY, Chen WY, Liao JW, Chao TH, Mao FC. Rapamycin protects against high fat diet-induced obesity in C57BL/6J mice. *J Pharmacol Sci*. 2009; 109:496–503. doi: 10.1254/jphs.08215FP
99. Leontieva OV, Paszkiewicz GM, Blagosklonny MV. Comparison of rapamycin schedules in mice on high-fat diet. *Cell Cycle*. 2014; 13:3350–56. doi: 10.4161/15384101.2014.970491
100. Makki K, Taront S, Molendi-Coste O, Bouchaert E, Neve B, Eury E, Lobbens S, Labalette M, Duez H, Staels B, Dombrowicz D, Froguel P, Wolowczuk I. Beneficial metabolic effects of rapamycin are associated with enhanced regulatory cells in diet-induced obese mice. *PLoS One*. 2014; 9:e92684. doi: 10.1371/journal.pone.0092684
101. Blagosklonny MV. Koschei the immortal and anti-aging drugs. *Cell Death Dis*. 2014; 5:e1552. doi: 10.1038/cddis.2014.520
102. Chang BD, Broude EV, Fang J, Kalinichenko TV, Abdryashitov R, Poole JC, Roninson IB. p21^{Waf1/Cip1/Sdi1}-induced growth arrest is associated with depletion of mitosis-control proteins and leads to abnormal mitosis and endoreduplication in recovering cells. *Oncogene*. 2000; 19:2165–70. doi: 10.1038/sj.onc.1203573
103. Broude EV, Swift ME, Vivo C, Chang BD, Davis BM, Kalurupalle S, Blagosklonny MV, Roninson IB. p21^(Waf1/Cip1/Sdi1) mediates retinoblastoma

protein degradation. *Oncogene*. 2007; 26:6954–58.
doi: 10.1038/sj.onc.1210516

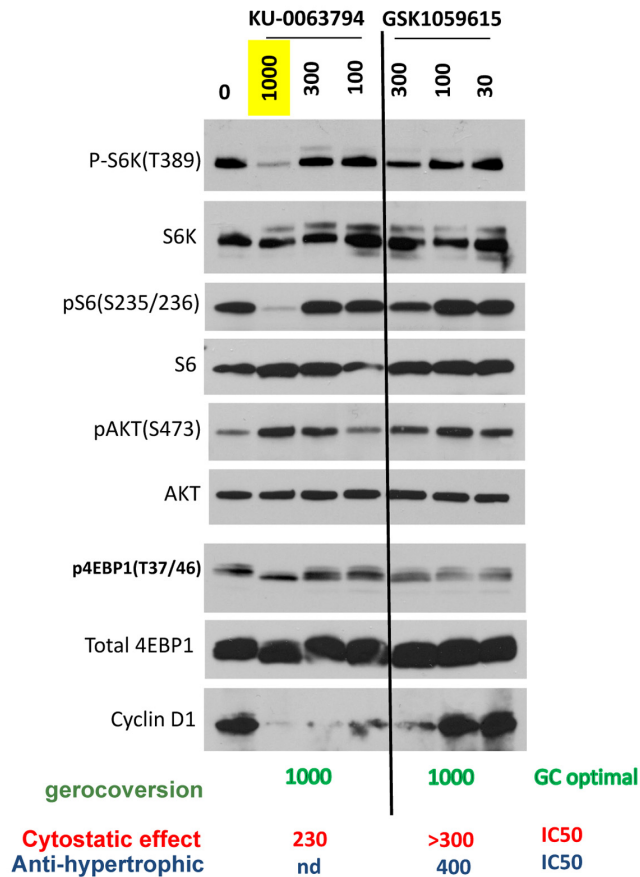
SUPPLEMENTARY MATERIAL



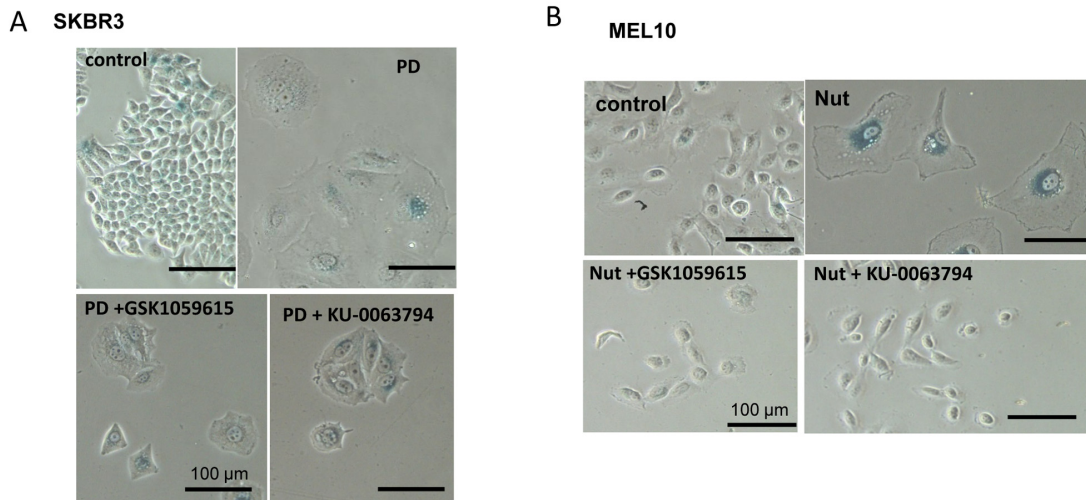
Supplementary Figure S1. Extended concentration ranges of TOR inhibitors to determine maximal optimal dose for gerosuppression in HT-p21 cellular model of senescence. HT-p21 cells were treated with IPTG and different concentrations of indicated TOR inhibitors. After 4 day-treatment, drugs were washed out and cells were incubated in drug-free medium For 7 days and counted. Data are mean ± SD from triplicate wells.



Supplementary Figure S2. Gerosuppressive effect mirrors cytostatic effect. of TOR inhibitors. HT-p21 cells were treated with serial dilutions of indicated drugs as described in Figure 1 A (for cytostatic effect, shown as filled markers) and in Fig. 1C (for gerosuppressive effect, shown as empty markers).



Supplementary Figure S3. HT-p21 cells were treated with range of concentrations of KU-0063794 and GSK1059615 for 24 h and lysed. Data present Immunoblotting with indicated antibodies.



Supplementary Figure S4. Effect of GSK1059615 and KU-0063794 on senescent morphology of SKBR3 (A) and MEL10 (B) cells. SKBR3 and MEL10 cells were induced to senesce by treatment with 10 μ M PD0332991 (PD) or 2.5 μ M nutlin 3a (Nut), respectively. Co-treatment with either 1000 nM of GSK1059615 or KU-0063794 prevent senescent morphology in these cells.

Towards specific inhibition of mTORC2

Elizabeth R. Murray and Angus JM. Cameron

The mammalian target of rapamycin (mTOR) serine/threonine protein kinase is a key regulator of eukaryotic cell growth, metabolism and survival. In mammals, mTOR functions in two distinct multi-subunit complexes, mTOR complex 1 (mTORC1) and mTOR complex 2 (mTORC2). These complexes integrate signals concerning the availability of cellular energy, nutrients and growth factors to affect metabolism, protein biosynthesis, lipid biosynthesis, cell proliferation and autophagy through the phosphorylation of distinct effectors, including members of the AGC kinase family. The target specificity of mTORC1 and mTORC2 can be attributed to the unique protein components of each complex. The mTORC1-specific subunit Raptor thus recruits mTORC1 substrates including 4EBP1 and p70S6 kinase. Amongst the various mTORC2-specific subunits, Sin1 has now been shown to recruit selected AGC kinase substrates including AKT. Both complexes are implicated in the aging process and multiple age-related diseases including cancer, cardiovascular disease, type II diabetes and neurodegenerative disorders.

Historically, investigation of mTOR complex function in aging and disease has been facilitated by genetic deletion of mTOR components, the small molecule inhibitor rapamycin, and ATP-competitive kinase inhibitors. Rapamycin is an acute inhibitor of mTORC1 but not mTORC2, and kinase inhibitors generally target both mTORC1 and mTORC2. Hence, whilst the role of mTORC1 in aging is relatively well defined – rapamycin is well established to extend the lifespan of mice – the study of mTORC2 function has been limited by a lack of specific mTORC2 inhibitors. This is complicated by the fact that chronic rapamycin treatment disrupts mTORC2 in a cell-type and context specific manner. For example, chronic rapamycin disrupts hepatic mTORC2 *in vivo*, leading to glucose intolerance and insulin resistance; attributed to mTORC2 as *Rictor* deletion alone also induces hepatic insulin resistance [1]. Intriguingly, *Rictor* deletion in mice is also deleterious for the longevity of males but does not negatively affect the lifespan of females, in a manner that is independent of glucose intolerance [2]. In a separate study, rapamycin treatment has been shown to increase the lifespan of both male and female mice, but to increase the lifespan of females more than males [3].

This suggests that chronic rapamycin-induced inhibition of mTORC2 limits the longevity benefits afforded by mTORC1 inhibition, specifically in male mice. Overall, these studies suggest caution in the use of non-specific mTOR complex inhibitors until more is understood with respect to the role of mTORC2 in aging and disease. Potential liabilities associated with targeting mTORC2, such as induction of diabetes and suppression of lifespan, require further study.

Excitingly, new mechanisms of selectively inhibiting mTORC2 are emerging (Figure 1). One approach via disruption of mTORC2 substrate recruitment shows promise. We previously identified the central highly conserved region in the middle (CRIM) domain of Sin1 as a direct binding partner of the mTORC2-specific substrates PKC ϵ and AKT [4]. Expression of Sin1 mutants, where the CRIM domain has been disrupted or deleted, is sufficient to displace endogenous Sin1 from mTORC2 and inhibit phosphorylation of the mTORC2-specific targets AKT, PKC α and PKC ϵ . In contrast, phosphorylation of the mTORC1-specific target, P70S6K Thr389 is unaffected. Recently, in a key paper by Tatebe et al., the CRIM domain of Sin1 was shown to form a discrete ubiquitin-fold domain that specifically binds and recruits mTORC2-specific substrate AGC kinases [5]. Target recognition requires interaction with a short acidic peptide, highly conserved in diverse eukaryote Sin1 orthologues, and previously shown by us to be required for AGC targeting [4]. In our most recent work [6], we have shown that expression of mutant Sin1 in DLD1 colon cancer cells inhibits AKT phosphorylation of the mTORC2 target site Ser473 and also on the PDK1 site Thr308. Furthermore, blocking mTORC2 substrate binding in DLD1 cells attenuated tumour growth, and tumour size correlated with the degree of AKT suppression *in vivo*. Thus, disrupting substrate recruitment provides a novel way to define mTORC2 complex-specific functions, and inhibitors of mTORC2-substrate interactions could be of therapeutic benefit for patients with cancer.

The next challenge is to identify feasible therapeutic strategies to selectively block mTORC2 function in the clinic. One possible approach is to target complex-specific protein-protein interactions, as pioneered recently with the identification of small molecules that inhibit the association of Rictor with mTOR [7]. These compounds inhibit the phosphorylation of mTORC2

targets AKT, NDRG1 and PKC α and critically, no effect on the phosphorylation of the mTORC1 substrate p70S6 kinase or mTORC1-dependent negative feedback loops was observed. In the same study, these small molecules inhibited cell growth, motility and invasion in glioblastoma cells *in vitro* and, *in vivo*, inhibited glioblastoma xenograft tumour growth. It is perhaps worth noting that pharmacological disruption or genetic ablation of the mTORC2 complex may not be the functional equivalent of blocking substrate recruitment (Figure 1). Indeed, a central highly conserved multi-protein complex such as mTORC2 is likely to have additional non-catalytic functions. Targeting substrate recruitment, either through CRIM domain mutation or with drugs, may thus provide a more nuanced view on mTORC2 function.

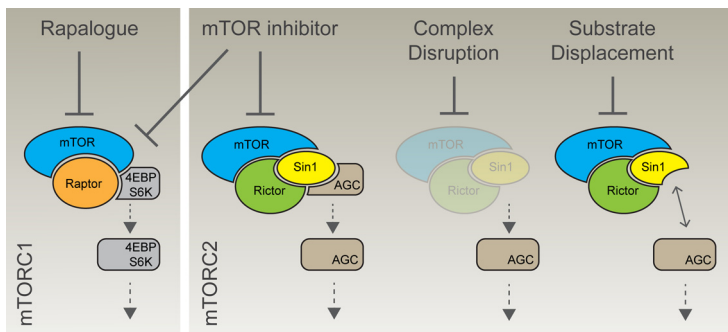


Figure 1. Distinct strategies for selective and unselective targeting of the mTOR complexes. Rapamycin and related rapalogues acutely target mTORC1 specifically, although chronic exposure can also limit mTORC2 function in a context specific manner. Alternatively, mTOR catalytic inhibitors do not discriminate between the complexes. Targeting complex-specific subunits provides an alternative route to specific blockade. mTORC2 complex disruption, either through genetic deletion of Rictor or with small molecules, leads to loss of the entire complex. Alternatively, disruption of substrate recruitment can uncouple mTORC2 from its targets, while leaving the complex intact. Contrasting these distinct approaches will help define therapeutic opportunities and liabilities associated with mTOR inhibition.

mTORC2 has emerged as a promising drug target, particularly in cancer, but the complex roles of mTORC2 in the aging process and age-related disorders remain potential liabilities. Progress in defining the molecular mechanisms underlying mTORC2 function has begun to identify selective strategies for targeting mTORC2, which will complement the mTORC1 directed rapalogues, as we continue to unravel the convoluted mTOR-signalling network.

REFERENCES

1. Lamming DW, et al. *Science*. 2012; 335:1638–43. <https://doi.org/10.1126/science.1215135>
2. Lamming DW, et al. *Aging Cell*. 2014; 13:911–17. <https://doi.org/10.1111/ace1.12256>
3. Miller RA, et al. *Aging Cell*. 2014; 13:468–77. <https://doi.org/10.1111/ace1.12194>
4. Cameron AJ, et al. *Biochem J*. 2011; 439:287–97. <https://doi.org/10.1042/BJ20110678>
5. Tatebe H, et al. *eLife*. 2017; 6. <https://doi.org/10.7554/eLife.19594>
6. Cameron AJ, et al. *Oncotarget*. 2017; 8:84685–96. <https://doi.org/10.18632/oncotarget.20086>
7. Benavides-Serrato A, et al. *PLoS One*. 2017; 12:e0176599. <https://doi.org/10.1371/journal.pone.0176599>

Angus J.M. Cameron: Kinase Biology Laboratory, Centre for Tumour Biology, Barts Cancer Institute, Queen Mary, University of London, John Vane Science Centre, Charterhouse Square, London, EC1M 6BQ, UK

Correspondence: Angus J.M. Cameron

Email: a.cameron@qmul.ac.uk

Keywords: mTOR, mTORC2, AGC kinases, AKT, PKC, Sin1

Copyright: Murray and Cameron. This is an open-access article distributed under the terms of the Creative Commons Attribution License (CC BY 3.0), which permits unrestricted use, distribution, and reproduction in any medium, provided the original author and source are credited

Received: December 6, 2017

Published: December 12, 2017

Fasting for stem cell rejuvenation

Cristina González-Estévez and Ignacio Flores

Throughout the centuries, humankind has relentlessly searched for ways to live longer and healthier lives. From the "fountain of youth" quest to novel senolytics, from alchemical recipes to modern diets, different approaches have been pursued to fulfil the human desire of prolonging life while maintaining good shape. Among all anti-aging interventions, calorie restricted diets and periods of fasting stand out as the most compelling and robust methods to prolong life and health span and to reduce the risk of diabetes, neurodegeneration, autoimmune disorders, spontaneous tumours and cardiovascular disease [1]. Furthermore, dietary interventions are also emerging as important enhancers of adult stem cell function [2]. However, little is known on how prolonged fasting alters the function and properties of adult stem cells. Since fasting outcomes are conserved across taxa [2], studying fasting in species that possess many stem cells and can cope with long periods of food deprivation can be exceedingly informative.

Planarians -better known for their impressive regenerative capacities- can be deprived of food for more than 3 months without showing an impairment in either physiology or activity levels. They handle prolonged periods of starvation or fasting by shrinking in size. Around 25% of the cells in their parenchyma are adult stem cells, which are kept in a constant ration respect their body size. Interestingly, refeeding allows fasted planarians to grow back to their original size [3]. Their stem cells do not show any signs of senescence and hence they are considered immortal. How fasting influences planarian stem cell properties is unknown.

We have recently reported the effect of fasting on planarian stem cells regarding telomere length [4]. Telomeres protect chromosomes from DNA degradation and misguided repair mechanisms. Proper telomere functioning requires a minimum length that is maintain by telomerase. However, telomerase activity levels in adult tissues are not sufficient to prevent progressive telomere shortening with age [5]. Therefore, telomere length is considered a cellular marker of aging. By measuring telomere length *in situ* on whole planarians we found that fasted planarians present a higher percentage of stem cells with the longest telomeres, indicating that fasting rejuvenates the stem cell pool [4]. Having a population of stem cells with very long telomeres allows planarians to quickly respond to any

injury even while fasting. It also allows them to mount a long-term proliferation response as soon as nutrients become available again. Therefore, natural cycles of fasting and feeding promote the maintenance of a healthy and always cycling stem cell population thus making planarians immortal (Figure 1).

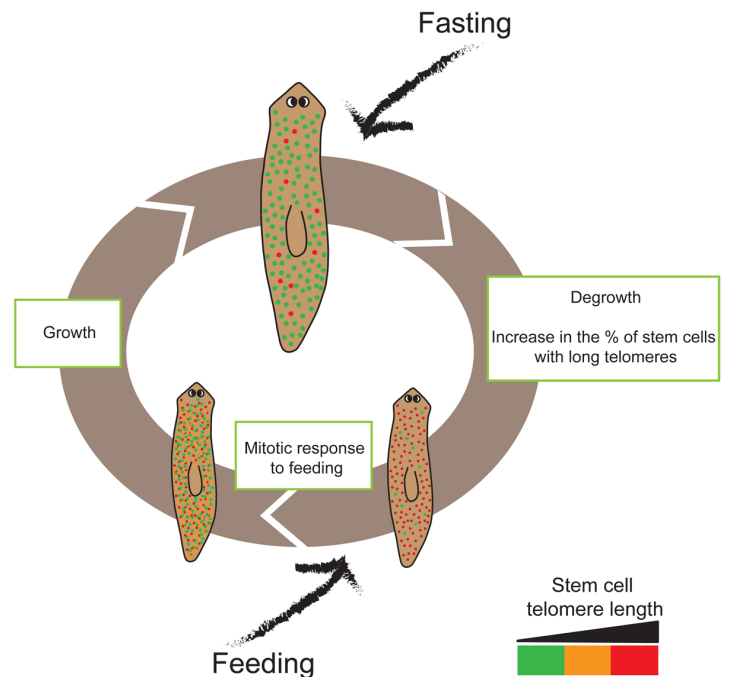


Figure 1. Schematic representation of the life cycle of *Schmidtea mediterranea* asexual strain. Cycles of feeding and fasting are common during planarian life. During fasting the percentage of stem cells with long telomeres increases. Feeding induces a rapid proliferative response. During growing due to feeding, the stem cell pool decreases its telomere length. Red cells indicate stem cells with the longest telomeres while the orange show medium length and the green ones the shortest telomeres. Planarians are not to scale.

Our data shows that the enrichment of stem cells with long telomeres during fasting occurs through the inhibition of mTOR signalling [4], a pathway known to enhance stem cell function during dietary restriction [2]. The easy explanation to understand how mTOR down-regulation elongates telomeres is through a reduction in mitosis. It is indeed known that mTOR signalling regulates the mitotic response to amputation and blastema growth [6]. However, while fasting increases

telomere length, the number of mitosis and stem cells remains constant [7]. Other factors than cell division may modulate telomere length, for instance exonucleases or oxygen levels [5]. It is also feasible that stem cells with the shortest telomeres are considered “less-fit” or “loser”, being selected to either die or differentiate and contributing in this way to a general increase in telomere length in the remaining stem cell pool. Interestingly, mTOR signalling has been linked to “cell competition” and an mTOR-controlled process, autophagy, has been shown to be required by “loser” cells to die [8]. The question still remains on whether fasting affects other molecular/cellular processes in planarian stem cells. Ongoing research will clarify this point.

Both activation of telomerase and long telomere length are known to positively correlate with stem cell pluripotency. Interestingly we find that the stem cell population is highly heterogeneous for telomere length, correlating with their known heterogeneity with regards to potency and lineage commitment [4]. We also find that fasting not only increases the percentage of stem cells with long telomeres but also increases the maximum telomere length in planarian stem cells [4]. Altogether leads to the attractive hypothesis that fasting, by modulating mTOR signalling, may increase pluripotency in planarians. Our work opens up many interesting endeavours which we predict will help in the understanding of regeneration and stem cell ageing.

REFERENCES

1. Longo VD, Mattson MP. *Cell Metab.* 2014; 19:181–92. <https://doi.org/10.1016/j.cmet.2013.12.008> PMID:24440038
2. Fontana L, Partridge L. *Cell.* 2015; 161:106–18. <https://doi.org/10.1016/j.cell.2015.02.020> PMID:25815989
3. Felix DA, et al. *Semin Cell Dev Biol.* 2019; 87:169–81. <https://doi.org/10.1016/j.semcdb.2018.04.010> PMID:29705301
4. Iglesias M, et al. *Stem Cell Reports.* 2019; 13:405–18. <https://doi.org/10.1016/j.stemcr.2019.06.005> PMID:31353226
5. Flores I, et al. *Genes Dev.* 2008; 22:654–67. <https://doi.org/10.1101/gad.451008> PMID:18283121
6. González-Estévez C, et al. *PLoS Genet.* 2012; 8:e1002619. <https://doi.org/10.1371/journal.pgen.1002619> PMID:22479207
7. González-Estévez C, et al. *Int J Dev Biol.* 2012; 56:83–91. <https://doi.org/10.1387/ijdb.113452cg>

PMID:22252539

8. Nagata R, et al. *Dev Cell.* 2019; 51:99–112.e4. <https://doi.org/10.1016/j.devcel.2019.08.018> PMID:31543447

Cristina González-Estévez: Leibniz Institute on Aging-Fritz Lipmann Institute (FLI), Jena 07745, Germany

Correspondence: Cristina González-Estévez, Ignacio Flores
Email: cristina.gonzalez.estevez@gmail.com, iflores@cnic.es

Keywords: planarian, mTOR, *Schmidtea mediterranea*, starvation, stem cell, telomere

Funding: CGE was funded by the FLI. The FLI is a member of the Leibniz Association and is financially supported by the Federal Government of Germany and the State of Thuringia. IF was funded by grants from the Spanish Ministry of Science and Innovation (SAF2016-80406-R) and the Comunidad de Madrid (S2017/BMD-3875). The CNIC is supported by the Ministerio de Ciencia, Innovación y Universidades and the Pro CNIC Foundation, and is a Severo Ochoa Center of Excellence (SEV-2015-0505)

Copyright: González-Estévez and Flores. This is an open-access article distributed under the terms of the Creative Commons Attribution License (CC BY 3.0), which permits unrestricted use, distribution, and reproduction in any medium, provided the original author and source are credited

Received: February 25, 2020

Published: March 6, 2020

BMAL1 knockdown triggers different colon carcinoma cell fates by altering the delicate equilibrium between AKT/mTOR and P53/P21 pathways

Yuan Zhang^{1,2}, Aurore Devocelle^{2,3}, Lucas Souza^{1,2}, Adlen Foudi^{1,2}, Sabrina Tenreira Bento^{1,2}, Christophe Desterke^{1,2}, Rachel Sherrard⁵, Annabelle Ballesta^{1,2}, Rene Adam^{1,2,4}, Julien Giron-Michel^{2,3}, Yunhua Chang^{1,2}

¹INSERM, UMR935, Malignant and Therapeutic Stem Cells Models, Villejuif, France

²Paris-Saclay University, Saint-Aubin, France

³INSERM, UMR1197 Interactions between Stem Cells and Their Niches in Physiology, Tumors and Tissue Repair, Villejuif, France

⁴Hôpital Paul Brousse AP-HP, Villejuif, France

⁵Sorbonne Université and CNRS, Institut de Biologie Paris Seine, UMR8256 Biological Adaptation and Aging (B2A), Paris, France

Correspondence to: Yunhua Chang; email: yunhua.chang-marchand@inserm.fr

Keywords: BMAL1, mTOR, P53, senescence, colorectal cancer1

Received: October 2, 2019

Accepted: March 24, 2020

Published: May 10, 2020

Copyright: Zhang et al. This is an open-access article distributed under the terms of the Creative Commons Attribution License (CC BY 3.0), which permits unrestricted use, distribution, and reproduction in any medium, provided the original author and source are credited.

ABSTRACT

Dysregulation of the circadian timing system (CTS) frequently appears during colorectal cancer (CRC) progression. In order to better understand the role of the circadian clock in CRC progression, this study evaluated *in vitro* how knockdown of a core circadian protein BMAL1 (BMAL1-KD) influenced the behavior of two primary human CRC cell lines (HCT116 and SW480) and a metastatic CRC cell line (SW620).

Unexpectedly, BMAL1-KD induced CRC cell-type specific responses rather than the same phenomenon throughout. First, BMAL1-KD increased AKT/mTOR activation in each CRC cell line, but to different extents. Second, BMAL1-KD-induced P53 activation varied with cell context. In a wild type P53 background, HCT116 BMAL1-KD cells quickly underwent apoptosis after shBMAL1 lentivirus transduction, while surviving cells showed less P53 but increased AKT/mTOR activation, which ultimately caused higher proliferation. In the presence of a partially functional mutant P53, SW480 BMAL1-KD cells showed moderate P53 and mTOR activation simultaneously with cell senescence. With a moderate increased AKT but unchanged mutant P53 activation, SW620 BMAL1-KD cells grew faster.

Thus, under different CRC cellular pathological contexts, BMAL1 knockdown induced relatively equal effects on AKT/mTOR activation but different effects on P53 activation, which finally triggered different CRC cell fates.

INTRODUCTION

The circadian timing system (CTS) exists in most living organisms with a basic molecular frame preserved from fungi to *Drosophila* and humans. This system coordinates behavior of the whole organism, including physiology and metabolism, with environmental cycles

of 24h. In mammals, the suprachiasmatic nuclei of the hypothalamus coordinate circadian rhythms via peripheral molecular clocks composed of at least fifteen genes that are expressed in every cell. Expression of these clock gene is regulated by transcription factors organized in positive (BMAL1 and CLOCK) or negative (PER and CRY) feedback loops. Briefly, the

transcriptional activator complex of BMAL1/CLOCK activates transcription of its target genes inducing expression of CRY and PER proteins, which in turn repress their own transcription through their interactions with the BMAL1/CLOCK heterodimer. The BMAL1/CLOCK heterodimer also activates the expression of REV-ERB α/β (NR1D1 and NR1D2) and ROR $\alpha/\beta/\gamma$, which repress and activate *BMAL1* transcription, respectively [1, 2]. Thus *BMAL1* is central to circadian timing and is the only clock gene whose deletion causes an immediate loss of behavioral circadian rhythmicity [1, 3].

This molecular circadian clock regulates multiple cellular processes, with ~43% of mammalian protein-coding genes showing rhythmic expression at least in one organ [4]. Also, 25% of protein phosphorylation [5] and nuclear accumulation of over 10% of nuclear proteins [6] exhibit circadian oscillation. Thus, by regulating many fundamental cellular processes, such as cell cycle, metabolism, senescence, apoptosis and DNA damage response, an intact circadian clock plays a crucial role in maintaining normal cell life and its dysfunction perturbs numerous cellular activities, thereby becoming a risk factor for disease, such as cancer [7, 8].

The link between circadian rhythms and cancer is indicated by an increased risk of cancer in people whose daily rhythms are disturbed by shift work or insufficient sleep [9]. Furthermore, circadian rhythmicity is often dysregulated in cancer patients and associated with poor prognosis and early mortality [10–13]. Although the BMAL1 exhibits a globally repressive function in many tumors, some studies also reveal that BMAL1 might favor tumorigenesis under certain circumstances. For example, compared to healthy tissue, colorectal cancers (CRC) often display higher CLOCK or BMAL1 expression, which is associated with liver metastasis and poorly differentiated or late-stage CRC cancer [14–16]. In addition, the majority of malignant pleural mesothelioma (MPM) cell lines, and a subset of MPM clinical specimens, expressed more BMAL1 compared to their non-cancer controls (non-tumorigenic mesothelial cell line - MeT-5A - and normal parietal pleura, respectively). Moreover, BMAL1 knockdown (BMAL1-KD) in MPM cell lines reduced cell growth and induced apoptosis [17, 18]. Therefore, the relationship between BMAL1 and cancer development is complex and requires deeper investigation to reveal molecular mechanistic insights.

CRC is one of the most common cancers. In 2012, there were 1.4 million new cases and 693,900 deaths worldwide from the disease [19]. In this study, we investigated the influence of BMAL1 deficiency in

CRC cell behavior in order to better understand the role of the circadian clock in colon cancer development at cellular and molecular levels. We have selected two primary colorectal adenocarcinoma cell lines, HCT116 and SW480, and a metastatic CRC cell line derived from the same patient as SW480 cells (SW620). Both primary CRC cell lines, HCT116 and SW480, express core-clock genes with circadian oscillation, whereas this oscillation is severely diminished in the metastatic cell line SW620 [20, 21, 22]. Using these three cell lines, we knocked down *BMAL1* expression by shRNA to investigate the influence of BMAL1 deficiency on CRC cell behavior.

Our results revealed that BMAL1-KD activated AKT/mTOR similarly in the three CRC cell lines (HCT116, SW480 or SW620), but had different effects on P53 activation. mTOR signaling is an evolutionarily conserved nutrient sensing pathway and a central regulator of mammalian metabolism. It has been hypothesized that increased mTOR activity could direct cell fate towards quiescence, cell death or senescence under varying P53 activation and P21 expression status [23–26]. Here, by altering the delicate equilibrium between AKT/mTOR and P53/P21 pathways, BMAL1-KD modulates CRC cell fates on the basis of their distinct cellular context.

RESULTS

Decreased BMAL1 altered expression of some circadian genes in primary CRC cell lines

Three CRC cell lines, two primary cell lines (HCT116 and SW480) and a metastatic cell line SW620, were transduced with lentiviruses encoding a scrambled shRNA (shScr) or a shRNA targeting BMAL1 (shBMAL1). After transduction, cells were selected by one-week puromycin treatment to remove non-transduced cells. Successful transduction was confirmed by flow cytometry of GFP expressing cells. The GFP positive cell population was used immediately for analysis as BMAL1-KD or control (Ctr) cells.

BMAL1 expression was significantly decreased compared to control at mRNA (Figure 1A, qRT-PCR) and protein levels (Figure 1B, Western blot) in all three BMAL1-KD cell lines, despite the fact that the two primary CRC cell lines exhibited much higher BMAL1 expression than the metastatic CRC cell line SW620.

Expression of BMAL1 target circadian genes (*NR1D1*, *PER2*, *CRY1* and *CRY2*) and its functional partner *CLOCK*, were also analyzed following BMAL1-KD. In the two primary BMAL1-KD CRC cell lines

(HCT116 and SW480), but not in BMAL1-KD SW620 cells, *NR1D1* expression was reduced and *CLOCK* expression was increased (Figure 1C, 1D). No significant modification of *PER2*, *CRY1* or *CRY2* expression was identified in any of the three cell lines (Data not shown).

BMAL1-KD thus modified circadian gene expression profile in two primary CRC cell lines (HCT116 and SW480) but not in the metastatic CRC cell line SW620.

BMAL1-KD increased AKT/mTOR activation in primary CRC cell lines

BMAL1 knockout mice manifest increased mTORC1 (mammalian target of rapamycin complex 1) activity and associated premature aging [27]. We thus investigated whether BMAL1-KD could modify AKT/mTOR signaling in CRC cell lines.

BMAL1-KD increased AKT activation in colon cancer cell lines. Compared to their controls, the percentage of AKT phosphorylation, measured by the ratio between phosphorylated AKT (pAKT) and total AKT, was greatly increased in the primary CRC lines, HCT116 BMAL1-KD ($p=0.0207$) and SW480 BMAL1-KD ($p=0.0302$), and slightly increased in

the metastatic SW620 BMAL1-KD ($p=0.0141$) cells (Figure 2A).

Moreover, mTOR activation, measured by the ratio between phosphorylated mTOR (pmTOR) and total mTOR, was significantly increased in HCT116 BMAL1-KD cells ($p=0.0298$) and in SW480 BMAL1-KD cells ($p=0.0291$) in comparison to their respective controls. However, SW620 BMAL1-KD cells only showed trend to increased mTOR activation ($p=0.0897$) (Figure 2B).

To further evaluate mTOR activity, we measured the phosphorylation of 40S Ribosomal protein S6, a major mTOR effector. Western blot analysis revealed a significant increase of S6 phosphorylation (pS6/S6 total) in HCT116 BMAL1-KD cells ($p=0.0324$) and in SW480 BMAL1-KD cells ($p=0.0052$) compared to controls. However, only a trend to increased phosphorylation was found in SW620 BMAL1-KD ($p=0.0634$; Figure 2C). These results were further confirmed by flow cytometry analysis, which revealed that the mean fluorescence intensity of pS6-APC staining increased significantly in HCT116 BMAL1-KD cells ($p=0.0316$) and in SW480 BMAL1-KD cells ($p<0.0001$), but not in SW620 BMAL1-KD cells ($p=0.4027$) compared to their own controls (Figure 2D).

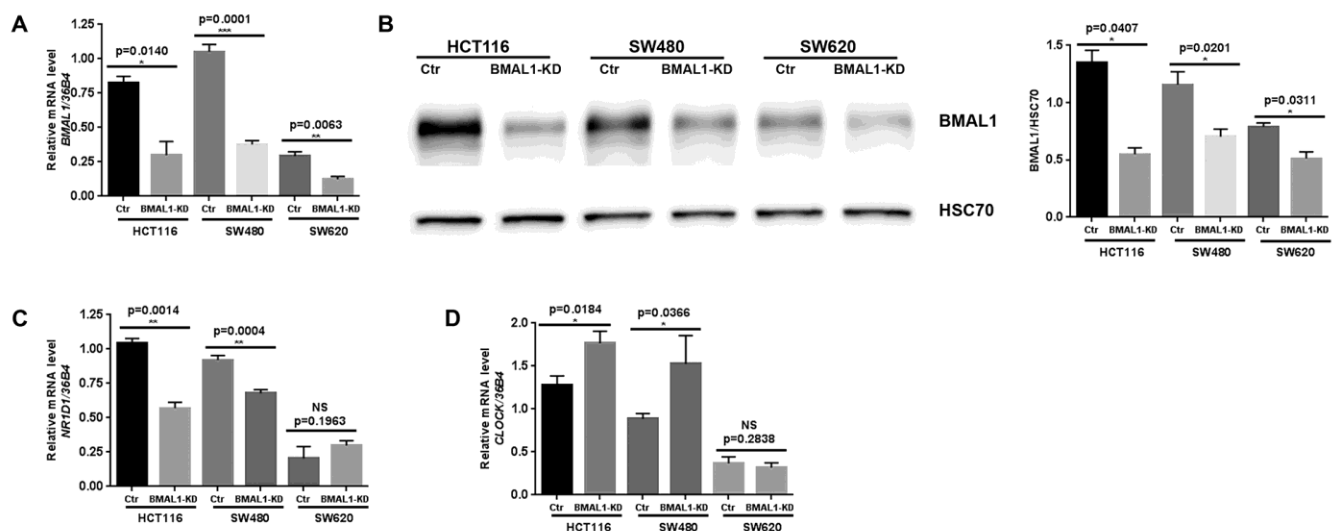


Figure 1. Lentiviral ShBMAL1 decreased BMAL1 expression in three CRC cell lines but only altered expression of some circadian genes in primary CRC cell lines. (A) Effect of shBMAL1 on BMAL1 mRNA level was ascertained by quantitative RT-PCR. *36B4* was used as a quantitative reference ($n=5$; $*p<0.05$; $***p<0.001$; $****p<0.0001$). **(B)** Effect of shBMAL1 on the level of BMAL1 protein was ascertained by Western-blot. *Left*, a representative immunoblot is shown. *Right*, Bar charts represent BMAL1 expression normalized to HSC70 ($n=3$; $*p<0.05$). Data are shown as mean \pm SEM. **(C)** Quantitative RT-PCR revealed decreased expression of *NR1D1* in two primary BMAL1-KD CRC cell lines (HCT116 and SW480) but not in the metastatic CRC cell line SW620. **(D)** Quantitative RT-PCR revealed increased expression of *CLOCK* in two primary BMAL1-KD CRC cell lines but not in the metastatic CRC cell line SW620.

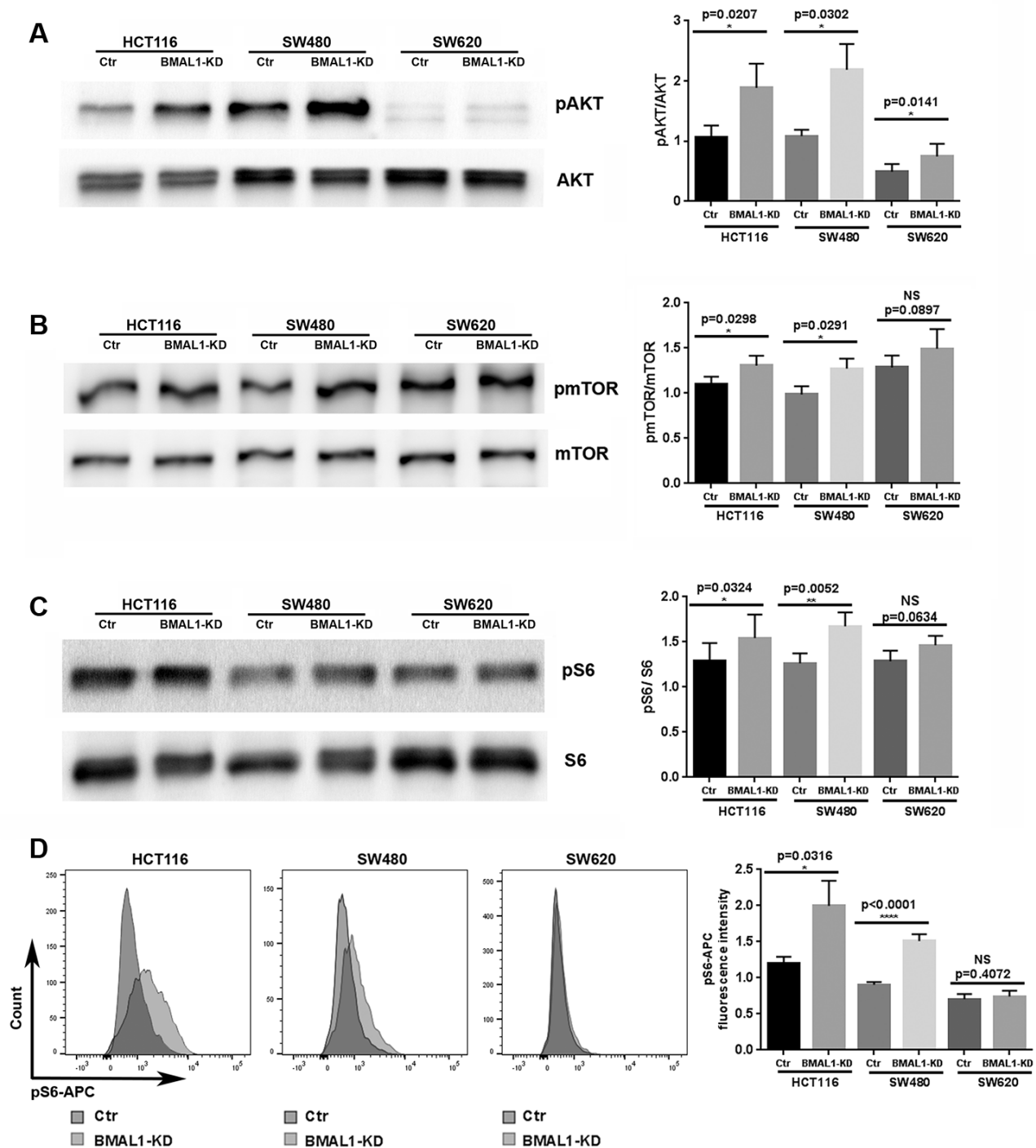


Figure 2. BMAL1-KD increased AKT/mTOR activation to varying degrees in the CRC cell lines. (A) Western-blot analysis revealed that BMAL1-KD increased AKT phosphorylation in the three CRC cell lines (n=5; *p<0.05; **p<0.01). The ratio of phosphorylated AKT to total AKT was used to indicate AKT activation level. (B) Western-blot analysis revealed that BMAL1-KD increased mTOR phosphorylation in HCT116 and SW480 (n=6; *p<0.05) but not in SW620 cells. The ratio between phosphorylated mTOR and total mTOR was used to indicate mTOR activation level. (C) Western-blot analysis revealed that knockdown BMAL1 increased 40S Ribosomal protein S6 phosphorylation in HCT116 and SW480 (n=6; ***p<0.001) but not in SW620 cells. The ratio between phosphorylated S6 and total S6 was used to evaluate mTOR activity. (A-C): *Left*, a representative immunoblot of independent experiments. *Right*, Bar charts represent the target protein expression level normalized to protein loading controls. (D) Flow cytometry analysis revealed increased phosphorylated S6 in HCT116 BMAL1-KD (*p<0.05) and SW480 BMAL1-KD (***p<0.0001) cells but not in SW620 BMAL1-KD cells compared to their proper controls. *Left*, representative staining of 7 independent experiments is shown. *Right*, Graphs represented the mean fluorescence intensity value of phosphorylated S6-APC (n=7). All data are shown as means \pm SEM.

BMAL1-KD induced different cell proliferation patterns in CRC cell lines

The activation of mTOR pathway by AKT kinase is implicated in many fundamental cell functions, such as survival, proliferation and growth [28]. We thus examined whether BMAL1-KD influenced CRC cell proliferation by using an MTT Cell Proliferation and Viability Assay (Figure 3A) and cytometry cell counts (Figure 3B).

In primary CRC cells, corresponding to their higher AKT/mTOR activity, MTT analysis showed that HCT116 BMAL1-KD cells exhibited greater proliferation from 72h in culture, compared to its control (72h, $p=0.0078$; 96h, $p<0.0001$). This result was confirmed by cell counts, which showed more HCT116 BMAL1-KD cells after 48h compared to control (48h, $p=0.0090$; 72h, $p=0.0317$; 96h, $p<0.0001$). In contrast, despite increased AKT/mTOR activity, the SW480 BMAL1-KD cell line did not show greater cell proliferation compared to its control. At 96h, cytometry cell counts even revealed fewer BMAL1-KD cells compared to control ($p=0.0259$).

In the metastatic SW620 BMAL1-KD cell line, there was slight increase of AKT activity but without evident increase of mTOR activity. However, this cell line did proliferate faster at 96h when compared to control (MTT: $p=0.0460$; cell count: $p=0.0090$).

BMAL1-KD increased senescence only in SW480 cells

Increased mTOR activity also leads to accelerated aging under certain conditions, as shown in *BMAL1* knockout mice [25–27]. SW480 BMAL1-KD cells demonstrated increased mTOR activity but no increased cellular proliferation, which led us to check whether BMAL1-KD induced senescence in these SW480 cells.

Of the three BMAL1-KD CRC cell lines, only SW480 BMAL1-KD cells showed an obvious increase of cell senescence, as identified by senescence-associated β -galactosidase activity (SA- β -gal) staining. These SA- β -gal-positive cells also demonstrated other senescence related alterations: enlarged cell size and flattened shape (Figure 4A). In contrast, compared to their controls, there was no evident increase in cellular senescence in HCT116 BMAL1-KD and SW620 BMAL1-KD lines.

Another common indicator of senescent cells is the marker of DNA double-strand breaks (DSB), phosphorylated H2AX (pH2AX) [29, 30]. Immunofluorescence (Figure 4B) and western blot (Figure 4C) analyses showed that phosphorylated H2AX was increased strongly in SW480 BMAL1-KD cells ($p=0.0209$) and only slightly in the SW620 BMAL1-KD cell line ($p=0.0269$).

Cell senescence is also mediated by, and can induce, P53/P21 activation [31]. Although P53 mRNA (Figure 5A,

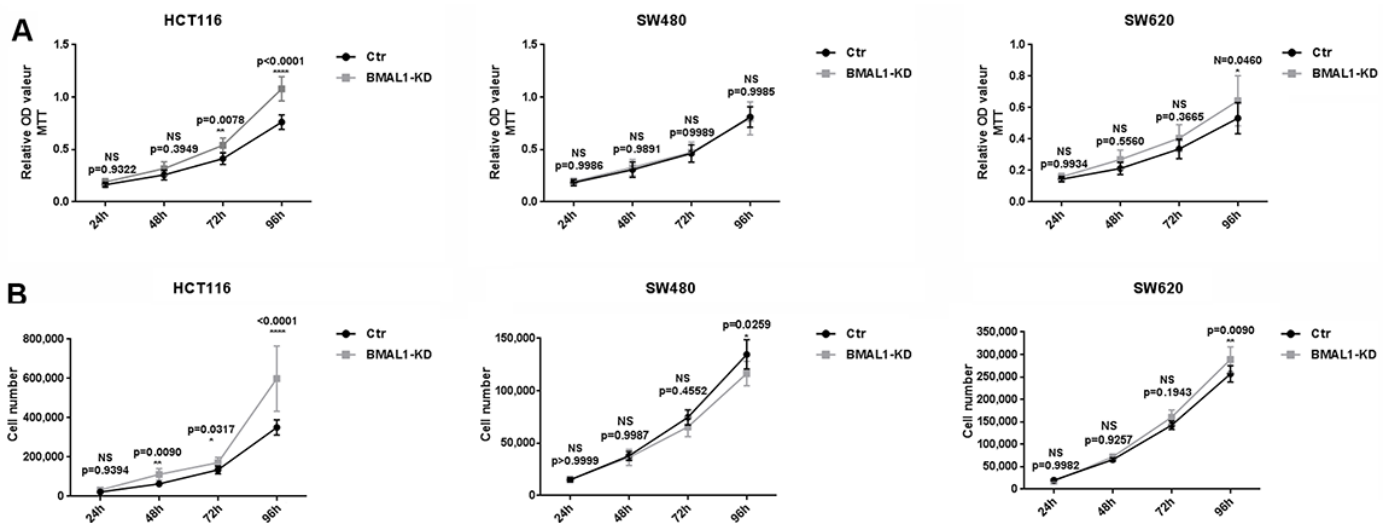


Figure 3. BMAL1-KD induced different cell proliferation patterns in CRC cell lines. MTT cell proliferation assay (A) and cell counts (B) were used to examine BMAL1-KD and control cells' proliferation rate for 96h. Stable HCT116 BMAL1-KD but not SW480 BMAL1-KD cells exhibited significantly higher cell counts compared to their control. SW620 BMAL1-KD cells only showed faster growth at 96h. (n=8; * $p<0.05$; ** $p<0.01$; *** $p<0.0001$). Error bar represented \pm SEM.

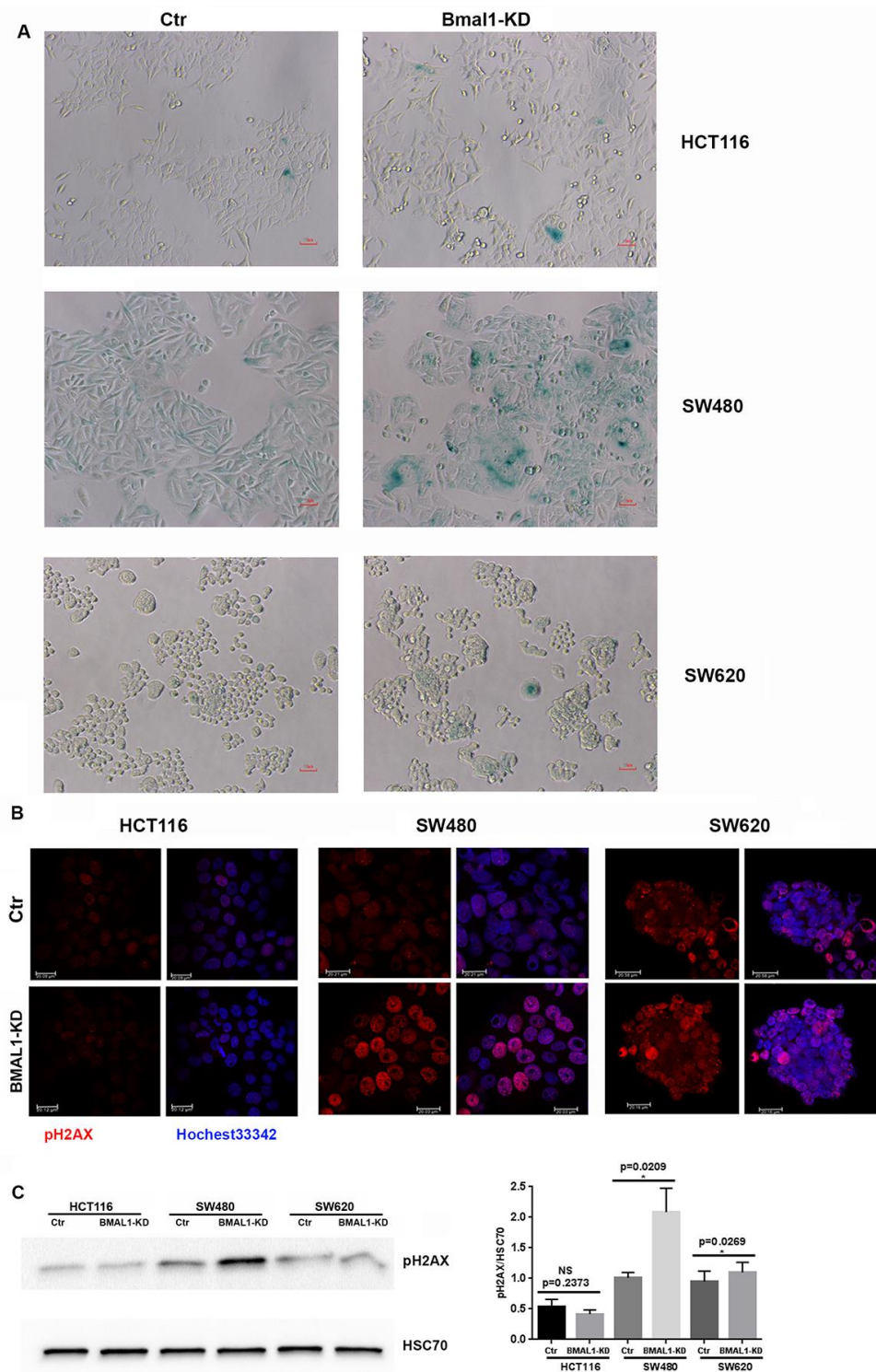


Figure 4. BMAL1-KD increased senescence in SW480 BMAL1-KD but not in HCT116 BMAL1-KD and SW620 BMAL1-KD cells. (A) Senescence-associated β -galactosidase (SA- β -gal) activity was obviously increased in SW480 BMAL1-KD cells, but not in HCT116 BMAL1-KD nor in SW620 BMAL1-KD cells. SA- β -gal activity was measured by β -galactosidase staining (blue). Scale Bar represents 10 μ M. Representative staining of three independent experiments was shown. (B) Immunofluorescence identified phosphorylated H2AX (pH2AX, red) in cell nuclei (Hoechst 33342, blue) of BMAL1-KD and control CRC cell lines. Representative staining of three independent experiments were shown. Scale bar, 20 μ m. (C) Western-blot revealed significant increase of pH2AX mainly in SW480 BMAL1-KD cells. *Left*, a representative immunoblot of three independent experiments was shown. *Right*, Bar charts represented pH2AX expression level normalized to HSC70 (n=7; *p<0.05; ***p<0.001). All data are shown as means \pm SEM.

qRT-PCR) and protein (Figure 5B, western blot) levels did not change in the three BMAL1-KD CRC cell lines, there was a change of P53 localization in SW480 BMAL1-KD cells. Compared to control, cytoplasmic P53 decreased ($p=0.0235$; Figure 5C) and P53 nuclear expression increased ($p=0.0183$; Figure 5D) in SW480 BMAL1-KD cells, suggesting P53 activation. In contrast, P53 cytoplasmic expression did not change in HCT116 BMAL1-KD and SW620 BMAL1-KD cells. Moreover, P53 nuclear localization in HCT116 BMAL1-KD cell line even decreased compared to its own control ($p=0.0249$; Figure 5D).

To confirm the link between cellular senescence and P53 expression in our cell lines, we analyzed expression of P53 targets, P21 and MDM2 (murine double minute homolog 2). In agreement with the different P53 activation, qRT-PCR (Figure 6A,

$p=0.0409$) and western-blot results revealed increased P21 (Figure 6B, $p=0.0291$) and MDM2 ($p=0.0160$; Figure 6C) expression only in SW480 BMAL1-KD cells compared to control. Moreover, MDM2 expression was even decreased in SW620 BMAL1-KD cells ($p=0.0122$).

In summary, after BMAL1-KD cellular senescence was only induced in one primary CRC line (SW480) in association with nuclear translocation of P53 and increased expression of P21 and MDM2.

BMAL1-KD increased apoptosis and P53 activation only in HCT116 cells

The previous results were performed on BMAL1-KD cell lines which were obtained after puromycin selection. However, phenomena such as apoptosis, will

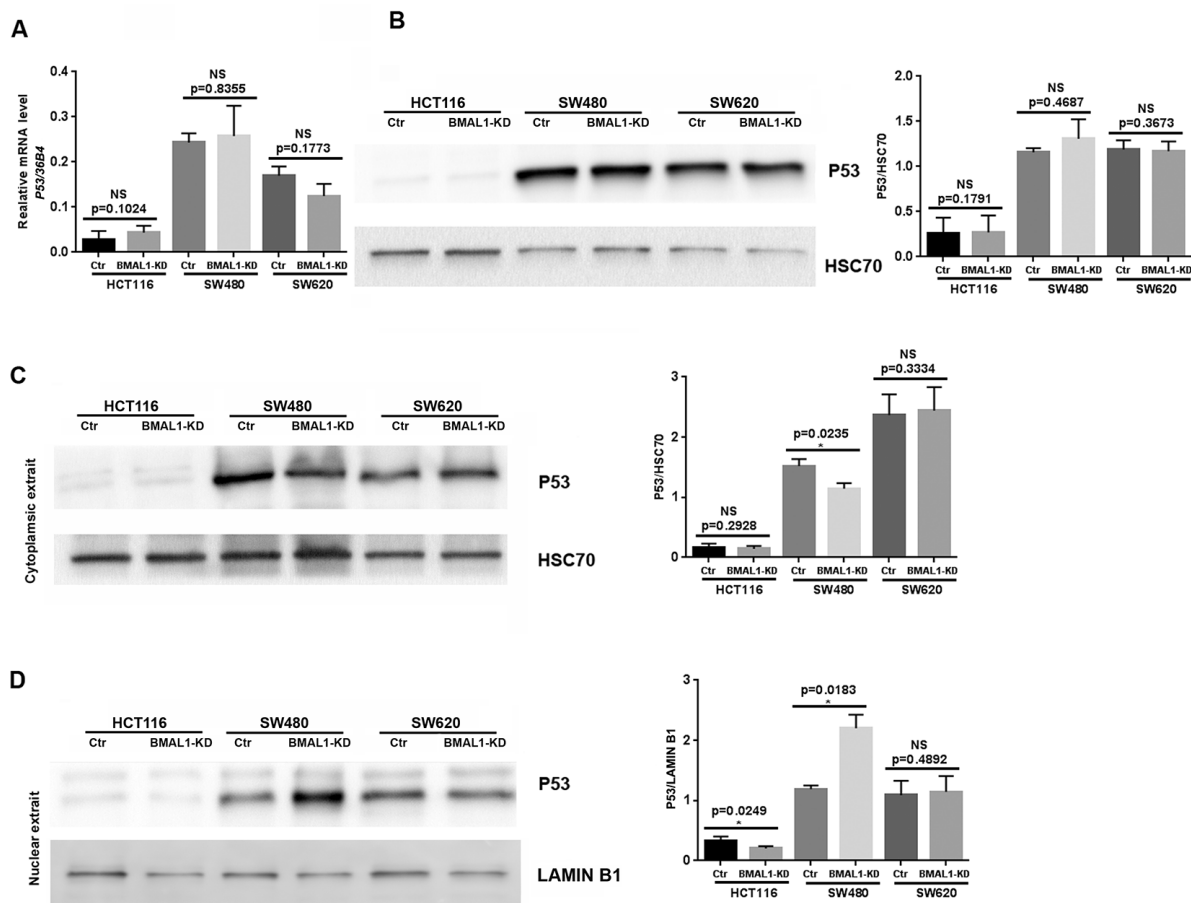


Figure 5. P53 expression status in CRC BMAL1-KD cell lines. (A) Quantitative RT-PCR revealed that no significant change of P53 mRNA levels in the three CRC cell lines. *36B4* was used as a quantitative reference for all quantitative RT-PCR analyses ($n=8$). (B) Western-blot analysis revealed no significant change of P53 protein levels in the three CRC cell lines ($n=7$). (C and D) Cytoplasmic (C) and nuclear (D) extracts from BMAL1-KD and control cell lines were analyzed by western-blot. Only SW480 BMAL1-KD cells exhibited a significant decrease of cytoplasmic P53 ($n=5$; $*p<0.05$) associated with a significant increased nuclear P53 ($n=5$; $*p<0.05$). Left, a representative immunoblot of 5 independent experiments was shown. Right, Bar charts represented P53 expression level normalized to HSC70 or LAMIN B1. All data are shown as means \pm SEM.

appear transiently after shBMAL1 begins to be expressed. GFP gene is incorporated in the lentivirus construction as a reporter of shRNA expression, and it becomes visible 24h post-transfection, indicating the onset of sh*BMAL1* expression. We thus tested for the onset of apoptosis with Annexin V labeling 48h after lentivirus transduction, i.e. around 24h after shBMAL1 expression begins.

Without puromycin selection, only GFP positive (GFP+) cells were considered as shRNA transduced. In the GFP+ population, the cells undergoing early apoptosis, i.e., Annexin V-positive and PI-negative cells, as well as the total apoptosis cells (Annexin V-positive cells) are all increased in shBMAL1 vs. shScr transduced HCT116 cells ($p=0.0054$ and $p=0.0393$). However, shBMAL1 transduced SW480 ($p=0.1858$ and $p=0.1149$) or SW620 ($p=0.1705$ and $p=0.2601$) cells only presented a trend to increase apoptosis (Figure 7A).

For HCT116 cells, we also measured P53 nuclear expression by flow cytometry, 48h after lentivirus transduction. For the GFP+ population, nuclei of shBMAL1 transduced cells exhibited increased P53 expression compared to shScr control cells ($p=0.0070$).

However, this difference was not observed in the GFP negative (shRNA non-transduced) population (Figure 7B).

DISCUSSION

In this study, we analyzed the consequences of circadian clock perturbation, specifically BMAL1-KD, on human colorectal cancer cell behavior. We used 3 experimental cell models corresponding to different colorectal cancer progression: two primary colorectal carcinoma cell lines (HCT116 and SW480) and SW620, a metastatic colorectal carcinoma cell line derived from the same patient as SW480. Our results reveal that BMAL1-KD triggers distinct cell fates in different colon cancer cell lines rather than the same phenomenon throughout.

BMAL1-KD appropriately alters expression of other core circadian genes

BMAL1-KD induced similar, and expected, gene expression changes in the two primary CRC cell lines: decreased *NR1D1* and increased *CLOCK* expression, but without modification of *PER2*, *CRY1* or *CRY2*. Reduced *NR1D1* expression is consistent with the exclusive control of its promoter by CLOCK-BMAL1

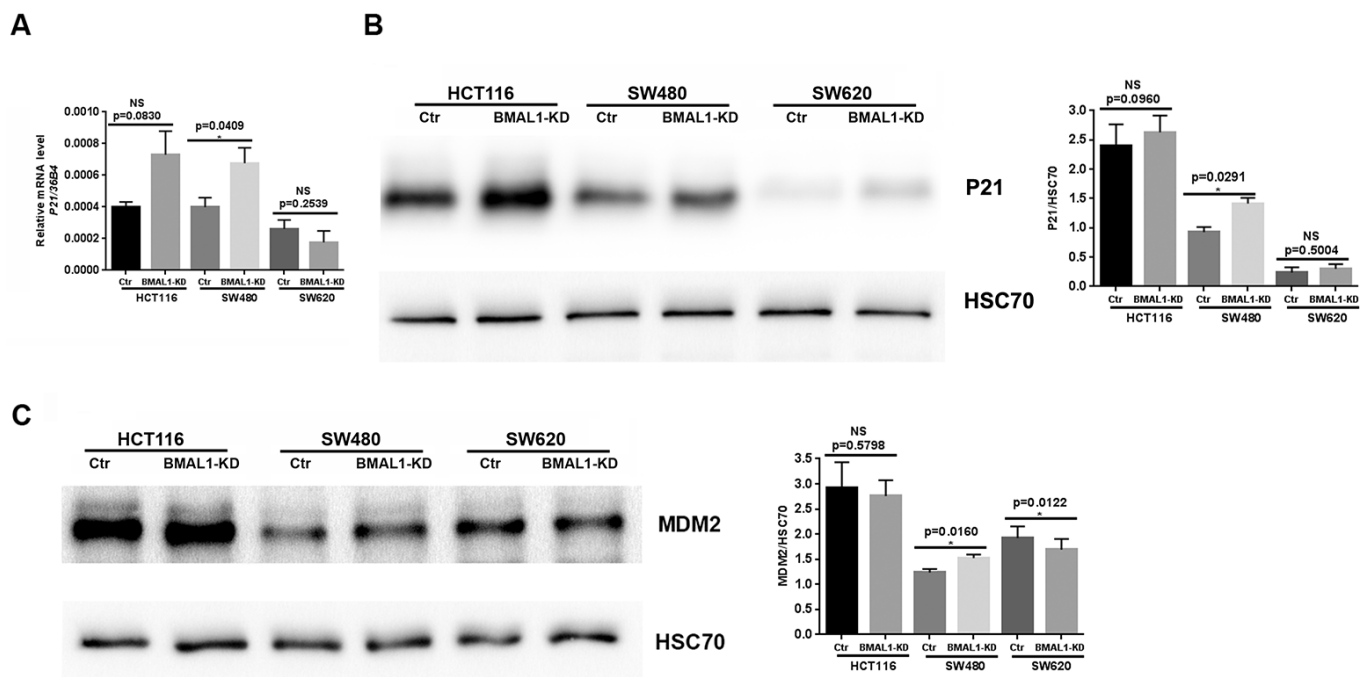


Figure 6. P21 and MDM2 expression status in CRC BMAL1-KD cell lines. (A) Quantitative RT-PCR revealed a significant increase of P21 mRNA in SW480 BMAL1-KD cells ($n=6$; $*p<0.05$) but not in HCT116 BMAL1-KD and SW620 BMAL1-KD cells. (B) Western-blot analysis revealed a significant increase of P21 protein in SW480 BMAL1-KD cells ($n=4$; $*p<0.05$) but not in HCT116 BMAL1-KD and SW620 BMAL1-KD cells. (C) Western-blot analysis revealed increased MDM2 protein in SW480 BMAL1-KD cells ($n=5$; $*p<0.05$) but not in HCT116 BMAL1-KD and SW620 BMAL1-KD cells. *Left*, a representative immunoblot of different independent experiments is shown. *Right*, Bar charts represent P21 or MDM2 expression normalized to HSC70. All data are shown as mean \pm SEM.

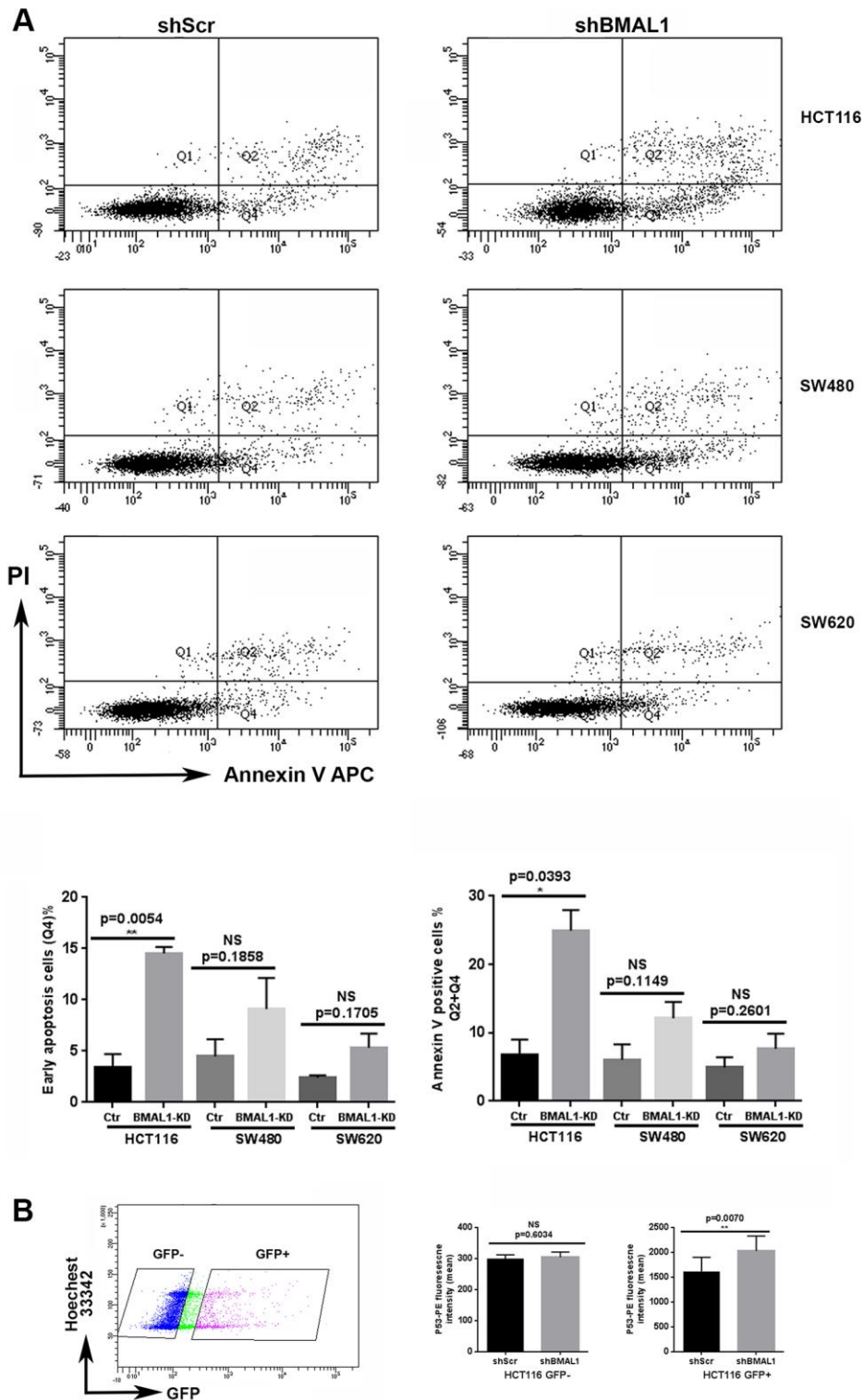


Figure 7. HCT116-shBMAL1 cells temporarily increased apoptosis and P53 activation after lentivirus transduction. (A) Flow cytometry analysis with Annexin V-APC and propidium iodide staining were applied to determine apoptosis ratio in different shRNA (shBMAL1 or shScr) transduced cells 48h after lentivirus transduction. *Upper panels*, a representative distribution of three independent experiments is shown. *Lower panels*, Graphs represent the percentage of early apoptosis cells (Q4) and total apoptosis cells (Q2+Q4) (3 independent for each analysis). A significant increase of apoptosis ratio is detected only in HCT116 cells after shBMAL1 transduction (** $p < 0.01$). (B) Flow cytometry analysis with P53-PE and Hoechst 33342 staining revealed that the nuclei of HCT116 shBMAL1 transduced cells (GFP positive population) exhibited an increased P53 expression compared to the nuclei of HCT116 shScr transduced cells ($n = 3$; ** $p < 0.01$). *Right*, Graphs represent the mean of P53 nuclei expression from three independent experiments. All data are shown as means \pm SEM.

binding to E-box regulatory elements [32] and the presence of two BMAL1 binding sites in the gene (Supplementary Figure 1) [33]. This contrasts with only one binding site for BMAL1 in *PER2*, *CRY1* or *CRY2* genes [33], and explains why *NR1D1* expression is more sensitive to the diminution of BMAL1. Similarly, NR1D1 (REV-ERBa) rapidly represses transcription of *BMAL1* and *CLOCK* genes via REV-ERBA response elements (RREs) [34, 35]. So, decreased *NR1D1* and increased *CLOCK* expression in the two primary BMAL1 knockdown CRC cells represent correct feedback regulation of core-clock gene expression [20–22].

BMAL1-KD increases mTOR activity in CRC cells

In the two primary CRC cell lines, BMAL1-KD increased activity of mTOR, a central regulator of cellular metabolism that links cellular energy and nutrients to cell division, growth, quiescence, senescence and death; and which is critically involved in cellular life, for example aging, diabetes and cancer [25, 26, 36]. Our result is coherent with observations in BMAL1 KO mice and the circadian rhythmicity of mTOR signaling [27, 37–39]. Moreover, we also demonstrate that BMAL1-KD increased phosphorylation of the mTOR effector, ribosomal S6 (Figure 2), whose protein kinase, S6K1, rhythmically phosphorylates BMAL1 so that it associates with cellular translational machinery for protein synthesis [39]. Thus our data support the links between BMAL1 and mTOR pathway, which suggests BMAL1 regulation of protein synthesis and the role of circadian timing in cancer development.

Different CRC cell fates triggered by BMAL1-KD depend not only on increased mTOR activity but also on P53 status of each cell line

BMAL1 knockout mice show increased mTOR activity, associated with age-related pathology and reduced lifespan, i.e. premature ageing [27, 40, 41]. Therefore, it is not surprising that cell senescence increased after BMAL1 knockdown and increased mTOR activity. However, why did this occur only in SW480 BMAL1-KD, but not HCT116 BMAL1-KD cells?

A possible explanation for this variance in cellular senescence between SW480 and HCT116 cells is their different P53 status. The HCT116 cell line expresses wild type (WT) P53, whereas the SW480 cell line carries a mutant P53 (R273H and P309S; mP53) which is only partially functional, such as inducing P21 expression [42]. Knockdown of this mP53 decreases colorectal cancer malignancy, indicating its important role in CRC development [43]. Blagosklonny et al. hypothesized that maximal P53 activity blocks mTOR, causing cellular quiescence or death, whereas partial P53 activity sustains mTOR activity and causes senescence [23–26]. In keeping with this hypothesis, we propose that the different P53 status (WT vs mutant) of HCT116 and SW480 cells underlies the different cell fates induced by mTOR activity after BMAL1-KD.

This proposal is supported by our findings. The reduction of BMAL1 in lentiviral transfected cells depends on the number of shRNA copies that are integrated, and will vary for each cell [44]. Thus just

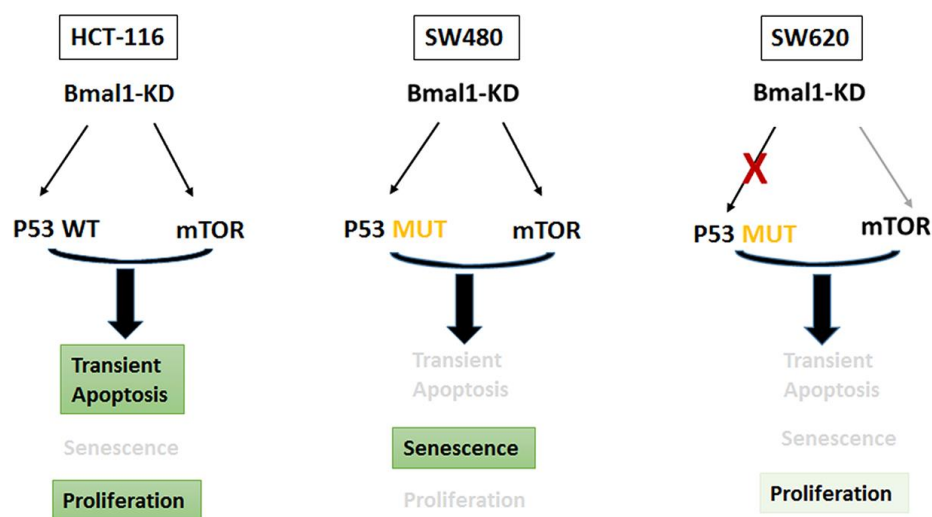


Figure 8. BMAL1-KD modified the delicate equilibrium between AKT/mTOR and P21/P53 pathways, which triggered the different cell fates based on distinct P53 and circadian rhythm status of every CRC cell line.

after lentiviral transfection, HCT116 BMAL1-KD and SW480 BMAL1-KD cultures will contain many cell populations each with distinct BMAL1, mTOR and P53 activation according to the number of integrated *shBMAL1* copies. Thus, in HCT116 cells which integrate a high number of *shBMAL1* copies, there will be high WT P53 activation, which can induce rapid apoptosis, as indeed we observed 24h after *shBMAL1* expression (Figure 7). Consequently, during the one-week puromycin selection for stable BMAL1-KD, the HCT116 BMAL1-KD cells with strong P53 activation would be removed by apoptosis, leaving those with less P53. Such P53 expression will in turn induce expression of MDM2, which directs P53 for proteasome degradation to limit its expression level and activity [45]. As our results showed, stable HCT116 BMAL1-KD cells had high MDM2 and low P53 expression, consistent with functional MDM2-P53 negative feedback. Finally, in the absence of increased P53 activity, increased AKT and mTOR activity in the stable HCT116 BMAL1-KD cells can increase cellular proliferation (Figure 3).

Alternatively, for SW480 cells, those which integrate many *shBMAL1* copies will stimulate mP53 activity, as demonstrated by nuclear translocation and expression of P21 and MDM2 (Figure 6). But mP53 has only partial function [42], as confirmed in our results by low expression of MDM2, which would limit MDM2-P53 negative feedback and explain the higher P53 expression in SW480 cells than HCT116 cells. Consequently, mTOR activity is sustained and provokes cell senescence. SW480 BMAL1-KD cells with fewer integrated *shBMAL1* will only moderately activate mP53, not block mTOR and promote cell survival or proliferation. Our results, showing only a relatively small decrease in SW480 BMAL1-KD cell counts (Figure 3) despite profound cellular senescence (Figure 4), are consistent with cultures being transduced by a range of *shBMAL1* copies.

Effect/influence of BMAL1 KD on CRC cell life requires functional circadian rhythm

In contrast to the two primary CRC cell lines, metastatic SW620 cells showed very little response to BMAL1-KD: a small increase in phosphorylated AKT without associated mTOR or S6 activation (Figures 2). A likely explanation for this muted response is an abnormal circadian timing system and low baseline expression of BMAL1 and other cell regulatory proteins (e.g. AKT, P21) in this cell line. In contrast to the two primary CRC cell lines (HCT116 and SW480), the metastatic cell line SW620 has severely diminished core-clock gene oscillation, indicating dysfunction of the transcription-translation feedback loops among different

circadian proteins [20–22]. Although SW480 and SW620 cell lines were derived from primary and metastatic sites of the same patient, there was only 5.5% overlap of genes with oscillating expression profiles, indicating the loss of intact circadian clock during tumor progression [22]. Consistent with this, BMAL1 knockdown in metastatic SW620 cells did not alter *NR1D1* and *CLOCK* expression, in contrast to the two primary CRC cells. Thus, a dysregulated core clock in SW620 cells, as indicated by poor oscillation of clock-controlled genes and low level of BMAL1 protein can explain why BMAL1-KD had less influence on SW620 cells than on SW480 cells in our experiments.

BMAL1 KD-associated oxidative stress reveals impaired P53 signaling in SW620 cells

Global deletion of BMAL1 induces an aging phenotype associated with oxidative stress [46], which damages DNA, including DNA strand breaks.

In stable HCT116 BMAL1-KD cells there was no evident oxidative stress (H2AX phosphorylation), consistent with vulnerable HCT116 BMAL1-KD cells with high WT P53 activation being eliminated by apoptosis just after *shBMAL1* transduction, and P53 activation in surviving cells being blocked by MDM2-P53 negative feedback.

In contrast, our results show phosphorylated H2AX in SW480 and SW620 BMAL1-KD cells, indicating oxidative stress. In SW480 BMAL1-KO cells, there was a large increase in phosphorylated H2AX and mP53 activation. In contrast, SW620 BMAL1-KD cells only slightly increased phosphorylated H2AX but without associated mP53 activation: no P53 nuclear translocation or P21 expression, and even decreased MDM2 expression (Figures 4–6), which suggested impaired P53 signaling in SW620 cells. In the absence of appropriate P53 activation and its induction of apoptosis or senescence, the moderate increase of AKT activity permits faster growth (Figure 8).

CONCLUSIONS

Briefly, our work provides a potential explanation for the different cell fates induced by BMAL1 knockdown in CRC cells, which is based on increased mTOR activation and different P53 status. However, these CRC cells also contain mutations in other cancer related genes (HCT116: *KRAS*, *PIK3CA*, *CTNNB1*, *BRCA2*, *CDKN2A* etc.; SW480 or SW620: *KRAS* and *APC* etc.) [47], which constitute a unique pathological context in every CRC cell. Thus, in addition to differences in core circadian clock status, P53 regulation and basal kinase activity that we demonstrate, all these distinct mutations

(including in *P53*) will contribute to the different cell fate induced by BMAL1 knockdown. Altogether, this work reveals the important role of BMAL1 in CRC cell behavior, in particular primary CRC cell fate decision. Knockdown of BMAL1 expression at different levels could potentially commit primary colon cancer cells towards different cell fates.

MATERIALS AND METHODS

Cell culture

HCT116, SW480 and SW620 cells were cultured in Dulbecco's modified Eagle medium (DMEM) supplemented with GlutaMAX (GIBCO, Life Technology, CA, USA) and 10% fetal bovine serum (FBS, Hyclone, UT, USA).

The shRNA sequence cloning in a lentiviral vector

A short hairpin RNA sequence (shRNA) against human BMAL1 (shBMAL1; Forward: 5'-CCGGAGAACCCA GGTTATCCATATTCTGCAGAATATGGATAACCT GGGTCTTTTTT-3'; Reverse: 5'-CTAGAAAAAA GAACCCAGGTTATCCATATTC TGCAGAATATGG ATAACCTGGGTTCT-3') or a control scrambled sequence (shScr) were inserted separately into a lentiviral vector (pLKO-shBMAL1-GFP-puro or pLKO-Scr-GFP-puro), which also encode the reporter protein GFP and the puromycin resistance gene.

Lentivirus production and cell transduction

Lentivirus particles were produced as previously described [48] but without concentration. After lentiviral production, the lentivirus supernatant was filtered with 0.45 μm filters and stored at -80°C . For target cell transduction, 1 mL filtered viral supernatant mixed with 1 mL DMEM (10% Fetal Bovine Serum, FBS) was added to each well of 6-well plates containing 50% confluent cells in the presence of 8 $\mu\text{g}/\text{mL}$ polybrene (Sigma, MO, USA) and incubated with for 24 hours.

Transduced cells were either used directly 48h after transfection, or after selection by adding 2 $\mu\text{g}/\text{mL}$ puromycin (Thermo Fisher) to the medium 72h after transfection and culturing for 1 week. After puromycin selection, flow cytometry analysis was performed to confirm that the entire cell population was GFP positive. These GFP positive cells, named as BMAL1-KD or control (Ctr) cells, were used for subsequent analysis.

Analyses with or without puromycin selection are repeated with the cells from three independent lentivirus transductions.

MTT cell proliferation assay

The BMAL1-KD or control CRC cell lines were seeded in 96-well plates at an initial density of 2×10^3 cells per well. Cell proliferation was measured daily during 4 days by Vybrant MTT Cell Proliferation Assay Kit (V13154, Molecular Probes, Invitrogen). Every time point was repeated 3-4 times in independent experiments. Two-way ANOVA was used for statistical analysis of 8 independent experiments.

Cell proliferation curve analysis

The BMAL1-KD or control CRC cell lines were seeded in 24-well plates at an initial density of 1×10^4 cells per well. After trypsinization (Trypsin-EDTA, Thermo Fisher, MA, USA) and suspension in PBS containing 0.5% bovine serum albumin (BSA) and 2 mM EDTA, the number of living cells from each well was counted over 4 days by a Miltenyi Biotec AutoMACS cytometry. Three independent experiments were statistically analyzed by two-way ANOVA.

Quantitative RT-PCR (qRT-PCR)

Cells were collected and total RNA was extracted as previously described [49]. Reverse transcription was performed with Superscript II RT-kit (Invitrogen, CA, USA). Quantitative real time PCR was performed by using LightCycler 480 SYBR Green I master kit (Roche, Bâle, Switzerland). Primers of *BMAL1* and *36B4* were used for gene amplification were previously described [49]. *P21* primer: Forward-GACACCACT GGAGGGTGACT and Reverse-CAGGTCCACATGG TCTTCCT. *P53* primer: Forward-GTTCCGAGAGCT GAATGAGG and Reverse-TCTGAGTCAGGCC TTCTGT.

The relative quantification of target RNA by using *36B4* as a reference was computed with the Relquant software (Roche, Bâle, Switzerland) with the "delta delta Ct" ($\Delta\Delta\text{Ct}$) method. T-test was used for statistical analysis.

Flow cytometry analysis of S6 phosphorylation

Cells were detached with Trypsin-EDTA (Thermo Fisher, MA, USA), fixed in ice-cold 70% ethanol, washed twice in ice-cold PBS and then centrifuged at 300g for 10 min. Cells were incubated with anti-Phospho-S6-APC (#14733; Cell Signaling, MA, USA) in PBS containing 0.5% bovine serum albumin (BSA) and 2 mM EDTA for 30 min at 4°C and labelled with Alexa Fluor® 647 or Alexa Fluor® 546 conjugated secondary antibodies (Molecular Probes) and Hoechst 33342 (B2261, Sigma MO, USA). After labelling, cells

were washed once time and analyzed in an LSR Fortessa™ cell analyzer (Becton Dickinson, NJ, USA).

Flow cytometry analysis of nuclear P53 expression

Cells were trypsinized and centrifuged at 1200 rpm for 5 min and suspended very gently in citrate solution (0.1% Trisodium citrate and 0.058% NaCl, pH=7.6) containing 0.001% NP40 and 10 mg/mL Hoechst 33342, incubated for at least 2h (maximum 24h) at 4°C to extract and stain cell nuclei. Cell nuclei were then incubated with anti-P53-PE (130-109-570, Miltenyi Biotec) in a PBS solution containing 0.5% BSA and 2 mM EDTA for 30 min at 4°C. After washing, nuclear P53 expression was analyzed by flow cytometry in an LSR Fortessa™ cell analyzer (Becton Dickinson, NJ, USA). T-test was used for statistical analysis.

Apoptosis assay

48h after viral transduction, transfected cells were trypsinized and then 10⁶ cells were washed in 1 mL of 1x Binding Buffer (130-092-820, Miltenyi Biotec, Germany) and centrifuged at 300g for 10 min. After 15 min incubation with anti-Annexin V-Alexa Fluor® 647 (640943, BioLegend, CA, USA), cells were washed and suspended in 500 µL 1x binding buffer, 10 mg/mL propidium iodide (PI) solution was added immediately prior to analysis by flow cytometry. All the experiments or solution are realized at 4°C. T-test was used for statistical analysis.

Immunofluorescence and confocal microscopy

The cells were cultured on 17 mm coverslip until desired confluence (around 50%), fixed with 4% PFA, permeabilized with 0.1% Triton and then blocked with 0.3% BSA before being incubated with primary (Anti-pH2AX 9718, Cell Signaling) and secondary antibodies. The confocal images were captured by a confocal LEICA SP5-AOBS microscope with a 63X/1.4 NA oil-immersion objective. Hoechst 33342 was used for nuclear staining.

Cytoplasmic and nuclear extracts preparation

Cytoplasmic and nuclear extracts of different cell lines were separated and prepared with NE-PER™ Nuclear and Cytoplasmic Extraction Reagents (78833, Thermo Fisher) by following the kit instruction. The different extracts were stored at -80°C until western-blot analysis by anti-P53 (2527, Cell signaling). HSC70 expression was used as a control of cytoplasmic protein loading (SPA-815, Stressgen) and LAMIN B1 (ab16048, Abcam) was used as nuclear protein loading.

Western blot

Western blot analysis was performed with sodium dodecyl sulfate polyacrylamide gel electrophoresis (SDS-PAGE) as previously described [49] with different primary antibodies: Anti-HSC70 (SPA-815, Stressgen), or anti-BMAL1 (14020), anti-Phospho-S6 ribosomal protein (Ser240/244; 5456), anti-S6 ribosomal protein (2317), anti-phospho-AKT (Ser473; 4060), anti-AKT(4691), anti-pmTOR (Ser2448; 2971), anti-mTOR (2972), anti-P21 Waf1/Cip1 (2947), anti-MDM2 (86934), anti-P53 (2527) all from Cell Signaling Technology. The results were quantified by Image J. T-test was used for statistical analysis.

CONFLICTS OF INTEREST

The authors declare no conflicts of interest.

FUNDING

Yuan Zhang is supported by the China Scholarship Council. A. Ballesta is funded by the Plan Cancer of the French National Cancer Institute (INCa), through the ATIP-Avenir program.

REFERENCES

1. Lowrey PL, Takahashi JS. Genetics of circadian rhythms in Mammalian model organisms. *Adv Genet.* 2011; 74:175–230.
<https://doi.org/10.1016/B978-0-12-387690-4.00006-4>
PMID:[21924978](https://pubmed.ncbi.nlm.nih.gov/21924978/)
2. Takahashi JS. Transcriptional architecture of the mammalian circadian clock. *Nat Rev Genet.* 2017; 18:164–79.
<https://doi.org/10.1038/nrg.2016.150>
PMID:[27990019](https://pubmed.ncbi.nlm.nih.gov/27990019/)
3. Bunger MK, Wilsbacher LD, Moran SM, Clendenin C, Radcliffe LA, Hogenesch JB, Simon MC, Takahashi JS, Bradfield CA. Mop3 is an essential component of the master circadian pacemaker in mammals. *Cell.* 2000; 103:1009–17.
[https://doi.org/10.1016/S0092-8674\(00\)00205-1](https://doi.org/10.1016/S0092-8674(00)00205-1)
PMID:[11163178](https://pubmed.ncbi.nlm.nih.gov/11163178/)
4. Zhang R, Lahens NF, Ballance HI, Hughes ME, Hogenesch JB. A circadian gene expression atlas in mammals: implications for biology and medicine. *Proc Natl Acad Sci U S A.* 2014; 111:16219–24.
<https://doi.org/10.1073/pnas.1408886111>
PMID:[25349387](https://pubmed.ncbi.nlm.nih.gov/25349387/)
5. Robles MS, Humphrey SJ, Mann M. Phosphorylation Is a Central Mechanism for Circadian Control of Metabolism and Physiology. *Cell Metab.* 2017; 25:118–27.

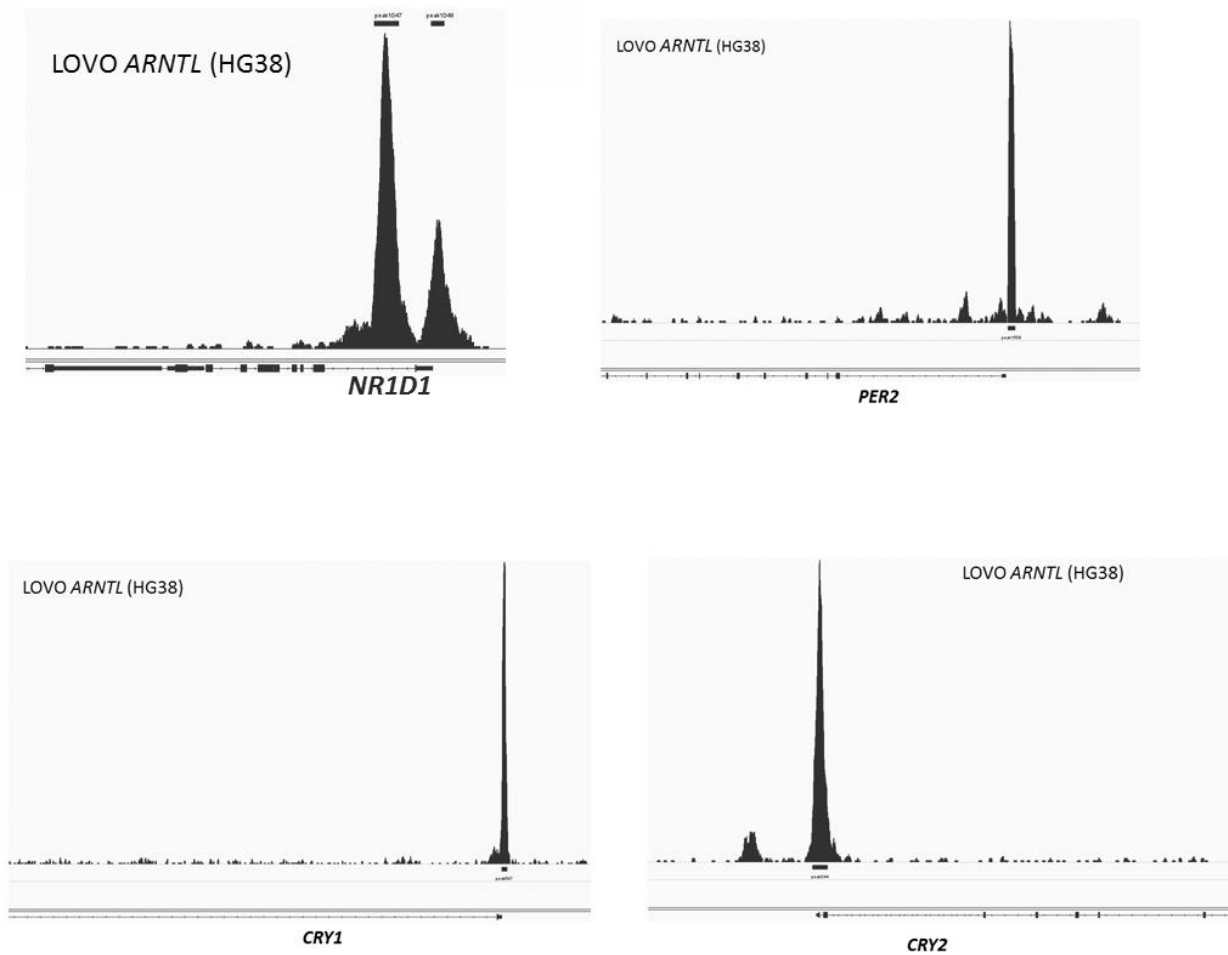
- <https://doi.org/10.1016/j.cmet.2016.10.004>
PMID:[27818261](https://pubmed.ncbi.nlm.nih.gov/27818261/)
6. Wang J, Mauvoisin D, Martin E, Atger F, Galindo AN, Dayon L, Sizzano F, Palini A, Kussmann M, Waridel P, Quadroni M, Dulić V, Naef F, Gachon F. Nuclear Proteomics Uncovers Diurnal Regulatory Landscapes in Mouse Liver. *Cell Metab.* 2017; 25:102–17.
<https://doi.org/10.1016/j.cmet.2016.10.003>
PMID:[27818260](https://pubmed.ncbi.nlm.nih.gov/27818260/)
 7. Fu L, Kettner NM. The circadian clock in cancer development and therapy. *Prog Mol Biol Transl Sci.* 2013; 119:221–82.
<https://doi.org/10.1016/B978-0-12-396971-2.00009-9>
PMID:[23899600](https://pubmed.ncbi.nlm.nih.gov/23899600/)
 8. Davis K, Roden LC, Leaner VD, van der Watt PJ. The tumour suppressing role of the circadian clock. *IUBMB Life.* 2019; 71:771–80.
<https://doi.org/10.1002/iub.2005>
PMID:[30674076](https://pubmed.ncbi.nlm.nih.gov/30674076/)
 9. Megdal SP, Kroenke CH, Laden F, Pukkala E, Schernhammer ES. Night work and breast cancer risk: a systematic review and meta-analysis. *Eur J Cancer.* 2005; 41:2023–32.
<https://doi.org/10.1016/j.ejca.2005.05.010>
PMID:[16084719](https://pubmed.ncbi.nlm.nih.gov/16084719/)
 10. Blakeman V, Williams JL, Meng QJ, Streuli CH. Circadian clocks and breast cancer. *Breast Cancer Res.* 2016; 18:89.
<https://doi.org/10.1186/s13058-016-0743-z>
PMID:[27590298](https://pubmed.ncbi.nlm.nih.gov/27590298/)
 11. Kettner NM, Katchy CA, Fu L. Circadian gene variants in cancer. *Ann Med.* 2014; 46:208–20.
<https://doi.org/10.3109/07853890.2014.914808>
PMID:[24901356](https://pubmed.ncbi.nlm.nih.gov/24901356/)
 12. Palesh O, Haitz K, Lévi F, Bjarnason GA, Deguzman C, Alizeh I, Ulusakarya A, Packer MM, Innominato PF. Relationship between subjective and actigraphy-measured sleep in 237 patients with metastatic colorectal cancer. *Qual Life Res.* 2017; 26:2783–91.
<https://doi.org/10.1007/s11136-017-1617-2>
PMID:[28656534](https://pubmed.ncbi.nlm.nih.gov/28656534/)
 13. El-Athman R, Relógio A. Escaping Circadian Regulation: An Emerging Hallmark of Cancer? *Cell Syst.* 2018; 6:266–67.
<https://doi.org/10.1016/j.cels.2018.03.006>
PMID:[29596780](https://pubmed.ncbi.nlm.nih.gov/29596780/)
 14. Wang L, Chen B, Wang Y, Sun N, Lu C, Qian R, Hua L. hClock gene expression in human colorectal carcinoma. *Mol Med Rep.* 2013; 8:1017–22.
<https://doi.org/10.3892/mmr.2013.1643>
PMID:[23970287](https://pubmed.ncbi.nlm.nih.gov/23970287/)
 15. Oshima T, Takenoshita S, Akaïke M, Kunisaki C, Fujii S, Nozaki A, Numata K, Shiozawa M, Rino Y, Tanaka K, Masuda M, Imada T. Expression of circadian genes correlates with liver metastasis and outcomes in colorectal cancer. *Oncol Rep.* 2011; 25:1439–46.
<https://doi.org/10.3892/or.2011.1207>
PMID:[21380491](https://pubmed.ncbi.nlm.nih.gov/21380491/)
 16. Karantanos T, Theodoropoulos G, Gazouli M, Vaiopoulou A, Karantanou C, Lymberi M, Pektasides D. Expression of clock genes in patients with colorectal cancer. *Int J Biol Markers.* 2013; 28:280–85.
<https://doi.org/10.5301/IJBM.5000033>
PMID:[23712462](https://pubmed.ncbi.nlm.nih.gov/23712462/)
 17. Røe OD, Anderssen E, Helge E, Pettersen CH, Olsen KS, Sandeck H, Haaverstad R, Lundgren S, Larsson E. Genome-wide profile of pleural mesothelioma versus parietal and visceral pleura: the emerging gene portrait of the mesothelioma phenotype. *PLoS One.* 2009; 4:e6554.
<https://doi.org/10.1371/journal.pone.0006554>
PMID:[19662092](https://pubmed.ncbi.nlm.nih.gov/19662092/)
 18. Elshazley M, Sato M, Hase T, Yamashita R, Yoshida K, Toyokuni S, Ishiguro F, Osada H, Sekido Y, Yokoi K, Usami N, Shames DS, Kondo M, et al. The circadian clock gene BMAL1 is a novel therapeutic target for malignant pleural mesothelioma. *Int J Cancer.* 2012; 131:2820–31.
<https://doi.org/10.1002/ijc.27598>
PMID:[22510946](https://pubmed.ncbi.nlm.nih.gov/22510946/)
 19. Torre LA, Bray F, Siegel RL, Ferlay J, Lortet-Tieulent J, Jemal A. Global cancer statistics, 2012. *CA Cancer J Clin.* 2015; 65:87–108.
<https://doi.org/10.3322/caac.21262>
PMID:[25651787](https://pubmed.ncbi.nlm.nih.gov/25651787/)
 20. Relógio A, Thomas P, Medina-Pérez P, Reischl S, Bervoets S, Gloc E, Riemer P, Mang-Fatehi S, Maier B, Schäfer R, Leser U, Herzog H, Kramer A, Sers C. Ras-mediated deregulation of the circadian clock in cancer. *PLoS Genet.* 2014; 10:e1004338.
<https://doi.org/10.1371/journal.pgen.1004338>
PMID:[24875049](https://pubmed.ncbi.nlm.nih.gov/24875049/)
 21. El-Athman R, Fuhr L, Relógio A. A Systems-Level Analysis Reveals Circadian Regulation of Splicing in Colorectal Cancer. *EBioMedicine.* 2018; 33:68–81.
<https://doi.org/10.1016/j.ebiom.2018.06.012>
PMID:[29936137](https://pubmed.ncbi.nlm.nih.gov/29936137/)
 22. Fuhr L, El-Athman R, Scrima R, Cela O, Carbone A, Knoop H, Li Y, Hoffmann K, Laukkanen MO, Corcione F, Steuer R, Meyer TF, Mazzocchi G, et al. The Circadian Clock Regulates Metabolic Phenotype Rewiring Via HKDC1 and Modulates Tumor Progression and Drug Response in Colorectal Cancer. *EBioMedicine.* 2018; 33:105–21.

- <https://doi.org/10.1016/j.ebiom.2018.07.002>
PMID:30005951
23. Leontieva OV, Gudkov AV, Blagosklonny MV. Weak p53 permits senescence during cell cycle arrest. *Cell Cycle*. 2010; 9:4323–27.
<https://doi.org/10.4161/cc.9.21.13584>
PMID:21051933
24. Leontieva OV, Blagosklonny MV. DNA damaging agents and p53 do not cause senescence in quiescent cells, while consecutive re-activation of mTOR is associated with conversion to senescence. *Aging (Albany NY)*. 2010; 2:924–35.
<https://doi.org/10.18632/aging.100265>
PMID:21212465
25. Dulic V. Senescence regulation by mTOR. *Methods Mol Biol*. 2013; 965:15–35.
https://doi.org/10.1007/978-1-62703-239-1_2
PMID:23296649
26. Terzi MY, Izmirli M, Gogebakan B. The cell fate: senescence or quiescence. *Mol Biol Rep*. 2016; 43:1213–20.
<https://doi.org/10.1007/s11033-016-4065-0>
PMID:27558094
27. Khapre RV, Kondratova AA, Patel S, Dubrovsky Y, Wrobel M, Antoch MP, Kondratov RV. BMAL1-dependent regulation of the mTOR signaling pathway delays aging. *Aging (Albany NY)*. 2014; 6:48–57.
<https://doi.org/10.18632/aging.100633>
PMID:24481314
28. Saxton RA, Sabatini DM. mTOR Signaling in Growth, Metabolism, and Disease. *Cell*. 2017; 168:960–76.
<https://doi.org/10.1016/j.cell.2017.02.004>
PMID:28283069
29. Sharma A, Singh K, Almasan A. Histone H2AX phosphorylation: a marker for DNA damage. *Methods Mol Biol*. 2012; 920:613–26.
https://doi.org/10.1007/978-1-61779-998-3_40
PMID:22941631
30. White RR, Vijg J. Do DNA Double-Strand Breaks Drive Aging? *Mol Cell*. 2016; 63:729–38.
<https://doi.org/10.1016/j.molcel.2016.08.004>
PMID:27588601
31. Noren Hooten N, Evans MK. Techniques to Induce and Quantify Cellular Senescence. *J Vis Exp*. 2017.
<https://doi.org/10.3791/55533>
PMID:28518126
32. Chiou YY, Yang Y, Rashid N, Ye R, Selby CP, Sancar A. Mammalian Period represses and de-represses transcription by displacing CLOCK-BMAL1 from promoters in a Cryptochrome-dependent manner. *Proc Natl Acad Sci USA*. 2016; 113:E6072–79.
<https://doi.org/10.1073/pnas.1612917113>
PMID:27688755
33. Yan J, Enge M, Whittington T, Dave K, Liu J, Sur I, Schmierer B, Jolma A, Kivioja T, Taipale M, Taipale J. Transcription factor binding in human cells occurs in dense clusters formed around cohesin anchor sites. *Cell*. 2013; 154:801–13.
<https://doi.org/10.1016/j.cell.2013.07.034>
PMID:23953112
34. Ueda HR, Chen W, Adachi A, Wakamatsu H, Hayashi S, Takasugi T, Nagano M, Nakahama K, Suzuki Y, Sugano S, Iino M, Shigeyoshi Y, Hashimoto S. A transcription factor response element for gene expression during circadian night. *Nature*. 2002; 418:534–39.
<https://doi.org/10.1038/nature00906> PMID:12152080
35. Preitner N, Damiola F, Lopez-Molina L, Zakany J, Duboule D, Albrecht U, Schibler U. The orphan nuclear receptor REV-ERB α controls circadian transcription within the positive limb of the mammalian circadian oscillator. *Cell*. 2002; 110:251–60.
[https://doi.org/10.1016/S0092-8674\(02\)00825-5](https://doi.org/10.1016/S0092-8674(02)00825-5)
PMID:12150932
36. Zoncu R, Efeyan A, Sabatini DM. mTOR: from growth signal integration to cancer, diabetes and ageing. *Nat Rev Mol Cell Biol*. 2011; 12:21–35.
<https://doi.org/10.1038/nrm3025>
PMID:21157483
37. Cornu M, Oppliger W, Albert V, Robitaille AM, Trapani F, Quagliata L, Fuhrer T, Sauer U, Terracciano L, Hall MN. Hepatic mTORC1 controls locomotor activity, body temperature, and lipid metabolism through FGF21. *Proc Natl Acad Sci U S A*. 2014; 111:11592–9.
<https://doi.org/10.1073/pnas.1412047111>
PMID:25082895
38. Jouffe C, Cretenet G, Symul L, Martin E, Atger F, Naef F, Gachon F. The circadian clock coordinates ribosome biogenesis. *PLoS Biol*. 2013; 11:e1001455.
<https://doi.org/10.1371/journal.pbio.1001455>
PMID:23300384
39. Lipton JO, Yuan ED, Boyle LM, Ebrahimi-Fakhari D, Kwiatkowski E, Nathan A, Güttler T, Davis F, Asara JM, Sahin M. The Circadian Protein BMAL1 Regulates Translation in Response to S6K1-Mediated Phosphorylation. *Cell*. 2015; 161:1138–51.
<https://doi.org/10.1016/j.cell.2015.04.002>
PMID:25981667
40. Kondratov RV, Kondratova AA, Gorbacheva VY, Vykhovanets OV, Antoch MP. Early aging and age-related pathologies in mice deficient in BMAL1, the core component of the circadian clock. *Genes Dev*. 2006; 20:1868–73.
<https://doi.org/10.1101/gad.1432206> PMID:16847346

41. Kondratov RV. A role of the circadian system and circadian proteins in aging. *Ageing Res Rev.* 2007; 6:12–27.
<https://doi.org/10.1016/j.arr.2007.02.003>
PMID:[17369106](https://pubmed.ncbi.nlm.nih.gov/17369106/)
42. Rochette PJ, Bastien N, Lavoie J, Guérin SL, Drouin R. SW480, a p53 double-mutant cell line retains proficiency for some p53 functions. *J Mol Biol.* 2005; 352:44–57.
<https://doi.org/10.1016/j.jmb.2005.06.033>
PMID:[16061257](https://pubmed.ncbi.nlm.nih.gov/16061257/)
43. Solomon H, Dinowitz N, Pateras IS, Cooks T, Shetzer Y, Molchadsky A, Charni M, Rabani S, Koifman G, Tarcic O, Porat Z, Kogan-Sakin I, Goldfinger N, et al. Mutant p53 gain of function underlies high expression levels of colorectal cancer stem cells markers. *Oncogene.* 2018; 37:1669–84.
<https://doi.org/10.1038/s41388-017-0060-8>
PMID:[29343849](https://pubmed.ncbi.nlm.nih.gov/29343849/)
44. Singer O, Verma IM. Applications of lentiviral vectors for shRNA delivery and transgenesis. *Curr Gene Ther.* 2008; 8:483–88.
<https://doi.org/10.2174/156652308786848067>
PMID:[19075631](https://pubmed.ncbi.nlm.nih.gov/19075631/)
45. Qian Y, Chen X. Senescence regulation by the p53 protein family. *Methods Mol Biol.* 2013; 965:37–61.
https://doi.org/10.1007/978-1-62703-239-1_3
PMID:[23296650](https://pubmed.ncbi.nlm.nih.gov/23296650/)
46. Kondratov RV, Vykhovanets O, Kondratova AA, Antoch MP. Antioxidant N-acetyl-L-cysteine ameliorates symptoms of premature aging associated with the deficiency of the circadian protein BMAL1. *Aging (Albany NY).* 2009; 1:979–87.
<https://doi.org/10.18632/aging.100113>
PMID:[20157581](https://pubmed.ncbi.nlm.nih.gov/20157581/)
47. Yeh JJ, Routh ED, Rubinas T, Peacock J, Martin TD, Shen XJ, Sandler RS, Kim HJ, Keku TO, Der CJ. KRAS/BRAF mutation status and ERK1/2 activation as biomarkers for MEK1/2 inhibitor therapy in colorectal cancer. *Mol Cancer Ther.* 2009; 8:834–43.
<https://doi.org/10.1158/1535-7163.MCT-08-0972>
PMID:[19372556](https://pubmed.ncbi.nlm.nih.gov/19372556/)
48. Lordier L, Bluteau D, Jalil A, Legrand C, Pan J, Rameau P, Jouni D, Bluteau O, Mercher T, Leon C, Gachet C, Debili N, Vainchenker W, et al. RUNX1-induced silencing of non-muscle myosin heavy chain IIB contributes to megakaryocyte polyploidization. *Nat Commun.* 2012; 3:717.
<https://doi.org/10.1038/ncomms1704> PMID:[22395608](https://pubmed.ncbi.nlm.nih.gov/22395608/)
49. Zhang Y, Giacchetti S, Parouchev A, Hadadi E, Li X, Dallmann R, Xandri-Monje H, Portier L, Adam R, Lévi F, Dulong S, Chang Y. Dosing time dependent in vitro pharmacodynamics of Everolimus despite a defective circadian clock. *Cell Cycle.* 2018; 17:33–42.
<https://doi.org/10.1080/15384101.2017.1387695>
PMID:[29099263](https://pubmed.ncbi.nlm.nih.gov/29099263/)

SUPPLEMENTARY MATERIALS

Supplementary Figure



Supplementary Figure 1. Two binding sites for BMAL1 in *NR1D1* gene have been mapped in LOVO CRC cell by in silico CHIP-seq analysis, but only one binding site of *PER* or *CRY* was identified.

BRD4 inhibition sensitizes renal cell carcinoma cells to the PI3K/mTOR dual inhibitor VS-5584

Ming Xu^{1,*}, Lijun Xu^{1,*}, Yin Wang^{2,*}, Guangcheng Dai¹, Boxin Xue¹, Yuan-yuan Liu³, Jianbing Zhu⁴, Jin Zhu¹

¹Department of Urology, the Second Affiliated Hospital of Soochow University, Suzhou, China

²Jiangsu Key Laboratory of Neuropsychiatric Diseases and Institute of Neuroscience, Soochow University, Suzhou, China

³Clinical Research and Laboratory Center, Affiliated Kunshan Hospital of Jiangsu University, Kunshan, China

⁴Department of Radiology, Suzhou Science and Technology Town Hospital, The Affiliated Suzhou Science and Technology Town Hospital of Nanjing Medical University, Suzhou, China

*Equal contribution

Correspondence to: Yuan-yuan Liu, Jianbing Zhu, Jin Zhu; **email:** 20194054004@stu.suda.edu.cn; zeno1839@126.com, <https://orcid.org/0000-0001-8186-9549>; urologistzhujin@163.com

Keywords: renal cell carcinoma, PI3K/AKT/mTOR, VS-5584, BRD4, chemosensitization

Received: May 21, 2020

Accepted: June 29, 2020

Published: October 13, 2020

Copyright: © 2020 Xu et al. This is an open access article distributed under the terms of the [Creative Commons Attribution License](https://creativecommons.org/licenses/by/3.0/) (CC BY 3.0), which permits unrestricted use, distribution, and reproduction in any medium, provided the original author and source are credited.

ABSTRACT

Activation of the PI3K/AKT/mTOR pathway promotes the progression of renal cell carcinoma (RCC). This study tested the anti-RCC cell activity of the PI3K/mTOR dual inhibitor, VS-5584. We show that VS-5584 inhibited PI3K/AKT/mTORC1/2 activation in established (786-O and A498 lines) and primary RCC cells, thereby suppressing cell survival, proliferation, migration and cell cycle progression. VS-5584 induced significant apoptosis in RCC cells. A daily single oral dose of VS-5584 (20 mg/kg) significantly inhibited 786-O tumor growth *in vivo*. VS-5584 treatment of 786-O tumor xenografts and RCC cells resulted in feedback upregulation of bromodomain-containing protein 4 (BRD4). Furthermore, BRD4 inhibition (by JQ1 and CPI203), knockdown or complete knockout potentiated VS-5584-induced RCC cell death and apoptosis. Conversely, forced overexpression of BRD4 attenuated the cytotoxicity of VS-5584 in 786-O cells. Collectively, VS-5584 potently inhibits RCC cell proliferation and survival. Its anti-tumor activity is further enhanced by the targeted inhibition of BRD4.

INTRODUCTION

Renal cell carcinoma (RCC) is the most common renal malignancy globally, causing significant human mortalities each year [1, 2]. In clinical practices, nephroureterectomy of the early-stage RCCs is yet the only curable treatment procedure [1]. However, a large proportion of RCC patients are diagnosed at advanced stages. Over 25% of them have local invasion and systematic metastasis [1, 3]. These patients often have a poor prognosis [1, 3].

Novel molecularly-targeted agents are needed for better RCC treatment [4, 5]. In RCC, PTEN depletion,

PI3KCA mutation, and receptor tyrosine kinases (RTKs) overactivation will result in sustained activation of phosphoinositide 3-kinase (PI3K)-AKT- mammalian target of rapamycin (mTOR) cascade [6–9]. This signaling is essential for cancer cell proliferation and migration, as well as angiogenesis and chemo-resistance [6, 9–11]. This cascade is now an established and critical therapeutic target of RCC. Temsirolimus and everolimus, two mTOR inhibitors, are approved by the FDA for the treatment of curtailed advanced RCC [6, 9–11]. Our group has previously shown that WYE-687, a AKT-mTORC1/2 inhibitor, potently suppressed RCC cell growth [12]. Recently, we demonstrated that a novel Akt inhibitor SC66 inhibited RCC cell

progression, but through AKT-dependent and AKT-independent mechanisms [13].

VS-5584 is a potent dual inhibitor of PI3K and mTOR [14]. It displays almost equivalent activity against PI3K and mTOR [14]. This dual inhibitor exhibits certain pharmacokinetic properties. It is well-tolerated in animal studies [14]. The current study tested the anti-RCC cell activity of VS-5584.

Bromodomain-containing protein 4 (BRD4), a member of the BET (bromodomain and extraterminal domain) family [15], binds acetylated-histones to participate in epigenetic processes [16–18]. It is required for chromatin structure formation in daughter cells in mitosis. BRD4 recruits positive transcription elongation factor b and phosphorylates RNA polymerase II. It is an essential step for transcription elongation and expression of several key oncogenes, including Bcl-2 and c-Myc [17, 19].

In cancer cells BRD4 overexpression promotes cell survival, proliferation, and resistance to apoptosis [20]. Recent studies have proposed a pivotal function of BRD4 in chemoresistance. The BRD4 inhibitor JQ1 sensitized highly chemo-resistant pleural mesothelioma cells to cisplatin [21], and pancreatic cancer cells to gemcitabine [22]. The results of this study demonstrated BRD4 is a key resistance factor of VS-5584 in RCC cells.

RESULTS

VS-5584 inhibits survival, proliferation, cell cycle progression and migration in RCC 786-O cells

The current study tested the potential anti-tumor activity of VS-5584, a novel dual inhibitor of PI3K/mTOR [14, 23], in RCC cells. 786-O RCC cells [12, 24] were treated with different concentrations (0.5–10 μM) of VS-5584. MTT cell viability assay results showed that VS-5584 treatment inhibited 786-O cell survival in a dose- and time-dependent manner (Figure 1A). The IC_{50} of VS-5584 was between 1–5 μM (at 72/96-h treatment, Figure 1A). A lower dose of VS-5584 (0.5 μM) was unable to significantly inhibit 786-O cell viability (Figure 1A). Results in Figure 1B demonstrated that VS-5584 dose-dependently inhibited PI3K/mTORC1/2 cascade activation in 786-O cells. As shown in Figure 1B, treatment with VS-5584 inhibited the activation of phosphorylated (“p-”) p85, an indicator of PI3K activation, as well as of p-S6K1 (Thr-389) and p-Akt (Ser-473), which are substrates of mTORC1 and mTORC2 [25], respectively. The total protein levels of p85, S6K1, and Akt1/2 remained unchanged (Figure 1B).

To test cell proliferation *in vitro*, BrdU ELISA and soft agar colony formation assays were performed. VS-5584 treatment (1–10 μM) significantly decreased BrdU ELISA OD (Figure 1C) and the number of 786-O colonies (Figure 1D). These results indicated its anti-proliferative activity. Furthermore, VS-5584 dose-dependently inhibited EdU incorporation in 786-O cells (Figure 1E), further confirming proliferation inhibition.

Analysis of cell cycle distribution by PI-FACS showed that treatment with VS-5584 (2/5 μM) increased the percentage of cells in the G0/G1 phases, while decreasing the percentage of cells in the S and G2/M phases (Figure 1F). Testing cell migration *in vitro*, using “Transwell” assays, confirmed that VS-5584 (1–10 μM) reduced the number of migrated 786-O cells (Figure 1G). At the lowest concentration (0.5 μM), VS-5584 again failed to inhibit 786-O cell migration *in vitro* (Figure 1G). Treatment with vehicle control (dimethyl sulfoxide, 0.1–0.5%), as expected, had no significant effect on 786-O cell survival, proliferation and migration (Figure 1C–1G). These results show that VS-5584 inhibited survival, proliferation, cell cycle progression, and migration in RCC 786-O cells.

VS-5584 induces apoptosis activation in RCC 786-O cells

Cell death assay results showed that VS-5584 dose-dependently induced LDH release into the culture medium (Figure 2A), indicating cell death. VS-5584 treatment (1–10 μM) of 786-O cells also increased single strand DNA (ssDNA) production (Figure 2B). Western blotting assay results, Figure 2C, demonstrated that VS-5584 dose-dependently induced cleavages of caspase-3, caspase-9 and PARP (poly ADP-ribose polymerase) in 786-O cells. Additional studies demonstrated that the percentage of TUNEL-positive nuclei was significantly increased with VS-5584 (1–10 μM) treatment (Figure 2D), thereby confirming apoptosis activation. Lower concentrations of VS-5584 (0.5 μM) failed to induce 786-O cell apoptosis (Figure 2A–2D). Collectively, our data suggest that VS-5584 induced apoptosis activation in 786-O RCC cells.

VS-5584 exerts anti-survival, anti-proliferative, and pro-apoptotic activity in the established and primary human RCC cells

The anti-tumor effects of VS-5584 were tested on the established human A498 RCC cells and two different primary human RCC cells, RCC1 and RCC2 (see our previous studies [13]). Western blotting results showed that activation of PI3K (“p-p85”), mTORC1 (“p-S6K1”), and mTORC2 (“p-Akt at Ser-473”) was inhibited by VS-5584 treatment (5 μM , 2 h) in A498

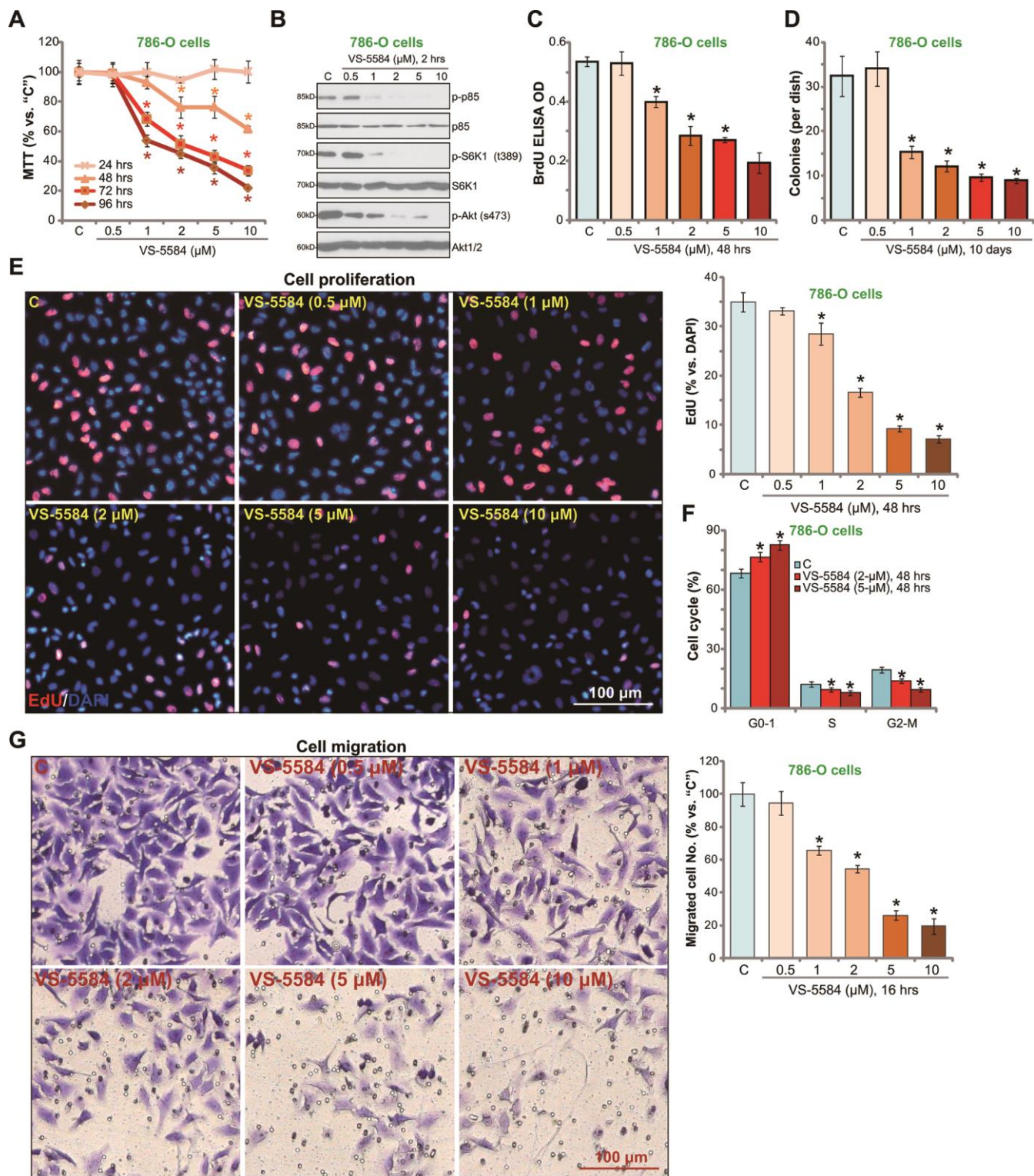


Figure 1. VS-5584 inhibits survival, proliferation, cell cycle progression and migration in RCC 786-O cells. RCC 786-O cells were either left untreated ("C", same for all Figures), or treated with applied concentrations of VS-5584 (0.5-10 μM), cells were further cultured for the indicated time; Cell survival (A, MTT assay), PI3K-mTORC1/2 activation (B, Western blotting), cell proliferation (C-E, BrdU EILSA, soft agar colony formation and EdU incorporation staining assays) and cell cycle progression (F, PI-FACS) were tested, with cell migration examined by "Transwell" assays (G). For "EdU" assays, at least 800 cells in five random views were included to calculate average number of migrated cells (same for all Figures). For "Transwell" assays five random views were included to calculate average number of migrated cells (same for all Figures). Data were presented as mean \pm standard deviation (SD, n=5). * p < 0.05 vs. "C" group. The *in vitro* experiments were repeated four times, and similar results were obtained. Bar = 100 μm (E, G).

and primary human RCC cells (Figure 3A). The basal PI3K/mTORC1/2 activity was low in HK-2 renal epithelial cells (Figure 3B). Treatment with VS-5584 (5 μ M) significantly inhibited the viability (MTT OD, Figure 3C) and proliferation (BrdU ELISA OD and nuclei EdU staining, Figure 3D, 3E) of A498 and primary RCC cells. Cell migration, tested by the “Transwell” assay, was largely inhibited in VS-5584-treated RCC cells (Figure 3F).

The ssDNA ELISA OD, an indicator of cell apoptosis, was increased in VS-5584-treated RCC cells (Figure 3G). To further confirm apoptosis activation we show that the ratio of TUNEL-positive nuclei was significantly increased with VS-5584 treatment in the RCC cells (Figure 3H). Whereas in HK-2 renal epithelial cells, the same VS-5584 treatment (5 μ M) failed to inhibit cell survival (Figure 3C), proliferation (Figure 3D, 3E) and migration (Figure 3F). Nor did it induce apoptosis activation (Figure 3G, 3H). Thus, VS-5584 induced anti-survival, anti-proliferative, anti-migration and pro-apoptotic activities in established (A498) and primary human RCC cells.

To test the anti-RCC activity of VS-5584 *in vivo*, nude mice were subcutaneously inoculated with 786-O cells to form xenografts. Tumor growth curve analysis showed that a daily single dose of VS-5584 (20 mg/kg, oral administration) significantly inhibited 786-O tumor growth (Figure 3I). By calculating the estimated daily tumor growth, using the formula (tumor volume at day35 – tumor volume at day0) \div 35, we show that 786-O xenograft growth *in vivo* was inhibited following treatment with VS-5584 (Figure 3J). The body weights of the experimental mice were not significantly different between the two groups (Figure 3K). There were no noticeable signs of apparent toxicity, suggesting that the VS-5584 treatment was well tolerated in the xenograft mouse model.

BRD4 inhibition potentiates VS-5584-induced RCC cell death and apoptosis

Although VS-5584 exerts anti-tumor effects against human RCC cells, its efficacy appears to be relatively low with an IC50 of 1-5 μ M (Figures 1, 2), suggesting that RCC cells show resistance to VS-558. The BET family protein BRD4 is required for transcription elongation [17]. The BRD4-dependent proteins, Bcl-2 [26] and c-Myc [27, 28], are key oncogenic proteins. To examine the potential activity of BRD4 in chemoresistance, Western blotting was used to analyze BRD4 protein levels in tumor tissue lysates (Figure 3I). Results showed that BRD4 protein levels were significantly increased in VS-5584-treated 786-O tumor tissues compared with those in vehicle control-treated tumor tissues (Figure 4A). Therefore, VS-5584 administration *in vivo* induced BRD4 expression. Similarly, the protein levels of BRD4, Bcl-2, and c-Myc were increased in VS-5584 (2/5 μ M)-treated 786-O cells *in vitro* (Figure 4B).

To confirm BRD4-induced RCC resistance to VS-5584, two known BRD4 inhibitors, JQ1 and CPI203, were utilized. Both BRD4 inhibitors blocked VS-5584 (5 μ M)-induced Bcl-2 and c-Myc upregulation (Figure 4B). Furthermore, treatment with JQ1 and CPI203 significantly enhanced the ability of VS-5584 (2/5 μ M) to decrease 786-O cell viability (Figure 4C) and to enhance apoptosis (Figure 4D). Treatment with JQ1 or CPI203 alone induced minor but significant 786-O cell death and apoptosis (Figure 4C, 4D).

In primary RCC cells (“RCC1”), VS-5584 treatment (5 μ M, 24 h) induced feedback upregulation of BRD4, Bcl-2, and c-Myc (Figure 4E). Furthermore, treatment with JQ1 or CPI203 potently enhanced the cytotoxicity of VS-5584 in primary cancer cells (Figure 4F, 4G). Co-treatment with VS-5584 and the BRD4 inhibitors

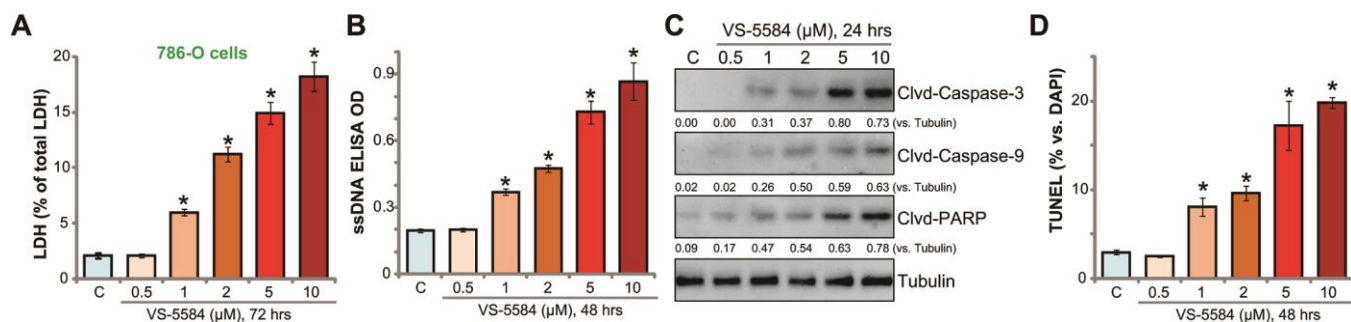


Figure 2. VS-5584 induces apoptosis activation in RCC 786-O cells. RCC 786-O cells were treated with applied concentrations of VS-5584 (0.5-10 μ M), cells were further cultured for the indicated time; Cell death was tested by LDH medium release assay (A); Cell apoptosis was tested by ssDNA ELISA (B), Western blotting testing apoptosis proteins (C), and nuclei TUNEL staining (D). Data were presented as mean \pm standard deviation (SD, n=5). * p < 0.05 vs. “C” group. The *in vitro* experiments were repeated four times, and similar results were obtained.

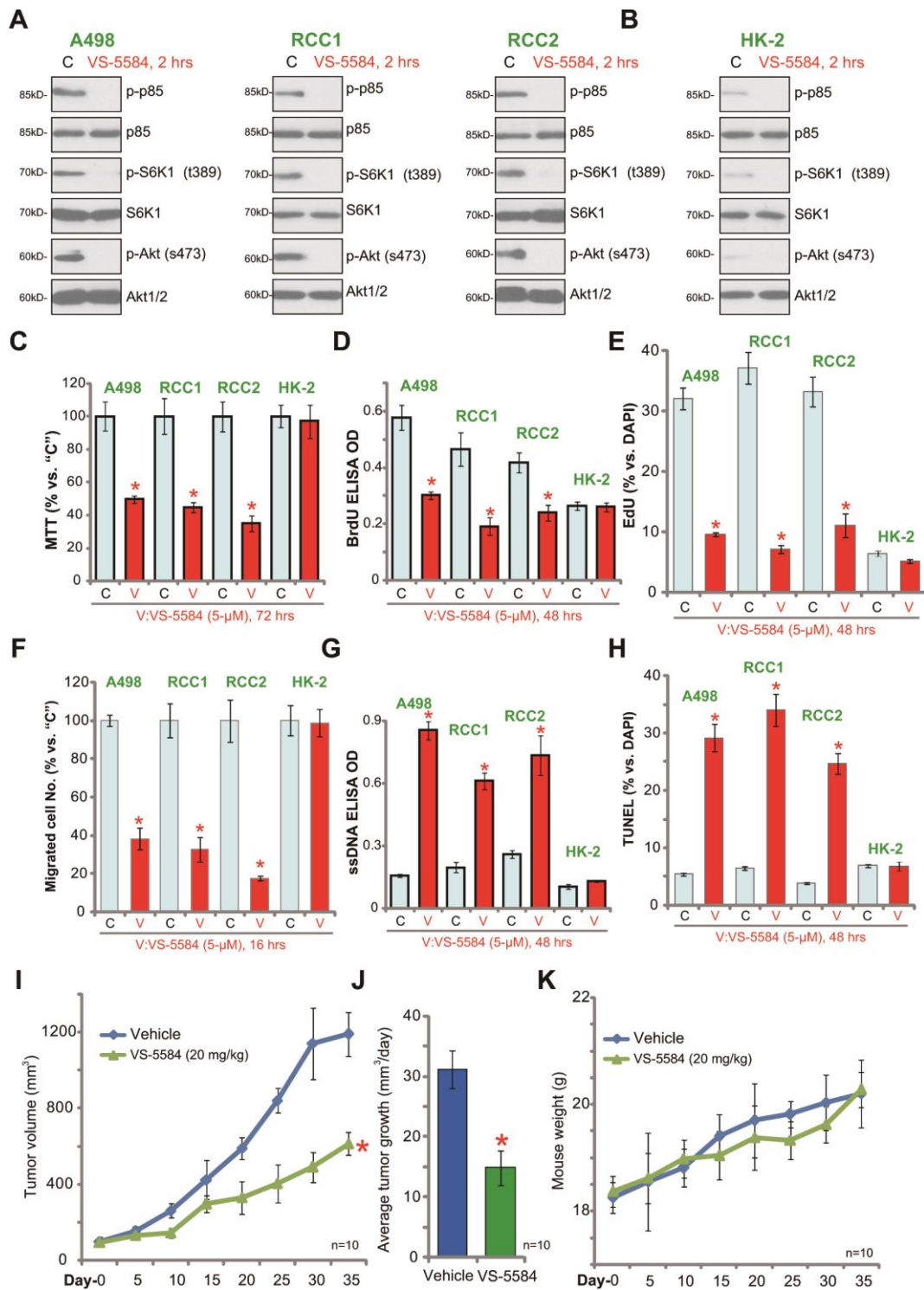


Figure 3. VS-5584 exerts anti-survival, anti-proliferative, and pro-apoptotic activity in the established and primary human RCC cells. A498 cells, the primary human RCC cells ("RCC1/RCC2") or HK-2 renal epithelial cells were treated with VS-5584 (5 μ M), cells were further cultured for indicated time; PI3K-mTORC1/2 activation (**A**, **B**, Western blotting), cell survival (C, MTT), proliferation (**D**, BrdU EILSA and **E**, nuclei EdU staining), migration (**F**, "Transwell" assay) and apoptosis (**G**, ssDNA ELISA and **H**, TUNEL staining) were tested. The 786-O xenograft tumor-bearing nude mice were administrated with vehicle control ("Vehicle", saline), VS-5584 (20 mg/kg, oral administration, daily), the tumor volumes (**I**) and mice body weights (**J**) were recorded every five days for a total of 35 days; The estimated daily tumor growth was calculated (**K**); Data were presented as mean \pm standard deviation (SD). * p < 0.05 vs. "C" group (C–H, n=5). * p < 0.05 vs. "Vehicle" (I, J, n=10). The *in vitro* experiments were repeated four times, and similar results were obtained. Bar = 100 μ m (E, F, H).

(JQ1/CPI203) failed to induce significant reduction in cell viability (Figure 4H) and apoptosis (Figure 4I) in HK-2 epithelial cells.

BRD4 is the primary resistance factor of VS-5584 in RCC 786-O cells

Because the pharmacological BRD4 inhibitors (JQ1 and CPI203) might have off-target toxicities, genetic strategies were employed to alter BRD4 expression in 786-O cells. Two lentiviral BRD4 shRNAs, with non-overlapping sequences (“sh-BRD4-S1/S2”), were transfected into 786-O cells. Western blotting results

showed that the protein expression of BRD4, as well as the BRD4-regulated c-Myc gene were significantly downregulated by BRD4 shRNA treatment (Figure 5A). Importantly, 786-O cells transduced with BRD4 shRNA were more vulnerable to VS-5584 treatment, showing an increased viability reduction (Figure 5B) and apoptosis (Figure 5C).

To confirm BRD4 knockdown results, a CRISPR-Cas9-BRD4-KO plasmid was transfected into RCC 786-O cells to completely knockout BRD4 protein in the stable cells. In BRD4-KO cells, no BRD4 protein expression was observed even with VS-5584 treatment (5 μM,

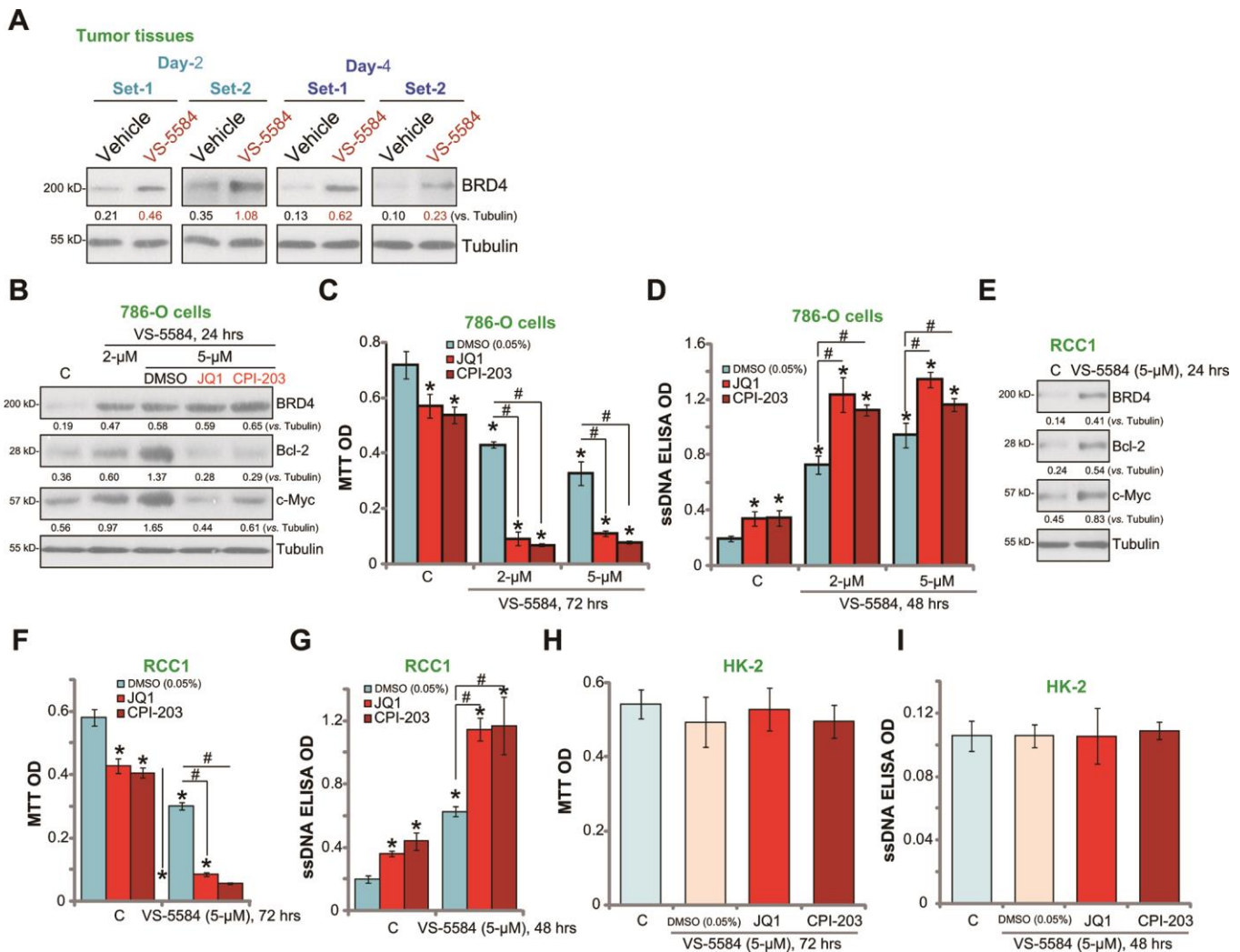


Figure 4. BRD4 inhibition potentiates VS-5584-induced RCC cell death and apoptosis. The 786-O xenograft tumor-bearing nude mice were administrated with vehicle control or VS-5584 (20 mg/kg, oral administration, daily), at treatment Day-2 and Day-4, 4 h after the VS-5584 or vehicle administration, two tumors (“Set-1/Set-2”) of each group were isolated, expression of BRD4 and Tubulin in tumor lysates was shown (A). 786-O cells (B) and primary human RCC cells (“RCC1”, E) were treated VS-5584 (or plus BRD4 inhibitors, B) for 24 h, listed proteins in total cell lysates were tested by Western blotting. 786-O cells (C, D), RCC1 primary cancer cells (F, G) or HK-2 cells (H, I) were pretreated with JQ1 (500 nM) or CPI203 (500 nM) for 30 min, followed by VS-5584 (2/5 μM) treatment for 48/72 h, cell survival and apoptosis were tested by MTT (C, F, H) and ssDNA ELISA (D, G, I), respectively. The listed proteins were quantified (B, E). Data were presented as mean ± standard deviation (SD, n=5). **p* < 0.05 vs. “C” group. #*p* < 0.05.

24 h; Figure 4D). c-Myc expression was significantly decreased (Figure 5D). Compared with control cells, BRD4-KO 786-O cells were significantly more sensitive to VS-5584 (Figure 5E, 5F).

Based on the above results, we predicted that forced BRD4 overexpression shall inhibit VS-5584 activity. To test this hypothesis, a lentiviral BRD4-expression vector was transfected into 786-O cells. After puromycin

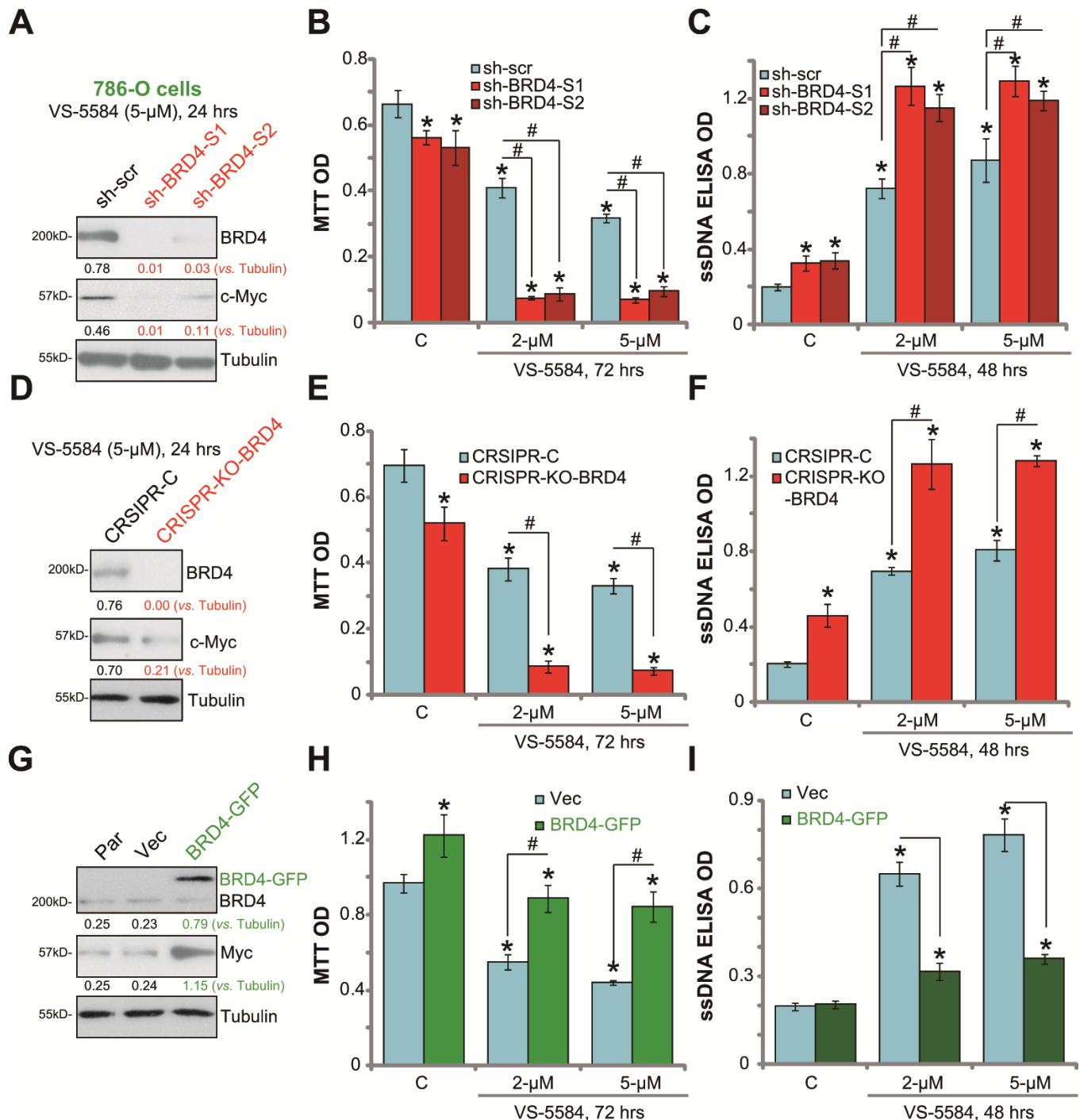


Figure 5. BRD4 is the primary resistance factor of VS-5584 in RCC 786-O cells. In VS-5584-treated stable 786-O cells with BRD4 shRNA (“sh-BRD4-S1/S2”, A–C), CRISPR-Cas9-BRD4-KO plasmid (D–F) or BRD4-expression vector (“BRD4-GFP”, G–I), BRD4, c-Myc and tubulin expression was shown (A, D, G). Cell survival and apoptosis were tested by MTT (after 72 h, B, E, H) and ssDNA ELISA (after 48 h, C, F, I), respectively. The listed proteins were quantified (A, D, G). Data were presented as mean \pm standard deviation (SD, n=5). *p< 0.05 vs. “C” group. #p< 0.05.

selection, the stable cells showed exogenous BRD4 expression (tagged with GFP, Figure 5G). c-Myc expression was increased in BRD4-overexpressing cells (Figure 5G). Compared with the vector control cells, BRD4-overexpressing cells showed significant reduction in cell death (Figure 5H) and apoptosis activation (Figure 5I) following VS-5584 treatment. Collectively, these results confirm that BRD4 is the primary factor of VS-5584 resistance in RCC cells.

DISCUSSION

There are two mTOR complexes, namely mTORC1 and mTORC2. mTORC1 inhibitors, such as everolimus, have been approved by the FDA for the clinical treatment of certain human RCCs [6, 9]. Yet, the clinical application of these inhibitors has several limitations. Rapamycin and its analogs can only partially inhibit mTORC1 activity [29, 30]. They fail to directly inhibit mTORC2, which is also important in the progression of RCC [7, 31].

VS-5584 is a novel PI3K/mTOR dual inhibitor, showing almost equivalent activity against PI3K and mTOR [14]. We found that VS-5584 blocked both mTORC1 and mTORC2 activation, as well as PI3K-Akt activity in RCC cells. We failed to observe feedback Erk-MAPK activation in VS-5584-treated RCC cells. A single daily oral dose of VS-5584 (20 mg/kg) significantly inhibited 786-O tumor growth *in vivo*. Hence, our data suggest that inhibition of the entire PI3K/AKT/mTOR cascade by VS-5584 could explain its superior anti-RCC cell activity.

Another important finding of this study was that BRD4, the BET family protein, is a key resistance factor against VS-5584 in RCC cells. VS-5584 treatment induced feedback upregulation of BRD4 in RCC cells, resulting in expression of BRD4 target proteins, Bcl-2 and c-Myc. Co-treatment with BRD4 inhibitors (JQ1/CPI203) potentiated VS-5584-induced RCC cell death and apoptosis. Furthermore, BRD4 knockdown or knockout enhanced VS-5584-induced cytotoxicity in RCC cells. Conversely, forced overexpression of BRD4 attenuated VS-5584-induced 786-O cell apoptosis.

The pharmacological and genetic evidence provided by this study indicate that BRD4 is a VS-5584 drug resistance factor in RCC cells. BRD4 inhibition may be an important strategy to sensitize RCC cells to VS-5584. The observed resistance to a PI3K-Akt inhibitor could be driven by the feedback activation of receptor tyrosine kinases (RTKs) [32]. It has been previously shown that BET inhibitors dissociated BRD4 from chromatin at the regulatory regions of multiple RTKs to reduce their expression level [32], thereby

sensitizing a broad range of tumor cell lines to PI3K-Akt inhibitors [32]. Wang et al. demonstrated that BRD4 inhibition suppressed Sonic hedgehog signaling to sensitize pancreatic ductal adenocarcinoma cells to gemcitabine [22]. Moreover, JQ1 in combination with cisplatin induced synergistic inhibitory effects on human malignant pleural mesothelioma cells, possibly via the promotion of cell senescence and apoptosis [21]. Further studies are needed to explore the underlying mechanisms of BRD4 upregulation by VS-5584, and how BRD4 inhibition sensitizes RCC cells to VS-5584.

In summary, VS-5584 potently inhibits RCC cell proliferation and survival. Its anti-tumor activity is further enhanced by the targeted inhibition of BRD4.

MATERIALS AND METHODS

Chemicals and reagents

VS-5584, JQ1, and CPI203 were obtained from Sigma-Aldrich (St. Louis, MO). Cell culture reagents were purchased from Gibco (Grand Island, NY). The antibodies were purchased from Cell Signaling Technology (Danvers, MA). Puromycin was obtained from Sigma-Aldrich.

Cell culture

Established human RCC cell lines (786-O and A498) as well as HK-2 human renal epithelial cells were obtained as described previously [13, 33]. The primary human RCC cells, derived from two different primary RCC patients (“RCC1” and “RCC2”, PTEN-null), were reported early [13]. The primary human cells were cultured in an appropriate medium as described previously [34].

Methylthiazol tetrazolium (MTT) assay

Cells were seeded onto a 96-well tissue culture plate (3×10^3 cells per well). MTT assay was performed to test cell viability, according to the manufacturer's instructions (Sigma-Aldrich). The MTT optical density (OD) at 590 nm was recorded.

Soft agar colony formation assay

A total of 10,000 RCC 786-O cells per treatment were seeded on the top layer of 0.35% solidified agar in complete medium in 10-cm culture dishes, with the bottom layer containing 0.8% agar. VS-5584 was added to the complete medium and replaced every two days for a total of 10 days. Following this, colonies were stained with crystal violet (Sigma) and counted.

BrdU (5-bromo-2-deoxyuridine) enzyme-linked immunosorbent assay (ELISA)

Cells were seeded onto 96-well tissue culture plates (3×10^3 cells per well). The BrdU ELISA kit (Roche Diagnostics, Basel, Switzerland) was utilized to test cell proliferation *in vitro*. The BrdU ELISA absorbance at 405 nm was recorded.

Cell cycle assay

The propidium iodide (PI; Invitrogen, Carlsbad, CA) flow cytometry assay was applied to test cell cycle distribution. Cells were seeded onto 6-well tissue culture plates (2×10^5 cells per well). Following the applied treatment, cells were washed, fixed, and incubated with DNase-free RNase and PI. Cells were tested using a FACSCalibur instrument (BD Biosciences, Shanghai, China).

***In vitro* cell migration assay**

As described human RCC cells or the HK-1 cells (4×10^4 cells of each condition in 200 μ L serum-free medium) were seeded on the upper surfaces of “Transwell” chambers, coated with Matrigel (Sigma) [35, 36]. The lower compartments were filled with FBS-containing complete medium. Following incubation, the migrated cells to the lower chambers were fixed, stained and counted.

EdU assay of cell proliferation

RCC cells or the HK-1 cells (1×10^5 cells/well) were seeded onto the six-well plates. An EdU (5-ethynyl-20-deoxyuridine) Apollo-488 *In Vitro* Imaging Kit (Ribo-Bio, Guangzhou, China) [37] was applied to examine and quantify cell proliferation. In brief, EdU (2.5 μ M) dye was added to RCC cells or the HK-1 cells for 6-8h. Cell nuclei were co-stained with DAPI for 15 min, and visualized via a fluorescent microscope (Leica).

Lactate dehydrogenase (LDH) assay for cell death

Cells were seeded onto 6-well tissue culture plates (2×10^5 cells per well). Cell death was examined by measuring the LDH content in the medium, using a 2-step enzymatic reaction LDH assay kit (Takara, Tokyo, Japan). Percentage of LDH release = LDH released in conditional medium \div (LDH released in conditional medium + LDH in cell lysates).

Terminal deoxynucleotidyl transferase dUTP nick-end labeling (TUNEL) assay

As described previously [33], cells were seeded onto 6-well tissue culture plates (2×10^5 cells per well).

TUNEL *In Situ* Cell Death Detection Kit (Roche Diagnostics, Shanghai, China) was utilized to quantify the number of TUNEL-labeled apoptotic nuclei.

Western blotting

After the applied treatment, cells were treated with lysis buffer [38]. The total cell protein lysates (30 μ g per treatment) were analyzed. Western blotting was performed following a previously described protocol [33]. Protein bands were visualized using enhanced chemiluminescence (ECL) reagents (Pierce, Suzhou, China), and quantified using the ImageJ software (National Institutes of Health).

Single stranded DNA (ssDNA) ELISA

ssDNA accumulation is a characteristic marker of cell apoptosis. For each treatment, 30 μ g of cell lysate (using the lysis buffer for western blotting) was analyzed. A ssDNA ELISA kit (Roche Diagnostics) was utilized to quantify DNA fragmentation. The ssDNA ELISA absorbance was recorded at 450 nm.

BRD4 shRNA

Two different lentiviral BRD4 shRNAs, with unique and non-overlapping sequences (“S1/S2”), were provided by Dr. Zhao [39]. 786-O cells were seeded onto 6-well tissue culture plates (2×10^5 cells per well). Cells were transfected with BRD4 shRNA lentivirus for 24 h. Puromycin (2 μ g/mL) was then used to select stable cells (4-5 passages). BRD4 knockdown in the stable cells was confirmed by Western blotting. Control cells were transfected with lentiviral scramble control shRNA (Santa Cruz Biotechnology).

Exogenous BRD4 overexpression

The pSUPER-puro-BRD4-GFP expression vector was provided by Dr. Zhao [39], and was transfected into HEK-293T cells together with the viral packaging proteins VSVG and Hit-60 (Promega, Shanghai, China). After 48 h, the medium containing the virus particles was filtered, and 786-O cells were incubated in this medium for additional 48 h. Puromycin was used to select the stable cells (4-5 passages). Exogenous BRD4 overexpression in stable cells was confirmed by western blotting.

BRD4 knockout (KO)

The CRISPR/Cas9 BRD4 KO plasmid (sc-400519-KO-2; Santa Cruz Biotechnology) was transfected to 786-O cells using Lipofectamine 2000 reagent (Invitrogen,

Shanghai, China), and selected with puromycin after 4-5 passages. Control cells were treated with an empty vector with control small guide RNA (sgRNA; Santa Cruz Biotechnology). BRD4 expression in stable cells was tested by western blotting.

Xenograft assay

The female nude mice were provided by the Animal Center of Chinese Academy of Science (Shanghai, China). 786-O cells were injected subcutaneously (*s.c.*) to the flanks of the nude mice. Within 20 days subcutaneous xenografts were established (around 100 mm³). Mice (n=10 each group) were treated with VS-5584. Mice body weight and bi-dimensional tumor measurements were taken every five days for a total of 35 days [40]. The animal protocol was approved by the Ethics Committee of Wenzhou Medical University.

Statistical analysis

Quantitative results were presented as mean ± standard deviation (SD). Results were compared by one-way analysis of variance (ANOVA) followed by Tukey's test (SPSS version 21.0, Chicago, IL). Values of *p* < 0.05 were considered as statistically significant.

AUTHOR CONTRIBUTIONS

MX, YW, LX, JZb, YL, JZ conceived, designed, and supervised the study. MX, YW, LX, GD, BX, JZb, YL, JZ collected samples, performed the experiments and analyzed the data. MX, YW, JZb, YL, JZ wrote the paper. All authors reviewed and approved the final manuscript.

CONFLICTS OF INTEREST

The authors listed no conflicts of interest.

FUNDING

The present study was supported by the National Natural Science Foundation of China (grant no. 81773221) for Professor Jin Zhu, the Natural Science Foundation of Jiangsu Province (grant no. BK20161222, BK20191170) for Professor Jin Zhu and Dr. Lijun Xu, by Suzhou Science and Technology Planed Projects (grant no. SS201857, SYS2018010, SYS2018062) for Professor Jin Zhu, Dr Jianbing Zhu, and Dr. Lijun Xu, by the grant for Key Young Talents of Medicine in Jiangsu (grant no.QNRC2016875) for Professor Jin Zhu, by Suzhou key clinical diseases diagnosis and treatment technology special project

(LCZX201930) for Dr. Jianbing Zhu, by Suzhou High-tech Zone Medical and Health Technology Plan Project (2017Z005) for Dr. Jianbing Zhu, and by the Pre Research Fund Project of The Second Affiliated Hospital of Soochow University (grant no. SDFEYBS1707) for Dr. Lijun Xu, Suzhou Program for Promoting health through science and education (KJXW2017069) and Kunshan Natural Science Foundation (KS1714).

REFERENCES

1. Siegel RL, Miller KD, Jemal A. Cancer statistics, 2018. *CA Cancer J Clin.* 2018; 68:7–30. <https://doi.org/10.3322/caac.21442> PMID:[29313949](https://pubmed.ncbi.nlm.nih.gov/29313949/)
2. Siegel RL, Miller KD, Jemal A. Cancer statistics, 2020. *CA Cancer J Clin.* 2020; 70:7–30. <https://doi.org/10.3322/caac.21590> PMID:[31912902](https://pubmed.ncbi.nlm.nih.gov/31912902/)
3. Wettersten HI, Weiss RH. Potential biofluid markers and treatment targets for renal cell carcinoma. *Nat Rev Urol.* 2013; 10:336–44. <https://doi.org/10.1038/nrurol.2013.52> PMID:[23545813](https://pubmed.ncbi.nlm.nih.gov/23545813/)
4. Mihaly Z, Sztupinszki Z, Surowiak P, Gyorffy B. A comprehensive overview of targeted therapy in metastatic renal cell carcinoma. *Curr Cancer Drug Targets.* 2012; 12:857–72. <https://doi.org/10.2174/156800912802429265> PMID:[22515521](https://pubmed.ncbi.nlm.nih.gov/22515521/)
5. Kapoor A, Gharajeh A, Sheikh A, Pinthus J. Adjuvant and neoadjuvant small-molecule targeted therapy in high-risk renal cell carcinoma. *Curr Oncol.* 2009 (Suppl 1); 16:S60–66. PMID:[19478895](https://pubmed.ncbi.nlm.nih.gov/19478895/)
6. Pal SK, Quinn DI. Differentiating mTOR inhibitors in renal cell carcinoma. *Cancer Treat Rev.* 2013; 39:709–19. <https://doi.org/10.1016/j.ctrv.2012.12.015> PMID:[23433636](https://pubmed.ncbi.nlm.nih.gov/23433636/)
7. Figlin RA, Kaufmann I, Brechbiel J. Targeting PI3K and mTORC2 in metastatic renal cell carcinoma: new strategies for overcoming resistance to VEGFR and mTORC1 inhibitors. *Int J Cancer.* 2013; 133:788–96. <https://doi.org/10.1002/ijc.28023> PMID:[23319457](https://pubmed.ncbi.nlm.nih.gov/23319457/)
8. Burgio SL, Fabbri F, Seymour IJ, Zoli W, Amadori D, De Giorgi U. Perspectives on mTOR inhibitors for castration-refractory prostate cancer. *Curr Cancer Drug Targets.* 2012; 12:940–49. <https://doi.org/10.2174/156800912803251234> PMID:[22831278](https://pubmed.ncbi.nlm.nih.gov/22831278/)

9. Husseinzadeh HD, Garcia JA. Therapeutic rationale for mTOR inhibition in advanced renal cell carcinoma. *Curr Clin Pharmacol*. 2011; 6:214–21.
<https://doi.org/10.2174/157488411797189433>
PMID:[21827395](https://pubmed.ncbi.nlm.nih.gov/21827395/)
10. Konings IR, Verweij J, Wiemer EA, Sleijfer S. The applicability of mTOR inhibition in solid tumors. *Curr Cancer Drug Targets*. 2009; 9:439–50.
<https://doi.org/10.2174/156800909788166556>
PMID:[19442061](https://pubmed.ncbi.nlm.nih.gov/19442061/)
11. Motzer RJ, Escudier B, Oudard S, Hutson TE, Porta C, Bracarda S, Grünwald V, Thompson JA, Figlin RA, Hollaender N, Urbanowitz G, Berg WJ, Kay A, et al, and RECORD-1 Study Group. Efficacy of everolimus in advanced renal cell carcinoma: a double-blind, randomised, placebo-controlled phase III trial. *Lancet*. 2008; 372:449–56.
[https://doi.org/10.1016/S0140-6736\(08\)61039-9](https://doi.org/10.1016/S0140-6736(08)61039-9)
PMID:[18653228](https://pubmed.ncbi.nlm.nih.gov/18653228/)
12. Pan XD, Gu DH, Mao JH, Zhu H, Chen X, Zheng B, Shan Y. Concurrent inhibition of mTORC1 and mTORC2 by WYE-687 inhibits renal cell carcinoma cell growth in vitro and in vivo. *PLoS One*. 2017; 12:e0172555.
<https://doi.org/10.1371/journal.pone.0172555>
PMID:[28257457](https://pubmed.ncbi.nlm.nih.gov/28257457/)
13. Xu M, Wang Y, Zhou LN, Xu LJ, Jin ZC, Yang DR, Chen MB, Zhu J. The therapeutic value of SC66 in human renal cell carcinoma cells. *Cell Death Dis*. 2020; 11:353.
<https://doi.org/10.1038/s41419-020-2566-1>
PMID:[32393791](https://pubmed.ncbi.nlm.nih.gov/32393791/)
14. Hart S, Novotny-Diermayr V, Goh KC, Williams M, Tan YC, Ong LC, Cheong A, Ng BK, Amalini C, Madan B, Nagaraj H, Jayaraman R, Pasha KM, et al. VS-5584, a novel and highly selective PI3K/mTOR kinase inhibitor for the treatment of cancer. *Mol Cancer Ther*. 2013; 12:151–61.
<https://doi.org/10.1158/1535-7163.MCT-12-0466>
PMID:[23270925](https://pubmed.ncbi.nlm.nih.gov/23270925/)
15. Wu X, Liu D, Gao X, Xie F, Tao D, Xiao X, Wang L, Jiang G, Zeng F. Inhibition of BRD4 suppresses cell proliferation and induces apoptosis in renal cell carcinoma. *Cell Physiol Biochem*. 2017; 41:1947–56.
<https://doi.org/10.1159/000472407> PMID:[28391274](https://pubmed.ncbi.nlm.nih.gov/28391274/)
16. White ME, Fenger JM, Carson WE 3rd. Emerging roles of and therapeutic strategies targeting BRD4 in cancer. *Cell Immunol*. 2019; 337:48–53.
<https://doi.org/10.1016/j.cellimm.2019.02.001>
PMID:[30832981](https://pubmed.ncbi.nlm.nih.gov/30832981/)
17. Devaiah BN, Singer DS. Two faces of brd4: mitotic bookmark and transcriptional lynchpin. *Transcription*. 2013; 4:13–17.
<https://doi.org/10.4161/trns.22542>
PMID:[23131666](https://pubmed.ncbi.nlm.nih.gov/23131666/)
18. Wu SY, Chiang CM. The double bromodomain-containing chromatin adaptor Brd4 and transcriptional regulation. *J Biol Chem*. 2007; 282:13141–45.
<https://doi.org/10.1074/jbc.R700001200>
PMID:[17329240](https://pubmed.ncbi.nlm.nih.gov/17329240/)
19. Hajmirza A, Emadali A, Gauthier A, Casasnovas O, Gressin R, Callanan MB. BET family protein BRD4: an emerging actor in NFκB signaling in inflammation and cancer. *Biomedicines*. 2018; 6:16.
<https://doi.org/10.3390/biomedicines6010016>
PMID:[29415456](https://pubmed.ncbi.nlm.nih.gov/29415456/)
20. Wang CY, Filippakopoulos P. Beating the odds: BETs in disease. *Trends Biochem Sci*. 2015; 40:468–79.
<https://doi.org/10.1016/j.tibs.2015.06.002>
PMID:[26145250](https://pubmed.ncbi.nlm.nih.gov/26145250/)
21. Zanellato I, Colangelo D, Osella D. JQ1, a BET inhibitor, synergizes with cisplatin and induces apoptosis in highly chemoresistant Malignant pleural mesothelioma cells. *Curr Cancer Drug Targets*. 2018; 18:816–28.
<https://doi.org/10.2174/1568009617666170623101722>
PMID:[28669341](https://pubmed.ncbi.nlm.nih.gov/28669341/)
22. Wang YH, Sui YN, Yan K, Wang LS, Wang F, Zhou JH. BRD4 promotes pancreatic ductal adenocarcinoma cell proliferation and enhances gemcitabine resistance. *Oncol Rep*. 2015; 33:1699–706.
<https://doi.org/10.3892/or.2015.3774> PMID:[25647019](https://pubmed.ncbi.nlm.nih.gov/25647019/)
23. Kolev VN, Wright QG, Vidal CM, Ring JE, Shapiro IM, Ricono J, Weaver DT, Padval MV, Pachter JA, Xu Q. PI3K/mTOR dual inhibitor VS-5584 preferentially targets cancer stem cells. *Cancer Res*. 2015; 75:446–55.
<https://doi.org/10.1158/0008-5472.CAN-14-1223>
PMID:[25432176](https://pubmed.ncbi.nlm.nih.gov/25432176/)
24. Zhu H, Mao JH, Wang Y, Gu DH, Pan XD, Shan Y, Zheng B. Dual inhibition of BRD4 and PI3K-AKT by SF2523 suppresses human renal cell carcinoma cell growth. *Oncotarget*. 2017; 8:98471–81.
<https://doi.org/10.18632/oncotarget.21432>
PMID:[29228703](https://pubmed.ncbi.nlm.nih.gov/29228703/)
25. Saxton RA, Sabatini DM. mTOR signaling in growth, metabolism, and disease. *Cell*. 2017; 168:960–76.
<https://doi.org/10.1016/j.cell.2017.02.004>
PMID:[28283069](https://pubmed.ncbi.nlm.nih.gov/28283069/)
26. Wang L, Wu X, Wang R, Yang C, Li Z, Wang C, Zhang F, Yang P. BRD4 inhibition suppresses cell growth, migration and invasion of salivary adenoid cystic carcinoma. *Biol Res*. 2017; 50:19.
<https://doi.org/10.1186/s40659-017-0124-9>
PMID:[28545522](https://pubmed.ncbi.nlm.nih.gov/28545522/)
27. Yao W, Yue P, Khuri FR, Sun SY. The BET bromodomain inhibitor, JQ1, facilitates c-FLIP degradation and

- enhances TRAIL-induced apoptosis independent of BRD4 and c-myc inhibition. *Oncotarget*. 2015; 6:34669–79.
<https://doi.org/10.18632/oncotarget.5785>
PMID:[26415225](https://pubmed.ncbi.nlm.nih.gov/26415225/)
28. Coudé MM, Braun T, Berrou J, Dupont M, Bertrand S, Masse A, Raffoux E, Itzykson R, Delord M, Riveiro ME, Herait P, Baruchel A, Dombret H, Gardin C. BET inhibitor OTX015 targets BRD2 and BRD4 and decreases c-MYC in acute leukemia cells. *Oncotarget*. 2015; 6:17698–712.
<https://doi.org/10.18632/oncotarget.4131>
PMID:[25989842](https://pubmed.ncbi.nlm.nih.gov/25989842/)
29. Zhou HY, Huang SL. Current development of the second generation of mTOR inhibitors as anticancer agents. *Chin J Cancer*. 2012; 31:8–18.
<https://doi.org/10.5732/cjc.011.10281>
PMID:[22059905](https://pubmed.ncbi.nlm.nih.gov/22059905/)
30. Vilar E, Perez-Garcia J, Tabernero J. Pushing the envelope in the mTOR pathway: the second generation of inhibitors. *Mol Cancer Ther*. 2011; 10:395–403.
<https://doi.org/10.1158/1535-7163.MCT-10-0905>
PMID:[21216931](https://pubmed.ncbi.nlm.nih.gov/21216931/)
31. Zheng B, Mao JH, Li XQ, Qian L, Zhu H, Gu DH, Pan XD. Over-expression of DNA-PKcs in renal cell carcinoma regulates mTORC2 activation, HIF-2 α expression and cell proliferation. *Sci Rep*. 2016; 6:29415.
<https://doi.org/10.1038/srep29415>
PMID:[27412013](https://pubmed.ncbi.nlm.nih.gov/27412013/)
32. Stratikopoulos EE, Dendy M, Szabolcs M, Khaykin AJ, Lefebvre C, Zhou MM, Parsons R. Kinase and BET inhibitors together clamp inhibition of PI3K signaling and overcome resistance to therapy. *Cancer Cell*. 2015; 27:837–51.
<https://doi.org/10.1016/j.ccell.2015.05.006>
PMID:[26058079](https://pubmed.ncbi.nlm.nih.gov/26058079/)
33. Ye X, Xie J, Huang H, Deng Z. Knockdown of MAGEA6 activates AMP-activated protein kinase (AMPK) signaling to inhibit human renal cell carcinoma cells. *Cell Physiol Biochem*. 2018; 45:1205–18.
<https://doi.org/10.1159/000487452>
PMID:[29448247](https://pubmed.ncbi.nlm.nih.gov/29448247/)
34. Chen MB, Zhang Y, Wei MX, Shen W, Wu XY, Yao C, Lu PH. Activation of AMP-activated protein kinase (AMPK) mediates plumbagin-induced apoptosis and growth inhibition in cultured human colon cancer cells. *Cell Signal*. 2013; 25:1993–2002.
<https://doi.org/10.1016/j.cellsig.2013.05.026>
PMID:[23712032](https://pubmed.ncbi.nlm.nih.gov/23712032/)
35. Zhou LN, Li P, Cai S, Li G, Liu F. Ninjurin2 overexpression promotes glioma cell growth. *Aging (Albany NY)*. 2019; 11:11136–47.
<https://doi.org/10.18632/aging.102515>
PMID:[31794427](https://pubmed.ncbi.nlm.nih.gov/31794427/)
36. Li G, Zhou LN, Yang H, He X, Duan Y, Wu F. Ninjurin 2 overexpression promotes human colorectal cancer cell growth in vitro and in vivo. *Aging (Albany NY)*. 2019; 11:8526–41.
<https://doi.org/10.18632/aging.102336>
PMID:[31597121](https://pubmed.ncbi.nlm.nih.gov/31597121/)
37. Fu D, Lu C, Qu X, Li P, Chen K, Shan L, Zhu X. LncRNA TTN-AS1 regulates osteosarcoma cell apoptosis and drug resistance via the miR-134-5p/MBTD1 axis. *Aging (Albany NY)*. 2019; 11:8374–85.
<https://doi.org/10.18632/aging.102325> PMID:[31600142](https://pubmed.ncbi.nlm.nih.gov/31600142/)
38. Cao C, Rioult-Pedotti MS, Migani P, Yu CJ, Tiwari R, Parang K, Spaller MR, Goebel DJ, Marshall J. Impairment of TrkB-PSD-95 signaling in angelman syndrome. *PLoS Biol*. 2013; 11:e1001478.
<https://doi.org/10.1371/journal.pbio.1001478>
PMID:[23424281](https://pubmed.ncbi.nlm.nih.gov/23424281/)
39. Xiang T, Bai JY, She C, Yu DJ, Zhou XZ, Zhao TL. Bromodomain protein BRD4 promotes cell proliferation in skin squamous cell carcinoma. *Cell Signal*. 2018; 42:106–13.
<https://doi.org/10.1016/j.cellsig.2017.10.010>
PMID:[29050985](https://pubmed.ncbi.nlm.nih.gov/29050985/)
40. Zheng B, Mao JH, Qian L, Zhu H, Gu DH, Pan XD, Yi F, Ji DM. Pre-clinical evaluation of AZD-2014, a novel mTORC1/2 dual inhibitor, against renal cell carcinoma. *Cancer Lett*. 2015; 357:468–75.
<https://doi.org/10.1016/j.canlet.2014.11.012>
PMID:[25444920](https://pubmed.ncbi.nlm.nih.gov/25444920/)

SPOCK1/SIX1 axis promotes breast cancer progression by activating AKT/mTOR signaling

Ming Xu¹, Xianglan Zhang², Songnan Zhang³, Junjie Piao¹, Yang Yang¹, Xinyue Wang¹, Zhenhua Lin¹

¹Department of Pathology and Cancer Research Center, Yanbian University Medical College, Yanji, China

²Oral Cancer Research Institute, Yonsei University College of Dentistry, Seoul, South Korea

³Department of Oncology, Yanbian University Affiliated Hospital, Yanji, China

Correspondence to: Zhenhua Lin; email: zhlin720@ybu.edu.cn

Keywords: SPOCK1, SIX1, EMT, breast cancer, AKT/mTOR signaling pathway

Received: March 28, 2020

Accepted: September 28, 2020

Published: December 3, 2020

Copyright: © 2020 Xu et al. This is an open access article distributed under the terms of the [Creative Commons Attribution License](https://creativecommons.org/licenses/by/3.0/) (CC BY 3.0), which permits unrestricted use, distribution, and reproduction in any medium, provided the original author and source are credited.

ABSTRACT

SPOCK1 is highly expressed in many types of cancer and has been recognized as a promoter of cancer progression. Its regulatory mechanism in breast cancer (BC) remains unclear. This study aimed to explore the precise function of SPOCK1 in BC progression and to identify the mechanism by which SPOCK1 is involved in cell proliferation and epithelial-mesenchymal transition (EMT). Immunohistochemistry (IHC) experiments and database analysis showed that high expression of SPOCK1 was positively associated with histological grade, lymph node metastasis (LN) and poor clinical prognosis in BC. A series of *in vitro* and *in vivo* assays elucidated that altering the SPOCK1 level led to distinct changes in BC cell proliferation and metastasis. Investigations of potential mechanisms revealed that SPOCK1 interacted with SIX1 to enhance cell proliferation, cell cycle progression and EMT by activating the AKT/mTOR pathway, whereas inhibition of the AKT/mTOR pathway or depletion of SIX1 reversed the effects of SPOCK1 overexpression. Furthermore, SPOCK1 and SIX1 were highly expressed in BC and might indicate poor prognoses. Altogether, the SPOCK1/SIX1 axis promoted BC progression by activating the AKT/mTOR pathway to accelerate cell proliferation and promote metastasis in BC, so the SPOCK1/SIX1 axis might be a promising clinical therapeutic target for preventing BC progression.

INTRODUCTION

Worldwide, breast cancer (BC) is the most frequently diagnosed and the most lethal gynecologic malignancy in women [1], and it is an increasing concern because of rising morbidity rates. Although major advances have been made in the treatment of BC, the prognosis for most patients would be significantly worse once metastasis occurs [2]. Metastasis is the impetus for most patient deaths and represents the fundamental challenge of clinical treatment for patients with BC. The initiation and metastasis of BC are intricate processes triggered by multiple genes and intracellular signal transduction cross-talk. Thus, looking for valid molecular hallmarks

and understanding the mechanisms of BC initiation and metastasis processes are urgently needed.

Sparg/osteonectin, cwcv and kazal-like domains proteoglycan 1 (SPOCK1), is also known as TIC1, SPOCK, and TESTICAN, and it belongs to the multidomain testicular proteoglycan family [3]. This protein family includes SPARC, TESTICAN-2, and TESTICAN-3, which are associated with cell proliferation and metastasis [4]. SPARC has been properly reported in a variety of cancers [5, 6], emphasizing its involvement in cell proliferation, angiogenesis and epithelial-to-mesenchymal transition (EMT). Recent discoveries have revealed that SPOCK1

is overexpressed in colorectal cancer, non-small cell lung cancer and glioblastoma [7–9]. Meanwhile, some reports revealed that SPOCK1 may promote the invasion and metastasis of gastric cancer and glioma [10, 11] and may confer a poor prognosis in urothelial carcinoma [12]. Nevertheless, the underlying mechanisms and functions of SPOCK1-induced BC activities, including cancer development and metastasis processes, are far from clear. Here, we described the oncogenicity of SPOCK1 and clarified the molecular mechanism of SPOCK1 involved in BC evolution.

EMT initially occurs in embryogenesis, and it is a kind of reversible and rapid change in cell phenotype, which is defined as changes in the epithelial phenotype into mesenchymal features [13], including loss of contact inhibition ability, promoting cell motility and invasiveness [14]. It is noteworthy that SIX homeobox 1 (SIX1), also known as BOS3, TIP39, and DFNA23, an indispensable transcription factor of organogenesis [15], plays a fatal role in promoting the cell EMT process [16–18]. SIX1 expression is negligible in normal adult organs, and its aberrant expression may lead to carcinogenesis [19]. Recently, SIX1 was found to be involved in cellular proliferation, invasion and the Warburg effect [16, 20]. In BC, SIX1 is highly expressed in half of primary cancers and 90% of cancer metastases [21]. In addition, SIX1 contributed to the initiation and prognosis of tumors [22]. To date, there are no similar reports regarding the association between SIX1 and SPOCK1 in BC evolution.

Herein, we aimed to reveal that overexpression of SPOCK1/SIX1 was related to BC cell proliferation and metastasis and predicted poor prognosis in BC patients via bioinformatic analysis of available BC datasets and immunohistochemical (IHC) assays. Additionally, we demonstrated that SPOCK1/SIX1 activated the PI3K/AKT/mTOR pathway, consequently promoting BC cell proliferation, accelerating cell cycle progression, and triggering the cell EMT program and metastasis, which provides new targets for BC therapies.

RESULTS

SPOCK1 was abnormally and strongly expressed and associated with metastasis and poor prognosis in BC

SPOCK1 was highly expressed in various cancers, including prostate cancer, pancreatic cancer, lung cancer and breast cancer (Figure 1A). We analyzed SPOCK1 mRNA expression across different datasets [23–25] from the Oncomine database and found that SPOCK1 was more highly expressed in BC than in

normal tissues (Figure 1B). The median rank of SPOCK1 in highly expressed genes of BC was 672.0 based on a meta-analysis across seven datasets for Oncomine algorithms ($P=1.06E-11$) (Figure 1C). Furthermore, the UALCAN database, which integrated TCGA samples, showed the same results (Figure 1D). UALCAN also showed mRNA expression of SPOCK1 in 33 kinds of cancers, in which several cancers, including breast cancer, exhibited increased SPOCK1 expression. In the HPA database, SPOCK1 protein expression was hardly detected in normal sections, but there were significantly higher levels in BC (Figure 1E).

To further confirm the expression pattern of SPOCK1 in BC, 80 BC tissues and 10 adjacent nontumor tissues were examined by IHC assay. IHC analysis showed that SPOCK1 was significantly more highly expressed in BC tissues than in adjacent nontumor tissues. The positive rate (93.8%; 75/80) and strongly positive rate (72.5%; 58/80) of SPOCK1 in BC were both significantly higher than in adjacent nontumor tissues (30.0%, 3/10 and 10%; 1/10) ($P<0.001$) (Figure 1F, Table 1), which confirmed that SPOCK1 was aberrantly upregulated in BC. Notably, aberrant SPOCK1 expression was associated with histological differentiation ($P=0.011$) and LN metastasis ($P=0.026$) but not with patient age or ER and PR status (Figure 1G, Table 2). Moreover, high SPOCK1 expression was markedly related to unfavorable outcomes in BC patients. We evaluated the relationship between the SPOCK1 expression level and OS, RFS, PPS and DMFS of patients with BC using the Kaplan-Meier plotter database. As shown in Figure 1H, high SPOCK1 expression resulted in shorter OS, RFS, PPS and DMFS in various datasets. Finally, the level of SPOCK1 was significantly higher in the high-risk group than in the low-risk group according to the SurvExpress database. In general, these results underscored that SPOCK1 was strongly expressed in BC and could serve as an outcome predictor in BCs.

SPOCK1 accelerated cell cycle progression and promoted cell proliferation in BC

To verify the potential oncogenic activity of SPOCK1 in BC, we surveyed endogenous SPOCK1 expression in a series of BC cell lines and a normal immortalized mammary gland cell line by western blot. Among the 7 cell lines, the MCF7 and SKBR3 cell lines exhibited high SPOCK1 expression, and the MDA-MB-231 and HS 578T cell lines showed low expression (Figure 2A). To explore the potential biological function of SPOCK1, we chose MCF7 and SKBR3 cell lines for SPOCK1 knockdown and MDA-MB-231 and HS 578T cell lines for stable SPOCK1 overexpression. The level of SPOCK1 expression in stable infected cell lines was

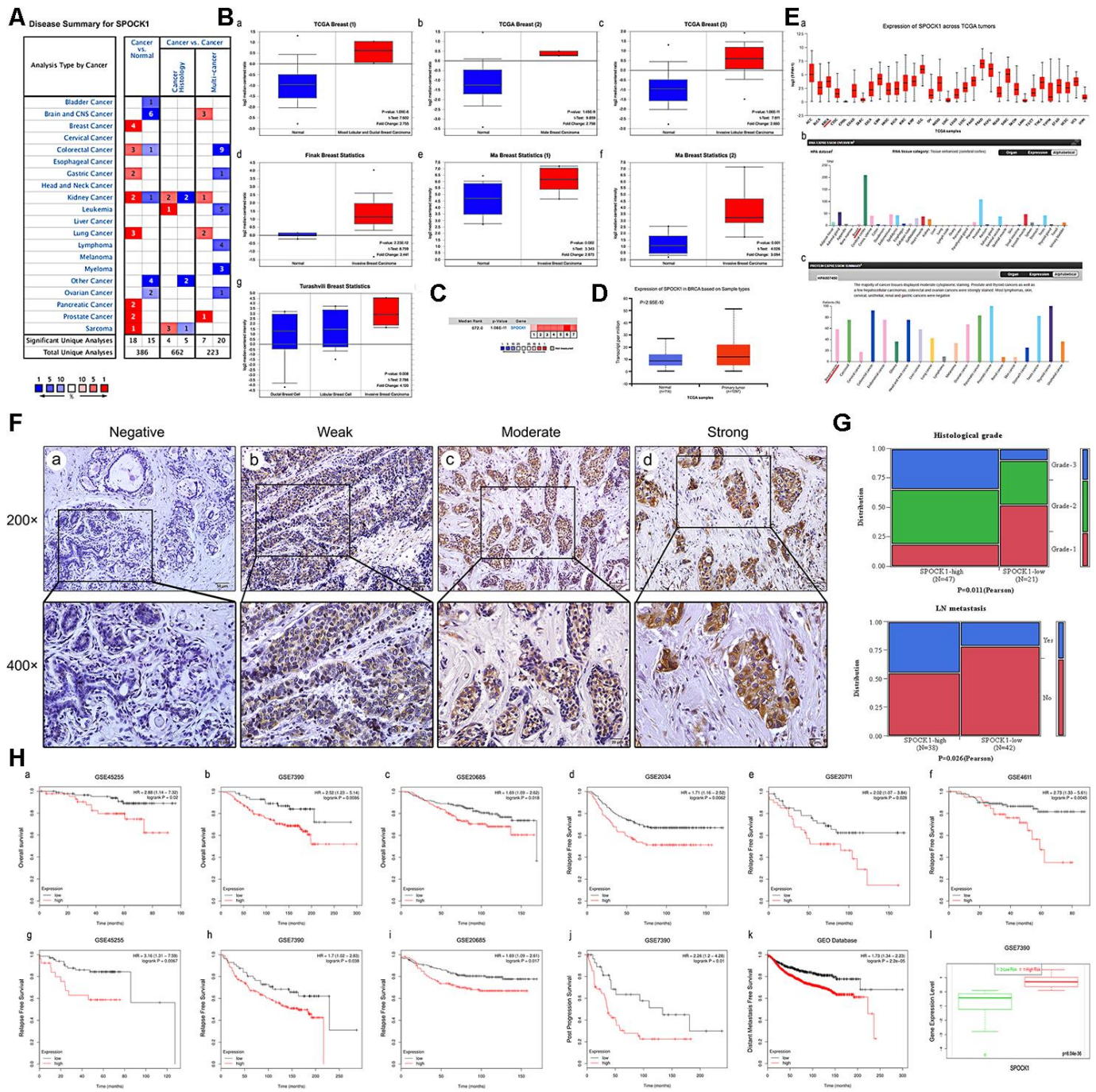


Figure 1. Overexpression of SPOCK1 is positively associated with histological grade, LN metastasis and poor prognosis in BC. (A) The graphic showed the numbers of datasets with statistically significant mRNA high expression (red) or down-expression (blue) of SPOCK1 (cancer vs. Normal tissue). The P -value threshold was 0.01. (B) Box plots derived from gene expression data in OncoPrint comparing expression of SPOCK1 in normal and BC tissue. The P -value was set up at 0.01 and fold change was defined as 2. (C) A meta-analysis of SPOCK1 gene expression from seven OncoPrint databases where colored squares indicated the median rank for SPOCK1 (vs. Normal tissue) across 7 analyses. (D) The expression of SPOCK1 was elevated in BC compared to normal breast tissues. Data derived from UALCAN database. (E) Expression of SPOCK1 across TCGA carcinomas from Ualcan database (a); overview of SPOCK1 protein levels in BC tissues and normal breast tissues (b-c). (F) IHC staining (negative, weak, moderate and strong expression) for SPOCK1 in BC tissues (a-d). (G) Relationships between SPOCK1 expression and clinicopathologically significant aspects of BC. (H) Overall survival (OS) (a-c), relapse free survival (RFS) (d-i), post progression survival (PPS) (j), distant metastasis free survival (DMFS) (k) and risk assessment curves (l) of patients with or without elevated SPOCK1 levels. Survival data derived from Kaplan–Meier (KM) plotter database. High SPOCK1 expression levels were found in high risk groups of BC patients. Box plots generated by SurvExpress showed the expression levels of SPOCK1 in indicated dataset and the P -value resulting from a t -test. Low-risk groups are denoted in green and high-risk groups in red, respectively.

Table 1. SPOCK1 expression in BC.

Diagnosis	No. of case	Positive cases				Positive rates	Strongly positive rates
		-	+	++	+++		
Breast cancer	80	5	17	26	32	93.8%	72.5%
Adjacent non-tumor	10	7	2	1	0	30.0%	10.0%
χ^2						31.262	15.377
P						0.000	0.000

Table 2. Relationship between SPOCK1 expression and clinicopathologic features of BC patients.

Variables	No. of case	SPOCK1 strongly positive cases (%)	χ^2	P value
Age				
≥52	43	74.4%(32/43)	0.172	0.679
<52	37	70.3%(26/37)		
Histological grade				
Grade-1	20	45%(9/20)	8.996	0.011*
Grade-2	30	73.3%(22/30)		
Grade-3	18	88.9%(16/18)		
ER				
Positive	50	70%(35/50)	0.418	0.518
Negative	30	76.7%(23/30)		
PR				
Positive	54	70.4%(38/54)	0.653	0.419
Negative	24	79.2%(19/24)		
LN metastasis				
Yes	26	65.4%(17/26)	4.941	0.026*
No	54	38.9%(21/54)		

* $P < 0.05$ and ** $P < 0.01$

verified by western blot (Figure 2B), and the transfection efficiency is shown in Figure 2C. The best silencing effect was obtained with the shSPOCK1#2 and shSPOCK1#3 constructs for MCF7 and SKBR3 cell lines. Meanwhile, stable overexpression of SPOCK1 in MDA-MB-231 and HS 578T cells was exhibited.

MTT and EdU incorporation assays were used to determine the potential function of SPOCK1 in BC proliferation. As shown in Figure 2D, 2E, silencing SPOCK1 significantly suppressed cell growth, whereas SPOCK1 overexpression promoted cell proliferation. Similarly, upregulation of SPOCK1 facilitated cell clonogenicity, while SPOCK1 knockdown resulted in smaller and fewer colonies than the controls (Figure 2F). We further analyzed the influence of the cell cycle on SPOCK1 expression at different levels. The flow cytometry assay indicated that cells with higher SPOCK1 expression accelerated the progression of G₂/M phase, compared with the respective control (Figure 2G). Additionally, SPOCK1 knockdown decreased the levels of Cyclin-B1, CDK1, C-myc and Survivin, which was coupled with a concomitant

increase in the expression of P21 and P27 (Figure 2H). Conversely, ectopic expression of SPOCK1 displayed harmful results. Together, the results demonstrated that SPOCK1 plays a crucial role in the BC cell cycle and proliferation *in vitro*.

In vivo, stable BC cells with modified SPOCK1 expression were subcutaneously injected into the fourth mammary fat pad of nude mice. The tumor volumes formed by cells with high SPOCK1 expression were significantly greater than those from cells with low SPOCK1 expression (Figure 2I). Additionally, the expression of Ki67 in the MCF7-NC group, SKBR3-NC group and MDA-MB-231-SPOCK1 group was much higher than it was in the negative control groups (Figure 2J). Overall, these findings suggested that SPOCK1 promoted BC cell growth *in vivo*.

SPOCK1 promoted BC metastasis via the EMT process

Next, we observed the metastatic ability of BC cells with different SPOCK1 expression. The wound-healing assay results indicated that cells with higher SPOCK1

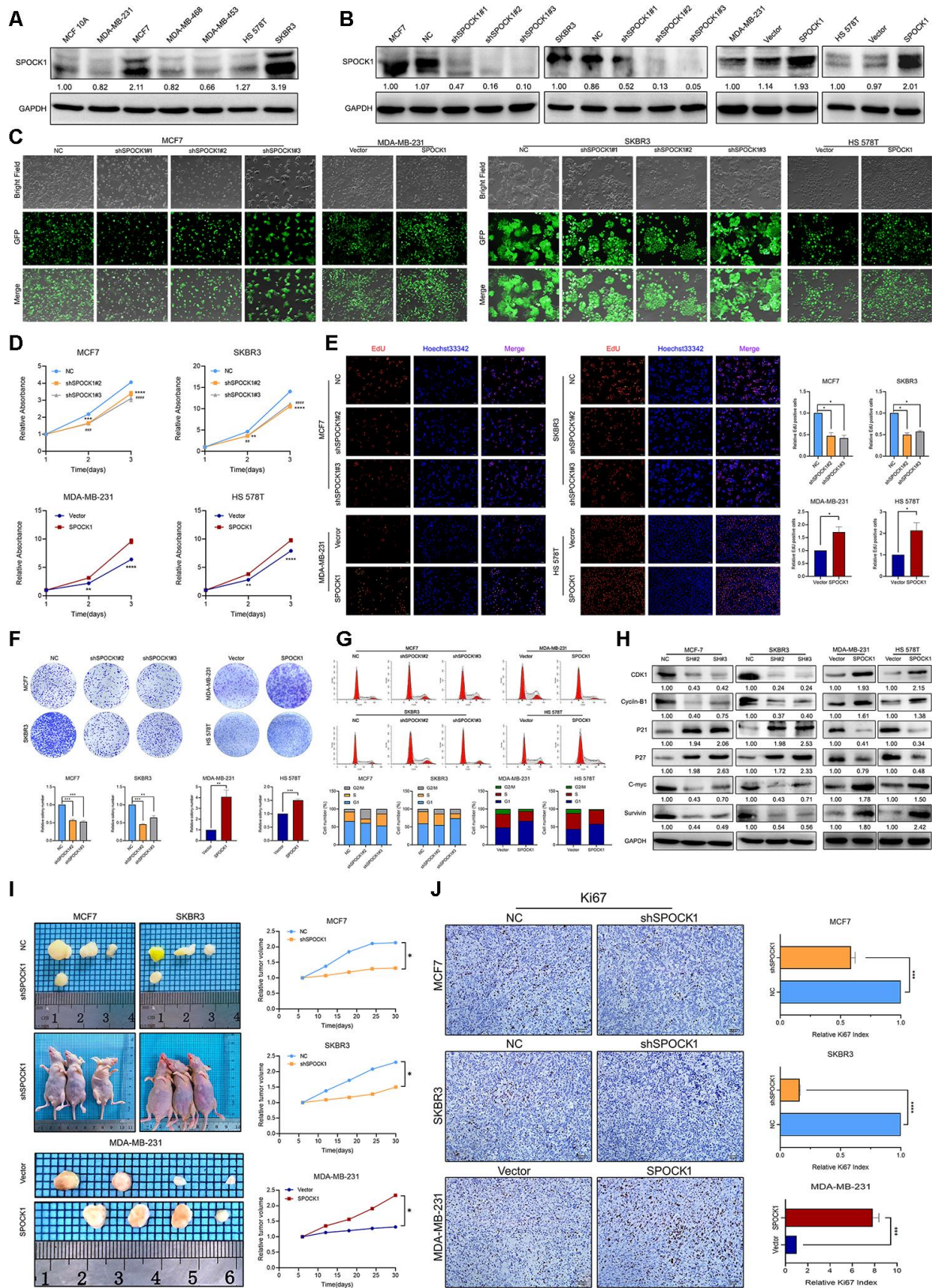


Figure 2. SPOCK1 influences BC cell growth. (A) Protein expression levels of SPOCK1 in BC cell lines as determined by western blot analysis. (B) MCF7/SKBR3 cells with SPOCK1 silencing and MDA-MB-231/HS 578T cells with SPOCK1 overexpression were established by viral transduction. The SPOCK1 levels in these established cell lines were verified by western blot analysis at 48 h after transfection. (C) Cells in bright light and GFP were captured to merge for displaying the transfection efficiency. (D) Cell viability was examined by MTT assay.

(E) Results of EdU assay on BC cells. Representative photographs are shown at the original magnification, $\times 100$. (F) Cell clonogenic capacity was measured by colony formation assay. (G) Flow-cytometry analysis was performed to detect cell cycle progression. (H) The expression of proteins related cell cycle (CDK1, Cyclin-B1, P21, P27, C-myc and Survivin) was determined by western blot analysis. GAPDH was used as a loading control. (I) Xenograft tumors formed by injecting the indicated cells. Relative tumor volume curves were summarized in the line chart ($*P < 0.05$). (J) IHC staining of the proliferation marker Ki67 in xenograft tumors. The relative percentage of Ki67-positive cells was summarized in the bar charts. The P values were obtained using t-tests ($***P < 0.001$, $****P < 0.0001$). All results are from three independent experiments. The error bars represent the SD.

expression displayed a more widespread wound closure area than the corresponding control (Figure 3A). Transwell assays provided evidence that was consistent with those findings (Figure 3B). To further explore the effect of SPOCK1 on BC metastasis *in vivo*, stable cells with modified SPOCK1 expression were injected into the tail veins of nude mice. The number of pulmonary metastases in the higher SPOCK1 expression group was significantly greater than that in the corresponding control, which was opposite to the result in the lower SPOCK1 expression group (Figure 3C). Moreover, we found that the cells with higher SPOCK1 expression lost cell polarity, displayed spindle-shaped and acquired mesenchymal morphology with stronger invasion and metastasis ability, but lower SPOCK1 expression tended to have the opposite morphology (Figure 3D).

To determine whether EMT is responsible for SPOCK1-mediated changes in BC metastasis, we analyzed a cohort of 1101 BC samples from the TCGA dataset by the UCSC Cancer Genomics Browser. As presented in Figure 3E, we found that the heat maps of SPOCK1 in BC were strikingly coincident with VIM, SNAI2, TWIST1, and ZEB1 and inversely proportional to CDH1 (E-cadherin). Similarly, the GEPIA2 database also showed positive correlations between SPOCK1 and mesenchymal proteins (Figure 3F). Western blot and IF assays showed that downregulation of SPOCK1 accelerated the expression of epithelial markers and was accompanied by a reduction in mesenchymal markers (Figure 3G, 3H). Consistently, the group with high SPOCK1 expression displayed inverse results. Additionally, IHC staining results showed a higher expression of E-Cadherin and lower expression of Vimentin in shSPOCK1 group tumor tissue. Conversely, sections with high SPOCK1 expression displayed the opposite effects (Figure 3I). Taken together, these findings indicated that SPOCK1 enhanced EMT progression and triggered BC metastasis *in vitro* and *in vivo*.

The oncogenic activity of SPOCK1 was significantly correlated with the AKT/mTOR pathway

The AKT/mTOR signaling pathway has vital roles in cancer evolution, and its activation has been found in most BCs [26–29]. Thus, we speculated that SPOCK1 is involved in the regulation of the AKT/mTOR pathway

in BC. Strikingly, depletion of SPOCK1 resulted in a decreased abundance of p-AKT, p-mTOR, p-S6 and p-4EBP1, where the total protein levels were not influenced (Figure 4A). Then, we further explored the role of the AKT/mTOR pathway in SPOCK1-mediated regulation of BC. We used the PI3K/AKT inhibitor LY 290042 and mTOR inhibitor rapamycin to block PI3K/AKT/mTOR activity and found that the inhibitors not only suppressed the activation of the PI3K/AKT/mTOR pathway but also reversed the promotion of SPOCK1 in the pathway. However, the inhibitors had no effects on SPOCK1 expression (Figure 4B). Indeed, LY290042 and rapamycin significantly suppressed the ability of SPOCK1 to accelerate BC cell proliferation and cell cycle progression (Figure 4C–4G). Similarly, inhibitors almost abolished the SPOCK1-mediated promotion of BC cell migration, invasion and EMT progression (Figure 4H–4J). These results demonstrated that SPOCK1 at least partly contributed to BC proliferation and EMT by activating the AKT/mTOR signaling pathway.

SIX1 was aberrantly expressed and interacted with SPOCK1 in BC

To further explore the molecular mechanisms underlying SPOCK1-induced BC proliferation and metastasis, we identified a potential target gene of SPOCK1 by bioinformatics strategies. We detected SPOCK1 protein-protein interactions by web-based databases, STRING and GeneMANIA, and intriguingly found that SPOCK1 was also associated with SIX1 (Figure 5A). The mechanism clarified that SIX1 could induce BC cells to undergo EMT progression and metastasis via the TGF- β pathway [30, 31]. Retrieval of the Oncomine database declared that SIX1 was highly expressed in breast cancer [23, 25] (Figure 5B–5E). The UALCAN and HPA databases showed the same results (Figure 5F). Moreover, HPA databases showed different positive staining intensities of SIX1 protein in BCs and negative staining in normal breast tissue (Figure 5G). Additionally, Kaplan Meier plotter and SurvExpress databases displayed that high levels of SIX1 expression resulted in poor OS, RFS and DMFS and acquired higher risk (Figure 5H). Overall, these data highlighted that SIX1 was highly expressed in BC and correlated with poor clinical outcome.

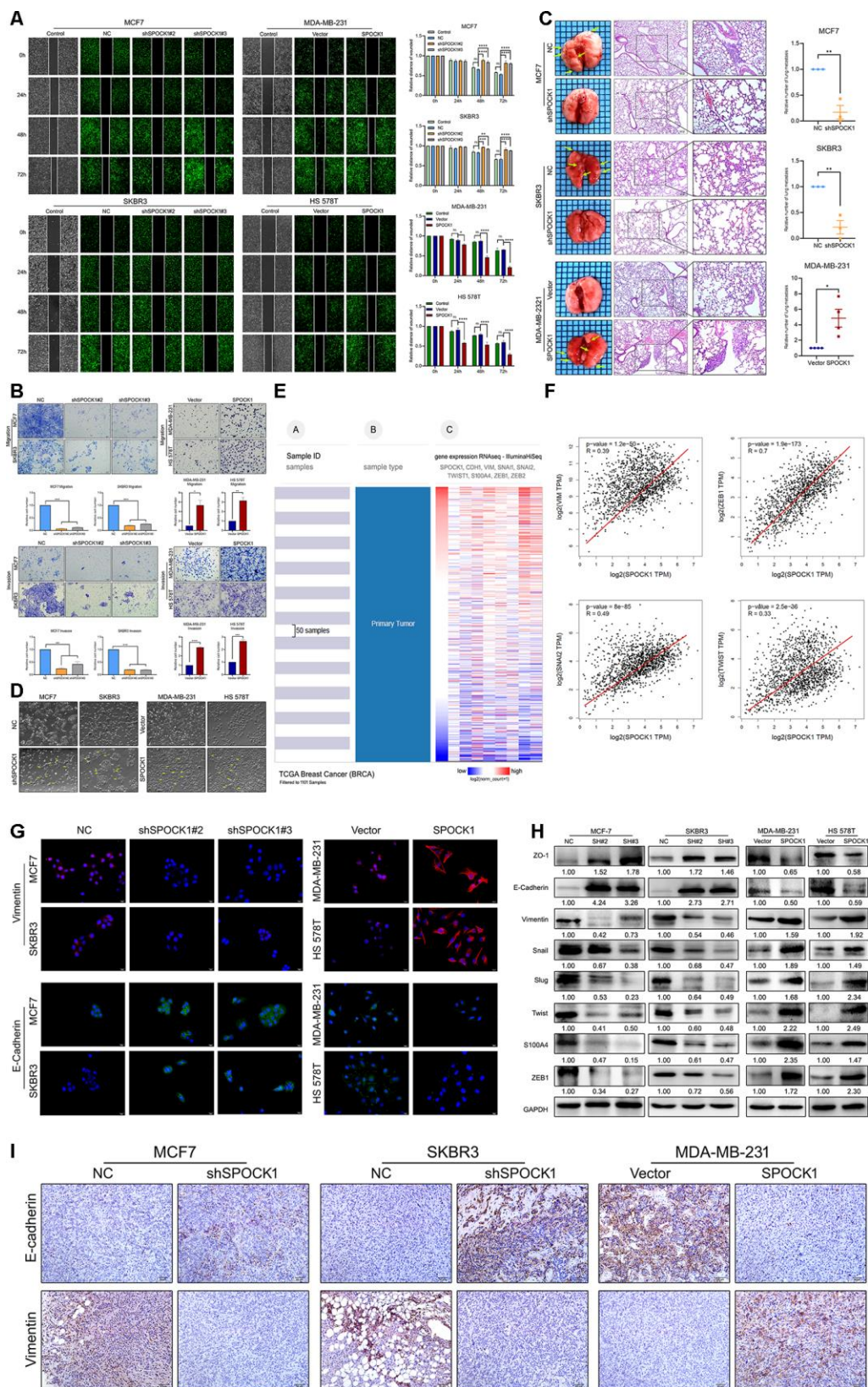


Figure 3. SPOCK1 promotes cellular invasion, metastasis and the EMT *in vitro* and *in vivo*. (A) A scratch wound-healing assay was used to determine the effects of SPOCK1 on BC cell motility. (B) Results of a transwell migration assay (a) and a Matrigel invasion assay (b) for cellular invasion. The mean number of cells in five fields per membrane is shown ($\times 200$). (C) Representative images of gross and hematoxylin and eosin (H&E) staining and relative numbers of lung surface metastatic foci detected in each group ($*P < 0.05$, $**P < 0.01$). The scale bar is 100

μM and $50 \mu\text{M}$. (D) Representative images showing the morphological changes in the indicated cell lines. (E) The heat maps of the correlation between SPOCK1 and EMT markers in the same cohort. (F) Positive relationships for SPOCK1 and EMT markers were showed on GEPIA2. (G) The expression of EMT markers was detected by immunofluorescence staining in BC cells. The scale bar is $20 \mu\text{M}$. (H) The expression of epithelial markers (E-cadherin and ZO-1) and mesenchymal markers (Vimentin, Snail, Slug, Twist, S100A4 and ZEB1) was determined by western blot analysis. GAPDH was used as a loading control. (I) IHC staining for E-cadherin and Vimentin protein in tumor specimens from xenografts (200 \times). The P values were obtained using Mann-Whitney U tests or t-tests ($*P<0.05$, $**P<0.01$, $***P<0.001$, $****P<0.0001$). All results are from three independent experiments. The error bars represent the SD.

According to these data, we wondered whether SPOCK1 enrichment in cells was linked to SIX1. Consistent with our conjecture, IF and western blot assays showed that SIX1 was enriched in SPOCK1-highly expressed cells, whereas SPOCK1 knockdown decreased the level of SIX1 expression (Figure 5I, 5J). To further explore the potential binding interaction between SPOCK1 and SIX1, a coimmunoprecipitation (Co-IP) assay was performed. As shown in Figure 5K, we discovered the physical interaction of SPOCK1 with SIX1. Additionally, IF staining showed colocalization of SPOCK1 and SIX1 in the cytoplasm (Figure 5L). Taken together, our findings indicated that SIX1 interacted with SPOCK1 in BC.

The SPOCK1/SIX1 axis regulated BC proliferation and metastasis via AKT/mTOR signaling activity

To explore the potential mechanism of SIX1 involved SPOCK1-induced proliferation, EMT and metastasis, we knocked down SIX1 expression in SPOCK1 stable overexpression cells by siRNA treatment (Figure 6A). As expected, silencing the expression of SIX1 effectively restrained SPOCK1-mediated cell proliferation, clone formation and cell cycle progression (Figure 6B–6E) and reversed SPOCK1-induced cell motility, migration and invasion (Figure 6F–6H). Furthermore, the downregulated expression of SIX1 substantially offset the SPOCK1-involved activation of AKT/mTOR signaling but did not affect the level of SPOCK1 expression (Figure 6I). Altogether, this evidence suggested that SIX1 silencing could, at least partially, abolish the biological behaviors that SPOCK1 induced in BC.

DISCUSSION

SPOCK1 is a highly conserved extracellular matrix glycoprotein, with structural diversity and extensive tissue distribution that may be involved in multiple cell and extracellular matrix interactions [32]. A study has shown that SPOCK1 could enhance the expression and activity of MMP2 and MMP9, which can degrade extracellular matrix components and promote tumor cells to break through the cell barrier composed of the basement membrane and extracellular space matrix, thus causing tumor cells to migrate and invade

surrounding tissues to distant tissues [11]. Additionally, SPOCK1 has been regarded as a candidate oncogene and have been verified to be closely related to the tumorigenesis, tumor progression, adhesion and metastasis of various tumors [33, 34]. Many biological phenomena have been observed in the function of the SPOCK1 gene, but the molecular biological mechanisms behind these phenomena are rarely studied.

Chen et al. reported that SPOCK1 was involved in slug-induced EMT and promoted cell invasion and metastasis, and high SPOCK1 expression was also reported to be a prognostic factor for poor survival in gastric cancer [10]. The results of this study documented that SPOCK1 was highly expressed in BC cells and clinical specimens relative to normal ones, which paralleled the Oncomine, HPA and Ualcan databases. IHC analysis showed that SPOCK1 was related to tumor histological differentiation and LN metastasis. Moreover, Kaplan Meier plotter database showed that BC patients with high SPOCK1 expression had poor OS, RFS, PPS and DMFS. Our findings were similar to the results in urothelial carcinoma (UC), in which higher SPOCK1 expression was correlated with unfavorable clinicopathological parameters and conferred a poor prognosis in UC [12]. Evidence from the SurvExpress database further showed that high expression of SPOCK1 had a higher risk in BC. These observations illustrated that SPOCK1 might play a crucial role in the treatment and prognosis evaluation of BC.

Infinite proliferation and metastasis are responsible for malignant tumor phenotypes, while initiation of EMT is the early step of the metastatic cascade. Unquestionably, EMT is identified as the dominant program in BC initiation and metastatic spread [35, 36]. A previous study revealed that deregulating the expression of SPOCK1 suppressed colorectal cancer (CRC) proliferation *in vitro* and *vivo*, and SPOCK1 was involved in CRC malignant features [7]. Notably, SPOCK1 was altered by EPCR to mediate 3D growth, consequently promoting breast cancer progression [37]. Here, we detected the variation in BC cells by modifying SPOCK1 expression, which revealed that SPOCK1 overexpression improved the proliferative and metastatic properties of BC cells and that suppression of SPOCK1 had the opposite effect. Xenograft and lung

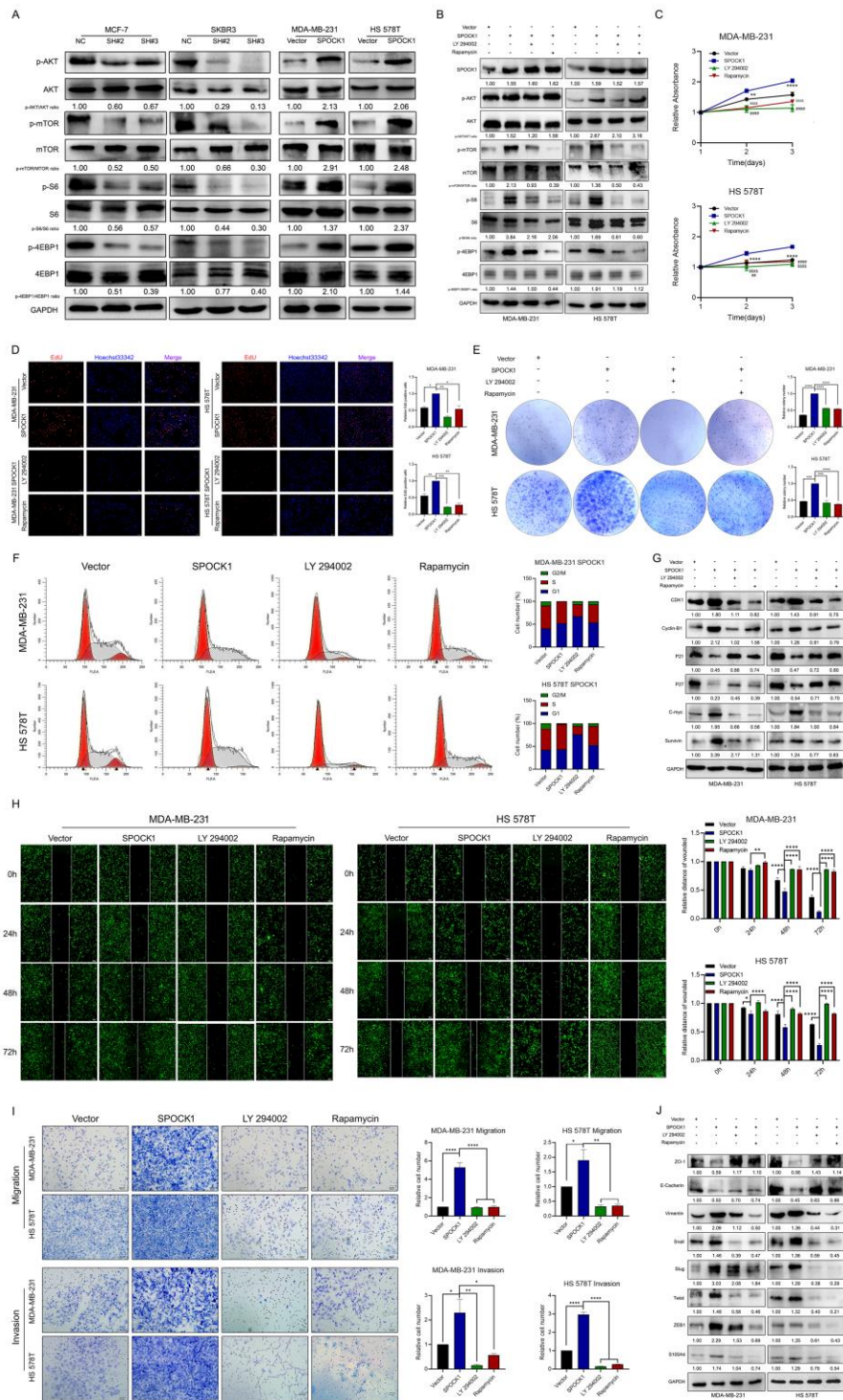


Figure 4. SPOCK1 activates the AKT/mTOR signaling pathway in BC cells. (A) Proteins level on AKT/mTOR pathway of indicated cells were assayed by western blotting. GAPDH was used as a loading control. (B) Stable BC cells were treated with LY 290042 or Rapamycin. Then indicated protein levels were assayed by western blotting. GAPDH was used as a loading control. (C–E) Cell viability was detected in SPOCK1-overexpressed cells after treatment with LY 290042 or Rapamycin by MTT assay (C), Edu staining (D) and colony formation (E) assays. (F) Cell cycle progression was assayed by flow-cytometry analysis after dealing with LY 290042 or Rapamycin. (G) Stable BC cells were treated with LY 290042 or Rapamycin. Then cell cycle related protein levels were assayed by western blotting. GAPDH was used as a loading control. (H–I) Cell motility and invasion capacities was detected in SPOCK1-overexpressed cells after treatment with rapamycin or LY294002. (J) Stable BC cells were treated with LY 290042 or Rapamycin. Then levels of EMT-related proteins were assayed by western blotting. GAPDH was used as a loading control. (* $P < 0.05$, ** $P < 0.01$, *** $P < 0.001$, **** $P < 0.0001$).

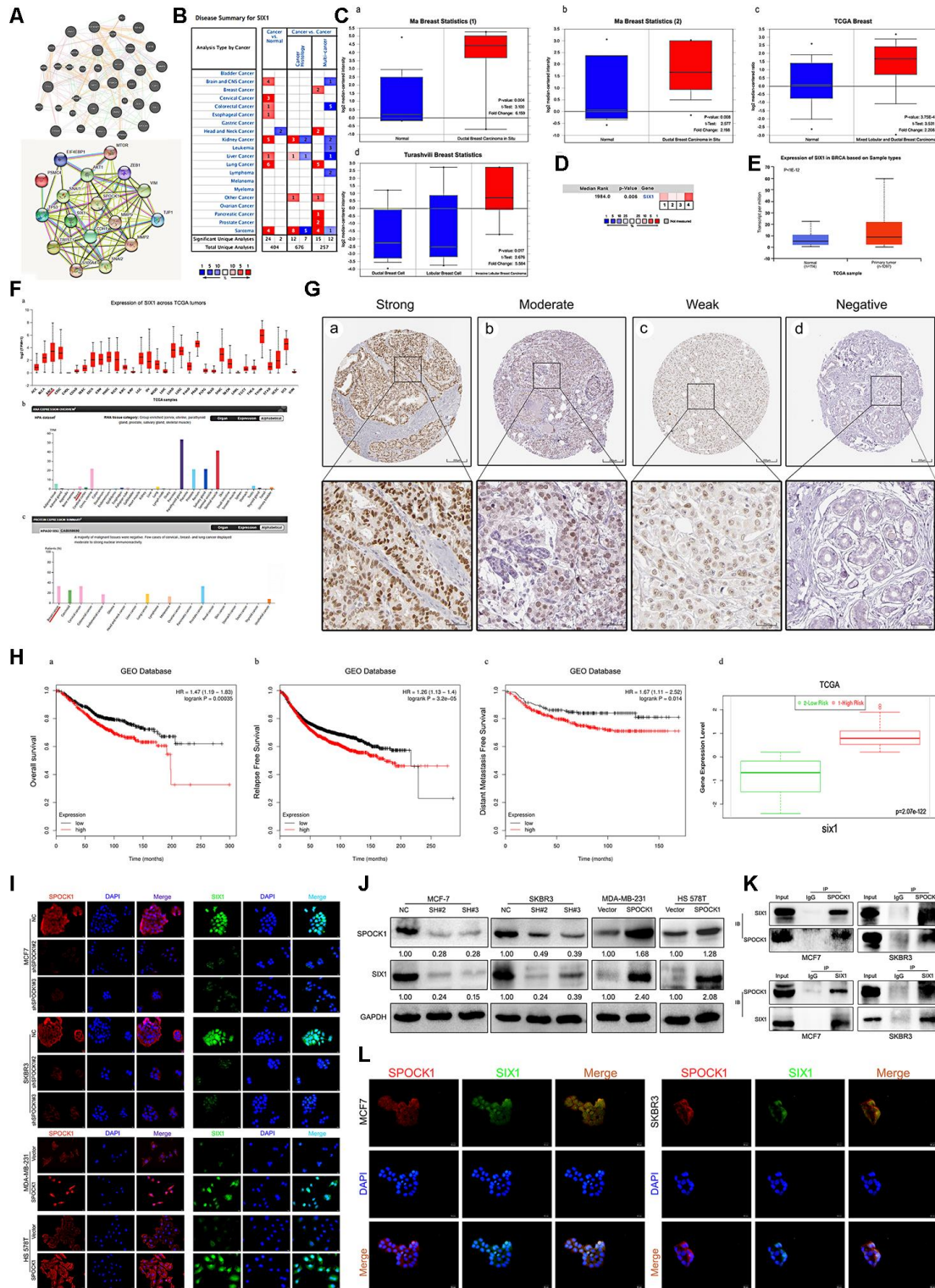


Figure 5. Identification of SIX1 as a downstream mediator of SPOCK1 in BC cells. (A) Network diagram of SPOCK1/SIX1 protein interaction by GeneMANIA (a) and STRING (b). (B) The graphic showed the numbers of datasets with statistically significant mRNA high expression (red) or down-expression (blue) of SIX1 (cancer vs. Normal tissue). The *P*-value threshold was 0.01. (C) Box plots derived from gene expression data in Onconome comparing expression of SIX1 in normal and BC tissue. The *p* value was set up at 0.01 and fold change was defined as 2. (D) A meta-analysis of SIX1 gene expression from four Onconome databases where colored squares indicated the median rank for SIX1 (vs. Normal tissue) across 4 analyses. (E) The expression of SIX1 was elevated in BC compared to normal breast tissues. Data derived from UALCAN database. (F) Expression of SIX1 across TCGA carcinomas from Ualcan database (a); overview of SIX1 protein levels in BC tissues and normal breast tissues (b-c). (G) IHC staining (negative, weak, moderate and strong expression) for SIX1 in BC tissues (a-d). Data derived

from HPA database. (H) Overall survival (OS) (a), relapse free survival (RFS) (b) and distant metastasis free survival (DMFS) (c) curves of patients with or without elevated SIX1 levels. Data derived from Kaplan–Meier (KM) plotter database. High SIX1 expression levels were found in high risk groups of BC patients (d). Data derived from SurvExpress database. (I, J) Expression levels of indicating cells were assayed by IF and western blotting. GAPDH was used as an internal control. (K) The interaction between endogenous SPOCK1 and SIX1 proteins was analyzed by coimmunoprecipitation in MCF7 and SKBR3 cells. (L) Immunofluorescence double-labeling experiments confirmed the existence of SPOCK1-SIX1 colocalization phenomena in the cytoplasm. The scale bar is 20 μ M.

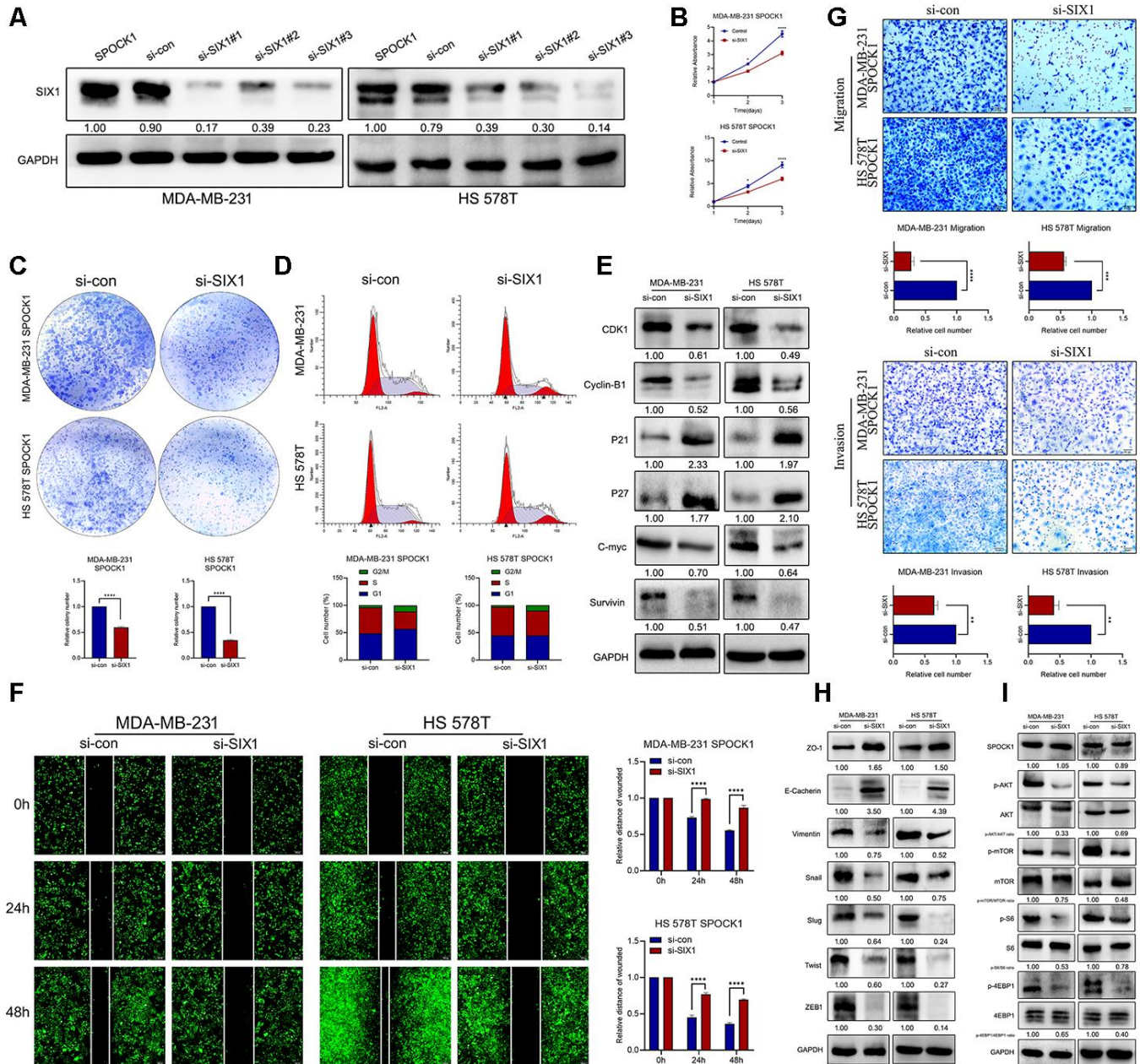


Figure 6. SIX1 involved in SPOCK1-mediated BC progression. (A) MDA-MB-231 and HS 578T cell line were transfected with si-con, si-SIX1#1, si-SIX1#2 and si-SIX1#3. The SIX1 levels in these were verified by western blot analysis after 48 h transfection. (B, C) Cell viability was detected in SPOCK1-overexpressed cells after transduction with si-RNAs by MTT assay (B) and colony formation (C) assay. (D) Cell cycle progression was assayed by flow-cytometry analysis after dealing with si-RNAs. (E) Stable BC cells were treated with si-RNAs. Then cell cycle related protein levels were assayed by western blotting. GAPDH was used as a loading control. (F, G) Cell motility and invasion capacities was detected in SPOCK1-overexpressed cells after treatment with si-RNAs. (H, I) Stable BC cells were treated with si-RNAs. The levels of EMT-related proteins and AKT/mTOR pathway were assayed by western blotting, respectively. GAPDH was used as a loading control. (* P <0.05, ** P <0.01, *** P <0.001, **** P <0.0001).

metastasis models further confirmed the *in vitro* results. Specifically, western blot and IF analyses showed that SPOCK1 increased the expression of mesenchymal markers and lost epithelial markers. Moreover, similar evidence was verified in xenograft mouse sections, suggesting that SPOCK1 triggered the EMT process both *in vitro* and *in vivo*.

The synthesis of multifarious signaling molecular events led to the oncogenesis of BC. Understanding and identifying these signaling mechanisms would restrain EMT progression to further therapeutically control cancer metastasis [38–40]. Previous studies reported that SPOCK1 could mediate EMT by the Wnt/ β -catenin signaling pathway in non-small cell lung cancer [8], the PI3K/AKT signaling pathway in colorectal cancer, among other pathways [7]. Moreover, SPOCK1 blocked gallbladder cancer (GBC) cell apoptosis and promoted cell proliferation and metastasis by activating PI3K/Akt signaling both *in vitro* and *in vivo* [41]. In addition to AKT signaling, mTOR plays a crucial role in tumor proliferation and growth. Recent evidence has reported that the mTOR signaling pathway also plays a key role in tumor motility, invasion, and metastasis [42]. In renal carcinoma, activation of mTOR signaling promoted cell invasion ability by inducing EMT [43]. It has been verified that the mTOR inhibitor rapamycin could suppress cell scratch and chemotactic migration. In addition, the inhibition of mTOR decreased the formation of lamellipodia [44]. Consistent with this,

pharmacologic and genetic inhibition of mTOR decreases colorectal cancer cell migration and invasion [45].

At present, targeting the PI3K/AKT/mTOR pathway as a therapeutic strategy to treat BC by is still an evolving field [46]. Thus, we were particularly interested in exploring the special role of SPOCK1 in the evolution of normal mammary glands to BC induced by the AKT/mTOR pathway. Our study revealed that SPOCK1 overexpression activates the AKT/mTOR pathway to promote the progression of BC. This was confirmed by the alterations of target proteins of the AKT/mTOR pathway, which was induced by depleting or overexpressing SPOCK1 expression and can be reversed by treatment with LY290042 or rapamycin, respectively. Furthermore, inhibition of the AKT/mTOR pathway by LY290042 or rapamycin treatment also impaired the effect of SPOCK1 upregulation on the cell cycle, proliferation and EMT process, verifying the effect of the AKT/mTOR pathway on SPOCK1-induced BC cell growth and metastasis.

SIX1 makes a notable contribution to tumor growth and metastasis [18, 47, 48]. SIX1 was identified to be involved in the oncogenic role of SPOCK1 in BC. Hyperactivation of SIX1 is widespread in a variety of human tumors and is associated with poor clinical efficacy. Emerging evidence has revealed that SIX1

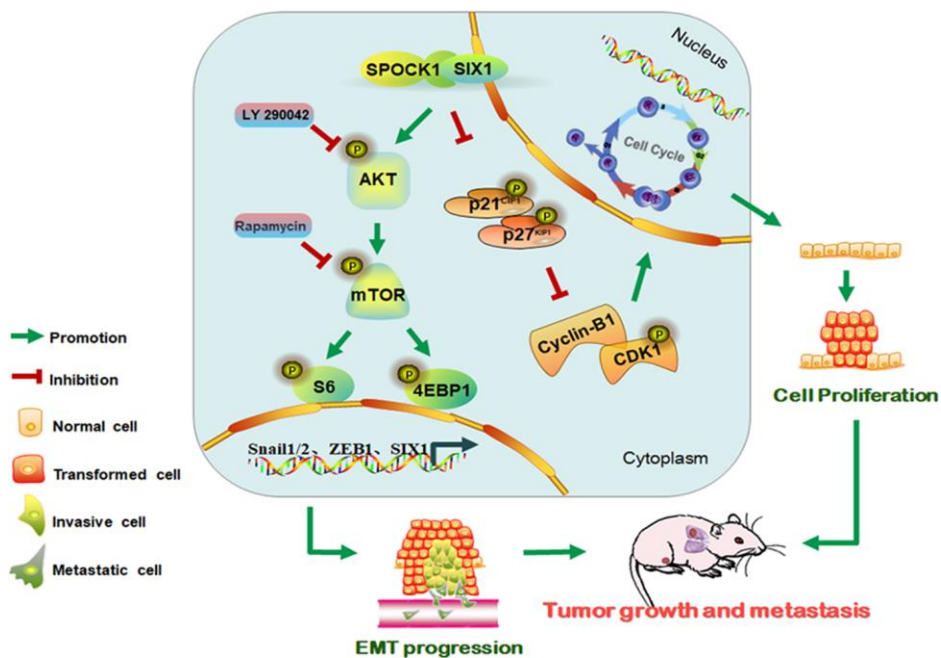


Figure 7. Schematic of the proposed molecular mechanism of SPOCK1/SIX1 axis-induced BC cancer cell growth and metastasis.

targets ERK and AKT signaling and promotes the malignant behavior of cancer cells [16, 49]. In accordance with this, we searched online databases and observed that SIX1 was frequently highly expressed in many cancers, including BC, and correlated with poor survival and high risk. Moreover, there was a statistically significant interaction between SPOCK1 and SIX1 that was identified by an online gene expression profiling interactive analysis tool. Based on these findings, we focused on the relationship between SPOCK1 and SIX1. As modified SPOCK1 expression led to significant changes in SIX1 levels, we then performed a Co-IP assay to confirm the interactive relationship. IF staining further showed that SPOCK1 and SIX1 were partly complexed together in the cytoplasm. Li et al. proposed that SIX1 participated in the transcriptional regulation of the Warburg effect in BC [20], providing critical evidence that SIX1 could act as a hallmark of cancer. Herein, to further identify the special role of SIX1 in SPOCK1-mediated BC evolution, we blocked the expression of SIX1 using siRNA and explored the effect on the cell cycle, proliferation, motility and EMT process. As we suspected, siSIX1 treatment significantly abolished SPOCK1-induced facilitation of BC progression without affecting the expression of SPOCK1 protein. Simply put, a large number of normative studies are still needed to clarify this molecular mechanism.

CONCLUSIONS

In summary, this study contributed to illuminating the molecular mechanism by which SPOCK1 overexpression in human BC potentiated tumor progression. Our findings indicated that SPOCK1 is aberrantly overexpressed in BC. SPOCK1/SIX1 axis stimulated the AKT/mTOR signaling pathway to accelerate cell cycle progression, promote cell proliferation, trigger EMT progression and facilitate metastasis in BC (Figure 7). SPOCK1 along with SIX1 might be prognostic factors for BC patients and promising therapeutic targets involved in strategies to prevent BC progression.

MATERIALS AND METHODS

SPOCK1/SIX1 expression pattern

We performed SPOCK1/SIX1 mRNA expression in different cancers and confirmed the expression pattern of SPOCK1/SIX1 in BC by Oncomine database (<https://www.oncomine.org/resource/login.html>).

The comparison of different SPOCK1/SIX1 expression in various normal and cancer tissues and the expression of SIX1 protein in BC were used The Human Protein

Atlas (HPA) (<https://www.proteinatlas.org/>) [50] and UALCAN (<http://ualcan.path.uab.edu/analysis.html>) [51] databases.

Survival analysis

SPOCK1/SIX1 prognostic value in BC, including relapse free survival (RFS), distant metastasis free survival (DMFS), post progression survival (PPS) and overall survival (OS), was calculated by Kaplan-Meier plotter (<http://kmplot.com/analysis/index.php?p=service&cancer=breast>). Risk assessment was further assessed by SurvExpress (<http://bioinformatica.mty.itesm.mx:8080/Biomatec/SurvivaX.jsp>).

Bioinformatics analysis

The protein and protein interaction networks in SPOCK1/SIX1 were established on the platform of GeneMANIA (<http://genemania.org/>) and Search Tool for the Retrieval of Interacting Genes (STRING) (<https://string-db.org/cgi/input.pl>) [52].

The heat map of the correlation between SPOCK1 and EMT markers in the same cohort was analyzed using UCSC Xena (<http://xena.ucsc.edu/>). The positive relationships for SPOCK1 and target genes were discerned and verified by Gene Expression Profiling Interactive Analysis 2 (GEPIA2) (<http://gepia2.cancer-pku.cn/#index>) [53].

Cell culture

Human BC cell lines MCF7, MDA-MB-231, MDA-MB-453, MDA-MB-468, HS 578T, SKBR3 and normal immortalized mammary gland cell line MCF10A were cultured in Dulbecco Modified Essential Medium (DMEM) (Gibco, USA) with 10% FBS and 100 units penicillin and 100 mg/mL streptomycin.

Plasmid construction and transfection

Human Lenti-shSPOCK1-GFP, Lenti-SPOCK1-GFP and negative control (Lenti-shNC and Lentivector control) were designed and packaged by Genechem (Co. Ltd., Shanghai, China). The target sequences of Lenti-shSPOCK1 were shown: 5'-TTTCGAGACGATGATTA TT-3' for shSPOCK1#2 and 5'-GCTGGATGACCTAGA ATAT-3' for shSPOCK1#3. The sequence of negative control was 5'-TTCTCCGAACGTGTACAGT-3'.

2×10^4 BC cells were inoculated into 24-well plates for stable infection, then produce stably transfected cells by puromycin (2 μ g/mL) after 48 h infection. The infection efficiency was identified by GFP gene reporter and western blot.

Cell proliferation assay

The 3-(4,5-dimethyl-2-thiazolyl)-2,5-diphenyl-2-H-tetrazolium bromide (MTT) assay was used to detect BC cell proliferation. Briefly, infected BC cells were seeded in plates and grown to 80% confluences for staining with MTT (0.5 mg/mL; 100 μ L; Dako, Denmark) and dissolved the crystal by dimethylsulfoxide per 24 h for 5 d. Three wells per group at least were analyzed and repeated three times.

Colony formation assay

BC cells were inoculated in 6-well plates for incubating about 15 d. Then fixed the cells by methanol after being washed with cold PBS (Phosphate-buffered saline solution, Boster, China) and staining with Giemsa. Counting the colonies directly.

5-ethynyl-2'-deoxyuridine (EdU) incorporation assay

5×10^3 BC cells seeded and grown in 96-well plates overnight and 100 μ L 50 μ M EdU medium (RiboBio, Guangzhou, China) per well were cultured for 2 h. Then the cells were fixed by methanol for 30 min and washing with PBS for 5 min twice. After permeabilizing with 0.5% TritonX-100 for 10 min twice and washing with PBS for 5 min, 1 \times Apollo dye was used to stain the cells for 30 min, repeated washing. Finally, the signal was visualized and recorded by a microscope after Hoechst 33342 counterstaining.

Flow cytometry assay

Washing the cells with 10 mL cold PBS, then centrifuging at 1000 rpm for 10 minutes and discarding the supernatant. Added 5 mL of 75% ethanol and incubated at -20° C overnight. Next day, washed twice with cold PBS to remove the ethanol, and centrifuged the cells for 10 minutes at 1500 rpm and discarded supernatant. Resuspension the cell pellets in 0.5 mL of PI/RNase Staining Buffer. After incubating 15 min at room temperature, stored tubes on ice freed from light prior to analyzing. Finally, samples were analyzed on the flow cytometer (BD Accuri C6) and used Modfit LT4.1 Software (Verity Software House, Inc., Topsham, ME, USA) to record the cell cycle distribution.

Immunofluorescence (IF)

BC cells were attached with 4% paraformaldehyde. Permeabilizing cells with 0.5% TritonX-100 for 15 min and blocking with 3% Albumin Bovine V (Solarbio, Beijing, China) for 2 h. Then incubating primary antibodies overnight at 4° C. Incubating with second antibodies (A1108, Invitrogen, USA), and counterstaining

by DAPI with an Antifade Mounting Medium (Beyotime, Shanghai, China) the next day. Finally, cover-slips signal was captured by the microscope.

Wound healing assay

BC cells were seeded and grown in 6-well plates at approximately 80% confluences, scratching the monolayer uniformly on the surface by 200 μ L. The scratched areas were recorded by microscope at 0h, 24h, 48h, and 72h. The migration distances were measured by Image J software for analyzing.

Migration and invasion assay

3×10^4 BC cells were inoculated onto the upper chambers with or without coating Matrigel (BD Biosciences) containing 1% with serum in DMEM. Filling 20% fetal bovine serum/DMEM media into the lower chamber. The chambers were attached with 4% paraformaldehyde for 5 min after incubation for 24-48 h at 37° C, 5% CO_2 . Then staining with Giemsa after washing with cold PBS. The migrated cells were counted by a microscope. The experiment was performed three times to reduce the possible effects of biological variability.

siRNA transfection

The sequence of si-SIX1 was SIX1-siRNA: 5'-GGG AGAACACCGAAAACAA-3'. BC cells were transfected with SIX1 siRNAs or control siRNA using LipofectamineTM 3000 Reagent (Invitrogen, USA) according to the manufacturer's instruction.

Western blot

BSA Protein Assay Kit (A8020-5, Roche, Basel, Switzerland) was applied to measure the protein concentration after lysing BC cells with RIPA buffer. The total protein was dissolved by SDS-PAGE loading buffer and transferred onto poly vinylidene fluoride (PVDF) membranes (Millipore, Billerica, MA, USA). The primary antibodies (Table 3) were incubated overnight at 4° C. Second day, the HRP-conjugated secondary antibodies (CST, Danvers, MA, USA) were incubating for an hour, then antibody-reactive bands were visualized via enhanced chemiluminescence (ECL) system (Millipore, USA) in an Imager.

Co-immunoprecipitation (Co-IP)

In brief, added lysis buffer and incubated on ice for 30 min after washing the cell pellet with cold PBS. Scraped cells and centrifuged about 5 min, 15000 rpm, then transfer supernatant to a new microcentrifuge. Preclear the Protein A/G PLUS-Agarose beads (Santa Cruz,

Table 3. The information of antibodies.

Antibodies	Source company	Dilution ration
Anti-SPOCK1	R&D Systems, USA	1:1000
Anti-GAPDH	Proteintech, Wuhan, China	1:1000
Anti-p21(CDNK1A)	Proteintech, Wuhan, China	1:1000
Anti-p27[Kip1]	Proteintech, Wuhan, China	1:1000
Anti-CDK1	Proteintech, Wuhan, China	1:1000
Anti-Cyclin-B1	Cell signaling Technology, USA	1:1000
Anti-Survivin	Cell signaling Technology, USA	1:1000
Anti-C-myc	Santa Cruz, Dallas, Texas, USA	1:1000
Anti-Slug	Elibscience, Wuhan, China	1:1000
Anti-E-cadherin	Elibscience, Wuhan, China	1:10000
Anti-Vimentin	Cell signaling Technology, USA	1:1000
Anti-Snail	Cell signaling Technology, USA	1:1000
Anti-ZO-1	Cell signaling Technology, USA	1:1000
Anti-Twist	Abcam, USA	1:500
Anti-S100A4	Abcam, USA	1:1000
Anti-ZEB1	Proteintech, Wuhan, China	1:1000
Anti-SIX1	Sigma, USA	1:1000
Anti-p-AKT	Cell signaling Technology, USA	1:2000
Anti-AKT	Cell signaling Technology, USA	1:1000
Anti-p-mTOR	Cell signaling Technology, USA	1:1000
Anti-mTOR	Cell signaling Technology, USA	1:1000
Anti-p-S6	Cell signaling Technology, USA	1:1000
Anti-S6	Cell signaling Technology, USA	1:1000
Anti-p-4EBP1	Cell signaling Technology, USA	1:1000
Anti-4EBP1	Cell signaling Technology, USA	1:1000

USA) with cold PBS and pre-blocked with BSA (Bovine serum albumin fraction V, Solarbio, China) to reduce non-specific immunoglobulin binding. Pellet beads, control IgG and 200 μ L cell lysate incubated at 4° C about 1 h, transfer supernatant to a fresh microcentrifuge tube on ice and added 5 μ L primary antibody and incubate overnight at 4° C, after centrifugation at 6500 rpm for 1 min at 4° C. Cap tubes and incubated at 4° C on a rocker platform overnight. Collected immunoprecipitates by centrifugation at 2500 rpm for 1 min at 4° C. Aspirated and discarded supernatant carefully. Washed pellet 3 times with lysis buffer, each time repeating centrifugation step above. After final wash, carefully aspirated and discarded supernatant and resuspended pellet in 20 μ L of 3 \times electrophoresis sample buffer. Boiled samples for 5 minutes and analyze 25 μ L aliquots by western blot.

Mouse xenograft model

To establish the orthotopic BC model, MDA-MB-231 cells stably overexpressing SPOCK1 (MDA-MB-231-

SPOCK1) and MCF7 and SKBR3 cells stably silenced SPOCK1 (MCF7-shSPOCK1; SKBR3-shSPOCK1) as well as their negative control (MDA-MB-231-Vector; MCF7-NC; SKBR3-NC) were implanted in the mammary gland fat pad of BALB/c nude female mice (Viatal Rivers, Beijing, China). Injecting 10⁶ cells into the tail vein of 5-week-old nude mice for vivo lung metastasis models. Tumor sizes were monitored per 5 days, and volumes were calculated with a formula: Volume (mm³) = 0.5 \times length \times width². About 5 weeks, all mice were sacrifices, then tumors and lungs were removed. The number of lung metastases was counted on the surface of the lungs. Finally, dissected tumors and lungs were hematoxylin and eosin staining.

IHC staining analysis

In brief, tissue sections were deparaffinized, rehydrated and incubated with 3% H₂O₂ for 15 min. Then performing in sodium citrate buffer (pH 6.0) at 95° C for antigen retrieval. After returning to the room

Table 4. Immunohistochemical scoring according to immune-staining intensity and area.

Staining area(%) Staining intensity	"0" (0-5%)	"1" (5%-25%)	"2" (25%-50%)	"3" (50%-75%)	"4" (75%-100%)
"0"(Negative)	Score0	Score0	Score0	Score0	Score0
"1"(Weak)	Score0	Score1	Score2	Score3	Score4
"2"(Moderate)	Score0	Score2	Score4	Score6	Score8
"3"(Strong)	Score0	Score3	Score6	Score9	Score12

temperature, the slides were incubated with primary antibodies overnight. Next day, secondary antibody was incubated for 2 h. The slides were developed in the reaction with a 3, 3'-diaminobenzidine chromogen and counterstained with Mayer's hematoxylin. Positive control and isotope control selected the tonsil and Rabbit IgG, respectively. Negative control treated positive tissue sections with PBS instead of primary antibody. Immunostaining for SPOCK1 was judged by a double semi-quantitative scoring system (Table 4). Specific reference to our previous research [54].

Statistical analysis

Statistical analyses were carried out by SPSS version 17.0 software and Prism 8.0 for Windows. Chi-square tests (χ^2) was used to compare the correlations between SPOCK1 expression and clinicopathological parameters. All data were displayed by mean \pm standard deviation, which calculated for thrice experiments. One-way Anova was used to compare data between multiple groups, and pairwise comparisons between groups were performed by t-test. We considered $P < 0.05$ as statistically significant.

Ethics statement

Our study complied the Declaration of Helsinki and approved by the Human Ethics Committee and the Research Ethics Committees of Yanbian University in China. All patients signed informed consent, which included consent to use the resection specimens for scientific research. All the specimens were kept in our tissue specimen bank and we promised to provide privacy protection for patients.

Animal care and experimental procedures in this study were approved by the Institutional Animal Care and Use Committee (IACUC) of Changchun Weishi testing technology service co. LTD and performed in accordance with the institutional guidelines.

AUTHOR CONTRIBUTIONS

Z. L. conceived this study and takes responsibility for the quality of the data. M. X., X. W. and Y. Y.

participated in the experiments. S. Z. and Z. L. played an important role in interpreting the results. M. X. and J. P. performed the data analysis. M. X. wrote the manuscript and X. Z. helped to modify the manuscript. All authors read and approved the final manuscript.

CONFLICTS OF INTEREST

The authors declare no conflicts of interest.

FUNDING

This study was supported by grants from the Special Funds for Local Science and Technology Development Guided by the Central Committee, basic research project of Jilin Province (202002021JC), National Natural Science Funds of China (No. 31760313), The Funds of Tumen River Scholar Project and Key Laboratory of the Science and Technology Department of Jilin Province (No. 20170622007JC).

REFERENCES

1. Siegel RL, Miller KD, Jemal A. Cancer statistics, 2020. *CA Cancer J Clin.* 2020; 70:7–30. <https://doi.org/10.3322/caac.21590> PMID:31912902
2. Lee ES, Jung SY, Kim JY, Kim JJ, Yoo TK, Kim YG, Lee KS, Lee ES, Kim EK, Min JW, Han W, Noh DY, Moon HG. Identifying the potential long-term survivors among breast cancer patients with distant metastasis. *Ann Oncol.* 2016; 27:828–33. <https://doi.org/10.1093/annonc/mdw036> PMID:26823524
3. Bradshaw AD, Sage EH. SPARC, a matricellular protein that functions in cellular differentiation and tissue response to injury. *J Clin Invest.* 2001; 107:1049–54. <https://doi.org/10.1172/JCI12939> PMID:11342565
4. Li Y, Chen L, Chan TH, Liu M, Kong KL, Qiu JL, Li Y, Yuan YF, Guan XY. SPOCK1 is regulated by CHD1L and blocks apoptosis and promotes HCC cell invasiveness and metastasis in mice. *Gastroenterology.* 2013; 144:179–91.e4. <https://doi.org/10.1053/j.gastro.2012.09.042> PMID:23022495

5. Naczki C, John B, Patel C, Lafferty A, Ghoneum A, Afify H, White M, Davis A, Jin G, Kridel S, Said N. SPARC inhibits metabolic plasticity in ovarian cancer. *Cancers (Basel)*. 2018; 10:385.
<https://doi.org/10.3390/cancers10100385>
PMID:[30332737](https://pubmed.ncbi.nlm.nih.gov/30332737/)
6. Ma J, Gao S, Xie X, Sun E, Zhang M, Zhou Q, Lu C. SPARC inhibits breast cancer bone metastasis and may be a clinical therapeutic target. *Oncol Lett*. 2017; 14:5876–82.
<https://doi.org/10.3892/ol.2017.6925> PMID:[29113221](https://pubmed.ncbi.nlm.nih.gov/29113221/)
7. Zhang J, Zhi X, Shi S, Tao R, Chen P, Sun S, Bian L, Xu Z, Ma L. SPOCK1 is up-regulated and promotes tumor growth via the PI3K/AKT signaling pathway in colorectal cancer. *Biochem Biophys Res Commun*. 2017; 482:870–76.
<https://doi.org/10.1016/j.bbrc.2016.11.126>
PMID:[27889608](https://pubmed.ncbi.nlm.nih.gov/27889608/)
8. Wang T, Liu X, Tian Q, Liang T, Chang P. Reduced SPOCK1 expression inhibits non-small cell lung cancer cell proliferation and migration through Wnt/ β -catenin signaling. *Eur Rev Med Pharmacol Sci*. 2018; 22:637–44.
https://doi.org/10.26355/eurrev_201802_14288
PMID:[29461591](https://pubmed.ncbi.nlm.nih.gov/29461591/)
9. Yu F, Li G, Gao J, Sun Y, Liu P, Gao H, Li P, Lei T, Chen Y, Cheng Y, Zhai X, Sayari AJ, Huang H, Mu Q. SPOCK1 is upregulated in recurrent glioblastoma and contributes to metastasis and temozolomide resistance. *Cell Prolif*. 2016; 49:195–206.
<https://doi.org/10.1111/cpr.12241> PMID:[26923184](https://pubmed.ncbi.nlm.nih.gov/26923184/)
10. Chen D, Zhou H, Liu G, Zhao Y, Cao G, Liu Q. SPOCK1 promotes the invasion and metastasis of gastric cancer through slug-induced epithelial-mesenchymal transition. *J Cell Mol Med*. 2018; 22:797–807.
<https://doi.org/10.1111/jcmm.13357> PMID:[28940639](https://pubmed.ncbi.nlm.nih.gov/28940639/)
11. Yang J, Yang Q, Yu J, Li X, Yu S, Zhang X. SPOCK1 promotes the proliferation, migration and invasion of glioma cells through PI3K/AKT and Wnt/ β -catenin signaling pathways. *Oncol Rep*. 2016; 35:3566–76.
<https://doi.org/10.3892/or.2016.4757> PMID:[27108836](https://pubmed.ncbi.nlm.nih.gov/27108836/)
12. Ma LJ, Wu WJ, Wang YH, Wu TF, Liang PI, Chang IW, He HL, Li CF. SPOCK1 overexpression confers a poor prognosis in urothelial carcinoma. *J Cancer*. 2016; 7:467–76.
<https://doi.org/10.7150/jca.13625> PMID:[26918061](https://pubmed.ncbi.nlm.nih.gov/26918061/)
13. Kalluri R, Weinberg RA. The basics of epithelial-mesenchymal transition. *J Clin Invest*. 2009; 119:1420–28.
<https://doi.org/10.1172/JCI39104> PMID:[19487818](https://pubmed.ncbi.nlm.nih.gov/19487818/)
14. Elzamy S, Badri N, Padilla O, Dwivedi AK, Alvarado LA, Hamilton M, Diab N, Rock C, Elfar A, Teleb M, Sanchez L, Nahleh Z. Epithelial-Mesenchymal Transition Markers in Breast Cancer and Pathological Response after Neoadjuvant Chemotherapy. *Breast Cancer (Auckl)*. 2018; 12:1178223418788074.
<https://doi.org/10.1177/1178223418788074>
PMID:[30083055](https://pubmed.ncbi.nlm.nih.gov/30083055/)
15. Ikeda K, Kageyama R, Suzuki Y, Kawakami K. Six1 is indispensable for production of functional progenitor cells during olfactory epithelial development. *Int J Dev Biol*. 2010; 54:1453–64.
<https://doi.org/10.1387/ijdb.093041ki> PMID:[21302255](https://pubmed.ncbi.nlm.nih.gov/21302255/)
16. Xie Y, Jin P, Sun X, Jiao T, Zhang Y, Li Y, Sun M. SIX1 is upregulated in gastric cancer and regulates proliferation and invasion by targeting the ERK pathway and promoting epithelial-mesenchymal transition. *Cell Biochem Funct*. 2018; 36:413–19.
<https://doi.org/10.1002/cbf.3361>
PMID:[30379332](https://pubmed.ncbi.nlm.nih.gov/30379332/)
17. Nishimura T, Tamaoki M, Komatsuzaki R, Oue N, Taniguchi H, Komatsu M, Aoyagi K, Minashi K, Chiwaki F, Shinohara H, Tachimori Y, Yasui W, Muto M, et al. SIX1 maintains tumor basal cells via transforming growth factor- β pathway and associates with poor prognosis in esophageal cancer. *Cancer Sci*. 2017; 108:216–25.
<https://doi.org/10.1111/cas.13135>
PMID:[27987372](https://pubmed.ncbi.nlm.nih.gov/27987372/)
18. Zhou H, Blevins MA, Hsu JY, Kong D, Galbraith MD, Goodspeed A, Culp-Hill R, Oliphant MUJ, Ramirez D, Zhang L, Trinidad-Pineiro J, Mathews Griner L, King R, et al. Identification of a Small-Molecule Inhibitor That Disrupts the SIX1/EYA2 Complex, EMT, and Metastasis. *Cancer Res*. 2020; 80:2689–2702.
<https://doi.org/10.1158/0008-5472.CAN-20-0435>
PMID:[32341035](https://pubmed.ncbi.nlm.nih.gov/32341035/)
19. Kumar JP. The sine oculis homeobox (SIX) family of transcription factors as regulators of development and disease. *Cell Mol Life Sci*. 2009; 66:565–83.
<https://doi.org/10.1007/s00018-008-8335-4>
PMID:[18989625](https://pubmed.ncbi.nlm.nih.gov/18989625/)
20. Li L, Liang Y, Kang L, Liu Y, Gao S, Chen S, Li Y, You W, Dong Q, Hong T, Yan Z, Jin S, Wang T, et al. Transcriptional regulation of the warburg effect in cancer by SIX1. *Cancer Cell*. 2018; 33:368–85.e7.
<https://doi.org/10.1016/j.ccell.2018.01.010>
PMID:[29455928](https://pubmed.ncbi.nlm.nih.gov/29455928/)
21. Ford HL, Kabingu EN, Bump EA, Mutter GL, Pardee AB. Abrogation of the G2 cell cycle checkpoint associated with overexpression of HSIX1: a possible mechanism of breast carcinogenesis. *Proc Natl Acad Sci USA*. 1998; 95:12608–13.
<https://doi.org/10.1073/pnas.95.21.12608>
PMID:[9770533](https://pubmed.ncbi.nlm.nih.gov/9770533/)

22. Kahlert C, Lerbs T, Pecqueux M, Herpel E, Hoffmeister M, Jansen L, Brenner H, Chang-Claude J, Bläker H, Kloor M, Roth W, Pilarsky C, Rahbari NN, et al. Overexpression of SIX1 is an independent prognostic marker in stage I-III colorectal cancer. *Int J Cancer*. 2015; 137:2104–13.
<https://doi.org/10.1002/ijc.29596> PMID:25951369
23. Turashvili G, Bouchal J, Baumforth K, Wei W, Dziechciarkova M, Ehrmann J, Klein J, Fridman E, Skarda J, Srovnal J, Hajduch M, Murray P, Kolar Z. Novel markers for differentiation of lobular and ductal invasive breast carcinomas by laser microdissection and microarray analysis. *BMC Cancer*. 2007; 7:55.
24. Finak G, Bertos N, Pepin F, Sadekova S, Souleimanova M, Zhao H, Chen H, Omeroglu G, Meterissian S, Omeroglu A, Hallett M, Park M. Stromal gene expression predicts clinical outcome in breast cancer. *Nat Med*. 2008; 14:518–27.
<https://doi.org/10.1038/nm1764> PMID:18438415
25. Ma XJ, Dahiya S, Richardson E, Erlander M, Sgroi DC. Gene expression profiling of the tumor microenvironment during breast cancer progression. *Breast Cancer Res*. 2009; 11:R7.
<https://doi.org/10.1186/bcr2222> PMID:19187537
26. Pascual J, Turner NC. Targeting the PI3-kinase pathway in triple-negative breast cancer. *Ann Oncol*. 2019; 30:1051–60.
<https://doi.org/10.1093/annonc/mdz133> PMID:31050709
27. Kilbas PO, Akcay IM, Doganay GD, Arisan ED. Bag-1 silencing enhanced chemotherapeutic drug-induced apoptosis in MCF-7 breast cancer cells affecting PI3K/Akt/mTOR and MAPK signaling pathways. *Mol Biol Rep*. 2019; 46:847–60.
<https://doi.org/10.1007/s11033-018-4540-x> PMID:30661182
28. Corti F, Nichetti F, Raimondi A, Niger M, Prinzi N, Torchio M, Tamborini E, Perrone F, Pruneri G, Di Bartolomeo M, de Braud F, Pusceddu S. Targeting the PI3K/AKT/mTOR pathway in biliary tract cancers: a review of current evidences and future perspectives. *Cancer Treat Rev*. 2019; 72:45–55.
<https://doi.org/10.1016/j.ctrv.2018.11.001> PMID:30476750
29. Cheng Y, Pan Y, Pan Y, Wang O. MNX1-AS1 is a functional oncogene that induces EMT and activates the AKT/mTOR pathway and MNX1 in breast cancer. *Cancer Manag Res*. 2019; 11:803–12.
<https://doi.org/10.2147/CMAR.S188007> PMID:30697072
30. Micalizzi DS, Wang CA, Farabaugh SM, Schiemann WP, Ford HL. Homeoprotein Six1 increases TGF-beta type I receptor and converts TGF-beta signaling from suppressive to supportive for tumor growth. *Cancer Res*. 2010; 70:10371–80.
<https://doi.org/10.1158/0008-5472.CAN-10-1354> PMID:21056993
31. Micalizzi DS, Christensen KL, Jedlicka P, Coletta RD, Baron AE, Harrell JC, Horwitz KB, Billheimer D, Heichman KA, Welm AL, Schiemann WP, Ford HL. The Six1 homeoprotein induces human mammary carcinoma cells to undergo epithelial-mesenchymal transition and metastasis in mice through increasing TGF-beta signaling. *J Clin Invest*. 2009; 119:2678–90.
32. Iozzo RV, Murdoch AD. Proteoglycans of the extracellular environment: clues from the gene and protein side offer novel perspectives in molecular diversity and function. *FASEB J*. 1996; 10:598–614.
33. Wang Y, Wang W, Qiu E. SPOCK1 promotes the growth of osteosarcoma cells through mTOR-S6K signaling pathway. *Biomed Pharmacother*. 2017; 95:564–70.
<https://doi.org/10.1016/j.biopha.2017.08.116> PMID:28869894
34. Veenstra VL, Damhofer H, Waasdorp C, Steins A, Kocher HM, Medema JP, van Laarhoven HW, Bijlsma MF. Stromal SPOCK1 supports invasive pancreatic cancer growth. *Mol Oncol*. 2017; 11:1050–64.
<https://doi.org/10.1002/1878-0261.12073> PMID:28486750
35. Bill R, Christofori G. The relevance of EMT in breast cancer metastasis: correlation or causality? *FEBS Lett*. 2015; 589:1577–87.
<https://doi.org/10.1016/j.febslet.2015.05.002> PMID:25979173
36. Puisieux A, Brabletz T, Caramel J. Oncogenic roles of EMT-inducing transcription factors. *Nat Cell Biol*. 2014; 16:488–94.
<https://doi.org/10.1038/ncb2976> PMID:24875735
37. Perurena N, Zanduetta C, Martínez-Canarias S, Moreno H, Vicent S, Almeida AS, Guruceaga E, Gomis RR, Santisteban M, Egeblad M, Hermida J, Lecanda F. EPCR promotes breast cancer progression by altering SPOCK1/testican 1-mediated 3D growth. *J Hematol Oncol*. 2017; 10:23.
<https://doi.org/10.1186/s13045-017-0399-x> PMID:28103946
38. Li H, Batth IS, Qu X, Xu L, Song N, Wang R, Liu Y. IGF-IR signaling in epithelial to mesenchymal transition and targeting IGF-IR therapy: overview and new insights. *Mol Cancer*. 2017; 16:6.
<https://doi.org/10.1186/s12943-016-0576-5> PMID:28137302

39. Goswami MT, Reka AK, Kurapati H, Kaza V, Chen J, Standiford TJ, Keshamouni VG. Regulation of complement-dependent cytotoxicity by TGF- β -induced epithelial-mesenchymal transition. *Oncogene*. 2016; 35:1888–98.
<https://doi.org/10.1038/onc.2015.258>
PMID:26148233
40. Ghahhari NM, Babashah S. Interplay between microRNAs and WNT/ β -catenin signalling pathway regulates epithelial-mesenchymal transition in cancer. *Eur J Cancer*. 2015; 51:1638–49.
<https://doi.org/10.1016/j.ejca.2015.04.021>
PMID:26025765
41. Shu YJ, Weng H, Ye YY, Hu YP, Bao RF, Cao Y, Wang XA, Zhang F, Xiang SS, Li HF, Wu XS, Li ML, Jiang L, et al. SPOCK1 as a potential cancer prognostic marker promotes the proliferation and metastasis of gallbladder cancer cells by activating the PI3K/AKT pathway. *Mol Cancer*. 2015; 14:12.
<https://doi.org/10.1186/s12943-014-0276-y>
PMID:25623055
42. Chen X, Cheng H, Pan T, Liu Y, Su Y, Ren C, Huang D, Zha X, Liang C. mTOR regulate EMT through RhoA and Rac1 pathway in prostate cancer. *Mol Carcinog*. 2015; 54:1086–95.
<https://doi.org/10.1002/mc.22177> PMID:25043657
43. Lamouille S, Connolly E, Smyth JW, Akhurst RJ, Derynck R. TGF- β -induced activation of mTOR complex 2 drives epithelial-mesenchymal transition and cell invasion. *J Cell Sci*. 2012; 125:1259–73.
<https://doi.org/10.1242/jcs.095299> PMID:22399812
44. Kwasnicki A, Jeevan D, Braun A, Murali R, Jhanwar-Uniyal M. Involvement of mTOR signaling pathways in regulating growth and dissemination of metastatic brain tumors via EMT. *Anticancer Res*. 2015; 35:689–96.
PMID:25667447
45. Gulhati P, Bowen KA, Liu J, Stevens PD, Rychahou PG, Chen M, Lee EY, Weiss HL, O'Connor KL, Gao T, Evers BM. mTORC1 and mTORC2 regulate EMT, motility, and metastasis of colorectal cancer via RhoA and Rac1 signaling pathways. *Cancer Res*. 2011; 71:3246–56.
<https://doi.org/10.1158/0008-5472.CAN-10-4058>
PMID:21430067
46. Costa RL, Han HS, Gradishar WJ. Targeting the PI3K/AKT/mTOR pathway in triple-negative breast cancer: a review. *Breast Cancer Res Treat*. 2018; 169:397–406.
<https://doi.org/10.1007/s10549-018-4697-y>
PMID:29417298
47. Xu H, Zhang Y, Peña MM, Pirisi L, Creek KE. Six1 promotes colorectal cancer growth and metastasis by stimulating angiogenesis and recruiting tumor-associated macrophages. *Carcinogenesis*. 2017; 38:281–292.
<https://doi.org/10.1093/carcin/bgw121>
PMID:28199476
48. Wu W, Ren Z, Li P, Yu D, Chen J, Huang R, Liu H. Six1: a critical transcription factor in tumorigenesis. *Int J Cancer*. 2015; 136:1245–53.
<https://doi.org/10.1002/ijc.28755> PMID:24488862
49. Xin X, Li Y, Yang X. SIX1 is overexpressed in endometrial carcinoma and promotes the malignant behavior of cancer cells through ERK and AKT signaling. *Oncol Lett*. 2016; 12:3435–40.
<https://doi.org/10.3892/ol.2016.5098>
PMID:27900017
50. Uhlén M, Fagerberg L, Hallström BM, Lindskog C, Oksvold P, Mardinoglu A, Sivertsson Å, Kampf C, Sjödstedt E, Asplund A, Olsson I, Edlund K, Lundberg E, et al. Proteomics. Tissue-based map of the human proteome. *Science*. 2015; 347:1260419.
<https://doi.org/10.1126/science.1260419>
PMID:25613900
51. Chandrashekar DS, Bashel B, Balasubramanya SA, Creighton CJ, Ponce-Rodriguez I, Chakvarathi BV, Varambally S. UALCAN: a portal for facilitating tumor subgroup gene expression and survival analyses. *Neoplasia*. 2017; 19:649–58.
<https://doi.org/10.1016/j.neo.2017.05.002>
PMID:28732212
52. Franceschini A, Szklarczyk D, Frankild S, Kuhn M, Simonovic M, Roth A, Lin J, Minguez P, Bork P, von Mering C, Jensen LJ. STRING v9.1: protein-protein interaction networks, with increased coverage and integration. *Nucleic Acids Res*. 2013; 41:D808–15.
<https://doi.org/10.1093/nar/gks1094> PMID:23203871
53. Tang Z, Kang B, Li C, Chen T, Zhang Z. GEPIA2: an enhanced web server for large-scale expression profiling and interactive analysis. *Nucleic Acids Res*. 2019; 47:W556–60.
<https://doi.org/10.1093/nar/gkz430> PMID:31114875
54. Xu M, Jin T, Chen L, Zhang X, Zhu G, Wang Q, Lin Z. Mortalin is a distinct bio-marker and prognostic factor in serous ovarian carcinoma. *Gene*. 2019; 696:63–71.

Deglycosylated EpCAM regulates proliferation by enhancing autophagy of breast cancer cells via PI3K/Akt/mTOR pathway

Liu Yang¹, Qijun Wang¹, Qian Zhao¹, Fan Yang¹, Tingjiao Liu², Xiaohua Huang³, Qiu Yan¹, Xuesong Yang¹

¹Department of Biochemistry and Molecular Biology, College of Basic Medicine Sciences, Dalian Medical University, Dalian, China

²Section of Oral Pathology, College of Stomatology, Dalian Medical University, Dalian, China

³Department of Clinical Biochemistry, College of Laboratory Science, Dalian Medical University, Dalian, China

Correspondence to: Xuesong Yang; email: yangxs@dlmedu.edu.cn

Keywords: EpCAM, glycosylation, autophagy, PI3K/Akt/mTOR, breast cancer

Received: January 1, 2021

Accepted: December 7, 2021

Published: January 4, 2022

Copyright: © 2021 Yang et al. This is an open access article distributed under the terms of the [Creative Commons Attribution License](https://creativecommons.org/licenses/by/3.0/) (CC BY 3.0), which permits unrestricted use, distribution, and reproduction in any medium, provided the original author and source are credited.

ABSTRACT

Autophagy is an important regulator of cellular homeostasis and its dysregulation often results in cancer. Aberrant glycosylation induced by oncogenic transformation contributes to tumor invasion and metastasis. In a previous study, we have demonstrated that EpCAM, a glycosylation protein, is associated with cell growth and metastasis in breast cancer. But the effect of EpCAM glycosylation on autophagy is not clear. The precise mechanism of regulation remains largely unknown. In this study, breast cancer cells were transfected with N-glycosylation mutation EpCAM plasmid to express deglycosylated EpCAM. The result showed that deglycosylated EpCAM promoted autophagy in breast cancer cells. We further confirmed this conclusion with the activator (Rapamycin, RAP) and inhibitor (Wortmannin) of autophagy. We also found that deglycosylated EpCAM promoted apoptosis and inhibited proliferation through activating autophagy by suppressing Akt/mTOR signaling pathway in breast cancer cells. These findings represent a novel mechanism by which deglycosylated EpCAM inhibits proliferation by enhancing autophagy of breast cancer cells via PI3K/Akt/mTOR pathway. In conclusion, the combination of autophagy modulation and EpCAM targeted therapy is a promising therapeutic strategy in the treatment of breast cancer.

INTRODUCTION

Breast cancer (BC) is the second most common malignancy among women [1]. The main cause of high mortality rate in BC is cancer recurrence, which origin from the metastasis of dormant tumor cells [2, 3]. Till now, surgical operation is the main treatment for breast cancer, which is effective for early stage of BC. But for the advanced, incurable stage of BC, transitional chemotherapeutic agents do not produce good results [4, 5]. Therefore, it is necessary to develop new targeted drugs for advanced BC as early as possible.

Epithelial cell adhesion molecule (EpCAM) is a glycoprotein expressing on the surface of epithelial cell and several tumor types, including colorectal cancer [6], endometrial carcinoma [7], lung carcinoma [8], gastric cancer, and BC [9]. It has been shown that there exists a close relationship between overexpression of EpCAM and advanced stages of BC [10]. Our study has demonstrated that decreased EpCAM caused a notable negative effect on cell proliferation, migration and invasion *in vitro* [11, 12]. EpCAM knockdown promoted apoptosis and raised the cytotoxic effect of 5-Fluorouracil in breast cancer cells through MAPK signaling pathway [13]. These results suggested that

EpCAM has a close relationship with malignant biological behaviors. But up to now, the relationship between EpCAM and autophagy has not been clear.

Autophagy is a self-degradative process and is important to maintain cellular homeostasis, development, differentiation, cell survival and death, which has been found to play an interesting role in cancer biology [14]. Autophagy has two mutually contradictory roles in tumors. These dual effects mean that we could find autophagy upregulation as well as autophagy downregulation in cancers. Therefore, autophagy show dual properties during malignant transformation, including oncogenic and tumor suppressor properties [15, 16]. Thus, it is essential to identify the key autophagy targets for new therapeutic agents.

Glycosylation modification on protein is the popular common form of post-translational modification. Tumor cells are usually accompanied by glycosylated modifications, which result in inhibition of apoptosis, uncontrolled proliferation, and metastasis. Recent data suggest that through the process of autophagy glycoconjugates could regulate physiology. For example, serum proteins showed hypoglycosylation and autophagy downregulated when the X-linked ATP6AP2 was mutated in the mouse liver [17]. Autophagy is inhibited by excessive O-GlcNAcylation and harmful to neurons [18]. We have learned that EpCAM is a glycoprotein which has three glycosylation sites [19]. EpCAM showed different glycosylation in normal tissues and in head and neck tumors [20]. Based on the above, we inferred that glycosylation of EpCAM may play a role on autophagy in breast cancer. But the regulatory mechanism of EpCAM glycosylation on autophagy remains unclear. Therefore, whether glycosylated EpCAM is associated with proliferation and apoptosis caused by autophagy needs to be studied further.

Thus, the role and mechanism of deglycosylation EpCAM on autophagy will be discussed in this paper. Overall, our study supposes that targeting autophagy may become an effective treatment for breast cancer.

RESULTS

Effect of glycosylation of EpCAM on autophagy

To elucidate glycosylation of EpCAM in BC on autophagy, an EpCAM overexpression plasmid and small interfering RNA-mediated silencing of EpCAM (si-EpCAM) were used to increase and reduce EpCAM expression in MCF-7 and MDA-MB-231 breast cancer cell lines, respectively. N-glycosylation mutation of

EpCAM plasmid was utilized to express deglycosylation EpCAM. Typical autophagosomal markers, Beclin 1, P62 and LC3, were detected by using Western blot. As shown in Figure 1A, the expression of LC3 I and P62 reduced and the expression of LC3-II and Beclin 1 increased after treated with deglycosylation of EpCAM in these two cells (MCF-7 and MDA-MB-231), suggesting that glycosylation modification in EpCAM may be associated with autophagy.

In addition, we used a GFP-LC3 expression vector to analyze the autophagy activity of cells. The punctate green fluorescent proteins expressed by this vector were mainly concentrated on autophagic vacuoles. We detected autophagosomes by studying GFP-LC3 fluorescence with fluorescence microscope. The group transfected with M-EpCAM plasmid showed higher percentage of punctate GFP, while the groups transfected EpCAM overexpression plasmid, si-EpCAM sequence, with showed primarily diffused (Figure 1B). The results were consistent with those obtained for LC3-II levels in the western blot experiments. We inferred that N-glycosylation of EpCAM influenced the sub-cellular distribution of LC3.

When autophagy occurs, autophagosomes with double-membrane vesicles will be formed. The autophagosomes can swallow other organelles and send them to the lysosome. This process can be observed by transmission electron microscopy [21]. As shown in Figure 1C–1b, 1d, in the MCF-7 cells treated with EpCAM overexpression plasmid and si-EpCAM sequence, the cytoplasm was filled with organelles of high electron density, which were not contained within vacuoles. These results suggested that there should be short of organelle autophagy. In contrast, cytoplasmic vacuoles containing high electron density organelles were abundant around the nuclear in MCF-7 cells transfected with M-EpCAM plasmid. This result (Figure 1C–1c) supported the hypothesis that formation of autophagosome was regulated by glycosylation modification of EpCAM. Taken together, it demonstrated that in breast cancer cells autophagy is associated with glycosylation of EpCAM.

Effect of regulators of autophagy on glycosylation of EpCAM

Based on above results, we have inferred N-glycosylation of EpCAM is important for autophagy. Next, inhibitor (Wortmannin) and agonist (Rapamycin) of autophagy were used to confirm the conclusion fatherly. Cells were treated with 100 nM Wortmannin or 200 nM Rapamycin for 12 hr accompanied with transfected with M-EpCAM plasmid. These data

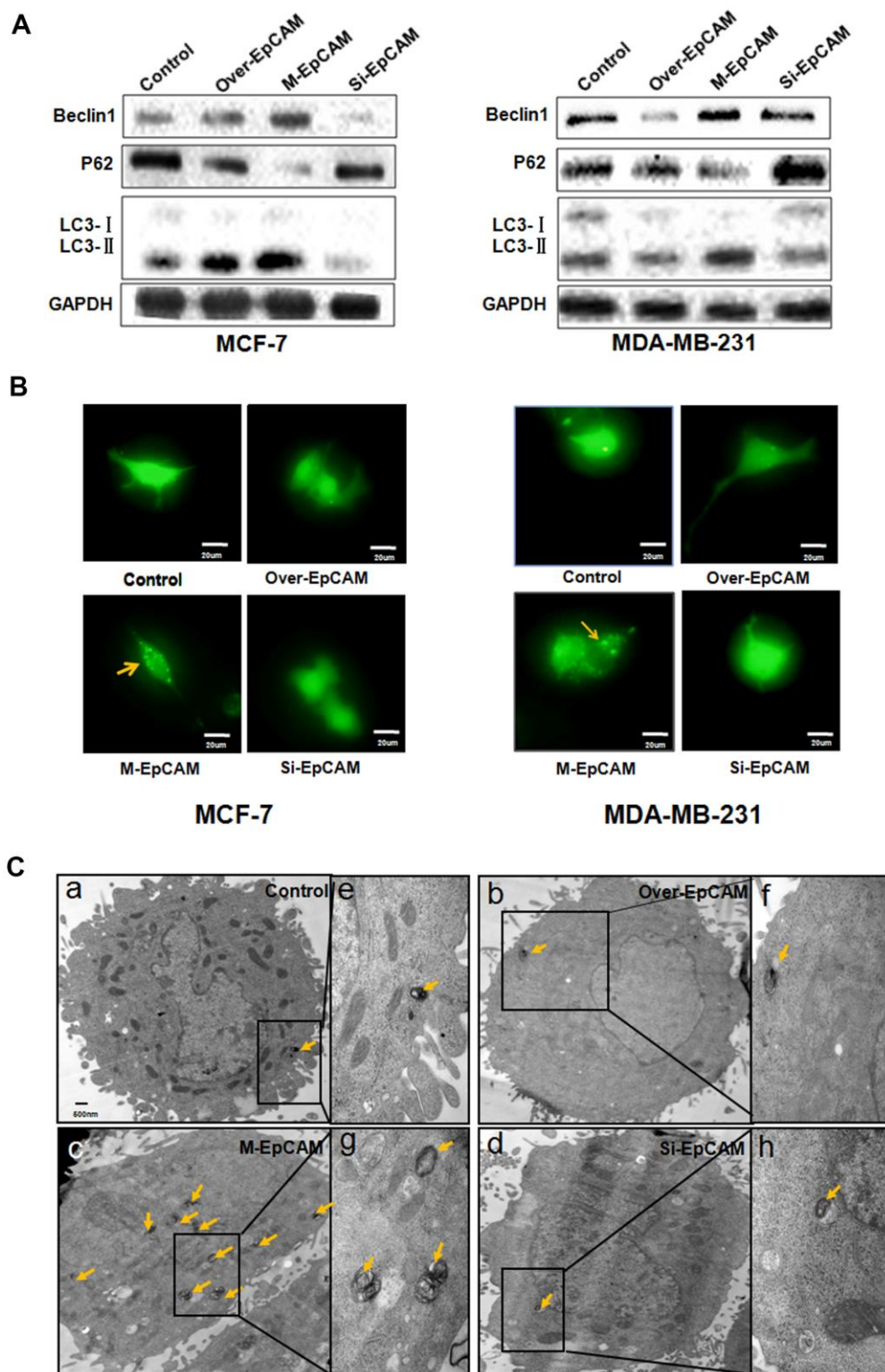


Figure 1. Effect of EpCAM on autophagy. (A) MCF-7 cells and MDA-MB-231 cells were treated with pCMV-SPORT 6-EpCAM plasmid, si-EpCAM sequence and M-EpCAM plasmid for 48 hr. Whole cell lysates were subjected to western blot to detect the expression of Beclin 1, p62 and the conversion from LC3-I to LC3-II. (B) MCF-7 cells and MDA-MB-231 cells were transfected with pCMV-SPORT 6-EpCAM plasmid or si-EpCAM sequence or M-EpCAM plasmid and pGFP-LC3 plasmid for 48 hr, images were collected. After transfection for 24 hr, the cells were observed under an inverted microscope. Arrow depicted the autophagosome. (C) Representative transmission electron microscopy images depicting ultrastructures of MCF-7 cells which were transfected with pCMV-SPORT 6-EpCAM plasmid, si-EpCAM sequence and M-EpCAM plasmid, respectively. (e–h) depicted boxed sections in panels (a–d) at a higher magnification, respectively. Arrows indicate autolysosomes.

(Figure 2) showed that the expression of Beclin1 and LC3-II were significantly decreased with Wortmannin treatment and increased with Rapamycin treatment for 12 hr, while the level of p62 had the opposite result. In addition, when Wortmannin accompanied with transfected with M-EpCAM plasmid, we found that the expressions of Beclin1 and LC3-II were decreased further and p62 was increased compared with

treatment of M--EpCAM plasmid. We also found that Rapamycin accompanied with transfected with M-EpCAM plasmid, the expression of Beclin1 and LC3-II were increased further and p62 was decreased compared with treatment of M-EpCAM plasmid. Collectively, these results suggest that deglycosylated EpCAM regulated autophagy in breast cancer cells.

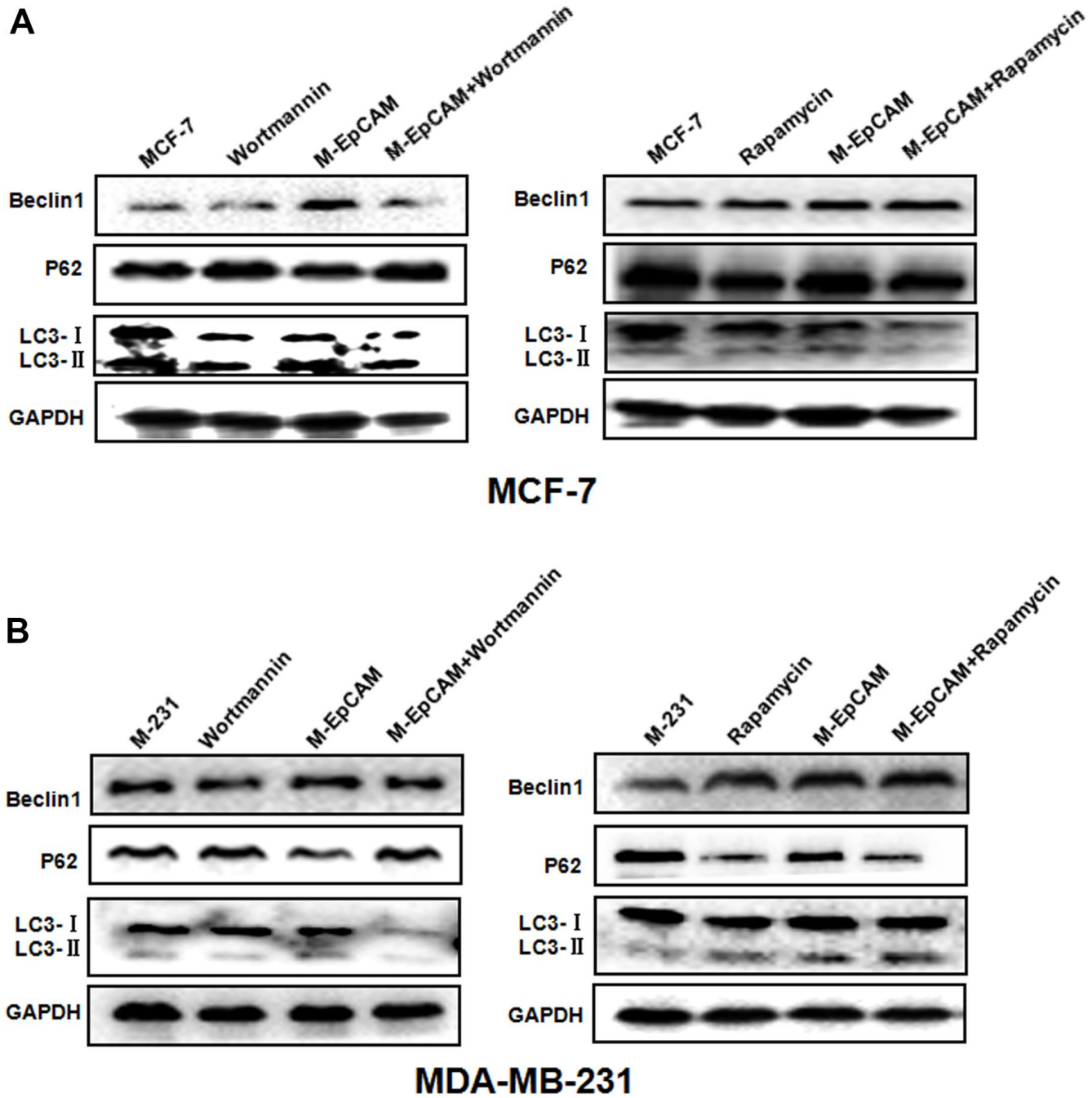


Figure 2. Effect of regulators of autophagy on glycosylation of EpCAM breast cancer cells. Treatment of MCF-7 (A) and MDA-MB-231 (B) cells were treated with 100 nM Wortmannin or 200 nM Rapamycin for 12 hr accompanied with transfected with M-EpCAM plasmid. Expressions of autophagy markers Beclin1, LC3, and p62 proteins were determined by western blot analysis.

The effect of inhibitor and activator of autophagy and deglycosylated EpCAM on apoptosis

We have demonstrated that deglycosylated-EpCAM strengthened the cytotoxic effect of 5-FU and promoted apoptosis in breast cancer cells [22]. It has been reported that autophagy is known to regulate cell cycle progression, survival and apoptosis [23]. Thus, we were interested in discussing the role of autophagy in deglycosylated EpCAM-mediated apoptosis in breast

cancer cells. We used Wortmannin and Rapamycin to inhibit and activate autophagy, respectively. The result showed that apoptosis-related proteins cleaved-caspase 3 and Bax increased and anti-apoptotic protein Bcl2 decreased when cells were transfected with plasmid of M-EpCAM. After M-EpCAM transfected cells were incubated with 100 nM Wortmannin for 24 hr, the expression of cleaved-caspase 3 and Bax decreased and Bcl2 increased compared with the cells transfected with M-EpCAM plasmid only (Figure 3A, 3C). Next,

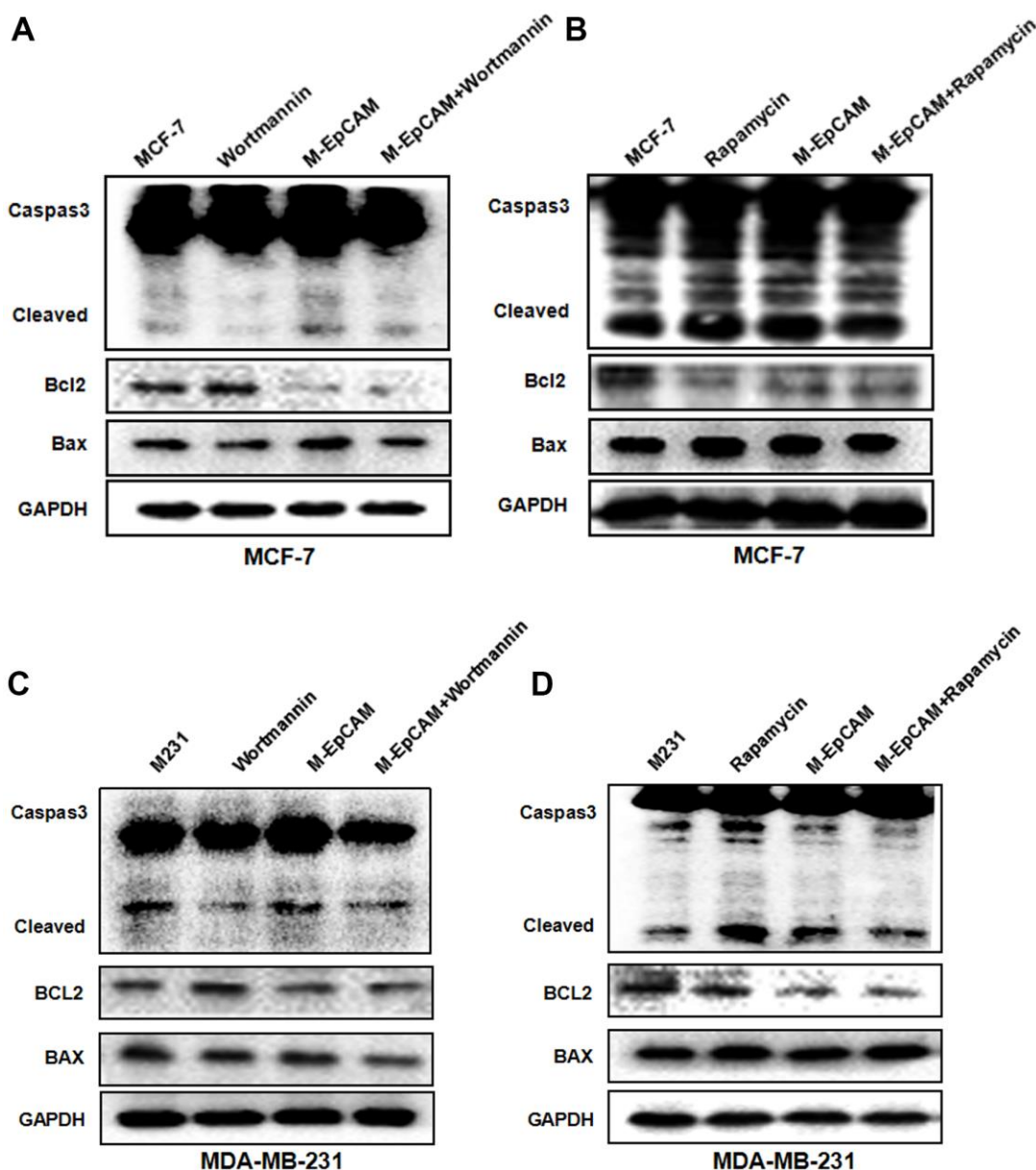


Figure 3. Effect of regulators of autophagy and deglycosylated EpCAM on apoptosis in breast cancer cells. (A, B) MCF-7 cells were incubated with 100 nM Wortmannin 200 nM Rapamycin for 12 hr after transfected with M-EpCAM plasmid. Expression of apoptosis related proteins Caspase 3, Bcl2 and Bax were detected with the method of Western blot. (C, D) MDA-MB-231 cells were incubated with 100 nM Wortmannin 200 nM Rapamycin for 12 hr after transfected with M-EpCAM plasmid. Expression of apoptosis related proteins Caspase 3, Bcl2 and Bax were detected with the method of Western blot.

we tested the effect of autophagy activator on the cell apoptosis. The western blot results showed that Rapamycin (activator) has the opposite effect compared to Wortmannin (inhibitor) (Figure 3B, 3D). Taken together, our findings proved that glycosylated EpCAM might regulate the apoptosis by influencing autophagy in breast cancer cells.

The effect of inhibitor and activator of autophagy and deglycosylated EpCAM on proliferation

Next, to further confirm that the effect of glycosylated EpCAM may participate in proliferation through

autophagy, we incubated MCF-7 and MDA-MB-231 cells with the autophagic inhibitor Wortmannin and stimulus Rapamycin, respectively. By monitoring the expression of proliferation maker PCNA, we found both cells showed Wortmannin increased and Rapamycin decreased the expression of PCNA. Deglycosylated EpCAM also decreased the PCNA expression. Synergistic effect of Wortmannin and deglycosylated EpCAM showed the callback of PCNA expression compared with using the Wortmannin only (Figure 4A, 4C). Then, we used Rapamycin (autophagic activator) to incubate these two breast cancer cells for 24 hr. The results showed that proliferation properties were

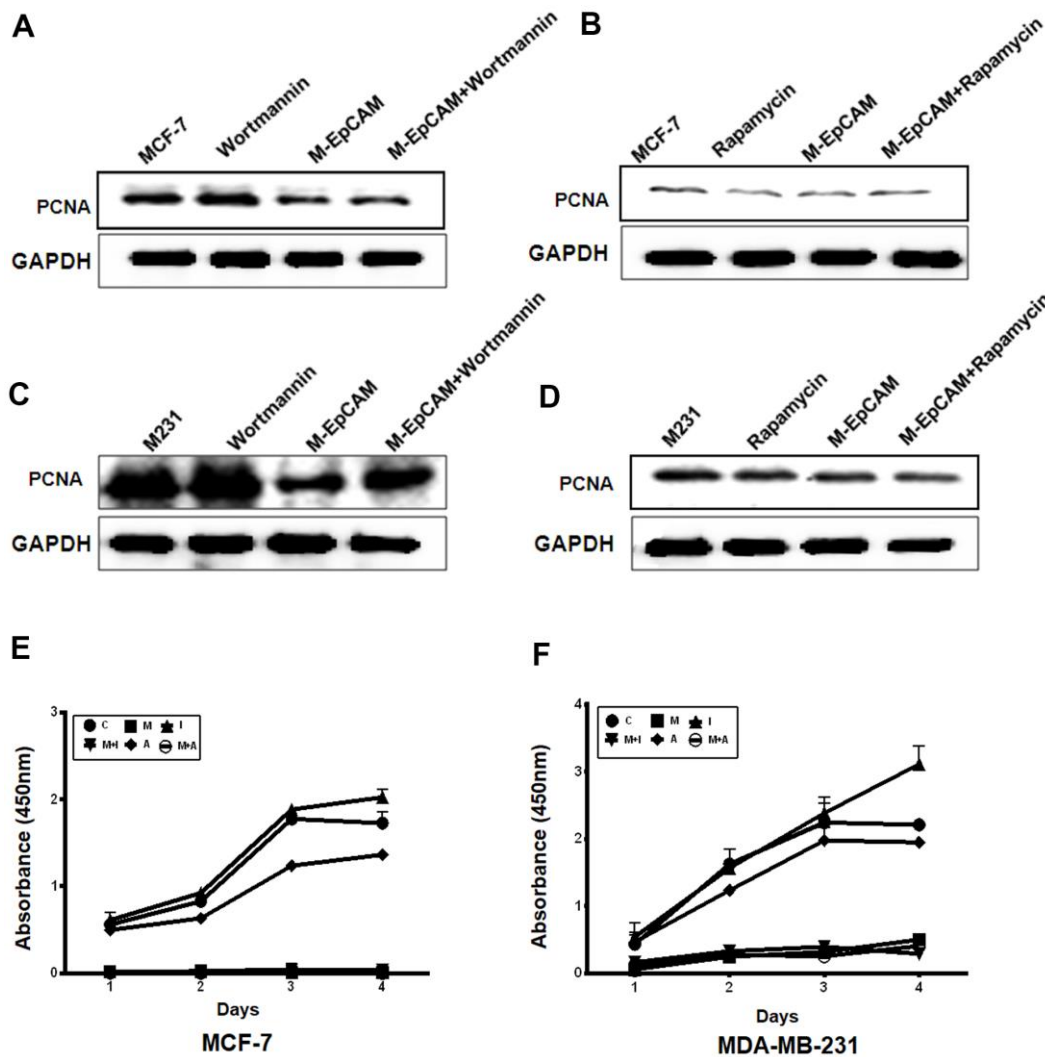


Figure 4. Effect of regulators of autophagy and deglycosylated EpCAM on proliferation in breast cancer cells. (A, B) MCF-7 cells were incubated with 100 nM Wortmannin or 200 nM Rapamycin for 12 hr after transfected with M-EpCAM plasmid. Expression of PCNA was detected with the method of Western blot. (C, D) MDA-MB-231 cells were incubated with 100 nM Wortmannin or 200 nM Rapamycin for 12 hr after transfected with M-EpCAM plasmid. Expression of PCNA was detected with the method of Western blot. (E, F) MCF-7 and MDA-MB-231 cells were incubated with 100 nM Wortmannin or 200 nM Rapamycin for 12 hr after transfected with M-EpCAM plasmid. The cells were cultured for another 4 days. The CCK8 assay used to evaluate the proliferation of the cells after transfection with the M-EpCAM plasmid or autophagic regulator.

inhibited after using the Rapamycin only. The results showed that proliferation properties were inhibited after using the Rapamycin only. Synergistic effect of Rapamycin and deglycosylated EpCAM showed the decrease of PCNA expression (Figure 4B, 4D). We also used CCK8 assay to evaluate the effect of glycosylated EpCAM and autophagy on proliferation, CCK8 assay results showed consistent with above western blot results of PCNA (Figure 4E, 4F). Over all, the finding suggested that glycosylated EpCAM might inhibit the proliferation through influencing autophagy in breast cancer cells.

Deglycosylated EpCAM regulates autophagy, apoptosis and proliferation by PI3K/AKT/mTOR signaling pathway

Many reports supported that autophagy is followed by the induction of apoptosis via PI3K/Akt/mTOR pathway [18, 24]. mTOR can be phosphorylated by phosphorylated-Akt to form p-mTOR, which plays a negative role in autophagy. Based on this, we explored the effect of glycosylation modification of EpCAM on Akt/mTOR signaling pathways. The result showed that deglycosylated EpCAM decreased the expression of pAkt (Figure 5). Next, to further confirm that PI3K/Akt/mTOR participated in this process, we incubated the cells with the Akt inhibitor MK2206 (1uM). The results showed that the levels of p-Akt and p-mTOR significantly declined when treated with MK2206. We also analyzed the effect of glycosylated EpCAM combined with MK2206. The results showed that deglycosylated EpCAM along with MK2206 decreased the expression of pAkt and pmTOR. Autophagy makers Beclin 1 and LC3-II

increased and P62 and LC3-I decreased when treated with M-EpCAM plasmid and MK2206 (Figure 6A). Furthermore, fluorescence result showed that increased granulation of GFP-LC3 during synergistic effect between deglycosylation of EpCAM and Akt inhibitor MK2206 (Figure 6B). Transmission electron microscopy has the same results as above (Figure 6C). Taken together, we deduced that deglycosylated EpCAM promote autophagy via PI3K/AKT/mTOR signaling pathway in breast cancer cells.

We also investigated the effect of glycosylation modification of EpCAM combined with inhibitor of Akt (MK2206) on apoptosis and proliferation in BC (Figure 7). In the MK2206 treated cells and M-EpCAM treated cells, cleaved-caspase 3 and BAX were increased and Bcl2 was decreased. When combined MK2206 and M-EpCAM, the results showed more effective. As shown in Figure 7C, 7D, PCNA expression in the MK2206 and M-EpCAM treated cells were decreased deeply. These data clearly demonstrated that glycosylated EpCAM plays a critical role in regulating autophagy, apoptosis and proliferation on breast cancer cells. Taken above, these data indicate that deglycosylated EpCAM-induced autophagy participated in the proliferation an apoptosis via I3K/Akt/mTOR signaling in breast cancer cells (Figure 8).

DISCUSSION

Autophagy is a catabolic process necessary for development, innate immunity, cellular stress responses, and cell death in physiology and pathology conditions. During this process, long-lived proteins overturn

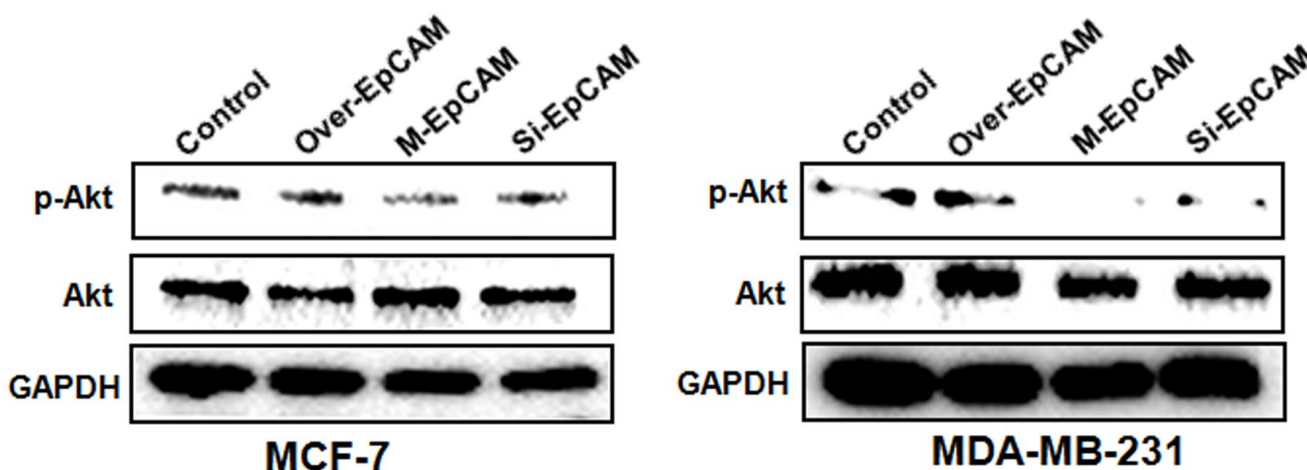


Figure 5. Effects of EpCAM on the PI3K/AKT/mTOR signaling pathway in MCF-7 and MDA-MB-231 cells. MCF-7 and MDA-MB-231 cells were transfected with pCMV-SPORT 6-EpCAM plasmid, si-EpCAM sequence and M-EpCAM plasmid for 48 hr, respectively. Expressions of pAkt and Akt were detected with method of Western blot.

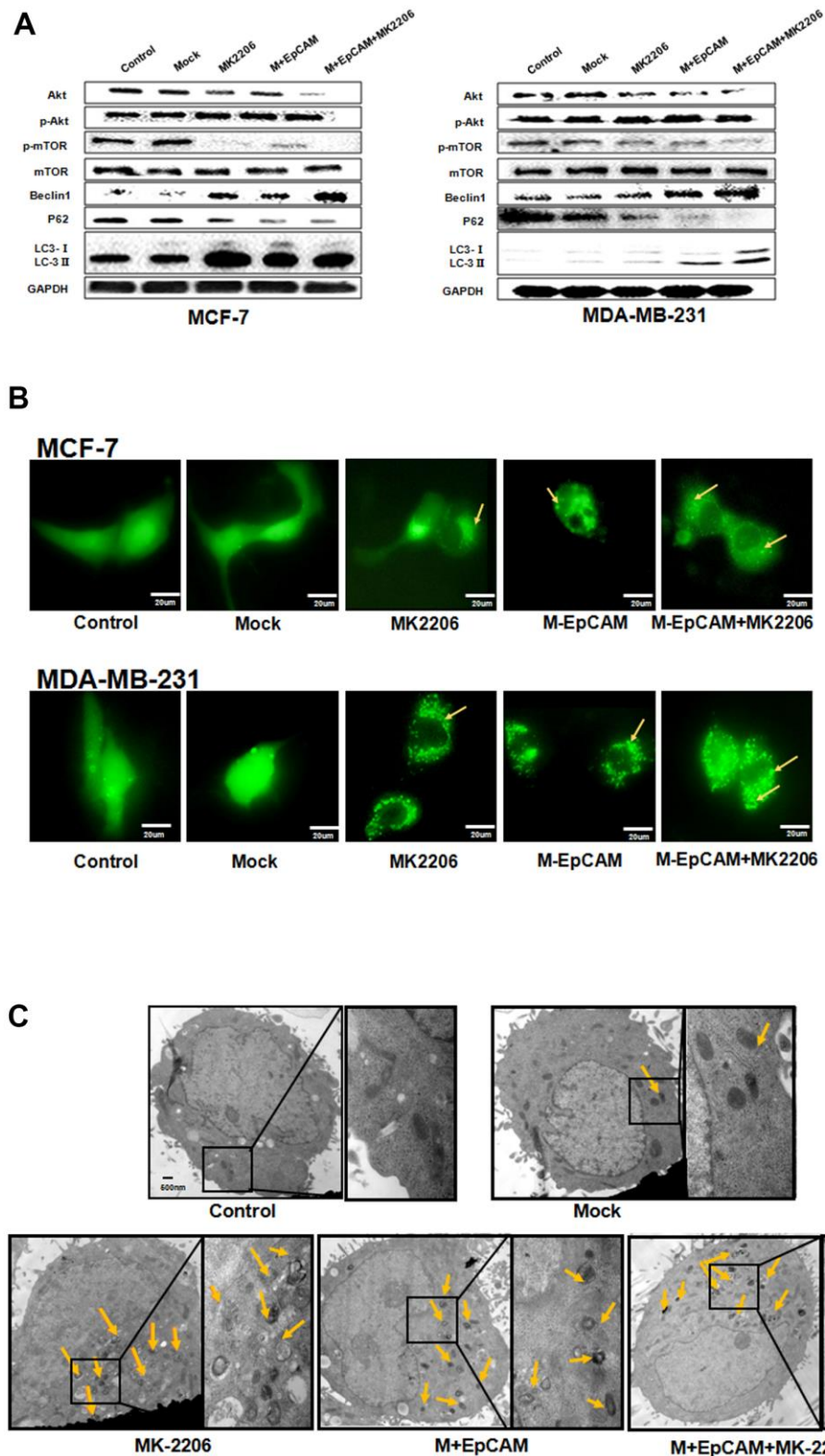


Figure 6. Effects of EpCAM on autophagy via PI3K/AKT/mTOR signaling pathway in MCF-7 and MDA-MB-231 cells. (A) MCF-7 cells and MDA-MB-231 cells were treated with M-EpCAM plasmid and MK2206 (1 μ M) for 48 h. Whole cell lysates were subjected to western blot to detect the expression of Beclin 1, p62 and the conversion from LC3-I to LC3-II. **(B)** MCF-7 cells and MDA-MB-231 cells were treated with M-EpCAM plasmid, pGFP-LC3 plasmid and MK2206 (1 μ M) for 48 hr. Cells were observed under an inverted microscope. Arrow depicted the autophagosome. **(C)** Representative transmission electron microscopy images depicting ultrastructures of MCF-7 cells which were transfected with M-EpCAM plasmid and MK2206 (1 μ M) for 48 h.

constitutively and macromolecules and organelles are damaged [2, 21, 25]. Autophagy plays an important physiological role to maintain cellular homeostasis [26]. Abnormal activation of autophagy can induce cell death [27]. Whether autophagy promotes cell survival or induces cell death is controversial. Through our study, we illustrated that autophagy and subsequent apoptosis were induced by deglycosylated EpCAM in breast cancer cells. Furthermore, we demonstrated the essential role of PI3K/Akt/mTOR signaling pathway in deglycosylated EpCAM-induced autophagy.

The dysregulation of autophagy has been identified in various diseases including cancer, cardiovascular

disease, and autoimmune disease [15]. Till now, many autophagy related proteins and modulators have been found to involve in the autophagy [28]. Autophagy plays a dual role in cell survival and death in both normal tissues and tumors [8]. The interplay between autophagy and cancer cell development and proliferation is complex. Autophagy has been implicated to be closely related to tumorigenesis [29]. Some evidence implicates autophagy as a tumor suppressor, while other evidence suggests that it promotes tumor proliferation. Thus, autophagy plays different roles in cancer biology depending on tumor type and context [9].

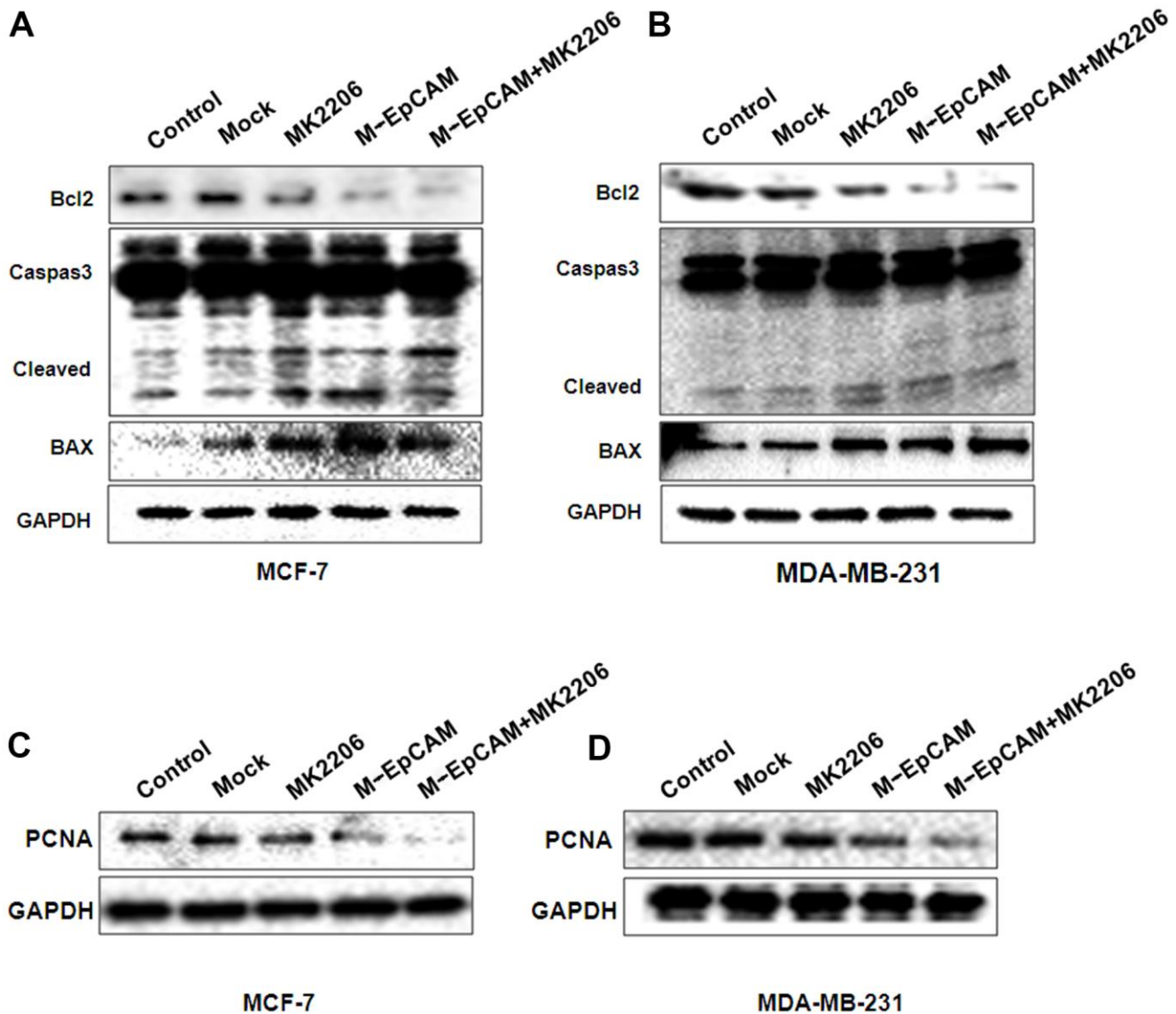


Figure 7. Effects of EpCAM and autophagy on proliferation and apoptosis via PI3K/AKT/mTOR signaling pathway in MCF-7 and MDA-MB-231 cells. MCF-7 (A, C) and MDA-MB-231 (B, D) cells were treated with M-EpCAM plasmid and MK2206 (1 μ M) for 48 h. Whole cell lysates were subjected to western blot to detect the expression of Caspase 3, Bcl2, Bax and PCNA.

Glycosylation is the common protein modification after translation. Abnormal glycosylation influence cancer development and metastasis. [30]. Tumor cells display a wide range of glycosylation alterations, and certain glycans are well-known markers of tumor progression, such as LeY, sLeX [14, 31]. Some data suggested that glycoconjugates influence physiological behavior by regulating autophagy. The mechanics of autophagosome formation was associated with glycoconjugates [32]. Many data have demonstrated that the relationship between the glycosylation and autophagy. Mutations in other crucial autophagy proteins have also been identified and support the idea that autophagy has a tumor suppressor function. For example, Zhu reported that O-GlcNAcase (OGA) inhibitors enhanced autophagy, which aided the brain in struggling with the accumulation of toxic protein species [17]. Li reported that knockdown of HIF-1 α regulated autophagy mediated glycosylation in oral squamous cells [33].

Autophagy and apoptosis, two important physiological behaviors, control cell survival and death in response to various stresses [34]. Autophagy is a conserved process to maintain cellular homeostasis, consisting of the degradation of organelles and abnormal proteins. Autophagy can be rapidly induced by hypoxia, and oxidative stress and so on [35]. Apoptosis is a process which show nuclear shrinkage, chromatin condensation

and apoptosis body [36]. In some cases, autophagy can inhibit apoptosis for cell survival, while in other cases autophagy may lead to cell death [37, 38]. Therefore, the combination of autophagy and apoptosis affects cell homeostasis. Many studies have shown the interaction between autophagy and apoptosis. This interaction is mainly reflected in the interaction between autophagy protein and apoptotic protein, such as Bcl-2/Beclin-1, Atgs, Caspases, p53, FLIP, and so on [39]. Therefore, it is of great significance to explore the interaction between autophagy proteins and apoptotic proteins. In general, autophagy predates apoptosis in maintaining cell homeostasis. Autophagy may become a guardian of apoptosis through surrounding microenvironment [40]. Existing literature reported that autophagy participated the process of cell apoptosis. For example, autophagy-dependent apoptosis was regulated by inhibition of SGK1 via the mTOR-Foxo3a pathway [41].

We reported that deglycosylated EpCAM induced autophagy and apoptosis in breast cancer cells in this study. Blockade of autophagy with autophagy inhibitor Wortmannin completely inhibited deglycosylated EpCAM-induced autophagy apoptosis in breast cancer cells. Activation of autophagy with autophagy activator Rapamycin got the opposite results. It has been demonstrated that a variety of integral cell signaling pathways are known to regulate autophagy.

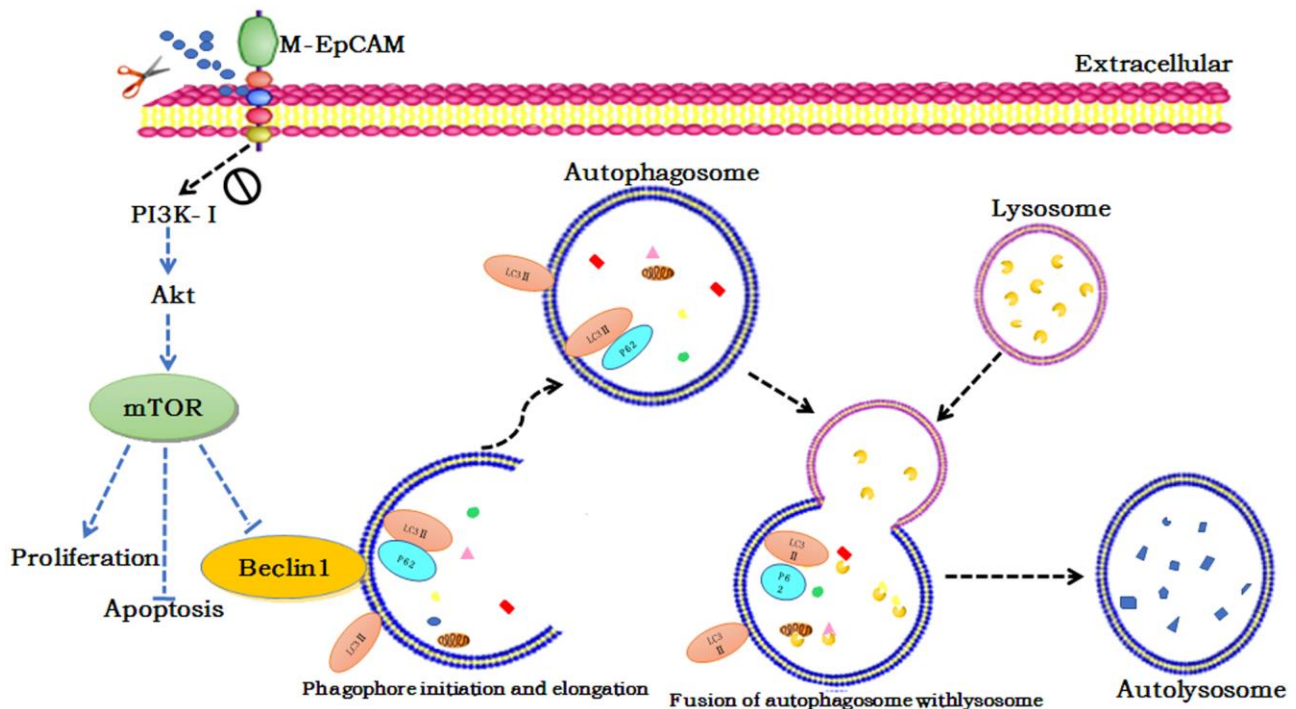


Figure 8. Schematic diagram of the proposed mechanism underlying deglycosylated EpCAM-induced autophagy participated in the proliferation an apoptosis via PI3K/Akt/mTOR signaling in breast cancer cells.

The PI3K/Akt/mTOR signaling pathway is the common way to regulate autophagy [42, 43]. Akt is phosphorylated and activated by PI3K. pAkt activates the downstream mTOR and make it phosphorylated, which is followed by down-regulation of phosphorylated p70S6K. The result induces autophagy [6, 13, 42, 44, 45]. To understand the mechanism of deglycosylated EpCAM-mediated autophagy in breast cancer cells, we analyzed the Akt-mTOR signaling pathway. Our study demonstrated that the effect of Akt-mTOR signaling on the regulation of autophagy in breast cancer cells. In addition, we also suggested that deglycosylated EpCAM facilitated cell apoptosis of breast cancer cells via PI3K/Akt signaling pathway.

CONCLUSIONS

In summary, we reported the autophagy disorder induced by three glycosylation point mutations in EpCAM in breast cancer cells. Deglycosylated EpCAM was found to be a functional marker that was required for AKT/mTOR mediated autophagy regulation in breast cancer cells. Our study further explore EpCAM functions and provides a theoretical basis for the treatment of breast cancer.

MATERIALS AND METHODS

Materials

MCF-7 and MDA-MB-231 cells were obtained from ATCC (Manassas, VA). DMEM/F12, fetal bovine serum (FBS), Lipofectamine™ Reagent was purchased from Invitrogen (Paisley, UK). The anti pAkt, Akt, pmTOR, mTOR, GAPDH and horseradish peroxidase (HRP)-conjugated anti-rabbit secondary antibody were obtained from Santa Cruz Biotechnology (Heidelberg, Germany). The anti Beclin 1, P62, ILC3, Caspase 3, Bcl2 and Bax were purchased from Proteintech (Wuhan, Hubei, China). Enhanced chemiluminescence (ECL) assay kit was purchased from Amersham (Louisville, Co).

Plasmid and RNAi sequence

EpCAM overexpression plasmid (pCMV-SPORT 6-EpCAM) was purchased from the Proteintech Group, Inc. (Wuhan, Hubei, China). siRNA for EpCAM is as follows: EpCAM-1: 5'-UGCUCUGAGCGAGUGAGA ATT-3'; EpCAM-2: 5'-UUCUCACUGCUCAGAGCA TT-3'. N-glycosylation mutant was made by replacing asparagine with glutamine in all the three N-glycosylation sites of EpCAM by TAKALA Company (Dalian, Liaoning, China). The mutation plasmid was named M-EpCAM plasmid.

Cell culture

Breast cancer cells (MCF-7 and MDA-MB-231) were cultured in medium DMEM/F12 plus 10% calf serum in a 5% CO₂ humidified atmosphere at 37° C.

Transfection

Transfection of cells with EpCAM overexpression plasmid, si-EpCAM sequence, M-EpCAM plasmid and pGFP-LC3 plasmid were performed using Lipofectamine™ Reagent according to the manufacturer's instruction.

Western blot

Cell extracts were prepared using with RIPA lysis buffer. After determination of concentration of protein, cell lysates were separated by 10% SDS-PAGE min-gel and transferred to a nitrocellulose membrane. Subsequently, the membrane was blocked using 5% non-fat milk for 2 h and then incubated with the primary antibodies overnight. After probed with horseradish peroxidase-conjugated secondary antibodies, immunoreactive proteins were visualized with ECL detection system.

Cell proliferation assay

Cells (1×10⁴ cells per well) were seeded in a 96-well plate. Cell viability was performed using an CCK8 assay, according to the manufacturer's instructions. The absorbance of OD_{450nm} was detected with a microplate reader.

Each sample was evaluated for three times for analysis.

Electron microscopy

Cells were treated with 2.5% glutaraldehyde in 0.1 M sodium cacodylate buffer, pH 7.4 for 30 minutes at room temperature and post-fixed with 1% osmium tetroxide in 0.1 M sodium cacodylate buffer, pH 7.4 for 1 hour, contrasted with 1% tannic acid in 0.05 M sodium cacodylate, followed by dehydration through graded alcohols and acetone and then embedded in EMbed 812. After using an UltraCut E ultramicrotome to cut into Ultrathin sections, samples were double-stained with 0.3% lead citrate and examined under a JEOL 1200EX electron microscope. Micrographs were taken at 60,000 or 200,000 magnifications.

Statistical analysis

The numerical data are expressed as means ± SD. Unpaired Student's t-tests were used to compare the

means of two groups. *P* value less than 0.05 was considered significant.

AUTHOR CONTRIBUTIONS

Liu Yang: Investigation, Formal analysis. Qijun Wang: Investigation, Formal analysis. Qian Zhao, Fan Yang: Investigation, Formal analysis. Tingjiao Liu: Conceptualization, Investigation. Xiaohua Huang: Investigation. Qiu Yan, Xuesong Yang: Investigation, Methodology, Writing - original draft, Visualization, Project administration, Funding acquisition.

CONFLICTS OF INTEREST

The authors declare that they have no conflicts of interest.

FUNDING

This work was supported by grants from the National Natural Science Foundation of Liaoning Province (NO. 201602242).

REFERENCES

1. Kolak A, Kamińska M, Sygit K, Budny A, Surdyka D, Kukielka-Budny B, Burdan F. Primary and secondary prevention of breast cancer. *Ann Agric Environ Med*. 2017; 24:549–53. <https://doi.org/10.26444/aaem/75943> PMID:29284222
2. Glick D, Barth S, Macleod KF. Autophagy: cellular and molecular mechanisms. *J Pathol*. 2010; 221:3–12. <https://doi.org/10.1002/path.2697> PMID:20225336
3. Hutchinson L. Breast cancer: challenges, controversies, breakthroughs. *Nat Rev Clin Oncol*. 2010; 7:669–70. <https://doi.org/10.1038/nrclinonc.2010.192> PMID:21116236
4. Jemal A, Bray F, Center MM, Ferlay J, Ward E, Forman D. Global cancer statistics. *CA Cancer J Clin*. 2011; 61:69–90. <https://doi.org/10.3322/caac.20107> PMID:21296855
5. Provenzano E, Ulaner GA, Chin SF. Molecular Classification of Breast Cancer. *PET Clin*. 2018; 13:325–38. <https://doi.org/10.1016/j.cpet.2018.02.004> PMID:30100073
6. Jung CH, Ro SH, Cao J, Otto NM, Kim DH. mTOR regulation of autophagy. *FEBS Lett*. 2010; 584:1287–95. <https://doi.org/10.1016/j.febslet.2010.01.017> PMID:20083114
7. Wen KC, Sung PL, Chou YT, Pan CM, Wang PH, Lee OK, Wu CW. The role of EpCAM in tumor progression and the clinical prognosis of endometrial carcinoma. *Gynecol Oncol*. 2018; 148:383–92. <https://doi.org/10.1016/j.ygyno.2017.11.033> PMID:29208367
8. Wilde L, Tanson K, Curry J, Martinez-Outschoorn U. Autophagy in cancer: a complex relationship. *Biochem J*. 2018; 475:1939–54. <https://doi.org/10.1042/BCJ20170847> PMID:29891531
9. Mowers EE, Sharifi MN, Macleod KF. Functions of autophagy in the tumor microenvironment and cancer metastasis. *FEBS J*. 2018; 285:1751–66. <https://doi.org/10.1111/febs.14388> PMID:29356327
10. Huang L, Yang Y, Yang F, Liu S, Zhu Z, Lei Z, Guo J. Functions of EpCAM in physiological processes and diseases (Review). *Int J Mol Med*. 2018; 42:1771–85. <https://doi.org/10.3892/ijmm.2018.3764> PMID:30015855
11. Gao J, Liu X, Yang F, Liu T, Yan Q, Yang X. By inhibiting Ras/Raf/ERK and MMP-9, knockdown of EpCAM inhibits breast cancer cell growth and metastasis. *Oncotarget*. 2015; 6:27187–98. <https://doi.org/10.18632/oncotarget.4551> PMID:26356670
12. Gao J, Yan Q, Wang J, Liu S, Yang X. Epithelial-to-mesenchymal transition induced by TGF-β1 is mediated by AP1-dependent EpCAM expression in MCF-7 cells. *J Cell Physiol*. 2015; 230:775–82. <https://doi.org/10.1002/jcp.24802> PMID:25205054
13. Paquette M, El-Houjeiri L, Pause A. mTOR Pathways in Cancer and Autophagy. *Cancers (Basel)*. 2018; 10:18. <https://doi.org/10.3390/cancers10010018> PMID:29329237
14. Varki A, Kannagi R, Toole B, Stanley P. Glycosylation Changes in Cancer. In: *Essentials of Glycobiology*. 3rd Edition, Varki A, Cummings RD, Esko JD, Stanley P, Hart GW, Aebi M, Darvill AG, Kinoshita T, Packer NH et al. editors. Cold Spring Harbor (NY): Cold Spring Harbor Laboratory Press; 2015–2017. Chapter 47. <https://www.ncbi.nlm.nih.gov/books/NBK453023/doi:10.1101/glycobiology.3e.047>
15. Marinković M, Šprung M, Buljubašić M, Novak I. Autophagy Modulation in Cancer: Current Knowledge on Action and Therapy. *Oxid Med Cell Longev*. 2018; 2018:8023821. <https://doi.org/10.1155/2018/8023821> PMID:29643976
16. Saha S, Panigrahi DP, Patil S, Bhutia SK. Autophagy in

- health and disease: A comprehensive review. *Biomed Pharmacother.* 2018; 104:485–95.
<https://doi.org/10.1016/j.biopha.2018.05.007>
 PMID:[29800913](https://pubmed.ncbi.nlm.nih.gov/29800913/)
17. Zhu Y, Shan X, Safarpour F, Erro Go N, Li N, Shan A, Huang MC, Deen M, Holicek V, Ashmus R, Madden Z, Gorski S, Silverman MA, Vocadlo DJ. Pharmacological Inhibition of O-GlcNAcase Enhances Autophagy in Brain through an mTOR-Independent Pathway. *ACS Chem Neurosci.* 2018; 9:1366–79.
<https://doi.org/10.1021/acschemneuro.8b00015>
 PMID:[29460617](https://pubmed.ncbi.nlm.nih.gov/29460617/)
 18. Lee HJ, Venkatarama Gowda Saralamma V, Kim SM, Ha SE, Raha S, Lee WS, Kim EH, Lee SJ, Heo JD, Kim GS. Pectolarigenin Induced Cell Cycle Arrest, Autophagy, and Apoptosis in Gastric Cancer Cell via PI3K/AKT/mTOR Signaling Pathway. *Nutrients.* 2018; 10:1043.
<https://doi.org/10.3390/nu10081043> PMID:[30096805](https://pubmed.ncbi.nlm.nih.gov/30096805/)
 19. Schnell U, Cirulli V, Giepmans BN. EpCAM: structure and function in health and disease. *Biochim Biophys Acta.* 2013; 1828:1989–2001.
<https://doi.org/10.1016/j.bbamem.2013.04.018>
 PMID:[23618806](https://pubmed.ncbi.nlm.nih.gov/23618806/)
 20. Pauli C, Münz M, Kieu C, Mack B, Breinl P, Wollenberg B, Lang S, Zeidler R, Gires O. Tumor-specific glycosylation of the carcinoma-associated epithelial cell adhesion molecule EpCAM in head and neck carcinomas. *Cancer Lett.* 2003; 193:25–32.
[https://doi.org/10.1016/s0304-3835\(03\)00003-x](https://doi.org/10.1016/s0304-3835(03)00003-x)
 PMID:[12691820](https://pubmed.ncbi.nlm.nih.gov/12691820/)
 21. Singh SS, Vats S, Chia AY, Tan TZ, Deng S, Ong MS, Arfuso F, Yap CT, Goh BC, Sethi G, Huang RY, Shen HM, Manjithaya R, Kumar AP. Dual role of autophagy in hallmarks of cancer. *Oncogene.* 2018; 37:1142–58.
<https://doi.org/10.1038/s41388-017-0046-6>
 PMID:[29255248](https://pubmed.ncbi.nlm.nih.gov/29255248/)
 22. Zhang D, Liu X, Gao J, Sun Y, Liu T, Yan Q, Yang X. The role of epithelial cell adhesion molecule N-glycosylation on apoptosis in breast cancer cells. *Tumour Biol.* 2017; 39:1010428317695973.
<https://doi.org/10.1177/1010428317695973>
 PMID:[28349835](https://pubmed.ncbi.nlm.nih.gov/28349835/)
 23. Salazar-Roa M, Malumbres M. Fueling the Cell Division Cycle. *Trends Cell Biol.* 2017; 27:69–81.
<https://doi.org/10.1016/j.tcb.2016.08.009>
 PMID:[27746095](https://pubmed.ncbi.nlm.nih.gov/27746095/)
 24. Zhang HW, Hu JJ, Fu RQ, Liu X, Zhang YH, Li J, Liu L, Li YN, Deng Q, Luo QS, Ouyang Q, Gao N. Flavonoids inhibit cell proliferation and induce apoptosis and autophagy through downregulation of PI3K mediated PI3K/AKT/mTOR/p70S6K/ULK signaling pathway in human breast cancer cells. *Sci Rep.* 2018; 8:11255.
<https://doi.org/10.1038/s41598-018-29308-7>
 PMID:[30050147](https://pubmed.ncbi.nlm.nih.gov/30050147/)
 25. White E, Mehnert JM, Chan CS. Autophagy, Metabolism, and Cancer. *Clin Cancer Res.* 2015; 21:5037–46.
<https://doi.org/10.1158/1078-0432.CCR-15-0490>
 PMID:[26567363](https://pubmed.ncbi.nlm.nih.gov/26567363/)
 26. Dikic I, Johansen T, Kirkin V. Selective autophagy in cancer development and therapy. *Cancer Res.* 2010; 70:3431–4.
<https://doi.org/10.1158/0008-5472.CAN-09-4027>
 PMID:[20424122](https://pubmed.ncbi.nlm.nih.gov/20424122/)
 27. Cagnol S, Chambard JC. ERK and cell death: mechanisms of ERK-induced cell death--apoptosis, autophagy and senescence. *FEBS J.* 2010; 277:2–21.
<https://doi.org/10.1111/j.1742-4658.2009.07366.x>
 PMID:[19843174](https://pubmed.ncbi.nlm.nih.gov/19843174/)
 28. Mizushima N, Yoshimori T, Levine B. Methods in mammalian autophagy research. *Cell.* 2010; 140:313–26.
<https://doi.org/10.1016/j.cell.2010.01.028>
 PMID:[20144757](https://pubmed.ncbi.nlm.nih.gov/20144757/)
 29. Thorburn A. Autophagy and disease. *J Biol Chem.* 2018; 293:5425–30.
<https://doi.org/10.1074/jbc.R117.810739>
 PMID:[29191833](https://pubmed.ncbi.nlm.nih.gov/29191833/)
 30. Cheng WK, Oon CE. How glycosylation aids tumor angiogenesis: An updated review. *Biomed Pharmacother.* 2018; 103:1246–52.
<https://doi.org/10.1016/j.biopha.2018.04.119>
 PMID:[29864905](https://pubmed.ncbi.nlm.nih.gov/29864905/)
 31. Pinho SS, Reis CA. Glycosylation in cancer: mechanisms and clinical implications. *Nat Rev Cancer.* 2015; 15:540–55.
<https://doi.org/10.1038/nrc3982> PMID:[26289314](https://pubmed.ncbi.nlm.nih.gov/26289314/)
 32. Fahie K, Zachara NE. Molecular Functions of Glycoconjugates in Autophagy. *J Mol Biol.* 2016; 428:3305–24.
<https://doi.org/10.1016/j.jmb.2016.06.011>
 PMID:[27345664](https://pubmed.ncbi.nlm.nih.gov/27345664/)
 33. Li YN, Hu JA, Wang HM. Inhibition of HIF-1 α Affects Autophagy Mediated Glycosylation in Oral Squamous Cell Carcinoma Cells. *Dis Markers.* 2015; 2015:239479.
<https://doi.org/10.1155/2015/239479> PMID:[26640316](https://pubmed.ncbi.nlm.nih.gov/26640316/)
 34. Maiuri MC, Zalckvar E, Kimchi A, Kroemer G. Self-eating and self-killing: crosstalk between autophagy and apoptosis. *Nat Rev Mol Cell Biol.* 2007; 8:741–52.
<https://doi.org/10.1038/nrm2239>
 PMID:[17717517](https://pubmed.ncbi.nlm.nih.gov/17717517/)
 35. Gatica D, Chiong M, Lavandero S, Klionsky DJ.

- Molecular mechanisms of autophagy in the cardiovascular system. *Circ Res.* 2015; 116:456–67.
<https://doi.org/10.1161/CIRCRESAHA.114.303788>
PMID:[25634969](https://pubmed.ncbi.nlm.nih.gov/25634969/)
36. Rogalińska M. Alterations in cell nuclei during apoptosis. *Cell Mol Biol Lett.* 2002; 7:995–1018.
PMID:[12511968](https://pubmed.ncbi.nlm.nih.gov/12511968/)
37. El-Khattouti A, Selimovic D, Haikel Y, Hassan M. Crosstalk between apoptosis and autophagy: molecular mechanisms and therapeutic strategies in cancer. *J Cell Death.* 2013; 6:37–55.
<https://doi.org/10.4137/JCD.S11034>
PMID:[25278778](https://pubmed.ncbi.nlm.nih.gov/25278778/)
38. Eisenberg-Lerner A, Bialik S, Simon HU, Kimchi A. Life and death partners: apoptosis, autophagy and the cross-talk between them. *Cell Death Differ.* 2009; 16:966–75.
<https://doi.org/10.1038/cdd.2009.33>
PMID:[19325568](https://pubmed.ncbi.nlm.nih.gov/19325568/)
39. Li M, Gao P, Zhang J. Crosstalk between Autophagy and Apoptosis: Potential and Emerging Therapeutic Targets for Cardiac Diseases. *Int J Mol Sci.* 2016; 17:332.
<https://doi.org/10.3390/ijms17030332>
PMID:[26950124](https://pubmed.ncbi.nlm.nih.gov/26950124/)
40. Liu G, Pei F, Yang F, Li L, Amin AD, Liu S, Buchan JR, Cho WC. Role of Autophagy and Apoptosis in Non-Small-Cell Lung Cancer. *Int J Mol Sci.* 2017; 18:367.
<https://doi.org/10.3390/ijms18020367>
PMID:[28208579](https://pubmed.ncbi.nlm.nih.gov/28208579/)
41. Liu W, Wang X, Liu Z, Wang Y, Yin B, Yu P, Duan X, Liao Z, Chen Y, Liu C, Li X, Dai Y, Tao Z. SGK1 inhibition induces autophagy-dependent apoptosis via the mTOR-Foxo3a pathway. *Br J Cancer.* 2017; 117:1139–53.
<https://doi.org/10.1038/bjc.2017.293> PMID:[29017179](https://pubmed.ncbi.nlm.nih.gov/29017179/)
42. Wu YT, Tan HL, Huang Q, Ong CN, Shen HM. Activation of the PI3K-Akt-mTOR signaling pathway promotes necrotic cell death via suppression of autophagy. *Autophagy.* 2009; 5:824–34.
<https://doi.org/10.4161/auto.9099> PMID:[19556857](https://pubmed.ncbi.nlm.nih.gov/19556857/)
43. Surviladze Z, Sterk RT, DeHaro SA, Ozbun MA. Cellular entry of human papillomavirus type 16 involves activation of the phosphatidylinositol 3-kinase/Akt/mTOR pathway and inhibition of autophagy. *J Virol.* 2013; 87:2508–17.
<https://doi.org/10.1128/JVI.02319-12> PMID:[23255786](https://pubmed.ncbi.nlm.nih.gov/23255786/)
44. Heinonen H, Nieminen A, Saarela M, Kallioniemi A, Klefström J, Hautaniemi S, Monni O. Deciphering downstream gene targets of PI3K/mTOR/p70S6K pathway in breast cancer. *BMC Genomics.* 2008; 9:348.
<https://doi.org/10.1186/1471-2164-9-348>
PMID:[18652687](https://pubmed.ncbi.nlm.nih.gov/18652687/)
45. Heras-Sandoval D, Pérez-Rojas JM, Hernández-Damián J, Pedraza-Chaverri J. The role of PI3K/AKT/mTOR pathway in the modulation of autophagy and the clearance of protein aggregates in neurodegeneration. *Cell Signal.* 2014; 26:2694–701.
<https://doi.org/10.1016/j.cellsig.2014.08.019>
PMID:[25173700](https://pubmed.ncbi.nlm.nih.gov/25173700/)

A comprehensive analysis of FOX family in HCC and experimental evidence to support the oncogenic role of FOXH1

Xiwu Ouyang¹, Lemeng Feng¹, Lei Yao¹, Jingyu Zhang¹, Yao Xiao², Guodong Liu³, Gewen Zhang¹, Zhiming Wang¹

¹Department of Liver Surgery, Xiangya Hospital, Central South University, Changsha 410008, Hunan, China

²Department of Pancreatic Surgery, Xiangya Hospital, Central South University, Changsha 410008, Hunan, China

³Department of Biliary Surgery, Xiangya Hospital, Central South University, Changsha 410008, Hunan, China

Correspondence to: Zhiming Wang; **email:** zhimingwang@csu.edu.cn

Keywords: FOX, HCC, FOXH1, prognosis, cell invasion

Received: April 20, 2020

Accepted: September 9, 2020

Published: March 7, 2022

Copyright: © 2022 Ouyang et al. This is an open access article distributed under the terms of the [Creative Commons Attribution License](https://creativecommons.org/licenses/by/3.0/) (CC BY 3.0), which permits unrestricted use, distribution, and reproduction in any medium, provided the original author and source are credited.

ABSTRACT

Hepatocellular carcinoma (HCC) remains the second leading cause of cancer related deaths worldwide. Understanding about the molecular biology of HCC and development of targeted therapies are still the main focuses of this type of disease. Here, by connecting the expression levels of FOX proteins with their associated clinical characteristics using TCGA LIHC dataset, we found that 27/40 FOX proteins were highly expressed in HCC tumors compared to normal liver tissues and their expression levels were tightly associated with HCC tumor stage, tumor grade and overall survival. Our experimental results also confirmed that FOXH1 indeed played an oncogenic role in HCC development by promoting cell growth and cell migration/invasion. Mechanistic dissection demonstrated that FOXH1-induced cell growth and cell migration/invasion relied on mTOR signaling because inhibition of mTOR signaling by rapamycin could attenuate FOXH1-mediated phenotypic alterations of HCC cells. The results from orthotopic mouse model also validated that FOXH1 promoted HA22T tumor growth via triggering mTOR activation. Overall, this study not only comprehensively examines the clinical values of FOX proteins in HCC but also provides experimental evidence to support the role of FOXH1 in HCC development, building rationale to develop more effective therapies to treat HCC patients.

INTRODUCTION

Hepatocellular carcinoma (HCC) is the most common primary hepatic cancer with an estimated 0.8 million incident cases in 2018 [1]. The majority of HCC occurs in people with either hepatitis B/C infection or aflatoxin exposure [2, 3]. Although current therapies including surgical dissection, liver transplantation, radiation therapy, targeted therapy and immune therapy improve patients' lives a lot [4], the mortality of HCC is still very high, with an estimated 0.7 million deaths in 2018, and is responsible for the second leading cause of cancer associated deaths worldwide [1, 5]. Therefore, there is an urgent need to

develop novel therapeutic strategies for better treatment of HCC patients.

As transcription factors, Forkhead Box (FOX) proteins are involved in various biological events such as proliferation, apoptosis, DNA repair and metabolism either alone or together with other transcription factors/cofactors [6]. Numerous studies have proved that the dysregulation of FOX proteins was tightly associated with cancer initiation, progression, and drug resistance [6–9]. For instance, the expression level of FOXC1 was significantly increased in HCC and it functioned as an independent predictor for HCC survival and tumor recurrence. FOXC1 promoted HCC tumor metastasis via

transactivating Snail [10], a central transcription factor regulating a bundle of metastasis-related genes. Besides, the oncogenic roles of FOXG1, FOXO3, FOXK1 and FOXM1 in HCC carcinogenesis have also been recognized in recent years [11–15], suggesting that FOX proteins may be the potentially therapeutic targets of HCC. However, few efforts have been taken to comprehensively evaluate the clinical values of FOX proteins and to unfold the role of FOXH1 in HCC.

The role of mTOR (mammalian target of rapamycin) signaling has been well documented in cancer development including HCC [16, 17]. The common subunits of mTOR complex at least include the mTOR kinase, mLST8 (the mammalian lethal with SEC13 protein 8), DEPTOR (DEP Domain Containing MTOR Interacting Protein), Tel2 (telomere maintenance 2) and Tti1 (Tel2-interacting protein 1) [18, 19]. RAPTOR in mTORC1 and RICTOR in mTORC2 make these two complexes different. In HCC patients, activation of the mTOR pathway was observed in 40-50% HCC patients and was closely associated with HCC poor prognosis and early recurrence [17, 20], which facilitated the development of mTOR inhibitors for clinical applications.

In this study, our analyses from TCGA dataset revealed that the majority of FOX proteins (27/40) was overexpressed in HCC patients and their expression levels were tightly correlated with tumor stage, tumor grade and overall survival of HCC patients. We also verified that FOXH1 was indeed highly expressed in our collected HCC samples compared to the corresponding adjacent tissues. And experimental results demonstrated that FOXH1 played an oncogenic role in HCC development, which was partially due to the activation of mTOR signaling. Indeed, inhibition of mTOR signaling with rapamycin could reverse FOXH1-induced HCC cell growth and cell invasion/migration. Furthermore, our *in vivo* animal data also confirmed that FOXH1 promoted HCC tumor growth. Overall, our study comprehensively analyzes the clinical values of FOX proteins in HCC and provides compelling rationale to develop FOX proteins either as diagnostic/prognostic or therapeutic biomarkers for better treatment of HCC patients.

RESULTS

Expression levels of FOX family members were increased in HCC patients

A lack of comprehensive analysis of FOX family members in HCC patients led us to examine their expression levels by using UALCAN (<http://ualcan.path.uab.edu>) online tool. As data presented in Figure 1,

27 FOX family members were highly expressed in HCC patients compared to normal liver tissues. Of note, other 13 FOX members failed to show this trend (Supplementary Figure 1): 7 FOX proteins (FOX B1, FOX B2, FOX G1, FOX I1, FOX N1, FOX R1 and FOX R2) were undetectable in both HCC and liver tissues; 4 FOX members (FOX D3, FOX F1, FOX O1 and FOX P2) were under expressed in HCC patients; FOX A3 and FOX P3 were indistinguishably expressed between HCC and normal liver tissues. Moreover, protein examination by Human Protein Atlas (<https://www.proteinatlas.org>) also confirmed that the majority of FOX proteins was overexpressed in HCC patients (Figure 2). Together, these analyses suggest that most FOX family proteins are highly expressed in HCC samples and they may serve as oncogenic factors to promote HCC progression.

The expression levels of FOX proteins were independent predictors for overall survival of HCC patients

To explore whether the expression levels of FOX proteins were associated with the prognosis of HCC, we first divided HCC patients into low-risk (n=181) and high-risk (n=180) group using the median expression level of individual FOX as a cutoff (Figure 3A). Cox overall survival analysis in SurvExpress (<http://bioinformatica.mty.itesm.mx:8080/Biomatec/SurvivaX.jsp>) demonstrated that high-risk group had poor overall survival compared to low risk group (Figure 3B, HR=2.16, P<0.001), indicating that the expression levels of these FOX proteins were highly associated with the overall survival of HCC. Also, the association of individual FOX protein with the overall survival of HCC was analyzed by UALCAN, which revealed that the majority of FOX proteins was highly expressed in HCC patients who had shorter overall survival time (Figure 3C). Furthermore, we also found that the expression levels of most FOX proteins were also tightly associated with tumor stage, tumor grade and metastatic status of HCC. Data showed that high grade, high stage or metastatic HCC patients tended to express high levels of FOX proteins (Supplementary Figures 2–4). Of note, although metastatic HCC expressed higher levels of FOX proteins, there was no statistically significant difference, largely due to the small sample size (n=4). Collectively, all these findings indicate that the expression levels of most FOX family members can serve as independent predictors for the prognosis of HCC patients.

Experimental evidence suggested that FOXH1 promoted HCC development

Next, we turned our focus on FOXH1 because its role in HCC progression has not yet been determined. The

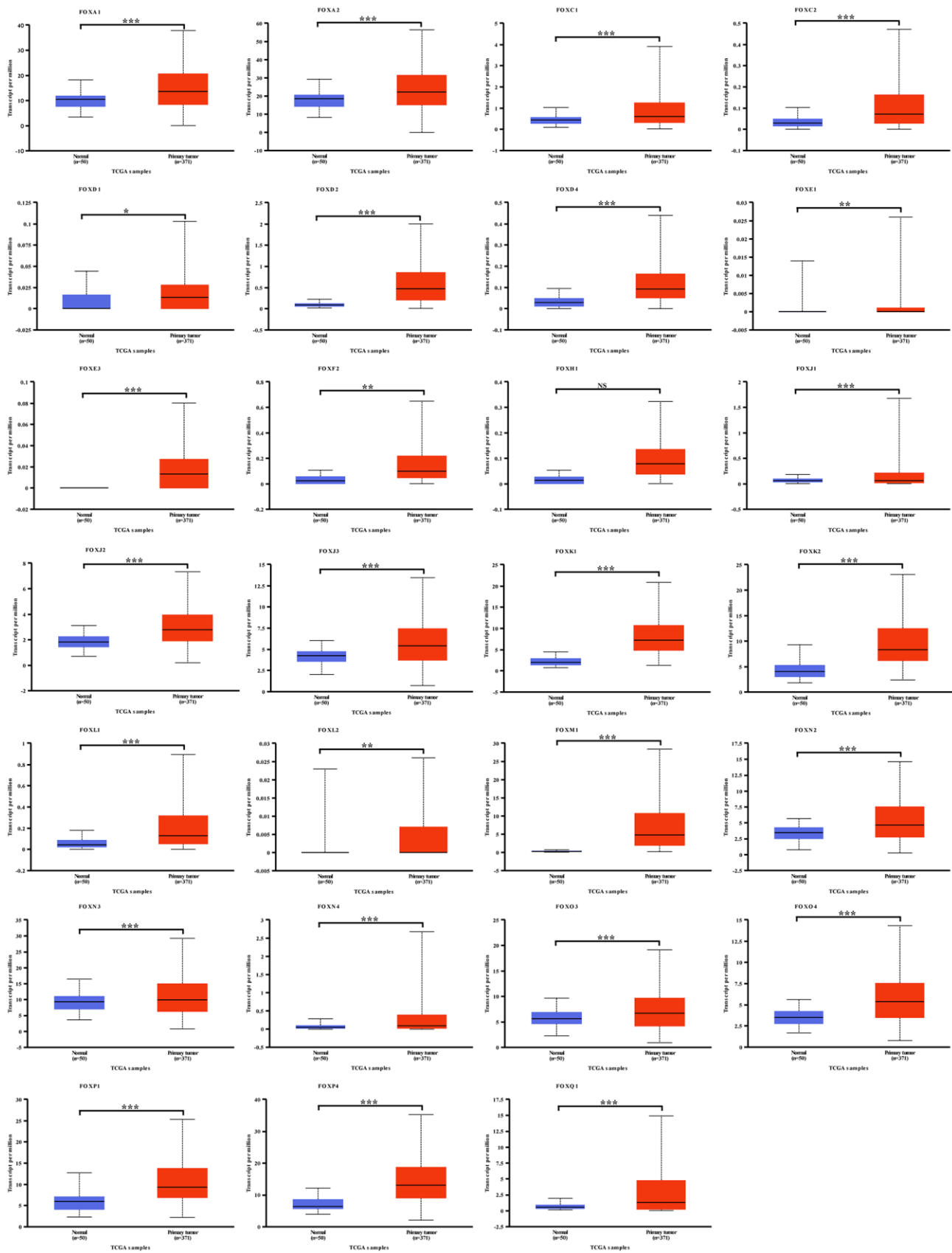


Figure 1. Expression levels of FOX family members were upregulated in HCC patients. 27 FOX proteins were upregulated in HCC patients compared to the normal liver tissues. *P<0.05, **P<0.01, ***P<0.001.

expression level of FOXH1 was tightly associated with tumor stage, tumor grade and overall survival of HCC (Figure 3C and Supplementary Figures 2–4). Indeed, overexpression of FOXH1 in HA22T promoted their growth, monitored by MTT assay (Figure 4A). Similar result was gained in SK-HEP-1 cells (Figure 4B). On the contrary, FOXH1 depletion by shRNAs suppressed cell growth of HA22T and SK-HEP-1 cells (Figure 4C, 4D). Also, our data revealed that overexpression of FOXH1 increased the colony forming ability of HA22T

cells (Figure 4E) while knockdown of FOXH1 inhibited the colony forming ability of HA22T cells (Figure 4F).

Next, we sought to investigate whether FOXH1 could regulate cell migration and cell invasion of HCC cells. Results from wound healing assay indicated that FOXH1 overexpression could increase cell migrating ability of both HA22T and SK-HEP-1 cells (Figure 4G) while FOXH1 depletion led to suppressed cell migration of HA22T and SK-HEP-1 cells (Figure 4H).

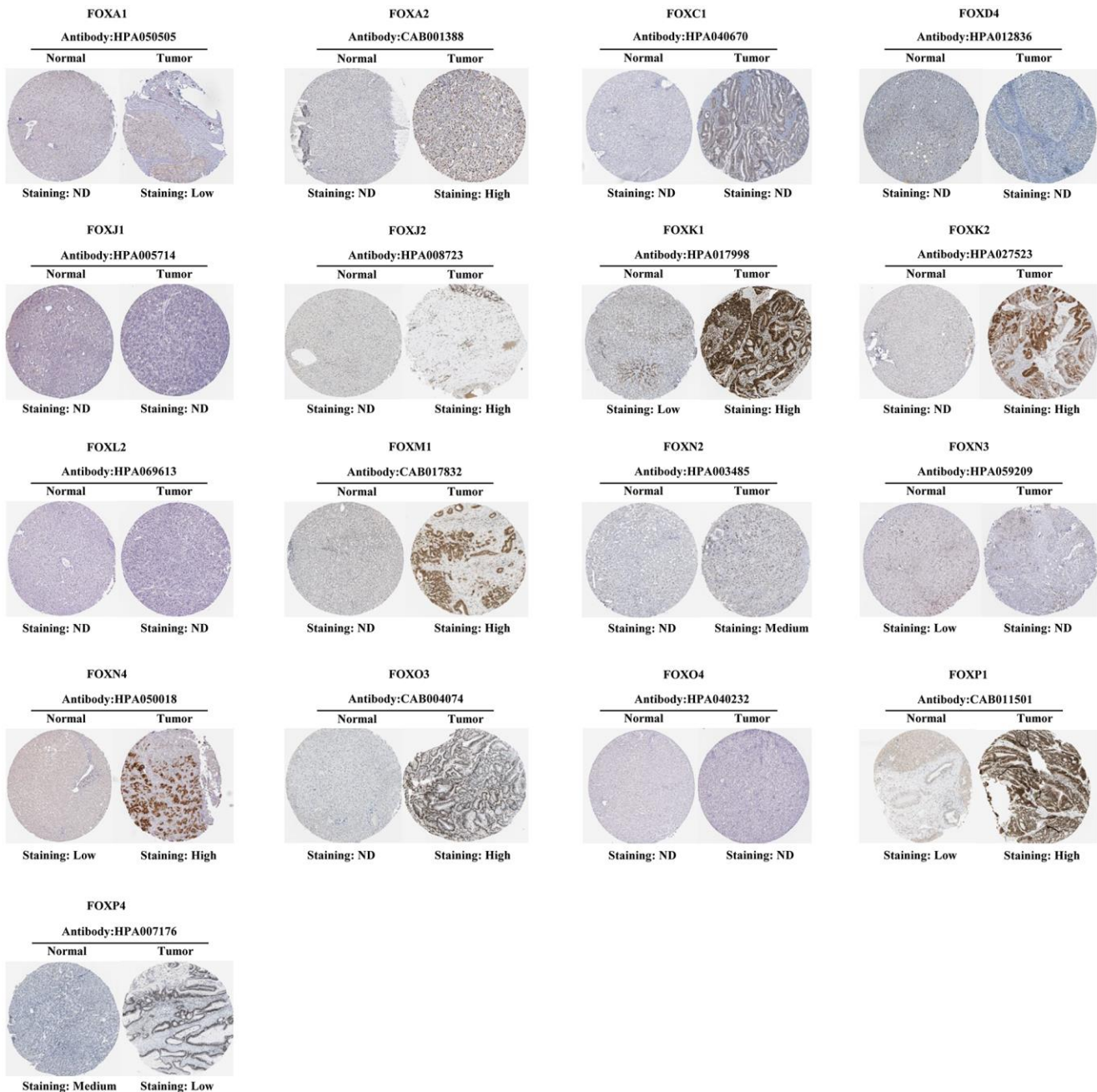


Figure 2. Representative immunohistochemical images of FOX proteins in HCC samples and the normal liver tissues. ND: Not detectable.

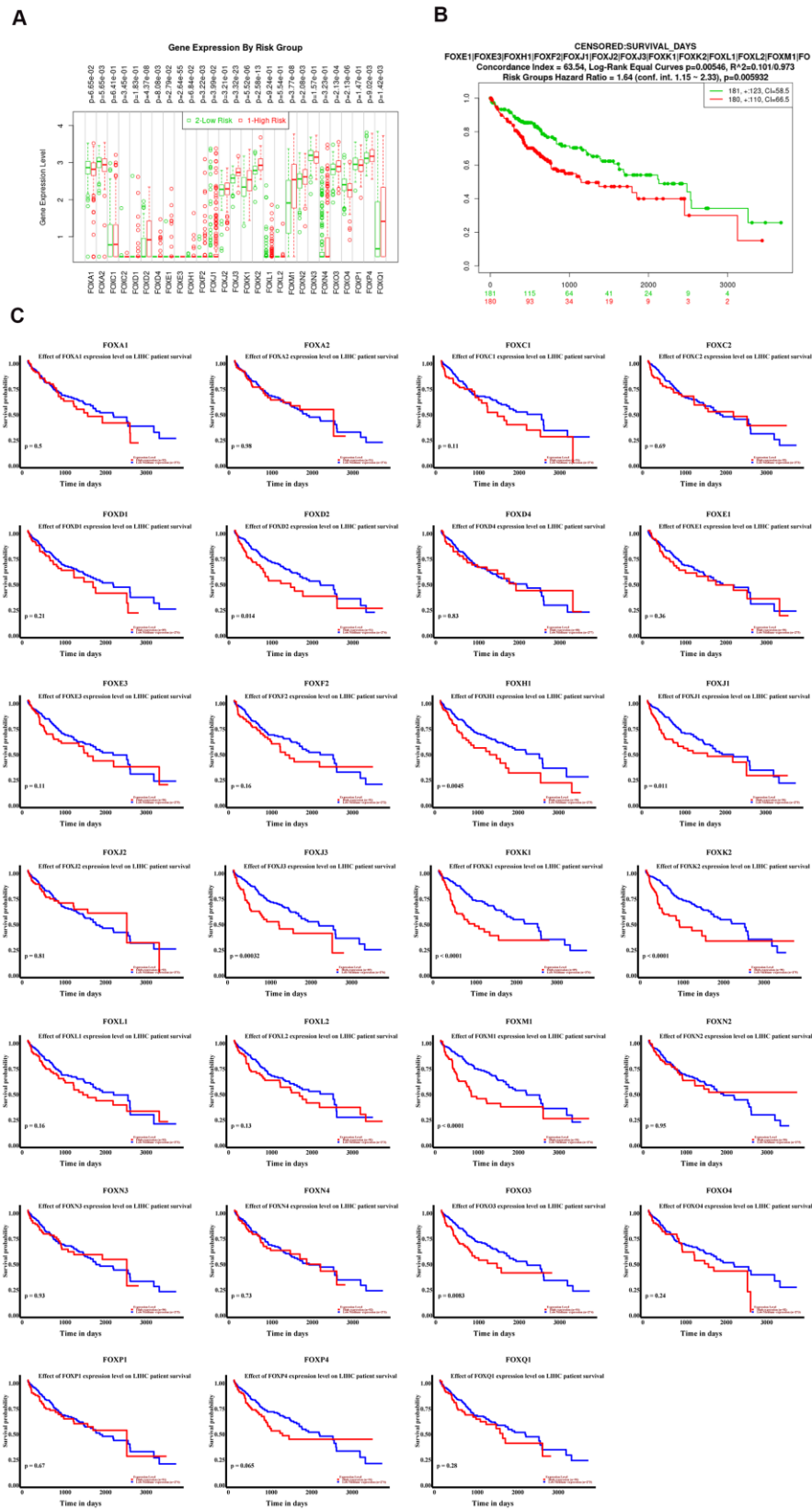


Figure 3. The expression levels of FOX proteins were independent predictors for overall survival of HCC patients. (A) The Box plots of individual FOX protein in low (green) and high (red) risk groups of TCGA-LIHC patients. **(B)** Cox overall survival analysis in SurvExpress showed that HCC patients with high expression levels of FOX proteins had shorter overall survival. **(C)** The association between Individual FOX protein expression level with overall survival of HCC. * $P < 0.05$, ** $P < 0.01$, *** $P < 0.001$.

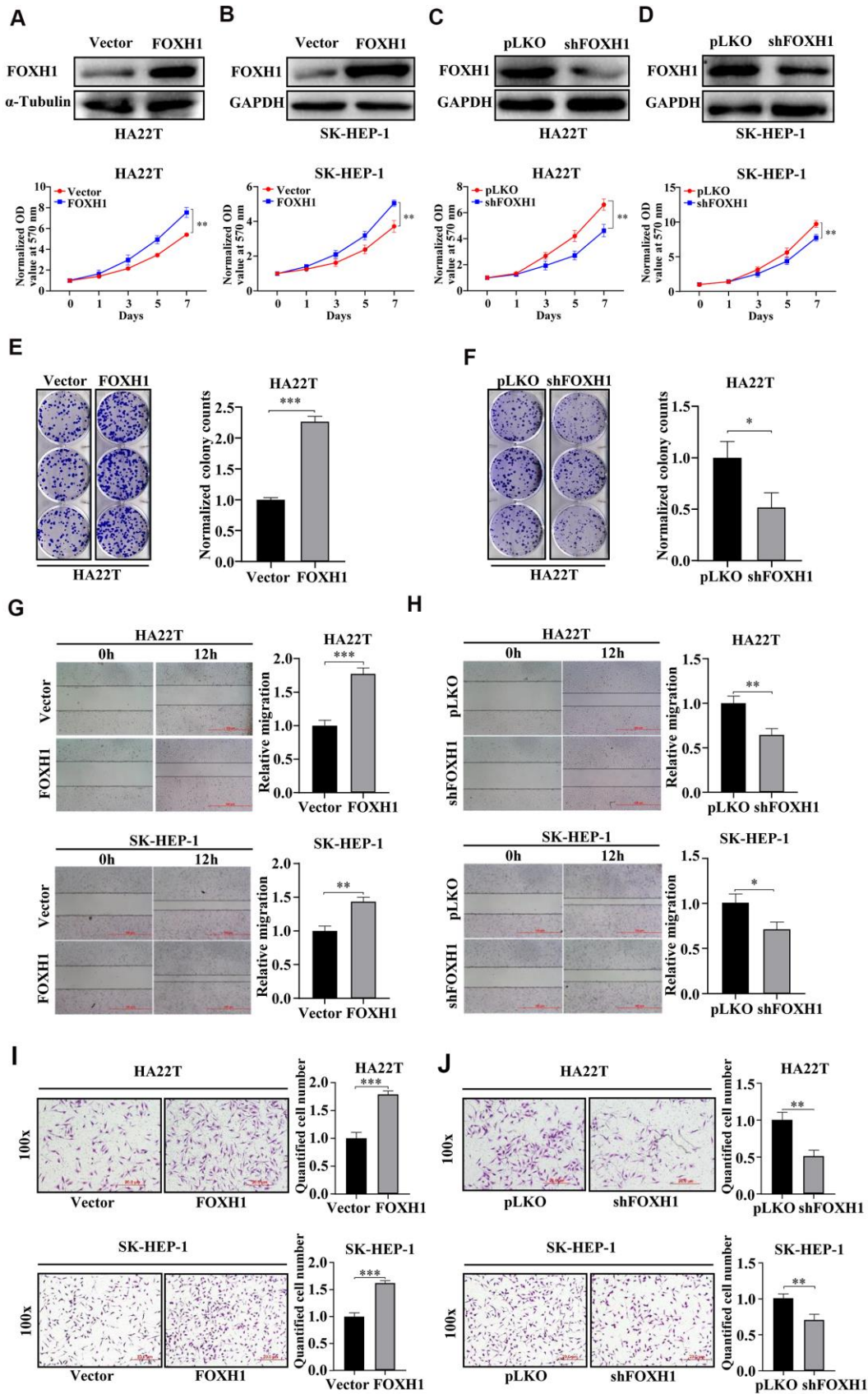


Figure 4. Experimental evidence suggested that FOXH1 promoted HCC development. (A, B) Top, the efficiency of FOXH1 overexpression. GAPDH was internal control. Bottom, MTT assay demonstrated that overexpression of FOXH1 promoted cell growth of

HA22T (A) and SK-HEP-1 cells (B). (C, D) Top, efficiency of FOXH1 knockdown. GAPDH was loading control. Bottom, MTT assay revealed that knockdown of FOXH1 reduced cell growth of HA22T (C) and SK-HEP-1 cells (D). (E) FOXH1 HA22T cells had better colony forming ability than Vector HA22T cells. Left, representative images of colonies. Right, statistical analysis. (F) FOXH1 depleted HA22T cells formed less colonies than the control cells. Left, representative images of colonies. Right, statistical analysis. (G) Overexpression of FOXH1 increased cell migrating ability of HA22T (top) and SK-HEP-1 cells (bottom) cells. Left, representative images of wounding healing assay. Right, statistical analysis. (H) FOXH1 knockdown suppressed the migrating ability of HA22T (top) and SK-HEP-1 cells (bottom) cells. Left, representative images of wounding healing assay. Right, statistical analysis. (I) Overexpression of FOXH1 promoted cell invasion of HA22T (top) and SK-HEP-1 (bottom) cells. Left, representative images of wounding healing assay. Right, statistical analysis. (J) Knockdown of FOXH1 decreased cell invasion of HA22T (top) and SK-HEP-1 (bottom) cells. Left, representative images of wounding healing assay. Right, statistical analysis. * $P < 0.05$, ** $P < 0.01$, *** $P < 0.001$.

Consistently, data from transwell invasion assay suggested that HA22T and SK-HEP-1 cells with FOXH1 overexpression had stronger invasive abilities compared to the corresponding control cells (Figure 4I). In contrast, knockdown of FOXH1 evidently suppressed cell invasion of HA22T and SK-HEP-1 cells (Figure 4J). Taken together, these results illustrate that FOXH1 plays an oncogenic role in HCC development by promoting cell growth and cell migration/invasion.

FOXH1 mediated cell growth and cell migration/cell invasion of HCC cells were dependent of mTOR signaling

To dissect the underlying mechanisms responsible for FOXH1 mediated cell growth and cell migration/invasion, we first performed GSEA KEGG pathway analysis to examine which signaling pathways were tightly associated with FOXH1 level. By dividing HCC patients into two groups ($n=187$ for each group) using the median expression level of FOXH1 as cutoff, we found that mTOR signaling was highly enriched in HCC patients with high level of FOXH1 (Figure 5A and Supplementary Figure 5, $p=0.003$). To end this, we performed the rescue assay by using mTOR specific inhibitor, rapamycin, to test whether FOXH1 mediated phenotypes of HCC cells were caused by mTOR activation. Expectedly, data revealed that FOXH1 lost its ability to increase cell growth of HA22T and SK-HEP-1 cells in the presence of 10 nM rapamycin (Figure 5B), monitored by MTT assay. Colony formation assay also showed that FOXH1 failed to increase the colony number of HA22T cells when these cells were treated with 10 nM rapamycin (Figure 5C). Moreover, inhibition of mTOR signaling with rapamycin could also reverse FOXH1 induced HCC cell migration and cell invasion of HA22T and SK-HEP-1 cells (Figure 5D, 5E). As the downstream indicator of mTOR signaling, the phosphorylation level of S6K1 was also increased by FOXH1 induction, which was attenuated by rapamycin treatment (Figure 5F). Together, all these data support the notion that FOXH1 mediated cell growth and cell migration/invasion are at least partially caused by the activation of mTOR signaling.

***In vivo* and clinical evidence confirmed the oncogenic role of FOXH1 in HCC development**

To test whether FOXH1 promoted HCC progression *in vivo*, we first orthotopically implanted luciferase-based Vector or FOXH1 HA22T (1X106) into the livers of nude mice and examined tumor growth by using IVIS system. Data showed that FOXH1 indeed could significantly promote HCC tumor growth (Figure 6A, 6B). Most importantly, FOXH1 HA22T tumors were considerably suppressed when we administrated them with 2 mg/kg rapamycin (Figure 6A, 6B), strengthening the notion that the contribution of FOXH1 to HCC progression was at least partially dependent of mTOR signaling. Immunohistochemical staining of mTOR signaling marker, p-S6K1, also confirmed that the tumor promoting role of FOXH1 in HA22T xenografted mouse model was dependent of mTOR activation (Figure 6C, 6D). Moreover, we collected HCC samples (clinical information was listed in Table 1) and the paired adjacent liver tissues to examine FOXH1 level. Consistent to our above results, high expression level of FOXH1 was observed in 16 HCC patients compared to the paired adjacent liver tissues (Figure 6E), which was also validated with immunohistochemical staining of FOXH1 in these 16 paired tissues (Figure 6F). Collectively, all these *in vivo* and clinical results demonstrate that FOXH1 serves as a tumor promoting factor controlling HCC tumor development.

DISCUSSION

Identification of novel diagnostic/prognostic or therapeutic biomarkers of HCC is still one of scientific focuses. In this study, we comprehensively analyzed the potential clinical value of individual FOX protein in HCC by using TCGA-LIHC dataset. Our data revealed that the majority of FOX proteins was highly expressed in HCC patients using the normal liver tissues as controls. Also, higher expression levels of FOX proteins were associated with higher stage, higher metastasis and shorter survival time of HCC. Importantly, our experimental confirmation using FOXH1 as example suggested that FOXH1 indeed promoted HCC progression by triggering mTOR activation. Our study not only pinpoints the clinical value of each FOX

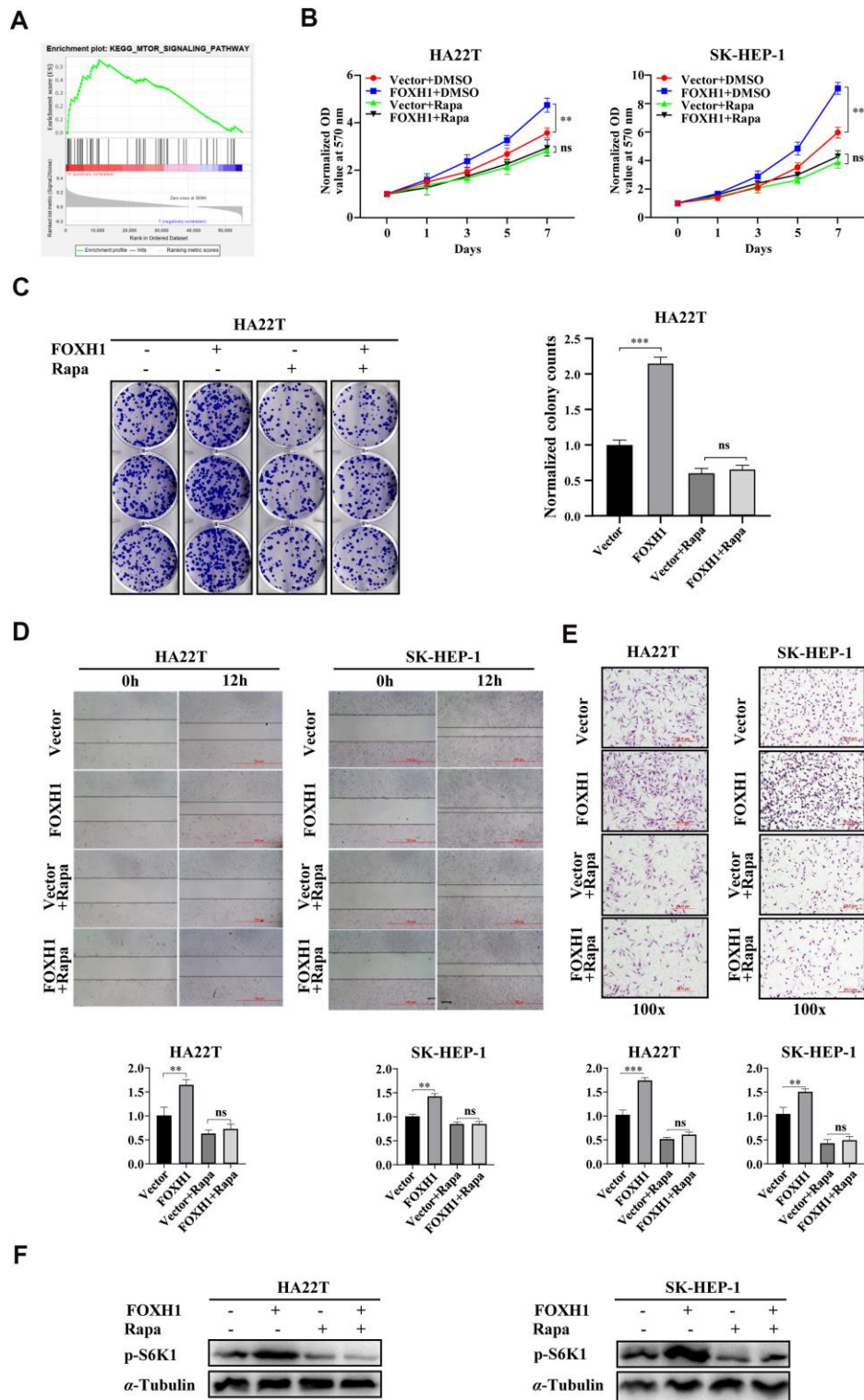


Figure 5. FOXH1 mediated cell growth and cell migration/cell invasion of HCC cells were dependent of mTOR signaling. (A) GSEA KEGG analysis showed that mTOR signaling was enriched in high FOXH1 HCC patients. (B) FOXH1 mediated cell growth of HA22T and SK-HEP-1 cells was blocked by mTOR inhibitor rapamycin (Rapa). (C) Colony formation assay showed that FOXH1 induced cell growth of HA22T cells was attenuated by rapamycin. Left, representative images of colonies. Right, statistical analysis. (D) FOXH1 lost the ability to increase cell migration of HA22T and SK-HEP-1 cells in the presence of rapamycin. Top, representative images of wounding healing assay. Bottom, statistical analysis. (E) FOXH1 failed to increase cell invasion of HA22T and SK-HEP-1 cells in the presence of rapamycin. Top, representative images of invading cells. Bottom, statistical analysis. (F) FOXH1 induced phosphorylation levels of S6K1 were blocked by rapamycin. GAPDH served as loading control. * $P < 0.05$, ** $P < 0.01$, *** $P < 0.001$.

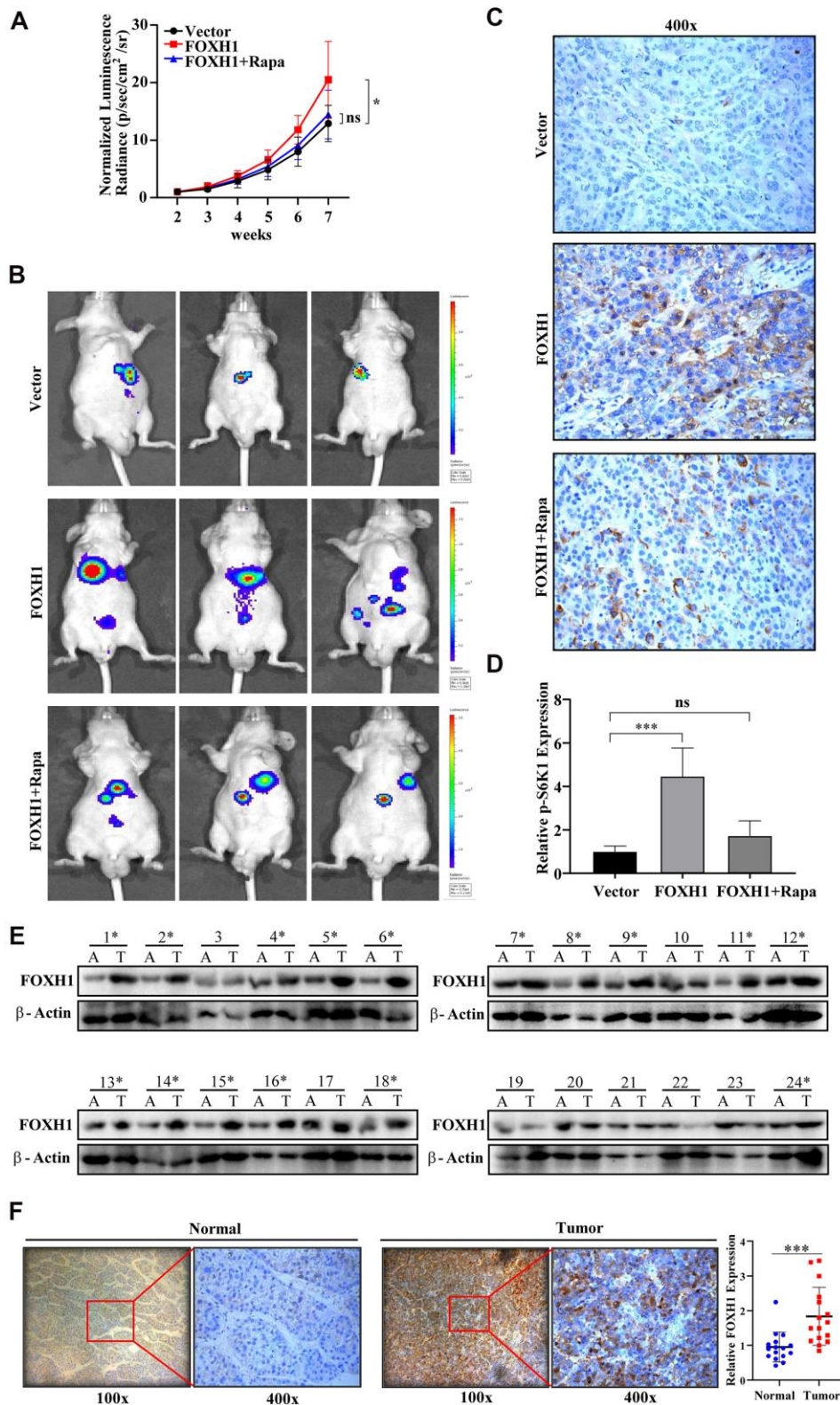


Figure 6. *In vivo* and clinical evidence confirmed the oncogenic role of FOXH1 in HCC development. (A) The HA22T tumor growth curve. (B) Representative images of HA22T tumors. (C) p-S6K1 staining showed that FOXH1 promoted HA22T tumor growth was dependent of mTOR activation. (D) A statistical analysis of p-S6K1 level. (E) Western blotting analysis of FOXH1 in 24 HCC samples with their paired adjacent liver tissues. (F) IHC staining of FOXH1 in HCC samples using their corresponding adjacent liver tissues as controls. Left, representative image of FOXH1 staining in slides made from patient 1#. Right, statistical analysis of FOXH1 staining. Scale bar: 25 μ m. * $P < 0.05$, ** $P < 0.01$, *** $P < 0.001$.

Table 1. Clinicopathological characteristics of HCC patients (N=24).

Patient code	Patient ID	Gender	Age, year	Tumor number	HBsAg	AFP, ng/mL	Liver cirrhosis	BCLC stage	TNM stage	Child-pugh
1	0008155592	Male	53	Multiple	Positive	>1210	Yes	B	III	A
2	0008146382	Male	54	Single	Positive	87.05	Yes	A	I	A
3	0000841294	Male	66	Single	Positive	>1210	Yes	0	I	A
4	0003476206	Male	56	Multiple	Positive	2.37	Yes	C	III	A
5	0008271060	Male	42	Single	Positive	4.39	Yes	A	I	A
6	0004865466	Male	20	Single	Positive	111.58	Yes	0	I	A
7	0008191254	Male	72	Single	Positive	850	Yes	A	II	A
8	0008292466	Male	64	Single	Positive	1.04	Yes	A	I	A
9	0008330242	Male	21	Multiple	Positive	>800	No	B	III	A
10	0000060449	Male	70	Single	Positive	4.99	Yes	0	I	A
11	0002543983	Male	59	Multiple	Positive	243.94	No	B	II	A
12	0004975402	Male	61	Single	Positive	400.6	Yes	A	I	A
13	0008366184	Male	54	Single	Positive	1.4	Yes	A	I	A
14	0002933746	Male	66	Single	Positive	1.18	No	A	I	A
15	0008075110	Male	41	Single	Positive	4.47	No	A	I	A
16	0001982601	Male	55	Single	Positive	2	Yes	A	I	A
17	0008435226	Female	65	Single	Positive	6.36	No	A	I	A
18	0008418675	Male	64	Single	Positive	14.15	Yes	A	I	A
19	0008464942	Male	48	Single	Positive	602.95	Yes	A	I	A
20	0008440382	Male	57	Single	Positive	>1210	Yes	A	I	A
21	0008465012	Male	50	Single	Positive	56.71	No	A	I	A
22	0003711350	Male	65	Single	Positive	>1210	Yes	A	I	A
23	0008509448	Male	56	Single	Positive	230.41	Yes	0	I	A
24	0008560310	Male	49	Multiple	Positive	9.92	No	B	III	A

protein in HCC but also strengthens the tumor promoting role of FOXH1 with both experimental and clinical evidence. Therefore, we believe development of FOX targeted therapeutic approaches may improve current treatments of HCC.

Recently, accumulating evidence suggested that FOX proteins were involved in cancer carcinogenesis. Immunohistochemical staining of FOXO3 demonstrated that FOXO3 was overexpressed in HCC samples, suggesting it may occupy a position in HCC development. Indeed, hepatic FOXO3a transgenic mice were much easier to develop tumorigenesis upon hepatotoxicin treatment compared to the control cohorts [21]. Study also documented that FOXG1 was highly expressed in HCC patients and its induction could promote EMT (epithelial-Mesenchymal transition) by activating beta-catenin signaling [11]. Moreover, the roles of FOXK1 and FOXQ1 in HCC in progression have also been well documented. An increased expression level of FOXK1 caused by DNA hypomethylation was observed in HCC patients [15]. FOXK1 upregulation in HCC cells led to expand the

population of cancer stem cells by increasing EpCAM and ALDH1 expression levels [15]. FOXQ1 upregulation could initiate HCC by enhancing the communication between cancer association fibroblasts (CAF) and tumor cells [22]. Our analyses of FOXK1, FOXQ1, FOXG1 and FOXO3a in TCGA LIHC dataset were consistent with previous findings. To summarize, the roles of FOX members in HCC initiation and progression are increasingly discovered. In this study, a comprehensive analysis of FOX members in HCC demonstrates that some FOX family members could serve as prognostic factors determining HCC progression.

Indeed, experimental validation demonstrated that FOXH1 promoted cell growth and cell invasion/migration of HCC cells. The *in vivo* animal data also confirmed the oncogenic role of FOXH1 in HCC development. Mechanistically, FOXH1 mediated HCC cell growth and cell invasion was partially caused by mTOR activation. As fact, the role of mTOR signaling in HCC progression has been well documented. Clinical data showed that mTOR signaling was activated in an approximate 40%

HCC patients [16, 17, 20], facilitating the clinical application of mTOR inhibitors into HCC treatment. Although mTOR inhibitors such as everolimus, temsirolimus and deforolimus have been approved for the treatment of RCC (renal cell carcinoma), HER2-negative breast cancer and pancreatic neuroendocrine tumor [23–25], they haven't obtained approval for treatment in HCC patients. Nevertheless, mTOR inhibitors have been showed to suppress HCC cell growth *in vitro* and *in vivo*. Most importantly, they are being clinically tested for the treatment of advanced HCC. Our results revealed that mTOR inhibitor rapamycin could block FOXH1 induced HCC cell growth *in vitro* and *in vivo*. All these facts build rationale to apply mTOR inhibitor for the treatment of HCC patients with high FOXH1 expression level.

In addition, we found that metastatic HCC patients preferred to highly express FOX proteins even though there was no statistically significant difference due to the small size of metastatic HCC patients (n=4), indicating FOX proteins may play critical roles in the development of HCC metastasis. Metastatic HCC is more lethal compared to localized HCC so that currently therapeutic options are less effective [26]. Our data showed that FOXH1 could enhance HCC cell migration and cell invasion, two essential steps during tumor metastasis, indicating targeting FOXH1 may overcome HCC metastasis. However, how to specifically target FOXH1 is still a scientific question. Fortunately, specific inhibitors towards FOX proteins were recently being developed. JBIR-141 and JBIR-142 have been identified as potent inhibitors specific for FOXO3a [27]. Given that FOX proteins are increased in metastatic HCC, it is worthy to develop their specific inhibitors for better treatment of this type of HCC.

Overall, our study comprehensively analyzed the correlations between the expression levels of FOX proteins and the clinical characteristics of HCC, pinpointing the prognostic values of FOX proteins in HCC progression. The experimental evidence also suggested that FOXH1 was truly a tumor promoting factor in HCC progression, strengthening the accuracy of our online analyses.

MATERIALS AND METHODS

Patient samples

HCC samples (24) and the paired adjacent liver tissues (24) were obtained from Department of Liver Surgery, Xiangya Hospital, Central South University. Resected tissues were stored in liquid nitrogen for further use. Informed consent was obtained from patients and study was approved by the Institutional Review board of Central South University.

Cell culture

HA22T, SK-HEP1 and 293T were purchased from Cell Bank in Chinese Academy of Sciences (Shanghai, China). 10% FBS DMEM (100 units/mL penicillin, 100 µg/mL streptomycin) was used to culture cells in humidified 5% CO₂ environment at 37° C.

Lentivirus generation

PLKO with shRNAs against FOXH1 or PWPI with FOXH1 cDNA was co-transfected with psPAX2 and pMD2.G into 293T cells using the standard calcium phosphate transfection method. 48 hours post-transfection, virus supernatant was collected and infected HCC cells. 8 µg/ml polybrene was used to enhance the efficiency of virus infection.

Real time qPCR

Total RNAs were isolated using Trizol reagent following the standard RNA extraction protocol. Reverse transcription was performed using two µg of total RNAs. Real time qRT-PCR was performed using a Bio-Rad CFX96 system with SYBR green to determine the mRNA expression levels of interested genes. GAPDH mRNA level was served as internal control.

Western blotting

Lysates from HA22T, SK-HEP1 cells were loaded into 10%-12% SDS-PAGE gel for electrophoresis before proteins were transferred to PVDF membrane. After being blocked with 10% milk in TBST, membrane was probed with specific primary antibody with approximate dilution at 4° C for at least 16 hours, followed by incubation with 1:5000 HRP conjugated secondary antibody for 1 hour at room temperature. After being washed with TBST, blots were analyzed using enhanced chemiluminescence. Anti-FOXH1 (ab189960, Abcam) and anti-GAPDH (sc-47724, Santa Cruz) were used in this study.

MTT cell growth assay

HA22T, SK-HEP1 cells were seeded into 24-well plates at a density of 5000 cells/well. Cells at different time points were incubated with 5 µg/ml 3-(4,5-Dimethylthiazolyl)-2,5-diphenyltetrazolium bromide (MTT, Abcam) for 3 hours, followed by 10 mins DMSO incubation and the absorbance was analyzed at 490 nm.

Wound healing assay

HA22T, SK-HEP1 cells with or without FOXH1 manipulation were scratched using a pipette tip. 48

hours later, images of these cells were taken by microscopy.

Transwell assay

HA22T, SK-HEP1 cells with or without FOXH1 manipulation were loaded into the upper chamber of the inserts pre-coated with 1:8 diluted matrigel (BD Bioscience, USA) at the density of 1×10^5 /well. 0% FBS medium in the lower chamber served as a chemoattractant. 24 hours later, the invading cells in inserts were stained with 0.1% crystal violet and imaged with inverted microscope (Olympus, Japan). Quantification of images was done with ImageJ.

In vivo xenografted mouse model

1×10^6 HA22T-luciferase cells were orthotopically implanted into nude mice to allow tumor growth. Tumors were measured by IVIS system every week. 4 weeks post-implantation, mice were sacrificed and tumors were removed for IHC staining.

Immunohistochemical staining (IHC)

Tissues were fixed in 10% (v/v) formaldehyde in PBS and embedded in paraffin. 5 μ m sections were made and treated with boiling citrate buffer (pH 6.0) for 30 mins to complete antigen retrieval. After incubation with 3% peroxidase and 10% goat serum blocking buffer, the slides were incubated with 1:100 diluted anti-FOXH1 (ab189960, Abcam) or anti-p-S6K1 (9234, CST) primary antibody at 4° C for at least 16 hours. Then the slides were incubated with biotin-labeled secondary antibody for another 30 min, and followed by 30 min streptavidin incubation (PK-4000, Vectastain, USA.) The FOXH1 signal was determined by DAB staining.

GSEA KEGG pathway analysis

The mRNA profile in TCGA-LIHC and the corresponding clinical information were downloaded from Xena Functional Genomics Explorer (<https://xenabrowser.net/heatmap/>) of the University of California Santa Cruz. KEGG pathway analysis was performed using GSEA online tool (<http://www.broadinstitute.org/gsea>) after dividing patients into two groups using the median expression level of FOXH1.

Statistical analysis

All statistical analyses were performed using GraphPad Prism software. Data were presented as mean \pm SE. Differences were analyzed with the Student t test, and

significance was set at $P < 0.05$. *, ** and *** indicates $P < 0.05$, $P < 0.01$ and $P < 0.001$, respectively.

AUTHOR CONTRIBUTIONS

Z.W. designed and monitored the production of the experiments and helped to revise the manuscript. X.O. conducted the experiments and completed the manuscript. L.F., L.Y., J. Z. and Y. X. helped to complete some of the experiments. G.L. and G.Z. helped to conduct the animal experiments.

CONFLICTS OF INTEREST

The authors declare that they have no conflicts of interest.

FUNDING

This study was supported by the grants from the National Nature Science Foundation of China (No.81372631), a project from the Chen Xiao-Ping Foundation for the Development of Science and Technology of Hubei Province under Grant (CXPJH11800001-2018208), National Natural Science Foundation of China (81903004).

REFERENCES

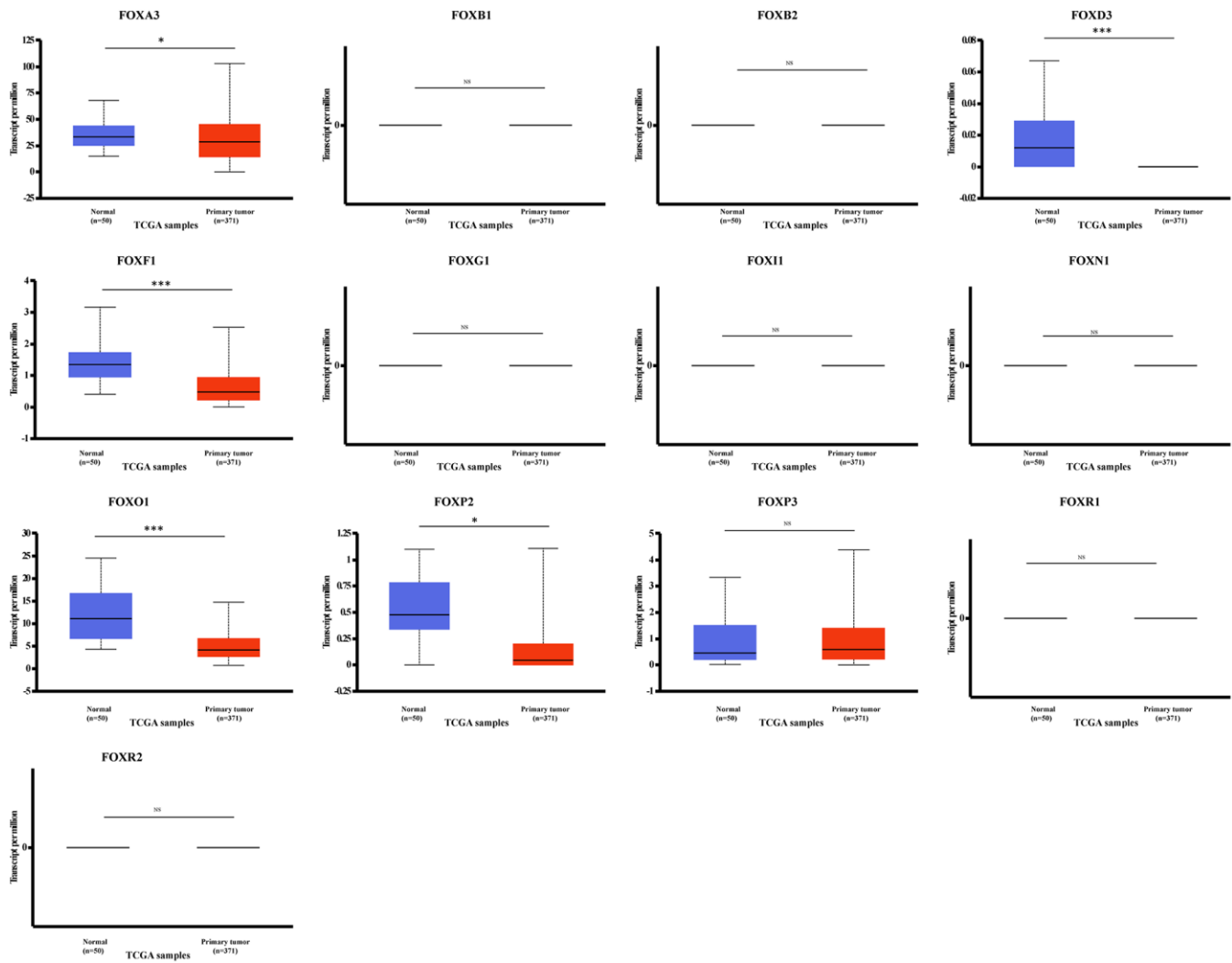
1. Bray F, Ferlay J, Soerjomataram I, Siegel RL, Torre LA, Jemal A. Global cancer statistics 2018: GLOBOCAN estimates of incidence and mortality worldwide for 36 cancers in 185 countries. *CA Cancer J Clin.* 2018; 68:394–424. <https://doi.org/10.3322/caac.21492> PMID:30207593
2. Rawla P, Sunkara T, Muralidharan P, Raj JP. Update in global trends and aetiology of hepatocellular carcinoma. *Contemp Oncol (Pozn).* 2018; 22:141–50. <https://doi.org/10.5114/wo.2018.78941> PMID:30455585
3. Anzola M. Hepatocellular carcinoma: role of hepatitis B and hepatitis C viruses proteins in hepatocarcinogenesis. *J Viral Hepat.* 2004; 11:383–93. <https://doi.org/10.1111/j.1365-2893.2004.00521.x> PMID:15357643
4. Daher S, Massarwa M, Benson AA, Khoury T. Current and future treatment of hepatocellular carcinoma: An updated comprehensive review. *J Clin Transl Hepatol.* 2018; 6:69–78. <https://doi.org/10.14218/JCTH.2017.00031> PMID:29607307
5. Raza A, Sood GK. Hepatocellular carcinoma review: current treatment, and evidence-based medicine. *World J Gastroenterol.* 2014; 20:4115–27.

- <https://doi.org/10.3748/wjg.v20.i15.4115>
PMID:24764650
6. Hannenhalli S, Kaestner KH. The evolution of Fox genes and their role in development and disease. *Nat Rev Genet.* 2009; 10:233–40.
<https://doi.org/10.1038/nrg2523>
PMID:19274050
 7. Bach DH, Long NP, Luu TT, Anh NH, Kwon SW, Lee SK. The dominant role of forkhead box proteins in cancer. *Int J Mol Sci.* 2018; 19:3279.
<https://doi.org/10.3390/ijms19103279>
PMID:30360388
 8. Myatt SS, Lam EW. The emerging roles of forkhead box (Fox) proteins in cancer. *Nat Rev Cancer.* 2007; 7:847–59.
<https://doi.org/10.1038/nrc2223> PMID:17943136
 9. Lam EW, Gomes AR. Forkhead box transcription factors in cancer initiation, progression and chemotherapeutic drug response. *Front Oncol.* 2014; 4:305.
<https://doi.org/10.3389/fonc.2014.00305>
PMID:25401090
 10. Xia L, Huang W, Tian D, Zhu H, Qi X, Chen Z, Zhang Y, Hu H, Fan D, Nie Y, Wu K. Overexpression of forkhead box C1 promotes tumor metastasis and indicates poor prognosis in hepatocellular carcinoma. *Hepatology.* 2013; 57:610–24.
<https://doi.org/10.1002/hep.26029> PMID:22911555
 11. Zheng X, Lin J, Wu H, Mo Z, Lian Y, Wang P, Hu Z, Gao Z, Peng L, Xie C. Forkhead box (FOX) G1 promotes hepatocellular carcinoma epithelial-mesenchymal transition by activating Wnt signal through forming T-cell factor-4/Beta-catenin/FOXG1 complex. *J Exp Clin Cancer Res.* 2019; 38:475.
<https://doi.org/10.1186/s13046-019-1433-3>
PMID:31771611
 12. Ahn H, Kim H, Abdul R, Kim Y, Sim J, Choi D, Paik SS, Shin SJ, Kim DH, Jang K. Overexpression of forkhead box O3a and its association with aggressive phenotypes and poor prognosis in human hepatocellular carcinoma. *Am J Clin Pathol.* 2018; 149:117–27.
<https://doi.org/10.1093/ajcp/aqx132> PMID:29365018
 13. Chai N, Xie HH, Yin JP, Sa KD, Guo Y, Wang M, Liu J, Zhang XF, Zhang X, Yin H, Nie YZ, Wu KC, Yang AG, Zhang R. FOXM1 promotes proliferation in human hepatocellular carcinoma cells by transcriptional activation of CCNB1. *Biochem Biophys Res Commun.* 2018; 500:924–9.
<https://doi.org/10.1016/j.bbrc.2018.04.201>
PMID:29705704
 14. Xia L, Huang W, Tian D, Zhu H, Zhang Y, Hu H, Fan D, Nie Y, Wu K. Upregulated FoxM1 expression induced by hepatitis B virus X protein promotes tumor metastasis and indicates poor prognosis in hepatitis B virus-related hepatocellular carcinoma. *J Hepatol.* 2012; 57:600–12.
<https://doi.org/10.1016/j.jhep.2012.04.020>
PMID:22613004
 15. Cao H, Chu X, Wang Z, Guo C, Shao S, Xiao J, Zheng J, Zhang D. High FOXK1 expression correlates with poor outcomes in hepatocellular carcinoma and regulates stemness of hepatocellular carcinoma cells. *Life Sci.* 2019; 228:128–34.
<https://doi.org/10.1016/j.lfs.2019.04.068>
PMID:31054270
 16. Sahin F, Kannangai R, Adegbola O, Wang J, Su G, Torbenson M. mTOR and P70 S6 kinase expression in primary liver neoplasms. *Clin Cancer Res.* 2004; 10:8421–5.
<https://doi.org/10.1158/1078-0432.CCR-04-0941>
PMID:15623621
 17. Villanueva A, Chiang DY, Newell P, Peix J, Thung S, Alsinet C, Tovar V, Roayaie S, Minguez B, Sole M, Battiston C, Van Laarhoven S, Fiel MI, et al. Pivotal role of mTOR signaling in hepatocellular carcinoma. *Gastroenterology.* 2008; 135:1972–83.
<https://doi.org/10.1053/j.gastro.2008.08.008>
PMID:18929564
 18. Wullschlegel S, Loewith R, Hall MN. TOR signaling in growth and metabolism. *Cell.* 2006; 124:471–84.
<https://doi.org/10.1016/j.cell.2006.01.016>
PMID:16469695
 19. Kim LC, Cook RS, Chen J. mTORC1 and mTORC2 in cancer and the tumor microenvironment. *Oncogene.* 2017; 36:2191–201.
<https://doi.org/10.1038/onc.2016.363>
PMID:27748764
 20. Matter MS, Decaens T, Andersen JB, Thorgeirsson SS. Targeting the mTOR pathway in hepatocellular carcinoma: current state and future trends. *J Hepatol.* 2014; 60:855–65.
<https://doi.org/10.1016/j.jhep.2013.11.031>
PMID:24308993
 21. Lu M, Hartmann D, Braren R, Gupta A, Wang B, Wang Y, Mogler C, Cheng Z, Wirth T, Friess H, Kleeff J, Hüser N, Sunami Y. Oncogenic Akt-FOXO3 loop favors tumor-promoting modes and enhances oxidative damage-associated hepatocellular carcinogenesis. *BMC Cancer.* 2019; 19:887.
<https://doi.org/10.1186/s12885-019-6110-6>
PMID:31488102
 22. Luo Q, Wang CQ, Yang LY, Gao XM, Sun HT, Zhang Y, Zhang KL, Zhu Y, Zheng Y, Sheng YY, Lu L, Jia HL, Yu WQ, et al. FOXQ1/NDRG1 axis exacerbates

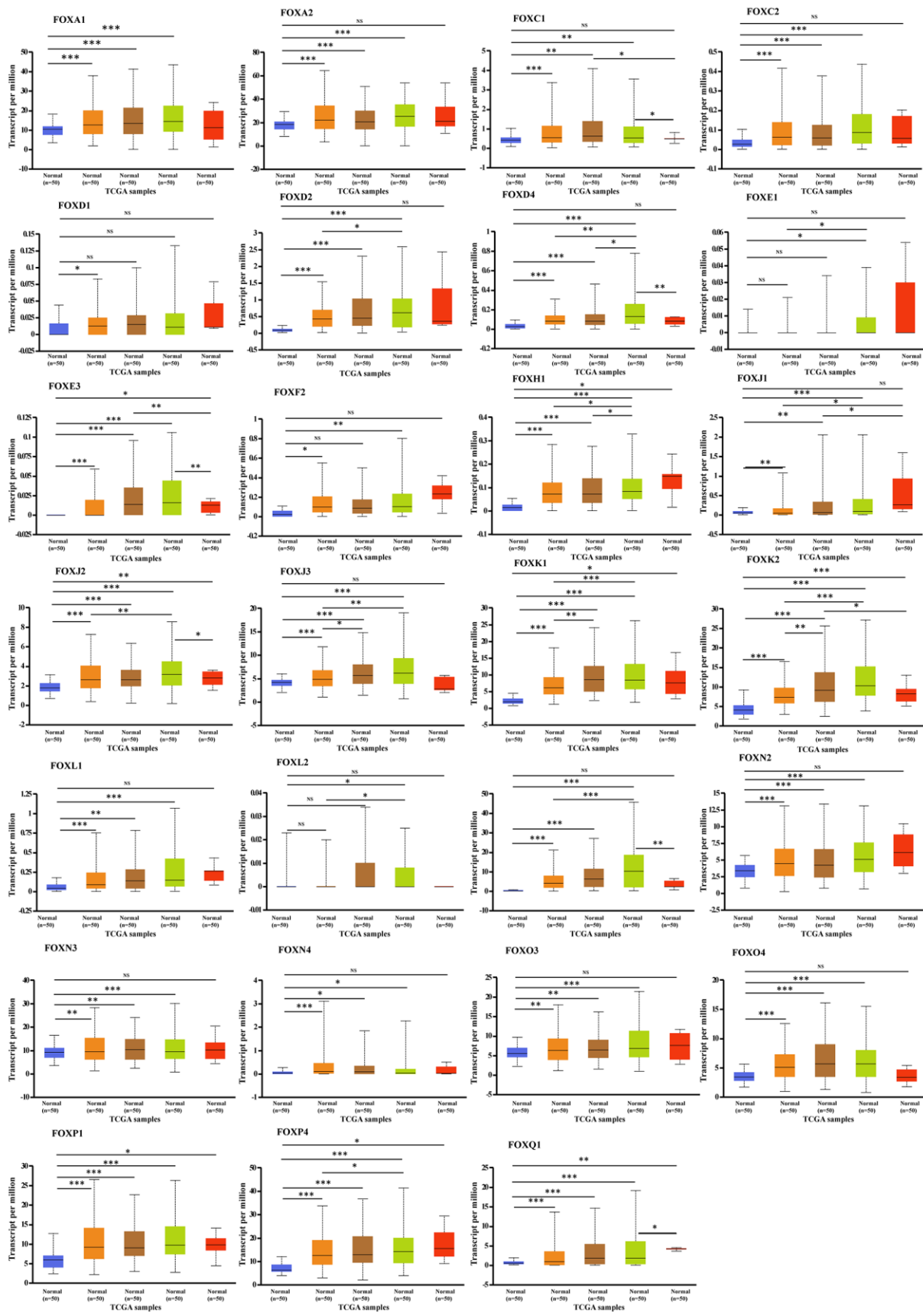
- hepatocellular carcinoma initiation via enhancing crosstalk between fibroblasts and tumor cells. *Cancer Lett.* 2018; 417:21–34.
<https://doi.org/10.1016/j.canlet.2017.12.021>
PMID:[29248714](https://pubmed.ncbi.nlm.nih.gov/29248714/)
23. Lee JJ, Loh K, Yap YS. PI3K/Akt/mTOR inhibitors in breast cancer. *Cancer Biol Med.* 2015; 12:342–54.
<https://doi.org/10.7497/j.issn.2095-3941.2015.0089>
PMID:[26779371](https://pubmed.ncbi.nlm.nih.gov/26779371/)
24. Battelli C, Cho DC. mTOR inhibitors in renal cell carcinoma. *Therapy.* 2011; 8:359–67.
<https://doi.org/10.2217/thy.11.32> PMID:[21894244](https://pubmed.ncbi.nlm.nih.gov/21894244/)
25. Orr-Asman MA, Chu Z, Jiang M, Worley M, LaSance K, Koch SE, Carreira VS, Dahche HM, Plas DR, Komurov K, Qi X, Mercer CA, Anthony LB, et al. mTOR kinase inhibition effectively decreases progression of a subset of neuroendocrine tumors that progress on rapalog therapy and delays cardiac impairment. *Mol Cancer Ther.* 2017; 16:2432–41.
<https://doi.org/10.1158/1535-7163.MCT-17-0058>
PMID:[28864682](https://pubmed.ncbi.nlm.nih.gov/28864682/)
26. Okusaka T, Okada S, Ishii H, Nose H, Nagahama H, Nakasuka H, Ikeda K, Yoshimori M. Prognosis of hepatocellular carcinoma patients with extrahepatic metastases. *Hepatogastroenterology.* 1997; 44:251–7.
PMID:[9058154](https://pubmed.ncbi.nlm.nih.gov/9058154/)
27. Kawahara T, Kagaya N, Masuda Y, Doi T, Izumikawa M, Ohta K, Hirao A, Shin-ya K. Foxo3a inhibitors of microbial origin, JBIR-141 and JBIR-142. *Org Lett.* 2015; 17:5476–9.
<https://doi.org/10.1021/acs.orglett.5b02842>
PMID:[26493489](https://pubmed.ncbi.nlm.nih.gov/26493489/)

SUPPLEMENTARY MATERIALS

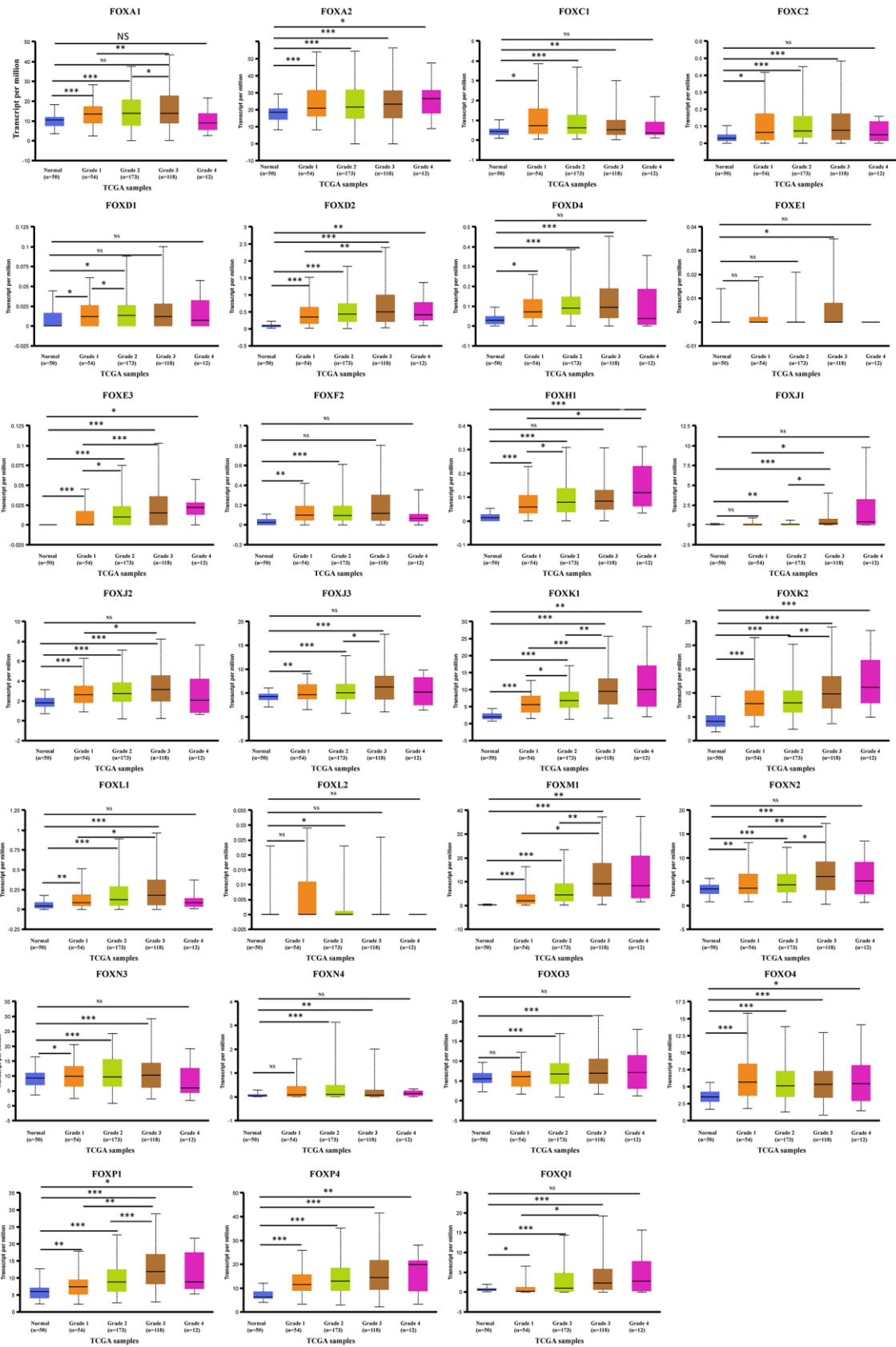
Supplementary Figures



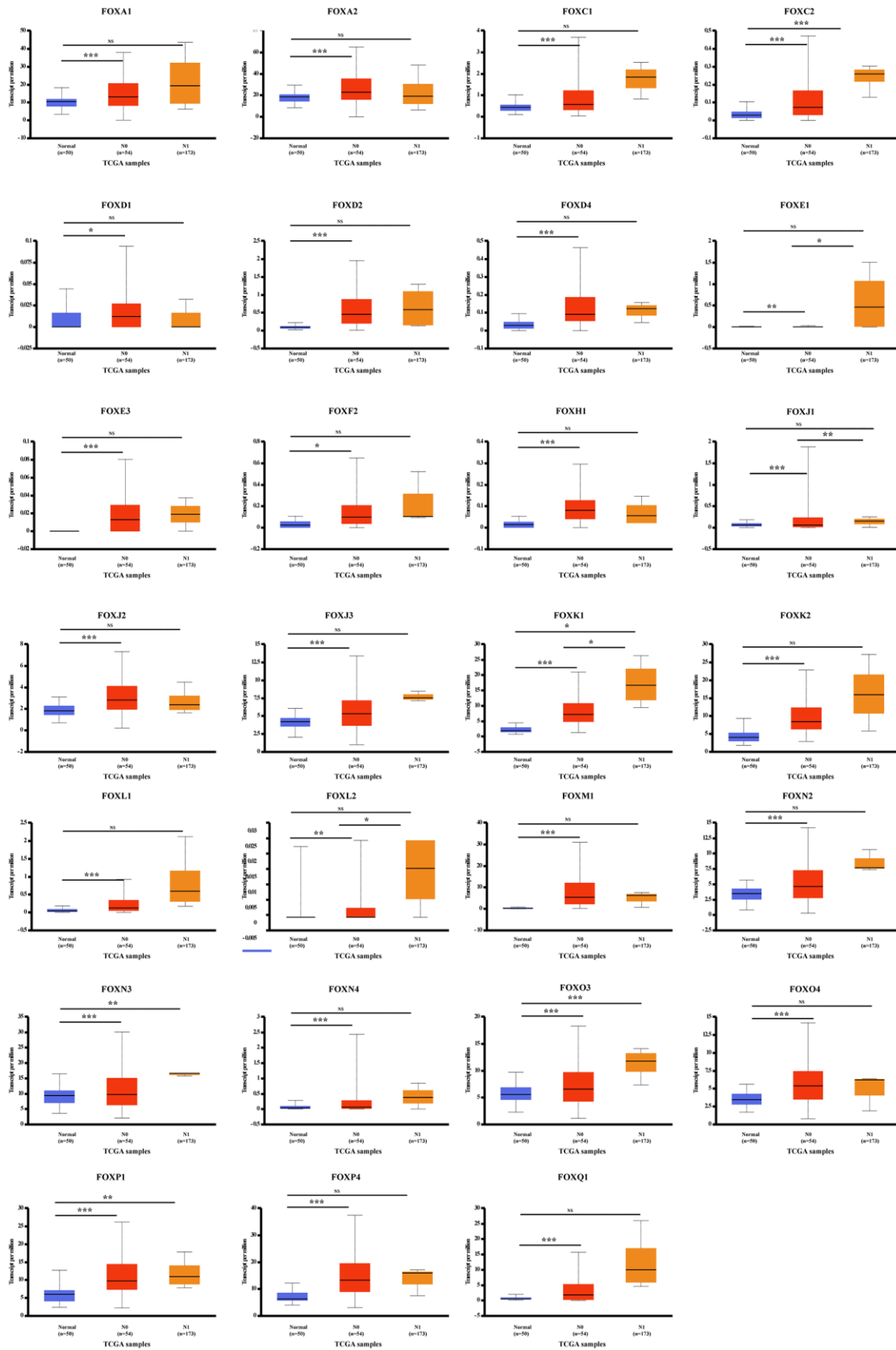
Supplementary Figure 1. 13/40 FOX proteins were not upregulated in HCC patients compared to the normal liver tissues.



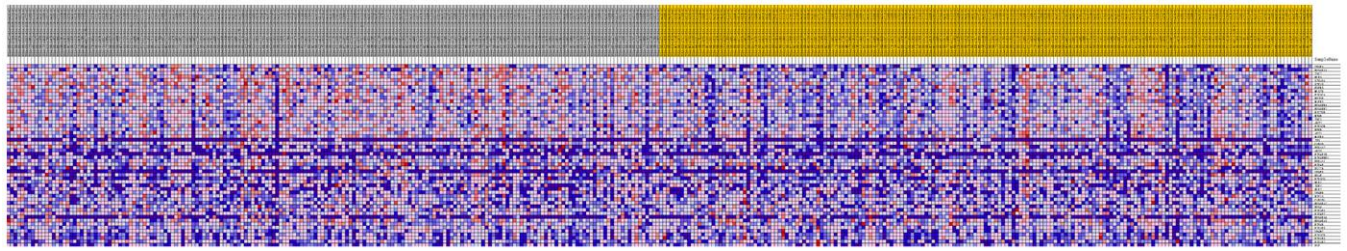
Supplementary Figure 2. The association of individual FOX mRNA level with tumor stage of HCC.



Supplementary Figure 3. The association of individual FOX mRNA level with tumor grade of HCC. * $P < 0.01$, ** $P < 0.01$, *** $P < 0.001$.



Supplementary Figure 4. The association of individual FOX mRNA level with tumor metastasis of HCC. *P<0.01, **P<0.01, *P<0.001. NS, no significant difference.**



Supplementary Figure 5. Expression heatmap of mTOR signaling related molecules in high FOXH1 and low FOXH1 HCC patients.

Ox-LDL-mediated ILF3 overexpression in gastric cancer progression by activating the PI3K/AKT/mTOR signaling pathway

Danping Sun¹, Mingxiang Zhang², Meng Wei¹, Zhaoyang Wang², Wen Qiao², Peng Liu¹, Xin Zhong¹, Yize Liang¹, Yuanyuan Chen³, Yadi Huang¹, Wenbin Yu¹

¹Department of Gastrointestinal Surgery, General Surgery, Qilu Hospital, Cheeloo College of Medicine, Shandong University, Jinan 250012, China

²The Key Laboratory of Cardiovascular Remodeling and Function Research, Chinese Ministry of Education, Chinese Ministry of Health and Chinese Academy of Medical Sciences, Department of Cardiology, Qilu Hospital, Cheeloo College of Medicine, Shandong University, Jinan 250012, China

³Department of Nursing Department, Qilu Hospital, Cheeloo College of Medicine, Shandong University, Jinan 250012, China

Correspondence to: Wenbin Yu; email: wenbin_yu2003@163.com, <https://orcid.org/0000-0001-7111-3780>

Keywords: gastric cancer, dyslipidemia, interleukin-enhancer binding factor 3 (ILF3), ox-LDL, PI3K/AKT/mTOR signaling pathway, biomarkers

Received: October 10, 2021

Accepted: April 21, 2022

Published: May 4, 2022

Copyright: © 2022 Sun et al. This is an open access article distributed under the terms of the [Creative Commons Attribution License](https://creativecommons.org/licenses/by/3.0/) (CC BY 3.0), which permits unrestricted use, distribution, and reproduction in any medium, provided the original author and source are credited.

ABSTRACT

Background: This study aimed to investigate the relationship of dyslipidemia and interleukin-enhancer binding factor 3 (ILF3) in gastric cancer, and provide insights into the potential application of statins as an agent to prevent and treat gastric cancer.

Methods: The expression levels of ILF3 in gastric cancer were examined with publicly available datasets such as TCGA, and western blotting and immunohistochemistry were performed to determine the expression of ILF3 in clinical specimens. The effects of ox-LDL on expression of ILF3 were further verified with western blot analyses. RNA sequencing, Kyoto Encyclopedia of Genes and Genomes (KEGG), Gene Ontology (GO), and Gene Set Enrichment Analysis (GSEA) pathway analyses were performed to reveal the potential downstream signaling pathway targets of ILF3. The effects of statins and ILF3 on PI3K/AKT/mTOR signaling pathway, cell proliferation, cell cycle, migration and invasion of gastric cancer cells were investigated with Edu assay, flow cytometry and transwell assay.

Results: Immunohistochemistry and western blot demonstrated that the positive expression rates of ILF3 in gastric cancer tissues were higher than adjacent mucosa tissues. The ox-LDL promoted the expression of ILF3 in a time-concentration-dependent manner. ILF3 promoted the proliferation, cell cycle, migration and invasion by activating the PI3K/AKT/mTOR signaling pathway. Statins inhibited the proliferation, cell cycle, migration and invasion of gastric cancer by inhibiting the expression of ILF3.

Conclusions: These findings demonstrate that ox-LDL promotes ILF3 overexpression to regulate gastric cancer progression by activating the PI3K/AKT/mTOR signaling pathway. Statins inhibits the expression of ILF3, which might be a new targeted therapy for gastric cancer.

INTRODUCTION

Gastric cancer (GC) is a major health burden worldwide, especially in Eastern and Western Asia [1]. Besides, the

incidence of GC ranks second in China [2]. Due to the lack of obvious symptoms, specific clinical, imaging, or pathological manifestations, patients are usually diagnosed at the advanced stage [3, 4]. Despite the

development in surgery, chemotherapy, immunotherapy, and targeted therapy, the overall survival rate and prognosis remain unsatisfactory in patients with GC, with a poor 5-year survival rate (<30%) [5, 6]. Among them, the metastasis and recurrence of GC are the main reasons for treatment failure and the patient death [7, 8]. Therefore, it is critical to study the underlying molecular of the development of GC, which also can help us identify more molecular markers for monitoring the prognosis of patients.

To date, conventional serum tumor markers are applied in GC screening, including carcinoembryonic antigen (CEA), alpha-fetoprotein (AFP), cancer antigen 19-9(CA19-9), cancer antigen 72-4(CA72-4) and cancer antigen 125(CA125), and are also used in the predicting of the prognosis, recurrence, or metastasis [9–11]. However, as a result of the lack of sensitivity and specificity, these biomarkers are not recommended for GC detection and prognostic follow-up [12].

The successful eradication of *Helicobacter pylori* (Hp) effectively lowered the morbidity of distal GC, while the number of gastric cancers at the esophagogastric junction and upper third was increasing year by year, and new cases were gradually showing a younger trend [13]. Studies found that obesity contributes greatly to the occurrence of proximal GC [14]. Obesity is a disorder of energy balance and abnormal lipid metabolism, which is mainly characterized with the upregulated blood concentration of low-density lipoprotein cholesterol (LDL-C) [15, 16]. LDL-C is delivered throughout the body in the form of LDL. LDL is very prone to be oxidized by reactive oxygen species (ROS) to form oxidized LDL (ox-LDL) [17, 18]. Therefore, excessive ox-LDL indicates the abnormal lipid conditions in obese subjects. It is well-known that ox-LDL negatively impacts on hypertension, atherosclerosis, and cardiovascular diseases [19]. More and more studies demonstrated that the increased ox-LDL was positively associated with cancer development such as colon, breast, and ovarian cancer [20–22]. Some studies have demonstrated that ox-LDL can induce mutagenesis, stimulate proliferation, initiate metastasis, and induce treatment of resistance [23, 24].

Although the occurrence and development of GC involves a wide range of metabolic pathways [25], little has been written about the roles of abnormal lipid metabolism in this regard. Thus, the mechanism remains unclear that how ox-LDL promotes the occurrence and development of GC.

Interleukin-enhancer binding factor 3 (ILF3) is known as NF90/NF110, a member of the double-stranded

RNA-binding proteins (DRBPs), which is crucial in RNA metabolism from transcription to degradation, including transcription, translation, maintaining the stability of mRNA and primary microRNA processing [26]. In recent years, ILF3 has been widely studied and been linked to multiple malignant tumors. For example, ILF3 facilitated the occurrence of colorectal cancer by regulating the mRNA stability of serine–glycine–one-carbon (SGOC) SGOC genes [27]. ILF3 overexpression was associated with poor clinical outcome for patients with lung cancer, and ILF3 can also be employed to guide the hierarchical postoperative management of patients with lung cancer [28]. ILF3 might serve as an important promoter in hepatocellular carcinoma proliferation and migration, and could be a potential therapeutic target in hepatocellular carcinoma [29]. ILF3 increased the expression of HIF-1 α /VEGFA in cervical cancer cells to promote angiogenesis through PI3K/AKT signaling pathway [30]. Moreover, it has been reported the important function of ILF3 in the development of acquired chemoresistance in GC patients [31].

In addition to contributing to carcinogenesis, ILF3 is also a risk factor for coronary artery disease, venous thromboembolism, and stroke [32]. Studies have reported that ILF3 was associated with the serum concentrations of LDL cholesterol, and has been found to be a candidate gene for myocardial infarction in Japanese individual [33, 34]. The reports on the relationship of ox-LDL and the expression of ILF3, and their relationship with the development and progress of GC have never been reported. Therefore, further research is required to explore the association of ox-LDL and ILF3 and the underlying molecular mechanism in the development of GC.

Statins are 3-hydroxy-3-methylglutaryl coenzyme A (HMG-CoA) reductase inhibitors, which are intensively used for dyslipidemia and cardiovascular disease prevention [35]. Besides, statins use also could reduce total cancer risk and lower cancer-specific mortality [36, 37]. In a large population-based retrospective cohort study, statins use reduced the risk of cancer and cancer-related mortality [38]. A meta-analysis revealed that statins was associated with 32% reduction in the risk of GC [39]. Recent years, *in vivo* and *in vitro* studies have demonstrated that statins may exert anti-cancer effects via a number of potential mechanisms including inhibition of mevalonate pathway, anti-inflammatory and anti-angiogenesis [40, 41], and could lower the cholesterol levels in human gastric cancer cell lines [42].

This is the first study to demonstrate that statins can downregulate the expression of ILF3 in GC treatment

by reducing blood lipid levels. Thus, we hypothesized that ox-LDL promoted ILF3 overexpression and promoted proliferation, cell cycle, migration, and invasion of gastric cancer cells via PI3K/AKT/mTOR signaling pathway, and that statins might be the targeted drugs to treat GC in clinical practice.

RESULTS

ILF3 was overexpressed in gastric cancer patients

To determine the expression level of ILF3 in GC samples, analysis of the mRNA expression data from The Cancer Genome Atlas (TCGA) including 375 GC

samples and 32 normal cases demonstrated that the ILF3 expression level was higher in cancer tissue than normal tissues (Figure 1A, $P < 0.05$).

To measure the ILF3 expression levels in clinical GC tissues, immunohistochemical staining of ILF3 was performed in a cohort of 33 human GC tissues and matched adjacent non-cancerous tissues. Patients with GC were divided into subgroups according to use of statins medication. The results revealed that the ILF3 expression in GC was higher than in no-neoplastic tissues. And the expression of ILF3 in patients taking statins was significantly lower than that without taking statins (Figure 1B, $P < 0.05$).

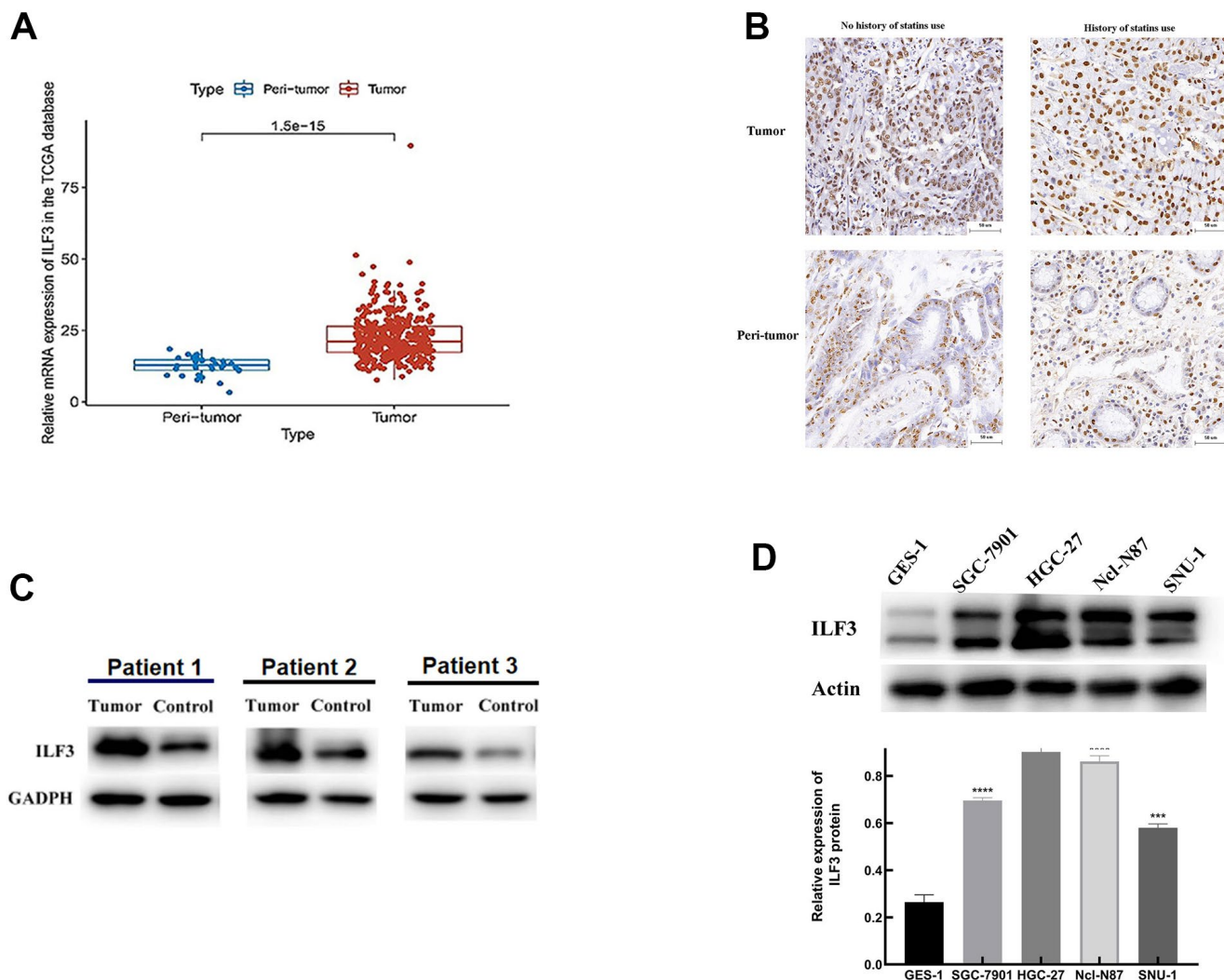


Figure 1. ILF3 was up-regulated in gastric cancer. (A) Expression of ILF3 mRNA in gastric cancer samples ($n = 375$) and normal samples ($n = 32$) from the TCGA data. (B) ILF3 protein expression was detected by IHC. ILF3 positive staining in tumor tissues was increased relative to non-cancerous tissues. (C) Western blot analysis of ILF3 in paired tumor tissues and non-cancerous tissues. The ILF3 expression level of mRNA was higher in cancer tissue than in normal tissues. (D) Western blot analysis of ILF3 protein in gastric epithelial cell line (GES-1) and gastric cancer cells lines (SGC-7901, HGC-27, Ncl-N87, and SNU-1). The ILF3 protein expression was significantly higher in gastric cancer cell lines than gastric epithelial cell line. $**P < 0.01$, $***P < 0.001$, $****P < 0.0001$.

Moreover, the ILF3 protein expression was quantified by western blot. As shown in Figure 1C, ILF3 protein level was significantly upregulated in tissues from GC ($P < 0.05$).

Expression of ILF3 protein was detected in all 4 gastric cancer cell lines (SGC-7901, HGC-27, Ncl-N87, and SNU-1) and gastric epithelial cell lines (GES-1). Western blotting found that GC cell lines expressed higher ILF3 protein than gastric epithelial cell line (GES-1) (Figure 1D, $P < 0.05$). Among the 4 cell lines of GC, the expressions of ILF3 in HGC-27 and Ncl-N87 were remarkably increased compared with other cell lines. Therefore, Ncl-N87 and HGC-27 cell lines were selected for subsequent experiments.

Whole-genome RNA-seq analysis of ILF3

Correlation analysis of the whole-genome RNA-sequencing (RNA-seq) of ILF3 was performed with small interference (si-ILF3) to explore potential biological effects of ILF3. The volcano map of transcriptomics analysis showed a global view of gene expression, and showed that ILF3 played important role in processing the environmental and genetic information, the cellular processes, metabolism, and organismal systems (Figure 2A, 2B).

Among all the differentially expressed genes (Supplementary Table 1), APOB and FGF19 were involved in the lipid biosynthetic process. APOB was also involved in the lipoprotein transport. Based on the result, we speculated that ILF3 may participate in the regulation of lipid metabolism by regulating the expression of APOB. Besides, DEPTOR was

overexpressed after knocking out ILF3 using ILF3-specific small interference RNA (si-ILF3), and previous studies have reported that DEPTOR is an endogenous mTOR inhibitor [43], whose expression was negatively regulated by mTOR. Therefore, the overexpressed DEPTOR may inhibit the mTOR signaling pathway and thus exerted a tumor suppressor effect (Figure 2C).

Functional characteristics of ILF3 in gastric cancer cells

GO analysis was applied to reveal the function characteristics of ILF3, including BPs (biological processes), CCs (cellular components), and MFs (molecular function) (Figure 3 and Supplementary Table 2).

For BP analysis, the functions of ILF3 were mainly involved in digestive system development, lipoprotein transport and localization, cell migration (T cell, leukocyte, lymphocyte etc.), cell-cell adhesion, cell proliferation (fibroblast, neural precursor cell, smooth muscle cell etc.), and DNA synthesis and transcription. For example, a number of investigators have proposed the role of lipoproteins in the promotion of cancer progression [44]. And LDL is the largest cholesterol transporter of the body [45]. The LDL receptor on tumor cells is overexpressed to meet the high demand of cholesterol which is necessary for the rapid cell proliferation and de novo membrane synthesis. And ox-LDL is an independent risk factor for GC. Thus, understanding the mechanism and function between ILF3 and ox-LDL facilitates the discovery of new targets for the treatment of GC.

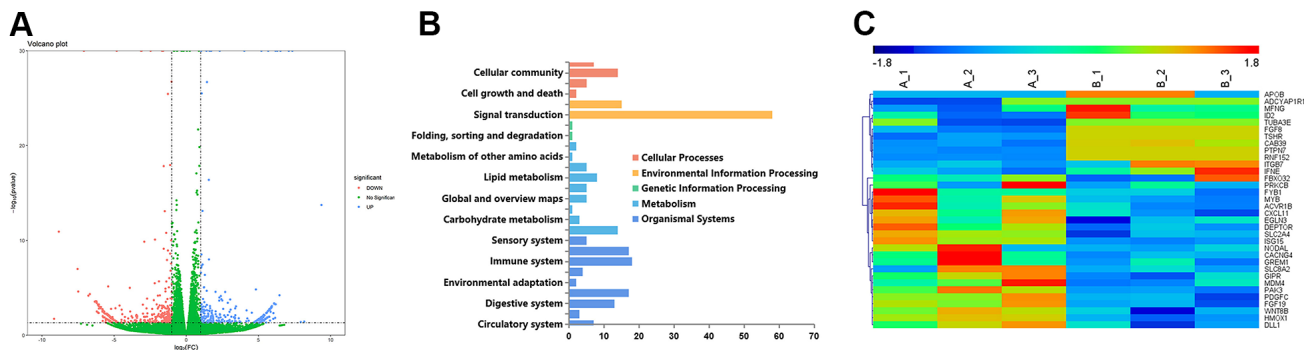


Figure 2. Volcano plot comparing gene expression between the interference group (infected with ILF3-specific siRNA) and the transfected negative control group in gastric cancer cell SGC-7901, respectively named si-ILF3 group and si-nc group. (A) The abscissa represents the logarithmic value of the fold change (\log_2FC) of the difference in the expression of a certain gene in the si-ILF3 group and si-nc group. The greater the absolute value of the abscissa, the greater the difference of expression between the two groups. The y-coordinate represents the negative log of p-value, namely the $-\log_{10}(p\text{-value})$. The higher the value of ordinate was, the more the differential expression of genes was reliable. **(B)** The potential important roles that ILF3 played in the gastric cancer cells. **(C)** Genes that were potentially regulated by ILF3 expression in whole-genome RNA sequencing.

For CC analysis, ILF3 was associated with membrane raft. Membrane rafts of lipid rafts are small, dynamic membrane domains which are enriched with cholesterol and sphingolipids [46]. Membrane rafts do not only occur in the plasma membrane but also in intracellular membranes and extracellular vesicles [47]. Membrane rafts are significant in cellular signal pathways, and regulating cell proliferation, migration, invasion and apoptosis, which are responsible for the initiation, development and progression of malignant tumors [48, 49]. Studies have shown that ox-LDL may destroy the severity of lipid rafts, leading to corresponding pathological processes, and promote the progression of cancer [50]. Further research to link the ox-LDL to impaired lipid raft function due to the interaction with the expression of ILF3 is needed.

For MF analysis, ILF3 was associated with Notch binding. Abnormal Notch signaling is associated with a variety of genetic and acquired disease, including

cancers [51]. Notch signaling pathway regulated cellular proliferation and differentiation in a variety of gastrointestinal tract tissues, including the stomach. [52, 53]. Studies have found that mTOR signaling was reduced after Notch inhibition suggesting that mTOR might be downstream of Notch in GC cells [54, 55]. Therefore, ILF3 may eventually activate the mTOR signaling pathway through the Notch signaling to promote the proliferation of GC cells.

ILF3 involved signaling pathway alterations in gastric cancer cells

KEGG pathway analysis of ILF3 identified 14 statistically significant signaling pathways, including African trypanosomiasis, Glycine, serine and threonine metabolism, Mineral absorption, Tryptophan metabolism, Arrhythmogenic right ventricular cardiomyopathy (ARVC), Gap junction, Hypertrophic cardiomyopathy (HCM), Systemic lupus erythematosus, Alcoholism,

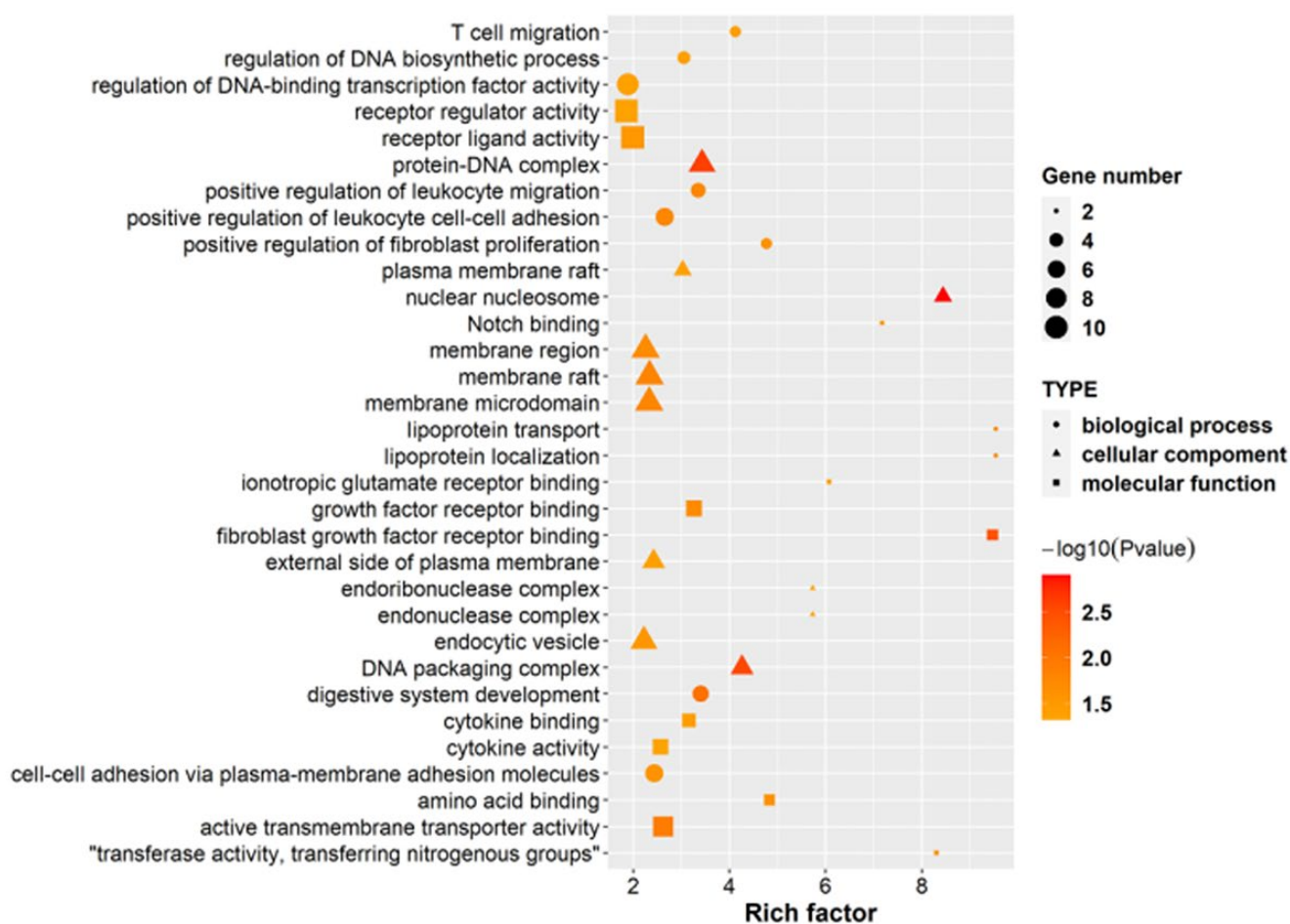


Figure 3. GO enrichment analysis between the si-ILF3 group and si-nc group in gastric cancer cell SGC-7901. GO enrichment analysis revealed the functions of ILF3 in gastric cancer cells, including BPs (biological processes), CCs (cellular components), and MFs (molecular function), which showed that ILF3 played important roles in the development of gastric cancer.

signaling pathways regulating stem cell pluripotency, TGF-beta signaling pathway, Dilated cardiomyopathy (DCM), Glycosaminoglycan biosynthesis - heparan sulfate / heparin and mTOR signaling pathway (Figure 4A and Supplementary Table 3).

To further investigate ILF3-mediated signaling pathways in gastric carcinogenesis, Gene Set Enrichment Analysis (GSEA) was performed, which found that ILF3 was positively associated with upregulation of mTOR signaling pathway. It is well-known that mTOR is an important downstream target of PI3K/AKT. Therefore, we need further experiments to prove that ILF3 can promote the occurrence and development of GC through PI3K/Akt/mTOR signaling pathway (Figure 4B).

ox-LDL promoted ILF3 overexpression in gastric cancer cells

To study the potential links between ox-LDL and ILF3, we set the concentration gradient of ox-LDL (0, 20, 40, 60, 80, and 100 µg/ml) and the time gradient (24, 48, and 72 h) of stimulation, respectively.

Western blotting showed that when the stimulation time was set to 48h, the protein expression of ILF3 was significantly upregulated after ox-LDL stimulation in 20, 40, 60, and 80 µg/ml concentration range compared with blank control group without ox-LDL stimulation. The protein expression of ILF3 was highest when the

concentration of ox-LDL was 40 µg/ml. When the concentration of ox-LDL is 100ug/ml, the protein expression of ILF3 is not statistically significant compared with control group (Figure 5A, P<0.05). Therefore, an ox-LDL concentration of 40 µg/ml was used for all subsequent experiments.

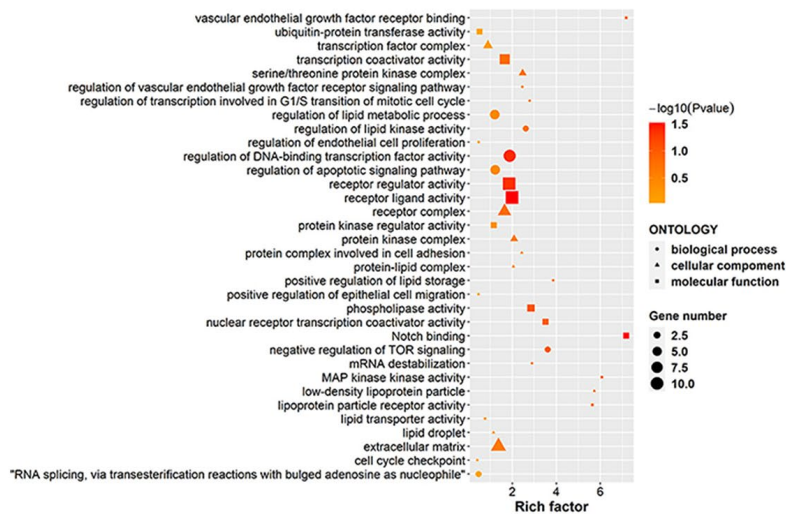
When the concentration of ox-LDL was set to 40 µg/ml, the expression of ILF3 was measured by western blot at 24h, 48h and 72h after stimulation. The expression of ILF3 was the highest when the stimulation time was 48h and it was statistically significant (Figure 5B, P<0.05).

To conduct loss-of-function assays to detect the effect of ILF3 on GC cells, ILF3 was knocked down with ILF3-specific small interference RNA (si-ILF3). Compared to the negative control (si-nc) group, mRNA and protein levels of ILF3 were lower (Figure 5C, P<0.05). Also, ILF3 was overexpressed with ILF3-overexpressed plasmids (flag-ILF3). Compared to the vector plasmids (CMV2) group, the ILF3 expression was significantly higher (Figure 5D, P<0.05).

ILF3 promoted proliferation, cell cycle, migration, and invasion of gastric cancer cells, and statins may exert an anti-tumor effect by inhibiting ILF3 expression in gastric cancer

Combined with BP (biological processes) analysis, to verify the role of ILF3 in promoting GC, *in vitro* experiments were conducted.

A



B

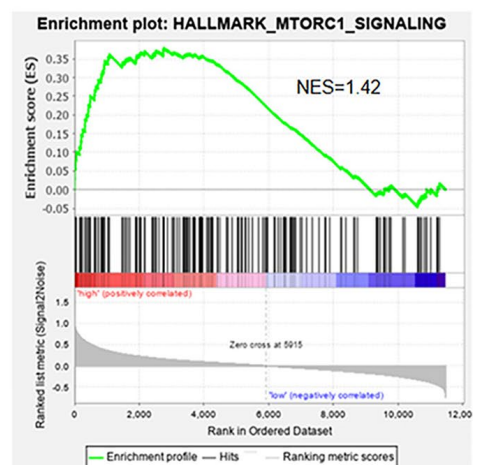


Figure 4. KEGG enrichment analysis between the si-ILF3 group and si-nc group in gastric cancer cell SGC-7901. (A) KEGG analysis showed the signaling pathways that ILF3 was involved in gastric cancer cell SGC-7901. **(B)** Results of the GSEA showed that ILF3 participated in the regulation of mTOR signaling pathway. NES = normalized enrichment score.

To further reveal the possible relationship between statins and ILF3, we set the concentration gradient of statins (0, 10, 20, 30, 40, and 50 $\mu\text{mol/L}$) to stimulate GC cells. Western blot assay showed that the expression of ILF3 was decreased with the increase in concentration of statins. Follow-up experiments chose 40 $\mu\text{mol/L}$ as the treatment concentration of statins treatment. And western blot analysis also found that ILF3-specific small interference RNA (si-ILF3) downregulated the protein expressions of ILF3 compared with blank control group (Figure 6A, $P < 0.05$). To reveal the role of ILF3 and the feasibility of statins in the treatment of GC, the changes of cell phenotype was analyzed after treatment with ox-LDL + si-nc, ox-LDL+ILF3-specific small interference RNA (si-ILF3) and ox-LDL + statins. And we set the ox-LDL + si-nc group as control group.

The effect of ILF3 on cell proliferation was evaluated by Edu assay (Figure 6B). The percentage of Edu-positive GC cells in the ILF3-specific small interference and statins treatment groups were lower than that in the control group. The PCNA expression was lower expressed in the ILF3-specific small interference and statins treatment groups compared to control (Figure 6B, 6C, $P < 0.05$).

Flow cytometry analyzed the effect of ILF3 on cell cycle of GC cells. Down-expression of ILF3 significantly increased the proportion of HGC-27 in the G0/G1 phase, and inhibited the proportion of HGC-27 in the S phase of cell cycle in the ILF3-specific small interference and

statins treatment groups compared to control group. Down-expression of ILF3 significantly inhibited the proportion of Ncl-N87 in the S phase of cell cycle in the ILF3-specific small interference and statins treatment groups compared to control group, but the proportion of Ncl-N87 in the G0/G1 phase was not statistically significant (Figure 6D, $P < 0.05$). Western blot analysis showed that the protein expression of cyclin-D1, the marker of G1-S phase transition, was lower expressed in the ILF3-specific small interference and statins treatment groups compared to control group (Figure 6E, $P < 0.05$).

The role of ILF3 on cell cycle was analyzed by flow cytometry. Inhibiting ILF3 expression significantly upregulated the proportion of HGC-27 and Ncl-N87 in the G0/G1 phase, and inhibited the percentage of HGC-27 and Ncl-N87 in the S phase in the ILF3-specific small interference and statins treatment groups compared to control group (Figure 6D, $P < 0.05$). As shown in Figure 6E, compared to control group, the protein level of cyclin-D1, the marker of G1-S phase transition, was lower expressed in the ILF3-specific small interference and statins treatment groups ($P < 0.05$).

Cell invasion and migration modulated by ILF3 were assessed by transwell assay. Less invasive and migrated GC cells were found in the ILF3-specific small interference and statins treatment groups compared to control group (Figure 6F, $P < 0.05$). The protein levels of MMP-2 and MMP-9 were lower expressed in the ILF3-specific small interference and statins treatment groups compared to control (Figure 6G, $P < 0.05$).

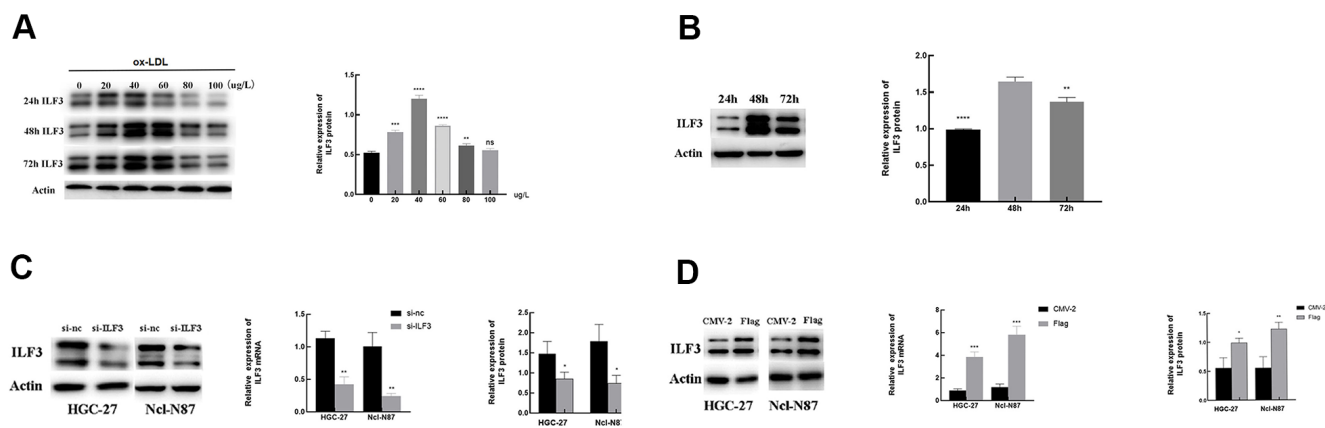


Figure 5. The relationship of the expression of ILF3 and ox-LDL. (A, B) ox-LDL promoted the expression of ILF3 in a time-concentration-dependent manner, the optimal concentration and intervention time was 40 $\mu\text{g/ml}$ and 48h. (C) ILF3 was knocked down by ILF3-specific small interference RNA (siRNA) in HGC-27 and Ncl-N87 cells. The mRNA and protein expression level of ILF3 was verified by RT-qPCR and western blot. The ILF3 expression at the mRNA and protein levels was significantly lower in the ILF3-siRNA group compared with the negative control group in HGC-27 and Ncl-N87 cells. (D) ILF3 was overexpressed by ILF3-overexpressed plasmids (flag-ILF3) in HGC-27 and Ncl-N87 cells. The mRNA and protein expression level of ILF3 was verified by RT-qPCR and western blot. The ILF3 expression at the mRNA and protein levels was significantly higher in the flag-ILF3 group compared with the negative control group in HGC-27 and Ncl-N87 cells. ** $P < 0.01$, *** $P < 0.001$, **** $P < 0.0001$ vs. 0 $\mu\text{g/L}$ or 48 h groups.

Knockdown of ILF3 inhibited the activity of PI3K/AKT/mTOR signaling pathway in gastric cancer cells

KEGG and GSEA analyses revealed that ILF3 affected GC through PI3K/AKT/mTOR signaling pathway.

Western blot analysis of p-PI3K/PI3K, p-AKT/AKT, and p-mTOR/mTOR found that p-PI3K, p-AKT, and p-mTOR were significantly downregulated ILF3-specific small interference and statins treatment groups compared to control group. And the expression of PI3K, AKT and mTOR did not change significantly

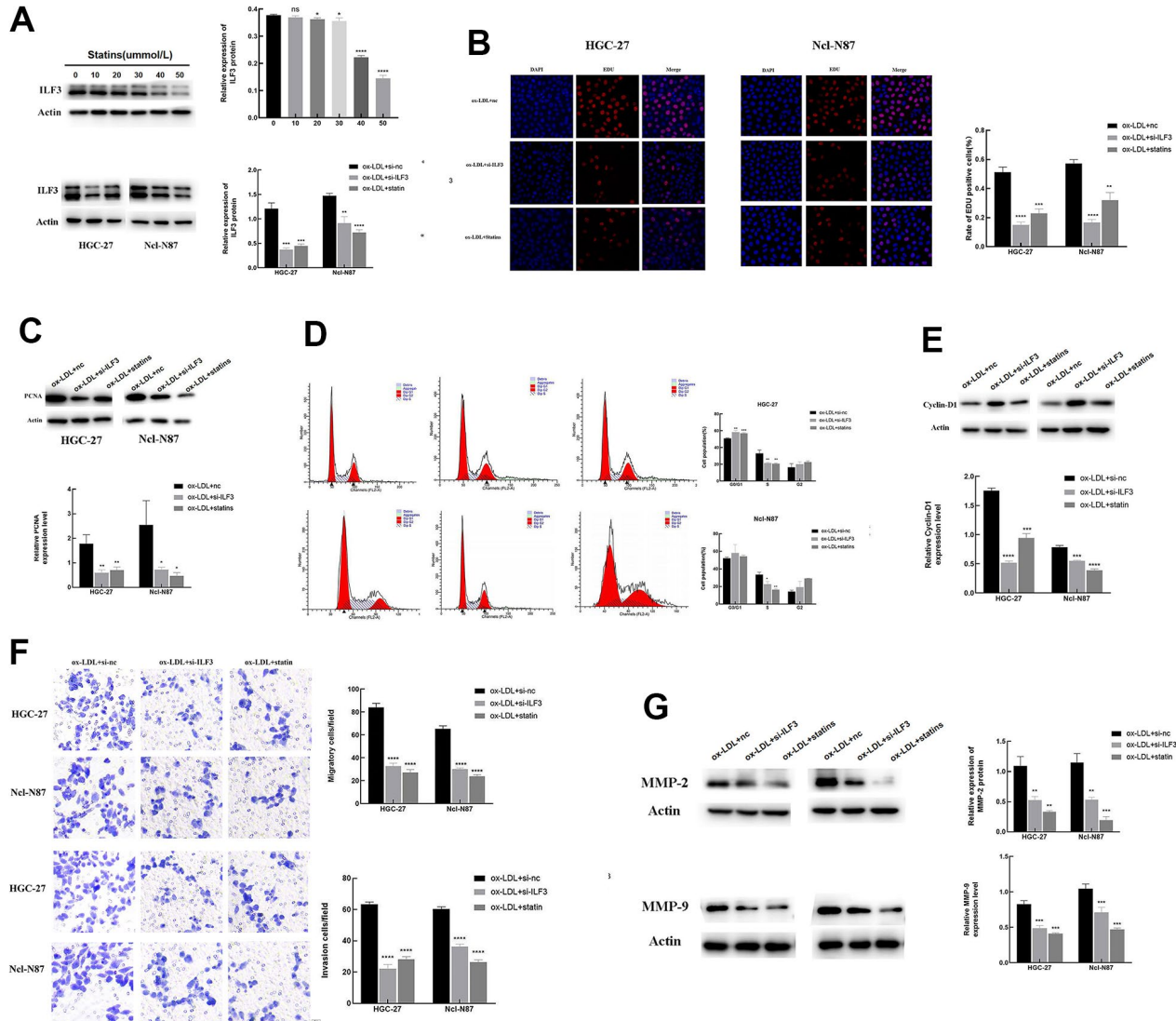


Figure 6. ILF3 promotes gastric cancer cells proliferation, cell cycle, migration, and invasion, and statins may exert an anti-tumor effect by inhibiting ILF3 expression in gastric cancer. (A) Statins inhibited the expression of ILF3 in a concentration-dependent manner, the optimal concentration was 40 μmol/L. The protein expression of ILF3 was significantly downregulated with ILF3-specific small interference RNA (si-ILF3) and statin treatment compared to control group. The expression level of ILF3 was analyzed with western blot. (B) Edu assay analyzed the effects of ILF3 on cell proliferation of gastric cancer cells. ILF3-specific small interference RNA (si-ILF3) and statins treatment inhibited the proliferation of HGC-27 and Ncl-N87 cells compared to control group. (C) The protein expression of PCNA was lower expressed in the ILF3-specific small interference and statins treatment groups compared to control group. (D) Flow cytometry analyzed the effect of ILF3 on cell cycle of gastric cancer cells. ILF3-specific small interference RNA (si-ILF3) and statins treatment inhibited the cell cycle of HGC-27 and Ncl-N87 cells compared to control group. (E) The protein expression of cyclin-D1 was lower expressed in the ILF3-specific small interference and statins treatment groups compared to control group. (F) Transwell assay analyzed the effect of ILF3 on cell migration and invasion. ILF3-specific small interference RNA (si-ILF3) and statins treatment inhibited the migration and invasion of HGC-27 and Ncl-N87 cells compared to control group. (G) The protein expression of MMP-2 and MMP-9 were lower expressed in the ILF3-specific small interference and statins treatment groups compared to control group. *P < 0.01, ***P < 0.001, ****P < 0.0001.

(Figure 7). These findings demonstrated that ILF3 regulated the proliferation, cell cycle, migration and invasion by activating the PI3K/AKT/mTOR signaling pathway.

ILF3 promoted gastric cancer cell proliferation, cell cycle, migration and invasion via PI3K/AKT/mTOR signaling pathway

To further define the role of PI3K/AKT/mTOR signaling pathway affected by ILF3 in the regulation of GC cell proliferation, cell cycle, migration, and invasion, the malignant biological of GC cells overexpressing ILF3 treated with PI3K/AKT inhibitor LY294002. ILF3-overexpressed plasmids (flag-ILF3) or vector plasmids (CMV2) were transfected into GC cells HGC-27 and Ncl-N87. The changes of cell phenotype were analyzed after treatment with ox-LDL+CMV2, ox-LDL+flag-ILF3, ox-LDL+flag-ILF3+PI3K/AKT inhibitor LY294002. And we set the ox-LDL+flag-ILF3 as the control group.

Western blotting found that p-PI3K, p-AKT, and p-mTOR were downregulated in ILF3-vector plasmids

(CMV2) and PI3K/AKT inhibitor LY294002 treatment groups compared to ILF3-overexpressed plasmids (flag-ILF3) group. And the expression of PI3K, AKT and mTOR did not change significantly (Figure 8A). These findings demonstrated that ILF3 activated the PI3K/AKT/mTOR signaling pathway. And the inhibition of the signaling pathway could reverse the gastric cancer-promoting effect of the overexpression of ILF3.

Edu assay analyzed the effects of PI3K/AKT/mTOR signaling pathway affected by ILF3 on cell proliferation of GC cells. The proportion of Edu-positive GC cells was higher than in the ILF3-overexpressed plasmids group compared to control group. LY294002 treatment reduced the proportion of Edu-positive GC cells compared to the ILF3-overexpressed plasmids group (Figure 8B, $P < 0.05$). The LY294002 treatment decreased the expression of PCNA compared to the ILF3-overexpressed plasmids group (Figure 8C, $P < 0.05$). Overall, inhibition of the signaling pathway impeded ILF3-mediated the proliferation of GC cells.

Flow cytometry analyzed the effects of the signaling pathway affected by ILF3 on the cell cycle. ILF3

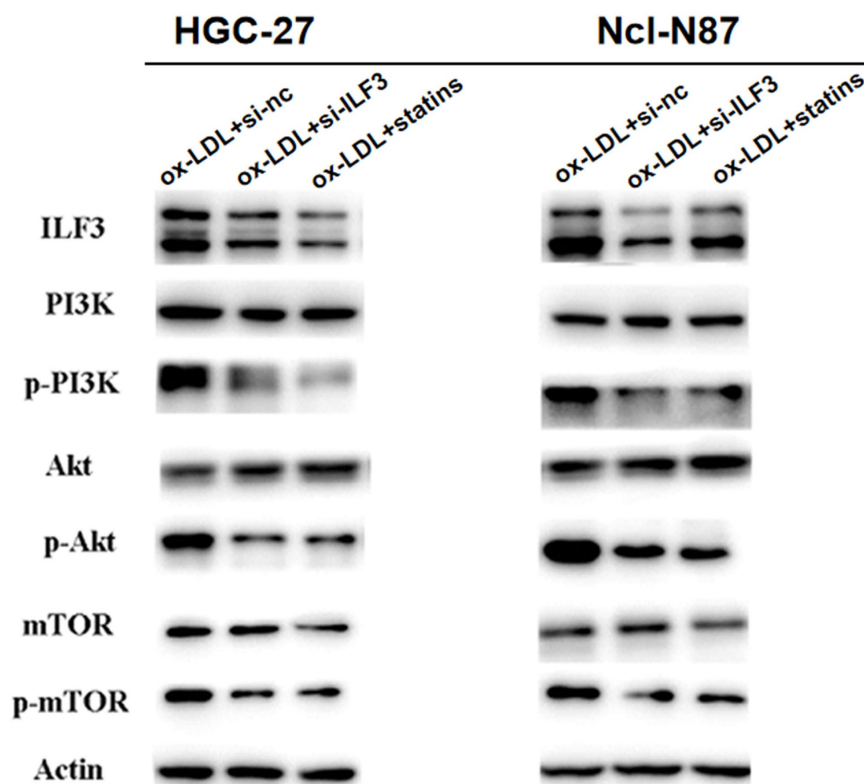


Figure 7. ILF3 was involved in the regulation of PI3K/AKT/mTOR signaling pathway. The effect of ILF3 on PI3K/AKT/mTOR signaling pathway was verified with western blot. ILF3-specific small interference RNA (si-ILF3) and statins treatment significantly inhibited PI3K/AKT/mTOR signaling pathway. The expression of p-PI3K/PI3K, p-AKT/AKT, and p-mTOR/mTOR were significantly downregulated compared to control group. And the expression of PI3K, AKT and mTOR and p-mTOR did not change significantly.

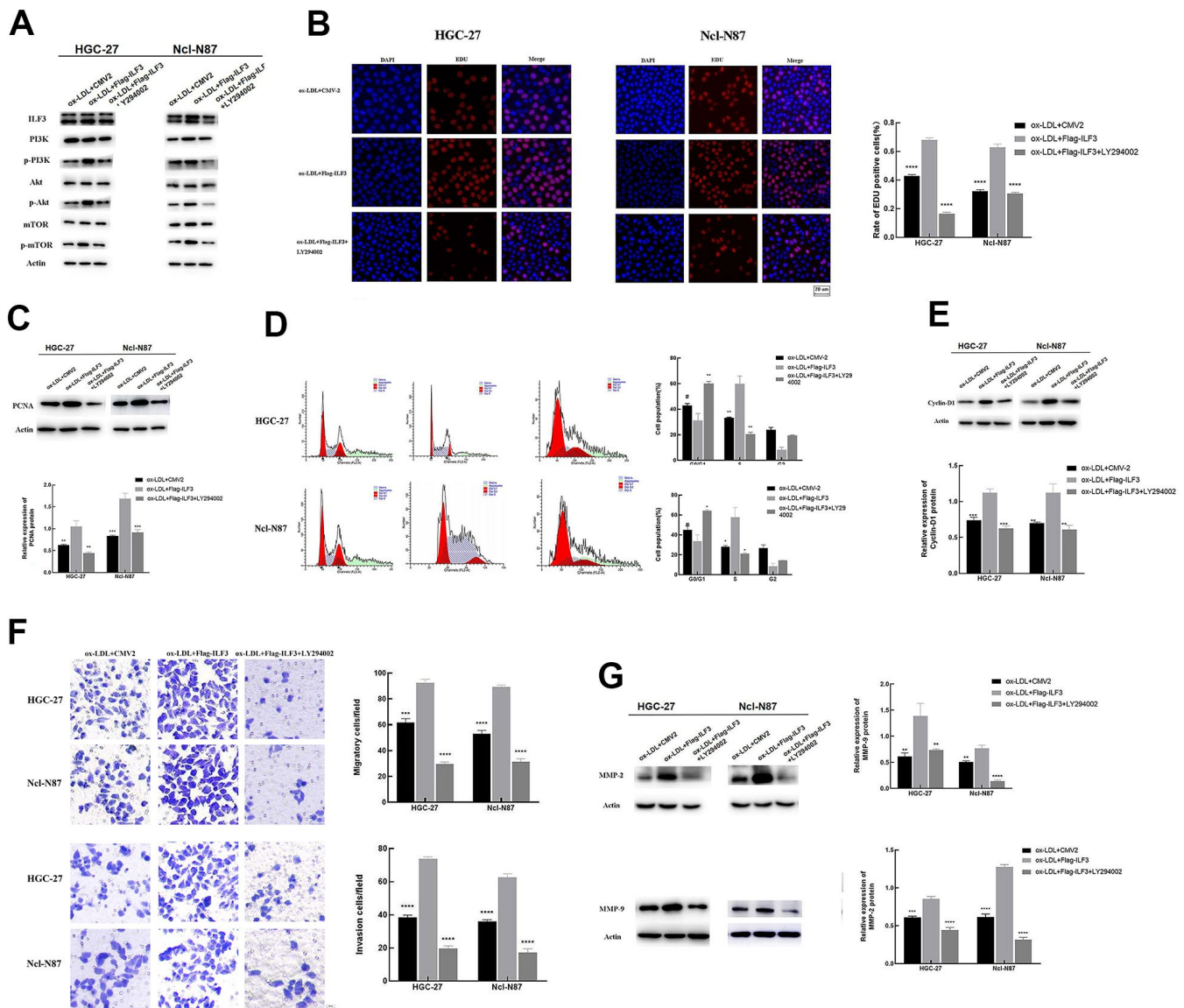


Figure 8. IL3 regulated gastric cancer cell proliferation, cell cycle, migration, and invasion via PI3K/AKT/mTOR signaling pathway. (A) The effect of ILF3 on PI3K/AKT/mTOR signaling pathway was verified with western blot. ILF3-overexpressed plasmids (flag-ILF3) treatment significantly activated PI3K/AKT/mTOR signaling pathway. The expression of p-PI3K/PI3K, p-AKT/AKT, and p-mTOR/mTOR were significantly upregulated compared to vector plasmids (CMV2) group. And PI3K/AKT inhibitor LY294002 treatment significantly inhibited the PI3K/AKT/mTOR signaling pathway. (B) Edu assay analyzed the effects of PI3K/AKT/mTOR signaling pathway affected by ILF3 on cell proliferation of gastric cancer cells. ILF3-overexpressed plasmids (flag-ILF3) treatment significantly promoted the proliferation of HGC-27 and Ncl-N87 cells. And PI3K/AKT inhibitor LY294002 treatment significantly inhibited the proliferation of HGC-27 and Ncl-N87 cells compared to control group ILF3-overexpressed plasmids (flag-ILF3) group. (C) The protein expression of PCNA was lower expressed in the PI3K/AKT inhibitor LY294002 treatment and vector plasmids (CMV2) groups compared to ILF3-overexpressed plasmids (flag-ILF3) group. (D) Flow cytometry analyzed the effects of PI3K/AKT/mTOR signaling pathway affected by ILF3 on cell cycle of gastric cancer cells. ILF3-overexpressed plasmids (flag-ILF3) treatment significantly promoted the cell cycle of HGC-27 and Ncl-N87 cells. And PI3K/AKT inhibitor LY294002 treatment significantly inhibited the cell cycle HGC-27 and Ncl-N87 cells compared to ILF3-overexpressed plasmids (flag-ILF3) group. (E) The protein expression of cyclin-D1 was lower expressed in the PI3K/AKT inhibitor LY294002 treatment and vector plasmids (CMV2) groups compared to ILF3-overexpressed plasmids (flag-ILF3) group. (F) Transwell assay analyzed the effects of PI3K/AKT/mTOR signaling pathway affected by ILF3 on migration and invasion of gastric cancer cells. ILF3-overexpressed plasmids (flag-ILF3) treatment significantly promoted the migration and invasion of HGC-27 and Ncl-N87 cells. And PI3K/AKT inhibitor LY294002 treatment significantly inhibited the migration and invasion HGC-27 and Ncl-N87 cells compared to ILF3-overexpressed plasmids (flag-ILF3) group. (G) The protein expression of MMP-2 and MMP-9 were lower expressed in the PI3K/AKT inhibitor LY294002 treatment and vector plasmids (CMV2) groups compared to ILF3-overexpressed plasmids (flag-ILF3) group. **P < 0.01, ***P < 0.001, ****P < 0.0001.

overexpression downregulated the proportion of HGC-27 and Ncl-N87 in the G0/G1 phase and increased the proportion of HGC-27 and Ncl-N87 in the S phase in the ILF3-overexpressed plasmids group compared to control group. LY294002 treatment increased the proportion of HGC-27 and Ncl-N87 in the G0/G1 phase and reduced the proportion of HGC-27 and Ncl-N87 in the S phase compared to the ILF3-overexpressed plasmids group (Figure 8D, $P < 0.05$). The LY294002 treatment downregulated the cyclin-D1 expression compared with ILF3-overexpressed group (Figure 8E, $P < 0.05$). Overall, inhibition of the PI3K/AKT/mTOR signaling pathway impeded ILF3-mediated the cell cycle of GC cells.

Transwell assay analyzed the effects of the signaling pathway affected by ILF3. The number of migrated and invasive GC cells was remarkably elevated in the ILF3-overexpressed plasmids group compared to control group (Figure 4F, $P < 0.05$). LY294002 treatment reduced the number of migrated and invasive GC cells compared to the ILF3-overexpressed plasmids group (Figure 8E, $P < 0.05$). The protein expression of MMP-2 and MMP-9 were higher in ILF3-overexpressed plasmids group compared to control group. LY294002 treatment decreased the expression of MMP-2 and MMP-9 compared to the ILF3-overexpressed plasmids group (Figure 8G, $P < 0.05$). Overall, suppress the PI3K/AKT/mTOR signaling pathway impeded ILF3-mediated the invasion and migration of GC cells.

ILF3 promoted tumorigenesis of *in vivo* gastric cancer cells

To test the consequent of ILF3 on the growth of GC cells *in vivo*, a xenograft tumor model was employed. Sixteen of twenty nude mice survived up to the end of the experiments. Tumors of the high-fat diets had larger volumes than those of the normal diets group. Tumors of statins treatment and YM-155 (ILF3 inhibitor) treatment groups had smaller volumes than those of the high-fat diets group (Figure 9A, $P < 0.05$). Immunohistochemistry showed that the expression of ILF3 in high-fat diets was significantly higher compared with the normal diet group. The expression of ILF3 in statins treatment and YM-155 (ILF3 inhibitor) treatment groups were lower than those of the high-fat diets group (Figure 9B, $P < 0.05$).

ILF3 was involved in the regulation of PI3K/AKT/mTOR signaling pathway in gastric cancer cell SGC-7901

The experiments were conducted in SGC-7901 cells to confirm the relationship of ILF3 and the related signaling pathway. Western blotting found that p-PI3K, p-AKT, and p-mTOR were significantly downregulated

ILF3-specific small interference and statins treatment groups compared to control group. The expression of PI3K, AKT and mTOR did not change significantly. The protein level of p-PI3K, p-AKT, and p-mTOR were significantly downregulated in ILF3-vector plasmids (CMV2) and PI3K/AKT inhibitor LY294002 treatment groups compared to control group. But the expression of PI3K, Akt and mTOR did not obviously changed (Figure 10).

DISCUSSION

Gastric cancer ranks fifth in the global incidence (5.6%) and fourth in tumor-related mortality (7.7%) [1]. Studies have investigated molecular mechanisms of GC. However, the pathogenesis needs to be further revealed. Therefore, more and more research has focused on patient-specific factors to provide more effective treatment to achieve precise treatment, thereby reducing morbidity and mortality [56]. Recently, studies have shown that lipid metabolism dysfunction plays significant role in gastric carcinogenesis [57], which provides a new research direction to predict, prevent, and early diagnosis of GC. High-fat diets and obesity have been regarded as risk factors of GC [58]. Therefore, dietary modifications and losing weight primary and secondary prevention strategies to reduce the risk of GC. In addition, this study focused on the molecular mechanism and targets of GC caused by abnormal lipid metabolism and find a new biomarker for early diagnoses of GC. In addition to formulating personalized treatment plans for targets, it is more important to find targeted drugs to successfully transform research results into results that benefit patients.

Obesity leads to diseases such as abnormal lipid metabolism and hyperlipidemia [59], and is an important risk factor for carcinogenesis. Some studies have demonstrated that improvement of blood lipid levels and obesity control reduced the occurrence rate of GC, colorectal cancer, and esophageal cancer [60–62]. Abnormal lipid metabolism triggers a cascade of molecular events to finally cause malignancy. So, understanding mechanisms that how obesity or abnormal lipid metabolism induce GC development is important to prevent and treat GC. A case-control study in South Korea has found the higher blood LDL in patients with GCs compared to healthy people [63]. And LDL can easily be oxidized to ox-LDL which is an important feature of abnormal lipid metabolism [64, 65]. While, ox-LDL is critical in the progress of atherosclerosis and non-alcoholic steatohepatitis [66, 67]. Recently, studies have revealed the function of ox-LDL in the cancer cell proliferation [24], cell cycle [68], EMT [69], angiogenesis [70] and metastasis [71]. However, the detailed mechanism of ox-LDL to regulate the

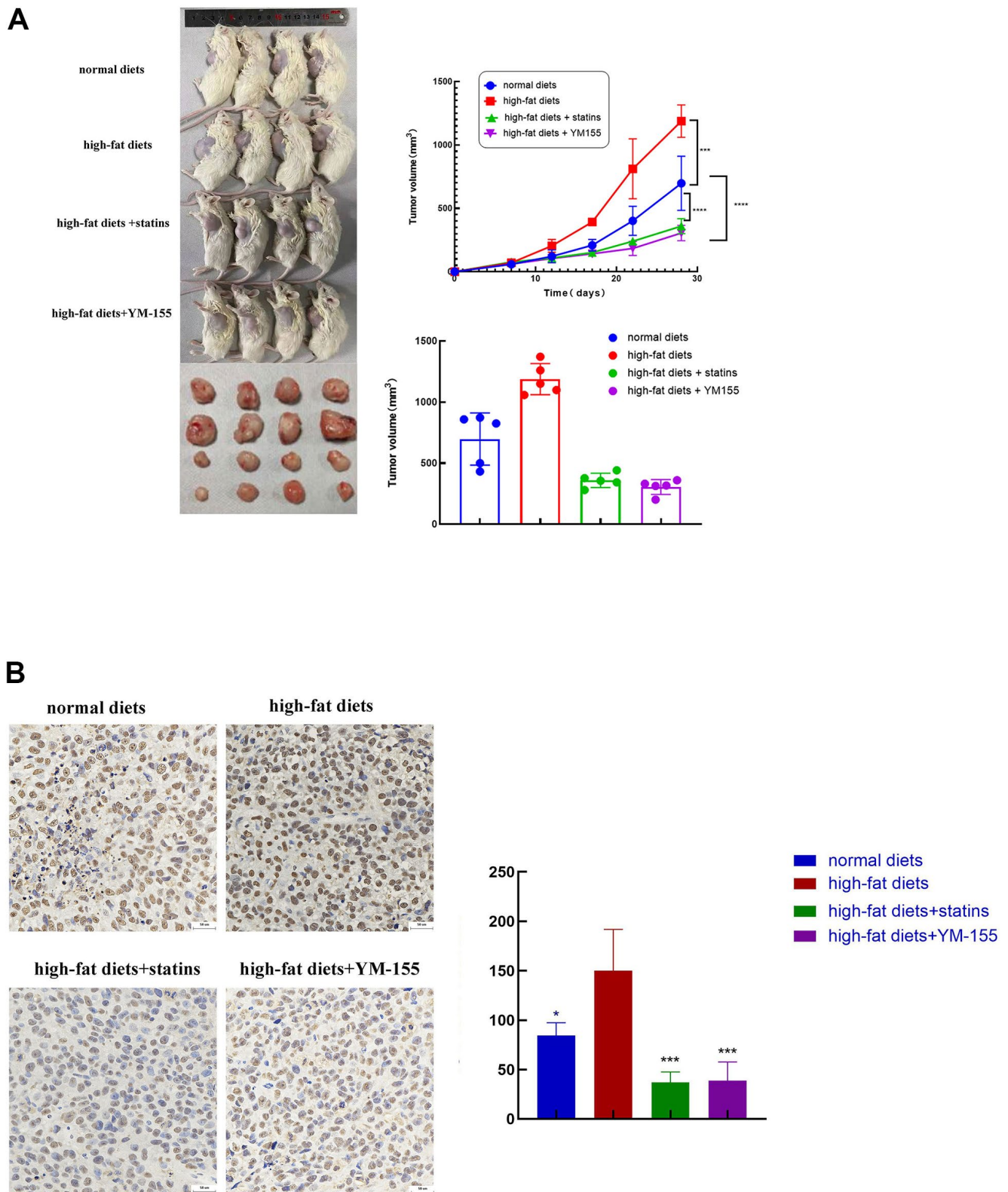


Figure 9. ILF3 promoted tumor cell growth *in vivo*. (A) Images of nude mouse tumorigenesis test after four weeks of implantation. Comparison of tumor volume between normal diets, high-fat diets, high-fat diets+statin and high-fat diets + ILF3 inhibitor-YM155. Tumors in high-fat diet group were bigger than normal diet group. Tumors in statin and ILF3 inhibitor-YM-155 groups were smaller than high-fat diet group. (B) Immunohistochemistry showed that the expression of ILF3 in normal diets, high-fat diets, high-fat diets+statin and high-fat diets + ILF3 inhibitor-YM155 groups. **P < 0.01, ***P < 0.001, ****P < 0.0001.

downstream gene expression or involved signaling pathways in GC is still unclear. It has been shown that ILF3 was associated with plasma LDL cholesterol, and has been considered as a candidate gene for the patients with acute myocardial infarction in Japanese [33, 34]. But the reports on the relationship of ox-LDL and the expression of ILF3, and their relationship with the occurrence and development of GC have never been reported. We found ox-LDL promoted the expression of ILF3 in a time-concentration dependent manner in GC cells, which provided a new research direction of the relationship of ox-LDL and GC.

Previous research has reported that ILF3 plays as a transcriptional coactivator and involves in proliferation and metastasis of tumor [72]. To further explore the function of ILF3, GO analysis on the sequencing results was performed to guide the next step of phenotyping experiments. GO analysis exhibited that ILF3 was vital in GC cell proliferation, migration and invasion, indicating the oncogenic role of ILF3. We showed that ILF3 promoted proliferation of GC *in vitro*, and ILF3

overexpression accelerated cell proliferation rate with upregulation of PCNA expression in GC cells, suggesting that ILF3 promotes GC progression. Previous research reported that downregulation of ILF3 could delay hepatocellular carcinoma cell cycle progression and inhibit cell proliferation [73]. And to a certain extent, the cell cycle reflects the proliferation status of GC cells. After ILF3 inhibition by ILF3-specific small interference, the proportion of GC cells in G0/G1 phase was increased, which indicated that ILF3 promoted the proliferation and cell cycle of GC cells.

Cell invasion and migration are typical hallmark of malignancies [74]. Consistent with previous study in melanoma, our results indicated that ILF3 could accelerate the invasion and migration of GC cells *in vitro* [75]. When ILF3 was down-regulated by siRNA, the migration and invasion of GC cells *in vitro* were significantly inhibited. Thereby, the results validated that ox-LDL promoted the overexpression of ILF3 to enhance proliferation, cell cycle, migration and invasion of GC cells, thereby promoting the occurrence and development of GC.

Statins can lower plasma cholesterol, and are extensively used to prevent cardiovascular diseases [76, 77]. Currently studies have found that statins have multiple functions, including anti-inflammatory, antioxidant, antithrombotic, anticancer, and cancer chemopreventive effects. Several studies found that statins improved chemosensitivity in a variety of cancers and was used as an adjuvant to chemotherapy [78]. A meta-analysis of studies supported the association between statin and GC risk [39]. A previous study found that Hp infection was the most common cause for GC [39], and cytotoxin-associated gene A (CagA) is the most-important virulence factor of Hp [79]. Hp can manipulate the cholesterol-rich microdomains (also called lipid rafts), which contributes to CagA functions and pathogenesis [80], and statins disrupt the lipid raft of cell membranes to inhibit pathogenic function of CagA [79]. A meta-analysis demonstrated that the inhibition of cancer by statins was more pronounced in distal than proximal GC, and that Hp infection is not the only risk factor for GC [42]. Besides, study had reported that the inhibition of the mevalonate pathway reverted the malignancy potential and reduce the invasiveness of cancers [81]. However, molecular mechanisms for the use of statins to treat GC remain unclear. Thus, it is crucial to find new targets to provide a reliable fundamental basis for statins against GC.

From CC analysis, the results showed that ILF3 was also associated with membrane raft. We proposed that statins may play anti-tumor effects in GC by acting on ILF3. To verify this hypothesis, in the present study we

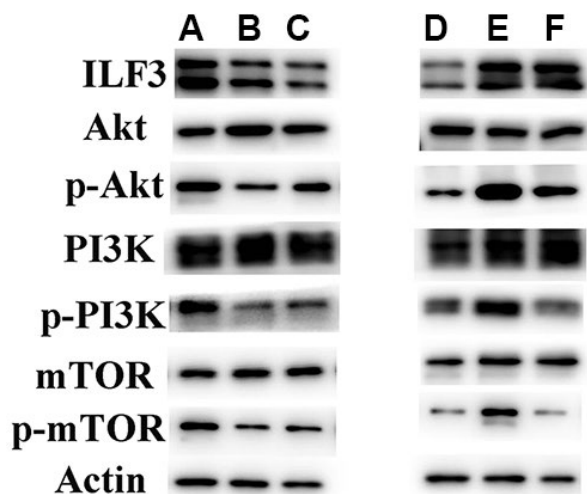


Figure 10. ILF3 was involved in the regulation of PI3K/AKT/mTOR signaling pathway in gastric cancer cell SGC-7901. (A:ox-LDL+si-nc;B:ox-LDL+si-ILF3;C:ox-LDL+statin; D:ox-LDL+CMV-2;E:ox-LDL+flag-ILF3;F:ox-LDL+flag-ILF3+PI3K/AKT inhibitor LY294002). (A–C) ILF3-specific small interference RNA (si-ILF3) and statins treatment significantly inhibited PI3K/AKT/mTOR signaling pathway. The expression of p-PI3K/PI3K, p-AKT/AKT, and p-mTOR/mTOR were significantly downregulated compared to control group. And the expression of PI3K, Akt and mTOR and p-mTOR did not change significantly. (D–F) ILF3-overexpressed plasmids (flag-ILF3) treatment significantly activated PI3K/AKT/mTOR signaling pathway. The expression of p-PI3K/PI3K, p-AKT/AKT, and p-mTOR/mTOR were significantly upregulated compared to vector plasmids (CMV2) group. PI3K/AKT inhibitor LY294002 treatment significantly inhibited the PI3K/AKT/mTOR signaling pathway.

conducted a series of experiments. We found statins treatment significantly inhibited the mRNA and protein expressions of ILF3 compared to control group in GC cells. The cell functional experiments revealed that statins treatment significantly inhibited the proliferation, cell cycle, migration and invasion of GC cells by inhibiting ILF3. The animal experiments revealed that ILF3 inhibitor (YM-155) and statins treatment not only the volume of subcutaneous, but also the expression of ILF3 were significantly reduced. These findings were consistent with previous findings that the expression of ILF3 was significantly lower in patients with taking statins when compared to patients who didn't take statins. Thereby, these data supported that ILF3 acted as a tumor promoter and served as a potential new target for the use of statins to treat GC patients, and ILF3 elimination is a significant target to prevent and intervene GC, providing rationale for the use of statins to treat GC.

Obesity-associated cancer is a major health burden and has been intensively studied. Researchers have identified multiple cancer risk factors including adipokines, cytokines, insulin/insulin-like growth factor axis, and other cellular signal pathways. Among them, lipids regulate some important oncogenic pathways such as PI3K/AKT/mTOR, Ras, or Wnt pathways [82, 83]. In this study, based on KEGG pathway enrichment analysis and GSEA analysis, the expression levels of ILF3 could regulate the activation of the PI3K/AKT/mTOR signaling pathway

The PI3K/AKT/mTOR signaling pathway is important in tumor progression, including cell proliferation, invasion, metastasis, cell cycle, apoptosis, and metabolic functions [84, 85]. Thus, discovery of new specific targets to activate PI3K/AKT/mTOR signaling pathway has become a hotspot of research among targeted interventions of GC. And the role of ILF3 in the modulation of PI3K/AKT/mTOR signaling pathway is unrevealed.

This study validated that interference of ILF3 and statins treatment downregulated the phosphorylation PI3K, AKT and mTOR, thereby inhibit the PI3K/AKT/mTOR signaling pathway in GC cells. The rescue experiments were designed, in which PI3K/AKT/mTOR signaling pathway inhibitors under the premise of overexpression of ILF3 were used to observe the phenotypic changes of GC cells. The rescue experiments demonstrated that the inhibitor of signaling pathway reversed overexpression effect of ILF3 on cell proliferation, cell cycle, migration, and invasion of GC cells. Therefore, ILF3 promoted cell proliferation, cell cycle, migration, and invasion by regulating PI3K/AKT/mTOR signaling pathway in GC cells.

ILF3 and its regulated PI3K/AKT/mTOR signaling pathway are valuable resource for GC in the field of abnormal lipid metabolism, providing insights into lipid metabolism and discovery of energy metabolism-based molecular biomarker pattern and new antitumor targets/drugs to effectively treat GC. ILF3 might be a new GC marker for risk stratification in people with obesity or abnormal lipid level. According to the individual risks, appropriate preventive measures can be taken. For high-risk group of GC, statins treatment improved blood lipid levels when inhibiting the expression of ILF3, and reduced the occurrence of GC. Statins combined with chemotherapy might aid personalized treatment of treatment of high-expressed ILF3 GC patients.

CONCLUSIONS

This study shows that ox-LDL promotes the expression of ILF3 through the PI3K/AKT/mTOR signaling pathway, thus facilitates the proliferation, cell cycle, migration and invasion of gastric cancer cells, providing a potential new biomarker for the early detection and the therapeutic target of gastric cancer patients.

MATERIALS AND METHODS

Clinical specimen acquisition and analysis

The data of mRNA sequencing and corresponding clinical information of 375 GC samples and 32 normal cases were obtained from The Cancer Genome Atlas (TCGA) database (<https://tcga-data.nci.nih.gov/>). The paired gastric cancer tissue and matched adjacent normal tissue were collected from 33 patients with GC admitted to Qilu Hospital, Cheeloo College of Medicine, Shandong University (Jinan, China) between January 2020 and December 2020 before surgery, these patients did not receive any other treatments, such as radiotherapy, chemotherapy, and targeted therapy. Informed consent was obtained from all participants.

Whole-genome RNA sequencing

The gastric cancer cells SGC-7901 were randomly divided into the interference group (infected with ILF3-specific siRNA) and the transfected negative control group. RNeasy mini kit (Qiagen, Germany) was applied to isolate total RNA. TruSeq™ RNA Sample Preparation Kit (Illumina, USA) was used to synthesize paired-end libraries. The final cDNA library was then created with PCR by purification and enrichment. The library construction and sequencing were implemented by Sinotech Genomics Co., Ltd (Shanghai, China). R package edgeR was carried out to analyze the mRNA differential expression. Differentially expressed RNAs

with $|\log_2(\text{fold-change})|$ value >1 and q value <0.05 were reserved for further analysis.

Functional enrichment analyses

We performed the Gene Ontology (GO) [86] and Kyoto Encyclopedia of Genes and Genomes (KEGG) pathway enrichment analyses based on the RNA sequencing, which included the biological processes (BP), cellular components (CC), molecular functions (MF), and pathways. The p value <0.05 were considered significant.

Gene Set Enrichment Analysis (GSEA) was performed to figure out the signaling pathway which may be regulated by ILF3. The normalized enrichment score (NES) >1 was considered as statistical significance.

Cell lines and cell culture

The gastric cancer cell lines GES, SGC-7901, HGC-27, Ncl-N87, and SNU-1 were obtained from Fuheng company, Shanghai, China, and were cultured in 1640 media (Gibco) supplemented with 10% fetal bovine serum (Gibco) and 1% penicillin/streptomycin (Millipore) in a humidified incubator with 5% CO₂ at 37° C.

ILF3-siRNA transfection and groupings

For the knockdown of ILF3, cells were transfected with ILF3-specific siRNA or scramble siRNA with lipofectamine 3000 reagents. Each targeting sequence was shown: si-ILF3: 5'-ACG UGA CAC GUU CGG AGA ATT-3'; si-nc: 5'-UUC UCC GAA CGU GUC ACG UTT-3'. According to the manufacturer's protocol, GC cells were seeded in a 6-well plate, and cultivated for 24h prior to transfection. And transfection was performed when the cells reached ~70% confluence. Subsequent experiments were performed at 48h post-transfection.

Plasmid construction and transfection

Human ILF3 Gene cDNA Clone (full-length ORF Clone) was cloned into Flag-ILF3 vector. For transfection, the Lipofectamine 3000 and OPTI-MEM (Gibco, Shanghai, China) were mixed with plasmids, transfected into cells and incubate for 24 hours.

Cell proliferation assay (Edu assay)

GC cells were seeded in 12-well plates to confluence and cultured with 10- μ M EdU for an additional 2h. Then 4% formaldehyde (PFA) was used to fix the cells for 30 min at room temperature (RT). After washing, Click-iTR EdU kit was used to detect EdU, with a detection time of ~30

min. After 10 min incubation with DAPI, the cells were observed with a fluorescence microscope (Olympus). The EdU incorporation rate was calculated by Image-Pro Plus 6.0 software (Media Cybernetics). The result was expressed as the ratio of EdU-positive cells to total DAPI-positive cells.

Flow cytometry for cell cycle analysis

Gastric cancer cells were centrifuged (1000g, 5 min, and 4° C), and rinsed with a volume (1 ml) of precooled PBS. Then a volume (1 ml) of precooled 70% ethanol was added, and the cells were maintained at 4° C for 2 h. The cell suspension was added with a volume (1 ml) of precooled PBS, and the supernatant was discarded after centrifugation (1000 g, 5 min, and 4° C). The cells were resuspended in a volume (500 μ l) of binding buffer with 25 μ l propidium Iodide (20 x) and 10 μ l RNase A (50 x) (RT, darkness, and 30min). Then the flow cytometry was performed.

Detection of cell migration and invasion

Human gastric cancer cell lines were collected, and suspended with 1640 medium (Gibco), made into 1.5×10^5 cells/ml. The cell suspension (200 μ l) was incubated into the upper chamber for migration (or precoated with 100 μ l Matrigel solution [BD] for invasion). A volume (600 μ l) of medium containing 20% FBS and specific treatment was applied to the lower chamber. After 24 h plating, the cells remaining on the upper chamber were removed with a cotton swab. The cells in the lower chamber were fixed and stained. And the number of migration and invasion cells was counted and photographed in three randomly selected view-fields.

Western blotting

The total proteins were collected from gastric cancer cells grown in a 6-well plate with specific treatment. Briefly, the cells were harvested and lysed with RIPA lysis buffer containing 1 \times protease inhibitor cocktail. A portion (5 μ l) of protein samples was separated by SDS-PAGE, and transferred onto PVDF membrane. PVDF membrane was blocked with 5% non-fat milk (1h, room temperature), and incubated with primary antibody (overnight, 4° C). The proteins on PVDF Membrane were incubated with secondary anti-rabbit antibodies (1h, room temperature). The levels of proteins and phosphoproteins were determined with WesternBright ECL. The primary antibodies were against ILF3 (Abcam, USA), PCNA (Abcam, USA), cyclinD1 (Abcam, USA), MMP9 (Abcam, USA), MMP2 (Abcam, USA), Akt (CST, USA), p-Akt (CST, USA), PI3K (CST, USA), p-PI3K (CST, USA), mTOR (CST, USA), and p- mTOR (CST, USA).

Immunohistochemistry staining (IHC)

Gastric cancer tissues and adjacent nonmalignant tissues were PFA-fixed, paraffin-embedded, and cut into 5- μ m-thick consecutive sections. Each section was then immersed in sodium citrate solution (pH 6.0, 20 min, 98° C) and washed three times with 1x PBS for 3 min/time to achieve deparaffinization and antigen recovery. The sections were permeabilized with PBS containing 0.5% Triton X-100 for 20 min at RT. After initial incubation in 4% normal goat serum (30 min, RT), primary antibody was used and incubated (4° C, overnight). After washing with PBS, each tissue section was incubated with secondary antibody for 1 h at RT, and then stained with diaminobenzidine (DAB). After washing in PBS, nuclei were stained with hematoxylin (Sigma-Aldrich) for 10 min, and washed in tap water. Immunohistochemistry for each sample was repeated thrice.

Real-time quantitative PCR (RT-qPCR)

RNAfast200 was applied to extract the total RNAs. Reverse transcription was performed in a total volume 20 μ l with reverse transcriptase. To remove genomic DNA, samples were mixed with gDNA wipeout buffer and incubated (42° C, 2min), and further incubated at 37° C for 15 min, and 85° C for 5 s to obtain cDNA. The prepared sample was stored at -20° C until use.

The quantification cycle (Cq) was calculated with the amplification curve. The experiments were repeated thrice. The primers for ILF3 were forward 5'-CATTACGCCATGAAACGCC-3', and reverse 5'-TAAAGATGGGGGCATGGACG-3'. The primers for GAPDH were forward 5'-GCACCGTCAAGGCTGAGAAC-3', and reverse 5'-TGGTGAAGACGCCAGTGGA-3'.

Xenograft tumor

Four-week-old male nude mice were obtained from Sibeifu Company (Beijing, China). A total of 1×10^7 HGC-27 cells were subcutaneously injected into nude mice (n = 5 per group). Nude mice were randomly divided into four groups (n = 5 per group): normal diets, high-fat diets, high-fat diets + statins treatment, and high-fat diets + ILF3 inhibitor-YM155 treatment. The tumor size was measured every 4 days with a vernier caliper starting from the day 7 after subcutaneous tumor. The treatment group were injected with statins (intraperitoneally, 5 mg/kg) or ILF3 inhibitor (intraperitoneally, 5 mg/kg) once every 3 days. The tumor volume was calculated with volume = $0.5 \times \text{length} \times \text{width}^2$. All animal experiments met the ethic regulations.

Statistical analysis and bioinformatics

SPSS 26.0 and GraphPad Prism 9.1.2 software were used to perform statistical analysis. Data was expressed as mean \pm SD of 3 independent biological replicates. Differences between two groups were analyzed by unpaired two-tailed Student's t-test. Multiple comparisons between groups were performed with ANOVA test. A P-value < 0.05 was considered as statistically significance.

Ethics approval

All investigations conformed to the principles outlined in the Declaration of Helsinki and were performed with permission by the responsible Medical Ethics Committee of Qilu Hospital of Shandong University.

Abbreviations

AFP: alpha-fetoprotein; Akt: serine-threonine kinase; BP: biological processes; CA125: cancer antigen 125; CA19-9: cancer antigen 19-9; CA72-4: cancer antigen 72-4; CC: cellular components; CEA: carcinoembryonic antigen; DRBPs: double-stranded RNA-binding proteins; GSEA: Gene Set Enrichment Analysis; ILF3: Interleukin-enhancer binding factor 3; LDL: low-density lipoprotein; LDL-C: low-density lipoprotein cholesterol; MF: molecular functions; MMP2: matrix metalloproteinase 2; MMP9: matrix metalloproteinase 9; mTOR: mammalian target of rapamycin; ox-LDL: oxidized low-density lipoprotein; p-Akt: phosphorylated serine-threonine kinase; PCNA: proliferating cell nuclear antigen; PI3K: phosphatidylinositol 3 kinase; p-mTOR: phosphorylated mammalian target of rapamycin; p-PI3K: phosphorylated phosphatidylinositol 3 kinases; ROS: reactive oxygen species; TCGA: The Cancer Genome Atlas; GSEA: Gene Set Enrichment Analysis.

AUTHOR CONTRIBUTIONS

D. S. performed most experiments. W.Y. and M.Z. designed the overall study. Z.W. and W.Q. supervised the experiments. D.S. wrote the paper. M.W. and Y. L. completed the collection and processing of clinical specimens. P.L., X. Z., Y. C. and Y.H. analyzed data. W.Y. revised the paper and acquired the funding. All authors read and approved the final manuscript.

ACKNOWLEDGMENTS

The authors also acknowledge Professor Mingxiang Zhang from The Key Laboratory of Cardiovascular Remodeling and Function Research, Chinese Ministry of Education, Chinese Ministry of Health and Chinese Academy of Medical Sciences, Department of Cardiology to assist in experimental design and guidance.

CONFLICTS OF INTEREST

The authors declare that they have no conflicts of interest.

FUNDING

This work was supported by Natural Science Foundation of Shandong Province, China (Grant/Award Number: ZR201911030023; and ZR2019LZL006).

REFERENCES

1. Sung H, Ferlay J, Siegel RL, Laversanne M, Soerjomataram I, Jemal A, Bray F. Global Cancer Statistics 2020: GLOBOCAN Estimates of Incidence and Mortality Worldwide for 36 Cancers in 185 Countries. *CA Cancer J Clin.* 2021; 71:209–49. <https://doi.org/10.3322/caac.21660> PMID:33538338
2. Cao W, Chen HD, Yu YW, Li N, Chen WQ. Changing profiles of cancer burden worldwide and in China: a secondary analysis of the global cancer statistics 2020. *Chin Med J (Engl).* 2021; 134:783–91. <https://doi.org/10.1097/CM9.0000000000001474> PMID:33734139
3. Sitarz R, Skierucha M, Mielko J, Offerhaus GJ, Maciejewski R, Polkowski WP. Gastric cancer: epidemiology, prevention, classification, and treatment. *Cancer Manag Res.* 2018; 10:239–48. <https://doi.org/10.2147/CMAR.S149619> PMID:29445300
4. Yang L, Li Y, Zhou T, Shi G, Pan J, Liu J, Wang G. Effect of the degree of gastric filling on the measured thickness of advanced gastric cancer by computed tomography. *Oncol Lett.* 2018; 16:2335–43. <https://doi.org/10.3892/ol.2018.8907> PMID:30008937
5. Chen S, Chen X, Nie R, Ou Yang L, Liu A, Li Y, Zhou Z, Chen Y, Peng J. A nomogram to predict prognosis for gastric cancer with peritoneal dissemination. *Chin J Cancer Res.* 2018; 30:449–59. <https://doi.org/10.21147/j.issn.1000-9604.2018.04.08> PMID:30210225
6. Torre LA, Bray F, Siegel RL, Ferlay J, Lortet-Tieulent J, Jemal A. Global cancer statistics, 2012. *CA Cancer J Clin.* 2015; 65:87–108. <https://doi.org/10.3322/caac.21262> PMID:25651787
7. Liu X, Chen L, Fan Y, Hong Y, Yang X, Li Y, Lu J, Lv J, Pan X, Qu F, Cui X, Gao Y, Xu D. IFITM3 promotes bone metastasis of prostate cancer cells by mediating activation of the TGF- β signaling pathway. *Cell Death Dis.* 2019; 10:517. <https://doi.org/10.1038/s41419-019-1750-7> PMID:31273201
8. Weng J, Li S, Lin H, Mei H, Liu Y, Xiao C, Zhu Z, Cai W, Ding X, Mi Y, Wen Y. PCDHGA9 represses epithelial-mesenchymal transition and metastatic potential in gastric cancer cells by reducing β -catenin transcriptional activity. *Cell Death Dis.* 2020; 11:206. <https://doi.org/10.1038/s41419-020-2398-z> PMID:32231199
9. Yu J, Zheng W. An Alternative Method for Screening Gastric Cancer Based on Serum Levels of CEA, CA19-9, and CA72-4. *J Gastrointest Cancer.* 2018; 49:57–62. <https://doi.org/10.1007/s12029-016-9912-7> PMID:28028765
10. Li Y, Yang Y, Lu M, Shen L. Predictive value of serum CEA, CA19-9 and CA72.4 in early diagnosis of recurrence after radical resection of gastric cancer. *Hepatogastroenterology.* 2011; 58:2166–70. PMID:22024091
11. He CZ, Zhang KH, Li Q, Liu XH, Hong Y, Lv NH. Combined use of AFP, CEA, CA125 and CA19-9 improves the sensitivity for the diagnosis of gastric cancer. *BMC Gastroenterol.* 2013; 13:87. <https://doi.org/10.1186/1471-230X-13-87> PMID:23672279
12. Wu D, Zhang P, Ma J, Xu J, Yang L, Xu W, Que H, Chen M, Xu H. Serum biomarker panels for the diagnosis of gastric cancer. *Cancer Med.* 2019; 8:1576–83. <https://doi.org/10.1002/cam4.2055> PMID:30873760
13. Gong X, Zhang H. Diagnostic and prognostic values of anti-helicobacter pylori antibody combined with serum CA724, CA19-9, and CEA for young patients with early gastric cancer. *J Clin Lab Anal.* 2020; 34:e23268. <https://doi.org/10.1002/jcla.23268> PMID:32118318
14. Shah MA, Khanin R, Tang L, Janjigian YY, Klimstra DS, Gerdes H, Kelsen DP. Molecular classification of gastric cancer: a new paradigm. *Clin Cancer Res.* 2011; 17:2693–701. <https://doi.org/10.1158/1078-0432.CCR-10-2203> PMID:21430069
15. Strader CD, MacIntyre DE, Candelore MR, Parker EM. Molecular approaches to the discovery of new treatments for obesity. *Curr Opin Chem Biol.* 1997; 1:204–9. [https://doi.org/10.1016/s1367-5931\(97\)80011-7](https://doi.org/10.1016/s1367-5931(97)80011-7) PMID:9667852
16. Liu G, Zheng X, Xu Y, Lu J, Chen J, Huang X. Long non-coding RNAs expression profile in HepG2 cells reveals the potential role of long non-coding RNAs in the cholesterol metabolism. *Chin Med J (Engl).* 2015; 128:91–7. <https://doi.org/10.4103/0366-6999.147824> PMID:25563320

17. Kuzu OF, Noory MA, Robertson GP. The Role of Cholesterol in Cancer. *Cancer Res.* 2016; 76:2063–70. <https://doi.org/10.1158/0008-5472.CAN-15-2613> PMID:[27197250](https://pubmed.ncbi.nlm.nih.gov/27197250/)
18. Lu M, Gursky O. Aggregation and fusion of low-density lipoproteins *in vivo* and *in vitro*. *Biomol Concepts.* 2013; 4:501–18. <https://doi.org/10.1515/bmc-2013-0016> PMID:[25197325](https://pubmed.ncbi.nlm.nih.gov/25197325/)
19. Chang C, Liu H, Wei C, Chang L, Liang J, Bei H, Li H, Liu S, Wu Y. Tongxinluo Regulates Expression of Tight Junction Proteins and Alleviates Endothelial Cell Monolayer Hyperpermeability via ERK-1/2 Signaling Pathway in Oxidized Low-Density Lipoprotein-Induced Human Umbilical Vein Endothelial Cells. *Evid Based Complement Alternat Med.* 2017; 2017:4198486. <https://doi.org/10.1155/2017/4198486> PMID:[28400842](https://pubmed.ncbi.nlm.nih.gov/28400842/)
20. Chimento A, Casaburi I, Avena P, Trotta F, De Luca A, Rago V, Pezzi V, Sirianni R. Cholesterol and Its Metabolites in Tumor Growth: Therapeutic Potential of Statins in Cancer Treatment. *Front Endocrinol (Lausanne).* 2019; 9:807. <https://doi.org/10.3389/fendo.2018.00807> PMID:[30719023](https://pubmed.ncbi.nlm.nih.gov/30719023/)
21. Koh WP, Dan YY, Goh GB, Jin A, Wang R, Yuan JM. Dietary fatty acids and risk of hepatocellular carcinoma in the Singapore Chinese health study. *Liver Int.* 2016; 36:893–901. <https://doi.org/10.1111/liv.12978> PMID:[26443688](https://pubmed.ncbi.nlm.nih.gov/26443688/)
22. Ioannou GN, Morrow OB, Conrole ML, Lee SP. Association between dietary nutrient composition and the incidence of cirrhosis or liver cancer in the United States population. *Hepatology.* 2009; 50:175–84. <https://doi.org/10.1002/hep.22941> PMID:[19441103](https://pubmed.ncbi.nlm.nih.gov/19441103/)
23. Zabirnyk O, Liu W, Khalil S, Sharma A, Phang JM. Oxidized low-density lipoproteins upregulate proline oxidase to initiate ROS-dependent autophagy. *Carcinogenesis.* 2010; 31:446–54. <https://doi.org/10.1093/carcin/bgp299> PMID:[19942609](https://pubmed.ncbi.nlm.nih.gov/19942609/)
24. Scoles DR, Xu X, Wang H, Tran H, Taylor-Harding B, Li A, Karlan BY. Liver X receptor agonist inhibits proliferation of ovarian carcinoma cells stimulated by oxidized low density lipoprotein. *Gynecol Oncol.* 2010; 116:109–16. <https://doi.org/10.1016/j.ygyno.2009.09.034> PMID:[19854496](https://pubmed.ncbi.nlm.nih.gov/19854496/)
25. Antalis CJ, Uchida A, Buhman KK, Siddiqui RA. Migration of MDA-MB-231 breast cancer cells depends on the availability of exogenous lipids and cholesterol esterification. *Clin Exp Metastasis.* 2011; 28:733–41. <https://doi.org/10.1007/s10585-011-9405-9> PMID:[21744083](https://pubmed.ncbi.nlm.nih.gov/21744083/)
26. Wen X, Liu X, Mao YP, Yang XJ, Wang YQ, Zhang PP, Lei Y, Hong XH, He QM, Ma J, Liu N, Li YQ. Long non-coding RNA DANCR stabilizes HIF-1 α and promotes metastasis by interacting with NF90/NF45 complex in nasopharyngeal carcinoma. *Theranostics.* 2018; 8:5676–89. <https://doi.org/10.7150/thno.28538> PMID:[30555573](https://pubmed.ncbi.nlm.nih.gov/30555573/)
27. Li K, Wu JL, Qin B, Fan Z, Tang Q, Lu W, Zhang H, Xing F, Meng M, Zou S, Wei W, Chen H, Cai J, et al. ILF3 is a substrate of SPOP for regulating serine biosynthesis in colorectal cancer. *Cell Res.* 2020; 30:163–78. <https://doi.org/10.1038/s41422-019-0257-1> PMID:[31772275](https://pubmed.ncbi.nlm.nih.gov/31772275/)
28. Xu Z, Huang H, Li X, Ji C, Liu Y, Liu X, Zhu J, Wang Z, Zhang H, Shi J. High expression of interleukin-enhancer binding factor 3 predicts poor prognosis in patients with lung adenocarcinoma. *Oncol Lett.* 2020; 19:2141–52. <https://doi.org/10.3892/ol.2020.11330> PMID:[32194712](https://pubmed.ncbi.nlm.nih.gov/32194712/)
29. Zhang C, Xie C, Wang X, Huang Y, Gao S, Lu J, Lu Y, Zhang S. Aberrant USP11 expression regulates NF90 to promote proliferation and metastasis in hepatocellular carcinoma. *Am J Cancer Res.* 2020; 10:1416–28. PMID:[32509388](https://pubmed.ncbi.nlm.nih.gov/32509388/)
30. Zhang W, Xiong Z, Wei T, Li Q, Tan Y, Ling L, Feng X. Nuclear factor 90 promotes angiogenesis by regulating HIF-1 α /VEGF-A expression through the PI3K/Akt signaling pathway in human cervical cancer. *Cell Death Dis.* 2018; 9:276. <https://doi.org/10.1038/s41419-018-0334-2> PMID:[29449553](https://pubmed.ncbi.nlm.nih.gov/29449553/)
31. Sun J, Zhao J, Yang Z, Zhou Z, Lu P. Identification of gene signatures and potential therapeutic targets for acquired chemotherapy resistance in gastric cancer patients. *J Gastrointest Oncol.* 2021; 12:407–22. <https://doi.org/10.21037/jgo-21-81> PMID:[34012635](https://pubmed.ncbi.nlm.nih.gov/34012635/)
32. Hinds DA, Buil A, Ziemek D, Martinez-Perez A, Malik R, Folkersen L, Germain M, Mälarstig A, Brown A, Soria JM, Dichgans M, Bing N, Franco-Cereceda A, et al, and METASTROKE Consortium, and INVENT Consortium. Genome-wide association analysis of self-reported events in 6135 individuals and 252 827 controls identifies 8 loci associated with thrombosis. *Hum Mol Genet.* 2016; 25:1867–74. <https://doi.org/10.1093/hmg/ddw037> PMID:[26908601](https://pubmed.ncbi.nlm.nih.gov/26908601/)
33. Yamada Y, Matsui K, Takeuchi I, Fujimaki T. Association of genetic variants with dyslipidemia and chronic kidney disease in a longitudinal population-based

- genetic epidemiological study. *Int J Mol Med*. 2015; 35:1290–300.
<https://doi.org/10.3892/ijmm.2015.2152>
PMID:25813695
34. Yoshida T, Kato K, Oguri M, Horibe H, Kawamiya T, Yokoi K, Fujimaki T, Watanabe S, Satoh K, Aoyagi Y, Tanaka M, Yoshida H, Shinkai S, et al. Association of polymorphisms of BTN2A1 and ILF3 with myocardial infarction in Japanese individuals with different lipid profiles. *Mol Med Rep*. 2011; 4:511–8.
<https://doi.org/10.3892/mmr.2011.441>
PMID:21468600
35. Krycer JR, Sharpe LJ, Luu W, Brown AJ. The Akt-SREBP nexus: cell signaling meets lipid metabolism. *Trends Endocrinol Metab*. 2010; 21:268–76.
<https://doi.org/10.1016/j.tem.2010.01.001>
PMID:20117946
36. Farwell WR, Scranton RE, Lawler EV, Lew RA, Brophy MT, Fiore LD, Gaziano JM. The association between statins and cancer incidence in a veterans population. *J Natl Cancer Inst*. 2008; 100:134–9.
<https://doi.org/10.1093/jnci/djm286>
PMID:18182618
37. Nielsen SF, Nordestgaard BG, Bojesen SE. Statin use and reduced cancer-related mortality. *N Engl J Med*. 2012; 367:1792–802.
<https://doi.org/10.1056/NEJMoa1201735>
PMID:23134381
38. Ren QW, Yu SY, Teng TK, Li X, Cheung KS, Wu MZ, Li HL, Wong PF, Tse HF, Lam CS, Yiu KH. Statin associated lower cancer risk and related mortality in patients with heart failure. *Eur Heart J*. 2021; 42:3049–59.
<https://doi.org/10.1093/eurheartj/ehab325>
PMID:34157723
39. Singh PP, Singh S. Statins are associated with reduced risk of gastric cancer: a systematic review and meta-analysis. *Ann Oncol*. 2013; 24:1721–30.
<https://doi.org/10.1093/annonc/mdt150>
PMID:23599253
40. Pelton K, Freeman MR, Solomon KR. Cholesterol and prostate cancer. *Curr Opin Pharmacol*. 2012; 12:751–9.
<https://doi.org/10.1016/j.coph.2012.07.006>
PMID:22824430
41. Juneja M, Kobelt D, Walther W, Voss C, Smith J, Specker E, Neuenschwander M, Gohlke BO, Dahlmann M, Radetzki S, Preissner R, von Kries JP, Schlag PM, Stein U. Statin and rottlerin small-molecule inhibitors restrict colon cancer progression and metastasis via MACC1. *PLoS Biol*. 2017; 15:e2000784.
<https://doi.org/10.1371/journal.pbio.2000784>
PMID:28570591
42. Lin CJ, Liao WC, Lin HJ, Hsu YM, Lin CL, Chen YA, Feng CL, Chen CJ, Kao MC, Lai CH, Kao CH. Statins Attenuate Helicobacter pylori CagA Translocation and Reduce Incidence of Gastric Cancer: *In Vitro* and Population-Based Case-Control Studies. *PLoS One*. 2016; 11:e0146432.
<https://doi.org/10.1371/journal.pone.0146432>
PMID:26730715
43. Doan H, Parsons A, Devkumar S, Selvarajah J, Miralles F, Carroll VA. HIF-mediated Suppression of DEPTOR Confers Resistance to mTOR Kinase Inhibition in Renal Cancer. *iScience*. 2019; 21:509–20.
<https://doi.org/10.1016/j.isci.2019.10.047>
PMID:31710966
44. Cruz PM, Mo H, McConathy WJ, Sabnis N, Lacko AG. The role of cholesterol metabolism and cholesterol transport in carcinogenesis: a review of scientific findings, relevant to future cancer therapeutics. *Front Pharmacol*. 2013; 4:119.
<https://doi.org/10.3389/fphar.2013.00119>
PMID:24093019
45. Bedin A, Maranhão RC, Tavares ER, Carvalho PO, Baracat EC, Podgaec S. Nanotechnology for the treatment of deep endometriosis: uptake of lipid core nanoparticles by LDL receptors in endometriotic foci. *Clinics (Sao Paulo)*. 2019; 74:e989.
<https://doi.org/10.6061/clinics/2019/e989>
PMID:31291391
46. Pike LJ. Rafts defined: a report on the Keystone Symposium on Lipid Rafts and Cell Function. *J Lipid Res*. 2006; 47:1597–8.
<https://doi.org/10.1194/jlr.E600002-JLR200>
PMID:16645198
47. Ripa I, Andreu S, López-Guerrero JA, Bello-Morales R. Membrane Rafts: Portals for Viral Entry. *Front Microbiol*. 2021; 12:631274.
<https://doi.org/10.3389/fmicb.2021.631274>
PMID:33613502
48. Hryniewicz-Jankowska A, Augoff K, Biernatowska A, Podkalicka J, Sikorski AF. Membrane rafts as a novel target in cancer therapy. *Biochim Biophys Acta*. 2014; 1845:155–65.
<https://doi.org/10.1016/j.bbcan.2014.01.006>
PMID:24480320
49. Zhang T, Wang Q, Wang Y, Wang J, Su Y, Wang F, Wang G. AIBP and APOA-I synergistically inhibit intestinal tumor growth and metastasis by promoting cholesterol efflux. *J Transl Med*. 2019; 17:161.
<https://doi.org/10.1186/s12967-019-1910-7>
PMID:31101050
50. Levitan I, Gooch KJ. Lipid rafts in membrane-cytoskeleton interactions and control of cellular

- biomechanics: actions of oxLDL. *Antioxid Redox Signal*. 2007; 9:1519–34.
<https://doi.org/10.1089/ars.2007.1686>
PMID:[17576163](https://pubmed.ncbi.nlm.nih.gov/17576163/)
51. Suckling RJ, Korona B, Whiteman P, Chillakuri C, Holt L, Handford PA, Lea SM. Structural and functional dissection of the interplay between lipid and Notch binding by human Notch ligands. *EMBO J*. 2017; 36:2204–15.
<https://doi.org/10.15252/emboj.201796632>
PMID:[28572448](https://pubmed.ncbi.nlm.nih.gov/28572448/)
52. Demitrack ES, Samuelson LC. Notch as a Driver of Gastric Epithelial Cell Proliferation. *Cell Mol Gastroenterol Hepatol*. 2017; 3:323–30.
<https://doi.org/10.1016/j.jcmgh.2017.01.012>
PMID:[28462374](https://pubmed.ncbi.nlm.nih.gov/28462374/)
53. Demitrack ES, Samuelson LC. Notch regulation of gastrointestinal stem cells. *J Physiol*. 2016; 594:4791–803.
<https://doi.org/10.1113/JP271667> PMID:[26848053](https://pubmed.ncbi.nlm.nih.gov/26848053/)
54. Hibdon ES, Razumilava N, Keeley TM, Wong G, Solanki S, Shah YM, Samuelson LC. Notch and mTOR Signaling Pathways Promote Human Gastric Cancer Cell Proliferation. *Neoplasia*. 2019; 21:702–12.
<https://doi.org/10.1016/j.neo.2019.05.002>
PMID:[31129492](https://pubmed.ncbi.nlm.nih.gov/31129492/)
55. He Y, Wang Y, Liu L, Liu S, Liang L, Chen Y, Zhu Z. Circular RNA circ_0006282 Contributes to the Progression of Gastric Cancer by Sponging miR-155 to Upregulate the Expression of FBXO22. *Onco Targets Ther*. 2020; 13:1001–10.
<https://doi.org/10.2147/OTT.S228216> PMID:[32099403](https://pubmed.ncbi.nlm.nih.gov/32099403/)
56. Ding S, Zhang Y. MicroRNA-539 inhibits the proliferation and migration of gastric cancer cells by targeting SRY-box 5 gene. *Mol Med Rep*. 2019; 20:2533–40.
<https://doi.org/10.3892/mmr.2019.10486>
PMID:[31322222](https://pubmed.ncbi.nlm.nih.gov/31322222/)
57. Luo X, Su KJ, Qiu C, Liu X, Yang F. Novel Prognostic Model for Gastric Cancer using 13 Co-Expression Long Non-Coding RNAs (LncRNAs). *Med Sci Monit*. 2020; 26:e923295.
<https://doi.org/10.12659/MSM.923295>
PMID:[32480397](https://pubmed.ncbi.nlm.nih.gov/32480397/)
58. Sun XJ, Shi JF, Guo LW, Huang HY, Yao NL, Gong JY, Sun YW, Liu GX, Mao AY, Liao XZ, Bai YN, Ren JS, Zhu XY, et al, and listed authors are on behalf of the Health Economic Evaluation Working Group, Cancer Screening Program in Urban China (CanSPUC). Medical expenses of urban Chinese patients with stomach cancer during 2002-2011: a hospital-based multicenter retrospective study. *BMC Cancer*. 2018; 18:435.
<https://doi.org/10.1186/s12885-018-4357-y>
PMID:[29665788](https://pubmed.ncbi.nlm.nih.gov/29665788/)
59. Yang D, Hu C, Deng X, Bai Y, Cao H, Guo J, Su Z. Therapeutic Effect of Chitooligosaccharide Tablets on Lipids in High-Fat Diets Induced Hyperlipidemic Rats. *Molecules*. 2019; 24:514.
<https://doi.org/10.3390/molecules24030514>
PMID:[30709014](https://pubmed.ncbi.nlm.nih.gov/30709014/)
60. Zakko L, Lutzke L, Wang KK. Screening and Preventive Strategies in Esophagogastric Cancer. *Surg Oncol Clin N Am*. 2017; 26:163–78.
<https://doi.org/10.1016/j.soc.2016.10.004>
PMID:[28279462](https://pubmed.ncbi.nlm.nih.gov/28279462/)
61. Bähr I, Goritz V, Doberstein H, Hiller GG, Rosenstock P, Jahn J, Pörtner O, Berreis T, Mueller T, Spielmann J, Kielstein H. Diet-Induced Obesity Is Associated with an Impaired NK Cell Function and an Increased Colon Cancer Incidence. *J Nutr Metab*. 2017; 2017:4297025.
<https://doi.org/10.1155/2017/4297025>
PMID:[28357137](https://pubmed.ncbi.nlm.nih.gov/28357137/)
62. Yasin HK, Taylor AH, Ayakannu T. A Narrative Review of the Role of Diet and Lifestyle Factors in the Development and Prevention of Endometrial Cancer. *Cancers (Basel)*. 2021; 13:2149.
<https://doi.org/10.3390/cancers13092149>
PMID:[33946913](https://pubmed.ncbi.nlm.nih.gov/33946913/)
63. Pih GY, Gong EJ, Choi JY, Kim MJ, Ahn JY, Choe J, Bae SE, Chang HS, Na HK, Lee JH, Jung KW, Kim DH, Choi KD, et al. Associations of Serum Lipid Level with Gastric Cancer Risk, Pathology, and Prognosis. *Cancer Res Treat*. 2021; 53:445–56.
<https://doi.org/10.4143/crt.2020.599>
PMID:[33253515](https://pubmed.ncbi.nlm.nih.gov/33253515/)
64. Jiang X, Li M, Yang Q, Du L, Du J, Zhou J. Oxidized low density lipoprotein and inflammation in gout patients. *Cell Biochem Biophys*. 2014; 69:65–9.
<https://doi.org/10.1007/s12013-013-9767-5>
PMID:[24068523](https://pubmed.ncbi.nlm.nih.gov/24068523/)
65. Bitorina AV, Oligschlaeger Y, Shiri-Sverdlov R, Theys J. Low profile high value target: The role of OxLDL in cancer. *Biochim Biophys Acta Mol Cell Biol Lipids*. 2019; 1864:158518.
<https://doi.org/10.1016/j.bbalip.2019.158518>
PMID:[31479734](https://pubmed.ncbi.nlm.nih.gov/31479734/)
66. Liu R, Cheng F, Zeng K, Li W, Lan J. GPR120 Agonist GW9508 Ameliorated Cellular Senescence Induced by ox-LDL. *ACS Omega*. 2020; 5:32195–202.
<https://doi.org/10.1021/acsomega.0c03581>
PMID:[33376857](https://pubmed.ncbi.nlm.nih.gov/33376857/)
67. Walenbergh SM, Koek GH, Bieghs V, Shiri-Sverdlov R. Non-alcoholic steatohepatitis: the role of oxidized low-density lipoproteins. *J Hepatol*. 2013; 58:801–10.

- <https://doi.org/10.1016/j.jhep.2012.11.014>
PMID:[23183522](https://pubmed.ncbi.nlm.nih.gov/23183522/)
68. Zettler ME, Prociuk MA, Austria JA, Massaeli H, Zhong G, Pierce GN. OxLDL stimulates cell proliferation through a general induction of cell cycle proteins. *Am J Physiol Heart Circ Physiol*. 2003; 284:H644–53.
<https://doi.org/10.1152/ajpheart.00494.2001>
PMID:[12529257](https://pubmed.ncbi.nlm.nih.gov/12529257/)
69. González-Chavarría I, Fernandez E, Gutierrez N, González-Horta EE, Sandoval F, Cifuentes P, Castillo C, Cerro R, Sanchez O, Toledo JR. LOX-1 activation by oxLDL triggers an epithelial mesenchymal transition and promotes tumorigenic potential in prostate cancer cells. *Cancer Lett*. 2018; 414:34–43.
<https://doi.org/10.1016/j.canlet.2017.10.035>
PMID:[29107109](https://pubmed.ncbi.nlm.nih.gov/29107109/)
70. González-Chavarría I, Cerro RP, Parra NP, Sandoval FA, Zuñiga FA, Omazabal VA, Lamperti LI, Jiménez SP, Fernandez EA, Gutiérrez NA, Rodríguez FS, Onate SA, Sánchez O, et al. Lectin-like oxidized LDL receptor-1 is an enhancer of tumor angiogenesis in human prostate cancer cells. *PLoS One*. 2014; 9:e106219.
<https://doi.org/10.1371/journal.pone.0106219>
PMID:[25170920](https://pubmed.ncbi.nlm.nih.gov/25170920/)
71. Ma C, Xie J, Luo C, Yin H, Li R, Wang X, Xiong W, Zhang T, Jiang P, Qi W, Zhou T, Yang Z, Wang W, et al. OxLDL promotes lymphangiogenesis and lymphatic metastasis in gastric cancer by upregulating VEGF-C expression and secretion. *Int J Oncol*. 2019; 54:572–84.
<https://doi.org/10.3892/ijo.2018.4648>
PMID:[30483757](https://pubmed.ncbi.nlm.nih.gov/30483757/)
72. Liu Y, Li Y, Zhao Y, Liu Y, Fan L, Jia N, Zhao Q. ILF3 promotes gastric cancer proliferation and may be used as a prognostic marker. *Mol Med Rep*. 2019; 20:125–34.
<https://doi.org/10.3892/mmr.2019.10229>
PMID:[31115508](https://pubmed.ncbi.nlm.nih.gov/31115508/)
73. Jiang W, Huang H, Ding L, Zhu P, Saiyin H, Ji G, Zuo J, Han D, Pan Y, Ding D, Ma X, Zhang Y, Wu J, et al. Regulation of cell cycle of hepatocellular carcinoma by NF90 through modulation of cyclin E1 mRNA stability. *Oncogene*. 2015; 34:4460–70.
<https://doi.org/10.1038/onc.2014.373> PMID:[25399696](https://pubmed.ncbi.nlm.nih.gov/25399696/)
74. Qu J, Liu B, Li B, Du G, Li Y, Wang J, He L, Wan X. TRIB3 suppresses proliferation and invasion and promotes apoptosis of endometrial cancer cells by regulating the AKT signaling pathway. *Onco Targets Ther*. 2019; 12:2235–45.
<https://doi.org/10.2147/OTT.S189001> PMID:[30988628](https://pubmed.ncbi.nlm.nih.gov/30988628/)
75. Gao G, Li W, Liu S, Han D, Yao X, Jin J, Han D, Sun W, Chen X. The positive feedback loop between ILF3 and lncRNA ILF3-AS1 promotes melanoma proliferation, migration, and invasion. *Cancer Manag Res*. 2018; 10:6791–802.
<https://doi.org/10.2147/CMAR.S186777>
PMID:[30588088](https://pubmed.ncbi.nlm.nih.gov/30588088/)
76. Maron DJ, Fazio S, Linton MF. Current perspectives on statins. *Circulation*. 2000; 101:207–13.
<https://doi.org/10.1161/01.cir.101.2.207>
PMID:[10637210](https://pubmed.ncbi.nlm.nih.gov/10637210/)
77. Liao JK. Effects of statins on 3-hydroxy-3-methylglutaryl coenzyme a reductase inhibition beyond low-density lipoprotein cholesterol. *Am J Cardiol*. 2005; 96:24F–33F.
<https://doi.org/10.1016/j.amjcard.2005.06.009>
PMID:[16126020](https://pubmed.ncbi.nlm.nih.gov/16126020/)
78. Ahmadi Y, Karimian R, Panahi Y. Effects of statins on the chemoresistance-The antagonistic drug-drug interactions versus the anti-cancer effects. *Biomed Pharmacother*. 2018; 108:1856–65.
<https://doi.org/10.1016/j.biopha.2018.09.122>
PMID:[30372891](https://pubmed.ncbi.nlm.nih.gov/30372891/)
79. Simons K, Toomre D. Lipid rafts and signal transduction. *Nat Rev Mol Cell Biol*. 2000; 1:31–9.
<https://doi.org/10.1038/35036052> PMID:[11413487](https://pubmed.ncbi.nlm.nih.gov/11413487/)
80. Lin CJ, Lai CK, Kao MC, Wu LT, Lo UG, Lin LC, Chen YA, Lin H, Hsieh JT, Lai CH, Lin CD. Impact of cholesterol on disease progression. *Biomedicine (Taipei)*. 2015; 5:7.
<https://doi.org/10.7603/s40681-015-0007-8>
PMID:[26048694](https://pubmed.ncbi.nlm.nih.gov/26048694/)
81. Freed-Pastor WA, Mizuno H, Zhao X, Langerød A, Moon SH, Rodriguez-Barrueco R, Barsotti A, Chicas A, Li W, Polotskaia A, Bissell MJ, Osborne TF, Tian B, et al. Mutant p53 disrupts mammary tissue architecture via the mevalonate pathway. *Cell*. 2012; 148:244–58.
<https://doi.org/10.1016/j.cell.2011.12.017>
PMID:[22265415](https://pubmed.ncbi.nlm.nih.gov/22265415/)
82. Chen J. Multiple signal pathways in obesity-associated cancer. *Obes Rev*. 2011; 12:1063–70.
<https://doi.org/10.1111/j.1467-789X.2011.00917.x>
PMID:[22093240](https://pubmed.ncbi.nlm.nih.gov/22093240/)
83. Hashmi S, Wang Y, Suman DS, Parhar RS, Collison K, Conca W, Al-Mohanna F, Gaugler R. Human cancer: is it linked to dysfunctional lipid metabolism? *Biochim Biophys Acta*. 2015; 1850:352–64.
<https://doi.org/10.1016/j.bbagen.2014.11.004>
PMID:[25450488](https://pubmed.ncbi.nlm.nih.gov/25450488/)
84. Bahrami A, Hasanazadeh M, Hassanian SM, ShahidSales S, Ghayour-Mobarhan M, Ferns GA, Avan A. The Potential Value of the PI3K/Akt/mTOR Signaling Pathway for Assessing Prognosis in Cervical Cancer and as a Target for Therapy. *J Cell Biochem*. 2017; 118:4163–9.
<https://doi.org/10.1002/jcb.26118> PMID:[28475243](https://pubmed.ncbi.nlm.nih.gov/28475243/)

85. Costa C, Pereira S, Lima L, Peixoto A, Fernandes E, Neves D, Neves M, Gaitero C, Tavares A, Gil da Costa RM, Cruz R, Amaro T, Oliveira PA, et al. Abnormal Protein Glycosylation and Activated PI3K/Akt/mTOR Pathway: Role in Bladder Cancer Prognosis and Targeted Therapeutics. PLoS One. 2015; 10:e0141253. <https://doi.org/10.1371/journal.pone.0141253> PMID:[26569621](https://pubmed.ncbi.nlm.nih.gov/26569621/)
86. The Gene Ontology Consortium. The Gene Ontology Resource: 20 years and still GOing strong. Nucleic Acids Res. 2019; 47:D330–8. <https://doi.org/10.1093/nar/gky1055> PMID:[30395331](https://pubmed.ncbi.nlm.nih.gov/30395331/)

SUPPLEMENTARY MATERIALS

Supplementary Tables

Please browse Full Text version to see the data of Supplementary Tables 1–3.

Supplementary Table 1. The differentially expressed genes between the control group and the si-ILF3 group.

Supplementary Table 2. The functional characteristics of ILF3 by GO analysis.

Supplementary Table 3. The significant signaling pathways that ILF3 identified by KEGG pathway analysis.

Hallmarks of cancer and hallmarks of aging

Mikhail V. Blagosklonny¹

¹Roswell Park Comprehensive Cancer Center, Buffalo, NY 14263, USA

Correspondence to: Mikhail V. Blagosklonny; email: Blagosklonny@oncotarget.com, Blagosklonny@rapalogs.com

Keywords: oncology, carcinogenesis, geroscience, mTOR, rapamycin, hyperfunction theory

Received: February 14, 2022

Accepted: May 2, 2022

Published: May 9, 2022

Copyright: © 2022 Blagosklonny. This is an open access article distributed under the terms of the [Creative Commons Attribution License](https://creativecommons.org/licenses/by/3.0/) (CC BY 3.0), which permits unrestricted use, distribution, and reproduction in any medium, provided the original author and source are credited.

ABSTRACT

A thought-provoking article by [Gems and de Magalhães](#) suggests that canonic hallmarks of aging are superficial imitations of hallmarks of cancer. I took their work a step further and proposed hallmarks of aging based on a hierarchical principle and the hyperfunction theory.

To do this, I first reexamine the hallmarks of cancer proposed by Hanahan and Weinberg in 2000. Although six hallmarks of cancer are genuine, they are not hierarchically arranged, i.e., molecular, intra-cellular, cellular, tissue, organismal and extra-organismal. (For example, invasion and angiogenesis are manifestations of molecular alterations on the tissue level; metastasis on the organismal level, whereas cell immortality is observed outside the host).

The same hierarchical approach is applicable to aging. Unlike cancer, however, aging is not a molecular disease. The lowest level of its origin is normal intracellular signaling pathways such as mTOR that drive developmental growth and, later in life, become hyperfunctional, causing age-related diseases, whose sum is aging. The key hallmark of organismal aging, from worms to humans, are age-related diseases. In addition, hallmarks of aging can be arranged as a timeline, wherein initial hyperfunction is followed by dysfunction, organ damage and functional decline.

Hallmarks of cancer: comparing apples and oranges

As depicted by Hanahan and Weinberg in 2000 [1], the circle schema of six hallmarks of cancer somewhat compares apples and oranges https://els-jbs-prod-cdn.jbs.elsevierhealth.com/cms/attachment/428dbc2e-657c-429d-98f4-9910c7df1678/gr1_lrg.jpg.

The hallmarks themselves are exact, but they are not equal. For example, limitless replicative potential (cell immortality) cannot be directly compared to sustained angiogenesis. Cell immortality is revealed outside the host (extra-organismal level), for example, in cell culture where clonal cell lines can proliferate indefinitely without interaction with normal tissues. In contrast, sustained angiogenesis requires interaction of cancer cells with normal cells of several tissues.

Angiogenesis can be only understood on the tissue level.

Second, cancer cells undergo Darwinian-type selection [2] for resistance to anti-growth signals, resistance to apoptosis and self-sufficiency in mitogenic signals. This trio represents three out of six hallmarks of cancer [1]. They can be combined in one super-hallmark: resistance to growth-limiting conditions [3]. (Note: The definition of oncogenic resistance to growth-limiting conditions was discussed previously [4]). Not only resistance to apoptosis and anti-growth signals but also self-sufficiency in mitogenic signals render cells resistant to growth-limiting conditions. Examples of growth-limiting conditions include lack of external mitogenic signals, cytostatic cytokines such as TGF-beta, cytotoxic carcinogens such as tobacco smoke, anti-cancer drugs, contact inhibition, glucose deprivation, cellular senescence, hypoxia, absence of nutrients and

growth factors [5, 6]. For example, glucose deprivation selects for oncogenic Ras [6].

Whereas normal cells do not proliferate in growth-limiting conditions, cancer cells do. Resistance to growth-limiting conditions provides an immediate selective advantage. But what immediate advantages can be provided by cellular immortality? The cell cannot tell the future, that it will live in cell culture one day. Cellular immortality is selected indirectly as derived hallmarks [3], because the same mutations that provide resistance to growth-limiting conditions also make cells immortal, angiogenic, invasive and metastatic [1, 7, 8]. Cellular immortality, angiogenesis, invasion and metastasis are derived hallmarks.

Third, molecular alterations (e.g., DNA mutations) are absent in the six-hallmark circle by Hanahan and Weinberg [1]. As discussed by Gems and de Magalhães, the hallmarks do not include mutations (or genetic instability) because this hallmark is implicitly taken for granted [9]. In fact, Hanahan and Weinberg called it an enabling hallmark in their revised paper published in 2011 [7].

In 2005, I explicitly included the molecular hallmark (mutations) and suggested the hierarchical principle to arrange these hallmarks from molecular to organismal levels [5].

Hierarchical model of hallmarks of cancer: arranging the oranges

Here I present the hallmarks of cancer, depicted as a circle by Hanahan and Weinberg [1], not as the circle but hierarchically, from molecular levels to the organism (Figure 1).

Molecular level: Somatically inheritable molecular alterations.

Genome instability is an enabling hallmark of cancer because it enables the acquisition of molecular alterations, such as DNA mutations, aneuploidy and epigenetic alterations [7]. Vogelstein et al. suggested that a typical human tumor contains relatively few driver gene mutations that each confers a growth advantage of 0.4% and numerous passenger gene mutations that confer no selective advantage [8, 10].

Intracellular signaling pathways: Oncogenic translation of ambivalent signaling

Signal-transduction pathways are ambivalent, causing opposite outcomes depending on cellular context. Oncogenic mutations re-wire signal transduction pathways. For example, MAPK pathways can simultaneously induce cyclin D1 and CDK inhibitors, leading either to cellular proliferation or senescence

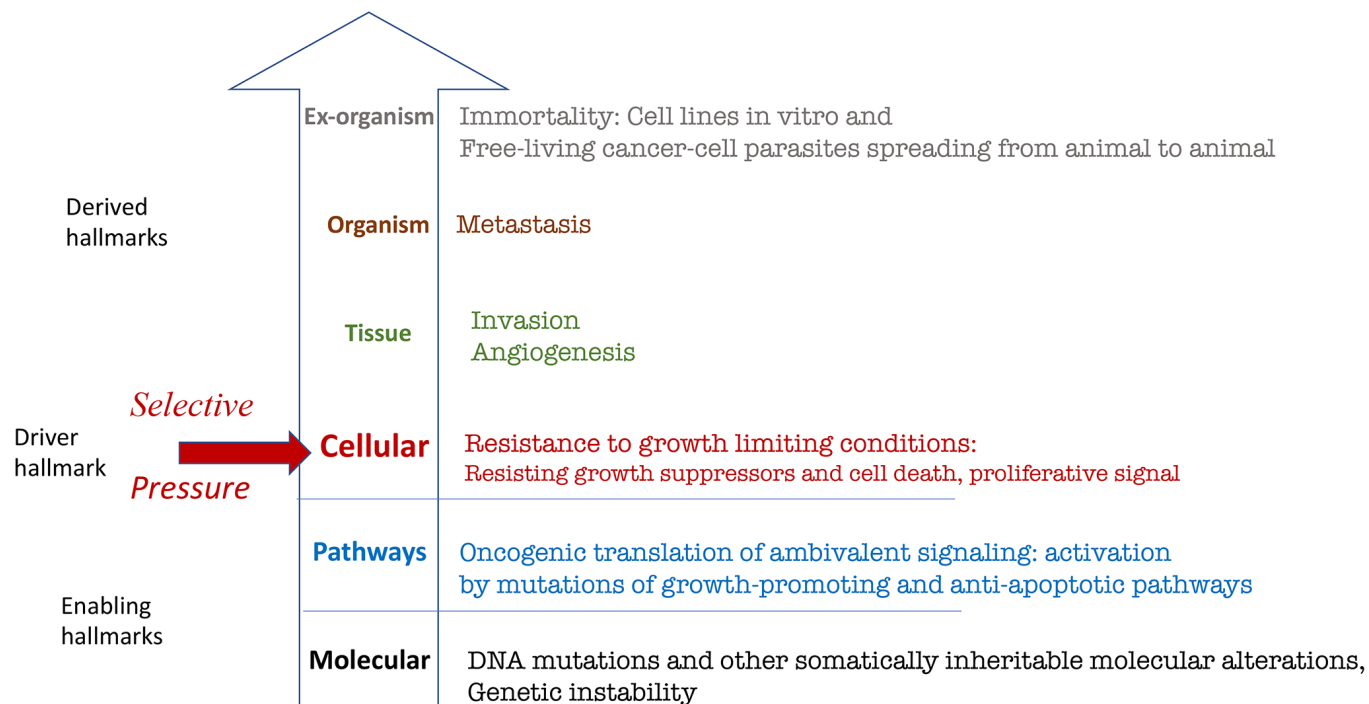


Figure 1. Hierarchical representation (from molecular to organismal levels) of the original hallmarks of cancer based on Hanahan and Weinberg. See text for explanation.

[11]. Inactivation of CDK inhibitors such as p16 may translate this ambivalent signaling into proliferation [3, 12]. TGF-beta inhibits normal cell proliferation, but in cancer it can induce proliferation and invasion [7, 13].

Growth-promoting and mitogen/nutrient-sensing signaling pathways are constantly activated by mutations to promote growth and proliferation as well as self-sufficiency in mitogen signaling. This, in turn, is manifested as three hallmarks of cancer on the next hierarchical level: cellular. This trio can be combined as one super-hallmark of resistance to growth-limiting conditions.

Cellular level: Resistance to growth-limiting conditions

Oncogenic mutations make cancer cells resistant to growth-limiting conditions (a definition of oncogenic-type of resistance was discussed previously [4]). This is the driver hallmark of cancer because it provides a selective advantage to cancer cells. Cells, capable of proliferation, are unicellular organisms in a Darwinian sense [2, 14, 15]. Selection can be “natural” (during carcinogenesis) and “artificial” (during cancer therapy) [14, 16]. For example, selection for therapy resistance increases oncogenic properties of cancer cells because many mutations in oncogenes and tumor suppressors that render cells drug-resistant also make them more oncogenic [5, 17–19]. Simultaneously, the same combination of mutations enables metastasis and other higher-level hallmarks. There is no direct selection for metastatic potential, angiogenesis and immortality. They are derived hallmarks.

Tissue level: Invasion and angiogenesis

Cancer cells produce cytokines and enzymes, which enable the cells to invade and to attract normal cells of different tissues in order to sustain angiogenesis [7].

Organismal level: Metastasis

Metastasis is the deadliest hallmark of cancer. Yet, there is no direct selection for metastatic potential. Direct selection for metastatic potential could take place only if metastases produced new metastases; in other words, if metastases reproduce. Simply, selection for cells resistant to growth-limiting conditions (survival and proliferation) brings about mutations that confer not only resistance, but also metastatic potential. There are no specific “metastasis” genes [8, 20]. They are the same oncogenes and tumor suppressors that act on cellular levels for the “trio” hallmark. Let us consider an analogy. If we select people for their ability to run faster, these selected people will also jump higher than

average, although selection was not for jumping ability. The fastest runners are the farthest jumpers.

Extra-organismal level: Cellular immortality

Some cancer cell lines live for more than half of a century in cell culture and for thousands of years in the wild. Originating in one animal, viable cancer cells are directly transmitted into unrelated hosts in a process similar to metastasis [21, 22]. Transmissible cancers have been observed in domestic dogs, the Tasmanian devil, hamsters and six bivalve species such as the soft-shell clam [23]. Canine transmissible venereal tumors (transmitted during sexual intercourse) may have originated thousands of years ago from the cells of a wolf or East Asian breed of dog [21–25]. The Tasmanian devil facial tumor disease [24] spreads through the Tasmanian devil population by transfer of cancer cells through biting [22]. [26]. Derived from a single original clam, leukemia-like cancer spreads among marine bivalves through sea water, leading to massive population loss [23, 27].

Six levels rather than six hallmarks

The number of hallmarks of cancer is arbitrary. Some can be combined, and others can be added. Numerous authors have re-visited the hallmarks of cancer, adding hallmarks or suggesting a new set of hallmarks [28–37].

Some hallmarks of cancer may be pseudo-hallmarks. For example, visiting an oncologist is a “hallmark” of cancer. We can be 99% sure that if someone has 20 appointments in an oncology clinic, then this person has cancer. However, it would be ridiculous to include this pseudo-hallmark in Figure 1. And the hierarchical principle makes this impossible, because there is no level (among the six levels) to include it.

Hallmarks of aging

To start with, let us depict the hallmarks of aging suggested by López-Otín et al. [38] based on the hierarchical principle. This representation renders hallmarks tangible but reveals three shortcomings (Figure 2).

First is the lack of hallmarks on the organismal level. Yet, the main hallmark of organismal aging is age-related diseases in all species from *C. elegans* [39–42] to humans [39, 43]. Aging is the sum of all age-related diseases, which cause death “from aging”.

Second, the relationship between hallmarks on different levels are unclear.

Third, the inclusion of genetic instability as a hallmark is based on the theory that aging is caused by accumulation of molecular damage. The molecular damage theory was refuted by key experiments, as discussed in detail [44–51].

Yes, damage accumulates and is harmful and potentially lethal [52–55] but it is not life-limiting because aging caused by hyper-functional signaling terminates life first. The reason why mTOR-driven aging is life-limiting has been discussed [49, 56, 57].

It was also suggested that the levels of DNA repair needed to avoid cancer at a young age greatly exceeds the levels that are needed to prevent damage-induced aging during a normal lifetime [58]. As previously discussed, the role of molecular damage in cancer supports the role of mTOR-driven hyperfunction in aging [59].

Let us depict hallmarks of aging, according to the hyperfunction theory of aging (Figure 3).

Hallmarks of aging and hyperfunction theory

The hyperfunction theory of aging was extensively reviewed previously [44, 45, 49, 56, 57, 60–66], and

responses [60, 67] to its critics [68, 69] were also provided.

According to hyperfunction theory, aging is a continuation of developmental and reproductive programs that were not turned off upon their completion. Continuously active signaling pathways that initially drive developmental growth, drive aging later in life. Signaling pathways establish feedback loops, involving also gene expression and epigenetic modifications. These pathways become hyperfunctional, meaning that their activity is higher than optimal for longevity.

How does normal function become a deadly hyperfunction? Consider an analogy. When you pump air into an inflatable balloon, it grows in size. But when it reaches its intended size and you continue to pump air at the same rate, it will not grow further but instead will burst. This event can be compared with a stroke due to hypertension, resulting in brain damage. The brain is not damaged by life-long accumulation of molecular damage, but by hyperfunction, such as hypertension and hypercoagulation, thrombosis.

Hyper-function does not necessarily mean increased function. Even unchanged or slightly decreased activity

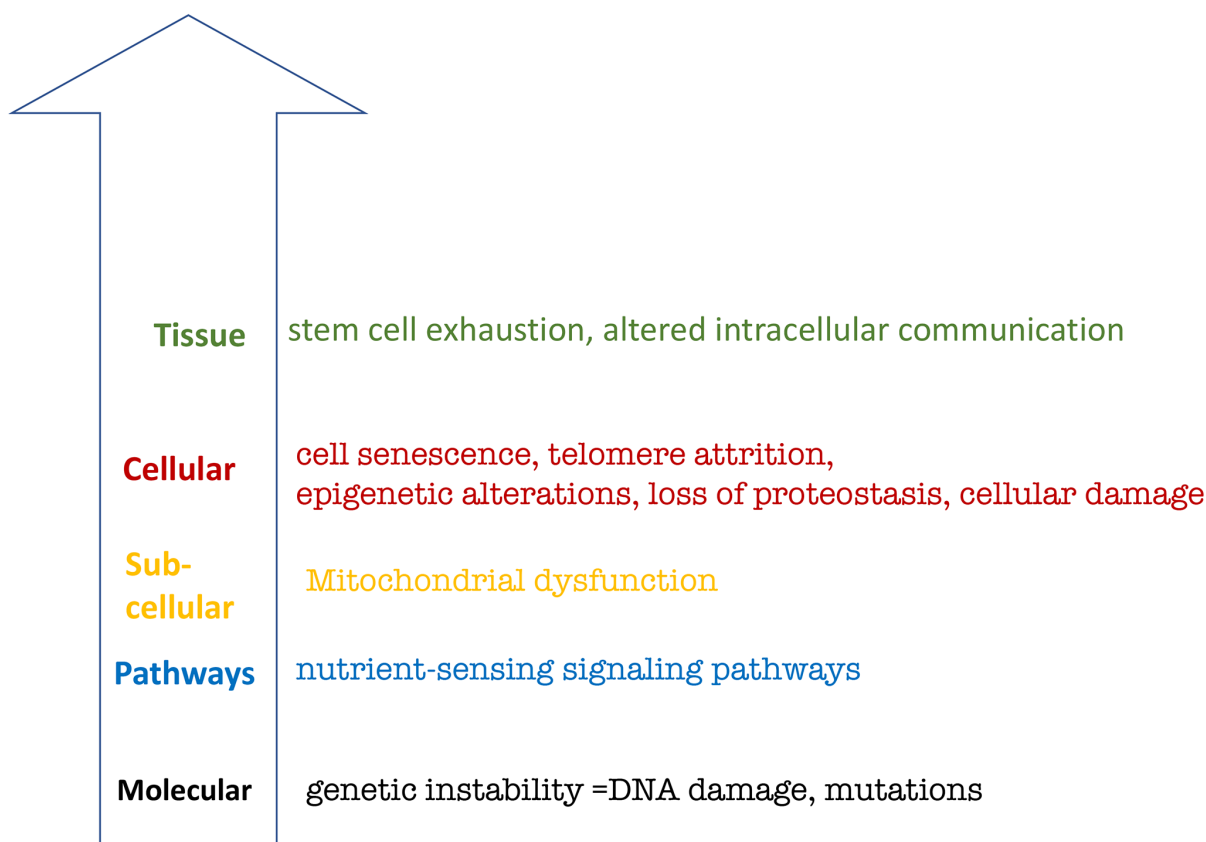


Figure 2. Hierarchical representation of the hallmarks of aging based on López-Otín et al. See text for explanation.

of growth-promoting pathways, such as mTOR, can be hyperfunctional when developmental growth is completed. As an analogy, 55 mph on the highway is not speeding, but even 40 mph on the driveway is too fast.

Hyperfunction causes organ damage and functional decline. The accumulation of molecular damage is associated with decline, but it is hyperfunction that causes decline during a normal lifetime.

Unlike cancer, aging is not a molecular disease. Development is not driven by accumulation of molecular damage or mutations in signaling pathways, and aging is not either. Nutrient-sensing pathways (e.g., mTOR) are not altered by random mutations.

The lowest level of hallmarks of aging is a continuous activation of normal signal transduction pathways. Deactivation of these pathways by knockout of a single gene extends lifespan in animals [70–73]. Rapamycin, a drug that inhibits normal mTOR signaling, extends lifespan [74–77].

Hyperfunctional signaling directly drives age-related diseases. There are no longevity pathways/mechanisms inhibitable by pro-aging pathways such as mTOR. Pro-

aging pathways do not drive aging by inhibiting longevity mechanisms. Why would nature create something that inhibits longevity mechanisms? Pro-aging pathways such as mTOR directly drive age-related diseases because they are a continuation of development.

The key to understanding aging: life-limiting vs. non-life-limiting hallmarks

Among numerous harmful processes, only one can be life-limiting in a particular individual. If an animal dies from one cause, it cannot die from another cause even a day later. If quasi-programmed (e.g., mTOR-driven) aging is life-limiting, then accumulation of random damages cannot kill the organism.

López-Otín et al. [38] suggested three criteria for hallmarks of aging but two of them are criteria for both life-limiting and non-life-limiting processes: (1) hallmarks are observed during normal aging and (2) its experimental aggravation should decrease lifespan. However, experimental aggravation can make any process life-limiting. Telomere shortening becomes life-limiting in mice lacking telomerase, but their symptoms are drastically different from normal age-related

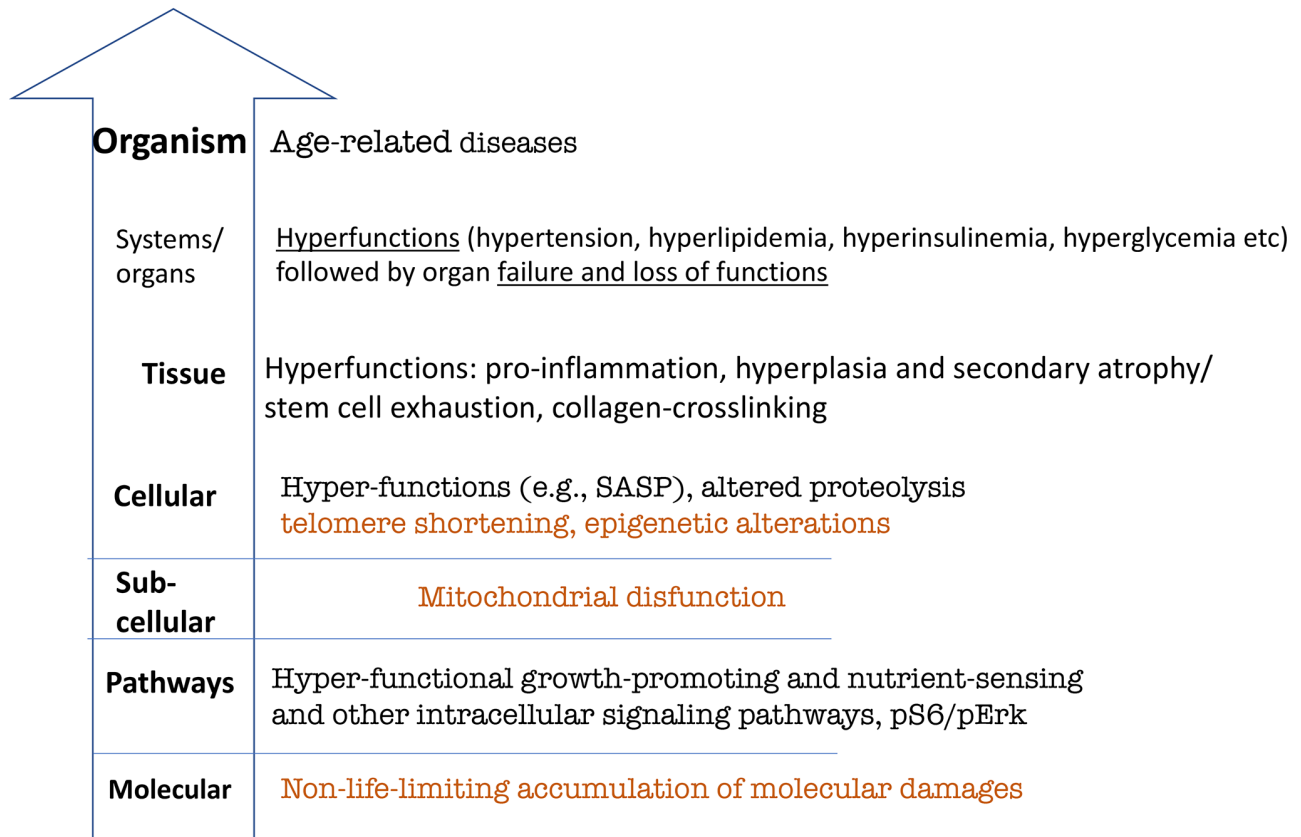


Figure 3. Hierarchical hallmarks of aging based on hyperfunction theory, applicable to humans. Non-life-limiting hallmarks are shown in brown color. See text for explanation.

diseases [78]. Although telomere shortening is associated with cardiovascular disease (CVD) in humans, patients with dyskeratosis congenita (DKC), a condition caused by short telomeres, do not die from CVD but from bone marrow failure (which is not a typical age-related disease) [79]. Hyperfunction theory explains how hyper-functional signaling leads to CVD in humans [80]. But telomere shortening cannot explain it.

Anything can shorten lifespan including starvation and the atomic bomb but they are not causes of aging. Only the third criterion matters: (3) its experimental amelioration should slow down aging and increase healthy lifespan. Not surprisingly, “the last criterion is the most difficult to achieve and not all of the hallmarks are fully supported yet by interventions,” as noted by López-Otín et al. [38]. In other words, they are not hallmarks of normal aging.

(Note: Even the third criterion is not sufficient to define a life-limiting hallmark.

Besides interventions may have off-target effects. For example, NAC, an antioxidant, is also a mTOR inhibitor [81]).

In conclusion, numerous deadly processes develop in parallel but only a few (or one) are life-limiting.

Therefore, non-limiting hallmarks are not included in the version of life-limiting hallmarks of aging (Figure 4). This final re-presentation is generic and can be applied to any species, from *C. elegans* to humans.

Aging as a selective force for cancer

Common cancers are age-related diseases. This cannot be explained by simple accumulation of mutations with age. For example, melanoma and lung cancer in smokers have atypically high mutation burden [8] but still develop at old age. Centenarians, who age slower, are protected from cancer. Rapamycin and calorie restriction slow aging in mice and prevent cancer.

As discussed, the selective force driving carcinogenesis is growth-limiting conditions, also named micro-environmental constraints in aging [16]. For example, the aging hematopoietic system selects for robust hematopoietic cells and such a preleukemic clone can originate leukemic clone [82]. Specifically, chronic inflammatory microenvironments in old age may select for cells harboring oncogenic mutations [83].

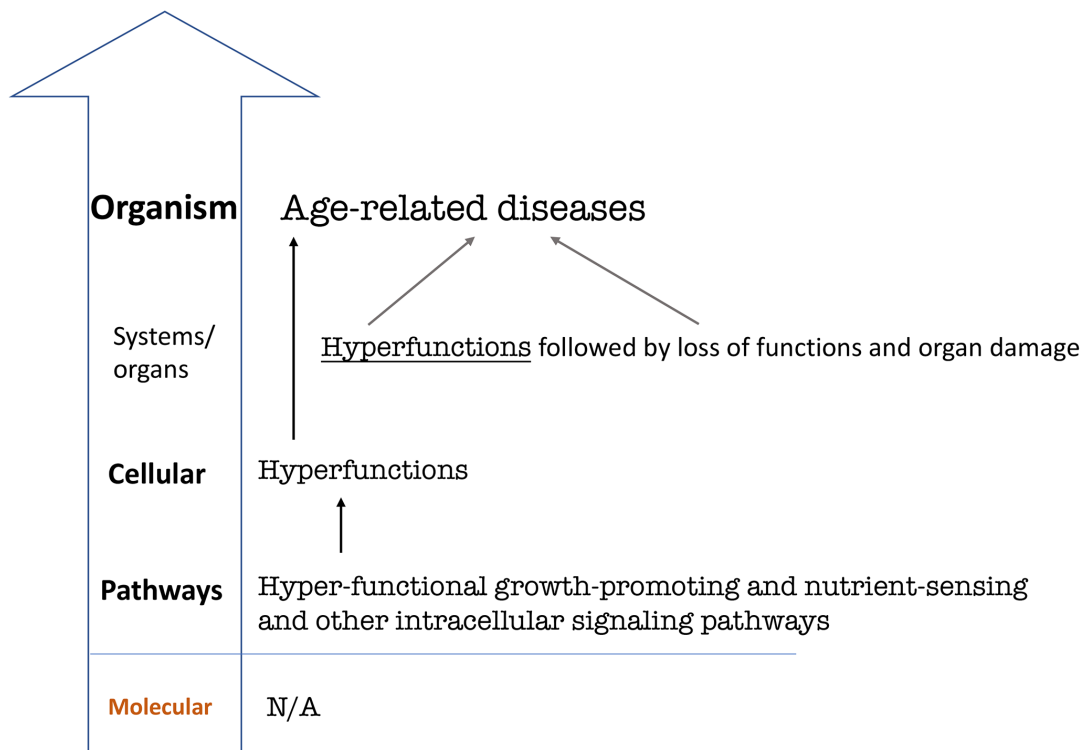


Figure 4. Hierarchical hallmarks of aging based on hyperfunction theory, universal. Hyperfunction of intracellular signaling pathways leads to cellular and systemic hyperfunctions, which in turn lead to age-related diseases on the organismal level [56]. Specific hyperfunctions and diseases may be different in different species and therefore are not shown. For example, human systemic hyperfunctions (e.g., hypertension, hyperlipidemia, hyperglycemia) and diseases (e.g., cardio-vascular diseases) differ from diseases in *C. elegans* [40, 41].

Chronic inflammation is a hyper-function and is in part mTOR-dependent [84–88]. An aging microenvironment puts stem cells on the path of hyper-activation [89] and geroconversion [90–92], leading to their exhaustion [89–92].

Mutations are necessary (with a few exceptions) but not sufficient for inducing cancer. The second requirement is selective force, favoring these mutations. Aging is a leading selective force.

One of the potential mechanisms of growth-limiting conditions that drive cancer progression is mTOR-dependent cellular senescence.

Common hallmarks of cancer, aging and cell senescence

Cellular senescence is a two-step process: cell cycle arrest followed by geroconversion [93]. Like organismal aging, geroconversion is a continuation of growth driven in part by hyperfunctional mTOR. When the cell cycle is blocked by p21/p16, but growth-promoting pathways such as mTOR and MAPK are active, the cells become hypertrophic (large cell morphology) and hyperfunctional: beta-Gal staining (lysosomal hyperfunction) and SASP. A hallmark of cellular senescence is active mTOR pathway in non-proliferating cells. Rapamycin suppresses geroconversion to senescence [93–97]. Figuratively, organismal aging is a quasi-growth after developmental growth is completed.

In cancer, the PI3K/mTOR pathway is almost universally activated by mutations [98–100]. Figuratively, cancer cells are proliferating senescent cells. In organismal aging, cancer and cellular senescence, the same key signaling pathways, such as mTOR, are involved. This is why the same drugs, such as rapamycin, can suppress all of them.

CONFLICTS OF INTERESTS

The authors declare no conflicts of interest related to this study.

REFERENCES

1. Hanahan D, Weinberg RA. The hallmarks of cancer. *Cell*. 2000; 100:57–70. [https://doi.org/10.1016/s0092-8674\(00\)81683-9](https://doi.org/10.1016/s0092-8674(00)81683-9) PMID:10647931
2. Cahill DP, Kinzler KW, Vogelstein B, Lengauer C. Genetic instability and darwinian selection in tumours. *Trends Cell Biol*. 1999; 9:M57–60. PMID:10611684
3. Blagosklonny MV. Molecular theory of cancer. *Cancer Biol Ther*. 2005; 4:621–7. <https://doi.org/10.4161/cbt.4.6.1818> PMID:15970666
4. Blagosklonny MV. Oncogenic resistance to growth-limiting conditions. *Nat Rev Cancer*. 2002; 2:221–5. <https://doi.org/10.1038/nrc743> PMID:11990858
5. Blagosklonny MV. Carcinogenesis, cancer therapy and chemoprevention. *Cell Death Differ*. 2005; 12:592–602. <https://doi.org/10.1038/sj.cdd.4401610> PMID:15818400
6. Yun J, Rago C, Cheong I, Pagliarini R, Angenendt P, Rajagopalan H, Schmidt K, Willson JK, Markowitz S, Zhou S, Diaz LA Jr, Velculescu VE, Lengauer C, et al. Glucose deprivation contributes to the development of KRAS pathway mutations in tumor cells. *Science*. 2009; 325:1555–9. <https://doi.org/10.1126/science.1174229> PMID:19661383
7. Hanahan D, Weinberg RA. Hallmarks of cancer: the next generation. *Cell*. 2011; 144:646–74. <https://doi.org/10.1016/j.cell.2011.02.013> PMID:21376230
8. Vogelstein B, Papadopoulos N, Velculescu VE, Zhou S, Diaz LA Jr, Kinzler KW. Cancer genome landscapes. *Science*. 2013; 339:1546–58. <https://doi.org/10.1126/science.1235122> PMID:23539594
9. Gems D, de Magalhães JP. The hoverfly and the wasp: A critique of the hallmarks of aging as a paradigm. *Ageing Res Rev*. 2021; 70:101407. <https://doi.org/10.1016/j.arr.2021.101407> PMID:34271186
10. Bozic I, Antal T, Ohtsuki H, Carter H, Kim D, Chen S, Karchin R, Kinzler KW, Vogelstein B, Nowak MA. Accumulation of driver and passenger mutations during tumor progression. *Proc Natl Acad Sci U S A*. 2010; 107:18545–50. <https://doi.org/10.1073/pnas.1010978107> PMID:20876136
11. Blagosklonny MV. A node between proliferation, apoptosis, and growth arrest. *Bioessays*. 1999; 21:704–9. [https://doi.org/10.1002/\(SICI\)1521-1878\(199908\)21:8<704::AID-BIES10>3.0.CO;2-5](https://doi.org/10.1002/(SICI)1521-1878(199908)21:8<704::AID-BIES10>3.0.CO;2-5) PMID:10440867
12. Maley CC, Galipeau PC, Li X, Sanchez CA, Paulson TG, Reid BJ. Selectively advantageous mutations and hitchhikers in neoplasms: p16 lesions are selected in Barrett's esophagus. *Cancer Res*. 2004; 64:3414–27.

- <https://doi.org/10.1158/0008-5472.CAN-03-3249>
PMID:[15150093](https://pubmed.ncbi.nlm.nih.gov/15150093/)
13. Liu X, Sun Y, Ehrlich M, Lu T, Kloog Y, Weinberg RA, Lodish HF, Henis YI. Disruption of TGF-beta growth inhibition by oncogenic ras is linked to p27Kip1 mislocalization. *Oncogene*. 2000; 19:5926–35.
<https://doi.org/10.1038/sj.onc.1203991>
PMID:[11127824](https://pubmed.ncbi.nlm.nih.gov/11127824/)
 14. Nowell PC. The clonal evolution of tumor cell populations. *Science*. 1976; 194:23–8.
<https://doi.org/10.1126/science.959840>
PMID:[959840](https://pubmed.ncbi.nlm.nih.gov/959840/)
 15. Merlo LM, Pepper JW, Reid BJ, Maley CC. Cancer as an evolutionary and ecological process. *Nat Rev Cancer*. 2006; 6:924–35.
<https://doi.org/10.1038/nrc2013>
PMID:[17109012](https://pubmed.ncbi.nlm.nih.gov/17109012/)
 16. Greaves M, Maley CC. Clonal evolution in cancer. *Nature*. 2012; 481:306–13.
<https://doi.org/10.1038/nature10762>
PMID:[22258609](https://pubmed.ncbi.nlm.nih.gov/22258609/)
 17. Blagosklonny MV. Antiangiogenic therapy and tumor progression. *Cancer Cell*. 2004; 5:13–7.
[https://doi.org/10.1016/s1535-6108\(03\)00336-2](https://doi.org/10.1016/s1535-6108(03)00336-2)
PMID:[14749122](https://pubmed.ncbi.nlm.nih.gov/14749122/)
 18. Blagosklonny MV. Why therapeutic response may not prolong the life of a cancer patient: selection for oncogenic resistance. *Cell Cycle*. 2005; 4:1693-8.
<https://doi.org/10.4161/cc.4.12.2259>
PMID:[16294046](https://pubmed.ncbi.nlm.nih.gov/16294046/)
 19. Pastò A, Pagotto A, Pilotto G, De Paoli A, De Salvo GL, Baldoni A, Nicoletto MO, Ricci F, Damia G, Bellio C, Indraccolo S, Amadori A. Resistance to glucose starvation as metabolic trait of platinum-resistant human epithelial ovarian cancer cells. *Oncotarget*. 2017; 8:6433–45.
<https://doi.org/10.18632/oncotarget.14118>
PMID:[28031535](https://pubmed.ncbi.nlm.nih.gov/28031535/)
 20. Reiter JG, Baretta M, Gerold JM, Makohon-Moore AP, Daud A, Iacobuzio-Donahue CA, Azad NS, Kinzler KW, Nowak MA, Vogelstein B. An analysis of genetic heterogeneity in untreated cancers. *Nat Rev Cancer*. 2019; 19:639–50.
<https://doi.org/10.1038/s41568-019-0185-x>
PMID:[31455892](https://pubmed.ncbi.nlm.nih.gov/31455892/)
 21. Murchison EP. Clonally transmissible cancers in dogs and Tasmanian devils. *Oncogene*. 2008 (Suppl 2); 27:S19–30.
<https://doi.org/10.1038/onc.2009.350>
PMID:[19956175](https://pubmed.ncbi.nlm.nih.gov/19956175/)
 22. Murchison EP, Schulz-Trieglaff OB, Ning Z, Alexandrov LB, Bauer MJ, Fu B, Hims M, Ding Z, Ivakhno S, Stewart C, Ng BL, Wong W, Aken B, et al. Genome sequencing and analysis of the Tasmanian devil and its transmissible cancer. *Cell*. 2012; 148:780–91.
<https://doi.org/10.1016/j.cell.2011.11.065>
PMID:[22341448](https://pubmed.ncbi.nlm.nih.gov/22341448/)
 23. Lister NC, Milton AM, Hanrahan BJ, Waters PD. Between the Devil and the Deep Blue Sea: Non-Coding RNAs Associated with Transmissible Cancers in Tasmanian Devil, Domestic Dog and Bivalves. *Noncoding RNA*. 2021; 7:72.
<https://doi.org/10.3390/ncrna7040072>
PMID:[34842768](https://pubmed.ncbi.nlm.nih.gov/34842768/)
 24. Ostrander EA, Davis BW, Ostrander GK. Transmissible Tumors: Breaking the Cancer Paradigm. *Trends Genet*. 2016; 32:1–15.
<https://doi.org/10.1016/j.tig.2015.10.001>
PMID:[26686413](https://pubmed.ncbi.nlm.nih.gov/26686413/)
 25. Cohen D. The canine transmissible venereal tumor: a unique result of tumor progression. *Adv Cancer Res*. 1985; 43:75–112.
[https://doi.org/10.1016/s0065-230x\(08\)60943-4](https://doi.org/10.1016/s0065-230x(08)60943-4)
PMID:[3887857](https://pubmed.ncbi.nlm.nih.gov/3887857/)
 26. McCallum H, Jones M, Hawkins C, Hamede R, Lachish S, Sinn DL, Beeton N, Lazenby B. Transmission dynamics of Tasmanian devil facial tumor disease may lead to disease-induced extinction. *Ecology*. 2009; 90:3379–92.
<https://doi.org/10.1890/08-1763.1>
PMID:[20120807](https://pubmed.ncbi.nlm.nih.gov/20120807/)
 27. Metzger MJ, Reinisch C, Sherry J, Goff SP. Horizontal transmission of clonal cancer cells causes leukemia in soft-shell clams. *Cell*. 2015; 161:255–63.
<https://doi.org/10.1016/j.cell.2015.02.042>
PMID:[25860608](https://pubmed.ncbi.nlm.nih.gov/25860608/)
 28. Hanahan D. Hallmarks of Cancer: New Dimensions. *Cancer Discov*. 2022; 12:31–46.
<https://doi.org/10.1158/2159-8290.CD-21-1059>
PMID:[35022204](https://pubmed.ncbi.nlm.nih.gov/35022204/)
 29. Fouad YA, Aanei C. Revisiting the hallmarks of cancer. *Am J Cancer Res*. 2017; 7:1016–36.
PMID:[28560055](https://pubmed.ncbi.nlm.nih.gov/28560055/)
 30. Senga SS, Grose RP. Hallmarks of cancer-the new testament. *Open Biol*. 2021; 11:200358.
<https://doi.org/10.1098/rsob.200358>
PMID:[33465324](https://pubmed.ncbi.nlm.nih.gov/33465324/)
 31. Munkley J, Elliott DJ. Hallmarks of glycosylation in cancer. *Oncotarget*. 2016; 7:35478–89.
<https://doi.org/10.18632/oncotarget.8155>
PMID:[27007155](https://pubmed.ncbi.nlm.nih.gov/27007155/)
 32. Flavahan WA, Gaskell E, Bernstein BE. Epigenetic plasticity and the hallmarks of cancer. *Science*. 2017;

- 357:eaal2380.
<https://doi.org/10.1126/science.aal2380>
PMID:[28729483](https://pubmed.ncbi.nlm.nih.gov/28729483/)
33. MacCarthy-Morrogh L, Martin P. The hallmarks of cancer are also the hallmarks of wound healing. *Sci Signal*. 2020; 13:eaay8690.
<https://doi.org/10.1126/scisignal.aay8690>
PMID:[32900881](https://pubmed.ncbi.nlm.nih.gov/32900881/)
34. Kroemer G, Pouyssegur J. Tumor cell metabolism: cancer's Achilles' heel. *Cancer Cell*. 2008; 13:472–82.
<https://doi.org/10.1016/j.ccr.2008.05.005>
PMID:[18538731](https://pubmed.ncbi.nlm.nih.gov/18538731/)
35. Colotta F, Allavena P, Sica A, Garlanda C, Mantovani A. Cancer-related inflammation, the seventh hallmark of cancer: links to genetic instability. *Carcinogenesis*. 2009; 30:1073–81.
<https://doi.org/10.1093/carcin/bgp127>
PMID:[19468060](https://pubmed.ncbi.nlm.nih.gov/19468060/)
36. Baraks G, Tseng R, Pan CH, Kasliwal S, Leiton CV, Shroyer KR, Escobar-Hoyos LF. Dissecting the Oncogenic Roles of Keratin 17 in the Hallmarks of Cancer. *Cancer Res*. 2022; 82:1159–66.
<https://doi.org/10.1158/0008-5472.CAN-21-2522>
PMID:[34921015](https://pubmed.ncbi.nlm.nih.gov/34921015/)
37. Rassy E, Assi T, Pavlidis N. Exploring the biological hallmarks of cancer of unknown primary: where do we stand today? *Br J Cancer*. 2020; 122:1124–32.
<https://doi.org/10.1038/s41416-019-0723-z>
PMID:[32042068](https://pubmed.ncbi.nlm.nih.gov/32042068/)
38. López-Otín C, Blasco MA, Partridge L, Serrano M, Kroemer G. The hallmarks of aging. *Cell*. 2013; 153:1194–217.
<https://doi.org/10.1016/j.cell.2013.05.039>
PMID:[23746838](https://pubmed.ncbi.nlm.nih.gov/23746838/)
39. Gems D. The aging-disease false dichotomy: understanding senescence as pathology. *Front Genet*. 2015; 6:212.
<https://doi.org/10.3389/fgene.2015.00212>
PMID:[26136770](https://pubmed.ncbi.nlm.nih.gov/26136770/)
40. Ezcurra M, Benedetto A, Sornda T, Gilliat AF, Au C, Zhang Q, van Schelt S, Petrache AL, Wang H, de la Guardia Y, Bar-Nun S, Tyler E, Wakelam MJ, Gems D. *C. elegans* Eats Its Own Intestine to Make Yolk Leading to Multiple Senescent Pathologies. *Curr Biol*. 2018; 28:2544–56.e5.
<https://doi.org/10.1016/j.cub.2018.06.035>
PMID:[30100339](https://pubmed.ncbi.nlm.nih.gov/30100339/)
41. Wang H, Zhang Z, Gems D. Monsters in the uterus: teratoma-like tumors in senescent *C. elegans* result from a parthenogenetic quasi-program. *Aging (Albany NY)*. 2018; 10:1188–9.
<https://doi.org/10.18632/aging.101486>
PMID:[29923830](https://pubmed.ncbi.nlm.nih.gov/29923830/)
42. Wang H, Zhao Y, Ezcurra M, Benedetto A, Gilliat AF, Hellberg J, Ren Z, Galimov ER, Athigapanich T, Girstmair J, Telford MJ, Dolphin CT, Zhang Z, Gems D. A parthenogenetic quasi-program causes teratoma-like tumors during aging in wild-type *C. elegans*. *NPJ Aging Mech Dis*. 2018; 4:6.
<https://doi.org/10.1038/s41514-018-0025-3>
PMID:[29928508](https://pubmed.ncbi.nlm.nih.gov/29928508/)
43. Blagosklonny MV. Validation of anti-aging drugs by treating age-related diseases. *Aging (Albany NY)*. 2009; 1:281–8.
<https://doi.org/10.18632/aging.100034>
PMID:[20157517](https://pubmed.ncbi.nlm.nih.gov/20157517/)
44. Gems D, de la Guardia Y. Alternative Perspectives on Aging in *Caenorhabditis elegans*: Reactive Oxygen Species or Hyperfunction? *Antioxid Redox Signal*. 2013; 19:321–9.
<https://doi.org/10.1089/ars.2012.4840>
PMID:[22870907](https://pubmed.ncbi.nlm.nih.gov/22870907/)
45. Gems D, Partridge L. Genetics of longevity in model organisms: debates and paradigm shifts. *Annu Rev Physiol*. 2013; 75:621–44.
<https://doi.org/10.1146/annurev-physiol-030212-183712>
PMID:[23190075](https://pubmed.ncbi.nlm.nih.gov/23190075/)
46. Doonan R, McElwee JJ, Matthijssens F, Walker GA, Houthoofd K, Back P, Matscheski A, Vanfleteren JR, Gems D. Against the oxidative damage theory of aging: superoxide dismutases protect against oxidative stress but have little or no effect on life span in *Caenorhabditis elegans*. *Genes Dev*. 2008; 22:3236–41.
<https://doi.org/10.1101/gad.504808>
PMID:[19056880](https://pubmed.ncbi.nlm.nih.gov/19056880/)
47. Ng LF, Ng LT, van Breugel M, Halliwell B, Gruber J. Mitochondrial DNA Damage Does Not Determine *C. elegans* Lifespan. *Front Genet*. 2019; 10:311.
<https://doi.org/10.3389/fgene.2019.00311>
PMID:[31031801](https://pubmed.ncbi.nlm.nih.gov/31031801/)
48. Blagosklonny MV. Aging: ROS or TOR. *Cell Cycle*. 2008; 7:3344–54.
<https://doi.org/10.4161/cc.7.21.6965>
PMID:[18971624](https://pubmed.ncbi.nlm.nih.gov/18971624/)
49. Blagosklonny MV. DNA- and telomere-damage does not limit lifespan: evidence from rapamycin. *Aging (Albany NY)*. 2021; 13:3167–75.
<https://doi.org/10.18632/aging.202674>
PMID:[33578394](https://pubmed.ncbi.nlm.nih.gov/33578394/)
50. Lapointe J, Hekimi S. When a theory of aging ages badly. *Cell Mol Life Sci*. 2010; 67:1–8.
<https://doi.org/10.1007/s00018-009-0138-8>

- PMID:[19730800](https://pubmed.ncbi.nlm.nih.gov/19730800/)
51. Ristow M, Schmeisser S. Extending life span by increasing oxidative stress. *Free Radic Biol Med*. 2011; 51:327–36.
<https://doi.org/10.1016/j.freeradbiomed.2011.05.010>
PMID:[21619928](https://pubmed.ncbi.nlm.nih.gov/21619928/)
52. Gladyshev VN. The free radical theory of aging is dead. Long live the damage theory! *Antioxid Redox Signal*. 2014; 20:727–31.
<https://doi.org/10.1089/ars.2013.5228>
PMID:[24159899](https://pubmed.ncbi.nlm.nih.gov/24159899/)
53. Golubev A, Hanson AD, Gladyshev VN. Non-enzymatic molecular damage as a prototypic driver of aging. *J Biol Chem*. 2017; 292:6029–38.
<https://doi.org/10.1074/jbc.R116.751164>
PMID:[28264930](https://pubmed.ncbi.nlm.nih.gov/28264930/)
54. Schumacher B, Pothof J, Vijg J, Hoeijmakers JHJ. The central role of DNA damage in the ageing process. *Nature*. 2021; 592:695–703.
<https://doi.org/10.1038/s41586-021-03307-7>
PMID:[33911272](https://pubmed.ncbi.nlm.nih.gov/33911272/)
55. MacRae SL, Croken MM, Calder RB, Aliper A, Milholland B, White RR, Zhavoronkov A, Gladyshev VN, Seluanov A, Gorbunova V, Zhang ZD, Vijg J. DNA repair in species with extreme lifespan differences. *Aging (Albany NY)*. 2015; 7:1171–84.
<https://doi.org/10.18632/aging.100866>
PMID:[26729707](https://pubmed.ncbi.nlm.nih.gov/26729707/)
56. Blagosklonny MV. Aging and immortality: quasi-programmed senescence and its pharmacologic inhibition. *Cell Cycle*. 2006; 5:2087–102.
<https://doi.org/10.4161/cc.5.18.3288>
PMID:[17012837](https://pubmed.ncbi.nlm.nih.gov/17012837/)
57. Blagosklonny MV. The hyperfunction theory of aging: three common misconceptions. *Oncoscience*. 2021; 8:103–7.
<https://doi.org/10.18632/oncoscience.545>
PMID:[34549076](https://pubmed.ncbi.nlm.nih.gov/34549076/)
58. de Grey AD. Protagonistic pleiotropy: Why cancer may be the only pathogenic effect of accumulating nuclear mutations and epimutations in aging. *Mech Ageing Dev*. 2007; 128:456–9.
<https://doi.org/10.1016/j.mad.2007.05.005>
PMID:[17588643](https://pubmed.ncbi.nlm.nih.gov/17588643/)
59. Blagosklonny MV. Molecular damage in cancer: an argument for mTOR-driven aging. *Aging (Albany NY)*. 2011; 3:1130–41.
<https://doi.org/10.18632/aging.100422>
PMID:[22246147](https://pubmed.ncbi.nlm.nih.gov/22246147/)
60. Blagosklonny MV. Response to the Thought-Provoking Critique of Hyperfunction Theory by Aubrey de Grey. *Rejuvenation Res*. 2021; 24:170–2.
<https://doi.org/10.1089/rej.2021.0018>
PMID:[33784825](https://pubmed.ncbi.nlm.nih.gov/33784825/)
61. Gems D. The hyperfunction theory: An emerging paradigm for the biology of aging. *Ageing Res Rev*. 2022; 74:101557.
<https://doi.org/10.1016/j.arr.2021.101557>
PMID:[34990845](https://pubmed.ncbi.nlm.nih.gov/34990845/)
62. Lind MI, Ravindran S, Sekajova Z, Carlsson H, Hinas A, Maklakov AA. Experimentally reduced insulin/IGF-1 signaling in adulthood extends lifespan of parents and improves Darwinian fitness of their offspring. *Evol Lett*. 2019; 3:207–16.
<https://doi.org/10.1002/evl3.108>
PMID:[31007945](https://pubmed.ncbi.nlm.nih.gov/31007945/)
63. Berman AE, Leontieva OV, Natarajan V, McCubrey JA, Demidenko ZN, Nikiforov MA. Recent progress in genetics of aging, senescence and longevity: focusing on cancer-related genes. *Oncotarget*. 2012; 3:1522–32.
<https://doi.org/10.18632/oncotarget.889>
PMID:[23455653](https://pubmed.ncbi.nlm.nih.gov/23455653/)
64. Iseghohi SO, Omage K. How ageing increases cancer susceptibility: A tale of two opposing yet synergistic views. *Genes Dis*. 2016; 3:105–9.
<https://doi.org/10.1016/j.gendis.2016.04.002>
PMID:[30258879](https://pubmed.ncbi.nlm.nih.gov/30258879/)
65. Scialò F, Sriram A, Naudí A, Ayala V, Jové M, Pamplona R, Sanz A. Target of rapamycin activation predicts lifespan in fruit flies. *Cell Cycle*. 2015; 14:2949–58.
<https://doi.org/10.1080/15384101.2015.1071745>
PMID:[26259964](https://pubmed.ncbi.nlm.nih.gov/26259964/)
66. Biliński T, Paszkiewicz T, Zadrag-Tecza R. Energy excess is the main cause of accelerated aging of mammals. *Oncotarget*. 2015; 6:12909–19.
<https://doi.org/10.18632/oncotarget.4271>
PMID:[26079722](https://pubmed.ncbi.nlm.nih.gov/26079722/)
67. Blagosklonny MV. Answering the ultimate question "what is the proximal cause of aging?". *Aging (Albany NY)*. 2012; 4:861–77.
<https://doi.org/10.18632/aging.100525>
PMID:[23425777](https://pubmed.ncbi.nlm.nih.gov/23425777/)
68. Zimniak P. What is the Proximal Cause of Aging? *Front Genet*. 2012; 3:189.
<https://doi.org/10.3389/fgene.2012.00189>
PMID:[23056007](https://pubmed.ncbi.nlm.nih.gov/23056007/)
69. de Grey ADN. Programs, Hyperfunction, and Damage: Why Definitions and Logic Matter So Much in Biogerontology. *Rejuvenation Res*. 2021; 24:83–5.
<https://doi.org/10.1089/rej.2021.0015>
PMID:[33784821](https://pubmed.ncbi.nlm.nih.gov/33784821/)
70. Kenyon CJ. The genetics of ageing. *Nature*. 2010;

- 464:504–12.
<https://doi.org/10.1038/nature08980>
 PMID:20336132
71. Vellai T, Takacs-Vellai K, Zhang Y, Kovacs AL, Orosz L, Müller F. Genetics: influence of TOR kinase on lifespan in *C. elegans*. *Nature*. 2003; 426:620.
<https://doi.org/10.1038/426620a>
 PMID:14668850
72. Bartke A, Quainoo N. Impact of Growth Hormone-Related Mutations on Mammalian Aging. *Front Genet*. 2018; 9:586.
<https://doi.org/10.3389/fgene.2018.00586>
 PMID:30542372
73. Selman C, Tullet JM, Wieser D, Irvine E, Lingard SJ, Choudhury AI, Claret M, Al-Qassab H, Carmignac D, Ramadani F, Woods A, Robinson IC, Schuster E, et al. Ribosomal protein S6 kinase 1 signaling regulates mammalian life span. *Science*. 2009; 326:140–4.
<https://doi.org/10.1126/science.1177221>
 PMID:19797661
74. Harrison DE, Strong R, Sharp ZD, Nelson JF, Astle CM, Flurkey K, Nadon NL, Wilkinson JE, Frenkel K, Carter CS, Pahor M, Javors MA, Fernandez E, Miller RA. Rapamycin fed late in life extends lifespan in genetically heterogeneous mice. *Nature*. 2009; 460:392–5.
<https://doi.org/10.1038/nature08221>
 PMID:19587680
75. Anisimov VN, Zabezhinski MA, Popovich IG, Piskunova TS, Semenchenko AV, Tyndyk ML, Yurova MN, Antoch MP, Blagosklonny MV. Rapamycin extends maximal lifespan in cancer-prone mice. *Am J Pathol*. 2010; 176:2092–7.
<https://doi.org/10.2353/ajpath.2010.091050>
 PMID:20363920
76. Bitto A, Ito TK, Pineda VV, LeTexier NJ, Huang HZ, Sutlief E, Tung H, Vizzini N, Chen B, Smith K, Meza D, Yajima M, Beyer RP, et al. Transient rapamycin treatment can increase lifespan and healthspan in middle-aged mice. *Elife*. 2016; 5:e16351.
<https://doi.org/10.7554/eLife.16351>
 PMID:27549339
77. Strong R, Miller RA, Bogue M, Fernandez E, Javors MA, Libert S, Marinez PA, Murphy MP, Musi N, Nelson JF, Petrascheck M, Reifsnnyder P, Richardson A, et al. Rapamycin-mediated mouse lifespan extension: Late-life dosage regimes with sex-specific effects. *Aging Cell*. 2020; 19:e13269.
<https://doi.org/10.1111/acer.13269>
 PMID:33145977
78. Herrera E, Samper E, Martín-Caballero J, Flores JM, Lee HW, Blasco MA. Disease states associated with telomerase deficiency appear earlier in mice with short telomeres. *EMBO J*. 1999; 18:2950–60.
<https://doi.org/10.1093/emboj/18.11.2950>
 PMID:10357808
79. Gramatges MM, Bertuch AA. Short telomeres: from dyskeratosis congenita to sporadic aplastic anemia and malignancy. *Transl Res*. 2013; 162:353–63.
<https://doi.org/10.1016/j.trsl.2013.05.003>
 PMID:23732052
80. Blagosklonny MV. Prospective treatment of age-related diseases by slowing down aging. *Am J Pathol*. 2012; 181:1142–6.
<https://doi.org/10.1016/j.ajpath.2012.06.024>
 PMID:22841821
81. Lai ZW, Hanczko R, Bonilla E, Caza TN, Clair B, Bartos A, Miklossy G, Jimah J, Doherty E, Tily H, Francis L, Garcia R, Dawood M, et al. N-acetylcysteine reduces disease activity by blocking mammalian target of rapamycin in T cells from systemic lupus erythematosus patients: a randomized, double-blind, placebo-controlled trial. *Arthritis Rheum*. 2012; 64:2937–46.
<https://doi.org/10.1002/art.34502>
 PMID:22549432
82. Shlush LI, Minden MD. Preleukemia: the normal side of cancer. *Curr Opin Hematol*. 2015; 22:77–84.
<https://doi.org/10.1097/MOH.000000000000111>
 PMID:25575035
83. Henry CJ, Casás-Selves M, Kim J, Zaberezhnyy V, Aghili L, Daniel AE, Jimenez L, Azam T, McNamee EN, Clambey ET, Klawitter J, Serkova NJ, Tan AC, et al. Aging-associated inflammation promotes selection for adaptive oncogenic events in B cell progenitors. *J Clin Invest*. 2015; 125:4666–80.
<https://doi.org/10.1172/JCI83024>
 PMID:26551682
84. Laberge RM, Sun Y, Orjalo AV, Patil CK, Freund A, Zhou L, Curran SC, Davalos AR, Wilson-Edell KA, Liu S, Limbad C, Demaria M, Li P, et al. mTOR regulates the pro-tumorigenic senescence-associated secretory phenotype by promoting IL1A translation. *Nat Cell Biol*. 2015; 17:1049–61.
<https://doi.org/10.1038/ncb3195>
 PMID:26147250
85. Choi YJ, Moon KM, Chung KW, Jeong JW, Park D, Kim DH, Yu BP, Chung HY. The underlying mechanism of proinflammatory NF- κ B activation by the mTORC2/Akt/IKK α pathway during skin aging. *Oncotarget*. 2016; 7:52685–94.
<https://doi.org/10.18632/oncotarget.10943>
 PMID:27486771
86. Wang R, Sunchu B, Perez VI. Rapamycin and the

- inhibition of the secretory phenotype. *Exp Gerontol*. 2017; 94:89–92.
<https://doi.org/10.1016/j.exger.2017.01.026>
 PMID:28167236
87. Wang R, Yu Z, Sunchu B, Shoaf J, Dang I, Zhao S, Caples K, Bradley L, Beaver LM, Ho E, Löhr CV, Perez VI. Rapamycin inhibits the secretory phenotype of senescent cells by a Nrf2-independent mechanism. *Aging Cell*. 2017; 16:564–74.
<https://doi.org/10.1111/acer.12587>
 PMID:28371119
88. Bent EH, Gilbert LA, Hemann MT. A senescence secretory switch mediated by PI3K/AKT/mTOR activation controls chemoprotective endothelial secretory responses. *Genes Dev*. 2016; 30:1811–21.
<https://doi.org/10.1101/gad.284851.116>
 PMID:27566778
89. Rodgers JT, King KY, Brett JO, Cromie MJ, Charville GW, Maguire KK, Brunson C, Mastey N, Liu L, Tsai CR, Goodell MA, Rando TA. mTORC1 controls the adaptive transition of quiescent stem cells from G0 to G(Alert). *Nature*. 2014; 510:393–6.
<https://doi.org/10.1038/nature13255>
 PMID:24870234
90. Sousa-Victor P, Gutarra S, García-Prat L, Rodriguez-Ubrea J, Ortet L, Ruiz-Bonilla V, Jardí M, Ballestar E, González S, Serrano AL, Perdiguero E, Muñoz-Cánoves P. Geriatric muscle stem cells switch reversible quiescence into senescence. *Nature*. 2014; 506:316–21.
<https://doi.org/10.1038/nature13013>
 PMID:24522534
91. Sousa-Victor P, Perdiguero E, Muñoz-Cánoves P. Geroconversion of aged muscle stem cells under regenerative pressure. *Cell Cycle*. 2014; 13:3183–90.
<https://doi.org/10.4161/15384101.2014.965072>
 PMID:25485497
92. Yue F, Bi P, Wang C, Li J, Liu X, Kuang S. Conditional Loss of Pten in Myogenic Progenitors Leads to Postnatal Skeletal Muscle Hypertrophy but Age-Dependent Exhaustion of Satellite Cells. *Cell Rep*. 2016; 17:2340–53.
<https://doi.org/10.1016/j.celrep.2016.11.002>
 PMID:27880908
93. Blagosklonny MV. Rapamycin, proliferation and geroconversion to senescence. *Cell Cycle*. 2018; 17:2655–65.
<https://doi.org/10.1080/15384101.2018.1554781>
 PMID:30541374
94. Demidenko ZN, Zubova SG, Bukreeva EI, Pospelov VA, Pospelova TV, Blagosklonny MV. Rapamycin decelerates cellular senescence. *Cell Cycle*. 2009; 8:1888–95.
<https://doi.org/10.4161/cc.8.12.8606>
 PMID:19471117
95. Dulic V. Senescence regulation by mTOR. *Methods Mol Biol*. 2013; 965:15–35.
https://doi.org/10.1007/978-1-62703-239-1_2
 PMID:23296649
96. Houssaini A, Breau M, Kebe K, Abid S, Marcos E, Lipskaia L, Rideau D, Parpaleix A, Huang J, Amsellem V, Vienney N, Validire P, Maitre B, et al. mTOR pathway activation drives lung cell senescence and emphysema. *JCI Insight*. 2018; 3:93203.
<https://doi.org/10.1172/jci.insight.93203>
 PMID:29415880
97. Maskey RS, Wang F, Lehman E, Wang Y, Emmanuel N, Zhong W, Jin G, Abraham RT, Arndt KT, Myers JS, Mazurek A. Sustained mTORC1 activity during palbociclib-induced growth arrest triggers senescence in ER+ breast cancer cells. *Cell Cycle*. 2021; 20:65–80.
<https://doi.org/10.1080/15384101.2020.1859195>
 PMID:33356791
98. Mossmann D, Park S, Hall MN. mTOR signalling and cellular metabolism are mutual determinants in cancer. *Nat Rev Cancer*. 2018; 18:744–57.
<https://doi.org/10.1038/s41568-018-0074-8>
 PMID:30425336
99. Millis SZ, Jardim DL, Albacker L, Ross JS, Miller VA, Ali SM, Kurzrock R. Phosphatidylinositol 3-kinase pathway genomic alterations in 60,991 diverse solid tumors informs targeted therapy opportunities. *Cancer*. 2019; 125:1185–99.
<https://doi.org/10.1002/cncr.31921>
 PMID:30582752
100. Schmidt-Kittler O, Zhu J, Yang J, Liu G, Hendricks W, Lengauer C, Gabelli SB, Kinzler KW, Vogelstein B, Huso DL, Zhou S. PI3Kα inhibitors that inhibit metastasis. *Oncotarget*. 2010; 1:339–48.
<https://doi.org/10.18632/oncotarget.166>
 PMID:21179398